Complexity

Uncertainty Models in Complex Systems 2022

Lead Guest Editor: Željko Stević
Guest Editors: Dragan Marinkovic and Siniša Sremac

Uncertainty Models in Complex Systems 2022

Complexity

Uncertainty Models in Complex Systems 2022

Lead Guest Editor: Željko Stević
Guest Editors: Dragan Marinkovic and Siniša Sremac

Contents

Hindawi
Complexity
Volume 2024, Article ID 1124822, 19 pages
https://doi.org/10.1155/2024/1124822

Research Article

A Multilevel Wavelet Decomposition Network Hybrid Model Utilizing Cyclic Patterns for Stock Price Prediction

H. R. Wen, Mingchuan Yuan, Shuxin Wang, Lixin Liang, and Xianghua Fu

Shenzhen Technology University, Shenzhen, China

Correspondence should be addressed to Shuxin Wang; wangshuxin@sztu.edu.cn

Received 16 September 2022; Revised 31 October 2023; Accepted 27 November 2023; Published 17 January 2024

Academic Editor: M. De Aguiar

Stock price prediction is an important and complex time-series problem in academia and financial industries. Stock market prices are voted by all kinds of investors and are influenced by various factors. According to the literature studies, such as Elliott's wave theory and Howard's market cycle investment theory, the cyclic patterns are significant characteristics of the stock market. However, even several studies that do consider cyclic patterns (or similar concepts) suffered from the data leakage or boundary problems, which could be impractical for real applications. Inspired by the abovementioned, we propose a hybrid deep learning model called mWDN-LSTM, which correctly utilizes the cyclic patterns' information to predict stock price while avoiding the data leakage and alleviating boundary problems. According to the experiments on two different datasets, our model mWDN-LSTM outperforms the well-known benchmarks such as CNN-LSTM on the same experimental setup and demonstrates the effectiveness of utilizing cyclic patterns in stock price prediction.

1. Introduction

Stock price prediction is a very important and complex problem in the field of financial time-series prediction [1]. Stock price fluctuations are influenced by corporate fundamentals, business cycles, stock market trading rules, international political events, investor sentiments, and other various factors. Due to the abovementioned reasons, stock price prediction is a challenging problem that has attracted more and more researcher's attention.

The main methods of stock price prediction could be classified into two major classes: traditional statistical methods and machine learning methods [2]. The traditional statistical methods have the advantages of solid statistical theory as support. Various statistical methods for stock price prediction such as exponential smoothing model (ESM) [3], vector autoregression (VAR) [4], autoregression integrated moving average (ARIMA) model [5], generalized autoregression conditional heteroskedasticity (GARCH) model [6], and radial basis function (RBF) [3] were proposed and widely adopted in econometrics. However, most of these methods are linear based on hand-crafted factors and are limited by the statistical assumptions that the data are smooth and normally distributed. In this case, such methods may face challenges when analyzing financial series data with large volume, highly noisy, nonlinear, and nonstationary characteristics [7].

Among machine learning methods, deep learning methods based on neural networks are more popular and of better performance [8]. The main advantage of deep learning models is their ability to learn representations from raw data without feature engineering conducted by experienced practitioners, and this advantage makes deep learning models especially suitable for complex systems such as the stock market. Moreover, deep learning models can provide a general approximation of functions for complex, nonlinear, and nonsmooth processes [9]. Therefore, deep learning models are quite worth exploring to deal with financial time-series data.

In addition to the main two classes of methods, some researchers proposed stock prediction methods based on fuzzy system theory. Wu et al. presented a fuzzy momentum contrarian uncertain characteristic system for the classification and quantification of stock characteristics [10]. Based

on the suitability index (SI) derived from fuzzy-set theory, Syu et al. presented a stock selection system called TripleS [11].

According to literature [12], the time series consists of four components: trend, cycle, seasonal, and irregular component. Trend is a long-run tendency characterizing the time series. It may be a linear increase or decrease in level over time. It may be stochastic, a result of a random process, or deterministic, a result of a prescribed mathematical function of time. Seasonal components or signals, by contrast, are distinguishable patterns of regular annual variations in a series. These may be due to changes in the precipitation or temperature and so on. Cycles are recurrent data movement patterns over periods. It is also a more or less regular long-range fluctuation above or below some equilibrium level or trend line. They have upswings, peaks, downswings, and troughs. They are studied for their turning points, duration, frequencies, depths, phases, and effects on related phenomena. For example, business cycles are postulated recurrent patterns of prosperity, recession, depression, and recovery. And what is left over after these components are extracted from the series is the irregular or error components.

In this paper, we refer to the cycles (or similar concepts) in the time series of stock prices generally as cyclic patterns. As far as we all know, signal decomposition methods in the data signal processing field can generate features of different frequencies from series data and perform time-frequency analysis on the series data. These features that contain upswings, peaks, downswings, troughs, and cycle information (or frequency information) can be considered as cyclic patterns. In order to capture cyclic patterns, we found, among the signal decomposition methods, discrete wavelet transform (DWT, or discrete wavelet decomposition) and empirical mode decomposition (EMD), which are considered to be effective methods for obtaining cyclic patterns [13].

However, we found that inappropriate procedures for applying the wavelet decomposition to time-series data easily lead to data leakage [14], which uses unobserved data, and its forecasting results would be of extremely high precision, and predictions based on these methods are unreliable. We also found that in order to curb the data leakage, a sliding window mechanism was proposed; however, the wavelet coefficients vary near the endpoint of the transformation window with its shifts and cause boundary problems. The boundary problem causes the generated subseries to be distorted, and the constructed hybrid models are less effective than simple prediction methods in prediction. In this study, we carefully investigate the calculation mechanism of wavelet decomposition and multilevel wavelet decomposition network methods to resolve the two problems mentioned above.

Currently, most hybrid neural network models that utilize cyclic pattern information did not take into consideration the data leakage and boundary problem during the utilization of signal decomposition techniques. Therefore, we would like to propose a hybrid neural network model that utilizes cyclic patterns to predict stock prices, avoiding the data leakage and alleviating boundary problems. We propose the mWDN-LSTM stock price prediction hybrid model, which utilizes the mWDN network to generate cyclic patterns and then uses the LSTM model to make time-series predictions.

The rest of this paper is organized as follows. Section 2 introduces the related research work. Section 3 introduces the proposed mWDN-LSTM in detail. Then, Section 4 and Section 5 present the experimental setup and discuss the experimental results. At last, Section 6 concludes this paper.

The main contributions of this paper are as follows:

(1) We propose a solution that avoids data leakage while alleviating the boundary problem. A multilevel wavelet decomposition neural network and its variants are investigated, which can adaptively adjust the wavelet coefficients.

(2) A new hybrid model combining the wavelet decomposition network and LSTM is proposed, which can effectively utilize the cyclic patterns, and experimental results demonstrate the effectiveness of our proposed model.

2. Related Work

Due to the success of deep learning in recent years, models based on neural networks have gained more and more attention for stock price prediction problems [15]. In 2010, Naeini et al. applied two neural networks, a feedforward multilayer perceptron (MLP) and an Elman recurrent network, to predict a company's stock value based on its history stock price [16]. In 2013, Ticknor proposed the model of feedforward neural networks with Bayesian regularization to predict stock prices, thereby reducing the possibility of model overfitting [17]. In 2015, Rather et al. achieved a high accuracy based on the RNN model for the prediction of 6 stock prices from NSE [18]. In 2016, Di Persio and Honchar employed CNN to predict the S&P 500 price movement. The results showed that CNN achieved better results for financial time series compared to MLP and RNN models [19]. In 2017, Selvin constructed several deep learning models to predict stock prices in the Indian stock market, and in this paper, the following neural network models were employed: deep recurrent neural network (RNN), long short-term memory (LSTM) neural network, and convolutional neural network (CNN). The results of the empirical analysis showed that these models achieved reasonable prediction accuracy for stock prices, and among them, LSTM performed the best [20]. In 2020, Lu et al. proposed a CNN-LSTM-based stock price prediction method. Meanwhile, the prediction models such as MLP, CNN, RNN, LSTM, and CNN-RNN were used to predict the SSE (Shanghai Stock Exchange) stock index, and the proposed CNN-LSTM model demonstrated the best results on MAE, RMSE, and R^2 evaluation criteria [21]. In 2021, Wu and Ming-Tai proposed the SACLSTM stock price prediction algorithm, which constructs a sequence array of historical data and its leading indicators and uses the array as the input image of the CNN framework, and this algorithm

has achieved excellent forecasting results for Taiwan and American stocks [22], which is similar to the work proposed by the authors in reference [23]. An LSTM-GA stock trading suggestion system in IOT was proposed, based on historical data and leading indicators [24]. In 2022, Zhang et al. proposed the novel transformer encoder-based attention network (TEANet) framework, which realizes the effective processing and analysis of stock prices to improve the accuracy of stock movement prediction [25].

Some researchers have constructed hybrid models based on signal decomposition techniques and neural networks to exploit the cyclic patterns in the stock market. However, the vast majority of researchers did not take into account the data leakage and boundary problem implicit in the utilization of signal decomposition techniques such as DWT for time-series prediction tasks. For example, in 2019, Qiu et al. decomposed the historical stock price time series using DWT and EMD and then analyzed the obtained subseries and generated prediction by the RVFL model [26]. Chandar decomposed the financial time series using DWT and subsequently inputted the decomposed subseries into ANFIS to predict closing prices [27]. In 2020, Li and Tang proposed the WT-FCD-MLGRU model and chose four major stock indices, S&P 500, IXIC, DJI, and SSE, to test the model performance [28]. In 2021, Wu et al. proposed a combination of ELM and DWT-based models to predict the stock price movements of 400 stocks in China [29]. In the abovementioned study that employed the signal decomposition techniques, the data decomposition of the whole data series, including the training and test sets, was performed before the model was trained. This decomposition operation leads to the problem of data leakage of future data. Therefore, the final results are unrealistic, and similar effects cannot be achieved in practical applications. In addition, in 2018, Hasumi and Kajita found that wavelet-based time-series predictions cannot even outperform a simple prediction when the time series is properly processed due to boundary problems [30]. Since the data leakage and boundary problem may lead to unreliable results, we will explain them in detail in Section 3.2.

There were also research works utilizing cyclic patterns (or similar concepts) in other time-series tasks. In 2018, Wang designed the mWDN network which implemented a multilevel discrete wavelet decomposition process through a neural network called mWDN. This model has a better prediction performance than SAE, RNN, and LSTM in cellphone user numbers and in ECG time-series prediction tasks [31]. In 2020, Zhang proposed a hybrid neural network model based on mWDN in an industrial productivity prediction task that was able to effectively improve the accuracy and granularity of the prediction [32].

3. Model

In this section, first, we introduce how to generate cyclic patterns in the stock market by the discrete wavelet decomposition techniques. Second, we explain the two major problems during the wavelet decomposition procedure that need to be overcome. Third, we introduce the proposed model and each of its components in detail. At last, the training and prediction of our model are introduced.

3.1. MDWD and Cyclic Patterns

3.1.1. MDWD. Multilevel discrete wavelet decomposition (MDWD), a typical discrete signal analysis method, is commonly applied to numerical analysis, time-frequency analysis, denoising, and so on. The process of multilevel discrete wavelet decomposition mainly includes convolution operation and downsampling. The convolution operation can decompose the series into low-frequency and high-frequency subseries. Downsampling was designed to reduce the redundancy of the data, and at the same time, it can keep the total amount of decomposed data consistent with the original data. However, if the translation-invariance of the decomposition process needs to be maintained (the length of each subseries obtained from the decomposition is equal to the length of the original series), this step can be left out.

The multilevel discrete wavelet decomposition process is shown in Figure 1, and the related parameters are shown in Table 1. The implementation steps are as follows:

(1) In the 1-th level of decomposition, the input series $\mathbf{x}$ will do convolution operations with the low-pass filter $\mathbf{l}$ and the high-pass filter $\mathbf{h}$ and generate the intermediate variable series $\mathbf{a}^l(1)$ and $\mathbf{a}^h(1)$, respectively. This step can also be represented in the form of matrix operations.

The formula for the i-th level convolution operation is as follows:

$$\begin{aligned} a_n^l(i+1) &= \sum_{k=1}^{K} x_{n+k-1}^l(i) * l_k, \\ a_n^h(i+1) &= \sum_{k=1}^{K} x_{n+k-1}^l(i) * h_k, \end{aligned} \tag{1}$$

where $x_n^l(i)$ is the n-th element of the low-frequency subseries in the i-th level and $\mathbf{x}^l(0)$ is set as the input series $\mathbf{x}$.

(2) 1/2 downsampling of the intermediate variable series $\mathbf{a}^l(1)$ and $\mathbf{a}^h(\mathbf{1})$ is performed to obtain the low-frequency and high-frequency subseries $\mathbf{x}^l(1)$ and $\mathbf{x}^h(1)$ of the 1-th level decomposition.

(3) The low-frequency subseries $\mathbf{x}^l(1)$ is set as the input series for the next level of decomposition.

(4) After pooling i times for step (1) to step (3), the decomposition result $\boldsymbol{\chi}(i)$ of the i-th level decomposition is obtained.

3.1.2. Cyclic Patterns. In order to utilize the cycle characteristic in the stock market, the first step is to generate cyclic patterns from the raw dataset. For example, discrete wavelet decomposition methods are employed to generate cyclic pattern information. The subseries obtained by discrete wavelet decomposition contain cyclic information (or frequency information), such as cycle fluctuation depth, fluctuation duration, and fluctuation turning point, rendering it consistent with the definition of a cyclic pattern in a time series.

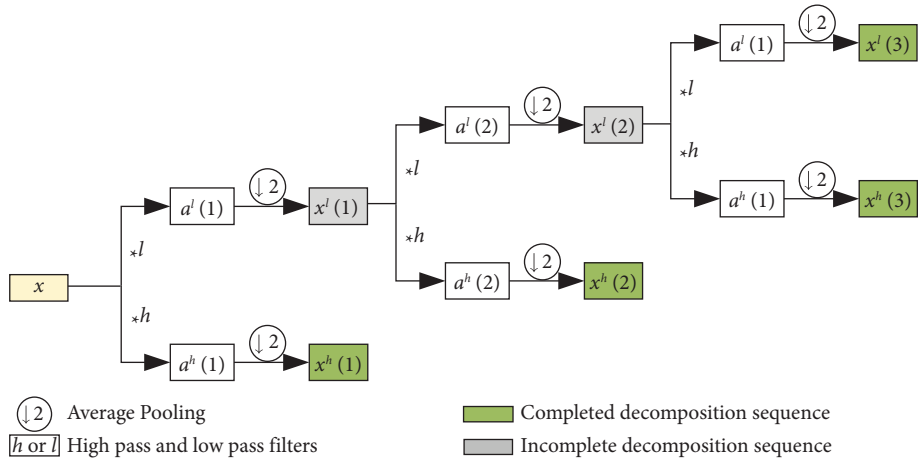

Figure 1: Multilevel discrete wavelet decomposition process.

Table 1: Parameters in the MDWD implementation process.

Parameter	Symbol
Input time series	$\mathbf{x} = \{x_1, \ldots x_t, \ldots, x_T\}$
Low and high subseries in the i-th level	$\mathbf{x}^l(i), \mathbf{x}^h(i)$
Low-pass filter	$\mathbf{l} = \{l_1, \ldots, l_k, \ldots, l_K\}, K \ll T$
High-pass filter	$\mathbf{h} = \{h_1, \ldots, h_k, \ldots, h_K\}, K \ll T$
Low-frequency intermediate variable series	$\mathbf{a}^l(i) = \{a_1^l(i), a_2^l(i), \ldots\}$
High-frequency intermediate variable series	$\mathbf{a}^h(i) = \{a_1^h(i), a_1^h(i), \ldots\}$
i-th level subseries/decomposed result	$\boldsymbol{\chi}(i) = \mathbf{x}^h(1), \mathbf{x}^h(2), \ldots, \mathbf{x}^h(i), \mathbf{x}^l(i)$

For example, we choose the series with a length of 200 and a decomposition level of 2 in Figure 2 to illustrate it. As shown in Figure 3, first, we can notice that the generated series fluctuates more or less regularly at the level of value 0, showing a cyclic fluctuation pattern. Although this series is not a rigorous cyclic series, it is a discrete combination of several cyclic series. Second, the series contains upward fluctuations and downward fluctuations, with the maximum upward fluctuations from $t = 5$ to $t = 18$ and the minimum downward fluctuations from $t = 95$ to $t = 100$. These unidirectional fluctuations are half of the cyclic fluctuations. Therefore, the series contains cyclic fluctuations with a minimum cycle of 10 days and a maximum cycle of 26 days. In addition, the series contains peaks and troughs, and the highest peak in this series is (195, 50.69) and the lowest trough is (5, −54.75). Therefore, the depth of the cyclic fluctuations in this series is between −54.75 and 50.69.

In conclusion, we can get the cycle information (or frequency information), cycle fluctuation depth information, fluctuation duration information, and fluctuation turning point information in the stock series data from the subseries decomposed by discrete wavelet decomposition methods, and it is consistent with the definition of a cycle in time series, so the subseries obtained by discrete wavelet decomposition is the cyclic pattern in the stock market that we need. In our model, the low-frequency subseries are long-term cyclic patterns and the high-frequency subseries are short-term cyclic patterns. We argue that cyclic patterns could be an enhancement for stock market prediction.

3.2. Data Leakage and Boundary Problem. We find that data leakage and boundary problems are two major problems when applying discrete wavelet decomposition in real stock price prediction applications. In the following, we describe these two problems in detail and introduce our method.

3.2.1. Data Leakage. Data leakage is the use of information in the model training process which would not be expected to be available at the prediction time, causing the predictive scores (metrics) to overestimate the model's utility when run in a production environment. We include the results of a method with data leakage in our experiments to demonstrate its easily overestimated effect.

When employing DWT with translation-invariance property, the length of the subseries is equal to the length of the original series, which makes many researchers mistakenly believe that they can decompose the original series in a one-time manner and then divide the dataset into the subseries. Based on this, model training and prediction are performed. This process is shown in Figure 4, and it contains data leakage. This is because the wavelet transform works by computing the convolution operation of the time series with

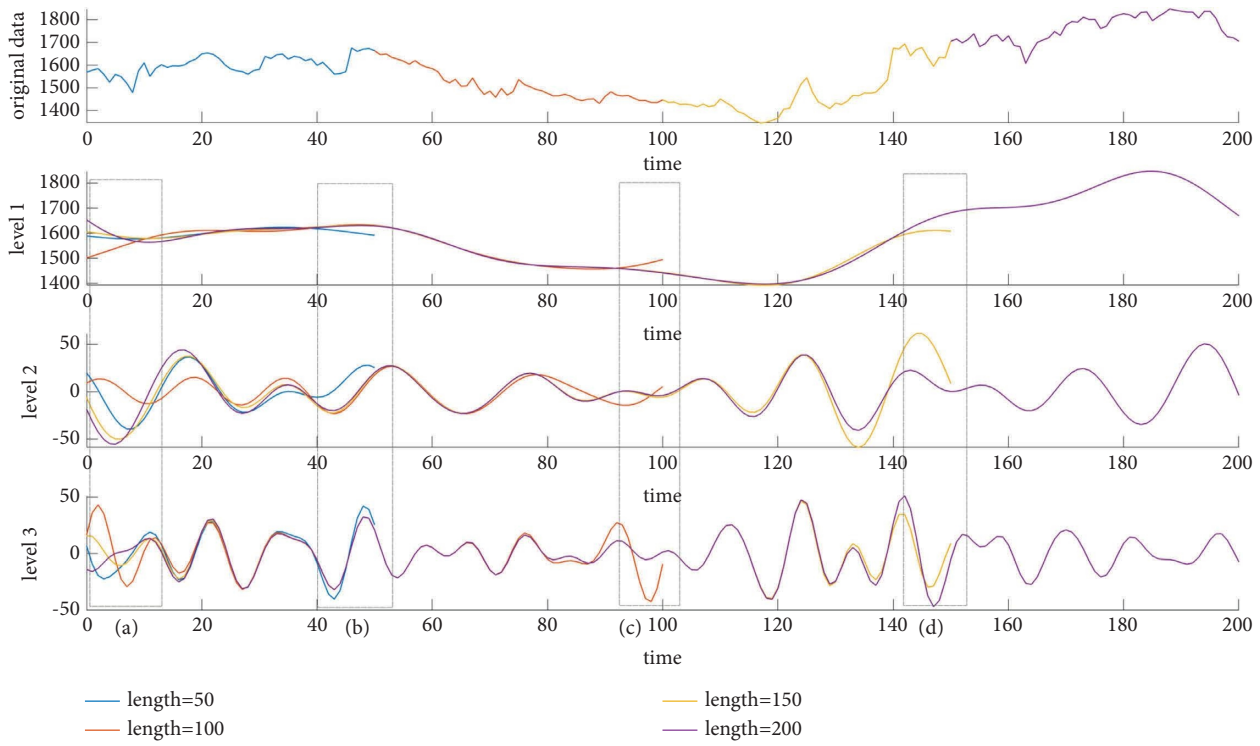

Figure 2: Comparison of series of different lengths after decomposition. (a) is the original data, (b) is the high-frequency subseries of level 3 decomposition, (c) is the high-frequency subseries of level 2 decomposition, and (d) is the high-frequency subseries of level 1 decomposition. The abovementioned decomposition has not been downsampled.

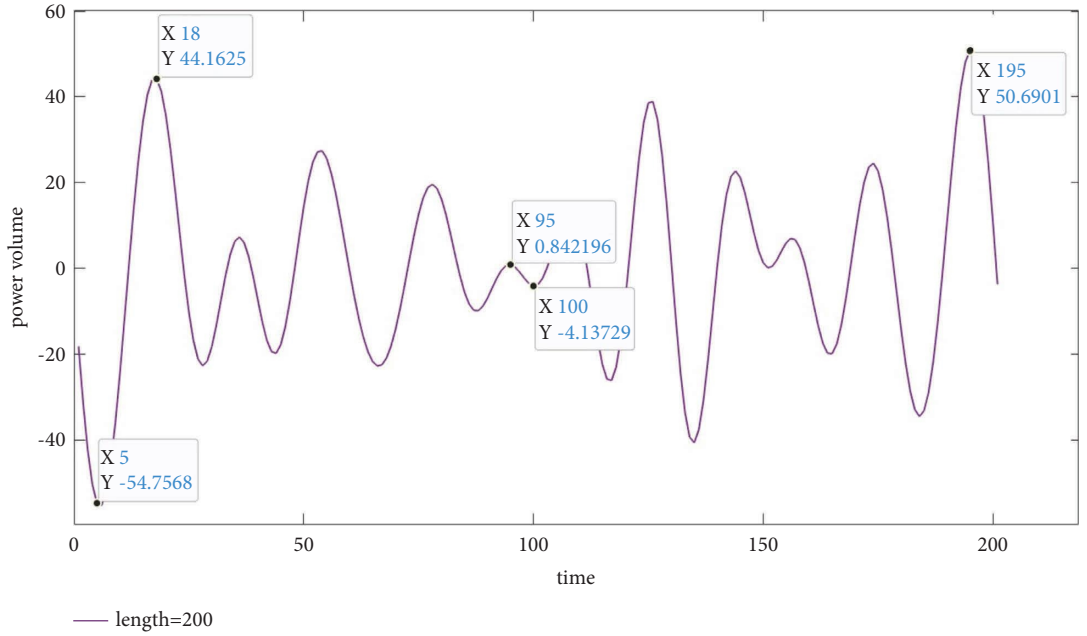

Figure 3: Level 2 decomposition series of length 200 series.

the selected wavelet function. When calculating the output of a point in a time series, it is necessary to convolve the wavelet function with that point and several points before and after it. As shown in the case of Figure 5, x_0 to x_9 are the time-series data arranged in a chronological order. The output of the data point x_1 needs to be obtained by convolution calculation with x_0, x_2, x_3, x_8, and x_9. The output of the data point x_3 needs to be obtained by convolution calculation with x_0, x_1, x_2, x_4, and x_5. So, the output of the convolution operation is a local combination of data points, and the decomposed components involve historical and future data. This is a typical data leakage problem.

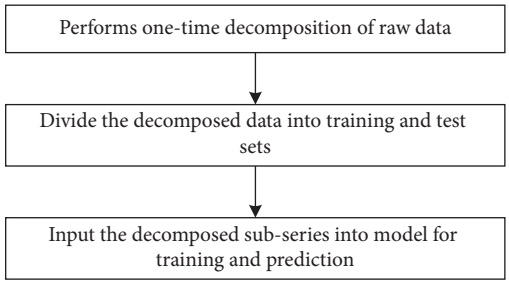

Figure 4: Wavelet decomposition-based prediction process in the existence of data leakage.

$$\begin{bmatrix} h_3 & h_4 & h_5 & 0 & 0 & 0 & 0 & h_0 & h_1 & h_2 \\ h_2 & h_3 & h_4 & h_5 & 0 & 0 & 0 & 0 & h_0 & h_1 \\ h_1 & h_2 & h_3 & h_4 & h_5 & 0 & 0 & 0 & 0 & h_0 \\ h_0 & h_1 & h_2 & h_3 & h_4 & h_5 & 0 & 0 & 0 & 0 \\ 0 & h_0 & h_1 & h_2 & h_3 & h_4 & h_5 & 0 & 0 & 0 \\ 0 & 0 & h_0 & h_1 & h_2 & h_3 & h_4 & h_5 & 0 & 0 \\ 0 & 0 & 0 & h_0 & h_1 & h_2 & h_3 & h_4 & h_5 & 0 \\ 0 & 0 & 0 & 0 & h_0 & h_1 & h_2 & h_3 & h_4 & h_5 \\ h_5 & 0 & 0 & 0 & 0 & h_0 & h_1 & h_2 & h_3 & h_4 \\ h_4 & h_5 & 0 & 0 & 0 & 0 & h_0 & h_1 & h_2 & h_3 \end{bmatrix} \begin{bmatrix} x_0 \\ x_1 \\ x_2 \\ x_3 \\ x_4 \\ x_5 \\ x_6 \\ x_7 \\ x_8 \\ x_9 \end{bmatrix} = \begin{bmatrix} y_0 \\ y_1 \\ y_2 \\ y_3 \\ y_4 \\ y_5 \\ y_6 \\ y_7 \\ y_8 \\ y_9 \end{bmatrix}$$

W X Y

Figure 5: Schematic diagram of wavelet transform convolution calculation. W is the regular wavelet convolution matrix case, X is the series data, and Y is the output.

This warns us that data decomposition should not involve prediction points and their subsequent data.

3.2.2. Boundary Problem. When we take measures to precisely control the decomposed series to avoid data leakage, such as sliding windows, the prediction results are significantly affected by the boundary problem and the model cannot generate accurate predictions.

In order to illustrate the boundary problem, we plot Figure 2 to show the difference in decomposing time series of different lengths. It also shows the difference of the corresponding output between whether the same point in time is at the boundary. The data are the SSE Composite Index data which are a part of the experimental dataset. We apply discrete wavelet decomposition to decompose the data into three components by expanding the number of data points from 50 to 200.

As can be seen from Figure 2, in the results of discrete wavelet decomposition of series data with lengths of 50, 100, 150, and 200, there are huge differences in the calculated results at the boundaries of the series. The subseries at the boundary are off-track and distorted. The subseries at the boundary are off-track and distorted, such as the four areas A, B, C, and D in Figure 2. This is caused by the assumption of circularity that the computation of the boundary involves the data at the other edge of the window. For example, the output of x_9 in Figure 5 needs to be calculated together with x_0 and x_1. The prediction of future data should be performed with the most recent data possible, rather than data from the other end of the sliding window, which would cause large biases in the prediction results.

We avoid data leakage by applying the sliding window mechanism with mWDN to replace the one-time wavelet decomposition. By establishing a new wavelet convolutional operation matrix and incorporating an adaptive adjustment mechanism for mWDN parameters, we aim to mitigate the impact of boundary problem on the prediction accuracy. This is elucidated in both the input layer and the mWDN component.

3.3. mWDN-LSTM Model. Our model mWDN-LSTM can be divided into four components: input layer, mWDN component, LSTM component, and output component. The model structure diagram is shown in Figure 6. In the first component, the input layer is designed to set up the sliding window and normalize the data. In the second component, the mWDN component is designed to implement wavelet decomposition and decompose the series data to generate cyclic patterns. In the third component, the LSTM component is utilized to learn and memorize long-term and short-term information and to make predictions. In the fourth component, the output component is a fully connected network that is utilized to convert the output vector into the final prediction.

3.3.1. Input Layer. In order to avoid data leakage and make the solution practically feasible, we can only decompose in real-time and predict while decomposing, so we use a sliding window mechanism as shown in Figure 7. The window is set up in front of the prediction point and moves forward one unit at a time until all data points are covered. mWDN also only decomposes the data within the window. This mechanism ensures that the decomposition process is real-time and does not include future data, which makes the prediction results realistic and reliable and can be deployed in real investment scenarios.

3.3.2. mWDN Component. In order to obtain cyclic patterns using discrete wavelet decomposition while alleviating the influence of boundary problems on prediction, we set up a new convolutional operation matrix and utilize mWDN with adaptive parameter adjustment capability to implement the discrete wavelet decomposition process.

(1) Redesign of the Convolutional Operation Matrix. When adopting the regular convolutional operation matrix (similar to Figure 5), the convolutional calculation at the boundary of the window involves data on the other side of the sliding window, causing the calculation results to be distorted. Therefore, we alleviate the impact of the boundary problem by shifting the wavelet parameters in the convolutional operation matrix so that the calculation results at the boundary near the prediction point are not distorted as much as possible. The redesigned matrix is shown in Figure 8. The redesigned matrix will be applied in mWDN.

The mWDN approximately implements an MDWD under a deep neural network framework. This neural network framework mainly consists of a perceptron model and an average pooling layer. mWDN implements the convolution operation in the MDWD by replacing the weight parameter matrix in the perceptron model using the wavelet function

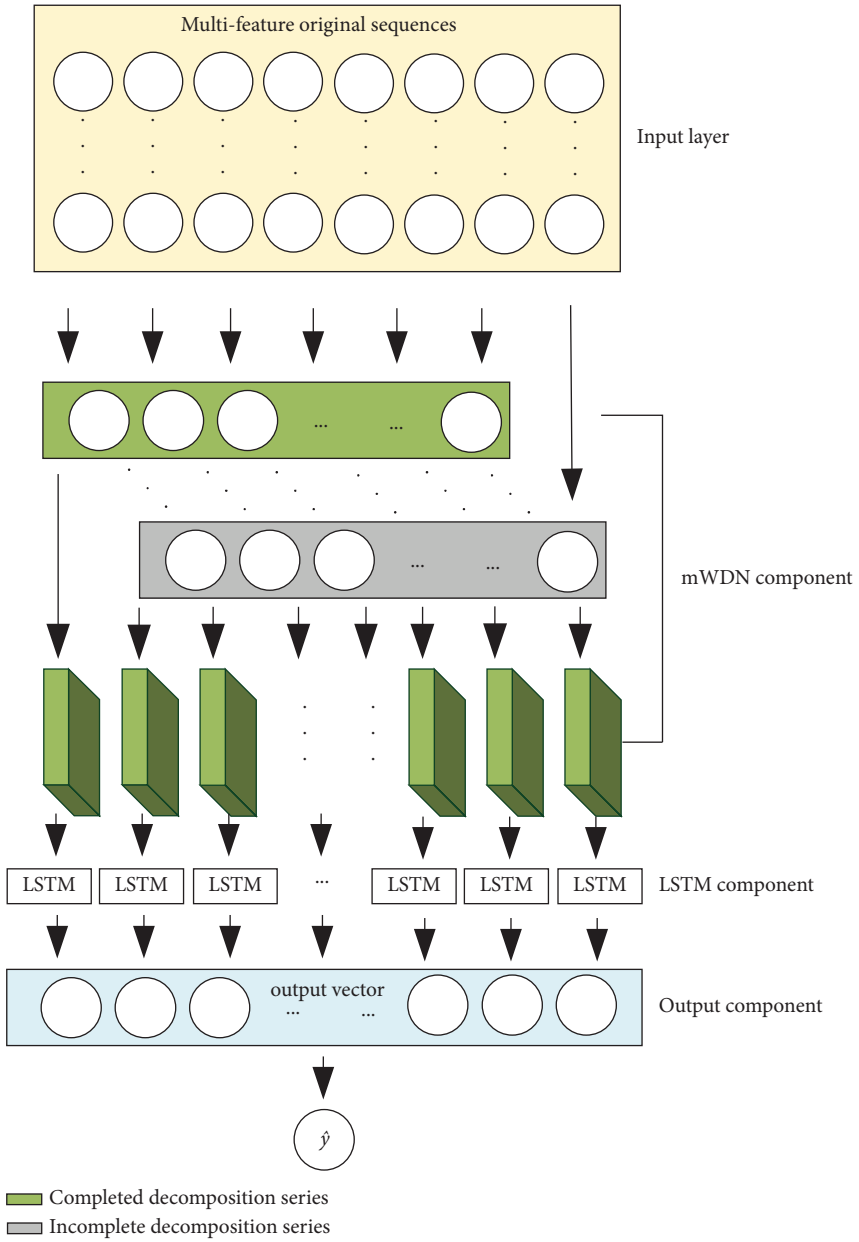

Figure 6: mWDN-LSTM structure diagram.

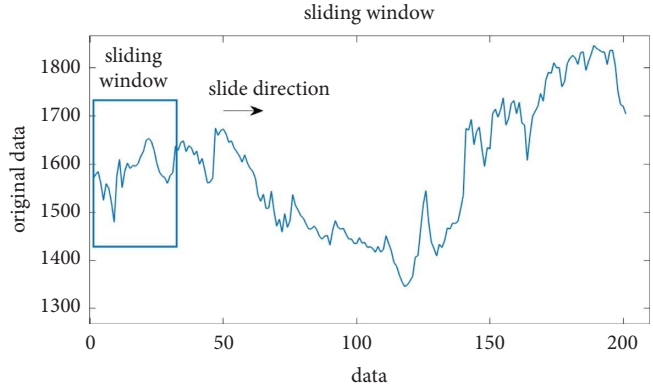

Figure 7: Diagram of the sliding window.

$$W^{l}(i)=\begin{bmatrix} l_K & \varepsilon & \cdots & \varepsilon & \varepsilon & \cdots & \varepsilon & \varepsilon & \varepsilon \\ l_{K-1} & l_K & \cdots & \varepsilon & \varepsilon & \cdots & \varepsilon & \varepsilon & \varepsilon \\ \vdots & \vdots & \ddots & \vdots & \vdots & \vdots & \vdots & \vdots & \vdots \\ l_1 & l_2 & \cdots & l_K & \varepsilon & \cdots & \varepsilon & \varepsilon & \varepsilon \\ \varepsilon & l_1 & \cdots & l_{K-1} & l_K & \cdots & \varepsilon & \varepsilon & \varepsilon \\ \vdots & \vdots & \vdots & \vdots & \vdots & \ddots & \vdots & \vdots & \vdots \\ \varepsilon & \varepsilon & \cdots & l_3 & l_4 & \cdots & l_K & \varepsilon & \varepsilon \\ \varepsilon & \varepsilon & \cdots & l_2 & l_3 & \cdots & l_{K-1} & l_K & \varepsilon \\ \varepsilon & \varepsilon & \cdots & l_1 & l_2 & \cdots & l_{K-2} & l_{K-1} & l_K \end{bmatrix}, \quad W^{h}(i)=\begin{bmatrix} h_K & \varepsilon & \cdots & \varepsilon & \varepsilon & \cdots & \varepsilon & \varepsilon & \varepsilon \\ h_{K-1} & h_K & \cdots & \varepsilon & \varepsilon & \cdots & \varepsilon & \varepsilon & \varepsilon \\ \vdots & \vdots & \ddots & \vdots & \vdots & \vdots & \vdots & \vdots & \vdots \\ h_1 & h_2 & \cdots & h_K & \varepsilon & \cdots & \varepsilon & \varepsilon & \varepsilon \\ \varepsilon & h_1 & \cdots & h_{K-1} & h_K & \cdots & \varepsilon & \varepsilon & \varepsilon \\ \vdots & \vdots & \vdots & \vdots & \vdots & \ddots & \vdots & \vdots & \vdots \\ \varepsilon & \varepsilon & \cdots & h_3 & h_4 & \cdots & h_K & \varepsilon & \varepsilon \\ \varepsilon & \varepsilon & \cdots & h_2 & h_3 & \cdots & h_{K-1} & h_K & \varepsilon \\ \varepsilon & \varepsilon & \cdots & h_1 & h_2 & \cdots & h_{K-2} & h_{K-1} & h_K \end{bmatrix}$$

FIGURE 8: Redesigned convolutional operation matrix, where $\mathbf{W}^{l}(i)$ and $\mathbf{W}^{h}(i) \in \mathbb{R}^{P\times P}$, P is the size of input series at the i-th level decomposition, ε are random values that satisfy $|\varepsilon| \ll |l|, \forall l \in l$, and $|\varepsilon| \ll |h|, \forall h \in h$.

matrix of the convolution operation. This makes mWDN different from MDWD with constant parameters and has the ability to fine-tune parameters such as convolutional operation matrix and bias vector to fit different learning tasks. Then, the downsampling process in MDWD is implemented by the average pooling layer. We hope to alleviate the impact of the wavelet decomposition boundary problem on the prediction results by optimizing the prediction effect based on the capability of mWDN to fine-tune the convolution calculation matrix and deviation vector. The schematic diagram for mWDN to implement the i-th level decomposition of the MDWD process is shown in Figure 9. The steps of the process are as follows:

(1) We set up weight matrices $\mathbf{W}^{l}(i)$ and $\mathbf{W}^{h}(i)$ according to the parameters of low-pass filter $\mathbf{l}$ and high-pass filter $\mathbf{h}$. The values of the low-pass filter and high-pass filter depend on the selected wavelet function. We initialize the bias vectors $\mathbf{b}^{\mathbf{l}}(i)$ and $\mathbf{b}^{\mathbf{h}}(i)$ as close-to-zero random values. We set the initial value of the weight matrices $\mathbf{W}^{l}(i)$ and $\mathbf{W}^{h}(i)$ at the i-th level decomposition as shown in Figure 8.

(2) We then multiply the weight matrix with the input series to implement the convolution operation described in Section 3.2.1 (1).

(3) The result of the previous step is then added to the bias vectors $\mathbf{b}^{\mathbf{l}}(i)$ and $\mathbf{b}^{\mathbf{h}}(i)$, and the addition result is input into the activation function to obtain the intermediate variable series $\mathbf{a}^{l}(i)$ and $\mathbf{a}^{h}(i)$.

The calculation process of step (2) and step (3) is shown in the following equation:

$$\begin{aligned} a^{l}(i) &= \sigma\left(W^{l}(i)x^{l}(i-1)+b^{l}(i)\right), \\ a^{h}(i) &= \sigma\left(W^{h}(i)x^{l}(i-1)+b^{h}(i)\right), \\ \mathbf{a}^{l}(i) &= \sigma\left(\mathbf{W}^{l}(i)\mathbf{x}^{l}(i-1)+\mathbf{b}^{l}(i)\right), \\ \mathbf{a}^{h}(i) &= \sigma\left(\mathbf{W}^{h}(i)\mathbf{x}^{l}(i-1)+\mathbf{b}^{h}(i)\right). \end{aligned} \tag{2}$$

(4) The intermediate variables $\mathbf{a}^{l}(i)$ and $\mathbf{a}^{h}(i)$ are downsampled using the average pooling layer as $x_j^{l}(i) = (a_{2j}^{l}(i) + a_{2j-1}^{l}(i))/2$, $x_j^{h}(i) = (a_{2j}^{h}(i) + a_{2j-1}^{h}(i))/2$, $j \in [0, P/2]$.

3.3.3. LSTM Component. In this component, we employ LSTM to model time-series data. LSTM is a special kind of recurrent neural network (RNN) proposed by Hochreiter and Schmidhuber [33]. Although RNN models can store history information by hiding states and effectively utilize history data information for prediction. However, RNNs can only learn short-term dependencies between features. The model has a problem of gradient explosion and gradient disappearance. LSTM is improved for the abovementioned problems by adding three gate structures and a memory cell on the basis of RNN. The three gates are the input gate, forget gate, and output gate. The role of these gate structures is to control the flow of information in the hidden state, learning long-term and short-term dependencies, which work quite well on time-series datasets.

3.4. mWDN-LSTM Training and Prediction Process. In order to train the mWDN-LSTM network, the training set needs to be standardized first. After standardization, the data are imported into the mWDN component for calculation based on the sliding window. The input data are decomposed into subseries of different frequencies after passing through the high-pass and low-pass filters. During decomposition, cyclic patterns are generated from the data. Then, the data are imported into the LSTM component for calculation. The input of each LSTM subnetwork is the output of the mWDN component. The LSTM component is calculated to obtain an output vector. The output vector is fed into a fully connected neural network to obtain the final prediction. After completing one model's calculation, the error function is utilized to calculate the error between the predicted value and the real value. Finally, the network is trained by propagating the calculated error values back to the network and using the optimizer to update the weights and biases of the network.

After the training is completed, the model is saved. Similarly, the test set first needs to be standardized. After standardization, the test set is imported into the saved model to calculate and obtain the predicted values. Since the obtained predicted values are standardized, standard restoration of the predicted values is required. Finally, the evaluation criteria are calculated based on the predicted and real values, and the predicted values and evaluation criteria are given as output.

The process of mWDN-LSTM training and prediction is shown in Figure 10.

4. Experiment

To demonstrate the effectiveness of mWDN-LSTM, we compare the model with MLP, CNN, RNN, LSTM, and

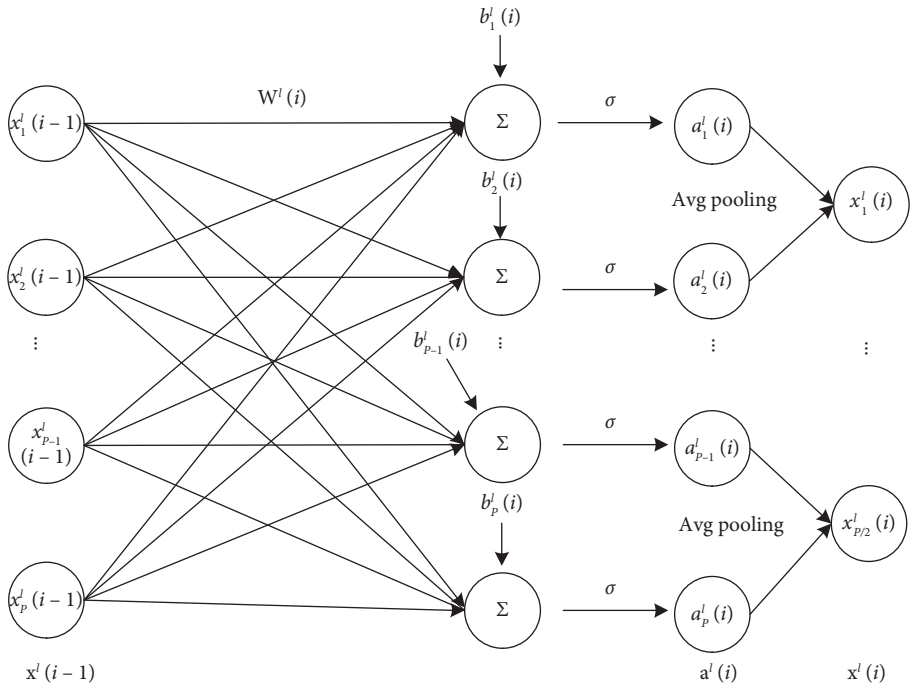

Figure 9: Schematic diagram of the mWDN implementation of MDWD process.

CNN- LSTM under the same environmental setup. In addition, we also show an experimental result of a model with data leakage (DWT-LSTM).

4.1. Dataset. The dataset settings for the experiment are as follows:

(1) Experimental subject: The experimental subject is SSE (Shanghai Stock Exchange) Composite Index (000001)

(2) Date range and data source: This includes daily transaction data for 7,127 trading days from July 1, 1991, to August 31, 2020, obtained from the wind database.

(3) Features included in each piece of data: The features include the opening price, highest price, lowest price, closing price, volume, turnover, ups and downs, and change. A sample of the data is shown in Table 2.

The dataset features can be described as follows:

(i) Opening price is the first price of any listed stock at the beginning of an exchange on a trading day.

(ii) High and low prices are the highest and lowest prices of the stock on that day. Generally, these data are applied by traders to measure the volatility of a stock.

(iii) Closing price is the price of the stock at the end of a trading day.

(iv) Volume is the total number of shares or contracts traded in the market during the day.

(v) Turnover is the total value of stocks or contracts traded in the market on that day.

(vi) Ups and downs are the values of the increase or decrease of the day's closing price relative to the previous day's closing price.

(vii) Change is the ratio of the increase or decrease of the day's closing price relative to the previous day's closing price.

(4) Prediction target: Prediction target is the closing price of the next day.

(5) Train and test set splits: We take the data of the first 6,627 trading days as the training set and the data of the last 500 trading days as the test set.

4.2. Experimental Setup. The data are standardized and restored by the z-score method. The standardization of data by using $ and the restoration of data are performed by using the following equations:

$$y_i = \frac{x_i - \overline{x}}{s}, \tag{3}$$

$$x_i = y_i * s + \overline{x}, \tag{4}$$

where x_i is the input data, x is the average of the input data, s is the standard deviation of the input data, and y_i is the standardized value.

For evaluation criteria, the mean absolute error (MAE), root mean square error (RMSE), and R-squared (R^2) are applied to evaluate the effectiveness. The MAE, RMSE, and R^2 calculation formulas are as follows:

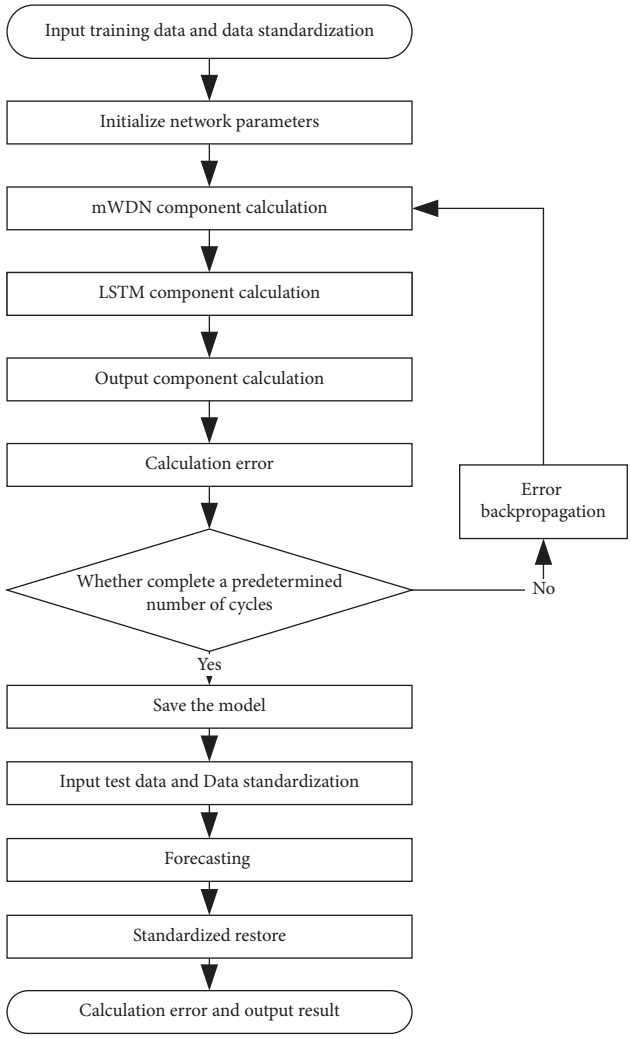

Figure 10: Flowchart of mWDN-LSTM training and prediction.

$$\begin{aligned}
\mathrm{MAE} &= \frac{1}{n}\sum_{i=1}^{n}\left|\widehat{y}_i - y_i\right|,\\
\mathrm{RMSE} &= \sqrt{\frac{1}{n}\sum_{i=1}^{n}\left(\widehat{y}_i - y_i\right)^2},\\
R^2 &= 1 - \frac{\mathrm{SS}_{\mathrm{Regression}}}{\mathrm{SS}_{\mathrm{Total}}}\\
&= 1 - \frac{\sum_{i=1}^{n}\left(y_i - \widehat{y}_i\right)^2}{\sum_{i=1}^{n}\left(y_i - \overline{y_i}\right)^2}, \quad R^2 \in (0, 1),
\end{aligned} \tag{5}$$

where $\widehat{y}_i$ is the predictive value, y_i is the real value, and $\overline{y_i}$ is the average value. The closer the MAE and RMSE values are to zero, the smaller the difference between the predicted and real values is, and the higher the prediction accuracy is. The closer the R^2 is to 1, the better the fitting degree of the model is.

4.3. Implementation of mWDN-LSTM. The parameter settings of our proposed model mWDN-LSTM are tuned one by one according to cross-validation. The parameters of this experiment are shown in Table 3.

The Fejer–Korovkin 4 wavelet function is a commonly adopted wavelet function with optimal asymptotic frequency localization [34]. So, we utilize the Fejer–Korovkin 4 as a wavelet function in our experiments, and the filter coefficients are set as

$$\begin{aligned}
\mathbf{l} = \{&0.3492,\ 0.7826,\ 0.4752, -0.0996,\\
&-0.1599,\ 0.0431,\ 0.0425, -0.0190\},\\
\mathbf{h} = \{&-0.0190, -0.0425,\ 0.04310,\ 0.1599,\\
&-0.0996, -0.4752,\ 0.7826, -0.3492\}.
\end{aligned} \tag{6}$$

According to the parameter settings of the mWDN-LSTM network, the data dimensions of input and output in each component of mWDN-LSTM are shown in Figure 11. The model structure is as follows: according to the size of the time_step and the dimension of the input data, the data of the input layer are a three-dimensional vector (none, 32, and 8). After the data are input into the mWDN component, the data are decomposed into subseries of different frequencies. The cyclic patterns in the data are generated. After 2-level decomposition, the data of length 32 will be decomposed into one subseries of length 16 and two subseries of length 8, for a total of three subseries. Therefore, the output of the mWDN component is two four-dimensional vectors: (none, 16, 1, 8) and (none, 8, 2, 8). Each subseries feeds an LSTM subnetwork. After the LSTM component is trained, an output vector (none and 48) will be output, where 48 is the number of hidden units in the LSTM component. Finally, the vector is fed into the output component to get the final predicted value.

5. Experiment Results

In this section, we will discuss our model's effectiveness compared with other benchmarks. With regard to benchmarks, to the best of our knowledge, there is no research that utilizes the cyclic pattern correctly in the stock price prediction task. So, we choose MLP, CNN, RNN, LSTM, and CNN-LSTM models as benchmarks. DWT-LSTM is used as a case study to describe the results of hybrid models in the existence of data leakage.

Our experiments exploit the training set data to train mWDN-LSTM, MLP, CNN, RNN, LSTM, and CNN-LSTM, respectively, and then exploit the test set data to generate predictions. Based on the experimental results, we plotted the comparison figure of predicted and real values (Figures 12–19), as well as the table of evaluation criteria (Table 4) and the comparison chart of evaluation criteria performance (Figures 20 and 21).

The results of DWT-LSTM, as shown in Figure 22 and Table 4, usually cause researchers to overestimate the performance of signal decomposition techniques such as wavelet decomposition, but similar hybrid models with data

Table 2: Head data in the SSE experimental data.

Date	Opening price	Highest price	Lowest price	Closing price	Volume (share)	Turnover (RMB)	Ups and downs	Change (%)
1991-7-1	136.64	138.62	136.56	136.85	2294000	12469884	−0.71	−0.5161
1991-7-2	135.91	135.96	135.69	135.96	283800	3794100	−0.89	−0.6503
1991-7-3	135.28	135.96	134.98	135.27	271500	1818504	−0.69	−0.5075
1991-7-4	136.63	136.63	134.19	136.63	1339400	8095138	1.36	1.0054
1991-7-5	136.01	137.68	135.9	135.96	1454000	9394861	−0.67	−0.4904
1991-7-8	135.26	135.28	134.93	135.28	587400	2925933	−0.68	−0.5001
1991-7-9	136.56	136.57	134.31	134.64	844200	4174836	−0.64	−0.4731
1991-7-10	134.4	135.6	133.72	133.99	602300	2894591	−0.65	−0.4828

Table 3: Parameter setting of mWDN-LSTM.

Parameters	Value
mWDN component decomposition level	2
mWDN component wavelet function	Fejer–Korovkin 4
mWDN component activation function	Sigmoid
Number of hidden units in LSTM component	48
LSTM component activation function	tanh
Time_step	32
Batch_size	64
Learning rate	0.001
Optimizer	Adam
Loss function	MAE
Epochs	150

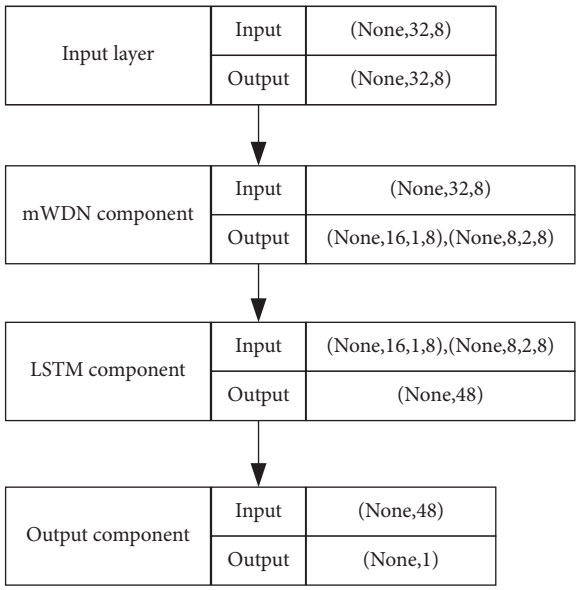

Figure 11: Data dimensions of input and output in each component of mWDN-LSTM.

leakage are unreliable in application scenarios. This is one of the motivations of our paper.

Furthermore, in order to clearly display and analyze the intersection of the constructed mWDN-LSTM stock index prediction model and the progress of the cutting-edge benchmark CNN-LSTM stock index prediction model, two time periods were selected from the test set results for enlarged display and comparison. If the first point of the test set is marked as t_1, the second point is marked as t_2, and so on, then the two time periods are "t301 to t400" and "t401 to t500". The result is as follows.

5.1. Results Demonstration. The comparison figure between predicted and real values can visually demonstrate the error between predicted and real values at the turning point and trend duration stage, as well as the degree of model fitting. From Figures 12–19, we can notice that mWDN-LSTM has the lowest error between the predicted and real values at the turning point and the trend duration phase stage compared to other models. So, the predicted value series of mWDN-LSTM has the highest degree of fitting with the real value series. Based on the diagram at the turning point and the trend duration phase, the descent order with regard to the fitting degree of all models is mWDN-LSTM, CNN-LSTM, LSTM, RNN, CNN, and MLP.

From the diagrams mentioned above, we can find that most models predict badly especially around the turning point, and our model mWDN-LSTM alleviates this problem by being guided by cyclic pattern information.

5.2. Result Analysis. The diagrams mentioned above demonstrate the prediction results visually. In this section, we calculated the evaluation criteria (MAE, RMSE, and R^2) based on the experiments carried out on the various models under the same experimental setup, so that we can more accurately evaluate the prediction error and model fitting degree. From the results presented in Table 4 and Figures 20 and 21, we can reach 3 major conclusions.

First, LSTM-based models outperform non-LSTM-based models, and this conclusion means that, generally, LSTM-based models are more suitable for time-series prediction tasks.

Among the non-LSTM-based models (CNN, RNN, and MLP), CNN and RNN have close prediction results with little differences between them, but they are significantly better than MLP. For example, compared to MLP, the MAE of CNN decreases from 37.757 to 30.397 by 19.5%, RMSE decreases from 49.371 to 41.492 by 16%, and R^2 improves by 1.59%. Therefore, the CNN and RNN models outperform the MLP.

Among the LSTM-based models (mWDN-LSTM, CNN-LSTM, and LSTM), LSTM performs worst but still, significantly improves the prediction results compared to CNN and RNN. For example, compared to CNN, the MAE of

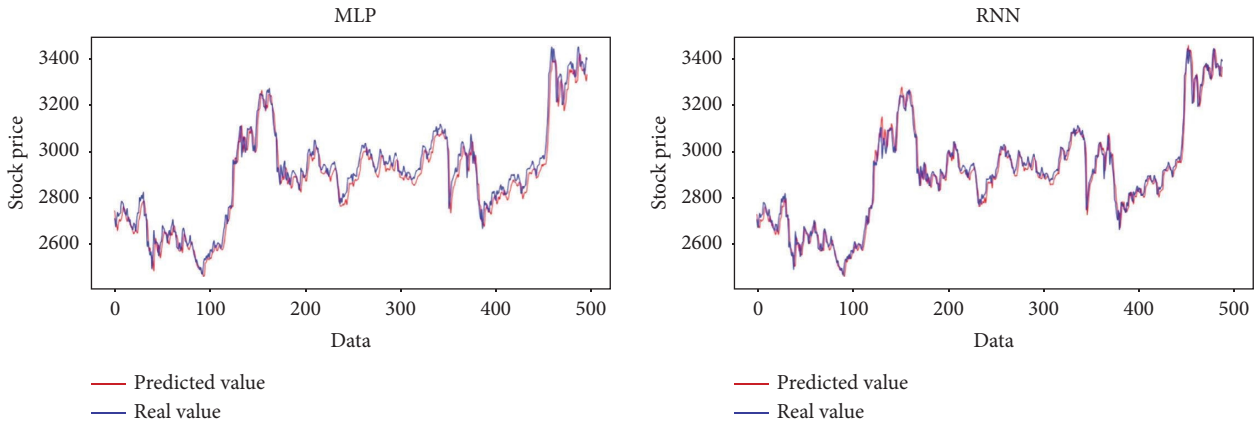

Figure 12: Comparison of the predicted value and the real value of the MLP and RNN models.

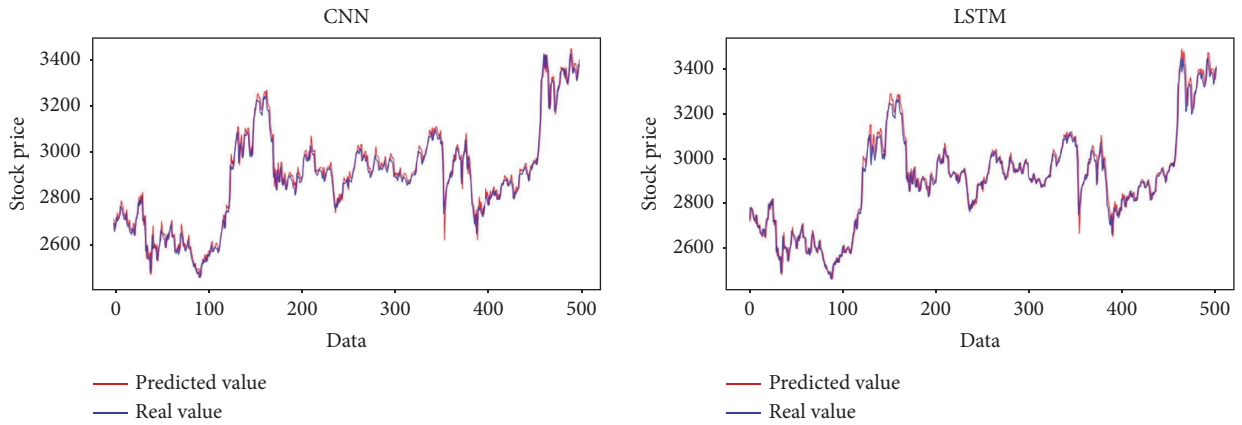

Figure 13: Comparison of the predicted value and the real value of the CNN and LSTM models.

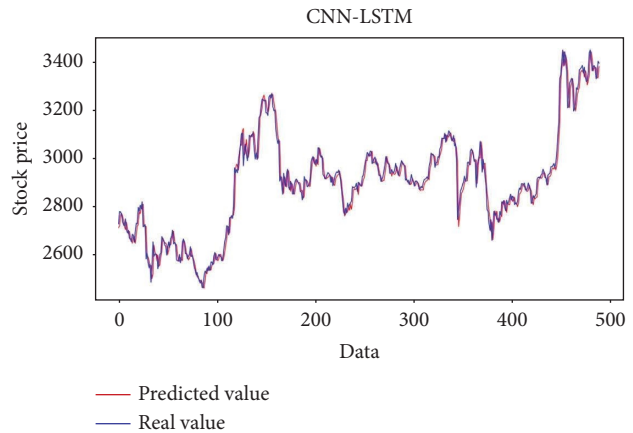

Figure 14: Comparison of the predicted value of the CNN-LSTM and the real value.

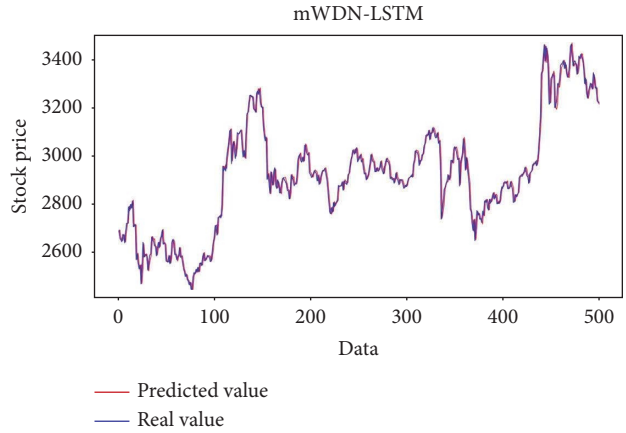

Figure 15: Comparison of the predicted value of the mWDN-LSTM and the real value.

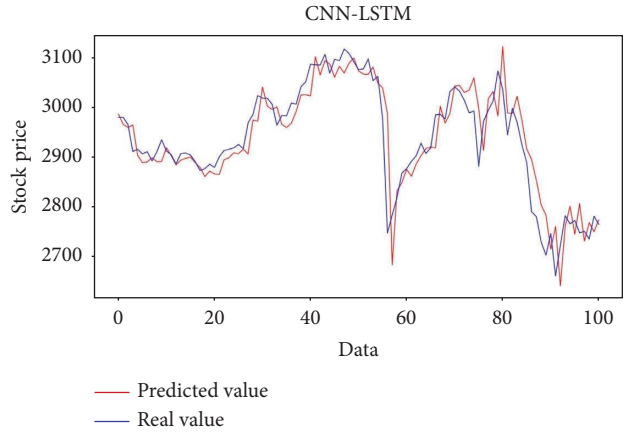

Figure 16: CNN-LSTM prediction result chart from t_{301} to t_{400}.

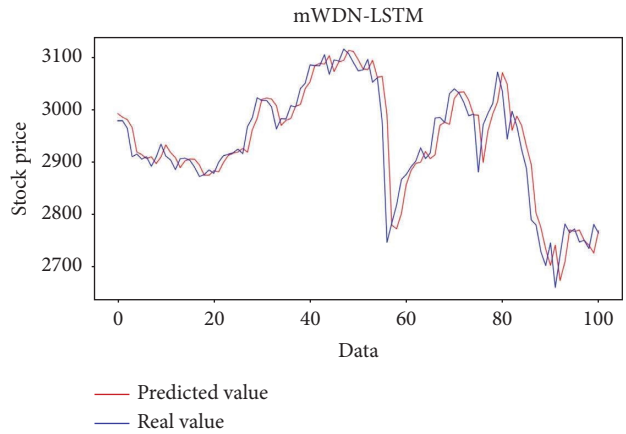

Figure 17: mWDN-LSTM prediction result chart from t_{301} to t_{400}.

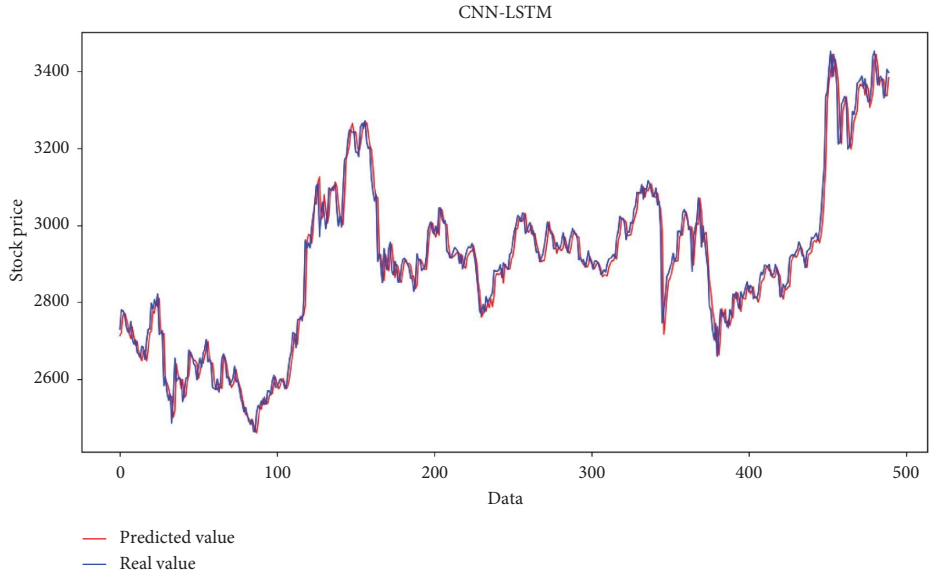

Figure 18: CNN-LSTM prediction result chart from t_{401} to t_{500}.

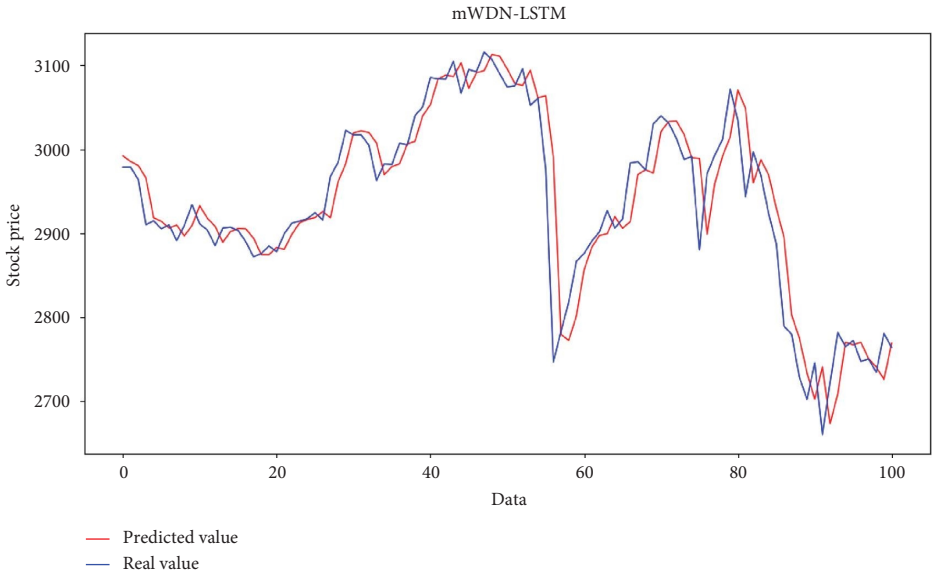

Figure 19: mWDN-LSTM prediction result chart from t_{401} to t_{500}.

LSTM decreased from 30.397 to 28.675 by 5.7%, RMSE decreased from 41.492 to 40.793 by 1.7%, and R^2 also improved by 0.13%.

Second, the hybrid models outperformed the nonhybrid model. This conclusion demonstrates that hybrid models designed for a specific task generally outperform general-purpose models.

Among all the hybrid models (CNN-LSTM and mWDN-LSTM), the CNN-LSTM model performs the worst. Among all the nonhybrid models (LSTM, RNN, CNN, and MLP), LSTM performs the best. For example, compared with LSTM, the MAE of CNN-LSTM decreased from 28.675 to 27.559 by 3.9%, and the RMSE decreased from 40.793 to 39.522 by 3.1%, and the R^2 also improved by 0.23%.

Finally, of all hybrid models, our model mWDN-LSTM performed the best. This demonstrates that correctly utilizing the cyclic patterns in a hybrid model can improve the prediction results.

We compare mWDN-LSTM with CNN-LSTM, which already achieve excellent prediction results among the benchmarks. Compared with CNN-LSTM, the MAE of the mWDN-LSTM model decreased by 4.8%, and the RMSE decreased by 3.1%, and the R^2 also improved by 0.48%.

Table 4: Comparison table of evaluation criteria.

Models	MAE	RMSE	R^2
mWDN-LSTM	26.244	38.290	0.9703
CNN-LSTM	27.559	39.522	0.9655
LSTM	28.675	40.793	0.9632
RNN	29.914	41.849	0.9612
CNN	30.397	41.492	0.9619
MLP	37.757	49.371	0.9460
DWT-LSTM	9.391	12.775	0.9964

Note. The DWT-LSTM model achieves high precision with data leakage, which is impractical in real applications.

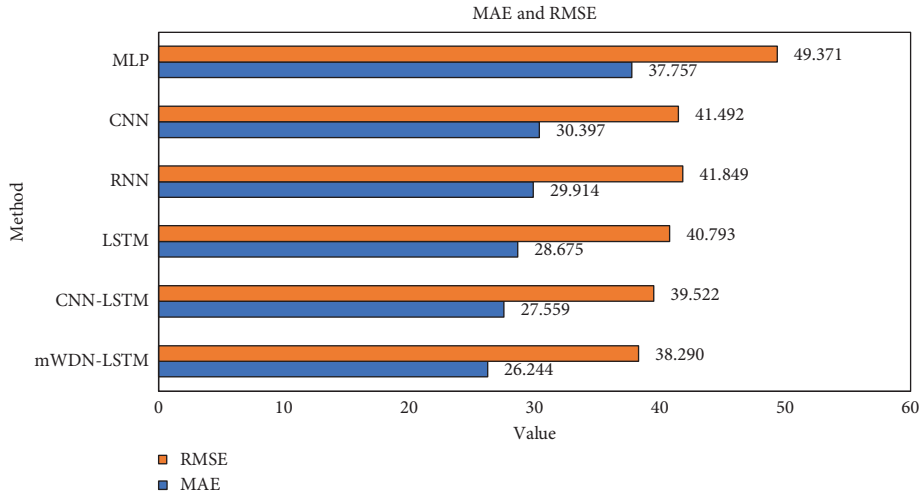

Figure 20: MAE and RMSE performance comparison chart.

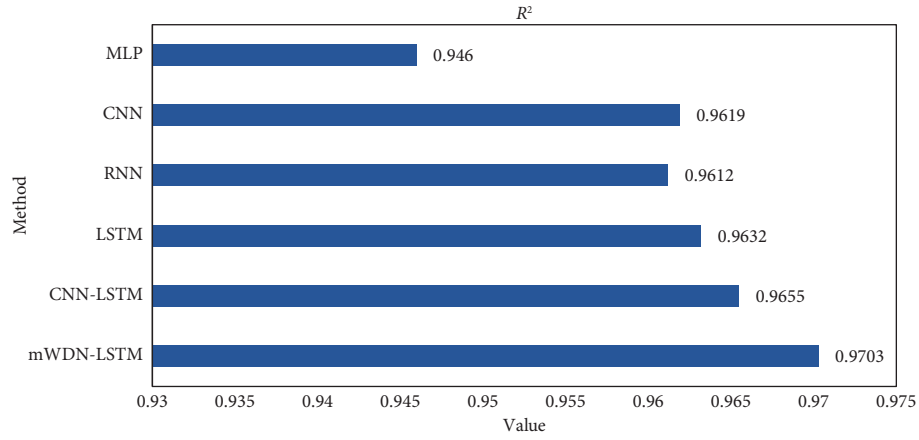

Figure 21: R^2 performance comparison chart.

5.3. Experimental Validation on Another Dataset. Furthermore, in order to validate our model, we conducted additional experiments and analysis on the Hang Seng Index (HSI) dataset in addition to the abovementioned SSE dataset. The HSI dataset has the same time frame as the SSE dataset, and the experimental setup such as dataset settings, model parameters, and experimental steps are also the same as the abovementioned experiments on the SSE dataset.

Based on the experimental results, the comparison figures of predicted values and real values (Figures 23 and 24) are plotted, as well as the table of evaluation criteria (Table 5) and the comparison charts of evaluation criteria performance (Figures 25 and 26).

From Figures 23–26 and Table 5, in experimental validation of the HSI dataset, we can see that the evaluation criteria, MAE and RMSE, of the mWDN-LSTM model are

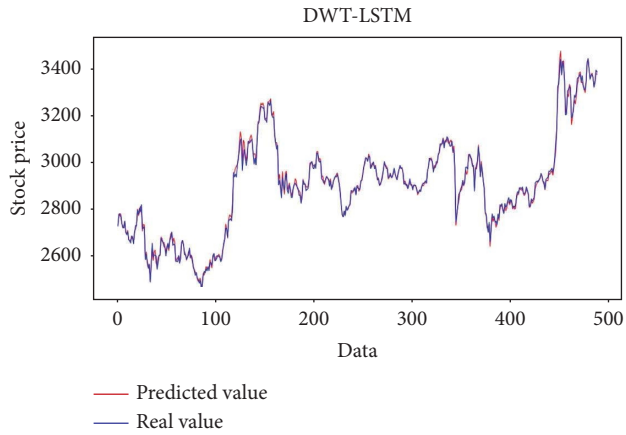

Figure 22: Experimental results with data leakage.

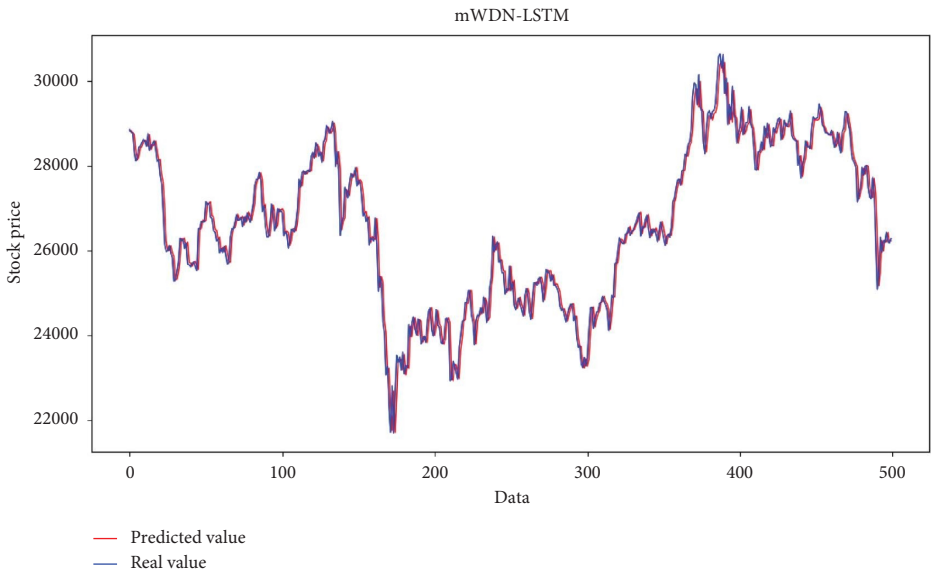

Figure 23: The comparison of the predicted value of the mWDN-LSTM and the real value (in HSI dataset's experimental validation).

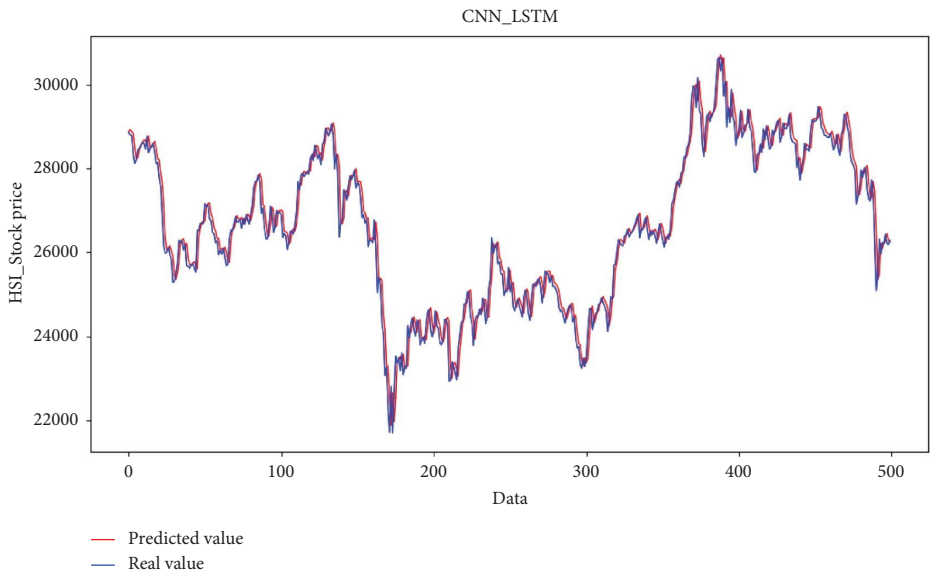

Figure 24: Comparison of the predicted value of the CNN-LSTM and the real value (in HSI dataset's experimental validation).

Table 5: Performance comparison table in HSI dataset.

Models	MAE	RMSE	R^2
mWDN-LSTM	256.488	353.775	0.9631
CNN-LSTM	263.764	363.186	0.9615
LSTM	273.402	367.061	0.9607
RNN	289.819	375.168	0.9589
CNN	290.474	376.101	0.9604
MLP	319.0930	416.251	0.9494

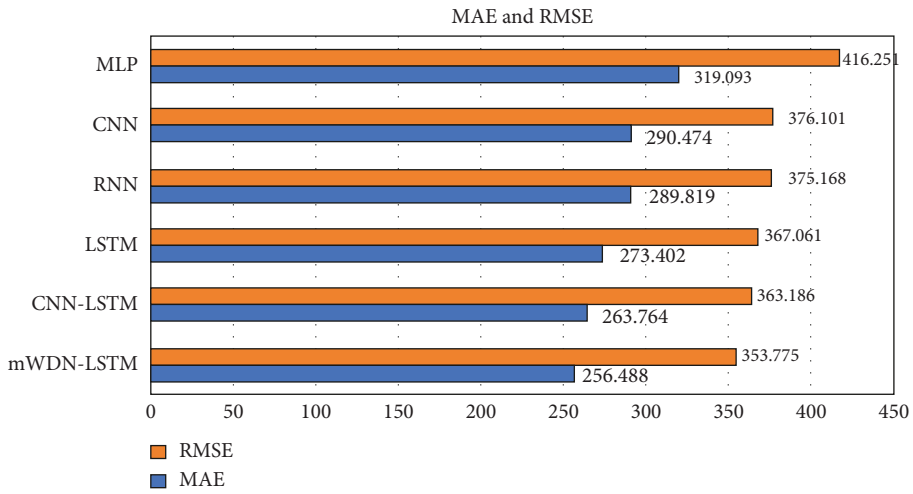

Figure 25: MAE and RMSE performance comparison chart (in HSI dataset's experimental validation).

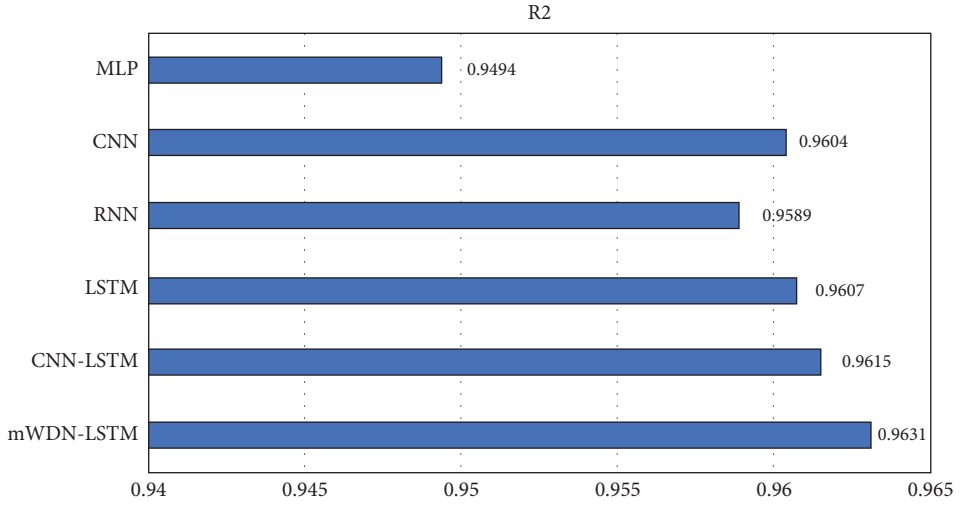

Figure 26: R^2 performance comparison chart in the HSI dataset (in HSI dataset's experimental validation).

the best, and R^2 is closest to 1; the mWDN-LSTM model also obtains excellent prediction results, and it has the highest degree of fitting compared to other benchmark models. It can be concluded that mWDN-LSTM has generalizability.

5.3.1. Summary. Our proposed mWDN-LSTM has outperformed all the other baseline models and is more effective for predicting the next day's closing price of stocks. Meanwhile, our experiments demonstrate the effectiveness of utilizing cyclic patterns while avoiding data leakage and alleviating the impact of boundary problems.

6. Conclusions

In this paper, we study the problem of stock price prediction which aims to predict the next day closing price of the stock using historical information. We have noticed that cyclic

patterns are important characteristics of the stock market. From this motivation, we propose the mWDN-LSTM model based on deep neural networks, which can effectively and correctly utilize the cyclic patterns in the stock market. Unlike other DWT-based hybrid models, our mWDN-LSTM model avoids the data leakage by sliding window mechanism, and through the adaptive parameter adjustment mechanism of mWDN and redesign of convolution matrix, the impact of boundary problem in wavelet decomposition on prediction performance is alleviated. Therefore, the model is both theoretically sound and practically feasible in stock price time-series prediction.

In addition, the model generates cyclic patterns with different frequencies from stock data by applying the mWDN network and then employing the LSTM model to learn the cyclic patterns and predict the next day's closing price. We compare mWDN-LSTM with baseline models to verify its effectiveness on the datasets of the SSE Composite Index and the Hang Seng Index. The experimental results show that the evaluation criteria, MAE and RMSE, of our model are the best, and R^2 is closest to 1. This means that our model mWDN-LSTM outperforms the benchmarks and demonstrates the effectiveness of utilizing cyclic patterns in stock price prediction tasks when avoiding data leakage and alleviating the impact of boundary problems.

Data Availability

The Shanghai Composite Index data used to support the findings of this study are collected publicly and are available from the corresponding author upon request.

Conflicts of Interest

The authors declare that they have no conflicts of interest regarding the publication of this paper.

Acknowledgments

This research work was funded by the Shenzhen Technology University.

References

[1] R. Vanaga, "Financial and capital market commission financing: aspects and challenges," *Journal of Logistics, Informatics and Service*, vol. 7, no. 1, pp. 17–30, 2020.

[2] D. Shah, H. Isah, and F. Zulkernine, "Stock market analysis: a review and taxonomy of prediction techniques," *International Journal of Financial Studies*, vol. 7, no. 2, p. 26, 2019.

[3] B. Billah, L. Maxwell, and R. D. Snyder, "Exponential smoothing model selection for forecasting," *International journal of forecasting Koehler*, vol. 22, no. 2, pp. 239–286, 2006.

[4] C. Jung and R. Boyd, "Forecasting UK stock prices," *Applied Financial Economics*, vol. 6, no. 3, pp. 279–286, 1996.

[5] A. A. Adebiyi, O. Aderemi, and C. K. Adewumi, "Stock price prediction using the arima model," in *Proceedings of the Uksim-Amss 16th International Conference on Computer Modelling and Simulation*, Cambridge, UK, March 2014.

[6] C. Zhang, X. Cheng, and M. Wang, "An empirical research in the stock market of Shanghai by GARCH model," *Operations Research and Management Science*, vol. 4, pp. 144–146, 2005.

[7] C. Shi and X. Zhuang, "A study concerning soft computing approaches for stock price fore- casting," *Axioms*, vol. 8, no. 4, p. 116, 2019.

[8] B. M. Henrique, V. A. Sobreiro, H. Kimura, and Kimura, "Literature review: machine learning techniques applied to financial market prediction," *Expert Systems with Applications*, vol. 124, pp. 226–251, 2019.

[9] G. Zhang, B. Eddy Patuwo, and M. Y Hu, "Forecasting with artificial neural networks," *International Journal of Forecasting*, vol. 14, no. 1, pp. 35–62, 1998.

[10] M. E. Wu, J. H. Syu, J. C. W. Lin, and J. M. Ho, "Effective fuzzy system for qualifying the characteristics of stocks by random trading," *IEEE Transactions on Fuzzy Systems*, vol. 30, no. 8, pp. 3152–3165, 2022.

[11] J.-H. Syu, J. C. W. Lin, C. J. Wu, and J. M. Ho, "Stock selection system through suitability index and fuzzy-based quantitative characteris tics," *IEEE Transactions on Fuzzy Systems*, vol. 31, no. 1, pp. 322–334, 2023.

[12] R. A. Yaffee and M. Mcgee, *An Introduction to Time Series Analysis and Forecasting*, Elsevier, Amsterdam, Netherlands, 2000.

[13] Z. Cui, W. Chen, and Y. Chen, "Multi-scale convolutional neural networks for time series classification," *Neural Networks*, vol. 136, 2016.

[14] R. Gao, L. Du, K. F. Yuen, and P. N. Suganthan, "Walk-forward empirical wavelet random vector functional link for time series forecasting," *Applied Soft Computing*, vol. 108, Article ID 107450, 2021.

[15] G. Duan, "Deep neural networks for stock price prediction," in *Proceedings of the 14th International Conference on Computer Research and Development (ICCRD)*, Shenzhen, China, January 2022.

[16] M. Naeini, H. Pakdaman, Taremian, H. Baradaran, and Hashemi, "Stock market value prediction using neural networks," in *Proceedings of the 2010 international conference on computer information systems and industrial management applications (CISIM)*, Krakow, Poland, October 2010.

[17] J. L. Ticknor, "A Bayesian regularized artificial neural network for stock market forecasting," *Expert Systems with Applications*, vol. 40, pp. 5501–5506, 2013.

[18] A. M. Rather, A. Agarwal, and V. Sastry, "Recurrent neural network and a hybrid model for prediction of stock returns," *Expert Systems with Applications*, vol. 42, no. 6, pp. 3234–3241, 2015.

[19] L. Di Persio and O. Honchar, "Artificial neural networks architectures for stock price prediction: comparisons and applications," *International journal of circuits, systems and signal processing*, vol. 10, pp. 403–413, 2016.

[20] S. Selvin, "Stock price prediction using LSTM, RNN and CNN-sliding window model," in *Proceedings of the 2017 International Conference on Advances in Computing, Communications and Informatics (ICACCI)*, IEEE, Udupi, India, September 2017.

[21] W. Lu, J. Li, Y. Li, A. Sun, and J. Wang, "A CNN-LSTM-based model to forecast stock prices," *Complexity*, vol. 2020, Article ID 6622927, 10 pages, 2020.

[22] J. Wu and Ming-Tai, "A graph-based CNN-LSTM stock price prediction algorithm with leading indicators," *Multimedia Systems*, vol. 29, pp. 1–20, 2021.

[23] J. M. Wu, Z. Li, G. Srivastava, M. Tasi, and J. C. Lin, "A graph-based convolutional neural network stock price prediction with leading indicators," *Software: Practice and Experience*, vol. 51, no. 3, pp. 628–644, 2021.

[24] J. M. T. Wu, L. Sun, G. Srivastava, and J. C. W. Lin, "A novel synergetic lstm-ga stock trading suggestion system in internet of things," *Mobile Information Systems*, vol. 2021, Article ID 6706345, 15 pages, 2021.

[25] Q. Zhang, C. Qin, Y. Zhang, F. Bao, C. Zhang, and P. Liu, "Transformer-based attention network for stock movement prediction," *Expert Systems with Applications*, vol. 202, Article ID 117239, 2022.

[26] X. Qiu, P. N. Suganthan, G. A. J. Amaratunga, and Amaratunga, "Fusion of multiple indi- cators with ensemble incremental learning techniques for stock price forecasting," *Journal of Banking and Financial Technology*, vol. 3, no. 1, pp. 33–42, 2019.

[27] S. K. Chandar, "Fusion model of wavelet transform and adaptive neuro fuzzy inference system for stock market prediction," *Journal of Ambient Intelligence and Humanized Computing*, vol. 2019, pp. 1–9, 2019.

[28] X. Li and P. Tang, "Stock index prediction based on wavelet transform and FCD-MLGRU," *Journal of Forecasting*, vol. 39, no. 8, pp. 1229–1237, 2020.

[29] D. Wu, X. Wang, and S. Wu, "A hybrid method based on extreme learning machine and wavelet transform denoising for stock prediction," *Entropy*, vol. 23, no. 4, p. 440, 2021.

[30] R. Hasumi and Y. Kajita, "Boundary problem and data leakage: a caveat for wavelet-based forecasting," 2018, https://www.jcer.or.jp/english/boundary-problem-and-data-leakage-a-caveat-for-wavelet-based-forecasting.

[31] J. Wang, "Multilevel wavelet decomposition network for interpretable time series analysis," in *Proceedings of the 24th ACM SIGKDD International Conference on Knowledge Discovery & Data Mining*, London, UK, July 2018.

[32] Y. Zhang, "Multivariate and multi-frequency lstm based fine-grained productivity forecasting for indus trial iot," in *Proceedings of the 2020 16th International Conference on Mobility, Sensing and Networking (MSN)*, Tokyo, Japan, December 2020.

[33] S. Hochreiter and J. Schmidhuber, "Long short-term memory," *Neural Computation*, vol. 9, no. 8, pp. 1735–1780, 1997.

[34] M. Nielsen, "On the construction and frequency localization of finite orthogonal quadrature filters," *Journal of Approximation Theory*, vol. 108, no. 1, pp. 36–52, 2001.

Hindawi
Complexity
Volume 2023, Article ID 3000653, 31 pages
https://doi.org/10.1155/2023/3000653

Research Article

Techniques for Finding Analytical Solution of Generalized Fuzzy Differential Equations with Applications

Mudassir Shams,[1] **Nasreen Kausar**,[2] **Naveed Yaqoob**,[1] **Nayyab Arif**,[1] **and Gezahagne Mulat Addis**[3]

[1]*Department of Mathematics and Statistics, Riphah International University, I-14, Islamabad 44000, Pakistan*
[2]*Department of Mathematics, Faculty of Arts and Sciences, Yildiz Technical University, Esenler 34220, Istanbul, Turkey*
[3]*Department of Mathematics, University of Gondar, P.O. Box: 196, Gondar, Ethiopia*

Correspondence should be addressed to Gezahagne Mulat Addis; gezahagne412@gmail.com

Received 31 August 2022; Revised 9 December 2022; Accepted 23 March 2023; Published 17 May 2023

Academic Editor: Zeljko Stevic

Engineering and applied mathematics disciplines that involve differential equations include classical mechanics, thermodynamics, electrodynamics, and general relativity. Modelling a wide range of real-world situations sometimes comprises ambiguous, imprecise, or insufficient situational information, as well as multiindex, uncertainty, or restriction dynamics. As a result, intuitionistic fuzzy set models are significantly more useful and versatile in dealing with this type of data than fuzzy set models, triangular, or trapezoidal fuzzy set models. In this research, we looked at differential equations in a generalized intuitionistic fuzzy environment. We used the modified Adomian decomposition technique to solve generalized intuitionistic fuzzy initial value problems. The generalized modified Adomian decomposition technique is used to solve various higher-order generalized trapezoidal intuitionistic fuzzy initial value problems, circuit analysis problems, mass-spring systems, steam supply control sliding value problems, and some other problems in physical science. The outcomes of numerical test applications were compared to exact technique solutions, and it was shown that our generalized modified Adomian decomposition method is efficient, robotic, and reliable, as well as simple to implement.

1. Introduction

Differential equation plays a vital role in every field of science and engineering. Differential equations are used to study bacterial growth, the motion of an object that moves to and fro, to calculate the flow of electricity, to explain the concept of thermodynamics, and to observe the propagation of heat or sound, fluid flow, temperature problems etc., [1–4].

In 1965, Zadeh [5] introduced the concept of fuzzy set theory as the extension of classical set theory. In classical set theory, we deal only with true or false values and do not analyze any values between them, whereas in fuzzy set theory, we deal with uncertain environmental conditions as membership values. The concept of fuzzy set theory has been applied to various fields of science and engineering to handle vagueness and uncertainty. In 1987, Kandel and Byatt introduced the fuzzy differential equations [6]. The fuzzy differential equations have been applied in numerous daily life problems [7]. Vasavi et al. [8] discussed fuzzy differential for cooling problems. Devi and Ganesan used fuzzy differential equations in modelling electric circuit problem [9]. Ahmad et al. [10] studied a mathematical method to find the solution of fuzzy integro-differential equations. Sadeghi et al. [11] studied the system of fuzzy differential equation. In 1986, Atanassov [12] introduced an extension of fuzzy set theory known as intuitionistic fuzzy set. The intuitionistic fuzzy set not only provides the information about membership values but also the nonmembership values, respectively, and so that the sum of both values is less than one. Intuitionistic fuzzy differential equations are being studied widely and being used in various fields of Physics,

Chemistry, Biology as well as among other fields of Science and Engineering. Melliani and Chadli obtained the approximate and numerical solutions of intuitionistic fuzzy differential equations with linear differential operators [13, 14]. Akin and Bayeg [15, 16] studied a method to find general solution of second-order intuitionistic fuzzy differential equation. Prasad Mondal and Kumar Roy [17–19] studied the generalized intuitionistic fuzzy Laplace transform method. Shams et al. used generalized trapezoidal intuitionistic fuzzy numbers and triangular intuitionistic fuzzy numbers in [20, 21] to solve a system of fuzzy initial value problems. The Adomian decomposition method (ADM) which is a semianalytical method was first presented by George Adomian in 1980s [22, 23]. This method is very efficient in finding the solutions of differential equations, algebraic equations as well as integral equations. In this article, we will propose the generalized modified Adomian decomposition method (GMADM) to find the solutions of generalized intuitionistic fuzzy differential equations with linear differential operators. This modification was proposed by Wazwaz [24]. He presented a reliable modification to the ADM. In this modification, Wazwaz divides the original function into two parts, one part assigned to the initial term of the series and the other to the second term. This modification results in a different series being generated. The efficiency of this method depends only on the choice of the parts into which the original function is to be divided.

Motivated by the aforesaid work, in this article, we use a GMADM to solve generalized trapezoidal intuitionistic fuzzy initial value problems (FIVPs).

The main contributions of this research work are summarized as follows:

(i) Using initial conditions as a generalized trapezoidal intuitionistic fuzzy number, a differential equation is solved using GMADM

(ii) The computational complexity of the proposed GMADM is described in order to solve problematic generalized trapezoidal intuitionistic fuzzy differential equations

(iii) Applications of generalized trapezoidal intuitionistic fuzzy differential equations in mechanical and electrical engineering are considered in a generalized trapezoidal intuitionistic fuzzy environment

(iv) The efficiency and applicability of the modified technique are assessed using computational tools

This paper is organized as follows: in Section 2, we recall some basic definitions which we will use in further sections. In Section 3, we introduced our proposed method and the efficiency of this method has been illustrated by applications. In the last section, we give conclusions.

2. Preliminaries

In this section, the fundamental definitions of fuzzy set and intuitionistic fuzzy set are presented.

Definition 1$_*$ [25]. Let X be the largest set under consideration, then A be a subset of X is said to be a fuzzy set if it is defined as follows:

$$\mu_{\overset{*}{A}}(x) = X \longrightarrow [0,1], \tag{1}$$

defines the degree of membership of an element $x\epsilon X$ to the set $\overset{*}{A}$ which is a subset of X.

Definition 2 [25]. α-cut of a fuzzy set $\overset{*}{A}$ is a crisp set $\overset{*}{A}_\alpha$ which is defined as follows:

$$\overset{*}{A}_\alpha = \left\{\left(x \mid \mu_{\overset{*}{A}}(x) \geq \alpha\colon\ x\epsilon X\right\}\right. . \tag{2}$$

Definition 3 [19]. If $\overset{*}{A}$ is a fuzzy set, then height of a fuzzy set is denoted by $h(\overset{*}{A})$ and is defined as the largest membership function obtained by any element in that set, i.e.,

$$h(\overset{*}{A}) = \sup \mu \overset{*}{A}(x). \tag{3}$$

Definition 4 [15]. Let X be a nonempty finite set of real numbers, then an intuitionistic fuzzy set $\overset{*}{F}$ on X is

$$\overset{*}{F} = \left\{\left(x, \mu_{\overset{*}{F}}(x), \upsilon_{\overset{*}{F}}(x)\right)\colon\ x\epsilon X\right\}, \tag{4}$$

where the functions

$$\begin{aligned} \mu_{\overset{*}{F}}(x) &= X \longrightarrow [0,1], \\ \upsilon_{\overset{*}{F}}(x) &= X \longrightarrow [0,1], \end{aligned} \tag{5}$$

define the degree of membership and degree of nonmembership, respectively, of an element $x\epsilon X$ to the set $\overset{*}{F}$ which is a subset of X, and for every $x\epsilon X$, the $0 \leq \mu_{\overset{*}{F}}(x) + \upsilon_{\overset{*}{F}}(x) \leq 1$, condition must be satisfied.

Definition 5 [19]. An intuitionistic fuzzy set $\overset{*}{F}$ is said to be normal if there exists an $x_0\epsilon X$, such that $\mu_{\overset{*}{F}}(x_0) = 1$ so $\upsilon_{\overset{*}{F}}(x_0) = 0$.

Definition 6 [19]. An intuitionistic fuzzy set $\overset{*}{F}$ is said to be convex set for the membership function if it satisfies the following condition:

$$\mu_{\overset{*}{F}}(x)(\eta x + (1-\eta)y) \geq \min\left(\mu_{\overset{*}{F}}(x), \mu_{\overset{*}{F}}(y)\right); \forall x, y\epsilon X, \eta\epsilon[0,1]. \tag{6}$$

Definition 7 [19]. An intuitionistic fuzzy set $\overset{*}{F}$ is said to be concave set for the nonmembership function if it satisfies the following condition:

$$\upsilon_{\overset{*}{F}}(x)(\eta x + (1-\eta)y) \geq \max\left(\upsilon_{\overset{*}{F}}(x), \upsilon_{\overset{*}{F}}(y)\right); \forall x, y\epsilon X, \eta\epsilon[0,1]. \tag{7}$$

2.1. Generalized Intuitionistic Fuzzy Number

Definition 8 [26]. A generalized intuitionistic fuzzy number

$$\overset{*}{N} = <(a_1, a_2, a_3, a_4; \nu_A); (b_1, b_2, b_3, b_4; \nu_B)>, \tag{8}$$

is said to be generalized trapezoidal intuitionistic fuzzy number (GTIFN) if its membership and nonmembership functions are defined as follows:

$$\mu_{\overset{*}{N}}(x) = \begin{cases} \nu_A\left(\dfrac{x-a_1}{a_2-a_1}\right), & a_1 \le x \le a_2, \\ \nu_A, & a_2 \le x \le a_3, \\ \nu_A\left(\dfrac{a_4-x}{a_4-a_3}\right), & a_3 \le x \le a_4, \\ 0, & \text{otherwise}, \end{cases}$$

$$\upsilon_{\overset{*}{N}}(x) = \begin{cases} \dfrac{(b_2-x)+\nu_B(x-b_1)}{b_2-b_1}, & b_1 \le x \le b_2, \\ \nu_B, & b_2 \le x \le b_3, \\ \dfrac{(x-b_3)+\nu_B(b_4-x)}{b_4-b_3}, & b_3 \le x \le b_4, \\ 1, & \text{otherwise}, \end{cases} \tag{9}$$

where $b_1 \le a_1 \le b_2 \le a_2 \le a_3 \le b_3 \le a_4 \le b_4, 0 \le \nu_A, \nu_B \le 1$ and $0 < \nu_A + \nu_B \le 1$.

Definition 9. (α, β)-Cut set [27] of GTIFN $\overset{*}{N} = <(a_1, a_2, a_3, a_4; \nu_A); (b_1, b_2, b_3, b_4; \nu_B)>$ is a crisp subset of X which is defined as follows:

$$\begin{aligned} \overset{*}{N}(\alpha, \beta) &= \left\{\left(x, \mu_{\overset{*}{N}}(x), \upsilon_{\overset{*}{N}}(x)\right): x \epsilon X, \mu_{\overset{*}{N}}(x) \ge \alpha, \upsilon_{\overset{*}{N}}(x) \le \beta\right\}, \\ &= \left\{\left[\overset{*}{N}_1(\alpha), \overset{*}{N}_2(\alpha)\right]; \left[\overset{*}{N}_1(\beta), \overset{*}{N}_2(\beta)\right]\right\}, \end{aligned} \tag{10}$$

where $\alpha + \beta < 1, \alpha \epsilon [0, \nu_A]$ and $\beta \epsilon [\nu_B, 1]$ as shown in Figure 1.

Figure 1 shows generalized trapezoidal intuitionistic fuzzy number.

Arithmetic operations on GTIFNs are defined as follows.

Definition 10 [28–30]. Let $\overset{*}{N}_1 = <(a_1, a_2, a_3, a_4; \nu_{A_1}); (b_1, b_2, b_3, b_4; \nu_{A_2})>$ and $\overset{*}{N}_2 = <(c_1, c_2, c_3, c_4; \nu_{B_1}); (d_1, d_2, d_3, d_4; \nu_{B_2})>$ be two GTIFNs and ω be a real number. Then,

(i) $\overset{*}{N}_1 + \overset{*}{N}_2 = <(a_1 + c_1, a_2 + c_2, a_3 + c_3, a_4 + c_4; \min\{\nu_{A_1}, \nu_{B_1}\}); (b_1 + d_1, b_2 + d_2, b_3 + d_3, b_4 + d_4; \max\{\nu_{A_2}, \nu_{B_2}\})>$,

(ii) $\overset{*}{N}_1 - \overset{*}{N}_2 = <(a_1 - c_4, a_2 - c_3, a_3 - c_2, a_4 - c_1; \min\{\nu_{A_1}, \nu_{B_1}\}); (b_1 - d_4, b_2 - d_3, b_3 - d_2, b_4 - d_1; \max\{\nu_{A_2}, \nu_{B_2}\})>$,

(iii) $\overset{*}{N}_1 \times \overset{*}{N}_2 = <(a_1c_1, a_2c_2, a_3c_3, a_4c_4; \min\{\nu_{A_1}, \nu_{B_1}\}); (b_1d_1, b_2d_2, b_3d_3, b_4d_4; \max\{\nu_{A_2}, \nu_{B_2}\})>$, where $\overset{*}{N}_1 > 0, \overset{*}{N}_2 > 0$.

(iv) $\overset{*}{N}_1 \times \overset{*}{N}_2 = <(a_1c_4, a_2c_3, a_3c_2, a_4c_1; \min\{\nu_{A_1}, \nu_{B_1}\}); (b_1d_4, b_2d_3, b_3d_2, b_4d_1; \max\{\nu_{A_2}, \nu_{B_2}\})>$, where $\overset{*}{N}_1 < 0, \overset{*}{N}_2 > 0$.

(v) $\overset{*}{N}_1 \times \overset{*}{N}_2 = <(a_4c_4, a_3c_3, a_2c_2, a_1c_1; \min\{\nu_{A_1}, \nu_{B_1}\}); (b_4d_4, b_3d_3, b_2d_2, b_1d_1; \max\{\nu_{A_2}, \nu_{B_2}\})>$, where $\overset{*}{N}_1 < 0, \overset{*}{N}_2 < 0$.

(vi) $\overset{*}{N}_1 \div \overset{*}{N}_2 = <(a_1/c_4, a_2/c_3, a_3/c_2, a_4/c_1; \min\{\nu_{A_1}, \nu_{B_1}\}); (b_1/d_4, b_2/d_3, b_3/d_2, b_4/d_4; \max\{\nu_{A_2}, \nu_{B_2}\})>$, where $\overset{*}{N}_2 > 0$.

(vii) $\omega\overset{*}{N}_1 = <(\omega a_1, \omega a_2, \omega a_3, \omega a_4; \min\{\nu_{A_1}, \nu_{B_1}\}); (\omega b_1, \omega b_2, \omega b_3, \omega b_4; \max\{\nu_{A_2}, \nu_{B_2}\})>$, where $\omega > 0$.

(viii) $\omega\overset{*}{N}_1 = <(\omega a_4, \omega a_3, \omega a_2, \omega a_1; \min\{\nu_{A_1}, \nu_{B_1}\}); (\omega b_4, \omega b_3, \omega b_4, \omega b_5; \max\{\nu_{A_2}, \nu_{B_2}\})>$, where $\omega < 0$.

3. The Generalized Modified Adomian Decomposition Method

A key concept is that the Adomian decomposition series expansion about the initial solution component function permits solution by recursion, in which the aforesaid rearrangement is accomplished through the choice of the recursion scheme. The modified ADM yields a rapidly convergent sequence of analytic functions as the approximate solutions of the original mathematical model. Thus, the modified Adomian decomposition method subsumes even the classic power series method while extending the class of amenable nonlinearity to include any analytic nonlinearity. Here, we generalized the MADM to GMADM to solve system of intuitionistic triangular fuzzy differential equation.

Let us consider the intuitionistic fuzzy differential equation with linear differential operator as follows [25]:

$$L\overset{*}{y}(t) + R\overset{*}{y}(t) + N(t, \overset{*}{y}(t)) = \overset{*}{f}(t), \tag{11}$$

where L is the highest order linear differential operator, R is the remaining part of the linear differential operator, N may be linear or nonlinear function of t and $\overset{*}{y}(t)$, and $\overset{*}{f}(t)$ is an intuitionistic fuzzy function. Here, in this case, we take N as a linear function of $\overset{*}{y}(t)$ and t.

Taking (α, β)-cut of (11), we get

$$\begin{aligned} &L\left(\left[\overset{*}{y}_1(t,\alpha); \overset{*}{y}_2(t,\alpha)\right]; \left[\overset{*}{y}_1(t,\beta); \overset{*}{y}_1(t,\beta)\right]\right) + R\left(\left[\overset{*}{y}_1(t,\alpha); \overset{*}{y}_1(t,\alpha)\right]; \left[\overset{*}{y}_1(t,\beta); \overset{*}{y}_2(t,\beta)\right]\right) \\ &+\left(\left[N_1\left(t, \overset{*}{y}_1(t,\alpha)\right); N_2\left(t, \overset{*}{y}_2(t,\alpha)\right)\right]; \left[N_1\left(t, \overset{*}{y}_1(t,\beta)\right); N_2\left(t, \overset{*}{y}_2(t,\beta)\right)\right]\right) = \left[\overset{*}{f}_1(t,\alpha); \overset{*}{f}_2(t,\alpha)\right]; \left[\overset{*}{f}_1(t,\beta); \overset{*}{f}_2(t,\beta)\right]. \end{aligned} \tag{12}$$

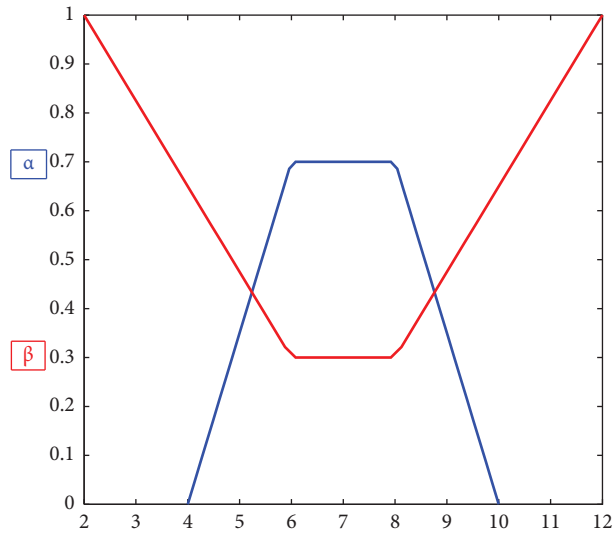

Figure 1: Generalized trapezoidal intuitionistic fuzzy number.

From (12), we obtain the following equations:

$$Ly_1^*(t,\alpha) + Ry_1^*(t,\alpha) + N_1\left(t, y_1^*(t,\alpha)\right) = f_1^*(t,\alpha), \tag{13}$$

$$Ly_2^*(t,\alpha) + Ry_2^*(t,\alpha) + N_2\left(t, y_2^*(t,\alpha)\right) = f_2^*(t,\alpha), \tag{14}$$

$$Ly_1^*(t,\beta) + Ry_1^*(t,\beta) + N_1\left(t, y_1^*(t,\beta)\right) = f_1^*(t,\beta), \tag{15}$$

$$Ly_2^*(t,\beta) + Ry_2^*(t,\beta) + N_1\left(t, y_2^*(t,\beta)\right) = f_2^*(t,\beta). \tag{16}$$

By taking L^{-1} operator on both sides of equations (13)–(16), we get

$$y_1^*(t,\alpha) = \Psi_1(t,\alpha) - L^{-1}\left(Ry_1^*(t,\alpha)\right) - L^{-1}\left(N_1\left(t, y_1^*(t,\alpha)\right) + L^{-1}\left(f_1^*(t,\alpha)\right)\right), \tag{17}$$

$$y_2^*(t,\alpha) = \Psi_2(t,\alpha) - L^{-1}\left(Ry_2^*(t,\alpha)\right) - L^{-1}\left(N_2\left(t, y_2^*(t,\alpha)\right) + L^{-1}\left(f_2^*(t,\alpha)\right)\right), \tag{18}$$

$$y_1^*(t,\beta) = \Psi_1(t,\beta) - L^{-1}\left(Ry_1^*(t,\beta)\right) - L^{-1}\left(N_1\left(t, y_1^*(t,\beta)\right) + L^{-1}\left(f_1^*(t,\beta)\right)\right), \tag{19}$$

$$y_2^*(t,\beta) = \Psi_2(t,\beta) - L^{-1}\left(Ry_2^*(t,\beta)\right) - L^{-1}\left(N_2\left(t, y_2^*(t,\beta)\right) + L^{-1}\left(f_2^*(t,\beta)\right)\right), \tag{20}$$

where

$$\begin{aligned} \Psi_i(t,\alpha) &= L\Psi_i(t,\alpha) \\ &= 0; i = 1,2, \\ \Psi_i(t,\beta) &= L\Psi_i(t,\beta) \\ &= 0; i = 1,2, \end{aligned} \tag{21}$$

the above functions are found by using the initial conditions.

Now by using the GMADM, the solutions of the (17)–(20) can be expressed in the form of an infinite series for the unknown functions as follows:

$$y_1^*(t,\alpha) = \sum_{n=0}^{\infty} y_{1_n}^*(t,\alpha), \tag{22}$$

$$y_2^*(t,\alpha) = \sum_{n=0}^{\infty} y_{2_n}^*(t,\alpha), \tag{23}$$

$$\overset{*}{y}_1\ (t,\beta) = \sum_{n=0}^{\infty} \overset{*}{y}_{1_n}(t,\beta), \tag{24}$$

$$\overset{*}{y}_2\ (t,\beta) = \sum_{n=0}^{\infty} \overset{*}{y}_{2_n}(t,\beta). \tag{25}$$

Using (22)–(25), in (17)–(20), we have

$$\sum_{n=0}^{\infty} \overset{*}{y}_{1_n}(t,\alpha) = \Psi_1(t,\alpha) - L^{-1}\left(R\sum_{n=0}^{\infty} \overset{*}{y}_{1_n}(t,\alpha)\right) - L^{-1}\left(N_1\left(t,\sum_{n=0}^{\infty} \overset{*}{y}_{1_n}(t,\alpha)\right)\right) + L^{-1}\left(\overset{*}{f}_1\ (t,\alpha)\right), \tag{26}$$

$$\sum_{n=0}^{\infty} \overset{*}{y}_{2_n}(t,\alpha) = \Psi_2(t,\alpha) - L^{-1}\left(R\sum_{n=0}^{\infty} \overset{*}{y}_{2_n}(t,\alpha)\right) - L^{-1}\left(N_2\left(t,\sum_{n=0}^{\infty} \overset{*}{y}_{2_n}(t,\alpha)\right)\right) + L^{-1}\left(\overset{*}{f}_2\ (t,\alpha)\right), \tag{27}$$

$$\sum_{n=0}^{\infty} \overset{*}{y}_{1_n}(t,\beta) = \Psi_1(t,\beta) - L^{-1}\left(R\sum_{n=0}^{\infty} \overset{*}{y}_{1_n}(t,\beta)\right) - L^{-1}\left(N_1\left(t,\sum_{n=0}^{\infty} \overset{*}{y}_{1_n}(t,\beta)\right)\right) + L^{-1}\left(\overset{*}{f}_1\ (t,\beta)\right), \tag{28}$$

$$\sum_{n=0}^{\infty} \overset{*}{y}_{2_n}(t,\beta) = \Psi_2(t,\beta) - L^{-1}\left(R\sum_{n=0}^{\infty} \overset{*}{y}_{2_n}(t,\beta)\right) - L^{-1}\left(N_2\left(t,\sum_{n=0}^{\infty} \overset{*}{y}_{2_n}(t,\beta)\right)\right) + L^{-1}\left(\overset{*}{f}_2\ (t,\beta)\right). \tag{29}$$

According to the GMADM, the recursive relation for the (26)–(29) is as follows:

$$\begin{aligned}
&\overset{*}{y}_{1_0}(t,\alpha) = \Psi_1(t,\alpha),\\
&\overset{*}{y}_{1_1}(t,\alpha) = L^{-1}\left(\overset{*}{f}_1\ (t,\alpha)\right) - L^{-1}\left(R\overset{*}{y}_{1_0}(t,\alpha)\right) - L^{-1}\left(N_1\left(t,\overset{*}{y}_{1_0}(t,\alpha)\right)\right),\\
&\overset{*}{y}_{1_{k+1}}(t,\alpha) = -L^{-1}\left(R\overset{*}{y}_{1_k}(t,\alpha)\right) - L^{-1}\left(N_1\left(t,\overset{*}{y}_{1_k}(t,\alpha)\right)\right), k\geq 1,\\
&\overset{*}{y}_{2_0}(t,\alpha) = \Psi_2(t,\alpha),\\
&\overset{*}{y}_{2_1}(t,\alpha) = L^{-1}\left(\overset{*}{f}_2\ (t,\alpha)\right) - L^{-1}\left(R\overset{*}{y}_{2_0}(t,\alpha)\right) - L^{-1}\left(N_2\left(t,\overset{*}{y}_{2_0}(t,\alpha)\right)\right),\\
&\overset{*}{y}_{2_{k+1}}(t,\alpha) = -L^{-1}\left(R\overset{*}{y}_{2_k}(t,\alpha)\right) - L^{-1}\left(N_2\left(t,\overset{*}{y}_{2_k}(t,\alpha)\right)\right), k\geq 1,\\
&\overset{*}{y}_{1_0}(t,\beta) = \Psi_1(t,\beta),\\
&\overset{*}{y}_{1_1}(t,\beta) = L^{-1}\left(\overset{*}{f}_1\ (t,\beta)\right) - L^{-1}\left(R\overset{*}{y}_{1_0}(t,\beta)\right) - L^{-1}\left(N_1\left(t,\overset{*}{y}_{1_0}(t,\beta)\right)\right),\\
&\overset{*}{y}_{1_{k+1}}(t,\beta) = -L^{-1}\left(R\overset{*}{y}_{1_k}(t,\beta)\right) - L^{-1}\left(N_1\left(t,\overset{*}{y}_{1_k}(t,\beta)\right)\right), k\geq 1,\\
&\overset{*}{y}_{2_0}(t,\beta) = \Psi_2(t,\beta),\\
&\overset{*}{y}_{2_1}(t,\beta) = L^{-1}\left(\overset{*}{f}_2\ (t,\beta)\right) - L^{-1}\left(R\overset{*}{y}_{2_0}(t,\beta)\right) - L^{-1}\left(N_2\left(t,\overset{*}{y}_{2_0}(t,\beta)\right)\right),\\
&\overset{*}{y}_{2_{k+1}}(t,\beta) = -L^{-1}\left(R\overset{*}{y}_{2_k}(t,\beta)\right) - L^{-1}\left(N_2\left(t,\overset{*}{y}_{2_k}(t,\beta)\right)\right), k\geq 1.
\end{aligned} \tag{30}$$

The nth term approximation to the solution is defined as follows:

$$\begin{cases} \phi_{1n}(t,\alpha) = \sum_{i=0}^{n-1} {}^{*}\ y_{1_i}(t,\alpha), \\ \phi_{2n}(t,\alpha) = \sum_{i=0}^{n-1} {}^{*}\ y_{2_i}(t,\alpha), \\ \phi_{1n}(t,\beta) = \sum_{i=0}^{n-1} {}^{*}\ y_{1_i}(t,\beta), \\ \phi_{2n}(t,\beta) = \sum_{i=0}^{n-1} {}^{*}\ y_{2_i}(t,\beta). \end{cases} \tag{31}$$

Hence,

$$\begin{cases} \lim_{n\longrightarrow\infty}(\phi_{1n}(t,\alpha)) = {}^{*}y_1\ (t,\alpha), \\ \lim_{n\longrightarrow\infty}(\phi_{2n}(t,\alpha)) = {}^{*}y_2\ (t,\alpha), \\ \lim_{n\longrightarrow\infty}(\phi_{1n}(t,\beta)) = {}^{*}y_1\ (t,\beta), \\ \lim_{n\longrightarrow\infty}(\phi_{2n}(t,\beta)) = {}^{*}y_2\ (t,\beta). \end{cases} \tag{32}$$

The complexity of the GMADM algorithm is approximately $O(N\log(N))$, according to numerical results using two or more fuzzy systems of intuitionistic differential equations.

3.1. Stability of the Proposed Scheme. When the solution produced by a technique is unaffected by small changes in the inputs and parameters and when it is expected that changes in the parameters carried on by impacts in equations and conditions, the method is said to be stable. By giving examples and analyzing the stability of the GMADM in this study, we suggested contrasting the GMADM with other existing methods, i.e., ADM and Taylor series method (TSM).

3.1.1. Applications. Here, we discuss some engineering applications [31–33] of generalized intuitionistic fuzzy environments.

Example 1. Series Circuit Problem (An Electrical Engineering Application).

Consider $\sigma_3 = <(11,12,13,14;0.8);(10,12,13,15;0.2)>$ volt battery is connected to a series circuit in which inductance is $\sigma_1 = <(0.4,0.5,0.6,0.7;0.8);(0.3,0.5,0.6,0.8;0.2)>$ henry, and the resistance is $\sigma_2 = <(8,9,10,11;0.8);(7,9,10,12;0.2)>$ ohms. Determine the current ${}^{*}i$ if the initial current is ${}^{*}i\ (0) = <(1,2,3,4;0.8);(0,2,3,5;0.2)>$.

The intuitionistic fuzzy differential equation related to above problem is as follows:

$$\begin{cases} \sigma_1 \dfrac{\mathrm{d}\,{}^{*}i\ (t)}{\mathrm{d}t} + \sigma_2 * {}^{*}i\ (t) = \sigma_3, \\ {}^{*}i\ (0) = \sigma_4. \end{cases} \tag{33}$$

In standard form, (33) can be written as follows:

$$\begin{cases} \dfrac{\mathrm{d}\,{}^{*}i\ (t)}{\mathrm{d}t} + \dfrac{\sigma_2}{\sigma_1} * {}^{*}i\ (t) = \dfrac{\sigma_3}{\sigma_1}, \\ {}^{*}i\ (0) = \sigma_4. \end{cases} \tag{34}$$

where $\sigma_2/\sigma_1 = <(11,15,20,28;0.8);(9,15,20,40;0.2)>$ and $\sigma_3/\sigma_1 = <(16,20,26,35;0.8);(13,20,26,50;0.2)>$.

By taking (α,β)-cut of (34), we obtain the following equations:

$$\frac{\mathrm{d}\,{}^{*}i_1\ (t,\alpha)}{\mathrm{d}t} + (5\alpha+11)\,{}^{*}i_1\ (t,\alpha) = 5\alpha+16, \qquad {}^{*}i_1\ (0,\alpha) = 1.25\alpha+1, \tag{35}$$

$$\frac{\mathrm{d}\,{}^{*}i_2\ (t,\alpha)}{\mathrm{d}t} + (28-10\alpha)\,{}^{*}i_2\ (t,\alpha) = 35-11.25\alpha, \qquad {}^{*}i_2\ (0,\alpha) = 4-1.25\alpha, \tag{36}$$

$$\frac{\mathrm{d}\,{}^{*}i_1\ (t,\beta)}{\mathrm{d}t} + (16.5-7.5\beta)\,{}^{*}i_1\ (t,\beta) = 21.75-8.75\beta, \qquad {}^{*}i_1\ (0,\beta) = -2.5\beta+2.5, \tag{37}$$

$$\frac{\mathrm{d}\,{}^{*}i_2\ (t,\beta)}{\mathrm{d}t} + (25\beta+15)\,{}^{*}i_2\ (t,\beta) = 30\beta+20, \qquad {}^{*}i_2\ (0,\beta) = 2.5\beta+2.5. \tag{38}$$

Here, $L = \mathrm{d}/\mathrm{d}t$ and by taking $L^{-1}(.) = \int_0^t (.)\mathrm{d}t$ on both sides of (35)–(38), and using the initial conditions, we obtain

$${}^{*}i_1\ (t,\alpha) = -5\int_0^t\int_0^t (\alpha+2.2)\,{}^{*}i_1\ (x,\alpha)\mathrm{d}x + 5\alpha t + 1.25\alpha + 16t + 1, \tag{39}$$

$${}^{*}i_2\ (t,\alpha) = 10\int_0^t (\alpha-2.8)\,{}^{*}i_2\ (x,\alpha)\mathrm{d}x - 11.25\alpha t - 1.25\alpha + 35t + 4, \tag{40}$$

$${}^{*}i_1\ (t,\beta) = 7.5\int_0^t (\alpha-2.2)\,{}^{*}i_1\ (x,\beta)\mathrm{d}x - 8.75\beta t + 21.75t - 2.5\beta + 2.5, \tag{41}$$

$$\overset{*}{i}_2\ (t,\beta) = -25\int_0^t (\alpha + 0.6)\overset{*}{i}_2\ (x,\beta)\mathrm{d}x + 30\beta t + 2.5\beta + 20t + 2.5. \tag{42}$$

Now by using GMADM, the solution of (39)–(42) can be expressed as follows:

$$\begin{cases} \overset{*}{i}_{1_0}(t,\alpha) = 1.25\alpha + 1, \\ \overset{*}{i}_{1_1}(t,\alpha) = \{(5\alpha + 16) - (5\alpha + 11)(1.25\alpha + 1)\}t, \\ \overset{*}{i}_{1_{k+1}}(t,\alpha) = -5\int_0^t (\alpha + 2.2)\,\overset{*}{i}_k(x,\alpha)dx, k \geq 1, \end{cases} \tag{43}$$

$$\begin{cases} \overset{*}{i}_{2_0}(t,\alpha) = -1.25\alpha + 4, \\ \overset{*}{i}_{2_1}(t,\alpha) = \{(-11.25\alpha + 35) + (10\alpha - 28)(-1.25\alpha + 4)\}t, \\ \overset{*}{i}_{2_{k+1}}(t,\alpha) = 10\int_0^t (\alpha - 2.8)\,\overset{*}{i}_{2_k}(x,\alpha)dx, k \geq 1, \end{cases} \tag{44}$$

$$\begin{cases} \overset{*}{i}_{1_0}(t,\beta) = -2.5\beta + 2.5, \\ \overset{*}{i}_{1_2}(t,\beta) = \{(-8.75\beta + 21.75) + (7.5\beta - 16.5)(-2.5\beta + 2.5)\}t, \\ \overset{*}{i}_{1_{k+1}}(t,\beta) = 7.5\int_0^t (\alpha - 2.2)\,\overset{*}{i}_{1_k}(x,\beta)dx, k \geq 1, \end{cases} \tag{45}$$

$$\begin{cases} \overset{*}{i}_{2_0}(t,\beta) = 2.5\beta + 2.5, \\ \overset{*}{i}_{2_1}(t,\beta) = \{(30\beta + 20) - (25\beta + 15)(2.5\beta + 2.5)\}t, \\ \overset{*}{i}_{2_{k+1}}(t,\beta) = -25\int_0^t (\alpha + 0.6)\,\overset{*}{i}_{2_k}(x,\beta)\mathrm{d}x, k \geq 1. \end{cases} \tag{46}$$

By solving (43)–(46), we get the closed form solution after four iterations as follows using GMADM:

$$\begin{aligned} \overset{*}{i}_1\ (t,\alpha) &= 1.25\alpha + 1 + \frac{1}{5\alpha + 11}[(5\alpha + 16) - (5\alpha + 11)(1.25\alpha + 1)]\left[1 - e^{-(5\alpha+11)t}\right], \\ \overset{*}{i}_2\ (t,\alpha) &= 4 - 1.25\alpha + \frac{1}{28 - 10\alpha}[(-11.25\alpha + 35) - (-10\alpha + 28)(-1.25\alpha + 4)]\left[1 - e^{-(-10\alpha+28)t}\right], \\ \overset{*}{i}_1\ (t,\beta) &= 2.5 - 2.5\beta + \frac{1}{16.5 - 7.5\beta}[(-8.75\beta + 21.75) - (-7.5\beta + 16.5)(-2.5\beta + 2.5)]\left[1 - e^{-(-7.5\beta+16.5)t}\right], \\ \overset{*}{i}_2\ (t,\beta) &= 2.5 + 2.5\beta + \frac{1}{25\beta + 15}[(30\beta + 20) - (25\beta + 15)(2.5\beta + 2.5)]\left[1 - e^{-(25\beta+15)t}\right]. \end{aligned} \tag{47}$$

The exact and approximate solutions of the IVP-I used in Example 1 are shown in Tables 1 and 2, respectively.

Figures 2(a) and 2(b) shows an approximate solution of the membership and nonmembership function for IVP-I used in Example 1.

The exact solution of Example 1 by classical method is given as follows:

$$
\begin{aligned}
\overset{*}{i}_1\ (t,\alpha) &= e^{-(5\alpha+11)t}\left(\frac{5}{4}\alpha+1-\frac{(5\alpha+16)}{(5\alpha+11)}\right)+\frac{(5\alpha+16)}{(5\alpha+11)},\\
\overset{*}{i}_2\ (t,\alpha) &= e^{2(5\alpha-14)t}\left(4-\frac{5}{4}\alpha-\frac{5}{8}\frac{(-28+9\alpha)}{(5\alpha-14)}\right)+\frac{5}{8}\frac{(-28+9\alpha)}{(5\alpha-14)},\\
\overset{*}{i}_1\ (t,\beta) &= e^{(3/2)(5\beta-11)t}\left(\frac{5}{2}-\frac{5}{2}\beta-\frac{1}{6}\frac{(-87+35\beta)}{(-11+5\beta)}\right)+\frac{1}{6}\frac{(-87+35\beta)}{(-11+5\beta)},\\
\overset{*}{i}_2\ (t,\beta) &= e^{-5(5\beta+3)t}\left(\frac{5}{2}\beta+\frac{5}{2}-\frac{2(3\beta+2)}{(5\beta+3)}\right)+\frac{2(3\beta+2)}{(5\beta+3)}.
\end{aligned}
\tag{48}
$$

Figure 3(a) depicts the exact solution of the membership function of the generalized intuitionistic fuzzy IVP-I, 3(b) depicts the exact solution of the nonmembership function, and 3(c) depicts the exact solution of the generalized intuitionistic fuzzy IVP-I as described in Example 1.

In Table 3, n represents the number of iterations, Err represents the residual error, and CPU time represents the computational time in seconds for finding the approximate solution of the generalized intuitionistic fuzzy IVP-I described in Example 1. Figures 2(a) and 2(b) show an approximate solution of the membership and nonmembership function for IVP-I used in Example 1. The exact solutions to the membership and nonmembership functions for IVP-I used in Example 1 are depicted in Figures 3(a)–3(c).

Example 2. Mass Spring System (Physical Engineering Application).

Consider a spring with a mass of $\overset{*}{m} = <(2,3,4,5;0.6);(1,3,4,6;0.3)>$ kg is held stretched $\overset{*}{s} = <(0.5,0.6,0.7,0.8;0.6);(0.4,0.6,0.7,0.9;0.3)>$ m beyond its natural length by a force of $\overset{*}{F} = <(19,20,21,23;0.6);(18,20,21,24;0.3)>$ N. If the spring begins at its equilibrium position, then a push gives it an initial velocity of $x_0^* = <(11,12,13,14;0.6);(10,12,13,15;0.3)>$ ms^{-1}.

The intuitionistic fuzzy initial value problem related to this problem is given as follows:

$$
\overset{*}{m}\frac{d^2x(t)}{dt^2}+\overset{*}{k}\overset{*}{x}(t)=0, \tag{49}
$$

with initial conditions:

$$
\begin{cases}
\overset{*}{x}(0) = <(5,6,7,8;0.6);(4,6,7,9;0.3)>,\\
\overset{*}{x}'(0) = <(11,12,13,14;0.6);(10,12,13,15;0.3)>.
\end{cases}
\tag{50}
$$

Here, $\overset{*}{k}$ is spring constant and its value is calculated as follows:

$$
\begin{aligned}
\overset{*}{k} &= \frac{\overset{*}{F}}{\overset{*}{s}} \\
&= <(24,29,35,46;0.8);(20,29,35,60;0.3)>.
\end{aligned}
\tag{51}
$$

Using the values of $\overset{*}{m}$ and $\overset{*}{k}$ in (49), we get the following intuitionistic fuzzy differential equation in standard form as follows:

$$
\frac{d^2\overset{*}{x}(t)}{dt^2}+<(5,7,12,23;0.6);(3,7,12,60;0.3)>\overset{*}{x}(t)=0. \tag{52}
$$

By taking (α,β)-cut of (50) and (52), we get

$$
\begin{aligned}
\frac{\mathrm{d}_1^2\overset{*}{x}(t,\alpha)}{\mathrm{d}t^2}+(3\alpha+5)\overset{*}{x}_1\ (t,\alpha)&=0,\\
\overset{*}{x}_1\ (0,\alpha)&=2\alpha+5,\\
\overset{*}{x}_1'(0,\alpha)&=2\alpha+11,
\end{aligned}
\tag{53}
$$

$$
\begin{aligned}
\frac{\mathrm{d}_2^2\overset{*}{x}(t,\alpha)}{\mathrm{d}t^2}+(23-18\alpha)\overset{*}{x}_2\ (t,\alpha)&=0,\\
x_2(0,\alpha)&=8-2\alpha,\\
\overset{*}{x}_2'(0,\alpha)&=14-2\alpha,
\end{aligned}
\tag{54}
$$

$$
\begin{aligned}
\frac{\mathrm{d}_1^2\overset{*}{x}(t,\beta)}{\mathrm{d}t^2}+(9-6\beta)\overset{*}{x}_1\ (t,\beta)&=0,\\
\overset{*}{x}_1\ (0,\beta)&=7-3\beta,\\
\overset{*}{x}_1'(0,\beta)&=13-3\beta,
\end{aligned}
\tag{55}
$$

$$
\begin{aligned}
\frac{\mathrm{d}_2^2\overset{*}{x}(t,\beta)}{\mathrm{d}t^2}+(69\beta-9)\overset{*}{x}_2\ (t,\beta)&=0,\\
\overset{*}{x}_2\ (0,\beta)&=3\beta+6,\\
\overset{*}{x}_2'(0,\beta)&=3\beta+12.
\end{aligned}
\tag{56}
$$

Here, $L=\mathrm{d}^2/\mathrm{d}t^2$ and by taking $L^{-1}(.)=\int_0^t\int_0^t(.)\mathrm{d}t\,\mathrm{d}t$ on both sides of (53)–(56), and using the initial conditions, we obtain

Table 1: Approximate solution of Example 1 at $t = 1$.

α	$\underline{i}_1^*(t,\alpha)$	$\underline{i}_2^*(t,\alpha)$	β	$\overline{i}_1^*(t,\beta)$	$\overline{i}_2^*(t,\beta)$
0	1.4546	1.2500	0.2	1.3333	1.3000
0.1	1.4348	1.2546	0.3	1.3421	1.2889
0.2	1.4167	1.2596	0.4	1.3519	1.2800
0.3	1.4000	1.2650	0.5	1.3627	1.2727
0.4	1.3846	1.2708	0.6	1.3750	1.2667
0.5	1.3704	1.2772	0.7	1.3889	1.2615
0.6	1.3571	1.28409	0.8	1.4048	1.2571
0.7	1.3448	1.2917	0.9	1.4231	1.2533
0.8	1.3333	1.3000	1.0	1.4444	1.2500

Table 2: Exact solution of Example 1 at $t = 1$.

α	$\underline{i}_1^*(t,\alpha)$	$\underline{i}_2^*(t,\alpha)$	β	$\overline{i}_1^*(t,\beta)$	$\overline{i}_2^*(t,\beta)$
0	1.4546	1.2500	0.2	1.3333	1.3000
0.1	1.4348	1.2546	0.3	1.3421	1.2889
0.2	1.4167	1.2596	0.4	1.3519	1.2800
0.3	1.4000	1.2650	0.5	1.3627	1.2727
0.4	1.3846	1.2708	0.6	1.3750	1.2667
0.5	1.3704	1.2772	0.7	1.3889	1.2615
0.6	1.3571	1.28409	0.8	1.4048	1.2571
0.7	1.3448	1.2917	0.9	1.4231	1.2533
0.8	1.3333	1.3000	1.0	1.4444	1.2500

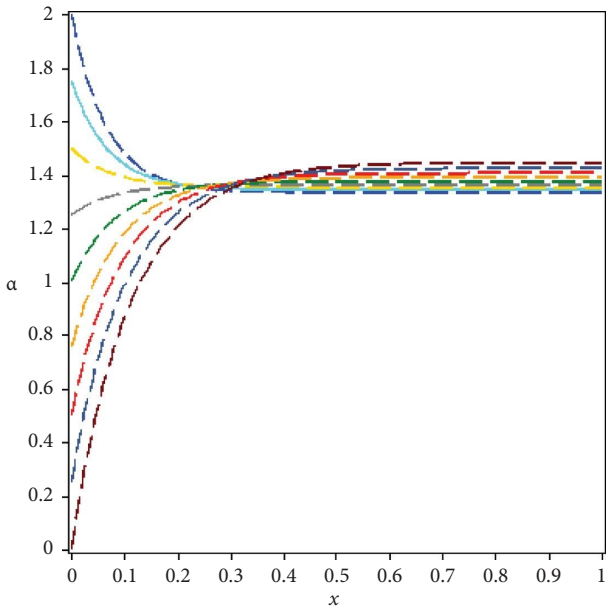

(a)

Figure 2: Continued.

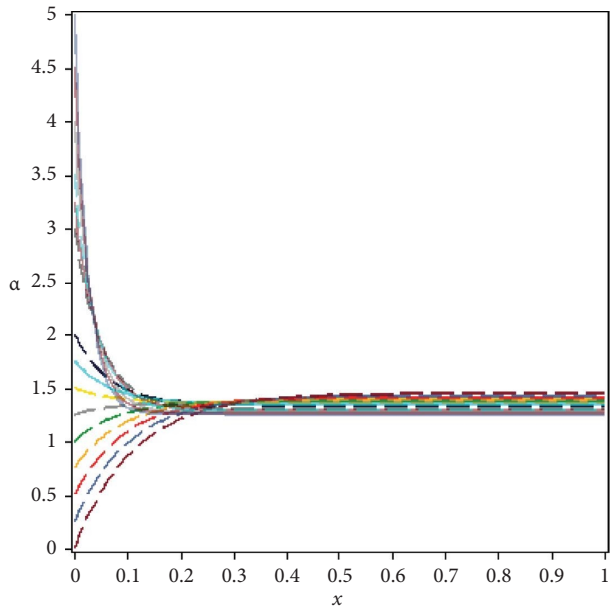

(b)

Figure 2: (a) Membership function and (b) nonmembership function.

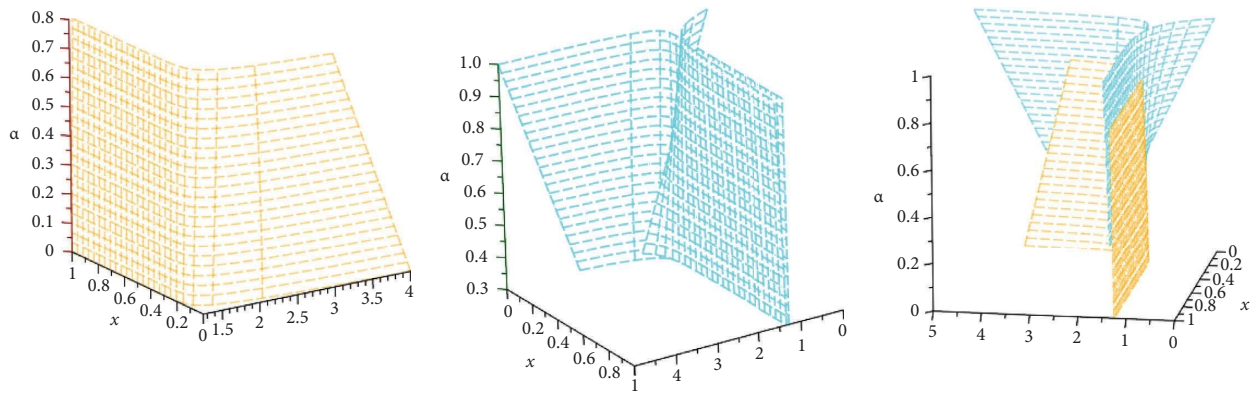

(a) (b) (c)

Figure 3: (a) Exact solution of membership function for GITF-IVP-I, (b) exact solution of nonmembership function for GITF-IVP-I, and (c) exact solution of GTIF-IVP-I.

Table 3: Error comparison of GMADM, ADM, and TSM for solving GTIF-IVP-I used in Example 1.

Methods	GMADM	ADM	TSM
n	04	17	08
Err	$1.2e-32$	$6.2e-15$	$7.1e-5$
CPU time	0.0123	0.2413	0.1452

$$\begin{cases} \overset{*}{x}_1\ (t,\alpha) = \int_0^t (-t+y)(3\alpha+5)\overset{*}{x}_1\ (y,\alpha)\mathrm{d}y + 2\alpha t + 2\alpha + 11t + 5, \\ \overset{*}{x}_2\ (t,\alpha) = \int_0^t \Big(-(-t+y)(-23+18\alpha)\overset{*}{x}_2\ (y,\alpha)\Big)\mathrm{d}y - 2\alpha t - 2\alpha + 14t + 8, \\ \overset{*}{x}_1\ (t,\beta) = \int_0^t \Big(-3(-t+y)(-3+2\beta)\overset{*}{x}_1\ (y,\beta)\Big)\mathrm{d}y - 3\beta t - 3\beta + 13t + 7, \\ \overset{*}{x}_2\ (t,\beta) = \int_0^t 3(-t+y)(-3+23\beta)\overset{*}{x}_2\ (y,\beta)\mathrm{d}y + 3\beta t + 3\beta + 12t + 6. \end{cases} \tag{57}$$

Now, by using GMADM, we get

$$\begin{cases} \overset{*}{x}_{1_0}(t,\alpha) = 5 + (2\alpha+11)t + 2\alpha, \\ \overset{*}{x}_{1_1}(t,\alpha) = -\alpha^2 t^3 - \frac{43}{6}\alpha t^3 - \frac{55}{6}t^3 - 3\alpha^2 t^2 - \frac{25}{2}\alpha t^2 - \frac{25}{2}t^2, \\ \overset{*}{x}_{1_{k+1}}(t,\alpha) = \int_0^t (-t+y)(3\alpha+5) *\ x_{1_k}(y,\alpha)\mathrm{d}y, k \geq 1. \end{cases} \tag{58}$$

$$\begin{cases} \overset{*}{x}_{2_0}(t,\alpha) = 8 + (14-2\alpha)t - 2\alpha, \\ \overset{*}{x}_{2_1}(t,\alpha) = -6\alpha^2 t^3 - \frac{149}{3}\alpha t^3 - \frac{161}{3}t^3 - 18\alpha^2 t^2 + 95\alpha t^2 - 92t^2, \\ \overset{*}{x}_{2_{k+1}}(t,\alpha) = \int_0^t \Big(-(-t+y)(-23+18\alpha) *\ x_{2_k}(y,\alpha)\mathrm{d}y, k \geq 1. \end{cases} \tag{59}$$

$$\begin{cases} \overset{*}{x}_{1_0}(t,\beta) = 7 + (13-3\beta)t - 3\beta, \\ \overset{*}{x}_{1_2}(t,\beta) = -3\beta^2 t^3 + \frac{35}{2}\beta t^3 - \frac{39}{2}t^3 - 9\beta^2 t^2 + \frac{69}{2}\beta t^2 - \frac{63}{2}t^2, \\ \overset{*}{x}_{1_{k+1}}(t,\beta) = \int_0^t \int_0^t \Big(-3(-t+y)(-3+2\beta) *\ x_{1_k}(y,\beta)\mathrm{d}y, k \geq 1. \end{cases} \tag{60}$$

$$\begin{cases} \overset{*}{x}_{2_0}(t,\beta) = 6 + (3\beta+12) + 3\beta, \\ \overset{*}{x}_{2_1}(t,\beta) = -\frac{69}{2}\beta^2 t^3 - \frac{267}{2}\beta t^3 + 18t^3 - \frac{207}{2}\beta^2 t^2 - \frac{387}{2}\beta t^2 + 27t^2, \\ \overset{*}{x}_{2_{k+1}}(t,\beta) = \int_0^t 3(-t+y)(-3+23\beta) *\ x_{2_k}(y,\beta)\mathrm{d}y, k \geq 1. \end{cases} \tag{61}$$

By solving the (58)–(61), we get the approximate solution after four iterations as follows:

$$\begin{aligned}
\overset{*}{x}_2(t,\alpha) &= 8-2\alpha+14t-2\alpha t+\frac{279841}{25920}t^9+\frac{625}{8064}t^8-\frac{161}{3}t^3-92t^2+\frac{3703}{60}t^5+\frac{529}{3}t^4-\frac{12167}{360}t^7-\frac{12167}{90}t^6-\frac{81}{140}t^9\alpha^5+\frac{981}{140}t^9\alpha^4\\
&-\frac{7383}{280}t^9\alpha^3+\frac{28037}{630}t^9\alpha^2-\frac{6412009}{181440}t^9\alpha-\frac{729}{140}t^8\alpha^5+\frac{3321}{70}t^8\alpha^4-\frac{44091}{280}t^8\alpha^3+\frac{69299}{280}t^8\alpha^2-\frac{3783937}{20160}t^8\alpha-\frac{81}{35}t^7\alpha^4+\frac{351}{14}t^7\alpha^3\\
&-\frac{10281}{140}t^7\alpha^2+\frac{212129}{2520}t^7\alpha-\frac{81}{5}t^6\alpha^4+\frac{1269}{10}t^6\alpha^3-\frac{1311}{4}t^6\alpha^2+\frac{126431}{360}t^6\alpha-\frac{27}{5}t^5\alpha^3+\frac{258}{5}t^5\alpha^2-\frac{1265}{12}t^5\alpha-27t^4\alpha^3+177t^4\alpha^2\\
&-\frac{3841}{12}t^4\alpha-6t^3\alpha^2+\frac{149}{3}t^3\alpha-18t^2\alpha^2+95t^2\alpha,\\
\overset{*}{x}_1(t,\beta) &= 7-3\beta+13t-3\beta t+\frac{1053}{4480}t^9+\frac{729}{640}t^8-\frac{39}{2}t^3-\frac{63}{2}t^2+\frac{351}{40}t^5+\frac{189}{8}t^4-\frac{1053}{560}t^7-\frac{567}{80}t^6-\frac{3}{280}t^9\beta^5+\frac{31}{80}t^9\beta^4-\frac{237}{560}t^9\beta^3\\
&+\frac{27}{35}t^9\beta^2-\frac{3051}{4480}t^9\beta-\frac{27}{280}t^8\beta^5+\frac{45}{56}t^8\beta^4-\frac{297}{112}t^8\beta^3+\frac{243}{56}t^8\beta^2-\frac{3159}{896}t^8\beta-\frac{9}{70}t^7\beta^4+\frac{159}{140}t^7\beta^3-\frac{27}{8}t^7\beta^2+\frac{2349}{560}t^7\beta-\frac{9}{10}t^6\beta^4\\
&+\frac{123}{20}t^6\beta^3-\frac{621}{40}t^6\beta^2+\frac{1377}{80}t^6\beta-\frac{9}{10}t^5\beta^3+\frac{33}{5}t^5\beta^2-\frac{549}{40}t^5\beta-\frac{9}{2}t^4\beta^3+24t^4\beta^2-\frac{333}{8}t^4\beta-3t^3\beta^2+\frac{35}{2}t^3\beta-9t^2\beta^2+\frac{69}{2}t^2\beta.
\end{aligned} \tag{62}$$

The exact and approximate solutions of the IVP-II used in Example 2 are shown in Tables 4 and 5, respectively.

Figures 4(a) and 4(b) show an approximate solution of the membership and nonmembership functions for IVP-II used in Example 2.

The exact solution of Example 2 given by classical method is as follows:

$$\begin{aligned}
x_1(t,\alpha) &= \frac{(2\alpha+11)\sin\sqrt{3\alpha+5}t}{\sqrt{3\alpha+5}}+(5+2\alpha)\cos\sqrt{3\alpha+5}t,\\
x_2(t,\alpha) &= \frac{2\sqrt{-18\alpha+23}(\alpha-7)\sin\sqrt{-18\alpha+23}t}{-18\alpha+23}+(8-2\alpha)\cos\sqrt{-18\alpha+23}t,\\
x_1(t,\beta) &= \frac{1}{3}\,\frac{2\sqrt{-6\beta+9}(3\beta-13)\sin\sqrt{-6\beta+9}t}{2\beta-3}+(7-3\beta)\cos\sqrt{-6\beta+9}t,\\
x_2(t,\beta) &= \frac{\sqrt{69\beta-9}(\beta+4)\sin\sqrt{69\beta-9}t}{23\beta-3}+(6=3\beta)\cos\sqrt{69\beta-9}t.
\end{aligned} \tag{63}$$

Figure 5(a) depicts the exact solution of the membership function of the generalized intuitionistic fuzzy IVP-II, 5(b) depicts the exact solution of the nonmembership function, and 5(c) depicts the exact solution of the generalized intuitionistic fuzzy IVP-I1 described in Example 2.

In Table 6, n represents the number of iterations, Err represents the residual error, and CPU time represents the computational time in seconds for finding the approximate solution of the generalized intuitionistic fuzzy IVP-II described in Example 2. Figures 4(a) and 4(b) show an approximate solution of the membership and nonmembership function for IVP-II used in Example 2. The exact solutions to the membership and nonmembership functions for IVP-II used in Example 2 are depicted in Figures 5(a)–5(c).

Example 3. Steam Supply Control Slide Value Problem (Mechanical Engineering Application).

The motion $\overset{*}{y}(t)$ of a steam supply control slide valve is governed by the third-order differential equation as follows:

$$m\frac{\mathrm{d}^3\overset{*}{y}}{\mathrm{d}t^3}+f\frac{\mathrm{d}^2\overset{*}{y}}{\mathrm{d}t^2}+k\frac{\mathrm{d}\overset{*}{y}}{\mathrm{d}t}+h\frac{\alpha}{I}\overset{*}{y}=0, \tag{64}$$

where m is mass of the valve, f is friction, k is a constant characterizing the properties of the slide valve spring, h is a constant depending on the dimensions of the equipment, α is a proportionality constant relating the motion and the acceleration of the control valve, and I is the moment of inertia of the turbine. If we neglect the friction and take $m = 50\text{kg}$, $k = 25$ $h = 1, \alpha = 6$, and $I = 0.8$, then the (64) becomes

$$50\frac{\mathrm{d}^3\overset{*}{y}}{\mathrm{d}t^3}+25\frac{\mathrm{d}\overset{*}{y}}{\mathrm{d}t}+\frac{6}{0.8}\overset{*}{y}=0, \tag{65}$$

with initial conditions

Table 4: Approximate solution of Example 2 at $t = 1$.

α	$x_1(t,\alpha)$	$x_2(t,\alpha)$	β	$x_1(t,\beta)$	$x_2(t,\beta)$
0	6.6109	−3.8972	0.3	5.7772	2.7760
0.1	6.5617	−2.9696	0.4	6.0440	−1.4241
0.2	6.5010	−1.9884	0.5	6.2821	−4.5497
0.3	6.4290	−0.9561	0.6	6.4899	−6.6794
0.4	6.3461	0.1248	0.7	6.6661	−7.8787
0.5	6.2525	1.2514	0.8	6.8090	−8.1914
0.6	6.1483	2.4206	0.9	6.9174	−7.6319
			1.0	6.9895	−6.1758

Table 5: Exact solution of Example 2 at $t = 1$.

α	$x_1(t,\alpha)$	$x_2(t,\alpha)$	β	$x_1(t,\beta)$	$x_2(t,\beta)$
0	6.6109	−3.8972	0.3	5.7772	2.7760
0.1	6.5617	−2.9696	0.4	6.0440	−1.4241
0.2	6.5010	−1.9884	0.5	6.2821	−4.5497
0.3	6.4290	−0.9561	0.6	6.4899	−6.6794
0.4	6.3461	0.1248	0.7	6.6661	−7.8787
0.5	6.2525	1.2514	0.8	6.8090	−8.1914
0.6	6.1483	2.4206	0.9	6.9174	−7.6319
			1.0	6.9895	−6.1758

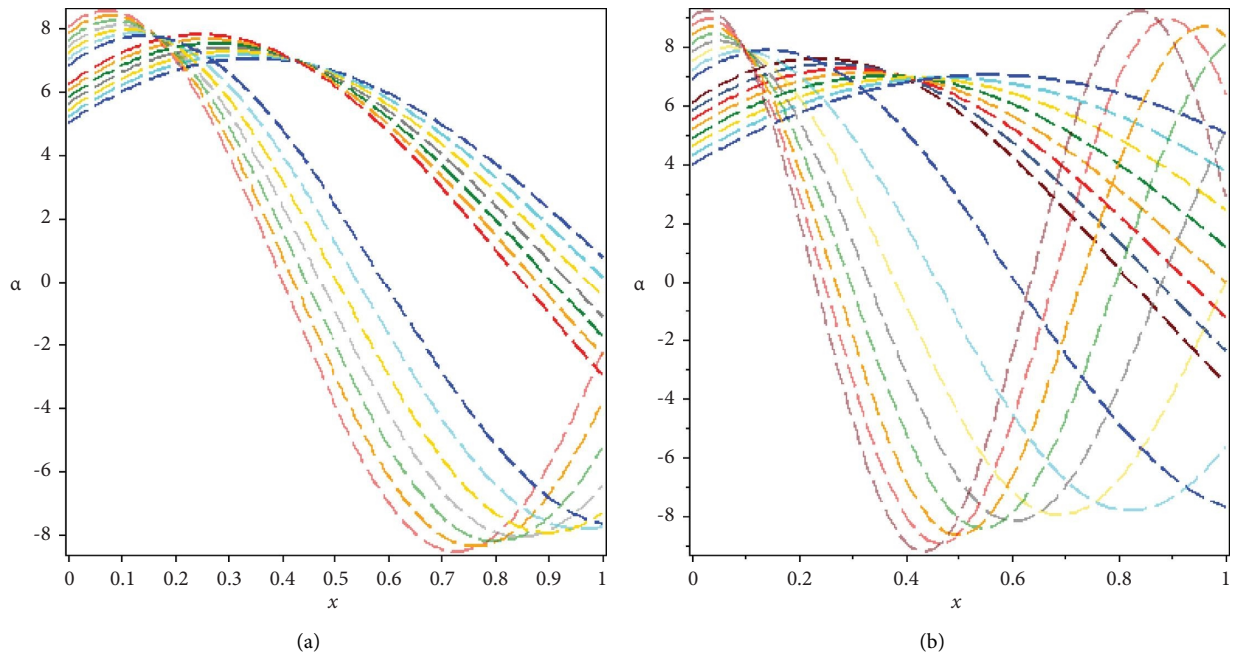

Figure 4: (a) Membership function and (b) nonmembership function.

$$\begin{aligned}
\overset{*}{y}(0) &= <(1,2,3,4;0.5);\ (0,2,3,5;0.3)>,\\
\overset{*}{y}'(0) &= <(7,8,9,10;0.5);\ (6,8,9,11;0.3)>,\\
\overset{*}{y}''(0) &= <(21,22,23,24;0.5);\ (20,22,23,25;0.3)>.
\end{aligned} \tag{66}$$

In standard form, (65) can be written as follows:

$$\frac{\mathrm{d}^3 \overset{*}{y}}{\mathrm{d}t^3} + \frac{1}{5}\frac{\mathrm{d}\overset{*}{y}}{\mathrm{d}t} + \frac{3}{20}\overset{*}{y} = 0. \tag{67}$$

By taking (α, β)-cut of (67) and (66), we get the following equations:

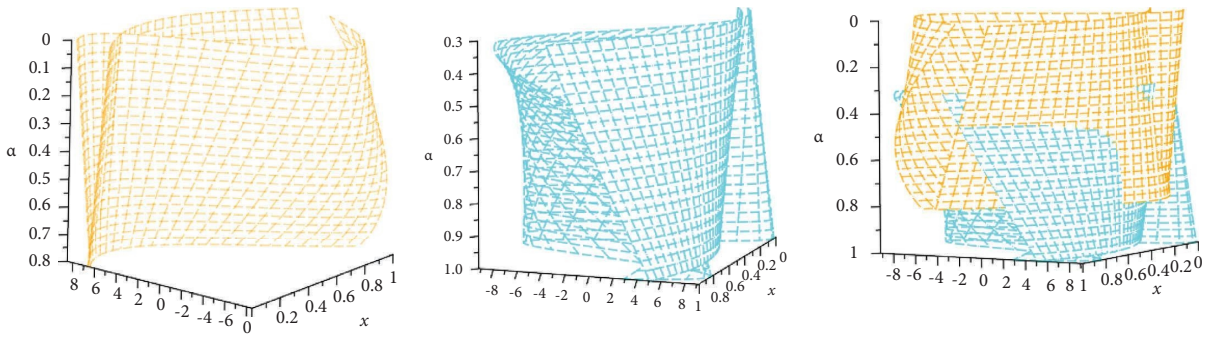

Figure 5: (a) Exact solution of membership function for GITF-IVP-II, (b) exact solution of nonmembership function for GITF-IVP-II, and (c) exact solution of GTIF-IVP-II.

Table 6: Error comparison of GMADM, ADM, and TSM for solving GTIF-IVP-II used in Example 2.

Methods	GMADM	ADM	TSM
n	04	14	06
Err	$4.2e-45$	$1.2e-19$	$0.1e-7$
CPU time	0.0143	0.2113	0.1872

$$\begin{cases} \dfrac{d^3 y_1^*(t,\alpha)}{dt^3} + \dfrac{1}{5}\dfrac{dy_1^*(t,\alpha)}{dt} + \dfrac{3}{20} y_1^*(t,\alpha) = 0, \\ y_1^*(0,\alpha) = 1 + 2\alpha, \\ y_1^{*\prime}(0,\alpha) = 7 + 2\alpha, \\ y_1^{*\prime\prime}(0,\alpha) = 21 + 2\alpha, \end{cases} \tag{68}$$

$$\begin{cases} \dfrac{d^3 y_2^*(t,\alpha)}{dt^3} + \dfrac{1}{5}\dfrac{dy_2^*(t,\alpha)}{dt} + \dfrac{3}{20} y_2^*(t,\alpha) = 0, y_2^*(0,\alpha) = 4 - 2\alpha, \\ y_2^{*\prime}(0,\alpha) = 10 - 2\alpha, y_2^{*\prime\prime}(0,\alpha) = 24 - 2\alpha, \end{cases} \tag{69}$$

$$\begin{cases} \dfrac{d^3 y_1^*(t,\beta)}{dt^3} + \dfrac{1}{5}\dfrac{dy_1^*(t,\beta)}{dt} + \dfrac{3}{20} y_1^*(t,\beta) = 0, \\ y_1^*(0,\beta) = 3 - 3\beta, \\ y_1^{*\prime}(0,\beta) = 9 - 3\beta, \\ y_1^{*\prime\prime}(0,\beta) = 23 - 3\beta, \end{cases} \tag{70}$$

$$\begin{cases} \dfrac{d^3 y_2^*(t,\beta)}{dt^3} + \dfrac{1}{5}\dfrac{dy_2^*(t,\beta)}{dt} + \dfrac{3}{20} y_2^*(t,\beta) = 0, \\ y_2^*(0,\beta) = 2 + 3\beta, \\ y_2^{*\prime}(0,\beta) = 8 + 3\beta, \\ y_2^{*\prime\prime}(0,\beta) = 22 + 3\beta. \end{cases} \tag{71}$$

Here, $L = d^3/dt^3$ and by taking $L^{-1}(.) = \int_0^t \int_0^t \int_0^t (.)dt\, dt\, dt$ on both sides of (68)–(71), and using the initial conditions, we obtain

$$\begin{aligned}
\overset{*}{y}_1\ (t,\alpha) &= \int_0^t -\frac{1}{40}\overset{*}{y}_1\ (x,\alpha)(x-t)(3x-3t-8)dx + 1 + \frac{53}{5}t^2 + \frac{6}{5}t^2\alpha + 2\alpha t + 2\alpha + 7t,\\
\overset{*}{y}_2\ (t,\alpha) &= \int_0^t -\frac{1}{40}\overset{*}{y}_2\ (x,\alpha)(x-t)(3x-3t-8)dx + 4 + \frac{62}{5}t^2 - \frac{6}{5}t^2\alpha - 2\alpha t - 2\alpha + 10t,\\
\overset{*}{y}_1\ (t,\beta) &= \int_0^t -\frac{1}{40}\overset{*}{y}_1\ (x,\beta)(x-t)(3x-3t-8)dx + 3 + \frac{59}{5}t^2 - \frac{9}{5}t^2\beta - 3\beta t - 3\beta + 9t,\\
\overset{*}{y}_2\ (t,\beta) &= \int_0^t -\frac{1}{40}\overset{*}{y}_2\ (x,\beta)(x-t)(3x-3t-8)dx + 2 + \frac{56}{5}t^2 + \frac{9}{5}t^2\beta + 3\beta t + 3\beta + 8t.
\end{aligned} \tag{72}$$

Now, by using GMADM, we get

$$\begin{cases}
\overset{*}{y}_{1_0}(t,\alpha) = 1 + \frac{1}{10}t^2(1+2\alpha) + \frac{1}{2}(21+2\alpha)t^2 + (7+2\alpha)t + 2\alpha,\\
\overset{*}{y}_{1_1}(t,\alpha) = -\frac{53}{2000}t^5 - \frac{3}{1000}t^5\alpha - \frac{529}{2400}t^4 - \frac{13}{400}t^4\alpha - \frac{31}{120}t^3 - \frac{7}{60}t^3\alpha - \frac{1}{10}t^2 - \frac{1}{5}t^2\alpha,\\
\overset{*}{y}_{1_{k+1}}(t,\alpha) = \int_0^t -\frac{1}{40}(x-t)(3x-3t-8)\overset{*}{y}_{1_k}(x,\alpha)dx, k \geq 1.
\end{cases} \tag{73}$$

$$\begin{cases}
\overset{*}{y}_{2_0}(t,\alpha) = 4 + \frac{1}{10}t^2(4-2\alpha) + \frac{1}{2}(24-2\alpha)t^2 + (10-2\alpha)t - 2\alpha,\\
\overset{*}{y}_{2_1}(t,\alpha) = -\frac{31}{1000}t^5 + \frac{3}{1000}t^5\alpha - \frac{323}{1200}t^4 + \frac{13}{400}t^4\alpha - \frac{31}{30}t^3 + \frac{7}{60}t^3\alpha - \frac{2}{5}t^2 + \frac{1}{5}t^2\alpha,\\
\overset{*}{y}_{2_{k+1}}(t,\alpha) = \int_0^t -\frac{1}{40}(x-t)(3x-3t-8)\overset{*}{y}_{2_k}(x,\alpha)dx, k \geq 1.
\end{cases} \tag{74}$$

$$\begin{cases}
\overset{*}{y}_{1_0}(t,\beta) = 3 + \frac{1}{10}t^2(3-2\beta) + \frac{1}{2}(23-3\beta)t^2 + (9-3\beta)t - 3\beta,\\
\overset{*}{y}_{1_1}(t,\beta) = -\frac{59}{2000}t^5 + \frac{9}{2000}t^5\beta - \frac{607}{2400}t^4 + \frac{39}{800}t^4\beta - \frac{3}{8}t^3 + \frac{7}{40}t^3\beta - \frac{3}{10}t^2 + \frac{3}{10}t^2\beta,\\
\overset{*}{y}_{1_{k+1}}(t,\beta) = \int_0^t -\frac{1}{40}(x-t)(3x-3t-8)\overset{*}{y}_{1_k}(x,\beta)dx, k \geq 1.
\end{cases} \tag{75}$$

$$\begin{cases}
\overset{*}{y}_{2_0}(t,\beta) = 2 + \frac{1}{10}t^2(2+3\beta) + \frac{1}{2}(22+3\beta)t^2 + (8+3\beta)t + 3\beta,\\
\overset{*}{y}_{2_1}(t,\beta) = -\frac{59}{2000}t^5 + \frac{9}{2000}t^5\beta - \frac{607}{2400}t^4 + \frac{39}{800}t^4\beta - \frac{3}{8}t^3 + \frac{7}{40}t^3\beta - \frac{3}{10}t^2 + \frac{3}{10}t^2\beta,\\
\overset{*}{y}_{2_{k+1}}(t,\beta) = \int_0^t -\frac{1}{40}(x-t)(3x-3t-8)\overset{*}{y}_{2_k}(x,\beta)dx, k \geq 1.
\end{cases} \tag{76}$$

By solving the (73)–(76), we get the approximate solution after four iterations as follows:

$$
\begin{aligned}
\overset{*}{y}_1(t,\alpha) &= 1 + t^2\alpha + 7t + \frac{1}{71751680000000}t^{14}\alpha + \frac{37}{30750720000000}t^{13}\alpha + \frac{41}{1013760000000}t^{12}\alpha - \frac{47381}{71751680000000}t^{10} - \frac{1}{750}t^5\alpha - \frac{7}{240}t^4\alpha \\
&\quad - \frac{7}{60}t^3\alpha - \frac{71}{3000}t^5 - \frac{7}{32}t^4 - \frac{31}{120}t^3 + \frac{2357}{1330560000000}t^{11} + \frac{57}{32000}t^6 - \frac{18539}{14515200000}t^9 + \frac{113}{26880000}t^8 + \frac{2711}{10080000}t^7 + \frac{137}{5040000}t^7\alpha \\
&\quad + \frac{53}{430510080000000}t^{14} + \frac{1801}{184504320000000}t^{13} + \frac{3967}{1330560000000}t^{12} + 2\alpha + \frac{109}{221760000000}t^{11}\alpha - \frac{71}{17280000000}t^{10}\alpha - \frac{1283}{7257600000}t^9\alpha \\
&\quad + \frac{21}{2}t^2 - \frac{1}{1612800}t^8\alpha + \frac{49}{144000}t^6\alpha 2t\alpha, \\
\overset{*}{y}_2(t,\alpha) &= 4 - t^2\alpha + 10t - \frac{1}{71751680000000}t^{14}\alpha - \frac{37}{30750720000000}t^{13}\alpha + \frac{1}{750}t^5\alpha - \frac{41}{1013760000000}t^{12}\alpha + \frac{7}{240}t^4\alpha + \frac{7}{60}t^3\alpha - \frac{77}{3000}t^5 - \frac{21}{80}t^4 \\
&\quad - \frac{13}{30}t^3 + \frac{1669}{665280000000}t^{11} - \frac{25927}{362880000000}t^{10} - \frac{5597}{3628800000}t^9 + \frac{11}{3360000}t^8 + \frac{223}{720000}t^7 + \frac{11}{4800}t^6 + \frac{31}{215255040000000}t^{14} - 2\alpha \\
&\quad + \frac{97}{8386560000000}t^{13} + \frac{1207}{3548160000000}t^{12} - \frac{109}{221760000000}t^{11}\alpha + \frac{71}{17280000000}t^{10}\alpha + \frac{1283}{7257600000}t^9\alpha + 12t^2 + \frac{1}{1612800}t^8\alpha \\
&\quad - \frac{137}{5040000}t^7\alpha - \frac{49}{144000}t^6\alpha - 2t\alpha, \\
\overset{*}{y}_2(t,\beta) &= 2 + \frac{3}{2}t^2\beta + 8t + \frac{3}{143503360000000}t^{14}\beta + \frac{37}{20500480000000}t^{13}\beta + \frac{41}{675840000000}t^{12}\beta - \frac{1}{500}t^5\beta - \frac{7}{160}t^4\beta - \frac{7}{40}t^3\beta - \frac{73}{3000}t^5 - \frac{7}{30}t^4 \\
&\quad - \frac{19}{60}t^3 + \frac{61}{30240000000}t^{11} - \frac{6109}{90720000000}t^{10} - \frac{9911}{7257600000}t^9 + \frac{157}{40320000}t^8 + \frac{89}{315000}t^7 + \frac{281}{144000}t^6 + \frac{1}{7687680000000}t^{14} \\
&\quad + \frac{239}{23063040000000}t^{13} + \frac{709}{2365440000000}t^{12} + 3\beta + \frac{109}{147840000000}t^{11}\beta - \frac{71}{11520000000}t^{10}\beta - \frac{1283}{4838400000}t^9\beta + 11t^2 - \frac{1}{1075200}t^8\beta \\
&\quad + \frac{137}{3360000}t^7\beta + \frac{49}{96000}t^6\beta + 3t\beta.
\end{aligned}
\tag{77}
$$

The exact and approximate solutions of the IVP-III used in Example 3 are shown in Tables 7 and 8, respectively.

Figures 6(a) and 6(b) show an approximate solution of the membership and nonmembership functions for IVP-III used in Example 3.

The exact solution of Example 3 given by classical method is as follows:

$$
\begin{aligned}
y_1^*(t,\alpha) &= \frac{1}{9}\frac{1}{\left((\xi)^{2/3}-60\right)(\chi)}\begin{pmatrix}
\begin{pmatrix}
168(\xi)^{7/3}+128887200000+7938000(\xi)^{2/3}\alpha+97200(\xi)^{2/3}\sqrt{19185}\,\alpha-818424000(\xi)^{1/3}\alpha-5832000(\xi)^{1/3}\\
\sqrt{19185}\,\alpha+48(\xi)^{7/3}\alpha-47871000(\xi)^{2/3}+48600(\xi)^{2/3}\sqrt{19185}-2864484000(\xi)^{1/3}-20412000(\xi)^{1/3}\sqrt{19185}+13258080000\alpha\\
+95904000\alpha\sqrt{19185}+10080(\xi)^{5/3}+2880(\xi)^{5/3}\alpha+930528000\sqrt{19185}
\end{pmatrix}\\
e^{(\sigma_2 t)}+\frac{2}{9}\frac{1}{\chi}\left(\sqrt{3}\left(84(\xi)^{5/3}+24(\xi)^{5/3}\alpha+7608(\xi)^{4/3}+302400(\xi)^{1/3}-456480(\xi)^{2/3}+816(\xi)^{4/3}\alpha+86400(\xi)^{1/3}\alpha-48960(\xi)^{2/3}\alpha\right)e^{\sigma_1 t}\sin(\sigma_3 t)\right)\\
-\frac{4}{9}\frac{1}{\left((\xi)^{2/3}-60\right)(\chi)}\begin{pmatrix}
\left(42(\xi)^{7/3}-8375400(\xi)^{2/3}\alpha-48600(\xi)^{2/3}\sqrt{19185}\,\alpha-204606000(\xi)^{1/3}\alpha-1458000(\xi)^{1/3}\sqrt{19185}\,\alpha+32532597000\right.\\
\left.+12(\xi)^{7/3}\alpha-17147700(\xi)^{2/3}-24300(\xi)^{2/3}\sqrt{19185}-716121000(\xi)^{1/3}-5103000(\xi)^{1/3}\sqrt{19185}+3936114000\alpha+28350000\alpha\right)e^{\sigma_1 t}\cos(\sigma_3 t)\\
\sqrt{19185}+2520(\xi)^{5/3}+720(\xi)^{5/3}\alpha+234819000\sqrt{19185}
\end{pmatrix}
\end{pmatrix},\\
y_2^*(t,\alpha) &= -\frac{2}{9}\frac{1}{\left((\xi)^{2/3}-60\right)(\chi)}\left(\begin{pmatrix}
24(\xi)^{7/3}\alpha+47952000\sqrt{19185}\,\alpha+6629040000\alpha+1440(\xi)^{5/3}\alpha-74387160000-409212000(\xi)^{1/3}\alpha-2916000(\xi)^{1/3}\\
\sqrt{19185}\,\alpha+48600(\xi)^{2/3}\sqrt{19185}\,\alpha+3969000(\xi)^{2/3}\alpha-120(\xi)^{7/3}-97200(\xi)^{2/3}\sqrt{19185}+17982000(\xi)^{2/3}+2046060000(\xi)^{1/3}+14580000(\xi)^{1/3}\sqrt{19185}-7200(\xi)^{5/3}-537192000\sqrt{19185}
\end{pmatrix}e^{\sigma_2 t}\right)\\
&\quad -\frac{4}{9}\frac{1}{\chi}\left(\sqrt{3}\left(12(\xi)^{5/3}\alpha+408(\xi)^{4/3}\alpha+43200(\xi)^{1/3}\alpha-24480(\xi)^{2/3}\alpha-60(\xi)^{5/3}-4416(\xi)^{4/3}-216000(\xi)^{1/3}+264960(\xi)^{2/3}\right)e^{\sigma_1 t}\sin(\sigma_3 t)\right)\\
&\quad +\frac{8}{9}\frac{1}{\left((\xi)^{2/3}-60\right)(\chi)}\left(\begin{pmatrix}
6(\xi)^{7/3}\alpha+1417500\sqrt{19185}\,\alpha+1968057000\alpha+360(\xi)^{5/3}\alpha-102303000(\xi)^{1/3}\alpha-729000(\xi)^{1/3}\sqrt{19185}\,\alpha-19218384000-4187700(\xi)^{2/3}\alpha\\
-243000(\xi)^{2/3}\sqrt{19185}\,\alpha-30\left(2025+15\sqrt{19185}\right)^{7/3}+14855400(\xi)^{2/3}+48600(\xi)^{2/3}\sqrt{19185}+511515000(\xi)^{1/3}+364500(\xi)^{1/3}\sqrt{19185}-1800(\xi)^{5/3}-138672000\sqrt{19185}
\end{pmatrix}e^{\sigma_1 t}\cos(\sigma_3 t)\right),\\
y_1^*(t,\beta) &= -\frac{1}{3}\frac{1}{\left((\xi)^{2/3}-60\right)(\chi)}\left(\begin{pmatrix}
24(\xi)^{7/3}\beta+47952000\beta\sqrt{19185}+662904000\beta+1440(\xi)^{5/3}\beta-409212000(\xi)^{1/3}\beta-2916000(\xi)^{1/3}\sqrt{19185}\,\beta\\
+3969000(\xi)^{2/3}\beta+48600(\xi)^{2/3}\sqrt{19185}\,\beta-72(\xi)^{7/3}+13311000(\xi)^{2/3}-48600(\xi)^{2/3}\sqrt{19185}+1227636000(\xi)^{1/3}+8748000(\xi)^{1/3}\\
\sqrt{19185}-4320(\xi)^{5/3}-47381760000-342144000\sqrt{19185}
\end{pmatrix}e^{\sigma_2 t}\right)\\
&\quad -\frac{2}{3}\frac{1}{(\chi)}\left(\sqrt{3}\left(12(\xi)^{5/3}\beta+408(\xi)^{4/3}\beta+43200(\xi)^{1/3}\beta-24480(\xi)^{2/3}\beta-36(\xi)^{5/3}-2808(\xi)^{4/3}-129600(\xi)^{1/3}+168480(\xi)^{2/3}\right)e^{\sigma_1 t}\sin(\sigma_3 t)\right)\\
&\quad +\frac{4}{3}\frac{1}{\left((\xi)^{2/3}-60\right)(\chi)}\left(\begin{pmatrix}
6(\xi)^{7/3}\beta+14175000\beta\sqrt{19185}+1968057000\beta+360(\xi)^{5/3}\beta-102303000(\xi)^{1/3}\beta-729000(\xi)^{1/3}\beta\sqrt{19185}-4187700(\xi)^{2/3}\beta+24300(\xi)^{2/3}\sqrt{19185}\,\beta-18(\xi)^{7/3}\\
8507700(\xi)^{2/3}+24300(\xi)^{2/3}\sqrt{19185}+306909000(\xi)^{1/3}+2187000(\xi)^{1/3}\sqrt{19185}-1080(\xi)^{5/3}-12156237000-87723000\sqrt{19185}
\end{pmatrix}e^{\sigma_1 t}\cos(\sigma_3 t)\right),\\
y_2^*(t,\beta) &= \frac{1}{9}\frac{1}{\left((\xi)^{2/3}-60\right)(\chi)}\left(\begin{pmatrix}
72(\xi)^{7/3}\beta+143856000\sqrt{19185}\,\beta+19887120000\beta+4320(\xi)^{5/3}\beta-1227636000(\xi)^{1/3}\beta-8748000(\xi)^{1/3}\sqrt{19185}\,\beta+11907000(\xi)^{2/3}\beta+145800(\xi)^{2/3}\sqrt{19185}\,\beta\\
+192(\xi)^{7/3}+135516240000-43902000(\xi)^{2/3}+97200(\xi)^{2/3}\sqrt{19185}-3273696000(\xi)^{1/3}-23328000(\xi)^{1/3}\sqrt{19185}+11520(\xi)^{5/3}+978480000\sqrt{19185}
\end{pmatrix}e^{\sigma_2 t}\right)\\
&\quad +\frac{2}{9}\frac{1}{(\chi)}\left(\sqrt{3}\left(36(\xi)^{5/3}\beta+1224(\xi)^{4/3}\beta+129600(\xi)^{1/3}\beta-73440(\xi)^{2/3}\beta+96(\xi)^{5/3}+8016(\xi)^{4/3}+345600(\xi)^{1/3}-480960(\xi)^{2/3}\right)e^{\sigma_1 t}\sin(\sigma_3 t)\right)\\
&\quad -\frac{4}{9}\frac{1}{\left((\xi)^{2/3}-60\right)(\chi)}\left(\begin{pmatrix}
18(\xi)^{7/3}\beta+42525000\beta\sqrt{19185}+5904171000\beta+1080(\xi)^{5/3}\beta-306909000(\xi)^{1/3}\beta-2187000(\xi)^{1/3}\sqrt{19185}\,\beta-1256310(\xi)^{2/3}\beta-72900(\xi)^{2/3}\sqrt{19185}\,\beta\\
+48(\xi)^{7/3}+34500654000-21335400(\xi)^{2/3}-48600(\xi)^{2/3}\sqrt{19185}-818424000(\xi)^{1/3}-5832000(\xi)^{1/3}\sqrt{19185}+2880(\xi)^{5/3}+248994000\sqrt{19185}
\end{pmatrix}e^{\sigma_1 t}\cos(\sigma_3 t)\right),
\end{aligned}
\tag{78}
$$

where

$$
\begin{aligned}
\sigma_1 &= \frac{1/60\left(2025+15\sqrt{19185}\right)^{2/3}-1}{\left(2025+15\sqrt{19185}\right)^{1/3}},\\
\sigma_2 &= \frac{-1/30\left(2025+15\sqrt{19185}\right)^{2/3}-60}{\left(2025+15\sqrt{19185}\right)^{1/3}},\\
\sigma_3 &= \frac{1/60\left(2025+15\sqrt{19185}\right)^{2/3}\sqrt{3}+60\sqrt{3}}{\left(2025+15\sqrt{19185}\right)^{1/3}},\\
\chi &= \frac{1}{2302200+16200\sqrt{19185}},\\
\xi &= 2025+15\sqrt{19185}.
\end{aligned}
\tag{79}
$$

Figure 7(a) depicts the exact solution of the membership function of the generalized intuitionistic fuzzy IVP-III, 7(b) depicts the exact solution of the nonmembership function, and 7(c) depicts the exact solution of the generalized intuitionistic fuzzy IVP-III described in Example 3.

In Table 9, n represents the number of iterations, Err represents the residual error, and CPU time represents the computational time in seconds for finding the approximate solution of the generalized intuitionistic fuzzy IVP-III described in Example 3. Figures 6(a) and 6(b) show an approximate solution of the membership and nonmembership functions for IVP-III used in Example 3. The exact solutions to the membership and nonmembership functions for IVP-III used in Example 3 are depicted in Figures 7(a) and 7(c).

Example 4. An Embedded Beam (A Physical Application).

A beam of length l is embedded at its left end and free at its right end. Find the deflection of the beam if a load $w_0 = 24EI$ is distributed along its length.

The intuitionistic fuzzy initial value problem related to above problem is given as follows:

Table 7: Approximate solution of Example 3 at $t = 1$.

α	$\underline{y}_1^*(t,\alpha)$	$\overline{y}_2^*(t,\alpha)$	β	$\underline{y}_1^*(t,\beta)$	$\overline{y}_2^*(t,\beta)$
0	18.00	25.28	0.3	20.67	22.61
0.1	18.49	24.80	0.4	19.94	23.34
0.2	18.97	24.31	0.5	19.21	24.07
0.3	19.46	23.83	0.6	18.49	24.80
0.4	19.94	23.35	0.7	17.76	25.52
0.5	20.43	22.85	0.8	17.03	26.25
			0.9	16.30	26.98
			1.0	15.57	27.71

Table 8: Exact solution of Example 3 at $t = 1$.

α	$\underline{y}_1^*(t,\alpha)$	$\overline{y}_2^*(t,\alpha)$	β	$\underline{y}_1^*(t,\beta)$	$\overline{y}_2^*(t,\beta)$
0	18.00	25.28	0.3	20.67	22.61
0.1	18.49	24.80	0.4	19.94	23.34
0.2	18.97	24.31	0.5	19.21	24.07
0.3	19.46	23.83	0.6	18.49	24.80
0.4	19.94	23.35	0.7	17.76	25.52
0.5	20.43	22.85	0.8	17.03	26.25
			0.9	16.30	26.98
			1.0	15.57	27.71

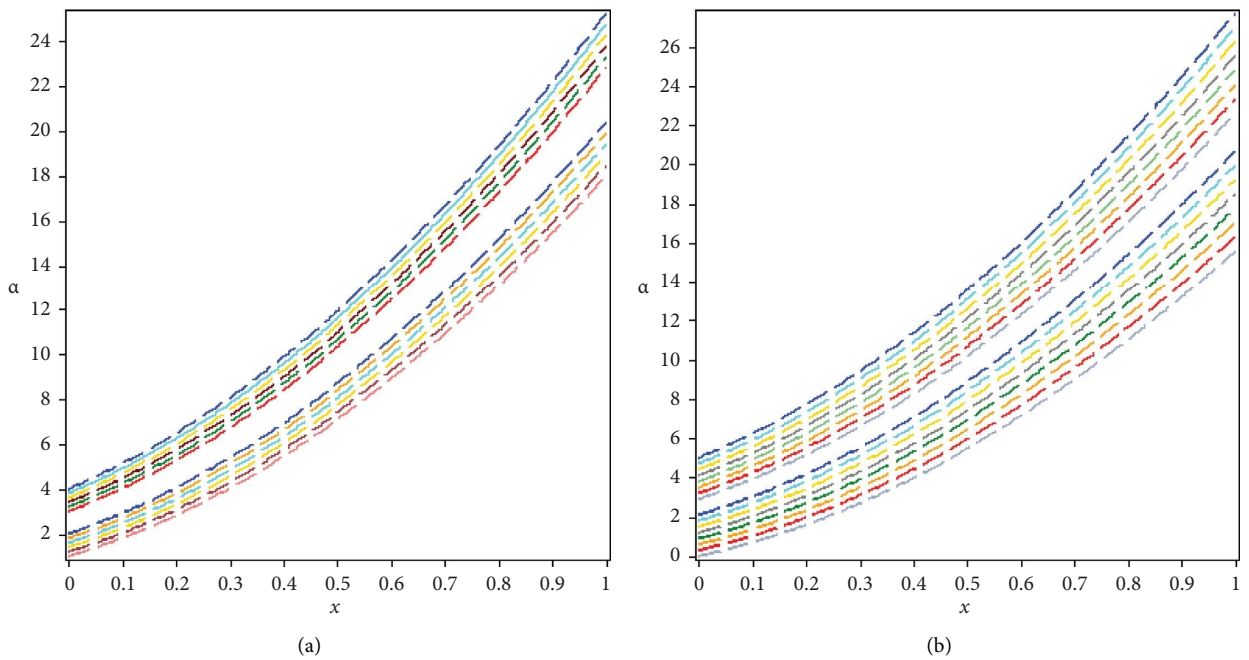

Figure 6: (a) Membership function and (b) nonmembership function.

$$EI\frac{d^4\overline{y}^*}{dx^4} = w_0, \tag{80}$$

Using the above value of w_0 in (80), and writing in standard form, we have

$$\frac{d^4\overline{y}^*}{dx^4} = 24, \tag{81}$$

with initial conditions:

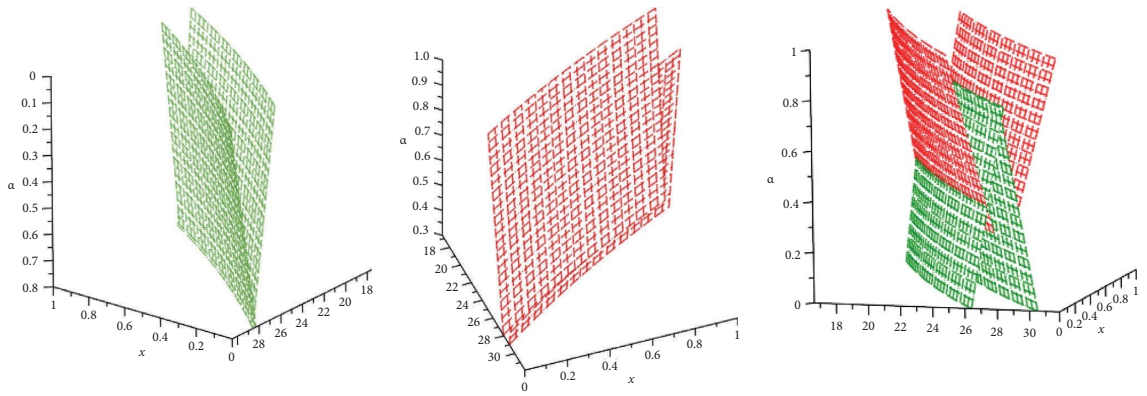

Figure 7: (a) Exact solution of membership function for GITF-IVP-III, (b) exact solution of nonmembership function for GITF-IVP-III, and (c) exact solution of GTIF-IVP-III.

Table 9: Error comparison of GMADM, ADM, and TSM for solving GTIF-IVP-III used in Example 3.

Methods	GMADM	ADM	TSM
n	04	13	06
Err	$5.2e-37$	$6.2e-28$	$1.0e-8$
CPU time	0.1123	0.2013	0.0452

$$\begin{cases} \overset{*}{y}(0) = <(1,2,3,4;0.5);(0,2,3,5;0.3)>, \\ \overset{*}{y}'(0) = <(7,8,9,10;0.5);(6,8,9,11;0.3)>, \\ \overset{*}{y}''(0) = <(21,22,23,24;0.5);(20,22,23,25;0.3)>, \\ \overset{*}{y}'''(0) = <(32,33,34,35;0.5);(31,33,34,36;0.3)>. \end{cases} \tag{82}$$

By taking (α,β)-cut of (81) and (82), we get

$$\begin{cases} \dfrac{d^4 \overset{*}{y}_1(x,\alpha)}{dx^4} = 24, \\ \overset{*}{y}_1(0,\alpha) = 2\alpha + 1, \\ \overset{*}{y}_1'(0,\alpha) = 2\alpha + 7, \\ \overset{*}{y}_1''(0,\alpha) = 2\alpha + 21, \\ \overset{*}{y}_1'''(0,\alpha) = 2\alpha + 32, \end{cases} \tag{83}$$

$$\begin{cases} \dfrac{d^4 \overset{*}{y}_1(x,\alpha)}{dx^4} = 24, \\ \overset{*}{y}_2(0,\alpha) = -2\alpha + 4, \\ \overset{*}{y}_2'(0,\alpha) = -2\alpha + 10, \\ \overset{*}{y}_2''(0,\alpha) = -2\alpha + 24, \\ \overset{*}{y}_2'''(0,\alpha) = -2\alpha + 35, \end{cases} \tag{84}$$

$$\begin{cases} \dfrac{\mathrm{d}^4 \overset{*}{y}_1\ (x,\alpha)}{\mathrm{d}x^4} = 24, \\ \overset{*}{y}_1\ (0,\beta) = -3\beta + 3, \\ \overset{*}{y}_1{}'(0,\beta) = -3\beta + 9, \\ \overset{*}{y}_1{}''(0,\beta) = -3\beta + 23, \\ \overset{*}{y}_1{}'''(0,\beta) = -3\beta + 34, \end{cases} \tag{85}$$

$$\begin{cases} \dfrac{\mathrm{d}^4 \overset{*}{y}_1\ (x,\alpha)}{\mathrm{d}x^4} = 24, \\ \overset{*}{y}_1\ (0,\beta) = -3\beta + 3, \\ \overset{*}{y}_1{}'(0,\beta) = -3\beta + 9, \\ \overset{*}{y}_1{}''(0,\beta) = -3\beta + 23, \\ \overset{*}{y}_1{}'''(0,\beta) = -3\beta + 34. \end{cases} \tag{86}$$

Here, $L = \mathrm{d}^4/\mathrm{d}x^4$, and by taking $L^{-1}(.) = \int_0^x \int_0^x \int_0^x \int_0^x (.)dx\,dx\,dx\,dx$ on both sides of (83)–(86), and using the initial conditions, we obtain

$$\begin{aligned} \overset{*}{y}_1\ (x,\alpha) &= x^4 + 2\alpha x + 2\alpha + 7x + 1 + x^2\alpha + \frac{21}{2}x^2 + \frac{1}{3}x^3\alpha + \frac{16}{3}x^3, \\ \overset{*}{y}_2\ (x,\alpha) &= x^4 + 4 - 2\alpha x - 2\alpha + 10x - x^2\alpha + 12x^2 - \frac{1}{3}x^3\alpha + \frac{35}{6}x^3, \\ \overset{*}{y}_1\ (x,\beta) &= x^4 + 3 - 3\beta x - 3\beta + 9x - \frac{3}{2}x^2\beta + \frac{23}{2}x^2 - \frac{1}{2}x^3\beta + \frac{17}{3}x^3, \\ \overset{*}{y}_2\ (x,\beta) &= x^4 + 3\beta x + 3\beta + 8x + 2 + \frac{3}{2}x^2\beta + 11x^2 + \frac{1}{2}x^3\beta + \frac{11}{2}x^3. \end{aligned} \tag{87}$$

Now, by using GMADM, we get

$$\begin{cases} \overset{*}{y}_{1_0}(x,\alpha) = 1 + 2\alpha x + 2\alpha + 7x + x^2\alpha + \dfrac{21}{2}x^2 + \dfrac{1}{3}x^3\alpha + \dfrac{16}{3}x^3, \\ \overset{*}{y}_{1_1}(x,\alpha) = x^4, \\ \overset{*}{y}_{1_{k+1}}(x,\alpha) = 0, k \geq 1. \end{cases} \tag{88}$$

$$\begin{cases} \overset{*}{y}_{2_0}(x,\alpha) = 4 - 2\alpha x - 2\alpha + 10x - x^2\alpha + 12x^2 - \dfrac{1}{3}x^3\alpha + \dfrac{35}{6}x^3, \\ \overset{*}{y}_{2_1}(x,\alpha) = x^4, \\ \overset{*}{y}_{2_{k+1}}(x,\alpha) = 0, k \geq 1. \end{cases} \tag{89}$$

$$\begin{cases} \overset{*}{y}_{1_0}(x,\beta) = 3 - 3\beta x - 3\beta + 9x - \frac{3}{2}x^2\beta + \frac{23}{2}x^2 - \frac{1}{2}x^3\beta + \frac{17}{3}x^3, \\ \overset{*}{y}_{1_1}(x,\beta) = x^4, \\ \overset{*}{y}_{1_{k+1}}(x,\beta) = 0, k \geq 1. \end{cases} \tag{90}$$

$$\begin{cases} \overset{*}{y}_{2_0}(x,\beta) = 2 + 3\beta x + 3\beta + 8x + \frac{3}{2}x^2\beta + 11x^2 + \frac{1}{2}x^3\beta + \frac{11}{2}x^3, \\ \overset{*}{y}_{2_1}(x,\beta) = x^4, \\ \overset{*}{y}_{2_{k+1}}(x,\beta) = 0, k \geq 1. \end{cases} \tag{91}$$

By solving the (88)–(91), we get the approximate solution after four iterations as follows:

$$\begin{aligned} \overset{*}{y}_{1_0}(x,\alpha) &= x^4 + 2\alpha x + 2\alpha + 7x + 1 + x^2\alpha + \frac{21}{2}x^2 + \frac{1}{3}x^3\alpha + \frac{16}{3}x^3, \\ \overset{*}{y}_{2_0}(x,\alpha) &= x^4 + 4 - 2\alpha x - 2\alpha + 10x - x^2\alpha + 12x^2 - \frac{1}{3}x^3\alpha + \frac{35}{6}x^3, \\ \overset{*}{y}_{1_0}(x,\beta) &= x^4 + 3 - 3\beta x - 3\beta + 9x - \frac{3}{2}x^2\beta + \frac{23}{2}x^2 - \frac{1}{2}x^3\beta + \frac{17}{3}x^3, \\ \overset{*}{y}_{2_0}(x,\beta) &= x^4 + 2 + 3\beta x + 3\beta + 8x + \frac{3}{2}x^2\beta + 11x^2 + \frac{1}{2}x^3\beta + \frac{11}{2}x^3. \end{aligned} \tag{92}$$

The exact and approximate solutions of the IVP-IV used in Example 4 are shown in Tables 10 and 11, respectively.

Figures 8(a) and 8(b) show an approximate solution of the membership and nonmembership functions for IVP-IV used in Example 4.

The exact solution of Example 4 determined by classical method is as follows:

$$\begin{aligned} \overset{*}{y}_{1_0}(x,\alpha) &= x^4 + 2\alpha x + 2\alpha + 7x + 1 + x^2\alpha + \frac{21}{2}x^2 + \frac{1}{3}x^3\alpha + \frac{16}{3}x^3, \\ \overset{*}{y}_{2_0}(x,\alpha) &= x^4 + 4 - 2\alpha x - 2\alpha + 10x - x^2\alpha + 12x^2 - \frac{1}{3}x^3\alpha + \frac{35}{6}x^3, \\ \overset{*}{y}_{1_0}(x,\beta) &= x^4 + 3 - 3\beta x - 3\beta + 9x - \frac{3}{2}x^2\beta + \frac{23}{2}x^2 - \frac{1}{2}x^3\beta + \frac{17}{3}x^3, \\ \overset{*}{y}_{2_0}(x,\beta) &= x^4 + 2 + 3\beta x + 3\beta + 8x + \frac{3}{2}x^2\beta + 11x^2 + \frac{1}{2}x^3\beta + \frac{11}{2}x^3. \end{aligned} \tag{93}$$

Figure 9(a) depicts the exact solution of the membership function of the generalized intuitionistic fuzzy IVP-IV, 9(b) depicts the exact solution of the nonmembership function, and 9(c) depicts the exact solution of the generalized intuitionistic fuzzy IVP-IV described in Example 4.

In Table 12, n represents the number of iterations, Err represents the residual error, and CPU time represents the computational time in seconds for finding the approximate solution of the generalized intuitionistic fuzzy IVP-IV described in Example 4. Figures 8(a) and 8(b) show an approximate solution of the membership and nonmembership functions for IVP-IV used in Example 4. The exact solutions to the membership and nonmembership functions for IVP-IV used in Example 4 are depicted in Figures 9(a)–9(c).

Table 10: Approximate solution of Example 4 at $x = 1$.

α	$\overset{*}{y}_1(x,\alpha)$	$\overset{*}{y}_2(x,\alpha)$	β	$\overset{*}{y}_1(x,\beta)$	$\overset{*}{y}_2(x,\beta)$
0	24.83	32.63	0.3	27.77	29.90
0.1	25.37	32.30	0.4	26.97	30.70
0.2	25.90	31.77	0.5	26.17	31.50
0.3	26.43	31.23	0.6	25.37	32.30
0.4	26.97	30.70	0.7	24.57	33.10
0.5	27.50	30.16	0.8	23.77	33.90
			0.9	22.97	34.70
			1.0	22.17	35.50

Table 11: Exact solution of Example 4 at $x = 1$.

α	$\overset{*}{y}_1(x,\alpha)$	$\overset{*}{y}_2(x,\alpha)$	β	$\overset{*}{y}_1(x,\beta)$	$\overset{*}{y}_2(x,\beta)$
0	24.83	32.83	0.3	27.77	29.90
0.1	25.37	32.30	0.4	26.97	30.70
0.2	25.90	31.77	0.5	26.17	31.50
0.3	26.43	31.23	0.6	25.37	32.30
0.4	26.97	30.70	0.7	24.57	33.10
0.5	27.50	30.16	0.8	23.77	33.90
			0.9	22.97	34.70
			1.0	22.17	35.50

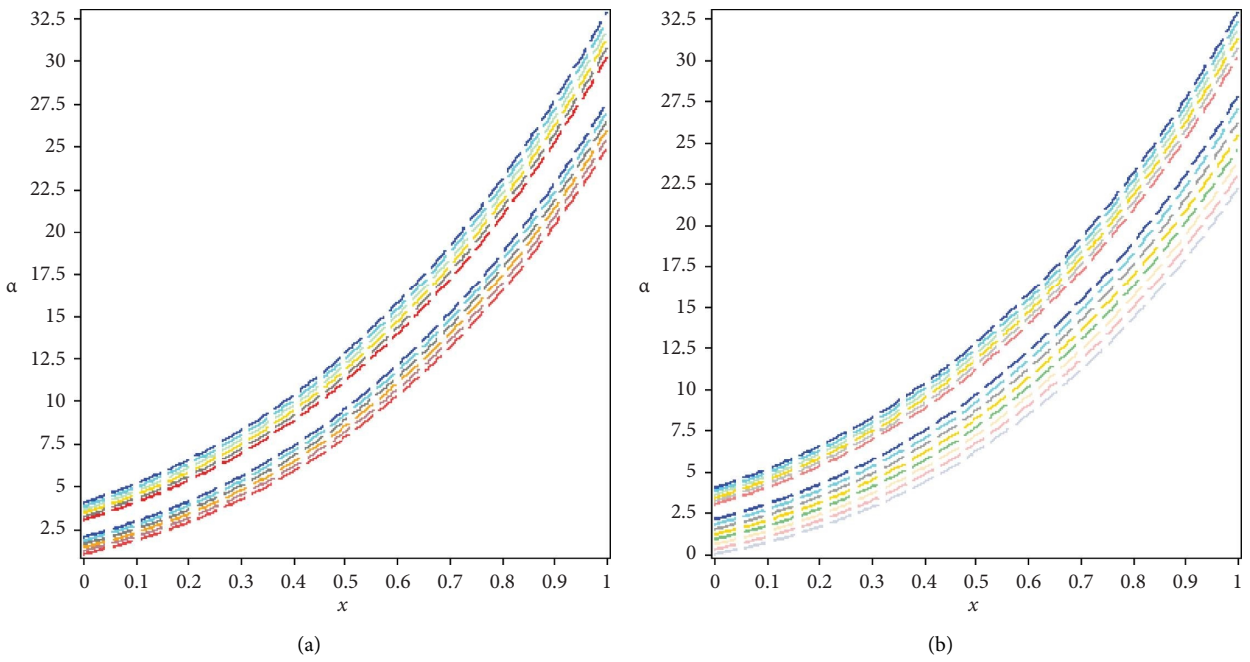

Figure 8: (a) Membership function and (b) nonmembership function.

Example 5. Higher-Order Generalized Intuitionistic Fuzzy Differential Equation.

Let us consider a generalized intuitionistic fuzzy initial value problem in which the coefficients are real crisp values and the initial conditions are generalized trapezoidal fuzzy numbers as follows:

$$\frac{d^5 \overset{*}{y}}{dx^4} + 4\frac{d\overset{*}{y}}{dx^3} + 4\frac{d\overset{*}{y}}{dx} = 0, \tag{94}$$

with initial conditions:

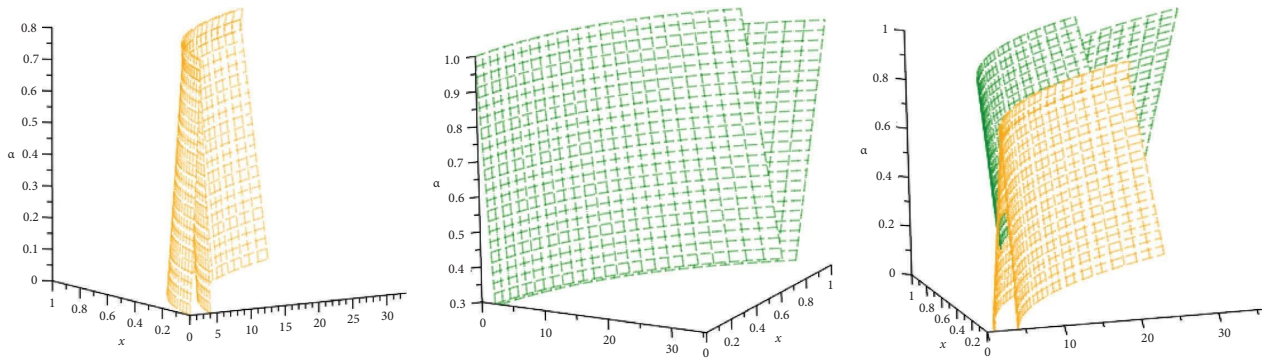

Figure 9: (a) Exact solution of membership function for GITF-IVP-IV, (b) exact solution of nonmembership function for GITF-IVP-IV, and (c) exact solution of GTIF-IVP-IV.

Table 12: Error comparison of GMADM, ADM, and TSM for solving GTIF-IVP-IV used in Example 4.

Methods	GMADM	ADM	TSM
n	04	13	05
Err	$7.2e-29$	$6.2e-11$	$7.1e-4$
CPU time	0.0163	0.0293	0.1352

$$\begin{cases} \overset{*}{y}(0) = <(1,2,3,4;0.5);(0,2,3,5;0.3)>, \\ \overset{*}{y}'(0) = <(7,8,9,10;0.5);(6,8,9,11;0.3)>, \\ \overset{*}{y}''(0) = <(21,22,23,24;0.5);(20,22,23,25;0.3)>, \\ \overset{*}{y}'''(0) = <(32,33,34,35;0.5);(31,33,34,36;0.3)>, \\ \overset{*}{y}^{(iv)} = <(16,17,18,19;0.5);(15,17,18,20;0.3)>. \end{cases} \tag{95}$$

By taking (α,β)-cut of (94) and (95), we get

$$\begin{cases} \dfrac{d^5 \overset{*}{y}_1(x,\alpha)}{dx^4} + 4\dfrac{d^3 \overset{*}{y}_1(x,\alpha)}{dx^3} + 4\dfrac{d\overset{*}{y}_1(x,\alpha)}{dx} = 0, \\ \overset{*}{y}_1(0,\alpha) = 2\alpha+1, \overset{*}{y}_1'(0,\alpha) = 2\alpha+7, \\ \overset{*}{y}_1''(0,\alpha) = 2\alpha+21, \overset{*}{y}_1'''(0,\alpha) = 2\alpha+32, \\ \overset{*}{y}_1^{(iv)}(0,\alpha) = 2\alpha+16, \end{cases}$$

$$\begin{cases} \dfrac{\mathrm{d}^5 \overset{*}{y}_1(x,\alpha)}{\mathrm{d}x^4} + 4\dfrac{\mathrm{d}^3 \overset{*}{y}_1(x,\alpha)}{\mathrm{d}x^3} + 4\dfrac{\mathrm{d}\overset{*}{y}_1(x,\alpha)}{\mathrm{d}x} = 0, \\ \overset{*}{y}_2(0,\alpha) = -2\alpha + 4, \overset{*}{y}_2'(0,\alpha) = -2\alpha + 10, \\ \overset{*}{y}_2''(0,\alpha) = -2\alpha + 24, \overset{*}{y}_2'''(0,\alpha) = -2\alpha + 35, \\ \overset{*}{y}_2^{(iv)}(0,\alpha) = -2\alpha + 19, \end{cases} \tag{97}$$

$$\begin{cases} \dfrac{\mathrm{d}^5 \overset{*}{y}_1(x,\alpha)}{\mathrm{d}x^4} + 4\dfrac{\mathrm{d}^3 \overset{*}{y}_1(x,\alpha)}{\mathrm{d}x^3} + 4\dfrac{\mathrm{d}\overset{*}{y}_1(x,\alpha)}{\mathrm{d}x} = 0, \\ \overset{*}{y}_1(0,\beta) = -3\beta + 3, \overset{*}{y}_1'(0,\beta) = -3\beta + 9, \\ \overset{*}{y}_1''(0,\beta) = -3\beta + 23, \overset{*}{y}_1'''(0,\beta) = -3\beta + 34, \\ \overset{*}{y}_1^{(iv)}(0,\beta) = -3\beta + 19, \end{cases} \tag{98}$$

$$\begin{cases} \dfrac{\mathrm{d}^5 \overset{*}{y}_1(x,\alpha)}{\mathrm{d}x^4} + 4\dfrac{\mathrm{d}^3 \overset{*}{y}_1(x,\alpha)}{\mathrm{d}x^3} + 4\dfrac{\mathrm{d}\overset{*}{y}_1(x,\alpha)}{\mathrm{d}x} = 0, \\ \overset{*}{y}_2(0,\beta) = 3\beta + 2, \overset{*}{y}_2'(0,\beta) = 3\beta + 8, \\ \overset{*}{y}_2''(0,\beta) = 3\beta + 22, \overset{*}{y}_2'''(0,\beta) = 3\beta + 33, \\ \overset{*}{y}_2^{(iv)}(0,\beta) = 3\beta + 17. \end{cases} \tag{99}$$

Here, $L = \mathrm{d}^5/\mathrm{d}x^5$ and by taking $L^{-1}(.) = \int_0^x \int_0^x \int_0^x \int_0^x \int_0^x (.)dx\,dx\,dx\,dx\,dx$ on both sides of (96)–(99), and using the initial conditions, we obtain

$$
\begin{aligned}
\overset{*}{y}_1\ (x,\alpha) &= \frac{2}{3}\int_0^x \overset{*}{y}_1\ (t,\alpha)(-x+t)\left(t^2-2tx+x^2+6\right)dt+1+\frac{3}{4}x^4\alpha\\
&\quad+\frac{13}{3}x^4+5x^2\alpha+2x\alpha+2\alpha+7x+\frac{25}{2}x^2+\frac{5}{3}x^3\alpha+10x^3,\\
\overset{*}{y}_2\ (x,\alpha) &= \frac{2}{3}\int_0^x \overset{*}{y}_2\ (t,\alpha)(-x+t)\left(t^2-2tx+x^2+6\right)dt+4-\frac{3}{4}x^4\alpha\\
&\quad+\frac{131}{24}x^4-5x^2\alpha-2x\alpha-2\alpha+10x+20x^2-\frac{5}{3}x^3\alpha+\frac{25}{2}x^3,\\
\overset{*}{y}_1\ (x,\beta) &= \frac{2}{3}\int_0^x \overset{*}{y}_1\ (t,\beta)(-x+t)\left(t^2-2tx+x^2+6\right)dt+3-\frac{9}{8}x^4\beta\\
&\quad+\frac{41}{8}x^4-\frac{15}{2}x^2\beta-3x\beta-3\beta+9x+\frac{35}{2}x^2-\frac{5}{2}x^3\beta+\frac{35}{3}x^3,\\
\overset{*}{y}_2\ (x,\beta) &= \frac{2}{3}\int_0^x \overset{*}{y}_2\ (t,\beta)(-x+t)\left(t^2-2tx+x^2+6\right)dt+2+\frac{9}{8}x^4\beta\\
&\quad+\frac{113}{24}x^4+\frac{15}{2}x^2\beta+3x\beta+3\beta+8x+15x^2+\frac{5}{2}x^3\beta+\frac{65}{6}x^3.
\end{aligned}
\tag{100}
$$

Now, by using GMADM, we get

$$
\begin{cases}
\overset{*}{y}_{1_0}(x,\alpha)=1+\frac{3}{4}x^4\alpha+\frac{13}{3}x^4+5x^2\alpha+2x\alpha+2\alpha+7x+\frac{25}{2}x^2\\
+\frac{5}{3}x^3\alpha+10x^3,\\
\overset{*}{y}_{1_1}(x,\alpha)=-2x^2-\frac{1}{560}x^8\alpha-\frac{1}{26}x^7\alpha-\frac{7}{45}x^6\alpha-\frac{2}{5}x^5\alpha-\frac{14}{3}x^3\\
-\frac{4}{3}x^3\alpha-2x^4\alpha-4x^2\alpha-\frac{13}{1260}x^8-\frac{1}{121}x^7-\frac{43}{60}x^6-\frac{67}{30}x^5-\frac{13}{3}x^4,\\
\overset{*}{y}_{1_{k+1}}(x,\alpha)=\frac{2}{3}\int_0^x(-x+t)\left(t^2-2tx+x^2+6\right)\overset{*}{y}_{1_k}(t,\alpha)dt,k\geq 1.
\end{cases}
\tag{101}
$$

$$
\begin{cases}
\overset{*}{y}_{2_0}(x,\alpha)=4-\frac{3}{4}x^4\alpha+\frac{131}{24}x^4-5x^2\alpha-2x\alpha-2\alpha+10x+20x^2\\
-\frac{5}{3}x^3\alpha+\frac{25}{2}x^3,\\
\overset{*}{y}_{2_1}(x,\alpha)=-8x^2+\frac{1}{560}x^8\alpha+\frac{1}{26}x^7\alpha+\frac{7}{45}x^6\alpha+\frac{2}{5}x^5\alpha-\frac{20}{3}x^3\\
+\frac{4}{3}x^3\alpha+2x^4\alpha+4x^2\alpha-\frac{131}{10080}x^8-\frac{5}{84}x^7-\frac{19}{20}x^6-\frac{17}{6}x^5-\frac{22}{3}x^4,\\
\overset{*}{y}_{2_{k+1}}(x,\alpha)=\frac{2}{3}\int_0^x(-x+t)\left(t^2-2tx+x^2+6\right)\overset{*}{y}_{2_k}(t,\alpha)dt,k\geq 1.
\end{cases}
\tag{102}
$$

$$\begin{cases} \overset{*}{y}_{1_0}(x,\beta) = 3 - \frac{9}{8}x^4\beta + \frac{41}{8}x^4 - \frac{15}{2}x^2\beta - 3x\beta - 3\beta + 9x + \frac{35}{2}x^2 \\ - \frac{5}{2}x^3\beta + \frac{35}{3}x^3, \\ \overset{*}{y}_{1_1}(x,\beta) = -6x^2 + \frac{3}{1120}x^8\beta + \frac{1}{84}x^7\beta + \frac{7}{30}x^6\beta + \frac{3}{5}x^5\beta - 6x^3 \\ + 2x^3\beta + 3x^4\beta + 6x^2\beta - \frac{41}{3360}x^8 - \frac{1}{18}x^7 - \frac{79}{90}x^6 - \frac{79}{30}x^5 - \frac{19}{3}x^4, \\ \overset{*}{y}_{1_{k+1}}(x,\beta) = \frac{2}{3}\int_0^x (-x+t)\left(t^2 - 2tx + x^2 + 6\right)\overset{*}{y}_{1_k}(t,\beta)dt, k \geq 1. \end{cases} \tag{103}$$

$$\begin{cases} \overset{*}{y}_{2_0}(x,\beta) = 2 + \frac{9}{8}x^4\beta + \frac{113}{24}x^4 + \frac{15}{2}x^2\beta + 3x\beta + 3\beta + 8x + 15x^2 \\ + \frac{5}{2}x^3\beta + \frac{65}{6}x^3, \\ \overset{*}{y}_{2_1}(x,\beta) = -4x^2 - \frac{3}{1120}x^8\beta - \frac{1}{84}x^7\beta - \frac{7}{30}x^6\beta - \frac{3}{5}x^5\beta - \frac{16}{3}x^3 \\ - 2x^3\beta - 3x^4\beta - 6x^2\beta - \frac{113}{10080}x^8 - \frac{13}{252}x^7 - \frac{143}{180}x^6 - \frac{73}{30}x^5 - \frac{16}{3}x^4, \\ \overset{*}{y}_{2_{k+1}}(x,\beta) = \frac{2}{3}\int_0^x (-x+t)\left(t^2 - 2tx + x^2 + 6\right)\overset{*}{y}_{2_k}(t,\beta)dt, k \geq 1. \end{cases} \tag{104}$$

By solving the (101)–(104), we get the approximate solution after three iterations as follows:

$$\begin{aligned} \overset{*}{y}_1(x,\alpha) = 1 + 7x + 2\alpha x &- \frac{17}{22680}x^{10}\alpha - \frac{1}{540}x^9\alpha - \frac{163}{14968800}x^{12}\alpha \\ &- \frac{67}{1247400}x^{11}\alpha - \frac{2}{42567525}x^{14}\alpha - \frac{1}{18162144000}x^{16}\alpha \\ &- \frac{1}{2043241200}x^{15}\alpha - \frac{2}{6081075}x^{13}\alpha - \frac{197}{22680}x^9 - \frac{181}{3742200}x^{12} \\ &- \frac{31}{103950}x^{11} - \frac{11}{5040}x^{10} - \frac{17}{8845200}x^{13} - \frac{1}{3143448000}x^{16} \\ &- \frac{1}{340540200}x^{15} - \frac{337}{1362160800}x^{14} - \frac{37}{180}x^6 - \frac{13}{10}x^5 + \frac{17}{2520}x^8 \\ &+ \frac{31}{315}x^7 + \frac{2}{3}x^4 + \frac{16}{3}x^3 + \frac{21}{2}x^2 + \frac{1}{3}x^3\alpha + \frac{1}{12}x^4\alpha + x^2\alpha + \frac{1}{90} \\ &\cdot x^7\alpha - \frac{1}{45}x^6\alpha - \frac{2}{15}x^5\alpha - \frac{19}{1680}x^8\alpha + 2\alpha, \end{aligned}$$

$$
\begin{aligned}
\overset{*}{y}_2\ (x,\alpha) &= 4 + 10x - 2\alpha x + \frac{17}{22680}x^{10}\alpha + \frac{1}{540}x^{9}\alpha + \frac{163}{14968800}x^{12}\alpha \\
&+ \frac{67}{1247400}x^{11}\alpha + \frac{2}{42567525}x^{14}\alpha + \frac{1}{18162144000}x^{16}\alpha \\
&+ \frac{1}{2043241200}x^{15}\alpha + \frac{2}{6081075}x^{13}\alpha - \frac{13}{1134}x^{9} - \frac{1937}{29937600}x^{12} \\
&- \frac{1}{2640}x^{11} - \frac{5}{1512}x^{10} - \frac{47}{19459440}x^{13} - \frac{131}{326918592000}x^{16} \\
&- \frac{1}{272432160}x^{15} - \frac{433}{1362160800}x^{14} - \frac{43}{180}x^{6} - \frac{3}{2}x^{5} - \frac{103}{10080}x^{8} \\
&+ \frac{29}{252}x^{7} + \frac{19}{24}x^{4} + \frac{35}{6}x^{3} + 12x^{2} - \frac{1}{3}x^{3}\alpha - \frac{1}{12}x^{4}\alpha \\
&- x^{2}\alpha - \frac{1}{90}x^{7}\alpha + \frac{1}{45}x^{6}\alpha + \frac{2}{15}x^{5}\alpha + \frac{19}{1680}x^{8}\alpha - 2\alpha,
\end{aligned}
$$

$$
\begin{aligned}
\overset{*}{y}_1\ (x,\beta) &= 3 + 9x - 3\beta x + \frac{17}{15120}x^{10}\beta + \frac{1}{360}x^{9}\beta + \frac{163}{9979200}x^{12}\beta \\
&+ \frac{67}{831600}x^{11}\beta + \frac{1}{14189175}x^{14}\beta + \frac{1}{12108096000}x^{16}\beta \\
&+ \frac{1}{1362160800}x^{15}\beta + \frac{1}{2027025}x^{13}\beta - \frac{239}{22680}x^{9} - \frac{17}{285120}x^{12} \\
&- \frac{439}{1247400}x^{11} - \frac{667}{226800}x^{10} - \frac{73}{32432400}x^{13} - \frac{41}{108972864000}x^{16} \\
&- \frac{1}{291891600}x^{15} - \frac{101}{340540200}x^{14} - \frac{7}{30}x^{6} - \frac{43}{30}x^{5} + \frac{43}{10080}x^{8} \\
&+ \frac{23}{210}x^{7} + \frac{19}{24}x^{4} + \frac{17}{3}x^{3} + \frac{23}{2}x^{2} - \frac{1}{2}x^{3}\beta - \frac{1}{8}x^{4}\beta - \frac{3}{2}x^{2}\beta \\
&- \frac{1}{60}x^{7}\beta + \frac{1}{30}x^{6}\beta + \frac{1}{5}x^{5}\beta + \frac{19}{1120}x^{8}\beta - 3\beta,
\end{aligned}
$$

$$
\begin{aligned}
\overset{*}{y}_2\ (x,\beta) &= 2 + 8x + 3\beta x - \frac{17}{15120}x^{10}\beta - \frac{1}{360}x^{9}\beta - \frac{163}{9979200}x^{12}\beta \\
&- \frac{67}{831600}x^{11}\beta - \frac{1}{14189175}x^{14}\beta - \frac{1}{12108096000}x^{16}\beta \\
&- \frac{1}{1362160800}x^{15}\beta - \frac{1}{2027025}x^{13}\beta - \frac{109}{11340}x^{9} - \frac{179}{3326400}x^{12} \\
&- \frac{811}{2494800}x^{11} - \frac{29}{11340}x^{10} - \frac{29}{13899600}x^{13} - \frac{113}{326918592000}x^{16} \\
&- \frac{1}{314344800}x^{15} - \frac{41}{151351200}x^{14} - \frac{13}{60}x^{6} - \frac{41}{30}x^{5} + \frac{11}{10080}x^{8} \\
&+ \frac{131}{1260}x^{7} + \frac{17}{24}x^{4} + \frac{11}{2}x^{3} + 11x^{2} + \frac{1}{2}x^{3}\beta + \frac{1}{8}x^{4}\beta + \frac{3}{2}x^{2}\beta \\
&+ \frac{1}{60}x^{7}\beta - \frac{1}{30}x^{6}\beta - \frac{1}{5}x^{5}\beta - \frac{19}{1120}x^{8}\beta + 3\beta.
\end{aligned}
\tag{105}
$$

The exact and approximate solutions of the IVP-V used in Example 5 are shown in Tables 13 and 14, respectively.

Figures 10(a) and 10(b) show an approximate solution of the membership and nonmembership functions for IVP-V used in Example 5.

The exact solution of Example 5 found by classical method is given as follows:

$$
\begin{aligned}
\overset{*}{y}_1\ (x,\alpha) &= \frac{9}{2}\alpha + 26 + \frac{7}{4}\sqrt{2}\sin(\sqrt{2}\,x)\alpha + \frac{37}{4}\sin(\sqrt{2}\,x)\sqrt{2} - \frac{5}{2}\sqrt{2}\cos(\sqrt{2}\,x)\alpha \\
&\quad - v25\cos(\sqrt{2}\,x) - \frac{3}{4}\sqrt{2}\sin(\sqrt{2}\,x)x\alpha - \frac{29}{4}\sqrt{2}\sin(\sqrt{2}\,x)x \\
&\quad - \frac{3}{2}\cos(\sqrt{2}\,x)x\alpha - \frac{23}{2}\cos(\sqrt{2}\,x)x, \\
\overset{*}{y}_2\ (x,\alpha) &= -\frac{9}{2}\alpha + \frac{131}{4} - \frac{7}{4}\sqrt{2}\sin(\sqrt{2}\,x)\alpha + \frac{95}{8}\sin(\sqrt{2}\,x)\sqrt{2} + \frac{5}{2}\sqrt{2}\cos \\
&\quad \cdot (\sqrt{2}\,x)\alpha - \frac{115}{4}\cos(\sqrt{2}\,x) + \frac{3}{4}\sqrt{2}\overset{*}{i}n(\sqrt{2}\,x)x\alpha - \frac{67}{8}\sqrt{2}\sin \\
&\quad \cdot (\sqrt{2}\,x)x + \frac{3}{2}\cos(\sqrt{2}\,x)x\alpha - \frac{55}{4}\cos(\sqrt{2}\,x)x, \\
\overset{*}{y}_1\ (x,\beta) &= -\frac{27}{4}\beta + \frac{123}{4} - \frac{21}{8}\sqrt{2}\sin(\sqrt{2}\,x)\beta + 11\sin(\sqrt{2}\,x)\sqrt{2} + \frac{15}{4}\sqrt{2}\cos \\
&\quad \cdot (\sqrt{2}\,x)\beta - \frac{111}{4}\cos(\sqrt{2}\,x) + \frac{9}{8}\sqrt{2}\sin(\sqrt{2}\,x)x\beta - \frac{65}{8}\sqrt{2}\sin \\
&\quad \cdot (\sqrt{2}\,x)x + \frac{9}{4}\cos(\sqrt{2}\,x)x\beta - 13\cos(\sqrt{2}\,x)x, \\
\overset{*}{y}_2\ (x,\beta) &= \frac{27}{4}\beta + \frac{113}{4} + \frac{21}{8}\sqrt{2}\sin(\sqrt{2}\,x)\beta + \frac{81}{8}\sin(\sqrt{2}\,x)\sqrt{2} - \frac{15}{4}\sqrt{2}\cos \\
&\quad \cdot (\sqrt{2}\,x)\beta - \frac{105}{4}\cos(\sqrt{2}\,x) - \frac{9}{8}\sqrt{2}\sin(\sqrt{2}\,x)x\beta - \frac{61}{8}\sqrt{2}\sin \\
&\quad \cdot (\sqrt{2}\,x)x - \frac{9}{4}\cos(\sqrt{2}\,x)x\beta - \frac{49}{4}\cos(\sqrt{2}\,x)x.
\end{aligned}
\tag{106}
$$

Figure 11(a) depicts the exact solution of the membership function of the generalized intuitionistic fuzzy IVP-V, 11(b) depicts the exact solution of the nonmembership function, and 11(c) depicts the exact solution of the generalized intuitionistic fuzzy IVP-V described in Example 5.

In Table 15, n represents the number of iterations, Err represents the residual error, and CPU time represents the computational time in seconds for finding the approximate solution of the generalized intuitionistic fuzzy IVP-V described in Example 5. Figures 10(a) and 10(b) show an approximate solution of the membership and nonmembership functions for IVP-V used in Example 5. The exact solutions to the membership and nonmembership functions for IVP-V used in Example 5 are depicted in Figures 11(a)–11(c).

3.1.2. Advantages of the GMADM

(i) When solving generalized trapezoidal intuitionistic fuzzy differential equations, it is found that GMADM converges faster and more efficient as compared to exact techniques

(ii) The fundamental benefit of the GMADM algorithm is that it can solve all types of fuzzy differential equations using more generalized fuzzy numbers, namely, generalized trapezoidal intuitionistic fuzzy number

(iii) The GMADM also offers the useful benefit of lowering computation costs while keeping improved numerical solution precision

Table 13: Approximate solution of Example 5 at $t = 1$.

α	$\underline{y}_1^*(x,\alpha)$	$\underline{y}_2^*(x,\alpha)$	β	$\overline{y}_1^*(x,\beta)$	$\overline{y}_2^*(x,\beta)$
0	23.09	30.98	0.3	26.02	28.08
0.1	23.61	30.45	0.4	25.23	28.87
0.2	24.14	29.92	0.5	24.44	29.66
0.3	24.67	29.40	0.6	23.65	30.45
0.4	25.19	28.87	0.7	22.86	31.24
0.5	25.72	28.35	0.8	22.07	32.03
			0.9	21.28	32.82
			1.0	20.50	33.60

Table 14: Exact solution of Example 5 at $x = 1$.

α	$\underline{y}_1^*(x,\alpha)$	$\underline{y}_2^*(x,\alpha)$	β	$\overline{y}_1^*(x,\beta)$	$\overline{y}_2^*(x,\beta)$
0	23.10	31.01	0.3	26.04	28.11
0.1	23.63	30.48	0.4	25.25	28.90
0.2	24.16	29.96	0.5	24.46	29.69
0.3	24.68	29.43	0.6	23.67	30.48
0.4	25.21	28.90	0.7	22.87	31.28
0.5	25.74	28.38	0.8	22.08	32.07
			0.9	21.29	32.86
			1.0	20.50	33.65

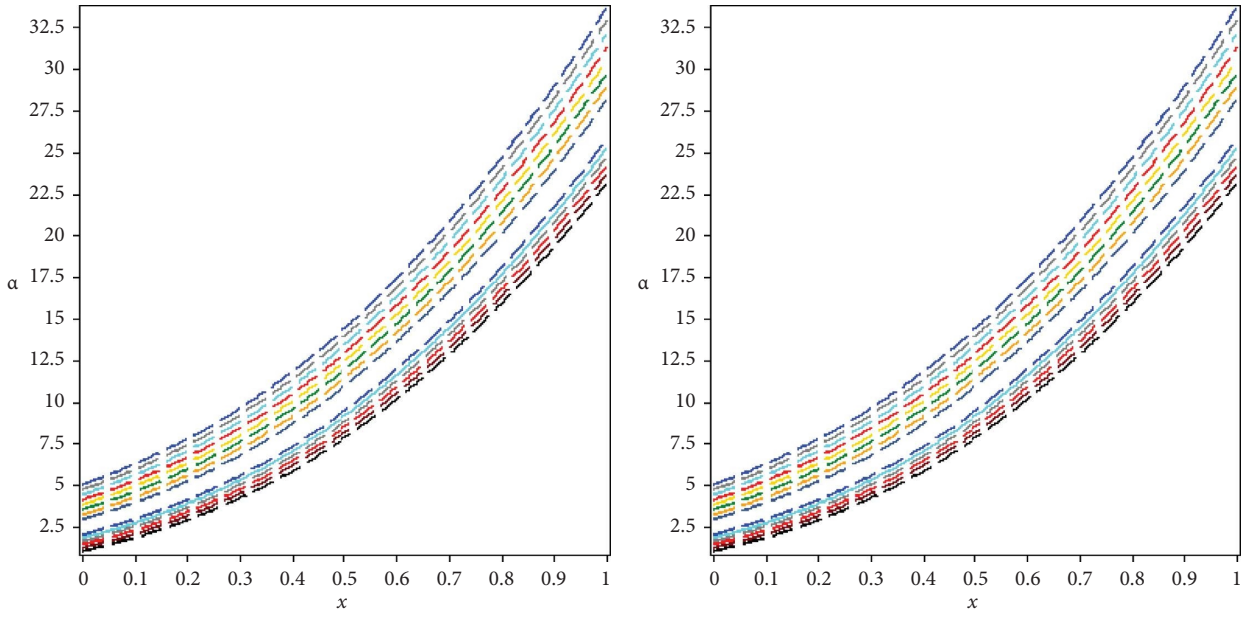

Figure 10: (a) Membership function and (b) nonmembership function.

(iv) GMADM can efficiently, rapidly, and accurately solve a large class of generalized trapezoidal intuitionistic fuzzy differential equations with closed form solutions that rapidly converge to exact solutions

(v) The GMADM has demonstrated to be very efficient and produces significant accuracy and computation time reductions, as illustrated in Figures 1–11 and Tables 1 to 15

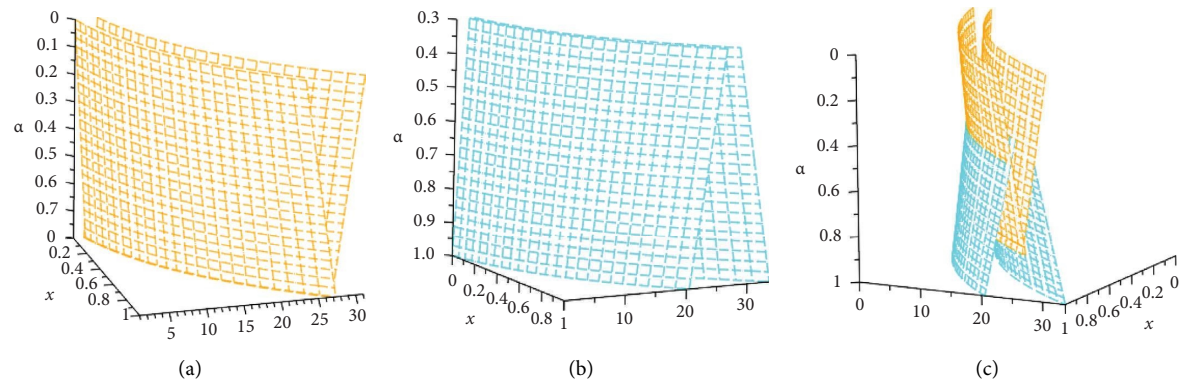

Figure 11: (a) Exact solution of membership function for GITF-IVP-V, (b) exact solution of nonmembership function for GITF-IVP-V, and (c) exact solution of GTIF-IVP-V.

Table 15: Error comparison of GMADM, ADM, and TSM for solving GTIF-IVP-V used in Example 5.

Methods	GMADM	ADM	TSM
n	03	19	07
Err	$0.2e-49$	$0.2e-21$	$7.9e-8$
CPU-time	0.0723	0.5403	0.4512

4. Conclusion

In this article, we solved the generalized trapezoidal intuitionistic fuzzy differential equations by applying the procedure of modified Adomian decomposition method with linear differential operator. We have applied this procedure to mechanical engineering problems. From all Tables 1 to 15 and Figures 1–11, it clearly shows the dominance efficiency of GMADM over exact technique in terms of computational time, number of iterations, and in errors. Moreover, we have shown that this method is more reliable by comparing the approximations with the exact solution. Future research will therefore focus on the solution of systems of linear and nonlinear first-order differential equations and their applications [34–36] in a generalized trapezoidal intuitionistic fuzzy environment, as well as systems of higher-order generalized trapezoidal intuitionistic fuzzy differential equations [37, 38].

Data Availability

The data supporting the current study are available from the corresponding author upon request.

Conflicts of Interest

The authors declare that there are no conflicts of interest.

Authors' Contributions

All authors contributed equally to the preparation of this manuscript.

References

[1] Y. Praroopa, A. S. Reddy, and P. B. Rao, "Review concept of application of differential equations," *International Journal of Latest Engineering Research and Applications*, vol. 1, no. 3, pp. 34–37, 2016.

[2] A. Hassan and Y. Zakari, "Application of first order differential equation in temperature problems," *Application of Differential Equations*, vol. 16, 2018.

[3] M. Shams, N. Kausar, P. Agarwal, S. Momani, and M. A. Shah, "Highly efficient numerical scheme for solving fuzzy system of linear and non-linear equations with application in differential equations," *Applied Mathematics in Science and Engineering*, vol. 30, no. 1, pp. 777–810, 2022.

[4] A. Elmoasry, M. Shams, N. Yaqoob, N. Kausar, Y. U. Gaba, and N. Rafiq, "Numerical scheme for finding roots of interval-valued fuzzy non-linear equation with application in optimization," *Journal of Function Spaces*, vol. 2021, Article ID 6369129, 16 pages, 2021.

[5] L. A. Zadeh, "Fuzzy sets," *Information and Control*, vol. 8, no. 3, pp. 338–353, 1965.

[6] A. Kandel and W. J. Byatt, "Fuzzy processes," *Fuzzy Sets and Systems*, vol. 4, no. 2, pp. 117–152, 1980.

[7] R. Alikhani and M. Mostafazadeh, "First order linear fuzzy differential equations with fuzzy variable coefficients," *Computational Methods for Differential Equations*, vol. 9, no. 1, pp. 1–21, 2021.

[8] C. H. Vasavi, G. S. Kumar, T. S. Rao, and B. V. AppaRao, "Application of fuzzy differential equations for cooling problems," *International Journal of Mechanical Engineering & Technology*, vol. 8, no. 12, pp. 712–721, 2017.

[9] S. S. Devi and K. Ganesan, "Modelling electric circuit problem with fuzzy differential equations," *Journal of Physics*, vol. 1377, pp. 1–7, 2019.

[10] J. Ahmad, A. Iqbal, and Q. M. U. L. Hassan, "Study of nonlinear fuzzy integro differential equations using mathematical methods and applications," *International Journal of Fuzzy Logic and Intelligent Systems*, vol. 21, no. 1, pp. 76–85, 2021.

[11] A. Sadeghi, A. I. M. Ismail, and A. Jameel, "Solving system of fuzzy differential equation," *International Mathematical Forum*, vol. 6, no. 42, pp. 2087–2100, 2011.

[12] K. T. Atanassov, "Intuitionistic fuzzy sets," *Fuzzy Sets and Systems*, vol. 20, no. 1, pp. 87–96, 1986.
[13] S. Melliani and L. S. Chadli, "Introduction to intuitionistic fuzzy differential equations," *Notes on Intuitionistic Fuzzy Sets*, vol. 7, pp. 39–42, 2001.
[14] B. B. Amma, S. Melliani, and L. S. Chadli, "Numerical solution of intuitionistic fuzzy differential equations by Euler and Taylor methods," *Notes on Intuitionistic Fuzzy Sets*, vol. 22, no. 2, pp. 71–86, 2016.
[15] O. Akin and S. Bayeg, "Intuitionistic fuzzy initial value problems - an application," *Hacettepe Journal of Mathematics and Statistics*, vol. 48, pp. 1682–1694, 2019.
[16] O. Akin and S. Bayeg, "System of intuitionistic fuzzy differential equations with intuitionistic fuzzy initial values," *Notes on Intuitionistic Fuzzy Sets*, vol. 24, no. 4, pp. 141–171, 2018.
[17] S. Prasad Mondal and T. Kumar Roy, "First order homogeneous ordinary differential equation with initial value as triangular intuitionistic fuzzy number," *Journal of Uncertainty in Mathematics Science*, vol. 2014, pp. 1–17, 2014.
[18] S. P. Mondal and T. K. Roy, "System of differential equation with initial value as triangular intuitionistic fuzzy number and its application," *International Journal of Algorithms, Computing and Mathematics*, vol. 1, no. 3, pp. 449–474, 2015.
[19] S. P. Mondal and T. K. Roy, "Generalized intuitionistic fuzzy laplace transform and its application in electric circuit," *Journal of Applied and Engineering Mathematics*, vol. 5, no. 1, pp. 30–45, 2015.
[20] M. Shams, N. Kausar, K. Alayyash, M. M. Al-Shamiri, N. Arif, and R. Ismail, "Semi-analytical scheme for solving intuitionistic fuzzy system of differential equations," *IEEE Access*, vol. 11, Article ID 33205, 2023.
[21] M. Shams, N. Kausar, S. Kousar, D. Pamucar, E. Ozbilge, and B. Tantay, "Computationally semi-numerical technique for solving system of intuitionistic fuzzy differential equations with engineering applications," *Advances in Mechanical Engineering*, vol. 14, no. 12, Article ID 168781322211421, 2022.
[22] G. Adomian, "Convergent series solution of nonlinear equations," *Journal of Computational and Applied Mathematics*, vol. 11, no. 2, pp. 225–230, 1984.
[23] G. Adomian, "A review of the decomposition method in applied mathematics," *Journal of Mathematical Analysis and Applications*, vol. 135, no. 2, pp. 501–544, 1988.
[24] A. M. Wazwaz, "A reliable modification of Adomian decomposition method," *Applied Mathematics and Computation*, vol. 102, no. 1, pp. 77–86, 1999.
[25] S. Biswas and T. K. Roy, "Adomian decomposition method for fuzzy differential equations with linear differential operator," *Journal of Information and Computing Science*, vol. 11, no. 4, pp. 243–250, 2016.
[26] G. Uthra, K. Thangavelu, and R. M. Umamageswari, "An optimal solution for generalized trapezoidal intuitionistic fuzzy transportation problem," *Advances in Fuzzy Mathematics*, vol. 12, no. 3, pp. 763–770, 2017.
[27] D. Chakraborty, D. K. Jana, and T. K. Roy, "Arithmetic operations on generalized intuitionistic fuzzy number and its applications to transportation problem," *Journal of the Operational Research Society of India*, vol. 52, no. 3, pp. 431–471, 2015.
[28] S. Banerjee and T. K. Roy, "Arithmetic operations on generalized trapezoidal fuzzy number and its applications," *Turkish Journal of Fuzzy Systems*, vol. 3, no. 1, pp. 16–44, 2012.
[29] M. R. Seikh, P. K. Nayak, and M. Pal, "Generalized triangular fuzzy numbers in intuitionistic fuzzy environment," *International Journal of Engineering Research and Development*, vol. 5, pp. 8–13, 2012.
[30] V. Ulucay, I. Deli, and M. Sahin, "Intuitionistic trapezoidal fuzzy multi-numbers and its application to multi-criteria decision-making problems," *Complex & Intelligent Systems*, vol. 5, no. 1, pp. 65–78, 2019.
[31] N. Rafiq, N. Yaqoob, N. Kausar et al., "Computer based fuzzy numerical method for solving engineering and real world applications," *Mathematical Problems in Engineering*, vol. 2021, Article ID 6916282, 13 pages, 2021.
[32] R. L. Burden and J. D. Faires, "Boundary-value problems for ordinary differential equations," in *Numerical Analysis*, pp. 1–863, Belmount Thomson Brooks/Cole Press, Boston, MA, USA, 91 edition, 2005.
[33] N. Khan, N. Yaqoob, M. Shams, Y. U. Gaba, and M. Riaz, "Solution of linear and quadratic equations based on triangular linear Diophantine Fuzzy numbers," *Journal of Function Spaces*, vol. 2021, Article ID 8475863, 14 pages, 2021.
[34] A. Ashraf, K. Ullah, A. Hussain, and M. Bari, "Interval-valued picture fuzzy Maclaurin symmetric mean operator with application in multiple attribute decision-making," *Reports in Mechanical Engineering*, vol. 3, no. 1, pp. 301–317, 2022.
[35] M. Shams, N. Rafiq, N. Kausar, N. Ahmad Mir, and A. Alalyani, "Computer oriented numerical scheme for solving engineering problems," *Computer Systems Science and Engineering*, vol. 42, no. 2, pp. 689–701, 2022.
[36] N. Martin, A. Velankanni Ananth, P. K. Sharmila, and T. Priya, "Fuzzy cognitive study on post pandemic impact on occupational shift in rural areas," *Journal of Fuzzy Extension and Applications*, vol. 3, no. 4, pp. 290–301, 2022.
[37] S. Mustafa, A. A. Bajwa, and S. Iqbal, "A new fuzzy grach model to forecast stock market technical analysis," *Operational Research in Engineering Sciences: Theory and Applications*, vol. 5, no. 1, pp. 185–204, 2022.
[38] M. Mollaei, "Fuzzy metric topology space and manifold," *Journal of Fuzzy Extension and Applications*, vol. 4, no. 1, pp. 18–27, 2023.

Hindawi
Complexity
Volume 2023, Article ID 6087990, 26 pages
https://doi.org/10.1155/2023/6087990

Research Article

A Novel Characterization of Fuzzy Soft Substructures in Quantales Theory

Saqib Mazher Qurashi,[1] **Muhammad Gulzar**,[1] **Rani Sumaira Kanwal**,[2] **Dilruba Akter**,[3] **and Muhammad Shawaiz Safdar**[1]

[1]*Government College University Faisalabad, Faisalabad, Pakistan*
[2]*Government College Women University Faisalabad, Faisalabad, Pakistan*
[3]*Department of Applied Mathematics, Gono Bishwabidyalay, Dhaka, Bangladesh*

Correspondence should be addressed to Muhammad Gulzar; 98kohly@gmail.com and Dilruba Akter; dilruba.amath@gonouniversity.edu.bd

Received 11 September 2022; Revised 6 October 2022; Accepted 15 October 2022; Published 5 May 2023

Academic Editor: Zeljko Stevic

In this paper, we use an algebraic structure quantale and define the idea of fuzzy soft substructures as a generalization of fuzzy substructures in quantale. These fuzzy soft substructures include fuzzy soft subquantales, fuzzy soft ideals, fuzzy soft prime ideals, fuzzy soft semiprime ideals, and fuzzy soft primary ideals. Furthermore, different characterizations of fuzzy soft substructures in quantales are introduced. Moreover, we extend this ideology to investigate that for each fuzzy soft substructure in quantale, there exists an α-soft substructure in quantales. These fuzzy soft subquantales and fuzzy soft ideals are characterized by their level subquantales and ideals, respectively. Finally, fuzzy soft image and fuzzy soft inverse image of fuzzy soft substructures under quantale homomorphism in quantale are discussed.

1. Introduction

Mulvey [1] was the first to present the quantale theory in 1986. Quantale theory provided a lattice framework for noncommutative C∗-algebra with algebraic structure, lattice order structures, and the initiation of quantum mechanics research. Yetter [2] created a relationship between quantale theory and linear logic in 1990, resulting in a comprehensive set of linear intuitionistic logic models. Quantale has applications in algebraic theory [3], rough set theory [4, 5], topological theory [6], theoretical computer science [7], and linear logic [8].

Zadeh [9] proposed the concept of fuzzy set (F Set) in 1965, and it has been used to generalize algebraic concepts. It provides an effective scientific and mathematical tool for explaining a framework that is both complex and confusing. Luo and Wang [10] proposed fuzzy ideals in quantales in 2014. They also explored rough fuzzy ideals in quantal. Generalization of rough fuzzy substructures and approximation of fuzzy substructures in quantales were investigated by Qurashi and Shabir [4, 11] in the form of $(\in, \in \vee q)$ and $(\in_\gamma, \in_\gamma \vee q\delta)$ in 2018 and 2020. In 2019, Farooq et al. [12] introduced several results relating to fuzzy hyper substructures of hyperquantales. The theory of F Set was extended by many authors to algebraic structures. Hussain et al. presented some results about rough Pythagorean fuzzy substructures in semigroups [13] in 2019.

In 1999, Molodtsov presented the soft set (S Set) theory [14] as a general scientific technique for managing vulnerability. Maji et al. explored some algebraic operations in S Set theory [15] in 2003, and Ali et al. [16] in 2009 discussed several new operations to combine the algebraic characteristics of S Set. Many significant problems were discussed by combining S Set theory and algebraic structures such as soft linear programming [17] in 2020, the roughness of bipolar S Set [18] in 2021, reduction of an information system [19] in 2019, soft ideals in semigroups [20] in 2019, representation of graphs based on neighborhood and S Set

[21] in 2017, and soft mappings [22] in 2022. Feng et al. described the link between soft, rough, and fuzzy sets and generate rough S Set, soft-rough set, and soft-rough$F$ Set [23, 24]. Ali et al. described the relationship between S Set and F Set in [16]. Kanwal and Shabir [25] applied soft relations to rough approximation of a F Set of semigroups. Moreover, Qurashi et al. [26] investigated the generalized roughness of fuzzy substructures in quantales w.r.t soft relations. Kanwal et al. [27] used soft relations to investigate the generalized approximation of substructures in quantales.

Maji et al. [28] defined the theory of fuzzy soft set (FSST), which was followed by research on picture FSST theory [29], time-neutrosophic$S$ Set theory [30, 31], possibility m-polarFSST theory [32], generalized intuitionistic FSST theory [33], inverse FSST theory [34], interval-valued picture FSST theory [35], generalized belief interval-valued$S$ Set theory [36], and generalized picture FSST theory [37]. Aygünoğlu and Aygün [38] explored fuzzy soft groups and discussed the applications of FSST to group theory. Shabir and Kanwal [39] discussed L-fuzzy soft ideals of nearrings. Habib et al. [40] introduced a new idea of the possibility F Soft ordered semigroups and their applications.

Majumdar and Samanta [41] introduced the notion of generalized FSST, which was immediately followed by studies on generalized multi-FSST [42], generalized F Set expert set [43], and generalized interval-valuedFSST [44]. Muhiuddin et al. [45] discussed FSST theory applied to commutative ideals of BCK-algebras in 2021. Jan et al. [46] proposed the multivalued picture F Set and multivalued picture FSST, which were modifications of the ideas of picture FSST and multi-FSST and their applications in group decision-making problems.

The remaining portion of the paper is designed using the following scheme. Section 2 connects some key explanations about quantales, their substructures, fuzzy substructures, soft substructures, and appropriate sequels. Notions of fuzzy soft substructures over quantale are discussed in section 3. In section 4, for each fuzzy soft substructures, there exists α-soft substructures are discussed. Additionally, fuzzy soft image and fuzzy soft inverse image are explained.

2. Preliminaries

In this section, some important notions and examples regarding substructures, fuzzy substructures, soft substructures, and their related results are discussed, which will be helpful in our following work.

Definition 1 (see [47]). A quantale $\mathscr{K}$ is a complete lattice equipped with an associative binary operation $\circledast$ distributing over arbitrary joins. That is $\forall e, e_i, f_i \in \mathscr{K}$, and $(i \in I)$, it holds that:

(i) $e\circledast(\vee_{i\in I} f_i) = \vee_{i\in I}(e\circledast f_i)$

(ii) $(\vee_{i\in I} e_i)\circledast f = \vee_{i\in I}(e_i\circledast f)$

Let $A_i, A, B \subseteq \mathscr{K}$, we define the following:

$$\begin{aligned} A\vee B &= \{e\vee f \mid e \in A, f \in B\},\\ A\circledast B &= \{e\circledast f \mid e \in A, f \in B\},\\ \bigvee_{i\in I} A_i &= \left\{\vee_{i\in I} e_i \,\middle|\, e_i \in A_i\right\}. \end{aligned} \tag{1}$$

Throughout the paper, quantales are denoted by $\mathscr{K}$ and $\mathfrak{b}$.

Example 1. The set $\mathscr{K} = \{0, g, h, 1\}$ is a quantale where binary operation on $\mathscr{K}$ and order relation are shown in Table 1 and Figure 1, respectively.

Definition 2 (see [47]). A set $Q \subseteq \mathscr{K}$ is called a subquantale $(\mathrm{Sub}_{\mathscr{K}})$ of quantale $\mathscr{K}$ if following hold:

(i) $\bigvee_{i\in I} q_i \in Q$

(ii) $q_1\circledast q_2 \in Q \forall q_1, q_2, q_i \in Q$

Example 2. Here the nonempty subset $Q = \{0, g, 1\}$ of quantale $\mathscr{K} = \{0, g, h, 1\}$ as shown in Example 1 is a subquantale of $\mathscr{K}$ where the binary operation on Q and order relation are shown in Table 2 and Figure 2, respectively.

Definition 3 (see [48]). A subset $\varnothing \neq \mathscr{I}$ of a quantale $\mathscr{K}$ is called an ideal (Id) of $\mathscr{K}$ if

(i) $e, f \in \mathscr{I}$, then $e\vee f \in \mathscr{I}$

(ii) $\forall e, f \in \mathscr{K}$ and $f \in \mathscr{I}$ such that $e \leq f \Longrightarrow e \in \mathscr{I}$

(iii) $\forall e \in \mathscr{K}$ and $f \in \mathscr{I} \Longrightarrow e\circledast f \in \mathscr{I}$ and $f\circledast e \in \mathscr{I}$

Definition 4 (see [48]). An ideal $\mathscr{I}$ of a quantale $\mathscr{K}$ is called prime ideal (P_I) if

$$e\circledast f \in \mathscr{I} \Longrightarrow e \in \mathscr{I} \text{ or } f \in \mathscr{I} \forall e, f \in \mathscr{K}. \tag{2}$$

Definition 5 (see [48]). An ideal $\mathscr{I}$ of a quantale $\mathscr{K}$ is called semiprime ideal (SP_I) if

$$f\circledast f \in \mathscr{I} \Longrightarrow f \in \mathscr{I} \forall f \in \mathscr{K}. \tag{3}$$

Definition 6 (see [48]). An ideal $\mathscr{I}$ of a quantale $\mathscr{K}$ is called primary ideal (PR_I) if $\mathscr{I} \neq \mathscr{K}$ and $\forall e, f \in \mathscr{K}$

$$e\circledast f \in \mathscr{I} \text{ and } e \notin \mathscr{I} \Longrightarrow f^n \in \mathscr{I} \forall e \in \mathscr{K}, \tag{4}$$

for some $n > 0$, where $f^n = f\circledast f\circledast \cdots \circledast f$.

Example 3. Consider Example 1. Order relation on $\mathscr{K}$ is shown in Figure 1. Let $\mathbb{I} = \{0, g\}$ be a subset of $\mathscr{K}$. It is easily verify that $\mathbb{I}$ is ideal, prime ideal, semiprime ideal, and primary ideal in quantale $\mathscr{K}$.

Definition 7 (see [9]). A F subset ρ of a quantale $\mathscr{K}$ is a function from $\mathscr{K}$ to the closed interval [0, 1], that is ρ: $\mathscr{K} \longrightarrow [0, 1]$.

Table 1: Binary operation subject to $\circledast$.

$\circledast$	0	g	h	1
0	0	0	0	0
g	0	g	0	g
h	0	0	h	h
1	0	g	h	1

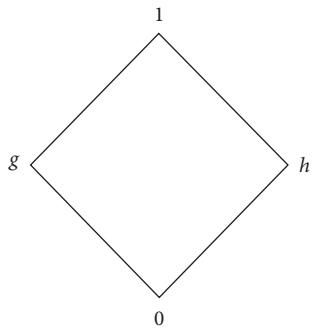

Figure 1: Illustration of $\mathcal{K}$.

Table 2: Binary operation subject to $\circledast$.

$\circledast$	0	g	1
0	0	0	0
g	0	g	g
1	0	g	1

Figure 2: Illustration of Q.

Definition 8 (see [11]). Suppose that ρ is a F subset of a quantale $\mathcal{K}$. Then ρ is a fuzzy subquantale $(F_S\mathcal{K})$ of $\mathcal{K}$ if

(i) $\rho(\vee_{i\in I}e_i) \geq \mathrm{Inf}_{i\in I}\rho(e_i)$

(ii) $\rho(e\circledast f) \geq \mathrm{Inf}(\rho(e),\rho(f))\forall e, e_i, f \in \mathcal{K}\,(i \in I)$

Definition 9 (see [10]). A nonempty F subset ρ of a quantale $\mathcal{K}$ is called fuzzy ideal (F_I) if

(i) $f \leq e \Longrightarrow \rho(e) \leq \rho(f)$

(ii) $\rho(e)\wedge\rho(f) \leq \rho(e\vee f)$

(iii) $\rho(e)\vee\rho(f) \leq \rho(e\circledast f)\forall e, f \in \mathcal{K}$

From (i) and (ii) in above definition, it is observed that $(e\vee f) = \rho(e)\wedge\rho(f)\forall e, f \in \mathcal{K}$. Thus a F subset ρ of a $\mathcal{K}$ is a F_I if and only if

(i) $\rho(e\vee f) = \rho(e)\wedge\rho(f)$and

(ii) $\rho(e)\vee\rho(f) \leq \rho(e\circledast f)\forall e, f \in \mathcal{K}$

Definition 10 (see [10]). A nonconstant $F_I\,\rho$ of a quantale $\mathcal{K}$ is called a fuzzy prime ideal (FP_I) of $\mathcal{K}$ if

$$\rho(e\circledast f) = \rho(e)\mathrm{or}\,\rho(f)\forall e, f \in \mathcal{K}. \tag{5}$$

Definition 11 (see [10]). A $F_I\,\rho$ of a quantale $\mathcal{K}$ is called fuzzy semiprime ideal (F_SP_I) of $\mathcal{K}$ if

$$\rho\left(e^2\right) = \rho(e)\forall e \in \mathcal{K}. \tag{6}$$

Definition 12 (see [10]). A nonconstant $F_I\,\rho$ of a quantale $\mathcal{K}$ is called fuzzy primary ideal (FPR_I) of $\mathcal{K}$ if

$$\rho(e\circledast f) = \rho(e)\mathrm{or}\,\rho\left(f^n\right)\forall e, f \in \mathcal{K}. \tag{7}$$

For some positive integer n.

Definition 13 (see [45]). Let U and E be an initial universe set and a set of parameters, respectively. Let $P(U)$ denotes the power set of U and $A\subseteq E$. A pair (F, A) is called a soft set over U, where F is a mapping given by $F\colon A \longrightarrow P(U)$.

Definition 14. Let (F, A) be a soft set over quantale $\mathcal{K}$. Then, (F, A) is called soft subquantale $(S_S\mathcal{K})$ over $\mathcal{K}$ if and only if $F(a)$ is a $\mathrm{Sub}_{\mathcal{K}}$ of $\mathcal{K}\forall a \in A$.

Definition 15. Let (F, A) be a S Set over quantale $\mathcal{K}$. Then, (F, A) is called soft ideal (S_I) over $\mathcal{K}$ if and only if $F(a)$ is an Id of $\forall a \in A$.

Definition 16. Let (F, A) be a S Set over quantale $\mathcal{K}$. Then, (F, A) is called soft prime ideal (STP_I) over $\mathcal{K}$ if and only if $F(a)$ is an P_I of $\forall a \in A$.

Definition 17. Let (F, A) be a S Set over quantale $\mathcal{K}$. Then, (F, A) is called soft semiprime ideal $(\mathrm{SSP_I})$ over $\mathcal{K}$ if and only if $F(a)$ is an SP_I of $\forall a \in A$.

Definition 18. Let (F, A) be a S Set over quantale $\mathcal{K}$. Then, (F, A) is called soft primary ideal (SPR_I) over $\mathcal{K}$ if and only if $F(a)$ is an PR_I of $\forall a \in A$.

Definition 19 (see [49]). Let ρ be a F subset of a quantale $\mathcal{K}$ and $\alpha \in [0, 1]$. Then,

$$\rho_\alpha = \{f \in \mathcal{K} \mid \rho(f) \geq \alpha\}, \tag{8}$$

is called $\alpha-$ level set of F subset ρ.

Definition 20 (see [28]). Let $\mathrm{FP}(U)$ denotes the set of all F subsets of U. A pair (F, A) is called a fuzzy soft set (FSST) over U, where F is a function given by $F\colon A \longrightarrow FP(U)$.

Definition 21 (see [50]). Let (Υ, I) and (η, J) be two FSST over the universe Ú. Union of (Υ, I) and (η, J) is the FSST, (χ, T) denoted by $(\Upsilon, I)\cup(\eta, J)$, where $T = I \cup J$ and $\forall d \in T$.

$$\chi(d) = \begin{cases} \Upsilon(d), & \text{if } d \in \frac{I}{J}, \\ \eta(d), & \text{if } d \in \frac{J}{I}, \\ \Upsilon(d)\check{}\eta(d), & \text{if } d \in I \cap J. \end{cases} \tag{9}$$

Definition 22 (see [50]). Let (Υ, I) and (η, J) be two FSST over the universe Ú. The restricted union of (Υ, I) and (η, J) is the FSST, (χ, T) denoted by $(\Upsilon, I)\uplus(\eta, J)$, where $T = I \cap J$ and $\forall d \in T$.

$$\chi(d) = \Upsilon(d)\vee\eta(d). \tag{10}$$

Definition 23 (see [50]). Let (Υ, I) and (η, J) be two FSST over the universe Ú. The extended intersection of (Υ, I) and (η, J) is the FSST, (χ, T) denoted by $(\Upsilon, I)\bar{\cap}(\eta, J)$, where $T = I \cup J$ and $\forall d \in T$.

$$\chi(d) = \begin{cases} \Upsilon(d), & \text{if } d \in \frac{I}{J}, \\ \eta(d), & \text{if } d \in \frac{J}{I}, \\ \Upsilon(d)\check{}\eta(d), & \text{if } d \in I \cap J. \end{cases} \tag{11}$$

Definition 24 (see [50]). Let (Υ, I) and (η, J) be two FSST over the universe Ú. The restricted intersection of (Υ, I) and (η, J) is the FSST, (χ, T) denoted by $(\Upsilon, I)\sqcap(\eta, J)$, where $T = I \cap J$ and χ: $I \cap J \longrightarrow \mathrm{SF}(\mathscr{K})\forall d \in T$.

$$\chi(d) = \Upsilon(d)\hat{}\eta(d). \tag{12}$$

Definition 25 (see [28]). Let (Υ, I) and (η, J) be two FSST over the universe Ú. "$(\Upsilon, I)\wedge(\eta, J)$" is the FSST, defined as $(\Upsilon, I)\wedge(\eta, J) = (\chi, T)$, where $T = I \times J$ and

$$\chi((i, j)) = \Upsilon(i)\wedge\eta(j)\forall(i, j) \in I \times J. \tag{13}$$

Definition 26 (see [28]). Let (Υ, I) and (η, J) be two FSST over the universe Ú. "$(\Upsilon, I)\vee(\eta, J)$" is the FSST, defined as $(\Upsilon, I)\vee(\eta, J) = (\chi, T)$, where $T = I \times J$ and

$$\chi((i, j)) = \Upsilon(i)\vee\eta(j)\forall(i, j) \in I \times J. \tag{14}$$

Definition 27. (see [28])Let P', P'' be the sets of parameters, $\varnothing \neq I \subseteq P'$ and $\varnothing \neq J \subseteq P''$. Let (Υ, I) and (η, J) be two FSST over a quantale $\mathscr{K}$ and $\mathfrak{Ƀ}$, respectively. The external product (E Product) of (Υ, I) and (η, J) is the FSST, (χ, T) over $\mathscr{K} \times \mathfrak{Ƀ}$ denoted by $(\Upsilon, I) \times (\eta, J)$ and defined as $(\chi, T) = (\Upsilon, I) \times (\eta, J)$ where $T = I \times J$ and

$$\chi((i, j)) = \Upsilon(i)\eta(j)\forall(i, j) \in I \times J. \tag{15}$$

Here ð is defined as follows:

$$\Upsilon(i)\eta(j)\left(d, d'\right) = \min\left\{(\Upsilon(i))(d), (\eta(j))\left(d'\right)\right\}. \tag{16}$$

3. Fuzzy Soft Substructure

In this section, we have discussed several key aspects relating to FSST substructures in quantale $\mathscr{K}$.

Definition 28. Let (Υ, J) be a FSST over a quantale $\mathscr{K}$. Then (Υ, J) is called fuzzy soft subquantale ($FS_S\mathscr{K}$) of $\mathscr{K}$ if $\Upsilon(q) \neq \varnothing$ is a $F_S\mathscr{K}$ of $\mathscr{K}\forall q \in J$.

Proposition 1. *Let $\{\mathscr{K}_i : i \in I\} \neq \varnothing$ be a family of quantales and $\{(\Upsilon_i, J_i) : i \in I\} \neq \varnothing$ be a family of* FSST *such that (Υ_i, J_i) is a $FS_S\mathscr{K}$ over $\mathscr{K}_i\forall i \in I$. Then E Product $\prod_{i\in I}(\Upsilon_i, J_i)$ is a $FS_S\mathscr{K}$ over $\prod_{i\in I}\mathscr{K}_i$.*

Proof. By definition, $\forall(q_i) \in \prod_{i\in I}J_i$

$(\prod_{i\in I}\Upsilon_i(q_i))(g) = \min_{i\in I}(\Upsilon_i(q_i))(g))$ where $(g) = (g_i) \in \prod_{i\in I}\mathscr{K}_i$ and $\Upsilon_i(q_i)$ is a $F_S\mathscr{K}$ of $\mathscr{K}_i\forall i \in I$.

Let $\prod_{i\in I}(\Upsilon_i, J_i) = (E, \prod_{i\in I}J_i)$ where $E((q_i)) = \prod_{i\in I}^{\sim}\Upsilon_i(q_i)\forall(q_i) \in \prod_{i\in I}J_i$. Then for all $(g_i)_1, (g_i)_2, \ldots, (g_i)_j \in \prod_{i\in I}\mathscr{K}_i\{E((q_i))\}(\vee_{j\in I}(g_i)_j) = (\prod_{i\in I}^{\sim}\Upsilon_i(q_i))$ $(\vee_{j\in I}(g_i)_j) = \min_{i\in I}\left\{(\Upsilon_i(q_i))(\underset{i\in I}{\vee}(g_i)_j)\right\}$

Since, $\Upsilon_i(q_i)$ is a $F_S\mathscr{K}$ of $\mathscr{K}_i$. So

$$\geq \min_{i\in I}\left\{\underset{j\in I}{\wedge}(\Upsilon_i(q_i))\left((g_i)_j\right)\right\} = \min_{i\in I}\left\{\left(\Upsilon_i^{i\in I}(q_i)((g_i)_1)\wedge(\Upsilon_i(q_i))\right)((g_i)_2)\wedge\ldots\wedge(\Upsilon_i(q_i))\left((g_i)_j\right)\right\}$$

$$= \left[\min_{i\in I}\{(\Upsilon_i(q_i))((g_i)_1)\}\right]\wedge\left[\min_{i\in I}\{(\Upsilon_i(q_i))((g_i)_2)\}\right]$$

$$\wedge\ldots\wedge\left[\min_{i\in I}\left\{(\Upsilon_i(q_i))\left((g_i)_j\right)\right\}\right]$$

$$\begin{aligned}&=\left(\tilde{\prod_{i\in I}}\Upsilon_i(q_i)\right)((g_i)_1)\wedge\left(\tilde{\prod_{i\in I}}\Upsilon_i(q_i)\right)((g_i)_2)\wedge\ldots\wedge\left(\tilde{\prod_{i\in I}}\Upsilon_i(q_i)\right)\left((g_i)_j\right)\\&=\{E((q_i))\}((g_i)_1)\wedge\{E((q_i))\}((g_i)_2)\wedge\ldots\wedge\{E((q_i))\}\left((g_i)_j\right).\end{aligned}\tag{17}$$

Now, for all $(g_i), (h_i)\in\prod_{i\in I}\mathscr{K}_i$

$$\begin{aligned}\{E((q_i))\}((g_i)\circledast(h_i))&=\left(\tilde{\prod_{i\in I}}\Upsilon_i(q_i)\right)((g_i)\circledast(h_i))\\&=\min_{i\in I}((\Upsilon_i(q_i))((g_i)\circledast(h_i)).\end{aligned}\tag{18}$$

Since, $\Upsilon_i(q_i)$ is a $F_S\mathscr{K}$ of $\mathscr{K}_i$. So

$$\begin{aligned}\geq\min_{i\in I}\{(\Upsilon_i(q_i))(g_i)\wedge(\Upsilon_i(q_i))(h_i)\}^{i\in I}&=\left[\min_{i\in I}\{(\Upsilon_i(q_i))(g_i)\}\right]\wedge\left[\min_{i\in I}\{(\Upsilon_i(q_i))(h_i)\}\right],\\&=\left(\tilde{\prod_{i\in I}}\Upsilon_i(q_i)\right)(g_i)\wedge\left(\tilde{\prod_{i\in I}}\Upsilon_i(q_i)\right)(h_i)\\&=\{E((q_i))\}(g_i)\wedge\{E((q_i))\}(h_i).\end{aligned}\tag{19}$$

This implies that $E((q_i))$ is a $F_S\mathscr{K}$ of $\prod_{i\in I}\mathscr{K}_i\forall(q_i)\in\prod_{i\in I}J_i$. Hence, $\prod_{i\in I}(\Upsilon_i,J_i)$ is a $FS_S\mathscr{K}$ over $\prod_{i\in I}\mathscr{K}_i$. □

Theorem 1. *Let $\{(\Upsilon_i,J_i):i\in I\}\neq\varnothing$ be a family of $FS_S\mathscr{K}$ over $\mathscr{K}$. Then $\underset{i\in I}{\cup}(\Upsilon_i,J_i)^{i\in I}$ with $(J_i\cap J_j)=\varnothing\forall i,j\in I$ is a $FS_S\mathscr{K}$ over $\mathscr{K}$.*

Proof. Let $\cup_{i\in I}(\Upsilon_i,J_i)=(E,\cup_{i\in I}J_i))$. Since $J_i\neq\varnothing$, so $\cup_{i\in I}J_i\neq\varnothing$. Then for any $q\in\cup_{i\in I}J_i$, this implies that $q\in J_j$ for some $j\in I$ and $E(q)=\Upsilon_j(q)$. Since, $\Upsilon_j(q)$ is a $F_S\mathscr{K}\forall q\in\cup_{i\in I}J_i$.

$\Rightarrow E(q)$ is a $F_S\mathscr{K}$ of $\mathscr{K}\forall q\in\cup_{i\in I}J_i$. Thus, $\cup_{i\in I}(\Upsilon_i,J_i)$ is a $FS_S\mathscr{K}$ over$\mathscr{K}$. □

Theorem 2. *Let $\{(\Upsilon_i,J_i):i\in I\}\neq\varnothing$ be a family of $FS_S\mathscr{K}$ over $\mathscr{K}$. Then $\bar{\cap}_{i\in I}(\Upsilon_i,J_i)$ is a $FS_S\mathscr{K}$ over $\mathscr{K}$.*

Proof. Let $\bar{\cap}_{i\in I}(\Upsilon_i,J_i)=(E,\underset{i\in I}{\cup}J_i)$ where $E(q)=\wedge_{j\in\Theta(q)}\Upsilon_j(q)\forall q\in\cup_{i\in I}J_i$. The set $\Theta(q)$ is defined as $\Theta(q)=\{j,q\in J_i\}$.

Then for all $g_1,g_2,\ldots,g_i\in\mathscr{K}$

$$\begin{aligned}\{E(q)\}(\overset{\vee}{}_{i\in I}g_i)&=\left\{\underset{j\in\Theta(q)}{\wedge}\Upsilon_j(q)\right\}\left(\underset{i\in I}{\vee}g_i\right)^{j\in\Theta(q)}\\&=\underset{j\in\Theta(q)}{\wedge}\left\{\Upsilon_j(q)\right\}\left(\underset{i\in I}{\vee}g_i\right)^{j\in\Theta(q)}.\end{aligned}\tag{20}$$

Since, $\Upsilon_j(q)$ is a $F_S\mathscr{K}$ of $\mathscr{K}$.

$$\begin{aligned}&\geq\underset{j\in\Theta(q)}{\wedge}\left\{\left(\Upsilon_j(q)\right)(g_1)\wedge\left(\Upsilon_j(q)\right)(g_2)\wedge\ldots\wedge\left(\Upsilon_j(q)\right)(g_i)\right\}\\&=\left[\underset{j\in\Theta(q)}{\wedge}\left\{\left(\Upsilon_j(q)\right)(g_1)\right\}\right]\wedge\left[\underset{j\in\Theta(q)}{\wedge}\left\{\left(\Upsilon_j(q)\right)(g_2)\right\}\right]\\&\wedge\ldots\wedge\left[\underset{j\in\Theta(q)}{\wedge}\left\{\left(\Upsilon_j(q)\right)(g_i)\right\}\right]\\&=\left[\underset{j\in\Theta(q)}{\wedge}\left\{\left(\Upsilon_j(q)\right)(g_1)\right\}\right]\wedge\left[\underset{j\in\Theta(q)}{\wedge}\left\{\left(\Upsilon_j(q)\right)(g_2)\right\}\right]\\&\wedge\ldots\wedge\left[\underset{j\in\Theta(q)}{\wedge}\left\{\left(\Upsilon_j(q)\right)(g_i)\right\}\right]\\&=\{(E(q))(g_1)\}\wedge\{(E(q))(g_2)\}\wedge\ldots\\&\wedge\{(E(q))(g_i)\}.\end{aligned}\tag{21}$$

Now, for all $g,h\in\mathscr{K}$

$$\begin{aligned}\{E(q)\}(g\circledast h)&=\left\{\underset{j\in\Theta(q)}{\wedge}\Upsilon_j(q)\right\}(g\circledast h)\\&=\left\{\underset{j\in\Theta(q)}{\wedge}\left(\Upsilon_j(q)\right)(g\circledast h)\right\}.\end{aligned}\tag{22}$$

Since, $\Upsilon_j(q)$ is a $F_S\mathscr{K}$ of $\mathscr{K}$.

$$\begin{aligned}
&\geq \underset{j\in\Theta(q)}{\wedge}\left\{\left(\Upsilon_j(q)\right)(g)\wedge\left(\Upsilon_j(q)\right)(h)\right\}\\
&=\left[\underset{j\in\Theta(q)}{\wedge}\left\{\left(\Upsilon_j(q)\right)(g)\right\}\right]\wedge\left[\underset{j\in\Theta(q)}{\wedge}\left\{\left(\Upsilon_j(q)\right)(g)\right\}\right]\\
&=\left[\underset{j\in\Theta(q)}{\wedge}\left\{\left(\Upsilon_j(q)\right)(g)\right\}\right]\wedge\left[\underset{j\in\Theta(q)}{\wedge}\left\{\left(\Upsilon_j(q)\right)(g)\right\}\right]\\
&=\{(E(q))(g)\}\wedge\{(E(q))(h)\},
\end{aligned}\tag{23}$$

$\Rightarrow E(q)$ is a $F_S\mathscr{K}$ of $\mathscr{K}\forall q\in\cup_{i\in I}J_i$. So $\bar{\cap}_{i\in I}(\Upsilon_i,J_i)$ is a $FS_S\mathscr{K}$ over $\mathscr{K}$. □

Theorem 3. *Let $\{(\Upsilon_i,J_i):i\in I\}\neq\varnothing$ be a family of $FS_S\mathscr{K}$ over $\mathscr{K}$. Then $\Cap_{i\in I}(\Upsilon_i,J_i)$ with $\cap_{i\in I}J_i\neq\varnothing$ is a $FS_S\mathscr{K}$ over $\mathscr{K}$.*

Proof. Let $\Cap_{i\in I}(\Upsilon_i,J_i)=(E,\cap_{i\in I}J_i)$ where $E(q)=\left\{\wedge_{j\in I}\Upsilon_j(q)\right\}\forall q\in\cap_{i\in I}J_i$.

Then for all $g_1,g_2,\ldots,g_i\in\mathscr{K}$

$$\begin{aligned}
\{E(q)\}\left(\underset{i\in I}{\vee}g_i\right)&=\left\{\underset{j\in I}{\wedge}\Upsilon_j(q)\right\}\left(\underset{i\in I}{\vee}g_i\right)\\
&=\underset{j\in I}{\wedge}\left\{\left(\Upsilon_j(q)\right)\left(\underset{i\in I}{\vee}g_i\right)\right\}.
\end{aligned}\tag{24}$$

Since, $\Upsilon_j(q)$ is a $F_S\mathscr{K}$ of $\mathscr{K}$.

$$\begin{aligned}
&\geq \underset{j\in I}{\wedge}\left\{\left(\Upsilon_j(q)\right)(g_1)\wedge\left(\Upsilon_j(q)\right)(g_2)\wedge\ldots\wedge\left(\Upsilon_j(q)\right)(g_i)\right\}\\
&=\left[\underset{j\in I}{\wedge}\left\{\left(\Upsilon_j(q)\right)(g_1)\right\}\right]\wedge\left[\underset{j\in I}{\wedge}\left\{\left(\Upsilon_j(q)\right)(g_2)\right\}\right]\wedge\ldots\wedge\left[\underset{j\in I}{\wedge}\left\{\left(\Upsilon_j(q)\right)(g_i)\right\}\right]\\
&=\left[\underset{j\in I}{\wedge}\left\{\Upsilon_j(q)\right\}(g_1)\right]\wedge\left[\left\{\underset{j\in I}{\wedge}\left(\Upsilon_j(q)\right)\right\}(g_2)\right]\wedge\left[\left\{\underset{j\in I}{\wedge}\left(\Upsilon_j(q)\right)\right\}(g_i)\right]\\
&=\{(E(q))(g_1)\}\wedge\{(E(q))(g_2)\}\wedge\ldots\wedge\{(E(q))(g_i)\}.
\end{aligned}\tag{25}$$

Now, for all $g,h\in\mathscr{K}$

$$\begin{aligned}
\{E(q)\}(g\circledast h)&=\left\{\underset{j\in I}{\wedge}\Upsilon_j(q)\right\}(g\circledast h)\\
&=\underset{j\in I}{\wedge}\left\{\left(\Upsilon_j(q)\right)(g\circledast h)\right\}.
\end{aligned}\tag{26}$$

Since, $\Upsilon_j(q)$ is a $F_S\mathscr{K}$ of $\mathscr{K}$.

$$\begin{aligned}
&\geq \underset{j\in I}{\wedge}\left\{\left(\Upsilon_j(q)\right)(g)\wedge\left(\Upsilon_j(q)\right)(h)\right\}\\
&=\left[\underset{j\in I}{\wedge}\left\{\left(\Upsilon_j(q)\right)(g)\right\}\right]\wedge\left[\left\{\underset{j\in I}{\wedge}\left(\Upsilon_j(q)\right)(g)\right\}(h)\right]\\
&=\{(E(q))(g)\}\wedge\{(E(q))(h)\},
\end{aligned}\tag{27}$$

$\Rightarrow E(q)$ is a $F_S\mathscr{K}$ of $\mathscr{K}\forall q\in\cap_{i\in I}J_i$. So, $\Cap_{i\in I}(\Upsilon_i,J_i)$ is a $FS_S\mathscr{K}$ over $\mathscr{K}$. □

Theorem 4. *Let $\{(\Upsilon_i,J_i):i\in I\}\neq\varnothing$ be a family of $FS_S\mathscr{K}$ over $\mathscr{K}$. Then $\wedge_{i\in I}(\Upsilon_i,J_i)$ is a $FS_S\mathscr{K}$ over $\mathscr{K}$.*

Proof. Let $\wedge_{i\in I}(\Upsilon_i,J_i)=(E,\prod_{i\in I}J_i)$ where $E(q)=\wedge_{j\in I}\Upsilon_j(q_j)\forall q_j\in\prod_{i\in I}J_i$.

Then for all $g_1,g_2,\ldots,g_i\in\mathscr{K}$.

$$\begin{aligned}
\{E(q)\}\left(\underset{i\in I}{\vee}g_i\right)&=\left\{\underset{j\in I}{\wedge}r_j(q_j)\right\}\left(\underset{i\in I}{\vee}g_i\right)\\
&=\underset{j\in I}{\wedge}\left\{\left(\Upsilon_j(q_j)\right)\left(\underset{i\in I}{\vee}g_i\right)\right\}.
\end{aligned}\tag{28}$$

Since, $\Upsilon_j(q_j)$ is a $F_S\mathscr{K}$ of $\mathscr{K}$.

$$\begin{aligned}
&\geq \underset{j\in I}{\wedge}\left\{\left(\Upsilon_j(q_j)\right)(g_1)\wedge\left(\Upsilon_j(q_j)\right)(g_2)\wedge\ldots\wedge\left(\Upsilon_j(q_j)\right)(g_i)\right\}\\
&=\left[\underset{j\in I}{\wedge}\left\{\left(\Upsilon_j(q_j)\right)(g_1)\right\}\right]\wedge\left[\underset{j\in I}{\wedge}\left\{\left(\Upsilon_j(q_j)\right)(g_2)\right\}\wedge\right]\ldots\wedge\left[\underset{j\in I}{\wedge}\left\{\left(\Upsilon_j(q_j)\right)(g_i)\right\}\right]\\
&=\left[\left\{\underset{j\in I}{\wedge}\left(\Upsilon_j(q_j)\right)\right\}(g_1)\right]\wedge\left[\left\{\underset{j\in I}{\wedge}\left(\Upsilon_j(q_j)\right)\right\}(g_2)\right]\ldots\wedge\left[\left\{\underset{j\in I}{\wedge}\left(\Upsilon_j(q_j)\right)\right\}(g_i)\right]\\
&=\left\{\left(E(q_j)\right)(g_1)\right\}\wedge\left\{\left(E(q_j)\right)(g_2)\right\}\wedge\ldots\wedge\left\{\left(E(q_j)\right)(g_i)\right\}.
\end{aligned}\tag{29}$$

Now, $\forall g, h \in \mathscr{K}$

$$\begin{aligned}\left\{E\left(q_j\right)\right\}(g \circledast h) &= \left\{\underset{j\in I}{\wedge}\left(\Upsilon_j\left(q_j\right)\right)\right\}(g \circledast h) \\ &\underset{j\in I}{\wedge}\left\{\left(\Upsilon_j\left(q_j\right)\right)(g \circledast h)\right\}\end{aligned} \tag{30}$$

Since, $\Upsilon_j(q_j)$ is a $F_S\mathscr{K}$ of $\mathscr{K}$.

$$\begin{aligned}&\geq \underset{j\in I}{\wedge}\left\{\left(\Upsilon_j\left(q_j\right)\right)(g) \wedge \left(\Upsilon_j\left(q_j\right)\right)(h)\right\} \\ &= \underset{j\in I}{\wedge}\left\{\left(\Upsilon_j\left(q_j\right)\right)(g)\right\} \wedge \underset{j\in I}{\wedge}\left\{\left(\Upsilon_j\left(q_j\right)\right)(h)\right\} \\ &\left[\left\{\underset{j\in I}{\wedge}\left(\Upsilon_j\left(q_j\right)\right)\right\}\right](g) \wedge \left[\left\{\underset{j\in I}{\wedge}\left(\Upsilon_j\left(q_j\right)\right)\right\}\right](h) \\ &= \left\{\left(E\left(q_j\right)\right)(g)\right\} \wedge \left\{\left(E\left(q_j\right)\right)(h)\right\},\end{aligned} \tag{31}$$

$\Rightarrow E(q_j)$ is a $F_S\mathscr{K}$ of $\mathscr{K} \forall q_j \in \prod_{i\in I} J_i$. So, $\wedge_{i\in I}(\Upsilon_i, J_i)$ is a $FS_S\mathscr{K}$ over $\mathscr{K}$. □

Remark 1. Let (Υ, I) and (η, J) be any two $FS_S\mathscr{K}$ over $\mathscr{K}$. Then $(\Upsilon, I) \uplus (\eta, J)$ and $(\Upsilon, I) \vee (\eta, J)$ may not be $FS_S\mathscr{K}$ over $\mathscr{K}$.

Example 4. Let $\mathscr{K}$ be a quantale of four elements $\{0, s, t, 1\}$ represented in Figure 3 and Table 3.

Let $I = \{l_1, l_2\}$ and $J = \{l_1, l_2, l_3\}$ be subsets of parameter $P = \{l_1, l_2, l_3\}$. Let (Υ, I) and (η, J) be $FS_S\mathscr{K}$ over $\mathscr{K}$ defined by Tables 4 and 5.

First, we have to show that $(\Upsilon, I) \uplus (\eta, J)$ is not a $FS_S\mathscr{K}$ over $\mathscr{K}$.

Let $(\Upsilon, I) \uplus (\eta, J) = (\check{\mathrm{D}}, \mathrm{I} \cap \mathrm{J})$ be defined in Table 6 as $\check{\mathrm{D}}(\mathrm{d}) = \Upsilon(\mathrm{l}) \vee \eta(\mathrm{l}) \forall \mathrm{l} \in \mathrm{I} \cap \mathrm{J}$. Then

From Table 6 we see that $\check{\mathrm{D}}(\mathrm{l}_1)\ (s \circledast t) = \check{\mathrm{D}}(\mathrm{l}_1)\ (0) = 0.6 \not\geq \check{\mathrm{D}}(\mathrm{l}_1)\ (s) \wedge \check{\mathrm{D}}(\mathrm{l}_1)\ (t) = 0.7 \wedge 0.7 = 0.7$ and $\check{\mathrm{D}}(\mathrm{l}_2)\ (s \circledast t) = \check{\mathrm{D}}(\mathrm{l}_2)\ (0) = 0.7 \not\geq \check{\mathrm{D}}(\mathrm{l}_2)\ (s) \wedge \check{\mathrm{D}}(\mathrm{l}_2)\ (t) = 0.9 \wedge 0.8 = 0.8$.

So, $(\Upsilon, I) \uplus (\eta, J)$ is not a $FS_S\mathscr{K}$ over $\mathscr{K}$.

Now, we have to show that $(\Upsilon, I) \vee (\eta, J)$ is not a $FS_S\mathscr{K}$ over $\mathscr{K}$.

Let $(\Upsilon, I) \vee (\eta, J) = (\dot{\mathrm{D}}, I \times J)$ be defined in Table 7.

$$\dot{\mathrm{D}}(l_1, l_2) = \Upsilon(l_1) \vee \eta(l_2) \forall (l_1, l_2) \in I \times J, \tag{32}$$

where $I \times J = \{(l_1, l_1), (l_1, l_2), (l_1, l_3), (l_2, l_1), (l_2, l_2), (l_2, l_3)\}$. Then

From Table 7 we see that

$$\begin{aligned}\left\{\dot{\mathrm{D}}\left((l_1, l_1)\right)\right\}(s \circledast t) &= \left\{\dot{\mathrm{D}}\left((l_1, l_1)\right)\right\}(0) = 0.6 \\ \left\{\dot{\mathrm{D}}\left((l_1, l_1)\right)\right\}(s) \wedge \left\{\dot{\mathrm{D}}\left((l_1, l_1)\right)\right\}(t) &= 0.7 \wedge 0.7 = 0.7.\end{aligned} \tag{33}$$

This implies that $\left\{\dot{\mathrm{D}}(l_1, l_1)\right\}(s \circledast t) \not\geq \left\{\dot{\mathrm{D}}(l_1, l_1)\right\}(s) \wedge \left\{\dot{\mathrm{D}}(l_1, l_1)\right\}(t)$.

Similarly,

$$\begin{aligned}\left\{\dot{\mathrm{D}}\left((l_1, l_1)\right)\right\}(s \circledast t) &\not\geq \left\{\dot{\mathrm{D}}\left((l_1, l_1)\right)\right\}(s) \wedge \left\{\dot{\mathrm{D}}\left((l_1, l_1)\right)\right\}(t), \\ \left\{\dot{\mathrm{D}}\left((l_1, l_1)\right)\right\} s \circledast t &\not\geq \left\{\dot{\mathrm{D}}\left((l_1, l_1)\right)\right\}(s) \wedge \left\{\dot{\mathrm{D}}\left((l_1, l_1)\right)\right\}(t),\end{aligned} \tag{34}$$

So, $(\Upsilon, I) \vee (\eta, J)$ is not a $FS_S\mathscr{K}$ over $\mathscr{K}$.

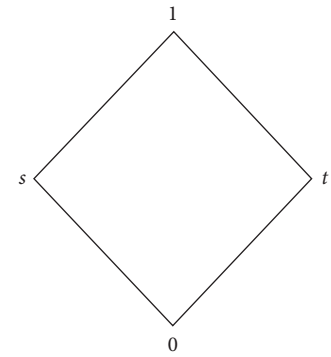

Figure 3: Illustration of $\mathscr{K}$.

Table 3: Binary operation subject to $\circledast$.

$\circledast$	0	s	t	1
0	0	0	0	0
s	0	s	0	s
t	0	0	t	t
1	0	s	t	1

Table 4: Binary operation subject to I.

I	l_1	l_2
0	0.6	0.7
s	0.1	0
t	0.7	0.8
1	0.8	0.9

Table 5: Binary operation subject to J.

J	l_1	l_2	l_3
0	0.3	0.5	1
s	0.7	0.9	0.2
t	0	0.2	0.4
1	0.6	1	0.8

Table 6: Binary operation subject to $\check{\mathrm{D}}$.

$\check{\mathrm{D}}$	l_1	l_2
0	0.6	0.7
s	0.7	0.9
t	0.7	0.8
1	0.8	1

Table 7: Binary operation subject to $\dot{\mathrm{D}}$.

$\dot{\mathrm{D}}$	(l_1, l_1)	(l_1, l_2)	(l_1, l_3)	(l_2, l_1)	(l_2, l_2)	(l_2, l_3)
0	0.6	0.6	1	0.7	0.7	1
s	0.7	0.9	0.2	0.7	0.9	0.2
t	0.7	0.7	0.7	0.8	0.8	0.8
1	0.8	1	0.8	0.9	1	0.9

Now some necessary characterizations about FS_I and some important results pertaining to this definition are elaborated here.

Definition 29. Let (Υ, J) be a FSST over a quantale $\mathscr{K}$. Then (Υ, J) is called fuzzy soft ideal (FS_I) of $\mathscr{K}$ if $\Upsilon(q) \neq \varnothing$ is a F_I of $\mathscr{K} \forall q \in J$.

Proposition 2. *Let $\{\mathscr{K}_i : i \in I\} \neq \varnothing$ be a family of quantales and $\{(E_i, H_i) : i \in I\} \neq \varnothing$ be a family of* FSST *such that (E_i, H_i) is a FS_I over $\mathscr{K}_i \forall i \in I$. Then E Product $\prod_{i\in I}(E_i, H_i)$ is a FS_I over $\prod_{i\in I}\mathscr{K}_i$.*

Proof. By definition, $\forall (q_i) \in \prod_{i\in I} H_i$

$$\left(\tilde{\prod_{i\in I}} E_i(q_i)\right)(g) = \min_{i\in I}\{(E_i(q_i))(g)\}, \tag{35}$$

where $(g) = (g_i) \in \prod_{i\in I}\mathscr{K}_i$ and $E_i(q_i)$ is a F_I of $\mathscr{K}_i \forall i \in I$.

Let $\prod_{i\in I}(E_i, H_i) = (C, \prod_{i\in I} H_i)$ where $C((q_i)) = \tilde{\prod_{i\in I}} E_i(q_i) \forall (q_i) \in \prod_{i\in I} H_i$.

Then for all (g_i), $(h_i) \in \prod_{i\in I}\mathscr{K}_i$

$$\begin{aligned} \{C((q_i))\}(g_i \vee h_i) &= \left(\tilde{\prod_{i\in I}} E_i(q_i)\right)((g_i \vee h_i)) \\ &= \min_{i\in I}(E_i(q_i)((g_i \vee h_i))). \end{aligned} \tag{36}$$

Since, $E_i(q_i)$ is a F_I of $\mathscr{K}_i$. So,

$$\begin{aligned} &= \min_{i\in I}\{(E_i(q_i))(g_i) \wedge (E_i(q_i))(h_i)\} \\ &= \left[\min_{i\in I}\{(E_i(q_i))(g_i)\}\right] \wedge \left[\min_{i\in I}\{(E_i(q_i))(h_i)\}\right] \\ &= \left(\tilde{\prod_{i\in I}} E_i(q_i)\right)((g_i)) \wedge \left(\tilde{\prod_{i\in I}} E_i(q_i)\right)((h_i)) \\ &= \{C((q_i))\}((g_i)) \wedge \{C((q_i))\}((h_i)). \end{aligned} \tag{37}$$

Now, for all (g_i), $(h_i) \in \prod_{i\in I}\mathscr{K}_i$

$$\begin{aligned} \{C((q_i))\}((g_i) \circledast (h_i)) &= \left(\tilde{\prod_{i\in I}} E_i(q_i)\right)((g_i) \circledast (h_i)) \\ &= \min_{i\in I}(E_i(q_i)((g_i) \circledast (h_i))). \end{aligned} \tag{38}$$

Since, $E_i(q_i)$ is a F_I of $\mathscr{K}_i$. So,

$$\begin{aligned}
&\geq \min_{i\in I}\{(E_i(q_i))(g_i)\vee(E_i(q_i))(h_i)\}\\
&=\left[\min_{i\in I}\{(E_i(q_i))(g_i)\}\right]\vee\left[\min_{i\in I}\{(E_i(q_i))(h_i)\}\right]\\
&==\left(\tilde{\prod_{i\in I}}E_i(q_i)\right)((g_i))\vee\left(\tilde{\prod_{i\in I}}E_i(q_i)\right)((h_i))\\
&=\{C((q_i))\}((g_i))\vee\{C((q_i))\}((h_i)).
\end{aligned}\tag{39}$$

This implies that $C((q_i))$ is a F_I of $\prod_{i\in I}\mathscr{K}_i\forall(q_i)\in\prod_{i\in I}H_i$. Hence, $\prod_{i\in I}(E_i,H_i)$ is a FS_I over $\prod_{i\in I}\mathscr{K}_i$. □

Theorem 5. *Let $\{(E_i,H_i)\colon i\in I\}\neq\varnothing$ be a family of FS_I over $\mathscr{K}$. Then, $\Cap_{i\in I}(E_i,H_i)$ with $\cap_{i\in I}H_i\neq\varnothing$ is a FS_I over $\mathscr{K}$.*

Proof. Let $\Cap_{i\in I}(E_i,H_i)=(C,\cap_{i\in I}H_i)$ where $C(q)=\wedge_{j\in I}E_jE_j(q)\forall q\in\cap_{i\in I}H_i$. Then for all $g,h\in\mathscr{K}$

$$\begin{aligned}
\{C(q)\}(g\vee h)&=\left\{\underset{j\in I}{\wedge}E_j(q)\right\}(g\vee h)\\
&=\underset{j\in I}{\wedge}\left\{\left(E_j(q)\right)(g\vee h)\right\}
\end{aligned}\tag{40}$$

Since, $E_j(q)$ is a F_I of $\mathscr{K}$.

$$\begin{aligned}
&=\underset{j\in I}{\wedge}\left\{\left(E_j(q)\right)(g)\wedge\left(E_j(q)\right)(h)\right\}\\
&=\left[\underset{j\in I}{\wedge}\left\{\left(E_j(q)\right)(g)\right\}\right]\wedge\left[\underset{j\in I}{\wedge}\left\{\left(E_j(q)\right)(h)\right\}\right]\\
&=\left[\left\{\underset{j\in I}{\wedge}\left(E_j(q)\right)\right\}(g)\right]\wedge\left[\left\{\underset{j\in I}{\wedge}\left(E_j(q)\right)\right\}(h)\right]\\
&=\{(C(q))(g)\}\wedge\{(C(q))(h)\}.
\end{aligned}\tag{41}$$

Now, for all $g,h\in\mathscr{K}$

$$\begin{aligned}
\{C(q)\}(g\circledast h)&=\left\{\underset{j\in I}{\wedge}E_j(q)\right\}(g\circledast h)\\
&=\underset{j\in I}{\wedge}\left\{\left(E_j(q)\right)(g\circledast h)\right\}.
\end{aligned}\tag{42}$$

Since, $E_j(q)$ is a F_I of $\mathscr{K}$.

$$\begin{aligned}
&\geq\underset{j\in I}{\wedge}\left\{\left(E_j(q)\right)(g)\vee\left(E_j(q)\right)(h)\right\}\\
&=\left[\underset{j\in I}{\wedge}\left\{\left(E_j(q)\right)(g)\right\}\right]\vee\left[\underset{j\in I}{\wedge}\left\{\left(E_j(q)\right)(h)\right\}\right]\\
&=\left[\left\{\underset{j\in I}{\wedge}\left(E_j(q)\right)\right\}(g)\right]\vee\left[\left\{\underset{j\in I}{\wedge}\left(E_j(q)\right)\right\}(h)\right]\\
&=\{(C(q))(g)\}\vee\{(C(q))(h)\},
\end{aligned}\tag{43}$$

$\Rightarrow C(q)$ is a F_I of $\mathscr{K}\forall q\in\cap_{i\in I}H_i$. So, $\Cap_{i\in I}(E_i,H_i)$ is a FS_I over $\mathscr{K}$. □

Theorem 6. *Let $\{(E_i,H_i)\colon i\in I\}\neq\varnothing$ be a family of FS_I over $\mathscr{K}$. Then $\Cup_{i\in I}(E_i,H_i)$ is a FS_I over $\mathscr{K}$.*

Proof. Let $\Cup_{i\in I}(E_i,H_i)=(C,\cup_{i\in I}H_i)$ where $C(q)=\wedge_{j\in\Theta(q)}E_j(q)\forall q\in\cap_{i\in I}H_i$. The set $\Theta(q)$ is defined as $\Theta(q)=\{j,q\in J_j\}$. Then for all $g,h\in\mathscr{K}$

$$\begin{aligned}
\{C(q)\}(g\vee h)&=\left\{\underset{j\in\Theta(q)}{\wedge}E_j(q)\right\}(g\vee h)\\
&=\underset{j\in\Theta(q)}{\wedge}\left\{\left(E_j(q)\right)(g\vee h)\right\}.
\end{aligned}\tag{44}$$

Since, $E_j(q)$ is a F_I of $\mathscr{K}$.

$$\begin{aligned}
&=\underset{j\in\Theta(q)}{\wedge}\left\{\left(E_j(q)\right)(g)\wedge\left(E_j(q)\right)(h)\right\}\\
&=\left[\underset{j\in\Theta(q)}{\wedge}\left\{\left(E_j(q)\right)(g)\right\}\right]\wedge\left[\underset{j\in\Theta(q)}{\wedge}\left\{\left(E_j(q)\right)(h)\right\}\right]\\
&=\left[\left\{\underset{j\in\Theta(q)}{\wedge}\left(E_j(q)\right)\right\}(g)\right]\wedge\left[\left\{\underset{j\in\Theta(q)}{\wedge}\left(E_j(q)\right)\right\}(h)\right]\\
&=\{(C(q))(g)\}\wedge\{(C(q))(h)\}.
\end{aligned}\tag{45}$$

Now, for all $g,h\in\mathscr{K}$

$$\begin{aligned}
\{C(q)\}(g\circledast h)&=\left\{\underset{j\in\Theta(q)}{\wedge}\left(E_j(q)\right)\right\}(g\circledast h)\\
&=\underset{j\in\Theta(q)}{\wedge}\left\{\left(E_j(q)\right)(g\circledast h)\right\}.
\end{aligned}\tag{46}$$

Since, $E_j(q)$ is a F_I of $\mathscr{K}$.

$$\begin{aligned}
&\geq\underset{j\in\Theta(q)}{\wedge}\left\{\left(E_j(q)\right)(g)\vee\left(E_j(q)\right)(h)\right\}\\
&=\left[\underset{j\in\Theta(q)}{\wedge}\left\{\left(E_j(q)\right)(g)\right\}\right]\vee\left[\underset{j\in\Theta(q)}{\wedge}\left\{\left(E_j(q)\right)(h)\right\}\right]\\
&=\left[\left\{\underset{j\in\Theta(q)}{\wedge}\left(E_j(q)\right)\right\}(g)\right]\vee\left[\left\{\underset{j\in\Theta(q)}{\wedge}\left(E_j(q)\right)\right\}(h)\right]\\
&=\{(C(q))(g)\}\vee\{(C(q))(h)\}.
\end{aligned}\tag{47}$$

$\Rightarrow C(q)$ is a F_I of $\mathscr{K}\forall q\in\cup_{i\in I}H_i$. So, $\Cup_{i\in I}(E_i,H_i)$ is a FS_I over $\mathscr{K}$. □

Theorem 7. *Let $\{(E_i, H_i): i \in I\} \neq \varnothing$ be a family of FS_I over $\mathscr{K}$. Then, $\uplus_{i\in I}(E_i, H_i)$ with $\cap_{i\in I}H_i \neq \varnothing$ is a FS_I over $\mathscr{K}$.*

Proof. Let $\uplus_{i\in I}(E_i, H_i) = (C, \cap_{i\in I}H_i)$ where $C(q) = \vee_{j\in I}E_j(q)\forall q \in \cup_{i\in I}H_i$. Then for all $g, h \in \mathscr{K}$

$$\begin{aligned}\{C(q)\}(g\vee h) &= \left\{\underset{j\in I}{\vee}E_j(q)\right\}(g\vee h)\\ &= \underset{j\in I}{\vee}\left\{\left(E_j(q)\right)(g\vee h)\right\}.\end{aligned} \tag{48}$$

Since, $E_j(q)$ is a F_I of $\mathscr{K}$.

$$\begin{aligned}&= \underset{j\in I}{\vee}\left\{\left(E_j(q)\right)(g)\wedge\left(E_j(q)\right)(h)\right\}\\ &= \left[\underset{j\in I}{\vee}\left\{\left(E_j(q)\right)(g)\right\}\right]\wedge\left[\underset{j\in I}{\vee}\left\{\left(E_j(q)\right)(h)\right\}\right]\\ &= \left[\left\{\underset{j\in I}{\vee}\left(E_j(q)\right)\right\}(g)\right]\wedge\left[\left\{\underset{j\in I}{\vee}\left(E_j(q)\right)\right\}(h)\right]\\ &= \{(C(q))(g)\}\wedge\{(C(q))(h)\}.\end{aligned} \tag{49}$$

Now, for all $g, h \in \mathscr{K}$

$$\begin{aligned}\{C(q)\}(g\circledast h) &= \left\{\underset{j\in I}{\vee}E_j(q)\right\}(g\circledast h)\\ &= \underset{j\in I}{\vee}\left\{\left(E_j(q)\right)(g\circledast h)\right\}.\end{aligned} \tag{50}$$

Since, $E_j(q)$ is a F_I of $\mathscr{K}$.

$$\begin{aligned}&\geq \underset{j\in I}{\vee}\left\{\left(E_j(q)\right)(g)\vee\left(E_j(q)\right)(h)\right\}\\ &= \left[\underset{j\in I}{\vee}\left\{\left(E_j(q)\right)(g)\right\}\right]\vee\left[\underset{j\in I}{\vee}\left\{\left(E_j(q)\right)(h)\right\}\right]\\ &= \left[\left\{\underset{j\in I}{\vee}\left(E_j(q)\right)\right\}(g)\right]\vee\left[\left\{\underset{j\in I}{\vee}\left(E_j(q)\right)\right\}(h)\right]\\ &= \{(C(q))(g)\}\vee\{(C(q))(h)\},\end{aligned} \tag{51}$$

$\Rightarrow C(q)$ is a F_I of $\mathscr{K}\forall q \in \cup_{i\in I}H_i$. So, $\uplus_{i\in I}(E_i, H_i)$ is a FS_I over $\mathscr{K}$. □

Theorem 8. *Let $\{(E_i, H_i): i \in I\} \neq \varnothing$ be a family of FS_I over $\mathscr{K}$. Then $\uplus_{i\in I}(E_i, H_i)$ is a FS_I over $\mathscr{K}$.*

Proof. Let $\uplus_{i\in I}(E_i, H_i) = (C, \cup_{i\in I}H_i)$ where $C(q) = \vee_{j\in\Theta(q)}E_j(q)\forall q \in \cup_{i\in I}H_i$. The set $\Theta(q)$ is defined as $\Theta(q) = \{j, q \in J_j\}$. Then for all $g, h \in \mathscr{K}$

$$\begin{aligned}\{C(q)\}(g\vee h) &= \left\{\underset{j\in\Theta(q)}{\vee}E_j(q)\right\}(g\vee h)\\ &= \underset{j\in\Theta(q)}{\vee}\left\{\left(E_j(q)\right)(g\vee h)\right\}.\end{aligned} \tag{52}$$

Since, $E_j(q)$ is a F_I of $\mathscr{K}$.

$$\begin{aligned}&= \underset{j\in\Theta(q)}{\vee}\left\{\left(E_j(q)\right)(g)\wedge\left(E_j(q)\right)(h)\right\}\\ &= \left[\underset{j\in\Theta(q)}{\vee}\left\{\left(E_j(q)\right)(g)\right\}\right]\wedge\left[\underset{j\in\Theta(q)}{\vee}\left\{\left(E_j(q)\right)(h)\right\}\right]\\ &= \left[\left\{\underset{j\in\Theta(q)}{\vee}\left(E_j(q)\right)\right\}(g)\right]\wedge\left[\left\{\underset{j\in\Theta(q)}{\vee}\left(E_j(q)\right)\right\}(h)\right]\\ &= \{(C(q))(g)\}\wedge\{(C(q))(h)\}.\end{aligned} \tag{53}$$

Now, for all $g, h \in \mathscr{K}$

$$\begin{aligned}\{C(q)\}(g\circledast h) &= \left\{\underset{j\in\Theta(q)}{\vee}E_j(q)\right\}(g\circledast h)\\ &= \underset{j\in\Theta(q)}{\vee}\left\{\left(E_j(q)\right)(g\circledast h)\right\}.\end{aligned} \tag{54}$$

Since, $E_j(q)$ is a F_I of $\mathscr{K}$.

$$\begin{aligned}&\geq \underset{j\in\Theta(q)}{\vee}\left\{\left(E_j(q)\right)(g)\vee\left(E_j(q)\right)(h)\right\}\\ &= \left[\underset{j\in\Theta(q)}{\vee}\left\{\left(E_j(q)\right)(g)\right\}\right]\vee\left[\underset{j\in\Theta(q)}{\vee}\left\{\left(E_j(q)\right)(h)\right\}\right]\\ &= \left[\left\{\underset{j\in\Theta(q)}{\vee}\left(E_j(q)\right)\right\}(g)\right]\vee\left[\left\{\underset{j\in\Theta(q)}{\vee}\left(E_j(q)\right)\right\}(h)\right]\\ &= \{(C(q))(g)\}\vee\{(C(q))(h)\},\end{aligned} \tag{55}$$

$\Rightarrow C(q)$ is a F_I of $\mathscr{K}\forall q \in \cup_{i\in I}H_i$. So, $\uplus_{i\in I}(E_i, H_i)$ is a FS_I over $\mathscr{K}$. □

Theorem 9. *Let $\{(E_i, H_i): i \in I\} \neq \varnothing$ be a family of FS_I over $\mathscr{K}$. Then $\wedge_{i\in I}(E_i, H_i)$ is a FS_I over $\mathscr{K}$.*

Proof. Let $\wedge_{i\in I}(E_i, H_i) = (C, \prod_{i\in I}H_i)\wedge_{i\in I}(E_i, H_i)$ where $C(q_j) = \wedge_{j\in I}E_j(q_j)\forall q_j \in \prod_{i\in I}H_i$.Then for all $g, h \in \mathscr{K}$

$$\begin{aligned}\left\{C\left(q_j\right)\right\}(g\vee h) &= \left\{\underset{j\in I}{\vee}E_j\left(q_j\right)\right\}(g\vee h)\\ &= \underset{j\in I}{\vee}\left\{\left(E_j\left(q_j\right)\right)(g\vee h)\right\}.\end{aligned} \tag{56}$$

Since, $E_j(q)$ is a F_I of $\mathscr{K}$.

$$\begin{aligned}&= \underset{j\in I}{\wedge}\left\{\left(E_j\left(q_j\right)\right)(g)\wedge\left(E_j\left(q_j\right)\right)(h)\right\}\\ &= \left[\underset{j\in I}{\wedge}\left\{\left(E_j\left(q_j\right)\right)(g)\right\}\right]\wedge\left[\underset{j\in I}{\wedge}\left\{\left(E_j\left(q_j\right)\right)(h)\right\}\right]\\ &= \left[\left\{\underset{j\in I}{\wedge}\left(E_j\left(q_j\right)\right)\right\}(g)\right]\wedge\left[\left\{\underset{j\in I}{\wedge}\left(E_j\left(q_j\right)\right)\right\}(h)\right]\\ &= \left\{\left(C\left(q_j\right)\right)(g)\right\}\wedge\left\{\left(C\left(q_j\right)\right)(h)\right\}.\end{aligned} \tag{57}$$

Now, for all $g, h \in \mathscr{K}$

$$\begin{aligned}\{C(q_j)\}(g\circledast h) &= \left\{\underset{j\in I}{\wedge} E_j(q_j)\right\}(g\circledast h)\\ &= \underset{j\in I}{\wedge}\{(E_j(q_j))(g\circledast h)\}.\end{aligned} \tag{58}$$

Since, $E_j(q)$ is a F_I of $\mathscr{K}$.

$$\begin{aligned}&\geq \underset{j\in I}{\wedge}\{(E_j(q_j))(g)\vee(E_j(q_j))(h)\}\\ &= \left[\underset{j\in I}{\wedge}\{(E_j(q_j))(g)\}\right]\vee\left[\underset{j\in I}{\wedge}\{(E_j(q_j))(h)\}\right]\\ &= \left[\underset{j\in I}{\wedge}\{(E_j(q_j))\}(g)\right]\vee\left[\underset{j\in I}{\wedge}\{(E_j(q_j))(h)\}\right]\\ &= \{(C(q_j))(g)\}\vee\{(C(q_j))(h)\},\end{aligned} \tag{59}$$

$\Rightarrow C(q_j)$ is a F_I of $\mathscr{K}\forall q_j \in \prod_{i\in I}H_i$. So, $\wedge_{i\in I}(E_i, H_i)$ is a FS_Iover. □

Theorem 10. *Let $\{(E_i, H_i): i \in I\} \neq \varnothing$ be a family of FS_I over $\mathscr{K}$. Then $\vee_{i\in I}(E_i, H_i)$ is a FS_I over $\mathscr{K}$.*

Proof. Let $\vee_{i\in I}(E_i, H_i) = (C, \prod_{i\in I}H_i)$ where $C(q_j) = \vee_{j\in I}E_j(q_j)\forall\, q_j \in \prod_{i\in I}H_i$. Then for all $g, h \in \mathscr{K}$

$$\{C(q_j)\}(g\vee h) = \left\{\left\{\underset{j\in I}{\vee} E_j(q_j)\right\}(g\vee h) = \underset{j\in I}{\vee}\{(E_j(q_j))(g\vee h)\}\right. . \tag{60}$$

Since, $E_j(q)$ is a F_I of $\mathscr{K}$.

$$\begin{aligned}&= \underset{j\in I}{\vee}\{(E_j(q_j))(g)\wedge(E_j(q_j))(h)\}\\ &= \left[\underset{j\in I}{\vee}\{(E_j(q_j))(g)\}\right]\left[\underset{j\in I}{\vee}\{(E_j(q_j))(h)\}\right]\\ &= \left[\left\{\underset{j\in I}{\vee}(E_j(q_j))\right\}\right]\wedge\left[\left\{\underset{j\in I}{\vee}(E_j(q_j))\right\}\right]\\ &= \{(C(q_j))(g)\}\wedge\{(C(q_j))(h)\}.\end{aligned} \tag{61}$$

Now, for all $g, h \in \mathscr{K}$

$$\begin{aligned}\{C(q_j)\}(g\circledast h) &= \left\{\left\{\underset{j\in I}{\vee} E_j(q_j)\right\}(g\circledast h)\right\}\\ &= \underset{j\in I}{\vee}\{\mathrm{E}_j(q_j)(g\circledast h)\}.\end{aligned} \tag{62}$$

Since, $E_j(q)$ is a F_I of $\mathscr{K}$.

$$\begin{aligned}&\geq \underset{j\in I}{\vee}\{(E_j(q_j))(g)\vee(E_j(q_j))(h)\}\\ &= \left[\underset{j\in I}{\vee}\{(E_j(q_j))(g)\}\right]\vee\left[\vee_{j\in I}\{(E_j(q_j))(h)\}\right]\\ &= \left[\left\{\underset{j\in I}{\vee}(E_j(q_j))\right\}(g)\right]\vee\left[\left\{\underset{j\in I}{\vee}(E_j(q_j))\right\}(h)\right]\\ &= \{(C(q_j))(g)\}\vee\{(C(q_j))(h)\},\end{aligned} \tag{63}$$

$\Rightarrow C(q_j)$ is a F_I of $\mathscr{K}\forall q_j \in \prod_{i\in I}H_i$. So, $\vee_{i\in I}(E_i, H_i)$ is a FS_Iover.

Now some necessary characterizations about FSP_I and some important results pertaining to this definition are elaborated here. □

Definition 30. Let (Υ, J) be a FSST over a quantale $\mathscr{K}$. Then (Υ, J) is called fuzzy soft prime ideal (FSP_I) of $\mathscr{K}$ if $\Upsilon(q) \neq \varnothing$ is a FP_I of $\mathscr{K}\forall q \in J$.

Proposition 3. *Let $\{\mathscr{K}_i: i \in I\} \neq \varnothing$ be a family of quantales and $\{(E_i, H_i): i \in I\} \neq \varnothing$ be a family of FSST such that (E_i, H_i) is a FSP_I over $\mathscr{K}_i \forall i \in I$. Then E Product $\prod_{i\in I}(E_i, H_i)$ is a FSP_I over $\prod_{i\in I}\mathscr{K}_i$.*

Proof. By definition, $\forall(q_i) \in \prod_{i\in I}H_i$

$$\left(\tilde{\prod_{i\in I}} E_i(q_i)\right)(g) = \min_{i\in I}((E_i(q_i))(g_i)), \tag{64}$$

where $(g) = (g_i) \in \prod_{i\in I}\mathscr{K}_i$ and $E_i(q_i)$ is a FP_I of $\mathscr{K}_i \forall i \in I$.

Let $\prod_{i\in I}(E_i, H_i) = (C, \prod_{i\in I}H_i)$ where $C((q_i)) = \tilde{\prod_{i\in I}}E_i(q_i)\forall(q_i) \in \prod_{i\in I}H_i$. By Proposition 2, $\prod_{i\in I}(E_i, H_i)$ is F_I of $\mathscr{K}_i$.

Now, for all (g_i), $(h_i) \in \prod_{i\in I}\mathscr{K}_i$

$$\begin{aligned}\{C((q_i))\}((g_i)\circledast(h_i)) &= \left(\tilde{\prod_{i\in I}} E_i(q_i)\right)((g_i)\circledast(h_i))\\ &= \min_{i\in I}\{(E_i(q_i))((g_i)\circledast(h_i))\}\Big\}.\end{aligned} \tag{65}$$

Since, $E_i(q_i)$ is a FP_I of $\mathscr{K}_i$. So,

$$\begin{aligned}
&= \min_{i\in I}\{(E_i(q_i))(g_i)\text{or}(E_i(q_i))(h_i)\}\\
&= \left[\min_{i\in I}\{(E_i(q_i)(g_i))\}\right]\text{or}\left[\min_{i\in I}\{(E_i(q_i)(h_i))\}\right]\\
&= \left(\tilde{\prod_{i\in I}} E_i(q_i)\right)((g_i))\text{or}\left(\tilde{\prod_{i\in I}} E_i(q_i)\right)((h_i))\\
&= \{C((q_i))\}((g_i))\text{or}\{C((q_i))\}((h_i)).
\end{aligned} \tag{66}$$

This implies that $C((q_i))$ is a FP_I of $\prod_{i\in I}\mathscr{K}_i \forall (q_i) \in \prod_{i\in I} H_i$. Hence, $\prod_{i\in I}(E_i, H_i)$ is a FSP_I over $\prod_{i\in I}\mathscr{K}_i$. □

Theorem 11. *Let* $\{(E_i, H_i): i \in I\} \neq \varnothing$ *be a family of* FSP_I *over* $\mathscr{K}$. *Then* $\Cap_{i\in I}(E_i, H_i)$ *with* $\cap_{i\in I} H_i \neq \varnothing$ *is a* FSP_I *over* $\mathscr{K}$.

Proof. Let $\Cap_{i\in I}(E_i, H_i) = (C, \cap_{i\in I} H_i)$ where $C(q) = \wedge_{j\in I} E_j(q) q \in \cap_{i\in I} H_i$. By Theorem 5, $\Cap_{i\in I}(E_i, H_i)$ is F_I of $\mathscr{K}$.

Now, for all $g, h \in \mathscr{K}$

$$\begin{aligned}
\{C(q)\}(g \circledast h) &= \left\{\underset{j\in I}{\wedge} E_j(q)\right\}(g \circledast h)\\
&= \underset{j\in I}{\wedge}\left\{\left(E_j(q)\right)(g \circledast h)\right\}.
\end{aligned} \tag{67}$$

Since, $E_j(q)$ is a FP_I of $\mathscr{K}$. So,

$$\begin{aligned}
&= \underset{j\in I}{\wedge}\left\{\left(E_j(q)\right)(g)\text{or}\left(E_j(q)\right)(h)\right\}\\
&= \left[\underset{j\in I}{\wedge}\left\{\left(E_j(q)\right)(g)\right\}\right]\text{or}\left[\underset{j\in I}{\wedge}\left\{\left(E_j(q)\right)(h)\right\}\right]\\
&= \left[\left\{\underset{j\in I}{\wedge}\left(E_j(q)\right)\right\}(g)\right]\text{or}\left[\left\{\underset{j\in I}{\wedge}\left(E_j(q)\right)\right\}(h)\right]\\
&= \{(C(q))(g)\}\text{or}\{(C(q))(h)\},
\end{aligned} \tag{68}$$

$\Rightarrow C(q)$ is a FP_I of $\mathscr{K} \forall q \in \cap_{i\in I} H_i$. Thus, $\Cap_{i\in I}(E_i, H_i)$ is a FSP_Iover. □

Theorem 12. *Let* $\{(E_i, H_i): i \in I\} \neq \varnothing$ *be a family of* FSP_I *over* $\mathscr{K}$. *Then* $\overline{\Cap}_{i\in I}(E_i, H_i)$ *is a* FSP_I *over* $\mathscr{K}$.

Proof. Let $\overline{\Cap}_{i\in I}(E_i, H_i) = (C, \cup_{i\in I} H_i)$ where $C(q) = \wedge_{j\in\Theta(q)} E_j(q) \forall q \in \cup_{i\in I} H_i$. The set $\Theta(q)$ is defined as $\Theta(q) = \{j, q \in J_j\}$. By Theorem 6, $\overline{\Cap}_{i\in I}(E_i, H_i)$ is F_I of $\mathscr{K}$. Now, for all $g, h \in \mathscr{K}$

$$\begin{aligned}
\{C(q)\}(g \circledast h) &= \left\{\underset{j\in\Theta(q)}{\wedge} E_j(q)\right\}(g \circledast h)\\
&= \underset{j\in\Theta(q)}{\wedge}\left\{\left(E_j(q)\right)(g \circledast h)\right\}.
\end{aligned} \tag{69}$$

Since, $E_j(q)$ is a FP_I of $\mathscr{K}$. So,

$$\begin{aligned}
&= \underset{j\in\Theta(q)}{\wedge}\left\{\left(E_j(q)\right)(g)\text{or}\left(E_j(q)\right)(h)\right\}\\
&= \left[\underset{j\in\Theta(q)}{\wedge}\left\{\left(E_j(q)\right)(g)\right\}\right]\text{or}\left[\underset{j\in\Theta(q)}{\wedge}\left\{\left(E_j(g)\right)(h)\right\}\right]\\
&= \left[\left\{\underset{j\in\Theta(q)}{\wedge}\left(E_j(q)\right)\right\}(g)\right]\text{or}\left[\left\{\underset{j\in\Theta(q)}{\wedge}\left(E_j(q)\right)\right\}(h)\right]\\
&= \{(C(q))(g)\}\text{or}\{(C(q))(h)\},
\end{aligned} \tag{70}$$

$\Rightarrow C(q)$ is a FP_I of $\mathscr{K} \forall q \in \cup_{i\in I} H_i$. Thus, $\overline{\Cap}_{i\in I}(E_i, H_i)$ is a FSP_Iover. □

Theorem 13. *Let* $\{(E_i, H_i): i \in I\} \neq \varnothing$ *be a family of* FSP_I *over* $\mathscr{K}$. *Then* $\Cup_{i\in I}(E_i, H_i)$ *with* $\cap_{i\in I} H_i \neq \varnothing$ *is a* FSP_I *over* $\mathscr{K}$.

Proof. Let $\Cup_{i\in I}(E_i, H_i) = (C, \cap_{i\in I} H_i)$ where $C(q) = \vee_{j\in I} E_j(q) \forall q \in \cap_{i\in I} H_i$. By Theorem 7, $\Cup_{i\in I}(E_i, H_i)$ is F_I of $\mathscr{K}$.

Now, for all $g, h \in \mathscr{K}$

$$\begin{aligned}
\{C(q)\}(g \circledast h) &= \left\{\underset{j\in I}{\vee} E_j(q)\right\}(g \circledast h)\\
&= \underset{j\in I}{\vee}\left\{\left(E_j(q)\right)(g \circledast h)\right\}.
\end{aligned} \tag{71}$$

Since, $E_j(q)$ is a FP_I of $\mathscr{K}$.

$$\begin{aligned}
&= \vee_{j\in I}\left\{\left(E_j(q)\right)(g)\text{or}\left(E_j(q)\right)(h)\right\}\\
&= \left[\underset{j\in I}{\wedge}\left\{\left(E_j(q)\right)(g)\right\}\right]\text{or}\left[\underset{j\in I}{\wedge}\left\{\left(E_j(q)\right)(h)\right\}\right]\\
&= \left[\left\{\underset{j\in I}{\wedge}\left(E_j(q)\right)\right\}(g)\right]\text{or}\left[\left\{\underset{j\in I}{\wedge}\left(E_j(q)\right)\right\}(h)\right]\\
&= \{(C(q))(g)\}\text{or}\{(C(q))(h)\}.
\end{aligned} \tag{72}$$

$\Rightarrow C(q)$ is a FP_I of $\mathscr{K} \forall q \in \cap_{i\in I} H_i$. So, $\Cup_{i\in I}(E_i, H_i)$ is a FSP_Iover. □

Theorem 14. *Let* $\{(E_i, H_i): i \in I\} \neq \varnothing$ *be a family of* FSP_I *over* $\mathscr{K}$. *Then* $\Cup_{i\in I}(E_i, H_i)$ *is a* FSP_I *over* $\mathscr{K}$.

Proof. Let $\Cup_{i\in I}(E_i, H_i) = (C, \cup_{i\in I} H_i)$ where $C(q) = \vee_{j\in\Theta(q)} E_j(d) \forall q \in \cup_{i\in I} H_i$. The set $\Theta(q)$ is defined as $\Theta(q) = \{j, q \in J_j\}$. By Theorem 8, $\Cup_{i\in I}(E_i, H_i)$ is F_I of $\mathscr{K}$. Now, for all $g, h \in \mathscr{K}$

$$\begin{aligned}\{C(q)\}(g\circledast h) &= \left\{\underset{j\in\Theta(q)}{\vee} E_j(q)\right\}(g\circledast h)\\ &= \underset{j\in\Theta(q)}{\vee}\left\{\left(E_j(q)\right)(g\circledast h)\right\}.\end{aligned} \tag{73}$$

Since, $E_j(q)$ is a FP_I of $\mathscr{K}$.

$$\begin{aligned}&= \underset{j\in\Theta(q)}{\vee}\left\{\left(E_j(q)\right)(g)\text{or}\left(E_j(q)\right)(h)\right\}\\ &= \left[\underset{j\in\Theta(q)}{\vee}\left\{\left(E_j(q)\right)(g)\right\}\right]\text{or}\left[\underset{j\in\Theta(q)}{\vee}\left\{\left(E_j(q)\right)(h)\right\}\right]\\ &= \left[\left\{\underset{j\in\Theta(q)}{\vee}\left(E_j(q)\right)\right\}(g)\right]\text{or}\left[\left\{\underset{j\in\Theta(q)}{\vee}\left(E_j(q)\right)\right\}(h)\right]\\ &= \{(C(q))(g)\}\text{or}\{(C(q))(h)\},\end{aligned} \tag{74}$$

$\Rightarrow C(q)$ is a FP_I of $\mathscr{K}\forall q \in \cup_{i\in I}H_i$. So, $\cup_{i\in I}(E_i,H_i)$ is a FSP_I over $\mathscr{K}$. □

Theorem 15. *Let* $\{(E_i,H_i): i\in I\}\neq\varnothing$ *be a family of* FSP_I *over* $\mathscr{K}$. *Then* $\wedge_{i\in I}(E_i,H_i)$ *is a* FSP_I *over* $\mathscr{K}$.

Proof. Let $\wedge_{i\in I}(E_i,H_i) = (C,\prod_{i\in I}H_i)$ where $C(q_j) = \wedge_{j\in I}E_j(q_j)\forall q_j\in\prod_{i\in I}H_i$. By Theorem 9, $\wedge_{i\in I}(E_i,H_i)$ is F_I of $\mathscr{K}$. Now, for all $g,h\in\mathscr{K}$

$$\begin{aligned}\left(C\left(q_j\right)\right)(g\circledast h) &= \left\{\underset{j\in I}{\wedge}E_j\left(q_j\right)\right\}(g\circledast h)\\ &= \underset{j\in I}{\wedge}\left\{\left(E_j\left(q_j\right)\right)(g\circledast h)\right\}.\end{aligned} \tag{75}$$

Since, $E_j(q)$ is a FP_I of $\mathscr{K}$.

$$\begin{aligned}&= \underset{j\in I}{\wedge}\left\{\left(E_j\left(q_j\right)\right)(g)\text{or}\left(E_j\left(q_j\right)\right)(h)\right\}\\ &= \left[\underset{j\in I}{\wedge}\left\{\left(E_j\left(q_j\right)\right)(g)\right\}\right]\text{or}\left[\underset{j\in I}{\wedge}\left\{\left(E_j\left(q_j\right)\right)(h)\right\}\right]\\ &= \left[\left\{\underset{j\in I}{\wedge}\left(E_j\left(q_j\right)\right)\right\}(g)\right]\text{or}\left[\left\{\underset{j\in I}{\wedge}\left(E_j\left(q_j\right)\right)\right\}(h)\right]\\ &= \left\{\left(C\left(q_j\right)\right)(g)\right\}\text{or}\left\{\left(C\left(q_j\right)\right)(h)\right\},\end{aligned} \tag{76}$$

$\Rightarrow C(q_j)$ is a FP_I of $\mathscr{K}\forall q_j\in\prod_{i\in I}H_i$. So, $\wedge_{i\in I}(E_i,H_i)$ is a FSP_Iover. □

Theorem 16. *Let* $\{(E_i,H_i): i\in I\}\neq\varnothing$ *be a family of* FSP_I *over* $\mathscr{K}$. *Then* $\wedge_{i\in I}(E_i,H_i)$ *is a* FSP_I *over* $\mathscr{K}$.

Proof. Let $\vee_{i\in I}(E_i,H_i) = (C,\prod_{i\in I}H_i)$ where $C(q_j) = \vee_{j\in I}E_j(q_j),\forall q_j\in\prod_{i\in I}H_i$. By Theorem 10, $\vee_{i\in I}(E_i,H_i)$ is F_I of $\mathscr{K}$. Now, for $g,h\in\mathscr{K}$

$$\begin{aligned}\left\{C\left(q_j\right)\right\}(g\circledast h) &= \left\{\underset{j\in I}{\vee}E_j\left(q_j\right)\right\}(g\circledast h)\\ &= \underset{j\in I}{\vee}\left\{\left(E_j\left(q_j\right)\right)(g\circledast h)\right\}.\end{aligned} \tag{77}$$

Since, $E_j(q)$ is a FP_I of $\mathscr{K}$.

$$\begin{aligned}&= \underset{j\in I}{\vee}\left\{\left(E_j\left(q_j\right)\right)(g)\text{or}\left(E_j\left(q_j\right)\right)(h)\right\}\\ &= \left[\underset{j\in I}{\vee}\left\{\left(E_j\left(q_j\right)\right)(g)\right\}\right]\text{or}\left[\underset{j\in I}{\vee}\left\{\left(E_j\left(q_j\right)\right)(h)\right\}\right]\\ &= \left[\left\{\underset{j\in I}{\vee}\left(E_j\left(q_j\right)\right)\right\}(g)\right]\text{or}\left[\left\{\underset{j\in I}{\vee}\left(E_j\left(q_j\right)\right)\right\}(h)\right]\\ &= \left\{\left(C\left(q_j\right)\right)g\right\}\text{or}\left\{\left(C\left(q_j\right)\right)(h)\right\},\end{aligned} \tag{78}$$

$\Rightarrow C(q_j)$ is a FP_I of $\mathscr{K}\forall q_j\in\prod_{i\in I}H_i$. So, $\vee_{i\in I}(E_i,H_i)$ is a FSP_I over $\mathscr{K}$.

Now some necessary characterizations about FSSP_I and some important results pertaining to this definition are elaborated here. □

Definition 31. Let (Υ,J) be a FSST over a quantale $\mathscr{K}$. Then (Υ,J) is called FSSP_I of $\mathscr{K}$ if $\Upsilon(q)\neq\varnothing$ is a F_SP_I of $\mathscr{K}\forall q\in J$.

Proposition 4. *Let* $\{\mathscr{K}_i: i\in I\}\neq\varnothing$ *be a family of quantales and* $\{(E_i,H_i): i\in I\}\neq\varnothing$ *be a family of* FSST *such that* (E_i,H_i) *is a* FSSP_I *over* $\mathscr{K}_i\forall i\in I$. *Then E Product* $\prod_{i\in I}(E_i,H_i)$ *is a* FSSP_I *over* $\prod_{i\in I}\mathscr{K}_i$.

Proof. By definition, $\forall(q_i)\in\prod_{i\in I}H_i$

$$\left(\tilde{\prod_{i\in I}}E_i(q_i)\right)(g) = \min_{i\in I}((E_i(q_i))(g_i)), \tag{79}$$

where $(g) = (g_i)\in\prod_{i\in I}\mathscr{K}_i$ and $E_i(q_i)$ is a F_SP_I of $\mathscr{K}_i\forall i\in I$.

Let $\prod_{i\in I}(E_i,H_i) = (C,\prod_{i\in I}H_i)$ where $C((q_i)) = \tilde{\prod_{i\in I}}E_i(q_i)\forall(q_i)\in\prod_{i\in I}H_i$. Since $\{(E_i,H_i): i\in I\}$ is FSSP_I. By Proposition 2, $\prod_{i\in I}(E_i,H_i)$ is F_I of $\mathscr{K}_i$.

Now, for all $(q_i)\in\prod_{i\in I}\mathscr{K}_i$

$$\begin{aligned}\{C((q_i))\}(g_i\circledast g_i) &= \left(\tilde{\prod_{i\in I}}E_i(q_i)\right)((g_i\circledast g_i))\\ &= \min_{i\in I}((E_i(q_i))(g_i\circledast g_i)).\end{aligned} \tag{80}$$

Since, $E_i(q_i)$ is a F_SP_I of $\mathscr{K}_i$. So,

$$\begin{aligned}&= \min_{i\in I}\{(E_i(q_i))(g_i)\}\\ &= \left[\min_{i\in I}\{(E_i(q_i))(g_i)\}\right]\\ &= \left(\tilde{\prod_{i\in I}}E_i(q_i)\right)((g_i))\\ &= \{C((q_i))\}((g_i)).\end{aligned} \tag{81}$$

This implies that $C((q_i))$ is a F_SP_I of $\prod_{i\in I}\mathscr{K}_i\forall(q_i)\in\prod_{i\in I}H_i$. Hence, $\prod_{i\in I}(E_i,H_i)$ is a FSSP_I over $\prod_{i\in I}\mathscr{K}_i$. □

Theorem 17. *Let* $\{(E_i, H_i): i \in I\} \neq \varnothing$ *be a family of* FSSP_I *over* $\mathscr{K}$. *Then* $\circledcirc_{i\in I}(E_i, H_i)$ *with* $\cap_{i\in I} H_i \neq \varnothing$ *is a* FSSP_I *over* $\mathscr{K}$.

Proof. Let $\circledcirc_{i\in I}(E_i, H_i) = (C, \cap_{i\in I} H_i)$ where $C(q) = \wedge_{j\in I} E_j(q) \forall q \in \cap_{i\in I} H_i$. Since $\{(E_i, H_i): i \in I\}$ is FSSP_I. By Theorem 5, $\circledcirc_{i\in I}(E_i, H_i)$ is F_I of $\mathscr{K}$.

Now, for all $g \in \mathscr{K}$

$$\begin{aligned}\{C(q)\}(g \circledast g) &= \left\{\bigwedge_{j\in I} E_j(q)\right\}(g \circledast g)\\ &= \bigwedge_{j\in I}\left\{\left(E_j(q)\right)(g \circledast g)\right\}.\end{aligned} \tag{82}$$

Since, $E_j(q)$ is a $F_S P_I$ of $\mathscr{K}$. So,

$$\begin{aligned}&= \bigwedge_{j\in I}\left\{\left(E_j(q)\right)(g)\right\}\\ &= \left[\left\{\bigwedge_{j\in I}\left(E_j(q)\right)\right\}(g)\right]\\ &= \{(C(q))(g)\},\end{aligned} \tag{83}$$

$\Rightarrow C(q)$ is a $F_S P_I$ of $\mathscr{K} \forall q \in \cap_{i\in I} H_i$. Thus, $\circledcirc_{i\in I}(E_i, H_i)$ is a FSSP_I over $\mathscr{K}$. □

Theorem 18. *Let* $\{(E_i, H_i): i \in I\} \neq \varnothing$ *be a family of* FSSP_I *over* $\mathscr{K}$. *Then* $\bar{\cap}_{i\in I}(E_i, H_i)$ *is a* FSSP_I *over* $\mathscr{K}$.

Proof. Let $\bar{\cap}_{i\in I}(E_i, H_i) = (C, \cup_{i\in I} H_i)$ where $C(q) = \wedge_{j\in\Theta(q)} E_j(q) \forall q \in \cup_{i\in I} H_i$. The set $\Theta(q)$ is defined as $\Theta(q) = \{j, q \in J_j\}$. By Theorem 6, $\bar{\cap}_{i\in I}(E_i, H_i)$ is F_I of $\mathscr{K}$. Now, for all $g \in \mathscr{K}$

$$\begin{aligned}\{C(q)\}(g \circledast g) &= \left\{\bigwedge_{j\in\Theta(q)} E_j(q)\right\}(g \circledast g)\\ &= \bigwedge_{j\in\Theta(q)}\left\{\left(E_j(q)\right)(g \circledast g)\right\}.\end{aligned} \tag{84}$$

Since, $E_j(q)$ is a $F_S P_I$ of $\mathscr{K}$. So,

$$\begin{aligned}&= \bigwedge_{j\in\Theta(q)}\left\{\left(E_j(q)\right)(g)\right\}\\ &= \left[\bigwedge_{j\in\Theta(q)}\left\{\left(E_j(q)\right)(g)\right\}\right]\\ &= \left[\left\{\bigwedge_{j\in\Theta(q)}\left(E_j(q)\right)\right\}(g)\right]\\ &= \{(C(q))(g)\},\end{aligned} \tag{85}$$

$\Rightarrow C(q)$ is a $F_S P_I$ of $\mathscr{K} \forall q \in \cup_{i\in I} H_i$. Thus, $\bar{\cap}_{i\in I}(E_i, H_i)$ is a FSSP_Iover. □

Theorem 19. *Let* $\{(E_i, H_i): i \in I\} \neq \varnothing$ *be a family of* FSSP_I *over* $\mathscr{K}$. *Then* $\uplus_{i\in I}(E_i, H_i)$ *with* $\cap_{i\in I} H_i \neq \varnothing$ *is a* FSSP_I *over* $\mathscr{K}$.

Proof. Let $\uplus_{i\in I}(E_i, H_i) = (C, \cap_{i\in I} H_i)$ where $C(q) = \vee_{j\in I} E_j(q) \forall q \in \cap_{i\in I} H_i$. By Theorem 7, $\uplus_{i\in I}(E_i, H_i)$ is F_I of $\mathscr{K}$. Now, for all $g \in \mathscr{K}$

$$\begin{aligned}\{C(q)\}(g \circledast g) &= \left\{\bigvee_{j\in I} E_j(q)\right\}(g \circledast g)\\ &= \bigvee_{j\in I}\left\{\left(E_j(q)\right)(g \circledast g)\right\}.\end{aligned} \tag{86}$$

Since, $E_j(q)$ is a $F_S P_I$ of $\mathscr{K}$.

$$\begin{aligned}&= \bigvee_{j\in I}\left\{\left(E_j(q)\right)(g)\right\}\\ &= \left[\bigvee_{j\in I}\left\{\left(E_j(q)\right)(g)\right\}\right]\\ &= \left[\left\{\bigvee_{j\in I}\left(E_j(q)\right)\right\}(g)\right]\\ &= \{(C(q))(g)\},\end{aligned} \tag{87}$$

$\Rightarrow C(q)$ is a $F_S P_I$ of $\mathscr{K} \forall q \in \cap_{i\in I} H_i$. So, $\uplus_{i\in I}(E_i, H_i)$ is a FSSP_I over $\mathscr{K}$. □

Theorem 20. *Let* $\{(E_i, H_i): i \in I\} \neq \varnothing$ *be a family of* FSSP_I *over* $\mathscr{K}$. *Then* $\cup_{i\in I}(E_i, H_i)$ *is a* FSSP_I *over* $\mathscr{K}$.

Proof. Let $\cup_{i\in I}(E_i, H_i) = (C, \cup_{j\in I} H_i)$ where $C(q) = \wedge_{j\in\Theta(q)} E_j(q) \forall q \in \cup_{j\in I} H_i$. The set $\Theta(q)$ is defined as $\Theta(q) = \{j, q \in J_j\}$. By Theorem 8, $\cup_{i\in I}(E_i, H_i)$ is F_I of $\mathscr{K}$. Now, for all $g \in \mathscr{K}$

$$\begin{aligned}\{C(q)\}(g \circledast g) &= \left\{\bigvee_{j\in\Theta(q)} E_j(q)\right\}(g \circledast g)\\ &= \bigvee_{j\in\Theta(q)}\left\{\left(E_j(q)\right)(g \circledast g)\right\}.\end{aligned} \tag{88}$$

Since, $E_j(q)$ is a $F_S P_I$ of $\mathscr{K}$.

$$\begin{aligned}&= \bigwedge_{j\in\Theta(q)}\left\{\left(E_j(q)\right)(g)\right\}\\ &= \left[\bigwedge_{j\in\Theta(q)}\left\{\left(E_j(q)\right)(g)\right\}\right]\\ &= \left[\left\{\bigwedge_{j\in\Theta(q)}\left(E_j(q)\right)\right\}(g)\right]\\ &= \{(C(q))(g)\},\end{aligned} \tag{89}$$

$\Rightarrow C(q)$ is a $F_S P_I$ of $\mathscr{K} \forall d \in \cup_{i\in I} H_i$. So, $\cup_{i\in I}(E_i, H_i)$ is a FSSP_Iover. □

Theorem 21. *Let* $\{(E_i, H_i): i \in I\} \neq \varnothing$ *be a family of* FSSP_I *over* $\mathscr{K}$. *Then* $\wedge_{i\in I}(E_i, H_i)$ *is a* FSSP_I *over* $\mathscr{K}$.

Proof. Let $\wedge_{i\in I}(E_i, H_i) = (C, \prod_{i\in I} H_i)$ where $C(q_j) = \wedge_{i\in I} E_j(q_j) \forall q_j \in \prod_{i\in I} H_i$. By Theorem 3.15, $\wedge_{i\in I}(E_i, H_i)$ is F_I of $\mathscr{K}$. Now, for all $g \in \mathscr{K}$

$$\begin{aligned}\{C(q_j)\}(g \circledast g) &= \left\{\underset{j\in I}{\wedge} E_j(q_j)\right\}(g \circledast g)\\ &= \underset{j\in I}{\wedge}\{(E_j(q_j))(g \circledast g)\}.\end{aligned} \tag{90}$$

Since, $E_j(q)$ is a $F_S P_I$ of $\mathscr{K}$.

$$\begin{aligned}&= \underset{j\in I}{\wedge}\{(E_j(q_j))(g)\}\\ &= \left[\underset{j\in I}{\wedge}\{(E_j(q_j))(g)\}\right]\\ &= \left[\left\{\underset{j\in I}{\wedge}(E_j(q_j))\right\}(g)\right]\\ &= \{(C(q_j))(g)\},\end{aligned} \tag{91}$$

$\Rightarrow C(q_j)$ is a $F_S P_I$ of $\mathscr{K} \forall d_j \in \prod_{i\in I} H_i$. So, $\wedge_{i\in I}(E_i, H_i)$ is a FSSP_Iover. □

Theorem 22. *Let* $\{(E_i, H_i): i \in I\} \neq \varnothing$ *be a family of* FSSP_I *over* $\mathscr{K}$. *Then* $\vee_{i\in I}(E_i, H_i)$ *is a* FSSP_I *over* $\mathscr{K}$.

Proof. Let $\vee_{i\in I}(E_i, H_i) = (C, \prod_{i\in I} H_i)$ where $C(q_j) = \vee_{j\in I} E_j(q_j) \forall q_j \in \prod_{i\in I} H_i$. By Theorem 10, $\vee_{i\in I}(E_i, H_i)$ is F_I of $\mathscr{K}$. Now, for all $g \in \mathscr{K}$

$$\begin{aligned}\{C(q_j)\}(g \circledast g) &= \left(\underset{j\in I}{\vee} E_j(q_j)\right)(g \circledast g)\\ &= \underset{j\in I}{\vee}\{(E_j(q_j))(g \circledast g)\}.\end{aligned} \tag{92}$$

Since, $E_j(q)$ is a $F_S P_I$ of $\mathscr{K}$.

$$\begin{aligned}&= \underset{j\in I}{\vee}\{(E_j(q_j))(g)\}\\ &= \left[\underset{j\in I}{\vee}\{(E_j(q_j))(g)\}\right]\\ &= \left[\left\{\underset{j\in I}{\vee}(E_j(q_j))\right\}(g)\right]\\ &= \{(C(q_j))(g)\},\end{aligned} \tag{93}$$

$\Rightarrow C(q_j)$ is a $F_S P_I$ of $\mathscr{K} \forall q_j \in \prod_{i\in I} H_i$. So, $\vee_{i\in I}(E_i, H_i)$ is a FSSP_Iover.

Now some necessary characterizations about FSPR_I and some important results pertaining to this definition are elaborated here. □

Definition 32. Let (Υ, J) be a FSST over a quantale $\mathscr{K}$. Then (Υ, J) is called fuzzy soft primary ideal FSPR_I of $\mathscr{K}$ if $\Upsilon(q) \neq \varnothing$ is a FPR_I of $\mathscr{K} \forall q \in J$.

Proposition 5. *Let* $\{\mathscr{K}_i: i \in I\} \neq \varnothing$ *be a family of quantales and* $\{(E_i, H_i): i \in I\} \neq \varnothing$ *be a family of* FSST, *such that* (E_i, H_i) *is a* FSPR_I *over* $\mathscr{K}_i \forall i \in I$. *Then E Product* $\prod_{i\in I}(E_i, H_i)$ *is a* FSPR_I *over* $\prod_{i\in I} \mathscr{K}_i$.

Proof. By definition, $\forall (q_i) \in \prod_{i\in I} H_i$

$$\left(\tilde{\prod_{i\in I}} E_i(q_i)\right)(g) = \min_{i\in I}((E_i(q_i))(g_i)), \tag{94}$$

where $(g) = (g_i) \in \prod_{i\in I} \mathscr{K}_i$ and $E_i(q_i)$ is a FPR_I of $\mathscr{K}_i \forall i \in I$.

Let $\prod_{i\in I}(E_i, H_i) = (C, \prod_{i\in I} H_i)$ where $C((q_i)) = \tilde{\prod_{i\in I}} E_i(q_i) \forall (q_i) \in \prod_{i\in I} H_i$. Since $\{(E_i, H_i): i \in I\}$ is a FSPR_I. By Proposition 2, $\prod_{i\in I}(E_i, H_i)$ is F_I of $\mathscr{K}_i$. Now, for all $(g_i), (h_i) \in \prod_{i\in I} \mathscr{K}_i$

$$\begin{aligned}\{C((q_i))\}((g_i) \circledast (h_i)) &= \left(\tilde{\prod_{i\in I}} E_i(q_i)\right)((g_i) \circledast (h_i))\\ &= \min_{i\in I}\left((E_i(q_i))(g_i) \circledast \left(h_i^{i\in I}\right)\right).\end{aligned} \tag{95}$$

Since, $E_i(q_i)$ is a FPR_I of $\mathscr{K}_i$. So,

$$\begin{aligned}&= \min_{i\in I}\{(E_i(q_i))(g_i) \text{or} (E_i(q_i))((h_i)^n)\}\\ &= \left[\min_{i\in I}\{(E_i(q_i))(g_i)\} \text{or} \min_{i\in I}\{(E_i(q_i))(h_i)^n\}\right]\\ &= \left(\tilde{\prod_{i\in I}} E_i(q_i)\right)((g_i)) \text{or} \left(\tilde{\prod_{i\in I}} E_i(q_i)\right)((h_i)^n)\\ &= \{C((q_i))\}((g_i)) \text{or} \{C((q_i))\}((h_i)^n),\end{aligned} \tag{96}$$

where

$$\begin{aligned}(h_i)^n &= h_i \circledast h_i \circledast \cdots \circledast h_i \in \{C(q_i)\}(h_i) \circledast \{C(q_i)\}(h_i) \circledast \cdots\\ &\circledast \{C(q_i)\}(h_i) = \{C(q_i)\}(h_i \circledast h_i \circledast \cdots \circledast h_i)\\ &= \{C(q_i)\}((h_i)^n),\end{aligned} \tag{97}$$

where $n \in \mathbb{N}$. This implies that $C((q_i))$ is a FPR_I of $\prod_{i\in I} \mathscr{K}_i \forall (q_i) \in \prod_{i\in I} H_i$. Thus, $\prod_{i\in I}(E_i, H_i)$ is a FSPR_I over $\prod_{i\in I} \mathscr{K}_i$. □

Theorem 23. *Let* $\{(E_i, H_i): i \in I\} \neq \varnothing$ *be a family of* FSPR_I *over* $\mathscr{K}$. *Then* $\Cap_{i\in I}(E_i, H_i)$ *with* $\cap_{i\in I} H_i \neq \varnothing$ *is a* FSPR_I *over* $\mathscr{K}$.

Proof. Let $\Cap_{i\in I}(E_i, H_i) = (C, \cap_{i\in I} H_i)$ where $C(q) = \wedge_{j\in I} E_j(q) \forall q \in \cap_{i\in I} H_i$. By Theorem 5, $\Cap_{i\in I}(E_i, H_i)$ is F_I of $\mathscr{K}$. Now, for all $g, h \in \mathscr{K}$

$$\begin{aligned}\{C(q)\}(g \circledast h) &= \underset{j\in I}{\wedge}\{E_j(q)\}(g \circledast h)\}\\ &= \underset{j\in I}{\wedge}\{E_j(q)\}(g \circledast h)\}.\end{aligned} \tag{98}$$

Since, $E_j(q)$ is a FPR_I of $\mathscr{K}$. So,

$$\begin{aligned}&= \underset{j\in I}{\wedge}\{(E_j(q))(g) \text{or} (E_j(q))(h^n)\}\\ &= \left[\underset{j\in I}{\wedge}\{(E_j(q))(g)\}\right] \text{or} \left[\underset{j\in I}{\wedge}\{(E_j(q))(h^n)\}\right]\\ &= \{(C(q))(g)\} \text{or} \{(C(q))(h^n)\},\end{aligned} \tag{99}$$

where

$$\begin{aligned}(h)^n &= h\circledast h\circledast\cdots\circledast h \in \{C(q)\}(h)\\ &\quad \circledast\{C(q)\}(h)\circledast\cdots\circledast\{C(q)\}(h)\\ &= \{C(q)\}(h\circledast h\circledast\ldots\circledast h)\\ &= \{C(q)\}(h^n),\end{aligned} \tag{100}$$

where $n \in \mathbb{N}$. This implies that $C(q)$ is a FPR_I of $\forall q \in \cap_{i\in I}H_i$. Thus, $\circledcirc_{i\in I}(E_i, H_i)$ is a FSPR_I over $\mathscr{K}$. □

Theorem 24. *Let $\{(E_i, H_i)\colon i \in I\} \neq \varnothing$ be a family of FSPR_I over $\mathscr{K}$. Then $\bar{\cap}_{i\in I}(E_i, H_i)$ is a FSPR_I over $\mathscr{K}$.*

Proof. Let $\bar{\cap}_{i\in I}(E_i, H_i) = (C, \cup_{i\in I}H_i)$ where $C(q) = \wedge_{j\in\Theta(q)}E_j(q)\forall q \in \cup_{i\in I}H_i$. The set $\Theta(q)$ is defined as $\Theta(q) = \{j, q \in J_j\}$. By Theorem 6, $\bar{\cap}_{i\in I}(E_i, H_i)$ is F_I of $\mathscr{K}$. Now, for all $g, h \in \mathscr{K}$

$$\begin{aligned}\{C(q)\}(g\circledast h) &= \left\{\underset{j\in\Theta(q)}{\wedge}E_j(q)\right\}(g\circledast h)\\ &= \underset{j\in\Theta(q)}{\wedge}\left\{\left(E_j(q)\right)(g\circledast h)\right\}.\end{aligned} \tag{101}$$

Since, $E_j(q)$ is a FPR_I of $\mathscr{K}$. So,

$$\begin{aligned}&\underset{j\in\Theta(q)}{\wedge}\left\{\left(E_j(q)\right)(g)\mathrm{or}\left(E_j(q)\right)(h^n)\right\}\\ &= \left[\underset{j\in\Theta(q)}{\wedge}\left\{\left(E_j(q)\right)(g)\right\}\right]\mathrm{or}\left[\underset{j\in\Theta(q)}{\wedge}\left\{\left(E_j(q)\right)(h^n)\right\}\right]\\ &= \left[\underset{j\in\Theta(q)}{\wedge}\left\{\left(E_j(q)\right)\right\}(g)\right]\mathrm{or}\left[\underset{j\in\Theta(q)}{\wedge}\left\{\left(E_j(q)\right)\right\}(h^n)\right]\\ &= \{(C(q))(g)\}\mathrm{or}\{(C(q))(h^n)\},\end{aligned} \tag{102}$$

where

$$\begin{aligned}(h)^n &= h\circledast h\circledast\cdots\circledast h \in \{C(q)\}(h)\\ &\quad \circledast\{C(q)\}(h)\circledast\cdots\circledast\{C(q)\}(h)\\ &= \{C(q)\}(h\circledast h\circledast\ldots\circledast h)\\ &= \{C(q)\}(h^n),\end{aligned} \tag{103}$$

where $n \in \mathbb{N}$. This implies that $C(q)$ is a FPR_I of $\forall q \in \cup_{i\in I}H_i$. Thus, $\bar{\cap}_{i\in I}(E_i, H_i)$ is a FSPR_I over $\mathscr{K}$. □

Theorem 25. *Let $\{(E_i, H_i)\colon i \in I\} \neq \varnothing$ be a family of FSPR_I over $\mathscr{K}$. Then $\uplus_{i\in I}(E_i, H_i)$ with $\overset{\cap}{i\in I}H_i \neq \varnothing$ is a FSPR_I over $\mathscr{K}$.*

Proof. Let $\uplus_{i\in I}(E_i, H_i) = (C, \cap_{i\in I}H_i)$ where $C(q) = \vee_{j\in I}E_j(q)\forall q \in \cap_{i\in I}H_i$. By Theorem 3.13, $\uplus_{i\in I}(E_i, H_i)$ is F_I of $\mathscr{K}$. Now, for all $g, h \in \mathscr{K}$

$$\begin{aligned}\{C(q)\}(g\circledast h) &= \left\{\underset{j\in I}{\vee}E_j(q)(g\circledast h)\right\}\\ &= \underset{j\in I}{\vee}\left\{\left(E_j(q)\right)(g\circledast h)\right\}.\end{aligned} \tag{104}$$

Since, $E_j(q)$ is a FPR_I of $\mathscr{K}$.

$$\begin{aligned}&= \overset{\vee}{j\in I}\left\{\left(E_j(q)\right)(g)\mathrm{or}\left(E_j(q)\right)(h^n)\right\}\\ &= \left[\overset{\vee}{j\in I}\left\{\left(E_j(q)\right)(g)\right\}\right]\mathrm{or}\left[\overset{\vee}{j\in I}\left\{\left(E_j(q)\right)(h^n)\right\}\right]\\ &= \left[\left\{\overset{\vee}{j\in I}\left(E_j(q)\right)(g)\right\}\right]\mathrm{or}\left[\left\{\overset{\vee}{j\in I}\left(E_j(q)\right)(h^n)\right\}\right]\\ &= \{(C(q))(g)\}\mathrm{or}\{(C(q))(h^n)\},\end{aligned} \tag{105}$$

where

$$\begin{aligned}(h)^n &= h\circledast h\circledast\cdots\circledast h \in \{C(q)\}(h)\\ &\quad \circledast\{C(q)\}(h)\circledast\cdots\circledast\{C(q)\}(h)\\ &= \{C(q)\}(h\circledast h\circledast\ldots\circledast h)\\ &= \{C(q)\}(h^n),\end{aligned} \tag{106}$$

where $n \in \mathbb{N}$. This implies that $C(q)$ is a FPR_I of $\forall q \in \overset{\cap}{i\in I}H_i$. So, $\overset{\uplus}{i\in I}(E_i, H_i)$ is a FSPR_I over $\mathscr{K}$. □

Theorem 26. *Let $\{(E_i, H_i)\colon i \in I\} \neq \varnothing$ be a family of FSPR_I over $\mathscr{K}$. Then $\overset{\cup}{i\in I}(E_i, H_i)$ is a FSPR_I over $\mathscr{K}$.*

Proof. Let $\overset{\cup}{i\in I}(E_i, H_i) = (C, \overset{\cup}{i\in I}H_i)$ where $C(q) = \overset{\vee}{j\in\Theta(q)}E_j(q)\forall q \in \overset{\cup}{i\in I}H_i$. The set $\Theta(q)$ is defined as $\Theta(q) = \{j, q \in J_j\}$. By Theorem 8, $\overset{\cup}{i\in I}(E_i, H_i)$ is F_I of $\mathscr{K}$. Now, for all $g, h \in \mathscr{K}$

$$\begin{aligned}\{C(q)\}(g\circledast h) &= \left\{\overset{\vee}{j\in\Theta(q)}E_j(q)\right\}(g\circledast h)\\ &= \overset{\vee}{j\in\Theta(q)}\left(E_j(q)(g\circledast h)\right).\end{aligned} \tag{107}$$

Since, $E_j(q)$ is a FPR_I of $\mathscr{K}$.

$$\begin{aligned}&= \overset{\vee}{j\in\Theta(q)}\left\{\left(E_j(q)\right)(g)or\left(E_j(q)\right)(h^n)\right\}\\ &= \left[\overset{\vee}{j\in\Theta(q)}\left\{\left(E_j(q)\right)(g)\right\}\right]\mathrm{or}\left[\overset{\vee}{j\in\Theta(q)}\left\{\left(E_j(q)\right)(h^n)\right\}\right]\\ &= \left[\left\{\overset{\vee}{j\in\Theta(q)}\left(E_j(q)\right)\right\}(g)\right]\mathrm{or}\left[\left\{\overset{\vee}{j\in\Theta(q)}\left\{\left(E_j(q)\right)\right\}(h^n)\right\}\right]\\ &= \{(C(q))(g)\}\mathrm{or}\{(C(q))(h^n)\},\end{aligned} \tag{108}$$

where

$$\begin{aligned}(h)^n &= h\circledast h\circledast\cdots\circledast h \in \{C(q)\}(h)\\ &\quad \circledast\{C(q)\}(h)\circledast\cdots\circledast\{C(q)\}(h)\\ &= \{C(q)\}(h\circledast h\circledast\ldots\circledast h)\\ &= \{C(q)\}(h^n),\end{aligned} \tag{109}$$

where $n \in \mathbb{N}$. This implies that $C(q)$ is a FPR_I of $\forall q \in \overset{\cup}{i\in I}H_i$. So, $\overset{\uplus}{i\in I}(E_i, H_i)$ is a FSPR_I over $\mathscr{K}$. □

Theorem 27. *Let $\{(E_i, H_i)\colon i \in I\} \neq \varnothing$ be a family of FSPR_I over $\mathscr{K}$. Then $\overset{\wedge}{i\in I}(E_i, H_i)$ is a FSPR_I over $\mathscr{K}$.*

Proof. Let $\overset{\wedge}{i\in I}(E_i, H_i) = (C, \prod_{i\in I}H_i)$ where $C(q_j) = \overset{\wedge}{j\in I}E_j(q_j)\forall q_j \in \prod_{i\in I}H_i$. By Theorem 9, $\overset{\wedge}{i\in I}(E_i, H_i)$ is F_I of $\mathscr{K}$. Now, for all $g, h \in \mathscr{K}$

$$\begin{aligned}\left\{C\left(q_j\right)\right\}(g\circledast h) &= \left\{\overset{\wedge}{}_{j\in I}E_j\left(q_j\right)\right\}(g\circledast h)\\ &= \overset{\wedge}{}_{j\in I}\left(E_j\left(q_j\right)(g\circledast h)\right).\end{aligned} \tag{110}$$

Since, $E_j(q)$ is a FPR_I of $\mathscr{K}$.

$$\begin{aligned}&= \overset{\wedge}{}_{j\in I}\left\{\left(E_j\left(q_j\right)\right)(g)\mathrm{or}\left(E_j\left(q_j\right)\right)(h^n)\right\}\\ &= \left[\overset{\wedge}{}_{j\in I}\left\{\left(E_j\left(q_j\right)\right)(g)\right\}\right]\mathrm{or}\left[\overset{\wedge}{}_{j\in I}\left\{\left(E_j\left(q_j\right)\right)(h^n)\right\}\right]\\ &= \left[\overset{\wedge}{}_{j\in I}\left\{\left(E_j\left(q_j\right)\right)\right\}(g)\right]\mathrm{or}\left[\left\{\overset{\wedge}{}_{j\in I}\left(E_j\left(q_j\right)\right)\right\}(h^n)\right]\\ &= \left\{\left(C\left(q_j\right)\right)(g)\right\}\mathrm{or}\left\{\left(C\left(q_j\right)\right)(h^n)\right\}.\end{aligned} \tag{111}$$

where

$$\begin{aligned}(h)^n &= h\circledast h\circledast\cdots\circledast h\in\{C(q)\}(h)\\ &\quad\circledast\{C(q)\}(h)\circledast\cdots\circledast\{C(q)\}(h)\\ &= \{C(q)\}(h\circledast h\circledast\cdots\circledast h)\\ &= \{C(q)\}(h^n),\end{aligned} \tag{112}$$

where $n\in\mathbb{N}$. This implies that $C(q_j)$ is a FPR_I of $\forall q_j\in\prod_{i\in I}H_i$. So, $\overset{\wedge}{}_{i\in I}(E_i,H_i)$ is a FSPR_I over $\mathscr{K}$. □

Theorem 28. *Let* $\{(E_i,H_i): i\in I\}\neq\varnothing$ *be a family of* FSPR_I *over* $\mathscr{K}$. *Then* $\overset{\wedge}{}_{i\in I}(E_i,H_i)$ *is a* FSPR_I *over* $\mathscr{K}$.

Proof. Let $\overset{\vee}{}_{i\in I}(E_i,H_i)=(C,\prod_{i\in I}H_i)$ where $C(q_j)=\overset{\vee}{}_{j\in I}E_j(q_j)\forall\prod_{i\in I}H_i$. By Theorem 10, $\overset{\vee}{}_{i\in I}(E_i,H_i)$ is F_I of $\mathscr{K}$. Now, for all $g,h\in\mathscr{K}$

$$\begin{aligned}\left\{C\left(q_j\right)\right\}(g\circledast h) &= \left\{\overset{\vee}{}_{j\in I}E_j\left(q_j\right)\right\}(g\circledast h)\\ &= \overset{\vee}{}_{j\in I}\left\{\left(E_j\left(q_j\right)\right)(g\circledast h)\right\}.\end{aligned} \tag{113}$$

Since, $E_j(q)$ is a FPR_I of $\mathscr{K}$.

$$\begin{aligned}&= \overset{\vee}{}_{j\in I}\left\{\left(E_j\left(q_j\right)\right)(g)\mathrm{or}\left(E_j\left(q_j\right)\right)(h^n)\right\}\\ &= \left[\overset{\vee}{}_{j\in I}\left\{\left(E_j\left(q_j\right)\right)(g)\right\}\right]\mathrm{or}\left[\overset{\vee}{}_{j\in I}\left\{\left(E_j\left(q_j\right)\right)(h^n)\right\}\right]\\ &= \left[\overset{\vee}{}_{j\in I}\left(E_j\left(q_j\right)\right)(g)\right]\mathrm{or}\left[\overset{\vee}{}_{j\in I}\left(E_j\left(q_j\right)\right)(h^n)\right]\\ &= \left\{\left(C\left(q_j\right)\right)(g)\right\}\mathrm{or}\left\{\left(C\left(q_j\right)\right)(h^n)\right\},\end{aligned} \tag{114}$$

where

$$\begin{aligned}(h)^n &= h\circledast h\circledast\cdots\circledast h\in\{C(q)\}(h)\\ &\quad\circledast\{C(q)\}(h)\circledast\cdots\circledast\{C(q)\}(h)\\ &= \{C(q)\}(h\circledast h\circledast\cdots\circledast h)\\ &= \{C(q)\}(h^n),\end{aligned} \tag{115}$$

where $n\in\mathbb{N}$. This implies that $C(q_j)$ is a FPR_I of $\forall q_j\in\prod_{i\in I}H_i$. So, $\overset{\vee}{}_{i\in I}(E_i,H_i)$ is a FSPR_I over $\mathscr{K}$. □

4. α-Soft Substructures, Fuzzy Soft Image, and Fuzzy Soft Inverse Image in Quantale

Two different quantales $\mathscr{K}$ and $\mathfrak{b}$ are being considered in this section and for each F Soft substructure in $\mathscr{K}$ there exist an α-soft substructures in $\mathscr{K}$ is investigated. These $\mathrm{FS}_S\mathscr{K}$ and FS_I are characterized by their level subquantales and ideals, respectively. F Soft image and F Soft inverse image of F Soft substructures in quantale are further explained.

Definition 33. (see [49])Let (C,J) be a FSST over $\mathscr{K}$. For each $\alpha\in[0,1]$, the set $(C,J)_\alpha=(C_\alpha,J)$ is called an α-level set of (C,J), where $C_\alpha(\mu)=\{x\in\mathscr{K}\mid C(\mu)(x)\geq\alpha\}$ for each $\mu\in J$. $(C,J)_\alpha$ is S Set over $\mathscr{K}$.

Some important results related to Definition 33 are expressed below.

Theorem 29. *Let* (C,J) *be a* FSST *over* $\mathscr{K}$. *Then for each* $\alpha\in[0,1]$, (C,J) *is a* $\mathrm{FS}_s\mathscr{K}$ *if and only if* $(C,J)_\alpha$ *is a* $S_s\mathscr{K}$ *over* $\mathscr{K}$.

Proof. Suppose (C,J) is a $\mathrm{FS}_s\mathscr{K}$. For each $\alpha\in[0,1],\sigma\in J$ and $x_i\in C_\alpha(\sigma)\forall i\in I$, then $C(\sigma)(x_i)\geq\alpha$. Since $C(\sigma)$ is a $F_S\mathscr{K}$ over $\mathscr{K}$. So,

$$C(\sigma)\left(\overset{\vee}{}_{i\in I}x_i\right)\geq\min_{i\in I}\{C(\sigma)(x_i)\}\geq\alpha. \tag{116}$$

This implies that $\overset{\vee}{}_{i\in I}x_i\in C_\alpha(\sigma)\forall i\in I$.

Now, for each $\alpha\in[0,1],\sigma\in J$ and $x_1,x_2\in C_\alpha(\sigma)$, then $C(\sigma)(x_1)\geq\alpha$ and $C(\sigma)(x_2)\geq\alpha$. Since $C(\sigma)$ is a $F_S\mathscr{K}$ over $\mathscr{K}$. So

$$C(\sigma)\left(x_1\circledast x_2\right)\geq\min\{C(\sigma)(x_1),C(\sigma)(x_2)\}\geq\alpha. \tag{117}$$

This implies that $x_1\circledast x_2\in C_\alpha(\sigma)$.

i.e., $C_\alpha(\sigma)$ is a $\mathrm{Sub}_{\mathscr{K}}$ over $\mathscr{K}$. So, by Definition 14, $C_\alpha(\sigma)$ is a $S_S\mathscr{K}$ over $\mathscr{K}$ for each $\alpha\in[0,1]$. Thus, $(C,J)_\alpha$ is a $S_s\mathscr{K}$ over $\mathscr{K}$.

Conversely, let $(C,J)_\alpha$ be a $S_s\mathscr{K}$ over $\mathscr{K}$. Then $C_\alpha(\sigma)$ is a $S_S\mathscr{K}$ over $\mathscr{K}$ for each $\alpha\in[0,1]$. For each $\sigma\in J$ and $x_i\in\mathscr{K}\forall i\in I$. Let $\alpha=\min_{i\in I}\{C(\sigma)(x_i)\}$ then $x_i\in C_\alpha(\sigma)\forall i\in I$. Since, $C_\alpha(\sigma)$ is a $\mathrm{Sub}_{\mathscr{K}}$ over $\mathscr{K}$. So,

$$\overset{\vee}{}_{i\in I}x_i\in C_\alpha(\sigma). \tag{118}$$

This means that

$$C(\sigma)\left(\overset{\vee}{}_{i\in I}x_i\right)\geq\min_{i\in I}\{C(\sigma)(x_i)\}=\alpha. \tag{119}$$

Now, for each $\sigma\in J$ and $x_1,x_2\in\mathscr{K}\forall i\in I$. Let $\alpha=\min\{C(\sigma)(x_1),C(\sigma)(x_2)\}$, then $x_1,x_2\in C_\alpha(\sigma)$. Since, $C_\alpha(\sigma)$ is a $\mathrm{Sub}_{\mathscr{K}}$ over $\mathscr{K}$. So,

$$x_1\circledast x_2\in C_\alpha(\sigma). \tag{120}$$

This means that

$$C(\sigma)\left(x_1\circledast x_2\right)\geq\min\{C(\sigma)(x_1),C(\sigma)(x_2)\}=\alpha. \tag{121}$$

i.e., $C(\sigma)$ is a $F_S\mathscr{K}$ over $\mathscr{K}\forall\sigma\in J$. Thus, (C,J) is a $\mathrm{FS}_s\mathscr{K}$ over $\mathscr{K}$.

Definition 33 are being employed to next theorem as follows: □

Theorem 30. *Let* (C,J) *be a* FSST *over* $\mathscr{K}$. *For each* $\alpha\in[0,1]$, (C,J) *is a* FS_I *if and only if* $(C,J)_\alpha$ *is a* S_I *over* $\mathscr{K}$.

Proof. Suppose (C, J) is a FS_I. For each $\alpha \in [0,1], \sigma \in J$ and $\forall x_1, x_2 \in C_\alpha(\sigma)$, we have $C(\sigma)(x_1) \geq \alpha$ and $C(\sigma)(x_2) \geq \alpha$. Since $C(\sigma)$ is a F_I over $\mathscr{K}$. So,

$$\begin{aligned} C(\sigma)(x_1 \vee x_2) &= \min \{C(\sigma)(x_1), C(\sigma)(x_2)\} \geq \alpha, \\ C(\sigma)(x_1 \circledast x_2) &\geq \min \{C(\sigma)(x_1), C(\sigma)(x_2)\} \geq \alpha. \end{aligned} \tag{122}$$

This implies that

$$\begin{aligned} x_1 \vee x_2 &\in C_\alpha(\sigma), \\ x_1 \circledast x_2 &\in C_\alpha(\sigma). \end{aligned} \tag{123}$$

i.e., $C_\alpha(\sigma)$ is Id over $\mathscr{K} \forall \sigma \in J$. Thus, $(C, J)_\alpha$ is a S_I over $\mathscr{K}$ for each $\alpha \in [0,1]$.

Conversely, assume that $(C, J)_\alpha$ is a S_I over $\mathscr{K}$. Then $C_\alpha(\sigma)$ is a S_I over $\mathscr{K}$ for each $\alpha \in [0,1]$. For each $\sigma \in J$ and $x_1, x_2 \in \mathscr{K}$, let $\alpha = \min \{C(\sigma)(x_1), C(\sigma)(x_2)\}$, then $x_1, x_2 \in C_\alpha(\sigma)$. Since, $C_\alpha(\sigma)$ is Id over $\mathscr{K}$. So,

$$\begin{aligned} x_1 \vee x_2 &\in C_\alpha(\sigma), \\ x_1 \circledast x_2 &\in C_\alpha(\sigma). \end{aligned} \tag{124}$$

This means that

$$\begin{aligned} C(\sigma)(x_1 \vee x_2) &= \min \{C(\sigma)(x_1), C(\sigma)(x_2)\} = \alpha, \\ C(\sigma)(x_1 \circledast x_2) &\geq \min \{C(\sigma)(x_1), C(\sigma)(x_2)\} = \alpha, \end{aligned} \tag{125}$$

i.e., $C(\sigma)$ is a F_I over $\mathscr{K} \forall \sigma \in J$. Thus, (C, J) is a FS_I over $\mathscr{K}$. □

Theorem 31. *Let (C, J) be a* FSST *over $\mathscr{K}$, (C, J) is a FSP_I if and only if $(C, J)_\alpha$ is a STP_I over $\mathscr{K}$ for each $\alpha \in [0,1]$.*

Proof. Suppose (C, J) is a FSP_I. For each $\alpha \in [0,1], \sigma \in J$ and $\forall x_1, x_2 \in C_\alpha(\sigma)$, we have $C(\sigma)(x_1) \geq \alpha$ and $C(\sigma)(x_2) \geq \alpha$. Since $C(\sigma)$ is a FP_I over $\mathscr{K}$. So,

$$\begin{aligned} C(\sigma)(x_1 \circledast x_2) &= C(\sigma)(x_1), \\ \text{or } C(\sigma)(x_2) &\geq \alpha. \end{aligned} \tag{126}$$

This implies that

$$\begin{aligned} x_1 &\in C_\alpha(\sigma), \\ \text{or } x_2 &\in C_\alpha(\sigma), \end{aligned} \tag{127}$$

i.e., $C_\alpha(\sigma)$ is P_I over $\mathscr{K} \forall \sigma \in J$. Thus, $(C, J)_\alpha$ is a STP_I over $\mathscr{K}$ for each $\alpha \in [0,1]$.

Conversely, assume that $(C, J)_\alpha$ is a STP_I over $\mathscr{K}$. Then $C_\alpha(\sigma)$ is a STP_I over $\mathscr{K}$ for each $\alpha \in [0,1]$. By Theorem 30, (C, J) is F_I over $\mathscr{K}$. Now, for each $\sigma \in J$ and $x_1, x_2 \in \mathscr{K}$, let $\alpha = C(\sigma)(x_1) \text{or } C(\sigma)(x_2)$, then $x_1 \in C_\alpha(\sigma) \text{or } x_2 \in C_\alpha(\sigma)$. Since, $C_\alpha(\sigma)$ is P_I over $\mathscr{K}$. So,

$$x_1 \circledast x_2 \in C_\alpha(\sigma). \tag{128}$$

This means that

$$\begin{aligned} C(\sigma)(x_1 \circledast x_2) &= C(\sigma)(x_1) \\ \text{or } C(\sigma)(x_2) &= \alpha, \end{aligned} \tag{129}$$

i.e., $C(\sigma)$ is a FP_I over $\mathscr{K} \forall \sigma \in J$. Thus, (C, J) is a FSP_I over $\mathscr{K}$. □

Theorem 32. *Let (C, J) be a* FSST *over $\mathscr{K}$, (C, J) is a FSSP_I if and only if $(C, J)_\alpha$ is a SSP_I over $\mathscr{K}$ for each $\alpha \in [0,1]$.*

Proof. Suppose (C, J) is a FSSP_I. For each $\alpha \in [0,1], \sigma \in J$ and $\forall x \in C_\alpha(\sigma)$, we have $C(\sigma)(x) \geq \alpha$. Since $C(\sigma)$ is a $F_S P_I$ over $\mathscr{K}$. So,

$$C(\sigma)(x \circledast x) = C(\sigma)(x) \geq \alpha. \tag{130}$$

This implies that

$$x \circledast x \in C_\alpha(\sigma) \Longrightarrow x \in C_\alpha(\sigma), \tag{131}$$

i.e., $C_\alpha(\sigma)$ is SP_I over $\mathscr{K} \forall \sigma \in J$. Thus, $(C, J)_\alpha$ is a SSP_I over $\mathscr{K}$ for each $\alpha \in [0,1]$.

Conversely, assume that $(C, J)_\alpha$ is a SSP_I over $\mathscr{K}$. Then $C_\alpha(\sigma)$ is a SSP_I over $\mathscr{K}$ for each $\alpha \in [0,1]$. By Theorem 30, (C, J) is F_I over $\mathscr{K}$. Now, for each $\sigma \in J$ and $x \in \mathscr{K}$, let $\alpha = C(\sigma)(x)$, then $x \in C_\alpha(\sigma)$. Since, $C_\alpha(\sigma)$ is SP_I over $\mathscr{K}$. So,

$$x \circledast x \in C_\alpha(\sigma). \tag{132}$$

This means that

$$C(\sigma)(x \circledast x) = C(\sigma)(x) = \alpha, \tag{133}$$

i.e., $C(\sigma)$ is a $F_S P_I$ over $\mathscr{K} \forall \sigma \in J$. Thus, (C, J) is a FSSP_I over $\mathscr{K}$. □

Theorem 33. *Let (C, J) be a* FSST *over $\mathscr{K}$, (C, J) is a FSPR_I if and only if $(C, J)_\alpha$ is a SPR_I over $\mathscr{K}$ for each $\alpha \in [0,1]$.*

Proof. Suppose (C, J) is a FSPR_I. For each $\alpha \in [0,1], \sigma \in J$ and $\forall x_1, x_2 \in C_\alpha(\sigma)$, we have $C(\sigma)(x_1) \geq \alpha$ and $C(\sigma)(x_2) \geq \alpha$. Since $C(\sigma)$ is a FPR_I over $\mathscr{K}$. So,

$$\begin{aligned} C(\sigma)(x_1 \circledast x_2) &= C(\sigma)(x_1), \\ \text{or } C(\sigma)(x_2^n) &\geq \alpha. \end{aligned} \tag{134}$$

This implies that

$$\begin{aligned} x_1 &\in C_\alpha(\sigma), \\ \text{or } x_2^n &\in C_\alpha(\sigma), \end{aligned} \tag{135}$$

i.e., $C_\alpha(\sigma)$ is PR_I over $\mathscr{K} \forall \sigma \in J$. Thus, $(C, J)_\alpha$ is a SPR_I over $\mathscr{K}$ for each $\alpha \in [0,1]$.

Conversely, assume that $(C, J)_\alpha$ is a STP_I over $\mathscr{K}$. Then $C_\alpha(\sigma)$ is a STP_I over $\mathscr{K}$ for each $\alpha \in [0,1]$. By Theorem 30, (C, J) is F_I over $\mathscr{K}$. Now, for each $\sigma \in J$ and $x_1, x_2 \in \mathscr{K}$, let $\alpha = C(\sigma)(x_1) \text{or } C(\sigma)(x_2^n)$, then $x_1 \text{ or } x_2^n \in C_\alpha(\sigma)$. Since, $C_\alpha(\sigma)$ is PR_I over $\mathscr{K}$. So,

$$x_1 \circledast x_2 \in C_\alpha(\sigma). \tag{136}$$

This means that

$$\begin{aligned} C(\sigma)(x_1 \circledast x_2) &= C(\sigma)(x_1), \\ \text{or } C(\sigma)(x_2^n) &= \alpha, \end{aligned} \tag{137}$$

i.e., $C(\sigma)$ is a FPR_I over $\mathscr{K} \forall \sigma \in J$. Thus, (C, J) is a FSPR_I over $\mathscr{K}$. □

Definition 34 (see [49]). Let U and R be finite. Then both are called a universe and a set of parameters, respectively. All F Soft sets over U with parameters from R is called F Soft class. We represent it by $(\widehat{U, R})$.

Further, discussion about image of a *FSST* is discussed below.

Definition 35 (see [49]). Let $(\widehat{X, R})$ and $(\widehat{Y, R'})$ be the F Soft classes over X and Y with parameters from R and R', respectively. Let $u: X \longrightarrow Y$ and $\rho: R \longrightarrow R'$ be two functions. For a $\mathrm{FSST}(C, I)$ in $(\widehat{X, R})$, where $I \subseteq R$, the image of (C, I) under the F Soft function $f = (u, \rho)$, denoted by $f(C, I)$, is the FSST over Y defined by $f(C, I) = (u(C), \rho(I))$, where

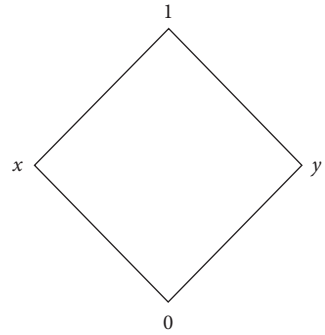

Figure 4: Illustration of $\mathscr{K}$.

$$u(C)(\beta)(y) = \left\{ \bigvee_{x \in u^{-1}(y)} \bigvee_{\theta \in \rho^{-1}(\beta) \cap I} C(\theta)(x), \text{if } u^{-1}(y) \neq \varnothing 0 \text{otherwise}, \forall \beta \in \rho(I), \forall y \in Y \right. \tag{138}$$

Furthermore, discussion about inverse image of a *FSST* is discussed below.

Definition 36 (see [49]). Let $(\widehat{X, R})$ and $(\widehat{Y, R'})$ be F Soft classes over X and Y with parameters from R and R', respectively. Let $u: X \longrightarrow Y$ and $\rho: R \longrightarrow R'$ be two functions. For a $\mathrm{FSST}(D, J)$ in $(\widehat{Y, R'})$, where $J \subseteq R'$, the inverse image of (D, J) under the F Soft function $f = (u, \rho)$, denoted by $f^{-1}(D, J)$, is the FSST over X defined by $f^{-1}(D, J) = (u^{-1}(D), \rho^{-1}(J))$, where

$$u^{-1}(D)(\alpha)(x) = D(\rho(\alpha))(u(x)), \forall \alpha \in \rho^{-1}(J), \forall x \in X. \tag{139}$$

The behavior of quantale homomorphism is being discussed below.

Definition 37 (see [26]). Let $(\mathscr{K}, \circledast_1)$ and $(\mathfrak{b}, \circledast_2)$ be two quantales. A mapping $\Xi: \mathscr{K} \longrightarrow \mathfrak{b}$ is called a quantale homomorphism if

(i) $\Xi(e \circledast_1 f) = \Xi(e) \circledast_2 \Xi(f)$

(ii) $\Xi(e \vee f) = \Xi(e) \vee \Xi(f) \forall e, f \in \mathscr{K}$

Theorem 34. *Let $(\widehat{\mathscr{K}, R})$ and $(\widehat{\mathfrak{b}, R'})$ be F Soft classes over quantales $\mathscr{K}$ and $\mathfrak{b}$ respectively. Let $f: (\widehat{\mathscr{K}, R}) \longrightarrow (\widehat{\mathfrak{b}, R'})$ and $\rho: R \longrightarrow R'$ be two functions and u be a quanatle homomorphic mapping from $\mathscr{K}$ to $\mathfrak{b}$. If (C, I) is a $\mathrm{FS}_S\mathscr{K}$ over $\mathfrak{b}$, then $f^{-1}(C, I)$ is a $\mathrm{FS}_S\mathscr{K}$ over $\mathscr{K}$.*

Proof. According to Definition 28, for each $\rho(\alpha) \in I$, $C(\rho(\alpha))$ is a $F_S\mathscr{K}$ over $\mathfrak{b}$. Then, for all $a_i \in \mathscr{K}$

$$\begin{aligned} u^{-1}(C)(\alpha)\left(\bigvee_{i \in I} a_i\right) &= C(\rho(\alpha))\left(u\left(\bigvee_{i \in I} a_i\right)\right) \\ &\geq C(\rho(\alpha))\left(\bigwedge_{i \in I} (u(a_i))\right) \\ &= \min_{i \in I}\{C(\rho(\alpha))(u(a_i))\} \\ &= \min_{i \in I}\left\{u^{-1}(C)(\alpha)(a_i)\right\} \end{aligned} \tag{140}$$

Now, for all $a, b \in \mathscr{K}$

$$\begin{aligned} u^{-1}(C)(\alpha)(a \circledast b) &= C(\rho(\alpha))(u(a \circledast b)) \\ &\geq C(\rho(\alpha))(u(a \wedge u(b)) \\ &= \min\ \{C(\rho(\alpha))(u(a)), C(\rho(\alpha))(u(b))\} \\ &= \min\ \left\{u^{-1}(C)(\alpha)(a), u^{-1}(C)(\alpha)(b)\right\}, \end{aligned} \tag{141}$$

$\Rightarrow u^{-1}(C)(\alpha)$ is a $F_S\mathscr{K}$ over $\mathscr{K}$. As α is arbitrary, so $f^{-1}(C, I)$ is a $\mathrm{FS}_S\mathscr{K}$ over $\mathscr{K}$ □

Remark 2. In the above theorem, if (C, I) is a $\mathrm{FS}_S\mathscr{K}$ over $\mathscr{K}$, then $f(C, I)$ is not a $\mathrm{FS}_S\mathscr{K}$ over $\mathfrak{b}$.

Example 5. Let $\mathscr{K}$ be a quantale having the order relation shown in Figure 4 and binary relation in Table 8.

Let $\mathfrak{b}$ be a quantale having the order relation shown in Figure 5 and binary relation in Table 9.

Table 8: Binary operation subject to $\circledast_1$.

$\circledast_1$	0	x	y	1
0	0	0	0	0
x	0	x	0	x
y	0	0	y	y
1	0	x	y	1

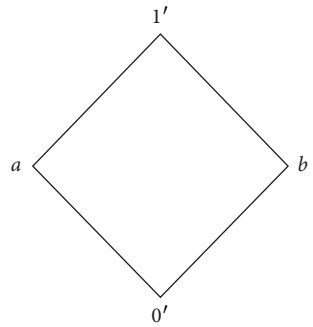

Figure 5: Illustration of $\mathfrak{Ł}$.

Table 9: Binary operation subject to $\circledast_2$.

$\circledast_2$	$0'$	a	b	$1'$
$0'$	$0'$	$0'$	$0'$	$0'$
a	$0'$	a	$0'$	a
b	$0'$	$0'$	b	b
$1'$	$0'$	a	b	$1'$

Let $R' = \{l_1', l_2', l_3', l_4'\}$ and $R = \{l_1, l_2, l_3, l_4\}$ and be set of parameters and $(\widehat{\mathscr{K}, R})$, $(\widehat{\mathfrak{Ł}, R'})$ be F Soft classes over quantales $\mathscr{K}$ and $\mathfrak{Ł}$, respectively. Define $\vartheta: \mathscr{K} \longrightarrow \mathfrak{Ł}$ and $\rho: R \longrightarrow R'$ as follows:

$$\begin{aligned}
\vartheta(0) &= 0', \\
\vartheta(x) &= a, \\
\vartheta(y) &= b, \\
\vartheta(1) &= 1', \\
\rho(l_1) &= l_1', \\
\rho(l_2) &= l_3', \\
\rho(l_3) &= l_1', \\
\rho(l_4) &= l_4'.
\end{aligned} \tag{142}$$

It is simple to check that ϑ is a homomorphic mapping from $\mathscr{K}$ to $\mathfrak{Ł}$. Now for $I \subseteq R$, take a $\mathrm{FS}_S\mathscr{K}$ over $\mathscr{K}$ as follows:

$$\begin{aligned}
C(l_1) &= \frac{0.4}{0} + \frac{0.7}{x} + \frac{0.1}{y} + \frac{0.2}{1}, \\
C(l_3) &= \frac{0.3}{0} + \frac{0.2}{x} + \frac{0.7}{y} + \frac{0.9}{1}.
\end{aligned} \tag{143}$$

According to the Definition 35, for $l_1' \in \rho(I) \subseteq R'$

$$\begin{aligned}
\vartheta(C)\left(l_1'\right) &= \frac{0.4}{0'} + \frac{0.7}{a} + \frac{0.7}{b} + \frac{0.9}{1'} \\
&\left(\because \{l_1, l_3\} = I \cap \rho^{-1}\left(l_1'\right)\right).
\end{aligned} \tag{144}$$

Since,

$$\vartheta(C)\left(l_1'\right)(a \circledast b) = \vartheta(C)\left(l_1'\right)\left(0'\right) = 0.4 \not\geq 0.7 = \min\left\{\vartheta(C)\left(l_1'\right)(a), \vartheta(C)\left(l_1'\right)(b)\right\}, \tag{145}$$

$\Rightarrow \vartheta(C)(l_1')$ is not a $F_S\mathscr{K}$ over $\mathfrak{Ł}$. Thus, the F Soft image $f(C, I)$ of $\mathrm{FS}_S\mathscr{K}(C, I)$ is not a $\mathrm{FS}_S\mathscr{K}$ over $\mathfrak{Ł}$

Theorem 35. *Let $(\widehat{\mathscr{K}, R})$ and $(\widehat{\mathfrak{Ł}, R'})$ be F Soft classes over quantales $\mathscr{K}$ and $\mathfrak{Ł}$ respectively. Let $f: (\widehat{\mathscr{K}, R}) \longrightarrow (\widehat{\mathfrak{Ł}, R'})$ be a function, $\rho: R \longrightarrow R'$ be an injective function and u be a quantale homomorphism from $\mathscr{K}$ to $\mathfrak{Ł}$. If (C, I) is a $\mathrm{FS}_S\mathscr{K}$ over $\mathscr{K}$, then $f(C, I)$ is a $\mathrm{FS}_S\mathscr{K}$ over $\mathfrak{Ł}$.*

Proof. By Theorem 29, we only prove that $(u(C), \rho(I))_\alpha$ is a $S_S\mathscr{K}$ over $\mathfrak{Ł}, \forall \alpha \in [0, 1]$. Since ρ is an injective, for each $\beta \in \rho(I)$, there exist $\gamma \in I$, such that $\rho(\gamma) = \beta$. Next we prove that $u(C)_\alpha(\beta)$ is a $\mathrm{Sub}_{\mathscr{K}}$ over $\mathfrak{Ł}$.

For all $z_i \in u(C)_\alpha(\beta)$

$$\begin{aligned}
u(C)(\beta)(z_i) &= \bigvee_{w \in u^{-1}(z_i)} \bigvee_{\theta \in \rho^{-1}(\beta) \cap I} C(\theta)(w) \\
&= \bigvee_{w \in u^{-1}(z_i)} C(\gamma)(w) \geq \alpha.
\end{aligned} \tag{146}$$

This implies that there exist $w_i \in \mathscr{K}$ such that $u(w_i) = z_i$ and $C(\gamma)(w_i) \geq \alpha$. Then,

$$\begin{aligned}
u(C)(\beta)\left(\bigvee_{i \in I} z_i\right) &= \bigvee_{w \in u^{-1}(z_i i \in I \vee)} \bigvee_{\theta \in \rho^{-1}(\beta) \cap I} C(\theta)(w) \\
&= \bigvee_{w \in u^{-1}(z_i i \in I \vee)} C(\gamma)(w) \\
&\geq C(\gamma)\left(\bigvee_{i \in I} w_i\right).
\end{aligned} \tag{147}$$

Since, $C(\gamma)$ is a $F_S\mathscr{K}$ over $\mathscr{K}$. So,

$$\geq \min_{i \in I}\{C(\gamma)(w_i)\} \geq \alpha. \tag{148}$$

Now, for all $z_1, z_2 \in u(C)_\alpha(\beta)$

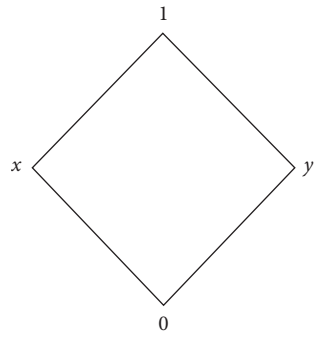

Figure 6: Illustration of $\mathscr{K}$.

Table 10: Binary operation subject to $\circledast_1$.

$\circledast_1$	0	x	y	1
0	0	0	0	0
x	0	x	0	x
y	0	0	y	y
1	0	x	y	1

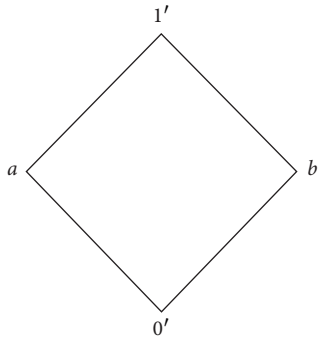

Figure 7: Illustration of $\mathfrak{b}$.

Table 11: Binary operation subject to $\circledast_2$.

$\circledast_2$	$0^{'}$	a	b	$1^{'}$
$0^{'}$	$0^{'}$	$0^{'}$	$0^{'}$	$0^{'}$
a	$0^{'}$	a	$0^{'}$	a
b	$0^{'}$	$0^{'}$	b	b
$1^{'}$	$0^{'}$	a	b	$1^{'}$

$$u(C)(\beta)(z_1) = \bigvee_{w\in u^{-1}(z_1)} \bigvee_{\theta\in \rho^{-1}(\beta)\cap I} C(\theta)(w) = \bigvee_{w\in u^{-1}(z_1)} C(\gamma)(w) \geq \alpha,$$
$$u(C)(\beta)(z_2) = \bigvee_{w\in u^{-1}(z_2)} \bigvee_{\theta\in \rho^{-1}(\beta)\cap I} C(\theta)(w) = \bigvee_{w\in u^{-1}(z_2)} C(\gamma)(w) \geq \alpha \tag{149}$$

This implies that there exist $w_1, w_2 \in \mathscr{K}$ such that $u(w_1) = z_1, u(w_2) = z_2,$ and $C(\gamma)(w_1) \geq \alpha, C(\gamma)(w_2) \geq \alpha$. Then,

$$\begin{aligned} u(C)(\beta)(z_1 \circledast z_2) &= \bigvee_{w\in u^{-1}(z_1\circledast z_2)} \bigvee_{\theta\in \rho^{-1}(\beta)\cap I} C(\theta)(w) \\ &= \bigvee_{w\in u^{-1}(z_1\circledast z_2)} C(\gamma)(w) \\ &\geq C(\gamma)(w_1 \circledast w_2). \end{aligned} \tag{150}$$

Since, $C(\gamma)$ is a $F_S\mathscr{K}$ over $\mathscr{K}$. So,

$$\geq C(\gamma)(w_1) \wedge C(\gamma)(w_2) \geq \alpha. \tag{151}$$

Thus, $\bigvee_{i\in I} z_i, z_1 \circledast z_2 \in u(C)_\alpha(\beta)$. This implies that $u(C)_\alpha(\beta)$ is a $\mathrm{Sub}_{\mathscr{K}}$ over $\mathscr{K}$. Since β is arbitrary, then $(u(C), \rho(I))_\alpha$ is a $S_S\mathscr{K}$ over $\mathfrak{b}, \forall \alpha \in [0,1]$. □

Theorem 36. *Let $(\widehat{\mathscr{K}}, R)$ and $(\widehat{\mathfrak{b}}, R')$ be F Soft classes over quantales $\mathscr{K}$ and $\mathfrak{b}$ respectively. Let f: $(\widehat{\mathscr{K}}, R) \longrightarrow (\widehat{\mathfrak{b}}, R')$ and ρ: $R \longrightarrow R'$ be two functions and u be a quantale homomorphic mapping from $\mathscr{K}$ to $\mathfrak{b}$. If (C, I) is a FS_I over $\mathfrak{b}$, then $f^{-1}(C, I)$ is a FS_I over $\mathscr{K}$.*

Proof. According to Definition 29, for each $\rho(\alpha) \in I$, $C(\rho(\alpha))$ is a F_I over $\mathfrak{b}$. Then for all $a, b \in \mathscr{K}$

$$u^{-1}(C)(\alpha)(a \vee b) = C(p(\alpha))(u(a \vee b)). \tag{152}$$

Since, $C(\rho(\alpha))$ is a F_I. So,

$$\begin{aligned} &= C(p(\alpha))(u(a) \wedge u(b)) \\ &= \min \{C(p(\alpha))(u(a)), C(p(\alpha))(u(b))\} \\ &= \min \left\{u^{-1}(C)(\alpha)(a), u^{-1}(C)(\alpha)(b)\right\}. \end{aligned} \tag{153}$$

Now, for all $a, b \in \mathscr{K}$

$$u^{-1}(C)(\alpha)(a \circledast b) = C(p(\alpha))(u(a \circledast b)). \tag{154}$$

Since, $C(\rho(\alpha))$ is a F_I. So,

$$\begin{aligned} &\geq C(p(\alpha))(u(a) \wedge u(b)) \\ &= \min \{C(p(\alpha))(u(a)), C(p(\alpha))(u(b))\} \\ &= \min \{u^{-1}(C)(\alpha)(a), u^{-1}(C)(\alpha)(b)\}, \end{aligned} \tag{155}$$

$\Longrightarrow u^{-1}(C)(\alpha)$ is a F_I over $\mathscr{K}$. As α is arbitrary, so $f^{-1}(C, I)$ is a FS_I over $\mathscr{K}$

In the above theorem, if (C, I) is a FS_I over $\mathscr{K}$, then $f(C, I)$ is not a FS_I over $\mathfrak{b}$. □

Example 6. Let $\mathscr{K}$ be a quantale having the order relation shown in Figure 6 and binary relation in Table 10.

Let $\mathfrak{b}$ be a quantale having the order relation shown in Figure 7 and binary relation in Table 11.

Let $R = \{l_1, l_2, l_3, l_4\}$ and $R' = \{l_1', l_2', l_3', l_4'\}$ be set of parameters and $(\widehat{\mathscr{K}}, R)$, $(\widehat{\mathfrak{b}}, R')$ be F Soft classes over quantales $\mathscr{K}$ and $\mathfrak{b}$, respectively. We define ϑ: $\mathscr{K} \longrightarrow \mathfrak{b}$ and ρ: $R \longrightarrow R'$ as follows:

$$\begin{aligned} \vartheta(0) &= 0^{'}, \\ \vartheta(x) &= a, \\ \vartheta(y) &= b, \\ \vartheta(1) &= 1^{'}, \\ \rho(l_1) &= l_1', \\ \rho(l_2) &= l_3', \\ \rho(l_3) &= l_1' \\ \rho(l_4) &= l_4'. \end{aligned} \tag{156}$$

It is simply to check that ϑ is a homomorphic mapping from $\mathscr{K}$ to $\mathfrak{L}$. Now for $I \subseteq R$, take a FS_I over $\mathscr{K}$ as follows:

$$C(l_1) = \frac{0.8}{0} + \frac{0.5}{x} + \frac{0.1}{y} + \frac{0.1}{1},$$
$$C(l_3) = \frac{0.9}{0} + \frac{0.2}{x} + \frac{0.7}{y} + \frac{0.2}{1}. \tag{157}$$

According to the Definition 4.5, for $l_1' \in \rho(I) \subseteq R'$

$$\vartheta(C)\left(l_1'\right) = \frac{0.9}{0'} + \frac{0.5}{a} + \frac{0.7}{b} + \frac{0.2}{1'},$$
$$\left(\because \{l_1, l_3\} = I \cap \rho^{-1}\left(l_1'\right)\right). \tag{158}$$

Since,

$$\vartheta(C)\left(l_1'\right)(a \vee b) = \vartheta(C)\left(l_1'\right)\left(1'\right) = 0.2 \neq 0.5$$
$$= \min\left\{\vartheta(C)\left(l_1'\right)(a), \vartheta(C)\left(l_1'\right)(b)\right\}, \tag{159}$$

$\Longrightarrow \vartheta(C)(l_1')$ is not a FS_I over $\mathfrak{L}$. Thus, the F Soft image $f(C, I)$ of $\mathrm{FS}_I(C, I)$ is not a FS_I over $\mathfrak{L}$

Theorem 37. *Let $(\widehat{\mathscr{K}}, R)$ and $(\widehat{\mathfrak{L}, R'})$ be F Soft classes over quantales $\mathscr{K}$ and $\mathfrak{L}$, respectively. Let f: $(\widehat{\mathscr{K}}, R) \longrightarrow (\widehat{\mathfrak{L}, R'})$ and ρ: $R \longrightarrow R'$ be two functions and u be a surjective quantale homomorphism from $\mathscr{K}$ to $\mathfrak{L}$. If (C, I) is a FS_I over $\mathscr{K}$, then $f(C, I)$ is a FS_I over $\mathfrak{L}$.*

Proof. By Theorem 30, we only prove that $(u(C), \rho(I))_\alpha$ is a S_I over $\mathfrak{L}, \forall \alpha \in [0, 1]$. For each $\beta \in \rho(I)$ and $\forall z_1, z_2 \in u(C)_\alpha(\beta)$

$$u(C)(\beta)(z_1) = \bigvee_{w \in u^{-1}(z_1)} \bigvee_{\gamma \in \rho^{-1}(\beta) \cap I} C(\gamma)(w) \geq \alpha,$$
$$u(C)(\beta)(z_2) = \bigvee_{w \in u^{-1}(z_2)} \bigvee_{\gamma \in \rho^{-1}(\beta) \cap I} C(\gamma)(w) \geq \alpha. \tag{160}$$

This implies that there exist $w_1, w_2 \in \mathscr{K}$ such that $u(w_1) = z_1, u(w_2) = z_2$, and $C(\gamma)(w_1) \geq \alpha, C(\gamma)(w_2) \geq \alpha$. Since u is a surjective, for each $z \in \mathfrak{L}$, there exist $w \in \mathscr{K}$, such that $u(w) = z$. Then

$$u(C)(\beta)(z_1 \vee z_2) = \bigvee_{w \in u^{-1}(z_1 \vee z_2)} \bigvee_{\gamma \in \rho^{-1}(\beta) \cap I} C(\gamma)(w) \geq C(\gamma)(w_1 \vee w_2). \tag{161}$$

Since, $C(\gamma)$ is a F_I over $\mathscr{K}$. So,

$$= C(\gamma)(w_1) \wedge C(\gamma)(w_2) \geq \alpha. \tag{162}$$

Now,

$$u(C)(\beta)(z_1 \circledast z_2) = \bigvee_{w \in u^{-1}(z_1 \circledast z_2)} \bigvee_{\gamma \in \rho^{-1}(\beta) \cap I} C(\gamma)(w) \geq C(\gamma)(w_1 \circledast w_2). \tag{163}$$

Since, $C(\gamma)$ is a F_I over $\mathscr{K}$. So,

$$\geq C(\gamma)(w_1) \wedge C(\gamma)(w_2) \geq \alpha. \tag{164}$$

Thus, $z_1 \vee z_2, z_1 \circledast z_2 \in u(C)_\alpha(\beta)$. This implies that $u(C)_\alpha(\beta)$ is an Id over $\mathscr{K}$. Since β is arbitrary, then $(u(C), \rho(I))_\alpha$ is a S_I over $\mathfrak{L}, \forall \alpha \in [0, 1]$. □

Theorem 38. *Let $(\widehat{\mathscr{K}}, R)$ and $(\widehat{\mathfrak{L}, R'})$ be F Soft classes over quantales $\mathscr{K}$ and $\mathfrak{L}$, respectively. Let f: $(\widehat{\mathscr{K}}, R) \longrightarrow (\widehat{\mathfrak{L}, R'})$ and ρ: $R \longrightarrow R'$ be two functions and u be a homomorphic mapping from $\mathscr{K}$ to $\mathfrak{L}$. If (C, I) is a FSP_I over $\mathfrak{L}$, then $f^{-1}(C, I)$ is a FSP_I over $\mathscr{K}$.*

Proof. According to Definition 30, for each $\rho(\alpha) \in I$, $C(\rho(\alpha))$ is a FP_I over $\mathfrak{L}$. Then for any $a, b \in \mathscr{K}$

$$u^{-1}(C)(\alpha)(a \circledast b) = C(p(\alpha))(u(a \circledast b)). \tag{165}$$

Since, $C(\rho(\alpha))$ is a FP_I. So,

$$= \{C(p(\alpha))(u(a))\} \text{or} \{C(p(\alpha))(u(b))\}$$
$$= (C)(\alpha)(a)\} \text{ or} \{u^{-1}(C)(\alpha)(b)\}, \tag{166}$$

$\Longrightarrow u^{-1}(C)(\alpha)$ is a FP_I over $\mathscr{K}$. As α is arbitrary, so $f^{-1}(C, I)$ is a FSP_I over $\mathscr{K}$ In the above theorem, if (C, I) is a FSP_I over $\mathscr{K}$, then $f(C, I)$ is not a FSP_I over $\mathfrak{L}$. □

Example 7. Let $\mathscr{K}$ be a quantale having the order relation shown in Figure 6 and binary relation in Table 10.

Let $\mathfrak{L}$ be a quantale having the order relation shown in Figure 7 and binary relation in Table 11.

Let $R = \{l_1, l_2, l_3, l_4\}$, $R' = \{l_1', l_2', l_3', l_4'\}$ be set of parameters and $(\widehat{\mathscr{K}}, R)$, and $(\widehat{\mathfrak{L}, R'})$ be F Soft classes over quantales $\mathscr{K}$ and $\mathfrak{L}$, respectively. We define ϑ: $\mathscr{K} \longrightarrow \mathfrak{L}$ and ρ: $R \longrightarrow R'$ as follows:

$$\begin{aligned} \vartheta(0) &= 0', \\ \vartheta(x) &= a, \\ \vartheta(y) &= b, \\ \vartheta(1) &= 1', \\ \rho(l_1) &= l_1', \\ \rho(l_2) &= l_3', \\ \rho(l_3) &= l_1', \\ \rho(l_4) &= l_4'. \end{aligned} \tag{167}$$

It is simply to check that ϑ is a homomorphic mapping from $\mathscr{K}$ to $\mathfrak{L}$. Now for $I \subseteq R$, take a FSP_I over $\mathscr{K}$ as

$$C(l_1) = \frac{0.5}{0} + \frac{0.5}{x} + \frac{0.1}{y} + \frac{0.1}{1},$$
$$C(l_3) = \frac{0.7}{0} + \frac{0.2}{x} + \frac{0.7}{y} + \frac{0.2}{1}. \tag{168}$$

According to the Definition 4.5, for $l_1' \in \rho(I) \subseteq R'$

$$\vartheta(C)(l_1') = \frac{0.7}{0'} + \frac{0.5}{a} + \frac{0.7}{b} + \frac{0.2}{1'} \because \{l_1, l_3\} = I \cap \rho^{-1}(l_1'). \tag{169}$$

Since,

$$\vartheta(C)(l_1')(a\vee b) = \vartheta(C)\left(l_1^{'}\right)\left(1^{'}\right) = 0.2 \neq 0.5 = \min\left\{\vartheta(C)\left(l_1^{'}\right)(a), \vartheta(C)(l_1')(b)\right\}, \tag{170}$$

$\Longrightarrow \vartheta(C)(l_1')$ is not a F_{I} over $\mathfrak{b}$. Thus, the F Soft image $f(C,I)$ of $\mathrm{FSP}_I(C,I)$ is not a FSP_I over $\mathfrak{b}$

Theorem 39. *Let $(\widehat{\mathscr{K}, R})$ and $(\widehat{\mathfrak{b}, R'})$ be F Soft classes over quantales $\mathscr{K}$ and $\mathfrak{b}$ respectively. Let f: $(\widehat{\mathscr{K}, R}) \longrightarrow (\widehat{\mathfrak{b}, R'})$ and ρ: $R \longrightarrow R^{'}$ be two functions and u be a surjective homomorphism from $\mathscr{K}$ to $\mathfrak{b}$. If (C,I) is a FSP_I over $\mathscr{K}$, then $f(C,I)$ is a FSP_I over $\mathfrak{b}$.*

Proof. By Theorem 31, we only prove that $(u(C), \rho(I))_\alpha$ is a STP_I over $\mathfrak{b}, \forall \alpha \in [0,1]$. For each $\beta \in \rho(I)$ and $\forall z_1, z_2 \in u(C)_\alpha(\beta)$

$$\begin{aligned} u(C)(\beta)(z_1) &= \overset{\vee}{w \in u^{-1}(z_1)} \overset{\vee}{\gamma \in \rho^{-1}(\beta)\cap I} C(\gamma)(w) \geq \alpha, \\ u(C)(\beta)(z_2) &= \overset{\vee}{w \in u^{-1}(z_2)} \overset{\vee}{\gamma \in \rho^{-1}(\beta)\cap I} C(\gamma)(w) \geq \alpha. \end{aligned} \tag{171}$$

This implies that there exist $w_1, w_2 \in \mathscr{K}$ such that $u(w_1) = z_1, u(w_2) = z_2$ and $C(\gamma)(w_1) \geq \alpha, C(\gamma)(w_2) \geq \alpha$. Since u is a surjective, for each $z \in \mathfrak{b}$, there exist $w \in \mathscr{K}$, such that $u(w) = z$. Then

$$u(C)(\beta)(z_1 \circledast z_2) = \overset{\vee}{w \in u^{-1}(z_1 \circledast z_2)} \overset{\vee}{\gamma \in \rho^{-1}(\beta)\cap I} C(\gamma)(w) \geq C(\gamma)(w_1 \circledast w_2). \tag{172}$$

Since, $C(\gamma)$ is a FP_I over $\mathscr{K}$. So,

$$\begin{aligned} &\geq C(\gamma)(w_1) \\ \text{or } &C(\gamma)(w_2) \geq \alpha. \end{aligned} \tag{173}$$

Thus, $z_1 \circledast z_2 \in u(C)_\alpha(\beta)$. This implies that $u(C)_\alpha(\beta)$ is an P_I over $\mathscr{K}$. Since β is arbitrary, then $(u(C), \rho(I))_\alpha$ is a STP_I over $\mathfrak{b}, \forall \alpha \in [0,1]$. □

Theorem 40. *Let $(\widehat{\mathscr{K}, R})$ and $(\widehat{\mathfrak{b}, R'})$ be F Soft classes over quantales $\mathscr{K}$ and $\mathfrak{b}$ respectively. Let f: $(\widehat{\mathscr{K}, R}) \longrightarrow (\widehat{\mathfrak{b}, R'})$ and ρ: $R \longrightarrow R^{'}$ be two functions and u be a homomorphic mapping from $\mathscr{K}$ to $\mathfrak{b}$. If (C,I) is a FSSP_I over $\mathfrak{b}$, then $f^{-1}(C,I)$ is a FSSP_I over $\mathscr{K}$.*

Proof. According to Definition 31, for each $\rho(\alpha) \in I$, $C(\rho(\alpha))$ is a $F_S P_I$ over $\mathfrak{b}$. Then for any $a \in \mathscr{K}$

$$u^{-1}(C)(\alpha)(a \circledast a) = C(p(\alpha))(u(a \circledast a)). \tag{174}$$

Since, $C(\rho(\alpha))$ is a $F_S P_I$. So,

$$\begin{aligned} &= \{C(p(\alpha))(u(a))\} \\ &= \{u^{-1}(C)(\alpha)(a)\}, \end{aligned} \tag{175}$$

$\Longrightarrow u^{-1}(C)(\alpha)$ is a $F_S P_I$ over $\mathscr{K}$. As α is arbitrary, so $f^{-1}(C,I)$ is a FSSP_I over $\mathscr{K}$

In the above theorem, if (C,I) is a FSSP_I over $\mathscr{K}$, then $f(C,I)$ is not a FSSP_I over $\mathfrak{b}$. □

Example 8. Let $\mathscr{K}$ be a quantale having the order relation shown in Figure 6 and binary relation in Table 10.

Let $\mathfrak{b}$ be a quantale having the order relation shown in Figure 7 and binary relation in Table 11.

Let $R = \{l_1, l_2, l_3, l_4\}$, $R^{'} = \{l_1', l_2', l_3', l_4'\}$ be set of parameters and $(\widehat{\mathscr{K}, R})$, and $(\widehat{\mathfrak{b}, R'})$ be F Soft classes over quantales $\mathscr{K}$ and $\mathfrak{b}$, respectively. Define ϑ: $\mathscr{K} \longrightarrow \mathfrak{b}$ and ρ: $R \longrightarrow R^{'}$ as follows:

$$\begin{aligned} \vartheta(0) &= 0^{'}, \\ \vartheta(x) &= a, \\ \vartheta(y) &= b, \\ \vartheta(1) &= 1^{'}, \\ \rho(l_1) &= l_1', \\ \rho(l_2) &= l_3', \\ \rho(l_3) &= l_1', \\ \rho(l_4) &= l_4'. \end{aligned} \tag{176}$$

It's simply to check that ϑ is a homomorphic mapping from $\mathscr{K}$ to $\mathfrak{b}$. Now for $I \subseteq R$, take a FSSP_I over $\mathscr{K}$ as follows:

$$\begin{aligned} C(l_1) &= \frac{0.7}{0} + \frac{0.5}{x} + \frac{0.3}{y} + \frac{0.3}{1}, \\ C(l_3) &= \frac{0.8}{0} + \frac{0.4}{x} + \frac{0.6}{y} + \frac{0.4}{1}. \end{aligned} \tag{177}$$

According to the Definition 4.5, for $l_1' \in \rho(I) \subseteq R^{'}$

$$\vartheta(C)(l_1') = \frac{0.8}{0^{'}} + \frac{0.5}{a} + \frac{0.6}{b} + \frac{0.4}{1^{'}} \because \{l_1, l_3\} = I \cap \rho^{-1}(l_1'). \tag{178}$$

Since,

$$\vartheta(C)\left(l_1^{'}\right)(a\vee b) = \vartheta(C)(l_1')\left(1^{'}\right) = 0.4 \neq 0.5 = \min\{\vartheta(C)(l_1')(a), \vartheta(C)(l_1')(b)\}, \tag{179}$$

$\Longrightarrow \vartheta(C)(l_1')$ is not a F_{I} over $\mathfrak{b}$. Thus, the F Soft image $f(C,I)$ of $\mathrm{FSSP}_I(C,I)$ is not a FSSP_I over $\mathfrak{b}$

Theorem 41. *Let $(\widehat{\mathscr{K}, R})$ and $(\widehat{\mathfrak{b}, R'})$ be F Soft classes over quantales $\mathscr{K}$ and $\mathfrak{b}$ respectively. Let f: $(\widehat{\mathscr{K}, R}) \longrightarrow (\widehat{\mathfrak{b}, R'})$ and ρ: $R \longrightarrow R^{'}$ be two functions and u be a surjective homomorphism from $\mathscr{K}$ to $\mathfrak{b}$. If (C,I) is a FSSP_I over $\mathscr{K}$, then $f(C,I)$ is a FSSP_I over $\mathfrak{b}$.*

Proof. By Theorem 32, we only prove that $(u(C), \rho(I))_\alpha$ is a SSP_I over $\mathfrak{b}, \forall \alpha \in [0,1]$. For each $\beta \in \rho(I)$ and $\forall z \in u(C)_\alpha(\beta)$

$$u(C)(\beta)(z) = \overset{\vee}{w \in u^{-1}(z)} \overset{\vee}{\gamma \in \rho^{-1}(\beta) \cap I} C(\gamma)(w) \geq \alpha. \tag{180}$$

This implies that there exist $w \in \mathscr{K}$ such that $u(w) = z$ and $C(\gamma)(w) \geq \alpha$. Since u is a surjective, for each $z \in \mathfrak{b}$, there exist $w \in \mathscr{K}$, such that $u(w) = z$. Thent

$$u(C)(\beta)(z \circledast z) = \overset{\vee}{w \in u^{-1}(z \circledast z)} \overset{\vee}{\gamma \in \rho^{-1}(\beta) \cap I} C(\gamma)(w) \geq C(\gamma)(w \circledast w). \tag{181}$$

Since, $C(\gamma)$ is a FP_I over $\mathscr{K}$. So,

$$\geq C(\gamma)(w) \geq \alpha. \tag{182}$$

Thus, $z \circledast z \in u(C)_\alpha(\beta)$. This implies that $u(C)_\alpha(\beta)$ is an SP_I over $\mathscr{K}$. Since β is arbitrary, then $(u(C), \rho(I))_\alpha$ is a SSP_I over $\mathfrak{b}, \forall \alpha \in [0,1]$. □

Theorem 42. *Let $(\widehat{\mathscr{K}, R})$ and $(\widehat{\mathfrak{b}, R'})$ be F Soft classes over quantales $\mathscr{K}$ and $\mathfrak{b}$ respectively. Let f: $(\widehat{\mathscr{K}, R}) \longrightarrow (\widehat{\mathfrak{b}, R'})$ and ρ: $R \longrightarrow R'$ be two functions and u be a homomorphic mapping from $\mathscr{K}$ to $\mathfrak{b}$. If (C, I) is a FSPR_I over $\mathfrak{b}$, then $f^{-1}(C, I)$ is a FSPR_I over $\mathscr{K}$.*

Proof. According to Definition 32, for each $\rho(\alpha) \in I$, $C(\rho(\alpha))$ is a FPR_I over $\mathfrak{b}$. Then for all $a, b \in \mathscr{K}$

$$u^{-1}(C)(\alpha)(a \circledast b) = C(p(\alpha))(u(a \circledast b)). \tag{183}$$

Since, $C(\rho(\alpha))$ is a FPR_I. So,

$$\begin{aligned} &= C(p(\alpha))(u(a) \text{ or } u(b^n)) \\ &= \{C(p(\alpha))(u(a))\} \text{or} \{C(p(\alpha))(u(b^n))\} \\ &= \left\{u^{-1}(C)(\alpha)(a)\right\} \text{or} \left\{u^{-1}(C)(\alpha)(b^n)\right\}, \end{aligned} \tag{184}$$

$\Longrightarrow u^{-1}(C)(\alpha)$ is a FPR_I over $\mathscr{K}$. As α is arbitrary, so $f^{-1}(C, I)$ is a FSPR_I over $\mathscr{K}$

In the above theorem, if (C, I) is a FSPR_I over $\mathscr{K}$, then $f(C, I)$ is not a FSPR_I over $\mathfrak{b}$. □

Example 9. Let $\mathscr{K}$ be a quantale having the order relation shown in Figure 6 and binary relation in Table 10.

Let $\mathfrak{b}$ be a quantale having the order relation shown in Figure 7 and binary relation in Table 11.

Let $R = \{l_1, l_2, l_3, l_4\}$, $R' = \{l_1', l_2', l_3', l_4'\}$ be set of parameters and $(\widehat{\mathscr{K}, R})$, $(\widehat{\mathfrak{b}, R'})$ be F Soft classes over quantales $\mathscr{K}$ and $\mathfrak{b}$, respectively. Define ϑ: $\mathscr{K} \longrightarrow \mathfrak{b}$ and ρ: $R \longrightarrow R'$ as follows:

$$\begin{aligned} \vartheta(0) &= 0', \\ \vartheta(x) &= a, \\ \vartheta(y) &= b, \\ \vartheta(1) &= 1', \\ \rho(l_1) &= l_1', \\ \rho(l_2) &= l_3', \\ \rho(l_3) &= l_{1,}', \\ \rho(l_4) &= l_4'. \end{aligned} \tag{185}$$

It is simply to check that ϑ is a homomorphic mapping from $\mathscr{K}$ to $\mathfrak{b}$. Now for $I \subseteq R$, take a FSPR_I over $\mathscr{K}$ as:

$$\begin{aligned} C(l_1) &= \frac{0.7}{0} + \frac{0.7}{x} + \frac{0.2}{y} + \frac{0.2}{1}, \\ C(l_3) &= \frac{0.9}{0} + \frac{0.4}{x} + \frac{0.9}{y} + \frac{0.4}{1}. \end{aligned} \tag{186}$$

According to the Definition 4.5, for $l_1' \in \rho(I) \subseteq R'$

$$\vartheta(C)(l_1') = \frac{0.9}{0'} + \frac{0.7}{a} + \frac{0.9}{b} + \frac{0.4}{1'} \because \{l_1, l_3\} = I \cap \rho^{-1}(l_1'). \tag{187}$$

Since,

$$\begin{aligned} \vartheta(C)(l_1')(a \vee b) &= \vartheta(C)(l_1')\left(1'\right) = 0.2 \neq 0.5 \\ &= \min\{\vartheta(C)(l_1')(a), \vartheta(C)(l_1')(b)\}. \end{aligned} \tag{188}$$

$\Longrightarrow \vartheta(C)(l_1')$ is not a F_I over $\mathfrak{b}$. Thus, the F Soft image $f(C, I)$ of $\mathrm{FSPR}_\mathrm{I}(C, I)$ is not a FSPR_I over $\mathfrak{b}$.

Theorem 43. *Let $(\widehat{\mathscr{K}, R})$ and $(\widehat{\mathfrak{b}, R'})$ be F Soft classes over quantales $\mathscr{K}$ and $\mathfrak{b}$ respectively. Let f: $(\widehat{\mathscr{K}, R}) \longrightarrow (\widehat{\mathfrak{b}, R'})$ and ρ: $R \longrightarrow R'$ be two functions and u be a surjective homomorphism from $\mathscr{K}$ to $\mathfrak{b}$. If (C, I) is a FSPR_I over $\mathscr{K}$, then $f(C, I)$ is a FSPR_I over $\mathfrak{b}$.*

Proof. By Theorem 33, we only prove that $(u(C), \rho(I))_\alpha$ is a SPR_I over $\mathfrak{b}, \forall \alpha \in [0,1]$. For each $\beta \in \rho(I)$ and $\forall z_1, z_2 \in u(C)_\alpha(\beta)$

$$\begin{aligned} u(C)(\beta)(z_1) &= \overset{\vee}{w \in u^{-1}(z_1)} \overset{\vee}{\gamma \in \rho^{-1}(\beta) \cap I} C(\gamma)(w) \geq \alpha, \\ u(C)(\beta)(z_2) &= \overset{\vee}{w \in u^{-1}(z_2)} \overset{\vee}{\gamma \in \rho^{-1}(\beta) \cap I} C(\gamma)(w) \geq \alpha. \end{aligned} \tag{189}$$

This implies that there exist $w_1, w_2 \in \mathscr{K}$ such that $u(w_1) = z_1, u(w_2) = z_2,$ and $C(\gamma)(w_1) \geq \alpha, C(\gamma)(w_2) \geq \alpha$. Since u is a surjective, for each $z \in \mathfrak{b}$, there exist $w \in \mathscr{K}$, such that $u(w) = z$. Then

$$\begin{aligned} u(C)(\beta)(z_1 \circledast z_2) &= \overset{\vee}{w \in u^{-1}(z_1 \circledast z_2)} \overset{\vee}{\gamma \in \rho^{-1}(\beta) \cap I} C(\gamma)(w) \\ &\geq C(\gamma)(w_1 \circledast w_2). \end{aligned} \tag{190}$$

Since, $C(\gamma)$ is a FPR_I over $\mathscr{K}$. So,

$$\begin{aligned} &= C(\gamma)(w_1) \\ \text{or } C(\gamma)(w_2^n) &\geq \alpha. \end{aligned} \tag{191}$$

Thus, $z_1 \circledast z_2 \in u(C)_\alpha(\beta)$. This implies that $u(C)_\alpha(\beta)$ is an PR_I over $\mathscr{K}$. Since β is arbitrary, then $(u(C), \rho(I))_\alpha$ is a SPR_I over $\mathfrak{b}, \forall \alpha \in [0,1]$. □

5. Conclusion

The theory of fuzzy sets and soft sets are very important area of mathematics and other sciences due to their applications. In this present paper, the effects of an algebraic structure quantale with fuzzy sets and soft sets are presented. The fuzzy soft substructures of quantales such

as fuzzy soft subquantale and fuzzy soft ideals, are discussed. The fuzzy soft substructures in quantales are the extended notion of fuzzy substructures in quantales. It is observed that fuzzy soft set over a quantale is a fuzzy soft substructures if and only if their α-level set is a soft substructures over quantale for any $\alpha \in [0, 1]$. Moreover, the results show that fuzzy soft image and fuzzy soft inverse image of fuzzy soft substructures in quantale under quantale homomorphism with certain conditions are obtained. Further work, using the idea of *FSST* in quantales, can be extended to different algebraic structures including the following:

(1) Picture fuzzy soft structures in quantale theory and its generalization

(2) Inverse ???? theory applied to the fuzzy substructures to the quantales

(3) Interval-valued picture ???? theory applied to the fuzzy substructures of quantales.

Data Availability

The paper includes the information used to verify the study's findings.

Conflicts of Interest

The authors declare that they have no conflicts of interest.

References

[1] C. J. Mulvey, "Rendiconti del circolo matematico di Palermo," *Lobachevskii Journal of Mathematics*, vol. 12, no. 2, pp. 99–104, 1986.

[2] D. N. Yetter, "Quantales and (noncommutative) linear logic," *The Journal of Symbolic Logic*, vol. 55, no. 1, pp. 41–64, 1990.

[3] D. Kruml and J. Paseka, "Algebraic and categorical aspects of quantales," *Handbook of Algebra*, vol. 5, pp. 323–362, 2008.

[4] S. M. Qurashi and M. Shabir, "Generalized approximations of $$\left(\in ,\in \vee q\right) $$ $\in$, $\in \vee$ q -fuzzy ideals in quantalesϵ,$\epsilon \vee$ q)-fuzzy ideals in quantales," *Computational and Applied Mathematics*, vol. 37, no. 5, pp. 6821–6837, 2018.

[5] Q. Xiao and Q. Li, "Generalized lower and upper approximations in quantales," *Journal of Applied Mathematics*, vol. 2012, Article ID 648983, 11 pages, 2012.

[6] U. Höhle, "Topological representation of right-sided and idempotent quantales," *Semigroup Forum*, vol. 90, no. 3, pp. 648–659, 2015.

[7] P. Resende, "Quantales, finite observations and strong bisimulation," *Theoretical Computer Science*, vol. 254, no. 1-2, pp. 95–149, Mar. 2001.

[8] J. Y. Girard, "Linear logic," *Theoretical Computer Science*, vol. 50, no. 1, pp. 1–101, 1987.

[9] L. A. Zadeh, "Fuzzy sets," *Information and Control*, vol. 8, no. 3, pp. 338–353, 1965.

[10] Q. Luo and G. Wang, "Roughness and fuzziness in quantales," *Information Sciences*, vol. 271, pp. 14–30, 2014.

[11] S. M. Qurashi and M. Shabir, "Some studies in the approximation of ($\epsilon\gamma$, $\epsilon\gamma \vee$??)-fuzzy substructures in quantales," *Computational and Applied Mathematics*, vol. 39, no. 2, pp. 1–21, 2020.

[12] M. Farooq, T. Mahmood, A. Khan, M. Izhar, and B. Davvaz, "Fuzzy hyperideals of hyperquantales," *Journal of Intelligent and Fuzzy Systems*, vol. 36, no. 6, pp. 5605–5615, 2019.

[13] A. Hussain, T. Mahmood, and M. I. Ali, "Rough Pythagorean fuzzy ideals in semigroups," *Computational and Applied Mathematics*, vol. 38, no. 2, pp. 67–15, Jun. 2019.

[14] D. Molodtsov, "Soft set theory first results," *Computers & Mathematics with Applications*, vol. 37, no. 4-5, pp. 19–31, Feb. 1999.

[15] P. K. Maji, R. Biswas, and A. R. Roy, "Soft set theory," *Computers & Mathematics with Applications*, vol. 45, no. 4-5, pp. 555–562, 2003.

[16] M. I. Ali, F. Feng, X. Liu, W. K. Min, and M. Shabir, "On some new operations in soft set theory," *Computers & Mathematics with Applications*, vol. 57, no. 9, pp. 1547–1553, 2009.

[17] M. I. Ali, N. Mehmood, J. Zhan, and N. Shah, "Soft linear programming: an application of soft vector spaces," *Journal of Information and Optimization Sciences*, vol. 41, no. 3, pp. 679–704, 2020.

[18] R. Gul, M. Shabir, M. Naz, and M. Aslam, "A novel approach toward roughness of bipolar soft sets and their applications in MCGDM," *IEEE Access*, vol. 9, pp. 135102–135120, 2021.

[19] M. Shabir, R. S. Kanwal, and M. I. Ali, "Reduction of an information system," *Soft Computing*, vol. 24, no. 14, pp. 10801–10813, 2020.

[20] R. S. Kanwal and M. Shabir, "Approximation of soft ideals by soft relations in semigroups," *Journal of Intelligent and Fuzzy Systems*, vol. 37, no. 6, pp. 7977–7989, 2019.

[21] M. I. Ali, M. Shabir, and F. Feng, "Representation of graphs based on neighborhoods and soft sets," *International Journal of Machine Learning and Cybernetics*, vol. 8, no. 5, pp. 1525–1535, 2017.

[22] G. M. Addis, D. A. Engidaw, and B. Davvaz, "Soft mappings: a new approach," *Soft Computing*, vol. 26, no. 8, pp. 3589–3599, 2022.

[23] F. Feng, C. Li, B. Davvaz, and M. I. Ali, "Soft sets combined with fuzzy sets and rough sets: a tentative approach," *Soft Computing*, vol. 14, no. 9, pp. 899–911, 2010.

[24] F. Feng, X. Liu, V. Leoreanu-Fotea, and Y. B. Jun, "Soft sets and soft rough sets," *Information Sciences*, vol. 181, no. 6, pp. 1125–1137, 2011.

[25] R. S. Kanwal and M. Shabir, "Rough approximation of a fuzzy set in semigroups based on soft relations," *Computational and Applied Mathematics*, vol. 38, no. 2, pp. 89–23, 2019.

[26] S. M. Qurashi, R. S. Kanwal, M. Shabir, and K. Ali, "Generalized roughness of fuzzy substructures in quantales with respect to soft relations," *Journal of Intelligent and Fuzzy Systems*, vol. 40, no. 6, pp. 10435–10452, 2021.

[27] R. S. Kanwal, S. M. Qurashi, and M. Shabir, "Generalized approximation of substructures in quantales by soft relations," *Computational and Applied Mathematics*, vol. 39, no. 1, pp. 24–22, Mar. 2020.

[28] P. K. Maji, R. K. Biswas, and A. Roy, "Fuzzy soft sets," *Journal of Fuzzy Mathematics*, vol. 9, no. 3, pp. 589–602, 2001.

[29] Y. Yang, C. Liang, S. Ji, and T. Liu, "Adjustable soft discernibility matrix based on picture fuzzy soft sets and its applications in decision making," *Journal of Intelligent and Fuzzy Systems*, vol. 29, no. 4, pp. 1711–1722, 2015.

[30] S. Alkhazaleh, "Time-neutrosophic soft set and its applications," *Journal of Intelligent and Fuzzy Systems*, vol. 30, no. 2, pp. 1087–1098, 2016.

[31] A. M. Khalil, S. Alkhazaleh, S. G. Li, F. You, and S. Q. Ma, "More on "Time-neutrosophic soft set and its applications,"

Journal of Intelligent and Fuzzy Systems, vol. 35, no. 5, pp. 5721–5728, 2018.

[32] A. M. Khalil, S. G. Li, H. X. Li, and S. Q. Ma, "Possibility m-polar fuzzy soft sets and its application in decision-making problems," *Journal of Intelligent and Fuzzy Systems*, vol. 37, no. 1, pp. 929–940, 2019.

[33] M. Agarwal, K. K. Biswas, and M. Hanmandlu, "Generalized intuitionistic fuzzy soft sets with applications in decision-making," *Applied Soft Computing*, vol. 13, no. 8, pp. 3552–3566, 2013.

[34] A. M. Khalil and N. Hassan, "Inverse fuzzy soft set and its application in decision making," *International Journal of Information and Decision Sciences*, vol. 11, no. 1, pp. 73–92, 2019.

[35] A. M. Khalil, S. G. Li, H. Garg, H. Li, and S. Ma, "New operations on interval-valued picture fuzzy set, interval-valued picture fuzzy soft set and their applications," *IEEE Access*, vol. 7, pp. 51236–51253, 2019.

[36] C. Cheng, Z. Cao, and F. Xiao, "A generalized belief interval-valued soft set with applications in decision making," *Soft Computing*, vol. 24, no. 13, pp. 9339–9350, 2020.

[37] M. J. Khan, P. Kumam, S. Ashraf, and W. Kumam, "Generalized picture fuzzy soft sets and their application in decision support systems," *Symmetry*, vol. 11, no. 3, p. 415, 2019.

[38] A. Aygünoğlu and H. Aygün, "Introduction to fuzzy soft groups," *Computers & Mathematics with Applications*, vol. 58, no. 6, pp. 1279–1286, 2009.

[39] M. Shabir and R. S. Kanwal, "On L-fuzzy soft ideals of nearrings," *Annals of fuzzy Mathematics and Informatics*, vol. 10, pp. 161–180, 2015.

[40] S. Habib, F. Muhammad Khan, and N. Yufeng, "A new concept of possibility fuzzy soft ordered semigroups via its applications," *Journal of Intelligent and Fuzzy Systems*, vol. 36, no. 4, pp. 3685–3696, 2019.

[41] P. Majumdar and S. K. Samanta, "Generalised fuzzy soft sets," *Computers & Mathematics with Applications*, vol. 59, no. 4, pp. 1425–1432, 2010.

[42] A. Dey and M. Pal, "Generalised multi-fuzzy soft set and its application in decision making," *Pacific Science Review A: Natural Science and Engineering*, vol. 17, no. 1, pp. 23–28, Jan. 2015.

[43] A. A. Hazaymeh, I. B. Abdullah, Z. T. Balkhi, and R. I. Ibrahim, "Generalized fuzzy soft expert set," *Journal of Applied Mathematics*, vol. 2012, Article ID 328195, 22 pages, 2012.

[44] S. Alkhazaleh and A. R. Salleh, "Generalised interval-valued fuzzy soft set," *Journal of Applied Mathematics*, vol. 2012, Article ID 870504, 18 pages, 2012.

[45] M. et al, D. Al-Kadi, H. Harizavi, and A. S. Albjedi, "Fuzzy soft set theory applied to commutative ideals of BCK-algebras," *International Journal of Advanced and Applied Sciences*, vol. 8, no. 6, pp. 48–56, 2021.

[46] N. Jan, T. Mahmood, L. Zedam, and Z. Ali, "Multi-valued picture fuzzy soft sets and their applications in group decision-making problems," *Soft Computing*, vol. 24, no. 24, pp. 18857–18879, 2020.

[47] K. I. Rosenthal, "Quantales and their applications, pittman research notes in mathematics 234," *Longman Scientific & Technical*, vol. 172, 1990.

[48] S. Q. Wang and B. Zhao, "Ideals of quantales," *Journal of Shanxi Normal University (Philosophy and Social Sciences edition)*, vol. 31, no. 4, pp. 7–10, 2003.

[49] C. F. Yang, "Fuzzy soft semigroups and fuzzy soft ideals," *Computers & Mathematics with Applications*, vol. 61, no. 2, pp. 255–261, 2011.

[50] M. I. Ali and M. Shabir, "Comments on De Morgan's law in fuzzy soft sets," *Journal of Fuzzy Mathematics*, vol. 18, no. 3, pp. 679–686, 2010.

Hindawi
Complexity
Volume 2023, Article ID 5912191, 22 pages
https://doi.org/10.1155/2023/5912191

WILEY | Hindawi

Research Article

Complex Dynamic Analysis, Circuit Design and Simplified Predefined Time Synchronization for a Jerk Absolute Memristor Chaotic System

Jindong Liu,[1] Zhen Wang,[1,2] Huaigu Tian,[1] and Fei Xie[1,3]

[1]*Xi'an Key Laboratory of Human-Machine Integration and Control Technology for Intelligent Rehabilitation, Xijing University, Xi'an 710123, China*
[2]*Shaanxi International Joint Research Center for Applied Technology of Controllable Neutron Source, Xijing University, Xi'an 710123, China*
[3]*Academy of Advanced Interdisciplinary Research, Xidian University, Xi'an 710071, China*

Correspondence should be addressed to Zhen Wang; williamchristian@163.com

Received 30 September 2022; Revised 9 November 2022; Accepted 22 March 2023; Published 18 April 2023

Academic Editor: Zeljko Stevic

In this parper, a 4D absolute memristor Jerk chaotic system is proposed. Firstly, complex dynamics are studied by phase diagram, Poincaré section, power spectrum, bifurcation diagram, 0-1 test, and Lyapunov exponent spectrum. Then, the period doubling bifurcation, degradation, and offset boosting are revealed. For the feasibility of practical application, the analog circuit and FPGA digital circuit are designed. Finally, a simplified predefined time synchronization scheme is proposed; comparing with the full control input synchronization scheme, the simplified predefined time synchronization scheme can not only reduce the controller inputs but also predefine the synchronization time.

1. Introduction

Nonlinear phenomena have a profound impact on the use of math-physical methods to describe our objective world, especially the use of chaotic theory to design and study circuits with simple structure, easily implementation, and complication in dynamics behavior, which is used in the fields of weak signal detection [1, 2], image encryption [3, 4], neural network [5–7], etc. As a new component describing the relationship between magnetic flux and charge, memristor was first proposed by Chua in 1971 [8]. Its rich nonlinear behavior and malleable have been widely used in recent years, including the design of memristor circuits with different orders and the construction of circuit models [9–12]. As a nonlinear dual-port element, memristor is added to the classical nonlinear system, such as Chua's circuit [13], Lorenz system [14], and Chen's system [15]. The memristor circuit composed of various classical nonlinear circuits shows colorful and unforgettable dynamic behaviors, including hidden attractors [16–18], hyperchaotic behaviors [19], symmetric attractors [13], and extreme multistability [20–23] with infinite number of coexistence attractors. The memristor model described by piecewise linear function [24], quadratic nonlinear function [25], and cubic nonlinear function [26] is a mathematical model often used by scholars. Different from the previous ones, this paper attempts to introduce a novel and interesting magnetic flux memristor model with absolute value function. These classes of memristors have uncertain two-sided characteristics due to its special properties, that is, it cannot only provide more flexibility in practical engineering but also may cause damage to the system.

The application of chaotic sequences is an extremely important link. In many cases, unipolar signals are often required in practical circuit applications, but the polarity conversion has become a thorny problem. In order to change this situation, Li [27] proposed a chaotic amplitude control method; by introducing a constant term into the system,

offset boosting can be achieved, which solves the problem of polarity conversion of chaotic signals; meanwhile, it does not change the dynamics of the system. Since then, many scholars have applied this method to the proposed chaotic systems, such as the offset boosting control of the integer order chaotic attractor [28, 29] and the fractional-order chaotic attractor [30, 31]. Here, the original system is converted into a self-replicating system, resulting in an infinite number of attractors with extreme multistability. Therefore, the application of chaotic system in engineering can be greatly enriched by offset boosting control, and the study on offset boosting control is becoming active increasingly.

It can be seen from the previous description that the multistability of memristor chaotic system brings many advantages in engineering; however, it will also lead to some undesirable things due to the "minor to damage" characteristics of chaos. In the past, scholars have proposed different control schemes to achieve the synchronization of memristor chaotic systems as follows: finite time synchronization schemes [16, 32–35]and fixed time synchronization schemes [18, 36, 37]. In addition, these proposed synchronization schemes require the same controller input dimension as the system dimension, which makes the controller more complex, and synchronization time cannot be given. In order to eliminate these defects, this paper considers introducing a simplified predefined time synchronization scheme, which synchronization time function is easier to realize than that of these previous synchronization schemes, and fewer controllers, so as to realize the control of "predefined" time for a class of Jerk systems with absolute value memristor.

Based on this, the main structure of this paper is as follows: Firstly, in Section 2, through the analog circuit realization and numerical simulation results of the absolute memristor, we can find that the absolute memristor has rich memristor characteristics and verify the influence of frequency and voltage amplitude on the area of hysteresis loop. Therefore, based on this, a novel 4D absolute memristor Jerk system is proposed. In Section 3, the dynamic analysis of the system is carried out, such as phase diagrams, Poincaré section, Lyapunov exponent spectrum, power spectrum, bifurcation diagram, 0-1 test, and offset boosting, revealing the rich dynamic behavior of the system. In Section 4, the analog circuit and FPGA digital circuit of the system are designed to verify the feasibility of the system. In Section 5, a simplified predefined time synchronization scheme is proposed innovatively, which overcomes the shortcomings that the synchronization time of finite time and fixed time synchronization schemes cannot be "predefined," and then compared with the full control input synchronization scheme, the simplified predefined time synchronization scheme can also reduce the controller input. Finally, the conclusion and the future work are given in the last section of this paper.

2. Properties of Absolute Memristor Model

2.1. Equivalent Circuit and Characteristic of Absolute Memristor. The memristor is a dual-port circuit element described by the equation $f(\varphi, q) = 0$; the mathematical expression of the magnetic control memristor described by a piecewise quadratic nonlinear function characteristic curve is as follows:

$$q(\varphi) = \alpha\varphi - 0.5\beta\varphi^2 \operatorname{sgn}(\varphi). \tag{1}$$

In equation (1), α, β are positive constants, and $\operatorname{sgn}(\cdot)$ is a symbolic function. We calculate the differential of time t at both ends of equation (1) at the same time, and the following relationship holds:

$$i(t) = W(\varphi)v(t) = (\alpha - \beta|\varphi|)v(t). \tag{2}$$

Here, $\mathrm{d}q/\mathrm{d}t = i(t)$, $\mathrm{d}\varphi/\mathrm{d}t = v(t)$, $W(\phi)$ is the magnetron absolute value type memristor as follows:

$$W(\varphi) = \frac{\mathrm{d}q(\varphi)}{\mathrm{d}\varphi} = \alpha - \beta|\varphi|. \tag{3}$$

That is, equation (2) is the VCR of the piecewise quadratic nonlinear magnetron memristor, and the absolute value type memristor is controlled by its internal state variable flux $\phi(t)$. The parameters are $\alpha = 1$, $\beta = 0.1$ in the equation (3), and the relationship between the driving voltage $v(t)$ and the current $i(t)$ can be obtained by applying the driving voltage $v(t)$ at both ends of equation (3). Furthermore, the absolute memristor circuit schematic diagram shown in Figure 1 can be designed according to the circuit theory.

According to the absolute memristor circuit schematic Figure 1, the circuit equation shown in equation (4) can be obtained. Moreover, the $t(s) - v(t)$ and $v(t) - i(t)$ curves of the absolute memristor are further realized according to the analog circuit simulation of the absolute memristor, as shown in Figure 2. The correctness of the tight hysteresis loop of the voltage and current origin contraction of the absolute value memristor is verified by circuit simulation.

$$i(t) = \frac{R_3}{R_2}\frac{R_8}{R_6}v(t) - \frac{R_3}{R_2}\frac{R_5}{R_4}\frac{R_8}{R_6}|x_4|v(t). \tag{4}$$

In order to further verify the correctness of the memristor characteristics realized by the analog circuit of absolute memristor, the driving voltages at both ends of the memristor are subjected to different excitation amplitudes and different excitation frequencies.

For the absolute memristor, the influence of the amplitude A and frequency F of the external excitation signal on the area of the memristor hysteresis loop is studied. Through the external input voltage V, its sinusoidal function $V = A\sin(2\pi F)$. It can be seen from the description in Figure 3 that the amplitude A of the sinusoidal excitation signal is positively correlated with the area of the hysteresis

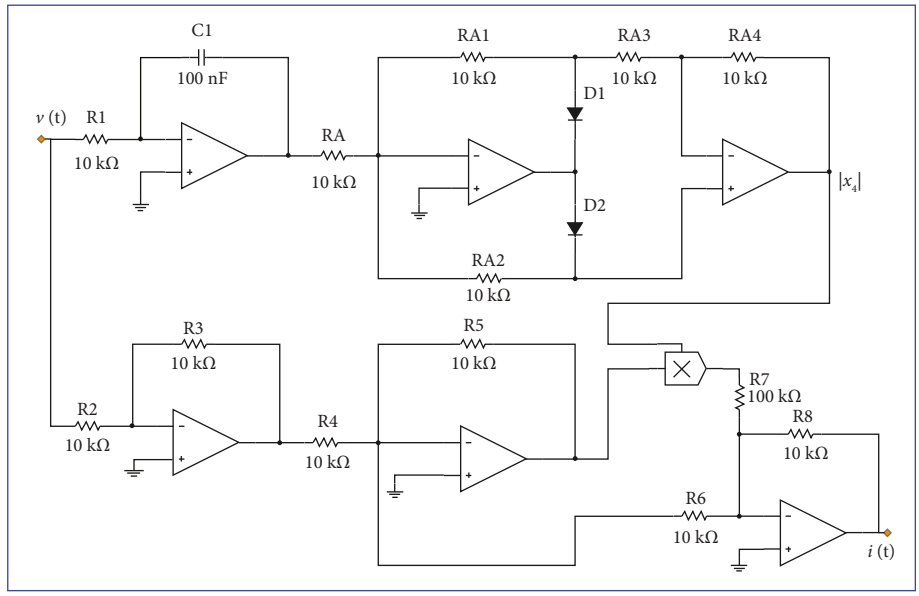

Figure 1: Circuit diagram of absolute memristor.

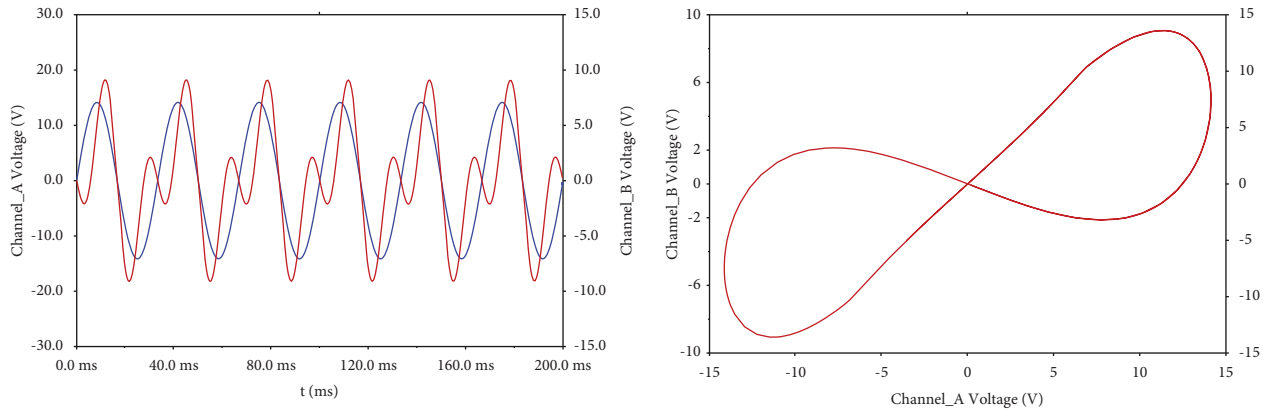

Figure 2: Absolute memristor hysteresis loop. (a) $t(s) - v(t)$ curve; (b) $v(t) - i(t)$ curve.

loop, and the frequency F is negatively correlated with the area of the hysteresis loop.

2.2. Modeling of a Absolute Memristor Jerk Chaotic System. In [38], there is a Jerk system, and the mathematical model is described as follows:

$$\begin{cases} \dot{x}_1 = x_2, \\ \dot{x}_2 = x_3, \\ \dot{x}_3 = |x_1| - x_2 - ax_3 - 1, \end{cases} \tag{5}$$

where a and b are the positive constant and x_1, x_2, and x_3 are the state variables. By introducing the new expression (2) to the degenerate Jerk system in (5), a novel class of degenerate chaotic Jerk system based on memristor can be described as follows:

$$\begin{cases} \dot{x}_1 = x_2 - b, \\ \dot{x}_2 = W(x_4)x_3, \\ \dot{x}_3 = |x_1| - x_2 - ax_3, \\ \dot{x}_4 = x_3 \end{cases} \tag{6}$$

where a and b are the positive constant and $W(x_4)$ is the memory derivative function of the previous absolute memristor equation (3). The nonlinear characteristics and dynamic behaviors of the novel memristor system (6) introduced in this paper are worth studying in the following sections.

3. Stability and Dynamics Analysis

3.1. Stability Analysis. Let $\dot{x}_1$, $\dot{x}_2$, $\dot{x}_3$ and $\dot{x}_4$ on the left side of equation (6) be equal to zero. It is easy to find that the set of equilibria of the system is $A = (\pm b, 0, 0, 0)$, where b is a real

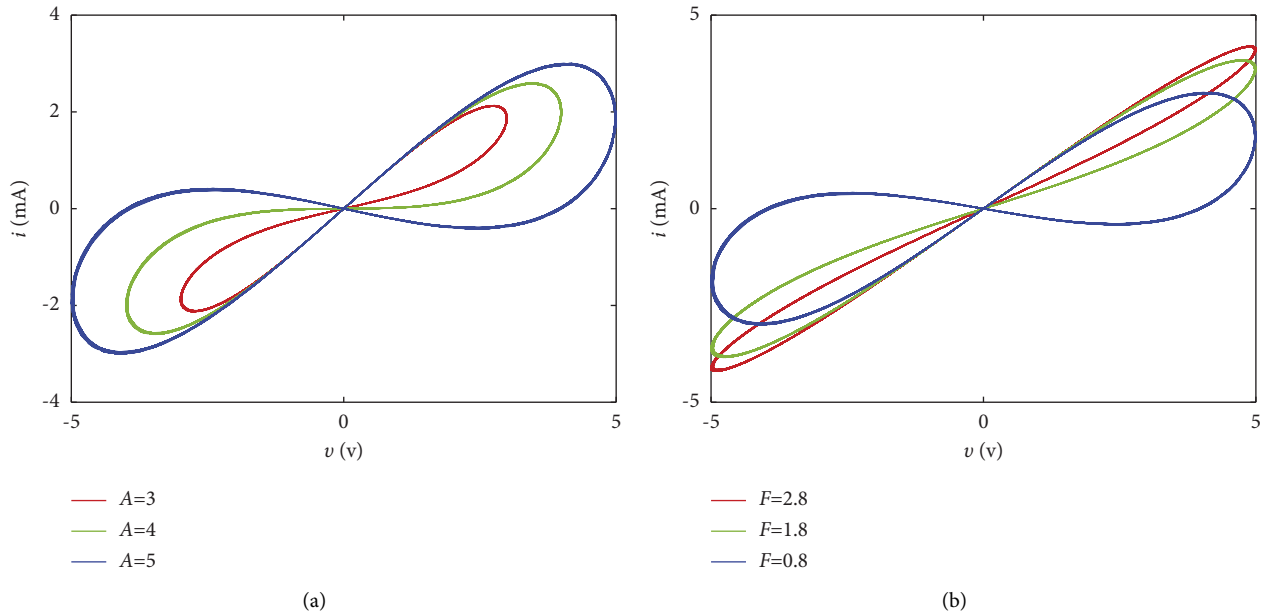

FIGURE 3: Numerical simulation of absolute memristor tight hysteresis loop. (a) Different amplitude A values; (b) different frequency F values.

constant. Linearize equation (6) at this set of equilibria to obtain the Jacobian matrix of the system is as follows:

$$J = \begin{bmatrix} 0 & 1 & 0 & 0 \\ 0 & 0 & -\beta \operatorname{sign}(x_4) & -\beta x_3 \operatorname{sign}(x_4) \\ \operatorname{sign}(x_1) & -1 & -a & 0 \\ 0 & 0 & 1 & 0 \end{bmatrix}. \quad (7)$$

Since the equilibrium is $A = (\pm b, 0, 0, 0)$, the characteristic polynomial of the system can be obtained as follows:

$$\lambda\left(\lambda^3 + a\right) = 0. \quad (8)$$

According to the Routh–Hurwitz stability condition, the necessary and sufficient condition for the existence of roots of equation (2) given above is $a > 0$. When the characteristic roots of equation (2) are $\lambda_1 < 0$, $\lambda_2 < 0$, $\lambda_3 < 0$, it is called a stable node. Therefore, the system can generate chaotic and rich dynamic behavior, and the parameter $a > 0$. It should be noted that the stability of equation (6) cannot be simply determined by equilibrium set $A = (\pm b, 0, 0, 0)$. Therefore, the dynamical behaviors of system (6) under other conditions are further analyzed below.

3.2. Dynamical Analysis

3.2.1. Phase Trajectory, Poincaré Section and Power Spectrum. The parameter selection for the system is $a = 0.6$, $b = 1.3$, $\alpha = 1$, $\beta = 0.1$ and initial value is $x_0 = (1, 0, 0, -1)$. The chaotic phase diagrams generated by the system under this parameter condition are shown in Figure 4. The corresponding Lyapunov exponent spectrum is calculated as $[0.0587, 0, -0.0028, -0.6560]$; the Wolf algorithm shows that the system exhibits chaos.

Similarly, under the condition that the parameters of system are consistent with the previous one, the Poincaré section and power spectrum characteristics are described, respectively, in Figures 5 and 6 to illustrate.

From the description in Figure 5, it is found that the Poincaré cross section is not a closed curve but a curve with phase diagram profile composed of dense points. The power spectrum in Figure 6 is found to be continuous without obvious wave peaks. It is concluded that the system is a chaotic system with complex dynamic behavior.

3.2.2. Bifurcation and Lyapunov Exponent Spectrum. In the system, to set the system parameter to $b = 1.3$, $\alpha = 1$, $\beta = 0.1$, and $x_0 = (0, 0, 0, -2)$ is the initial value of the system. When selecting system parameter a as system variable, the bifurcation diagram and Lyapunov exponent spectrum (LEs) of state variable x_1 can be obtained, as shown in Figures 7(a) and 7(b). When the system parameter a is increasing, the bifurcation diagram shows that the system has inverse period doubling bifurcation when the parameters $a = 0.65$ and $a = 0.73$, respectively. Similarly, the complex dynamic characteristics of the system can be described according to the Largest Lyapunov exponent (LLE). According to Figure 7(b), when $a < 0.65$, LLE > 0, and when $a > 0.65$, LLE $= 0$. In addition, the fourth value of LEs4 is always less than zero, which is not described in Figure 7(b). Therefore, the dynamic behavior is consistent when describing the change of parameter a in Figure 7.

According to the 0-1 test method, the periodic state or chaotic state of the system can be judged qualitatively under the influence of parameter a [39]. This method is mainly the a quantitative analysis method which is used to detect whether there is chaos in the system. When parameter $a = 0.6$, the trajectory of the system on the $p - s$ plane is

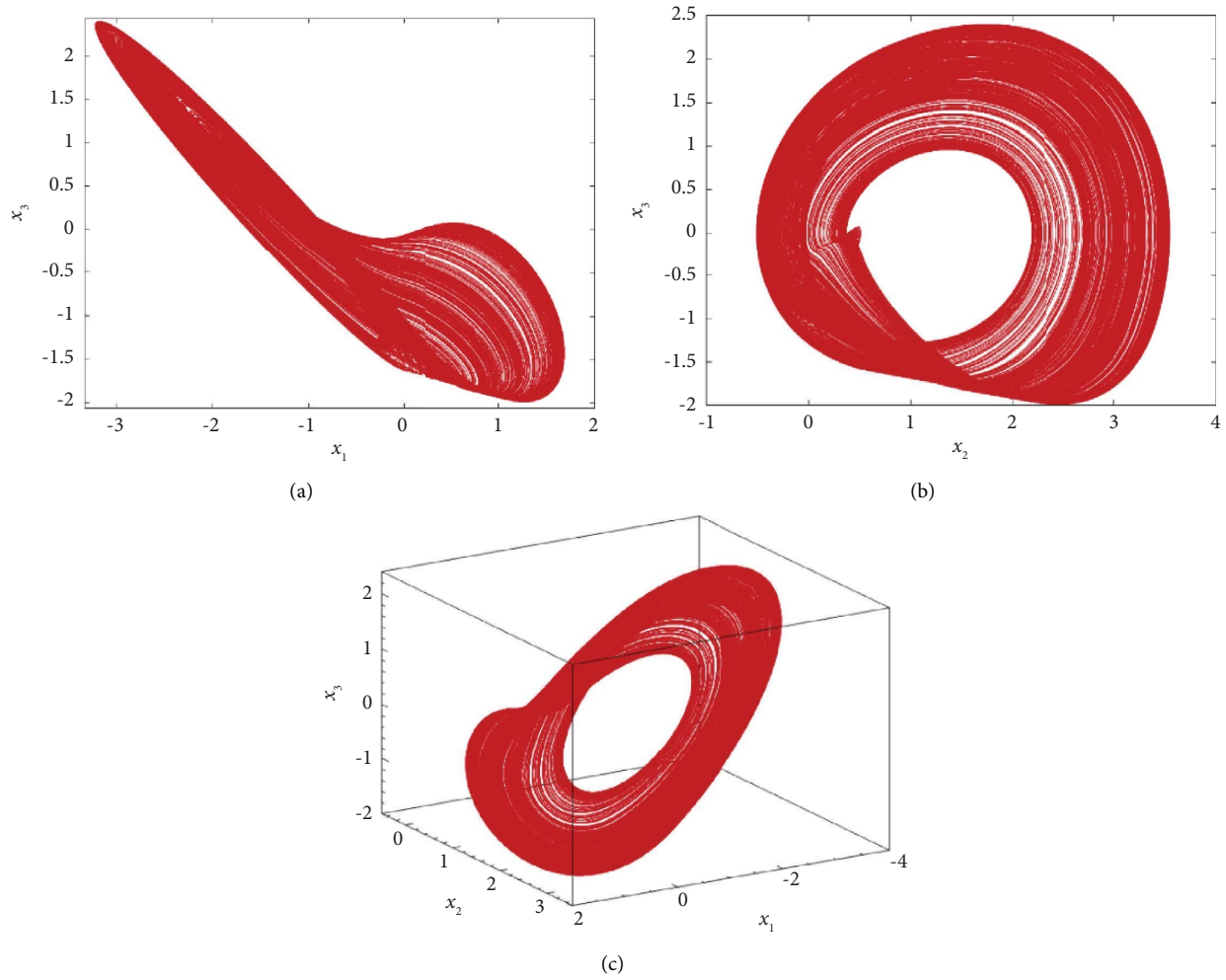

FIGURE 4: System phase diagram. (a) $x_1 - x_3$ plane; (b) $x_2 - x_3$ plane; (c) $x_1 - x_2 - x_3$ plane.

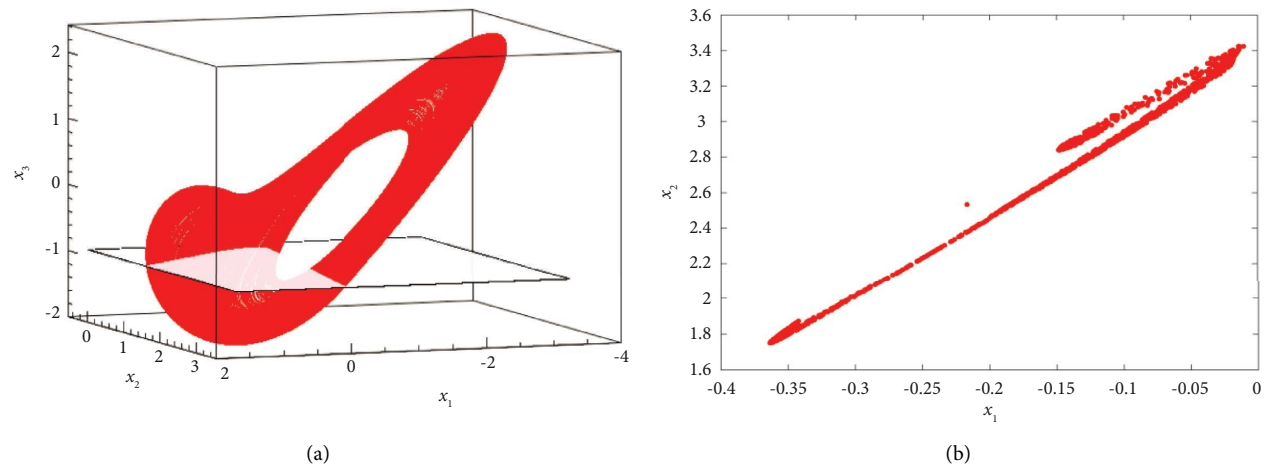

FIGURE 5: Poincaré section of phase diagram of the system. (a) $x_1 - x_2 - x_3$ plane phase diagram; (b) $x_3 = -1$ Poincaré section.

chaotic and irregular. When the parameter $a = 0.8$, the trajectory of the system on the $p - s$ plane is regular and orderly, as shown in Figure 8. The reflected dynamic behavior is the same as that in Figure 7.

Considering the dynamic phenomena caused by the change of initial value, fixed parameters are $a = 0.6$, $b = 1.3$, $\alpha = 1$, $\beta = 0.1$, and $x_0 = (0, x_2(0), 0, -2)$ is the initial value of the system, When $x_2(0) \in (0, 2)$ is selected, the chaotic

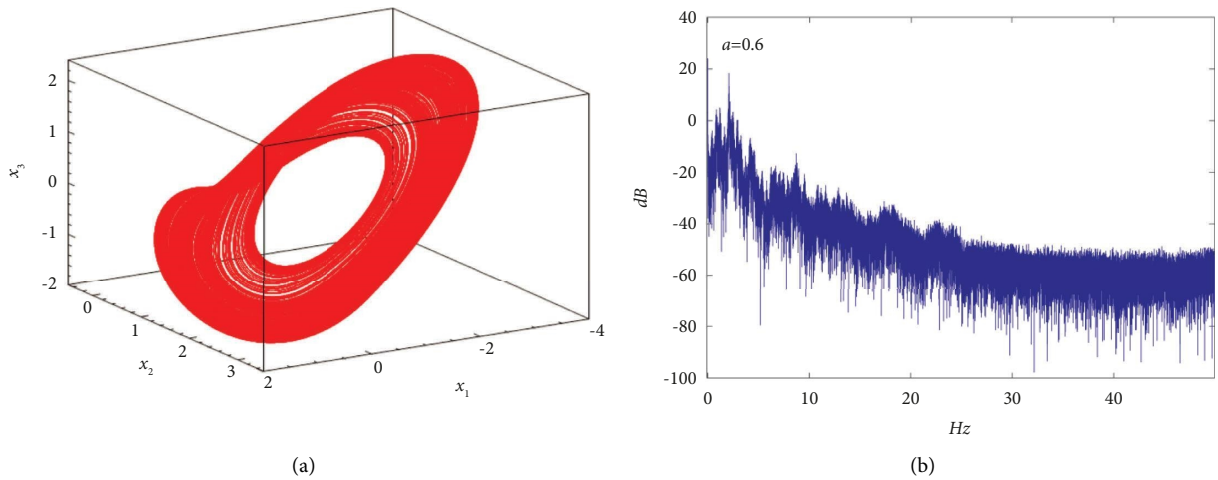

(a) (b)

Figure 6: Power spectrum of the system. (a) $x_1 - x_2 - x_3$ plane phase diagram; (b) power spectrum.

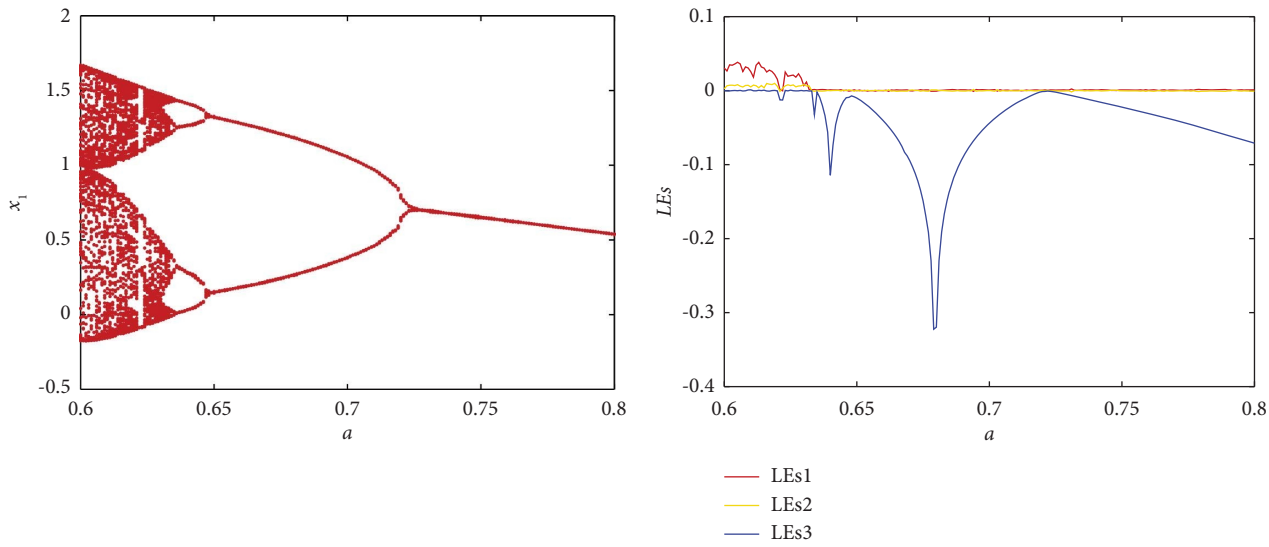

(a) (b)

Figure 7: Parameter a change. (a) Bifurcation diagram; (b) LEs.

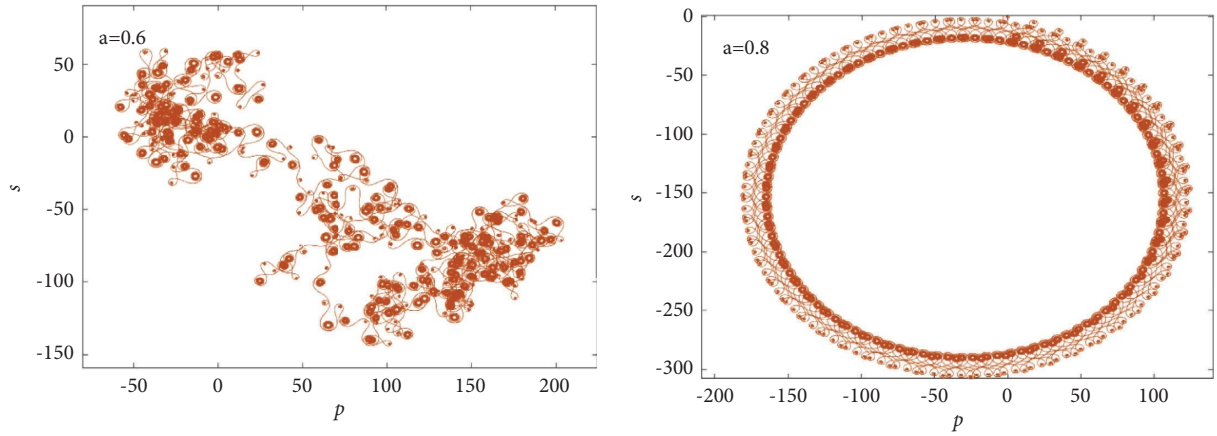

(a) (b)

Figure 8: $p - s$ plane trajectory of the system. (a) $a = 0.6$; (b) $a = 0.8$.

window and periodic window appear alternately, and the period doubling bifurcation phenomenon occurs when $x_2(0) = 1.21$. As it continues to increase to $x_2(0) = 1.48$, chaotic jump occurs and a short reverse period doubling bifurcation occurs until the end. The bifurcation diagram and LEs of system $x_2(0)$ as variable are drawn in Figure 9. They reflect the dynamic characteristics of $x_2(0)$ as independent variable, and the two reflect the same dynamic behavior.

Furthermore, the dynamic behavior of bifurcation diagram and LEs reaction is verified according to the type of phase diagram attractor of the system. The values of variable $x_2(0)$ are selected as 0.0, 1.5, and 2.0 in the system bifurcation diagram. The system phase diagram-type characteristics that can be drawn are shown in Figure 10.

When $x_4(0)$ is used as a system variable, other parameters remain the same as the previous one, when the variation range of $x_4(0)$ belongs to $[-3, 3]$. As can be seen from Figure 11(a), when the variable $x_4(0)$ increases, the system enters the large-scale chaotic window from the periodic window and ends with a short periodic window at the end. After variable $x_4(0) = 2.0$, the system enters the periodic window from the chaotic window. Then, there is a jumping chaotic band when $x_4(0) \in (2.32, 2.41)$, which then jump to the cycle window. Through the LEs depicting the change of the initial value variable $x_4(0)$ in Figure 11(b), it is found that the result is consistent with the dynamic phenomenon described in the bifurcation diagram in Figure 11(a).

Similarly, when $x_4(0)$ is $-3, -2.3, 0.0$, the phase diagram-type characteristics of the system is shown in Figure 12. It can be found that when the initial value $x_4(0) \in (-3, 3)$ changes, the system shows different characteristic types of chaotic attractors.

3.3. Transient Chaos of the System. The chaotic motion state of the system has limited life, and its main dynamic feature is that the system suddenly changes into a stable periodic motion in a short time of chaotic state, which can be called transient chaos [19], in order to reveal this transient chaotic phenomenon, by setting the system parameter to $a = 0.6$, $b = 1.3$, $\alpha = 1$, $\beta = 0.1$, and $x_0 = (1, 1, -2, -1)$ is the initial value of the system. According to the description in Figure 13, it can be found that the system is chaotic within $t < 2500s$ and periodic after $t > 2500s$. Therefore, the system has a short time of chaotic state and then degenerates into a periodic state.

Furthermore, the transient chaos behavior of the system is judged according to the characteristic type of the phase diagram. The chaotic phase diagram and periodic phase diagram of the system are drawn, respectively, in the time period of $t \in (500s - 2500s)$ and $t \in (4000s - 5000s)$ through Figure 14.

Transient chaos can also be described according to the time domain waveform of LEs of the system and the time domain waveform of state variable x_1 of the system, as shown in Figure 15. However, only the first and second curves are drawn in the time domain waveform of LEs, and the third and fourth curves are always less than zero. It is found from the LEs of the system in Figure 15(a) and the time t domain waveform of the state variable x_1 as shown in Figure 15(b). It can be seen that the system LLE > 0 before $t < 2500s$, LLE = 0 after $t > 2500s$. In addition, the time-domain waveform of the system state x_1 within $t \in (4000s, 5000s)$, and the system shows a periodic state in this interval, as shown in Figure 15(b). It further shows that the system has transient chaos.

3.4. Offset Boosting. In the memristor chaotic system, the position change of the attractor is changed by adding a constant term to the uncoupled term of the system. This phenomenon is a potential feature of the memristor chaotic system, which can control the chaotic attractor of the system through the constant term. It can be found in the system that state variables x_1 and x_2 are independent uncoupled state variables. Therefore, $|x_1|$ and x_2 in the system can be replaced by $|x_1 + k|$ and $(x_2 + l)$. We can know that k and l are the two control parameters of the offset boosting, and the system can be expressed as follows:

$$\begin{cases} \dot{x_1} = (x_2 + l) - b, \\ \dot{x_2} = (\alpha - \beta|x_4|)x_3, \\ \dot{x_3} = |x_1 + k| - (x_2 + l) - ax_3, \\ \dot{x_4} = x_3. \end{cases} \tag{9}$$

In equation (9), the parameter is set to $a = 0.6$, $b = 1.3$, $\alpha = 1$, $\beta = 0.1$. First, only one control parameter k is changed and parameter $l = 0$. Case 1: When $x_0 = (1, 0, 0, -1)$ is selected as the initial value of system (9), the offset boosting control parameters k take the values of $k = 0.0$, $k = 0.5$ and $k = -0.5$, respectively. Though Figure 16 shows the offset boosting phenomenon of system (9) under the influence of a single control parameter k, Figure 16(a) shows that the system phase diagrams move left and right along the x_1 direction on the $x_1 - x_2 - x_3$ space. Case 2: Select system (9) initial value as $x_0 = (1, 1, -2, -2)$, and the control parameters are the same as those in Case 1. Figure 16(b) shows that the system periodic phase diagrams move left and right along the x_1 direction on the $x_1 - x_3$ plane.

In order to study the offset boosting under the influence of another control parameter l, here, the parameter selection and initial value of system (9) are consistent with the previous research control parameter k. Case1: $l = 0.0$, $l = 1.0$, $l = -1.0$ as shown in Figure 17(a). Case2: $l = 0.0$, $l = 1.0$, $l = -1.0$ as shown in Figure 17(b). It can be seen that under the control parameter l, the phase diagrams of system (9) move left and right along the x_2 direction.

Similarly, when studying the offset boosting caused by the simultaneous change of double control parameters k and l, the selection of system (9) parameters and initial values are consistent with the previous one. The values of control parameters k and l are, respectively, $k = 0$, $l = 0.0$; $k = 0.5$, $l = 1.0$; $k = -0.5$, $l = -1.0$. It can be found from Figures 18(a) and 18(b) that system (9) phase diagrams can translate and enlarge in $x_1 - x_2 - x_3$ space and $x_1 - x_3$ plane under the

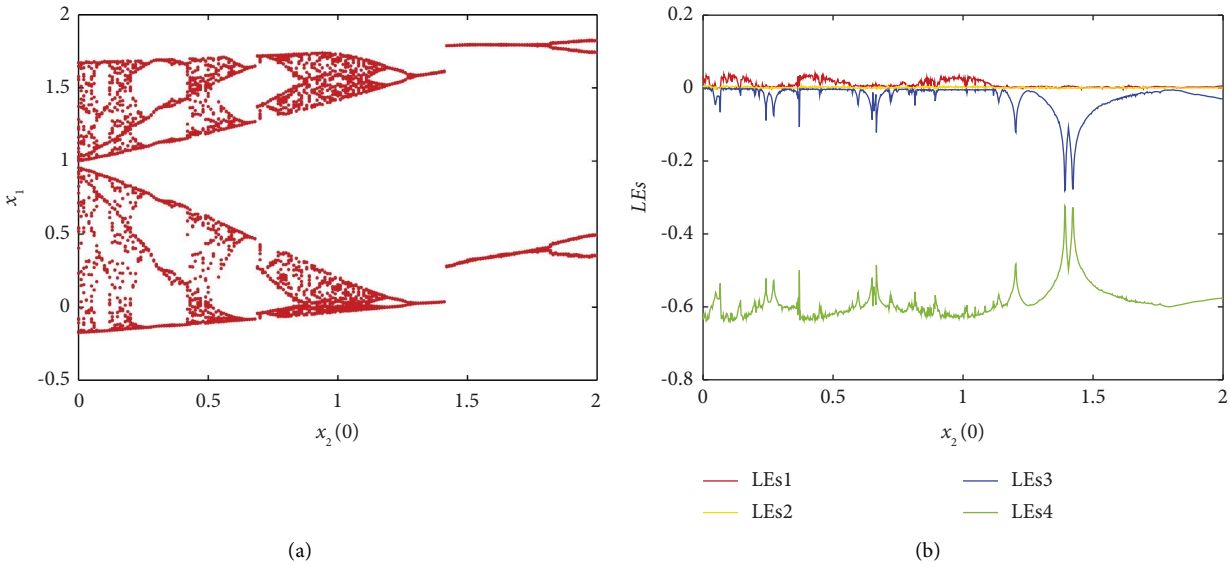

Figure 9: Initial value $x_2(0)$ change. (a) Bifurcation diagram; (b) LEs.

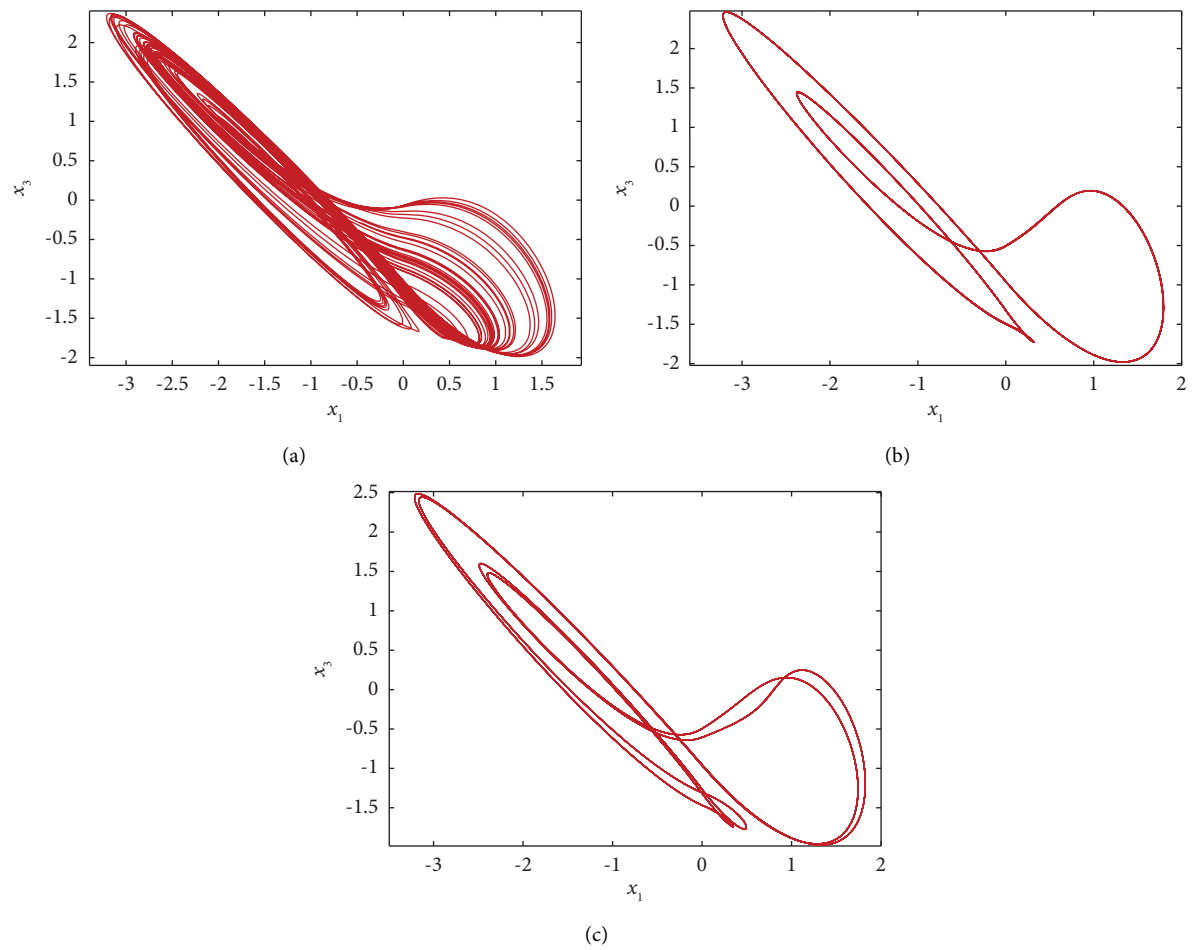

Figure 10: Types of the system phase diagrams with the change of the system initial value $x_2(0)$. (a) $x_2(0) = 0.0$ is $x_1 - x_3$ plane chaotic phase diagram; (b) $x_2(0) = 1.5$ is $x_1 - x_3$ plane periodic 1; (c) $x_2(0) = 2.0$ is $x_1 - x_3$ plane periodic 2.

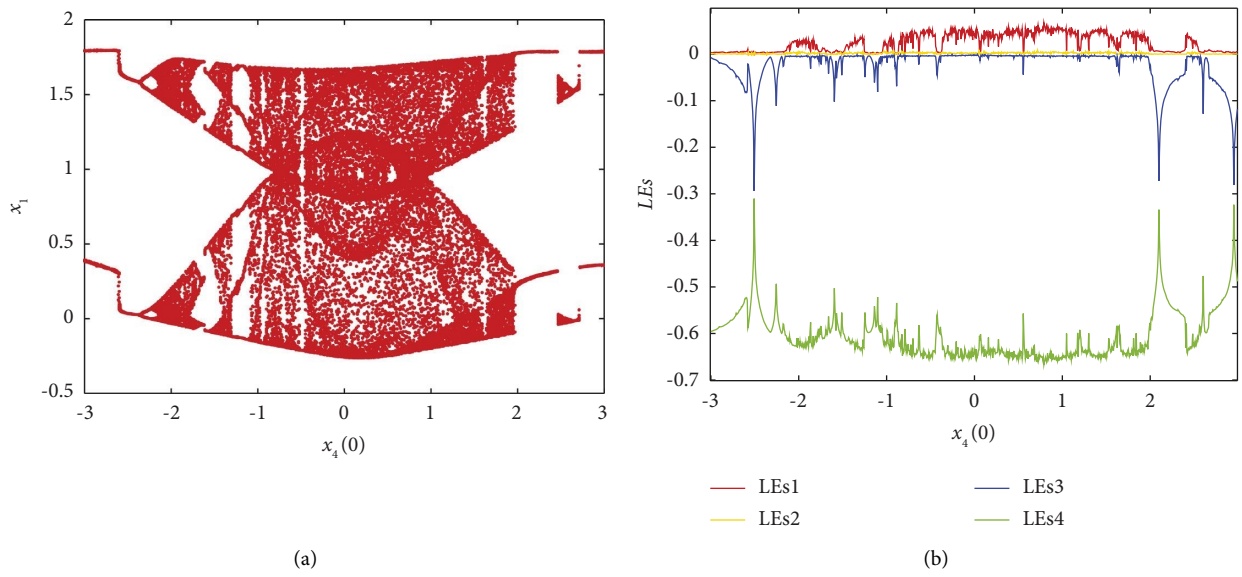

Figure 11: Initial value $x_4(0)$ change. (a) Bifurcation diagram; (b) LEs.

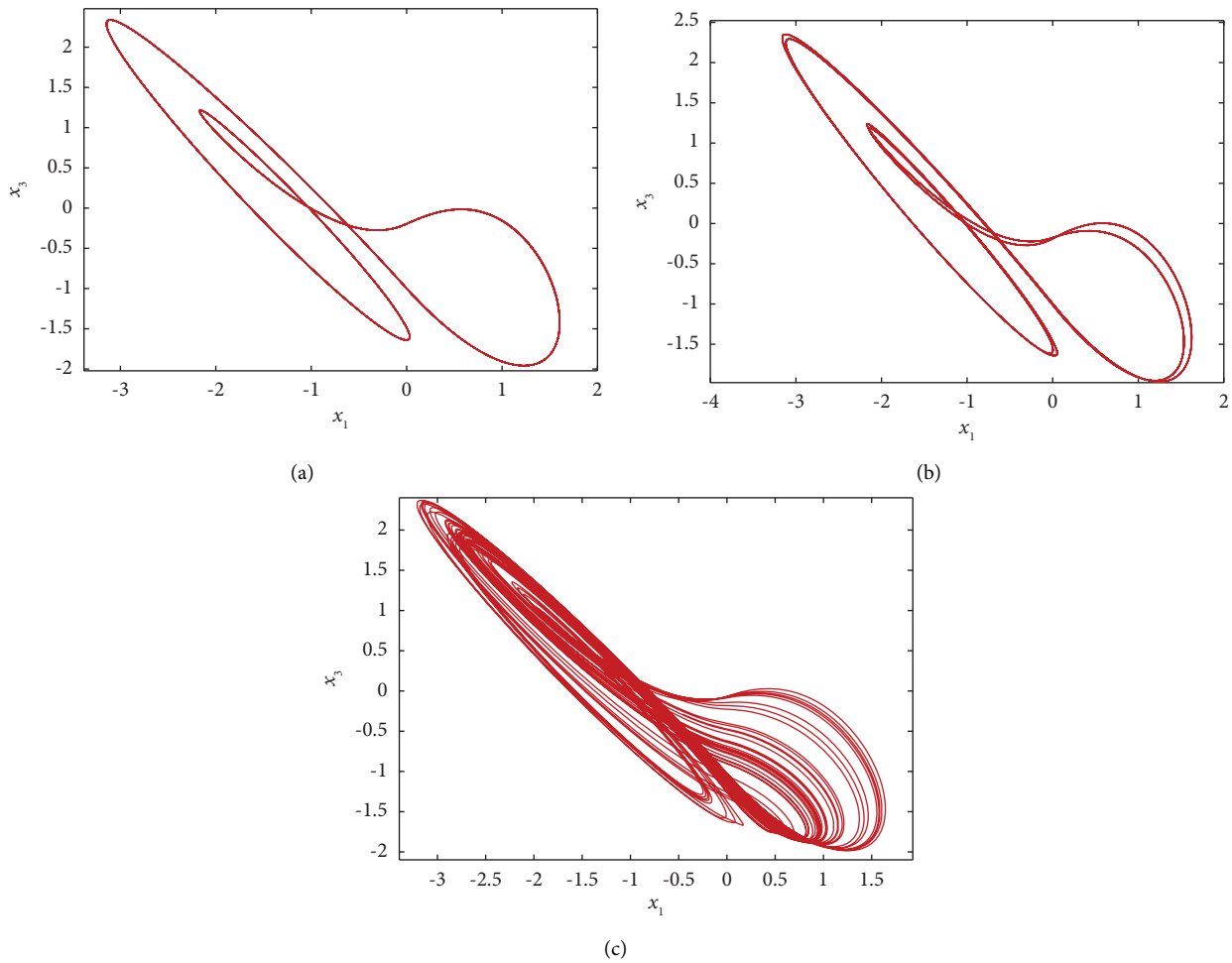

Figure 12: Types of the system phase diagrams with the change of the system initial value $x_4(0)$. (a) $x_4(0) = -3$ is $x_1 - x_3$ plane periodic 1; (b) $x_4(0) = -2.3$ is $x_1 - x_3$ plane periodic 2; (c) $x_4(0) = 0.0$ is $x_1 - x_3$ plane chaotic phase diagram.

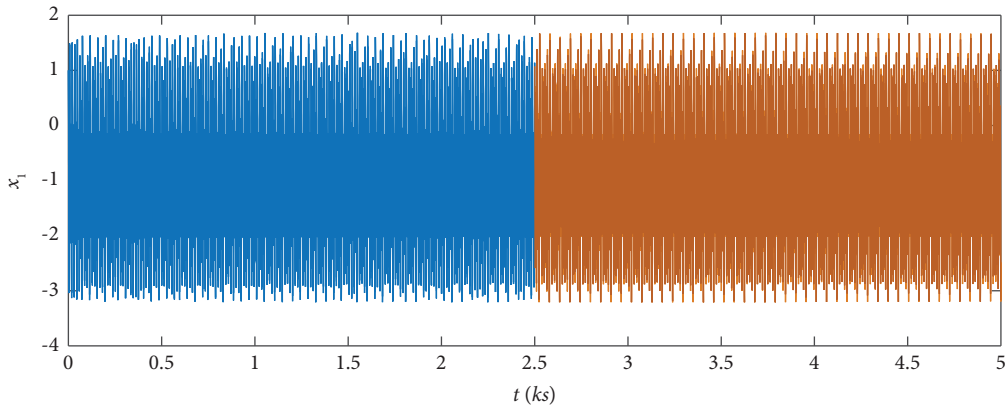

FIGURE 13: Time domain waveform of the system in time interval $t \in (0 - 5000\,\text{s})$.

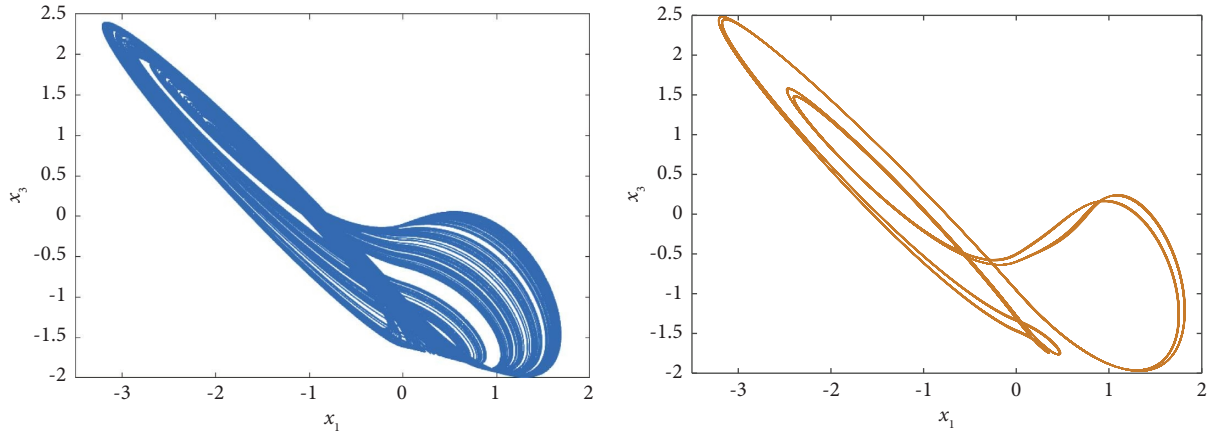

FIGURE 14: Phase diagrams of the system. (a) Phase diagram of $x_1 - x_3$ plane system in $t \in (500\,\text{s} - 2500\,\text{s})$ interval; (b) phase diagram of $x_1 - x_3$ plane system in $t \in (4000\,\text{s} - 5000\,\text{s})$ interval.

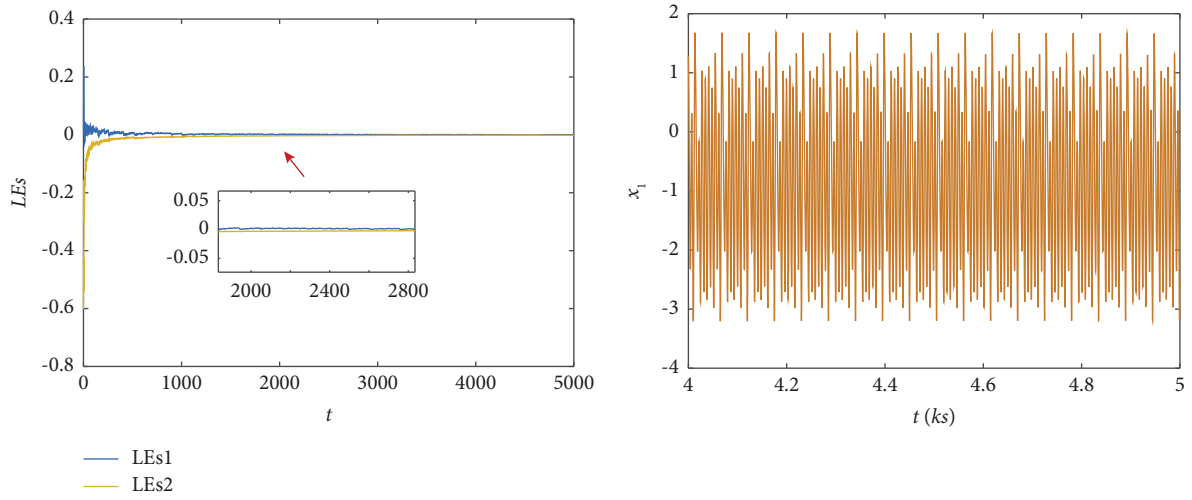

FIGURE 15: (a) The time domain waveform of LEs; (b) the time domain waveform of state variable x_1 in interval $t \in (4000\,\text{s}, 5000\,\text{s})$.

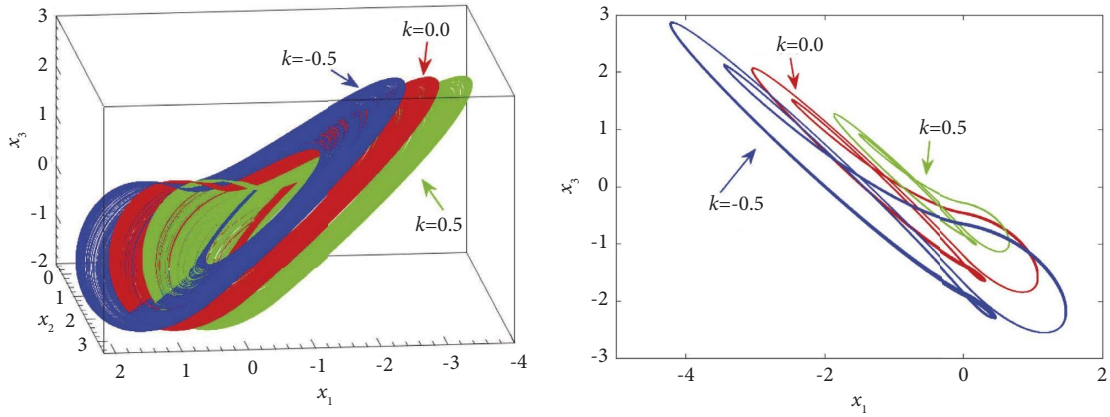

FIGURE 16: System phase diagrams with single control parameter k variation. (a) Chaotic phase diagrams of system (9) on space $x_1 - x_2 - x_3$; (b) periodic phase diagrams of system (9) on plane $x_1 - x_3$.

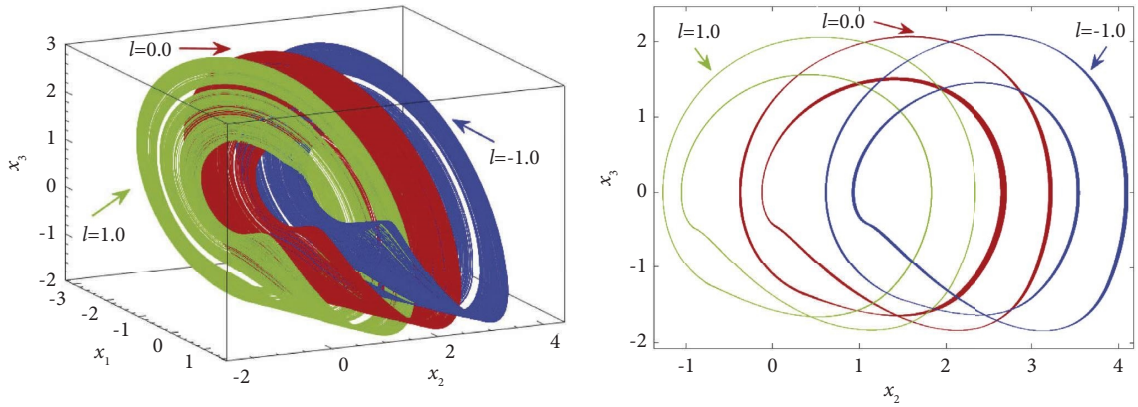

FIGURE 17: System phase diagrams with single control parameter l variation. (a) Chaotic phase diagrams of system (9) on space $x_1 - x_2 - x_3$; (b) periodic phase diagrams of system (9) on plane $x_2 - x_3$.

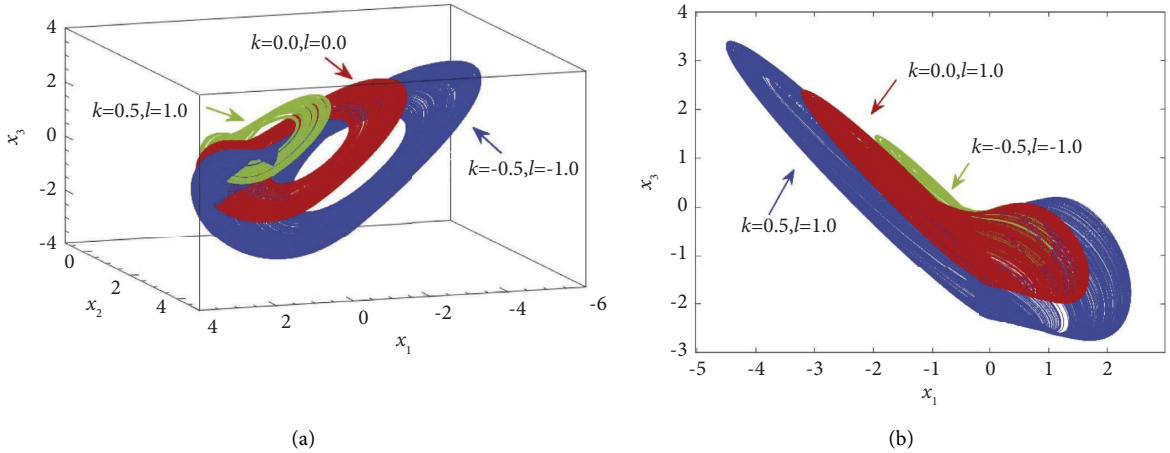

FIGURE 18: System phase diagrams with double control parameter k and l variation. (a) Chaotic phase diagrams of system (9) on plane $x_1 - x_2 - x_3$; (b) chaotic phase diagrams of system (9) on plane $x_1 - x_3$.

control of two parameters. It can be seen that the two parameter control of offset boosting mainly moves in the x_1 and x_2 directions in the $x_1 - x_2$ plane.

4. Circuit Implementation

4.1. Analog Circuit Design. The circuit realization of memristor chaotic systems is another method to study its dynamics and confirm its feasibility. Here, the analog circuit of the system is designed, and the circuit design schematic diagram is shown in Figure 19. During the design of the circuit principle, the common electronic analog components are designed based on the method of operational amplifier. The circuit includes 20 resistors and two absolute value modules designed by operational amplifier. Then, the capacitor is C1–C4, the multiplier is AD633, and the output coefficient is 0.1. The model of operational amplifier is TL8012 series. The analog circuit includes four channel circuits, and each channel is equipped with operation amplification circuit, integral operation amplification circuit, and inverse circuit. We add two absolute value circuit operation modules in the first and fourth channels of the circuit, and the circuit output states of the four channels are x_1, x_2, x_3, and x_4, respectively.

According to the circuit schematic diagram Figure 19 and Kirchhoff voltage law, the circuit equation of the following system can be obtained:

$$\begin{cases} \dfrac{\mathrm{d}x_1}{\mathrm{d}t} = \left(\dfrac{1}{R_2}x_1 + \dfrac{1}{R_1}V_1\right)\dfrac{R_3}{R_4C_1}, \\ \dfrac{\mathrm{d}x_2}{\mathrm{d}t} = \left(\dfrac{1}{R_5}x_3 + \dfrac{1}{R_6}x_3|x_4|\right)\dfrac{R_7}{R_8C_2}, \\ \dfrac{\mathrm{d}x_3}{\mathrm{d}t} = \left(\dfrac{1}{R_{11}}|x_1| + \dfrac{1}{R_{12}}\dfrac{R_{10}}{R_9}x_2 + \dfrac{1}{R_{13}}\dfrac{R_{17}}{R_{16}}x_3\right)\dfrac{R_{14}}{R_{15}C_3}, \\ \dfrac{\mathrm{d}x_4}{\mathrm{d}t} = \dfrac{1}{R_{18}}\dfrac{R_{19}}{R_{20}C_4}x_3. \end{cases} \tag{10}$$

The value of electronic components in circuit equation (10) is shown in Figure 19, and $\pm 15v$ power supply is adopted for all operational amplifiers. As shown in Figure 20, the chaotic phase diagrams captured by the system in the analog oscilloscope are described. The results show that the experimental results of the analog circuit are consistent with the numerical simulation results of the system, which shows the effectiveness of the analog circuit design.

4.2. FPGA Digital Circuit Implementation. Through the FPGA digital circuit experiment [11, 40], the chaotic phase diagram of the system is realized on the digital oscilloscope to illustrate the rationality of the system design. In this paper, an FPGA based on the Xilinx XC6SLX16-2FTG256I chip is chosen, which has the advantages of low statics, adjustable I/O port conversion rate, abundant logic resources, and large logic capacity. These advantages are very helpful for realizing the actual digital circuits that implement chaotic systems. In addition, the resource utilization of the chip is enumerated in Table 1.

Then, the system is discretized as shown in equation (11),

$$\begin{cases} x_1(\delta+1) = x_2(\delta) - 0.6, \\ x_2(\delta+1) = \left(\alpha - \beta|x_4(\delta)|\right)x_3(\delta), \\ x_3(\delta+1) = |x_1(\delta)| - x_2(\delta) - 0.6x_3(\delta), \\ x_4(\delta+1) = x_3(\delta). \end{cases} \tag{11}$$

In addition, the FPGA digital circuit of the system is designed, and the sampling time is 0.001. The continuous signal of the system can be obtained through the digital to analog conversion module. After debugging the digital oscilloscope, the chaotic phase diagrams of the system can be captured in the oscilloscope. The chaotic phase diagrams on the $x_1 - x_2$, $x_1 - x_3$ and $x_2 - x_3$ planes are shown in Figure 21. Therefore, the correctness of the analog circuit design and numerical simulation results of the system can be verified.

5. Synchronization Scheme Design of the System

In this paper, the simplified predefined time synchronization scheme is proposed, which not only reduces the controller inputs but also knows the synchronization time.

Lemma 1 [41]: *If the state τ is satisfied,*

$$\dot{\tau}\mathrm{sign}(\tau) \le -\frac{\pi/2}{T_f q}\left(|\tau|^{1-q} + |\tau|^{1+q}\right). \tag{12}$$

In equation (9), $T_f > 0$ and $0 < q < 1$. If $\tau(0) < M$ and M is bounded, then τ can converge to zero within the predefined time T_f.

$$\tau = 0, \text{ if } t \ge T_f. \tag{13}$$

5.1. Predefined Time Full Control Input Synchronization. It can be seen that the main system of the system is described as follows:

$$\begin{cases} \dot{x}_1 = x_2 - b, \\ \dot{x}_2 = \left(\alpha - \beta|x_4|\right)x_3, \\ \dot{x}_3 = |x_1| - x_2 - ax_3, \\ \dot{x}_4 = x_3, \end{cases} \tag{14}$$

The slave system of the system is

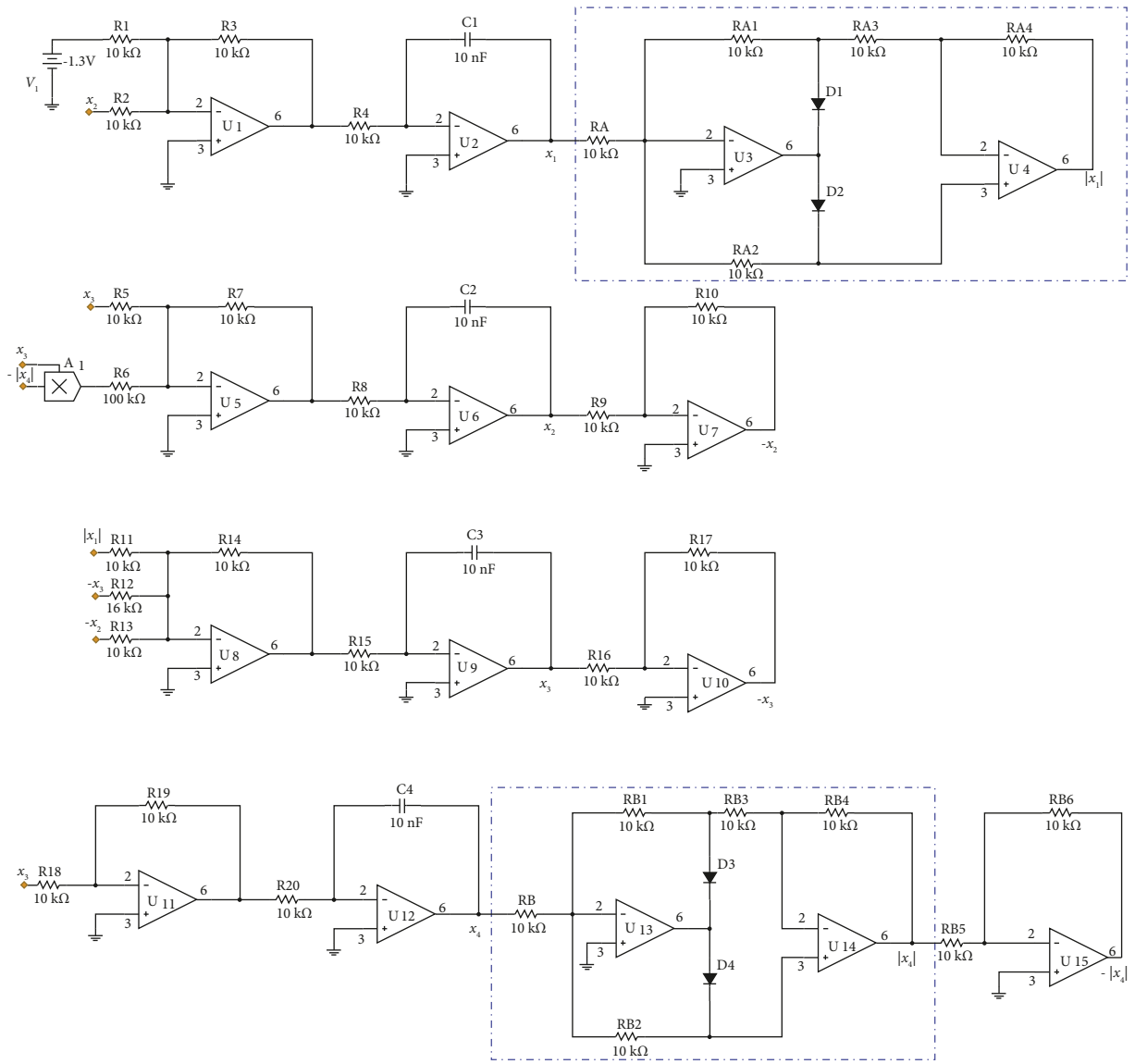

Figure 19: Schematic diagram of the system analog circuit implementation.

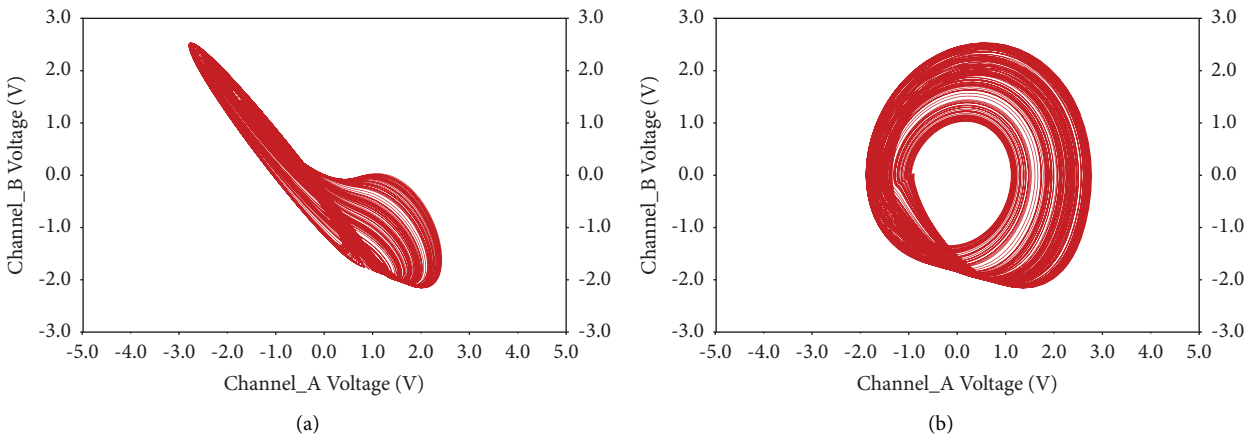

Figure 20: Chaotic phase diagrams of the system in analog oscillograph. (a) $x_1 - x_3$ plane; (b) $x_2 - x_3$ plane.

Table 1: The resource utilization of the chip.

Resource	FF	I/O	LUT	LUTRAM	BUFG
Already used	16200	45	13000	16200	1
Available	111010	150	47800	589824	30
Utilization (%)	14.55	31.33	27.24	2.74	3.11

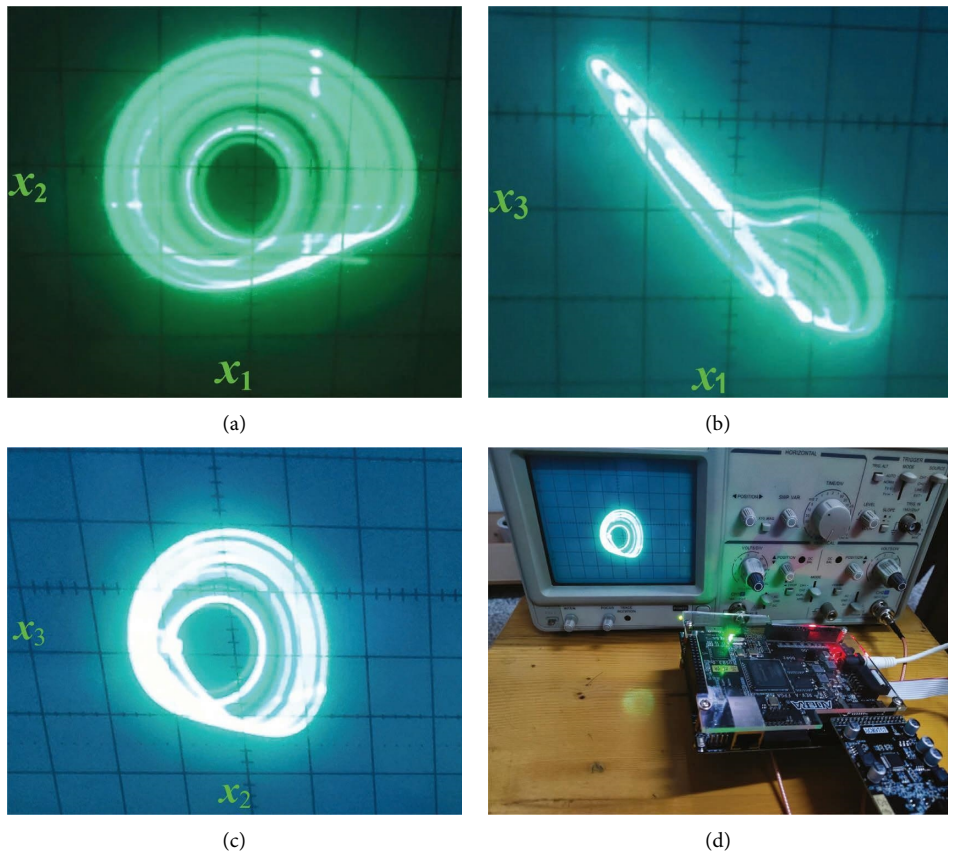

Figure 21: Implementation of FPGA digital circuit of the system.

$$\begin{cases} \dot{x}_{1s} = x_{2s} - b + u_{x_1}, \\ \dot{x}_{2s} = \left(\alpha - \beta\left|x_{4s}\right|\right)x_{3s} + u_{x_2}, \\ \dot{x}_{3s} = \left|x_{1s}\right| - x_{2s} - ax_{2s} + u_{x_3}, \\ \dot{x}_{4s} = x_{3s} + u_{x_4}, \end{cases} \tag{15}$$

where $x_i\,(i = 1s, 2s, 3s, 4s)$ are the status of the slave system, $u_i\,(i = x_1, x_2, x_3, x_4)$ are control input.

We define the synchronization error of the system as

$$\begin{cases} e_{x_1} = x_{1s} - x_1, \\ e_{x_2} = x_{2s} - x_2, \\ e_{x_3} = x_{3s} - x_3, \\ e_{x_4} = x_{4s} - x_4. \end{cases} \tag{16}$$

The time derivative of equation (16) is calculated as follows:

$$\begin{cases} \dot{e}_{x_1} = \dot{x}_{1s} - \dot{x}_1, \\ \dot{e}_{x_2} = \dot{x}_{2s} - \dot{x}_2, \\ \dot{e}_{x_3} = \dot{x}_{3s} - \dot{x}_3, \\ \dot{e}_{x_4} = \dot{x}_{4s} - \dot{x}_4. \end{cases} \tag{17}$$

By substituting equation (14) and equation (15) into equation (17),we can get

$$\begin{cases} \dot{e}_{x_1} = e_{x_2} + u_{x_1}, \\ \dot{e}_{x_2} = \left(\alpha - \beta\left|x_{4s}\right|\right)x_s - \left(\alpha - \beta\left|x_4\right|\right)x_3 + u_{x_2}, \\ \dot{e}_{x_3} = \left|x_{1s}\right| - \left|x_1\right| - e_{x_2} - ae_{x_3} + u_{x_3}, \\ \dot{e}_{x_4} = e_{x_4} + u_{x_4}. \end{cases} \tag{18}$$

Therefore, the controller design of the predefined time full control input synchronization scheme is as follows:

$$\begin{cases} u_{x_1} = -\dfrac{\pi/2}{T_{fx_1} q_{x_1}} \left(\left| e_{x_1} \right|^{1-q_{x_1}} + \left| e_{x_1} \right|^{1+q_{x_1}} \right) \operatorname{sign}\left(e_{x_1} \right) - e_{x_2}, \\ u_{x_2} = -\dfrac{\pi/2}{T_{fx_2} q_{x_2}} \left(\left| e_{x_2} \right|^{1-q_{x_2}} + \left| e_{x_2} \right|^{1+q_{x_2}} \right) \operatorname{sign}\left(e_{x_2} \right) - \left(\left(\alpha - \beta \left| x_{4s} \right| \right) x_{3s} - \left(\alpha - \beta \left| x_4 \right| \right) x_3 \right), \\ u_{x_3} = -\dfrac{\pi/2}{T_{fx_3} q_{x_3}} \left(\left| e_{x_3} \right|^{1-q_{x_3}} + \left| e_{x_3} \right|^{1+q_{x_3}} \right) \operatorname{sign}\left(e_{x_3} \right) - \left(\left| x_{1s} \right| - \left| x_1 \right| - e_{x_2} - a e_{x_3} \right), \\ u_{x_4} = -\dfrac{\pi/2}{T_{fx_4} q_{x_4}} \left(\left| e_{x_4} \right|^{1-q_{x_4}} + \left| e_{x_4} \right|^{1+q_{x_4}} \right) \operatorname{sign}\left(e_{x_4} \right) - e_{x_3}, \end{cases} \tag{19}$$

where $T_{fi} > 0$ and $0 < q_i < 1 \, (i = x_1, x_2, x_3, x_4)$.

We substitute equation (19) into equation (18) to obtain

$$\begin{cases} \dot{e}_{x_1} = -\dfrac{\pi/2}{T_{fx_1} q_{x_1}} \left(\left| e_{x_1} \right|^{1-q_{x_1}} + \left| e_{x_1} \right|^{1+q_{x_1}} \right) \operatorname{sign}\left(e_{x_1} \right), \\ \dot{e}_{x_2} = -\dfrac{\pi/2}{T_{fx_2} q_{x_2}} \left(\left| e_{x_2} \right|^{1-q_{x_2}} + \left| e_{x_2} \right|^{1+q_{x_2}} \right) \operatorname{sign}\left(e_{x_2} \right), \\ \dot{e}_{x_3} = -\dfrac{\pi/2}{T_{fx_3} q_{x_3}} \left(\left| e_{x_3} \right|^{1-q_{x_3}} + \left| e_{x_3} \right|^{1+q_{x_3}} \right) \operatorname{sign}\left(e_{x_3} \right), \\ \dot{e}_{x_4} = -\dfrac{\pi/2}{T_{fx_4} q_{x_4}} \left(\left| e_{x_4} \right|^{1-q_{x_4}} + \left| e_{x_4} \right|^{1+q_{x_4}} \right) \operatorname{sign}\left(e_{x_4} \right). \end{cases} \tag{20}$$

Therefore, considering that Lemma 1 is valid, through equation (20), the following relationship is established:

$$\begin{cases} \dot{e}_{x_1} \operatorname{sign}\left(e_{x_1} \right) = -\dfrac{\pi/2}{T_{fx_1} q_{x_1}} \left(\left| e_{x_1} \right|^{1-q_{x_1}} + \left| e_{x_1} \right|^{1+q_{x_1}} \right), \\ \dot{e}_{x_2} \operatorname{sign}\left(e_{x_2} \right) = -\dfrac{\pi/2}{T_{fx_2} q_{x_2}} \left(\left| e_{x_2} \right|^{1-q_{x_2}} + \left| e_{x_2} \right|^{1+q_{x_2}} \right), \\ \dot{e}_{x_3} \operatorname{sign}\left(e_{x_3} \right) = -\dfrac{\pi/2}{T_{fx_3} q_{x_3}} \left(\left| e_{x_3} \right|^{1-q_{x_3}} + \left| e_{x_3} \right|^{1+q_{x_3}} \right), \\ \dot{e}_{x_4} \operatorname{sign}\left(e_{x_4} \right) = -\dfrac{\pi/2}{T_{fx_4} q_{x_4}} \left(\left| e_{x_4} \right|^{1-q_{x_4}} + \left| e_{x_4} \right|^{1+q_{x_4}} \right), \end{cases} \tag{21}$$

According to Lemma 1, the synchronization error $e_i \, (i = x_1, x_2, x_3, x_4)$ realize synchronization within the predefined time $T_{fi} \quad (i = x_1, x_2, x_3, x_4)$, as shown in equation (22).

$$e_i = 0, \text{ if } t \geq T_{fi} \quad (i = x_1, x_2, x_3, x_4). \tag{22}$$

5.2. Simplified Predefined Time Synchronization. The main system of the system is equation (14), and the design of the slave system is as follows:

$$\begin{cases} \dot{x}_{1s} = x_{2s} - b, \\ \dot{x}_{2s} = \left(\alpha - \beta \left| x_{4s} \right| \right) x_{3s} + u_{x_2}, \\ \dot{x}_{3s} = \left| x_{1s} \right| - x_{2s} - a x_{3s} + u_{x_3}, \\ \dot{x}_{4s} = x_{3s}. \end{cases} \tag{23}$$

The slave system status $x_i \, (i = 1s, 2s, 3s, 4s)$ and $u_i \, (i = x_2, x_3)$ are the control input.

We define the system synchronization error as

$$\begin{cases} e_{x_1} = x_{1s} - x_1, \\ e_{x_2} = x_{2s} - x_2, \\ e_{x_3} = x_{3s} - x_3, \\ e_{x_4} = x_{4s} - x_4. \end{cases} \tag{24}$$

The time derivative of $e_i \, (i = x_1, x_2, x_3, x_4)$ is calculated as follows:

$$\begin{cases} \dot{e}_{x_1} = \dot{x}_{1s} - \dot{x}_1, \\ \dot{e}_{x_2} = \dot{x}_{2s} - \dot{x}_2, \\ \dot{e}_{x_3} = \dot{x}_{3s} - \dot{x}_3, \\ \dot{e}_{x_4} = \dot{x}_{4s} - \dot{x}_4. \end{cases} \tag{25}$$

Substituting equation (14) and equation (23) into equation (25) can obtain

$$\begin{cases} \dot{e}_{x_1} = e_{x_2}, \\ \dot{e}_{x_2} = \left(\alpha - \beta \left| x_{4s} \right| \right) x_{3s} - \left(\alpha - \beta \left| x_4 \right| \right) x_3 + u_{x_2}, \\ \dot{e}_{x_3} = \left| x_{1s} \right| - \left| x_1 \right| - e_{x_2} - a e_{x_3} + u_{x_3}, \\ \dot{e}_{x_4} = e_{x_3}. \end{cases} \tag{26}$$

In the case of satisfying the predefined time convergence algorithm of Lemma 1, the expected synchronization error $e_j \, (j = x_2, x_3)$ satisfies equation (27).

$$\begin{cases} e_{x_2} \longrightarrow -\dfrac{\pi/2}{T_{fx_1} q_{x_1}} \left(\left| e_{x_1} \right|^{1-q_{x_1}} \operatorname{sign}\left(e_{x_1}\right) + \left| e_{x_1} \right|^{1+q_{x_1}} \operatorname{sign}\left(e_{x_1}\right) \right). \\ e_{x_3} \longrightarrow -\dfrac{\pi/2}{T_{fx_4} q_{x_4}} \left(\left| e_{x_4} \right|^{1-q_{x_4}} \operatorname{sign}\left(e_{x_4}\right) + \left| e_{x_4} \right|^{1+q_{x_4}} \operatorname{sign}\left(e_{x_4}\right) \right). \end{cases} \tag{27}$$

Then, in order to satisfy (27), considering (26), the desired value of $e_m\,(m = x_2, x_3)$ can be defined as follows:

$$\begin{cases} e_{x_2 d} = -\dfrac{\pi/2}{T_{fx_1} q_{x_1}} \left(\left| e_{x_1} \right|^{1-q_{x_1}} \operatorname{sign}\left(e_{x_1}\right) + \left| e_{x_1} \right|^{1+q_{x_1}} \operatorname{sign}\left(e_{x_1}\right) \right), \\ e_{x_3 d} = -\dfrac{\pi/2}{T_{fx_4} q_{x_4}} \left(\left| e_{x_4} \right|^{1-q_{x_4}} \operatorname{sign}\left(e_{x_4}\right) + \left| e_{x_4} \right|^{1+q_{x_4}} \operatorname{sign}\left(e_{x_4}\right) \right). \end{cases} \tag{28}$$

To satisfy (28), two new errors $\overline{e}_{jd}\,(j = x_1, x_4)$ are defined

$$\begin{cases} \overline{e}_{x_2 d} = e_{x_2} - e_{x_2 d} = e_{x_2} + \dfrac{\pi/2}{T_{fx_1} q_{x_1}} \left(\left| e_{x_1} \right|^{1-q_{x_1}} \operatorname{sign}\left(e_{x_1}\right) + \left| e_{x_1} \right|^{1+q_{x_1}} \operatorname{sign}\left(e_{x_1}\right) \right), \\ \overline{e}_{x_3 d} = e_{x_3} - e_{x_3 d} = e_{x_3} + \dfrac{\pi/2}{T_{fx_4} q_{x_4}} \left(\left| e_{x_4} \right|^{1-q_{x_4}} \operatorname{sign}\left(e_{x_4}\right) + \left| e_{x_4} \right|^{1+q_{x_4}} \operatorname{sign}\left(e_{x_4}\right) \right). \end{cases} \tag{29}$$

Therefore, the controller design of the simplified predefined time synchronization scheme is as follows:

$$\begin{cases} u_{x_2} = -\dfrac{\pi/2}{T_{fx_1} q_{x_1}} \left(\left(1 - q_{x_1}\right) \left| e_{x_1} \right|^{-q_{x_1}} + \left(1 + q_{x_1}\right) \left| e_{x_1} \right|^{q_{x_1}} \right) e_{x_2} - \left[\left(\alpha - \beta \left| x_{4s} \right| \right) x_{3s} - \left(\alpha - \beta \left| x_4 \right| \right) x_3 \right] \\ -\dfrac{\pi/2}{\overline{T}_{fx_1} \overline{q}_{x_1}} \left(\left| \overline{e}_{x_2 d} \right|^{1-\overline{q}_{x_1}} \operatorname{sign}\left(\overline{e}_{x_2 d}\right) + \left| \overline{e}_{x_2 d} \right|^{1+\overline{q}_{x_1}} \operatorname{sign}\left(\overline{e}_{x_2 d}\right) \right), \\ u_{x_3} = -\dfrac{\pi/2}{T_{fx_4} q_{x_4}} \left(\left(1 - q_{x_4}\right) \left| e_{x_4} \right|^{-q_{x_4}} + \left(1 + q_{x_4}\right) \left| e_{x_4} \right|^{q_{x_4}} \right) e_{x_3} - \left[\left| x_{1s} \right| - \left| x_1 \right| - e_{x_2} - a e_{x_3} \right] \\ -\dfrac{\pi/2}{\overline{T}_{fx_4} \overline{q}_{x_4}} \left(\left| \overline{e}_{x_3 d} \right|^{1-\overline{q}_{x_4}} \operatorname{sign}\left(\overline{e}_{x_3 d}\right) + \left| \overline{e}_{x_3 d} \right|^{1+\overline{q}_{x_4}} \operatorname{sign}\left(\overline{e}_{x_3 d}\right) \right) \\ u_{x_1} = u_{x_4} = 0. \end{cases} \tag{30}$$

According to the proposed simplified predefined time synchronization scheme, if Lemma 1 is valid, the system achieves synchronization and error $e_i\,(i = x_1, x_2, x_3, x_4)$ converges to zero within the predefined time $T_{fi} \quad (i = x_1, x_2, x_3, x_4)$.

$$\begin{cases} e_{x_1} = 0, & \text{if } t \geq T_{x_1} \\ e_{x_2} = 0, & \text{if } t \geq T_{x_2} \\ e_{x_3} = 0, & \text{if } t \geq T_{x_3} \\ e_{x_4} = 0, & \text{if } t \geq T_{x_4,} \end{cases} \tag{31}$$

where $T_{x_1} = \overline{T}_{fx_1} + T_{fx_1}$, $T_{x_2} = \overline{T}_{fx_1} + T_{fx_1}$, $T_{x_3} = \overline{T}_{fx_4} + T_{fx_4}$ and $T_{x_4} = \overline{T}_{fx_4} + T_{fx_4}$. Combining the e_{x_2d} and e_{x_3d} functions in equation (29) and equation (26), equation (32) is established.

$$\begin{cases} \dot{\overline{e}}_{x_2d} = \dfrac{\pi/2}{T_{fx_1} q_{x_1}} \left(\left(1 - q_{x_1}\right) \left| e_{x_1} \right|^{-q_{x_1}} + \left(1 + q_{x_1}\right) \left| e_{x_1} \right|^{q_{x_1}} \right) e_{x_2} \\ + \left[\left(\alpha - \beta \left| x_{4s} \right| \right) x_{3s} - (\alpha - \beta x_4) x_3 \right] + u_{x_2}, \\ \dot{\overline{e}}_{x_3d} = \dfrac{\pi/2}{T_{fx_4} q_{x_4}} \left(\left(1 - q_{x_4}\right) \left| e_{x_4} \right|^{-q_{x_4}} + \left(1 + q_{x_4}\right) \left| e_{x_4} \right|^{q_{x_4}} \right) e_{x_3} \\ + \left[\left| x_{1s} \right| - \left| x_1 \right| - e_{x_2} - a e_{x_3} \right] + u_{x_3}. \end{cases} \tag{32}$$

Therefore, by substituting equation (30) into equation (32), we can get

$$\begin{cases} \dot{\overline{e}}_{x_2d} \operatorname{sign}\left(\overline{e}_{x_2d}\right) = -\dfrac{\pi/2}{\overline{T}_{fx_1} \overline{q}_{x_1}} \left(\left| \overline{e}_{x_2d} \right|^{1-\overline{q}_{x_1}} + \left| \overline{e}_{x_2d} \right|^{1+\overline{q}_{x_1}} \right). \\ \dot{\overline{e}}_{x_3d} \operatorname{sign}\left(\overline{e}_{x_3d}\right) = -\dfrac{\pi/2}{\overline{T}_{fx_4} \overline{q}_{x_4}} \left(\left| \overline{e}_{x_3d} \right|^{1-\overline{q}_{x_3}} + \left| \overline{e}_{x_3d} \right|^{1+\overline{q}_{x_4}} \right). \end{cases} \tag{33}$$

According to Lemma 1, from equation (33), it can be seen that the errors $\overline{e}_{x_2d}$ and $\overline{e}_{x_3d}$ are synchronization and converge to zero within the predefined time $\overline{T}_{fx_1}$ and $\overline{T}_{fx_4}$, respectively. Therefore, it can be proved that the synchronization error $e_i (i = x_1, x_2, x_3, x_4)$ achieves synchronization and converges to zero within the predefined time T_{fi} $(i = x_1, x_2, x_3, x_4)$, but the synchronization error $e_i (i = x_1, x_2, x_3, x_4)$ may diverge to infinity before the $\overline{e}_{x_2d}$ and $\overline{e}_{x_3d}$ synchronization errors converge to zero.

Considering the influence of $\overline{e}_{x_2d}$ and $\overline{e}_{x_3d}$, it is proved in two steps. In step 1, the proof is that the synchronization error $e_i (i = x_1, x_2, x_3, x_4)$ is bounded before $\overline{e}_{x_2d}$ and $\overline{e}_{x_3d}$ converge to zero. In step 2, the proof is that the synchronization error $e_i (i = x_1, x_2, x_3, x_4)$ can converge to zero to achieve synchronization before $\overline{e}_{x_2d}$ and $\overline{e}_{x_3d}$ converge to zero.

In step 1: According to equation (33), equation (34) is valid.

$$\begin{cases} \overline{e}_{x_2d} \dot{\overline{e}}_{x_2d} \le 0, \\ \overline{e}_{x_3d} \dot{\overline{e}}_{x_3d} \le 0. \end{cases} \tag{34}$$

Lassume there are

$$\begin{cases} \left| \overline{e}_{x_2d} \right| \le \left| \overline{e}_{x_2d}(0) \right|, \\ \left| \overline{e}_{x_3d} \right| \le \left| \overline{e}_{x_3d}(0) \right|. \end{cases} \tag{35}$$

Combining equation (25) and equation (29), we can get

$$\begin{cases} \overline{e}_{x_2d} = \dot{e}_{x_1} + \dfrac{\pi/2}{T_{fx_1} q_{x_1}} \left(\left| e_{x_1} \right|^{1-q_{x_1}} \operatorname{sign}\left(e_{x_1}\right) + \left| e_{x_1} \right|^{1+q_{x_1}} \operatorname{sign}\left(e_{x_1}\right) \right), \\ \overline{e}_{x_3d} = \dot{e}_{x_4} + \dfrac{\pi/2}{T_{fx_4} q_{x_4}} \left(\left| e_{x_4} \right|^{1-q_{x_4}} \operatorname{sign}\left(e_{x_4}\right) + \left| e_{x_4} \right|^{1+q_{x_4}} \operatorname{sign}\left(e_{x_4}\right) \right). \end{cases} \tag{36}$$

It can be further known from equations (35) and (36).

$$\begin{cases} -\dfrac{\pi/2}{T_{fx_1} q_{x_1}} \left(\left| e_{x_1} \right|^{1-q_{x_1}} \operatorname{sign}\left(e_{x_1}\right) + \left| e_{x_1} \right|^{1+q_{x_1}} \operatorname{sign}\left(e_{x_1}\right) \right) - \left| \overline{e}_{x_2d}(0) \right| \le \dot{e}_{x_1}, \\ \le -\dfrac{\pi/2}{T_{fx_1} q_{x_1}} \left(\left| e_{x_1} \right|^{1-q_{x_1}} \operatorname{sign}\left(e_{x_1}\right) + \left| e_{x_1} \right|^{1+q_{x_1}} \operatorname{sign}\left(e_{x_1}\right) \right) + \left| \overline{e}_{x_2d}(0) \right|, \\ -\dfrac{\pi/2}{T_{fx_4} q_{x_4}} \left(\left| e_{x_4} \right|^{1-q_{x_4}} \operatorname{sign}\left(e_{x_4}\right) + \left| e_{x_4} \right|^{1+q_{x_4}} \operatorname{sign}\left(e_{x_4}\right) \right) - \left| \overline{e}_{x_3d}(0) \right| \le \dot{e}_{x_4}, \\ \le -\dfrac{\pi/2}{T_{fx_4} q_{x_4}} \left(\left| e_{x_4} \right|^{1-q_{x_4}} \operatorname{sign}\left(e_{x_4}\right) + \left| e_{x_4} \right|^{1+q_{x_4}} \operatorname{sign}\left(e_{x_4}\right) \right) + \left| \overline{e}_{x_3d}(0) \right|. \end{cases} \tag{37}$$

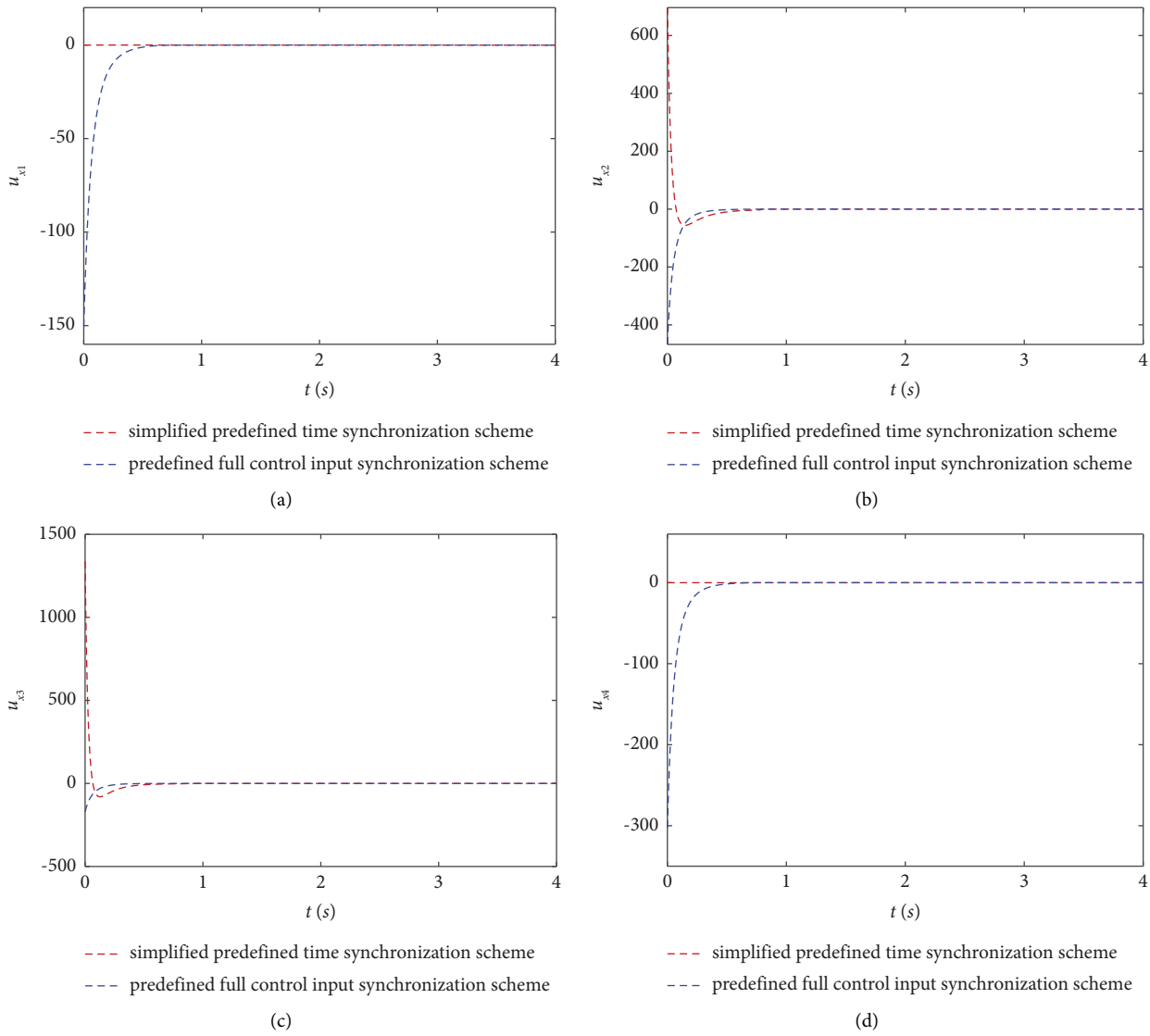

Figure 22: The system control input. (a) u_{x_1}; (b) u_{x_2}; (c) u_{x_3}; (d) u_{x_4}.

So, we can conclude that

$$\begin{cases} e_{x_1}\dot{e}_{x_1} \le 0; \quad \text{if} \left|e_{x_1}\right| \ge \left(\dfrac{T_{fx_1}q_{x_1}}{\pi/2}\left|\overline{e}_{x_2 d}(0)\right|\right)^{1/1+q_{x_1}} \\ e_{x_4}\dot{e}_{x_4} \le 0; \quad \text{if} \left|e_{x_4}\right| \ge \left(\dfrac{T_{fx_4}q_{x_4}}{\pi/2}\left|\overline{e}_{x_3 d}(0)\right|\right)^{1/1+q_{x_4}} \end{cases} \tag{38}$$

It can be concluded that e_{x_1} and e_{x_4} are bounded.

$$\begin{cases} \left|e_{x_1}\right| \le \max\left(\dfrac{T_{fx_1}q_{x_1}}{\pi/2}\left|\overline{e}_{x_2 d}(0)\right|, e_{x_1}(0)\right)^{1/1+q_{x_1}}, \\ \left|e_{x_4}\right| \le \max\left(\dfrac{T_{fx_4}q_{x_4}}{\pi/2}\left|\overline{e}_{x_3 d}(0)\right|, e_{x_4}(0)\right)^{1/1+q_{x_4}}. \end{cases} \tag{39}$$

In step 2: From Lemma 1, $\overline{e}_{x_2 d}(0)$ and $\overline{e}_{x_3 d}(0)$ are bounded, and according to equation (33), it can be known that the error $\overline{e}_{jd}\,(j = x_1, x_4)$ converge to zero to achieve synchronization at the predefined time $\overline{T}_{fx_1}$ and $\overline{T}_{fx_4}$, that is,

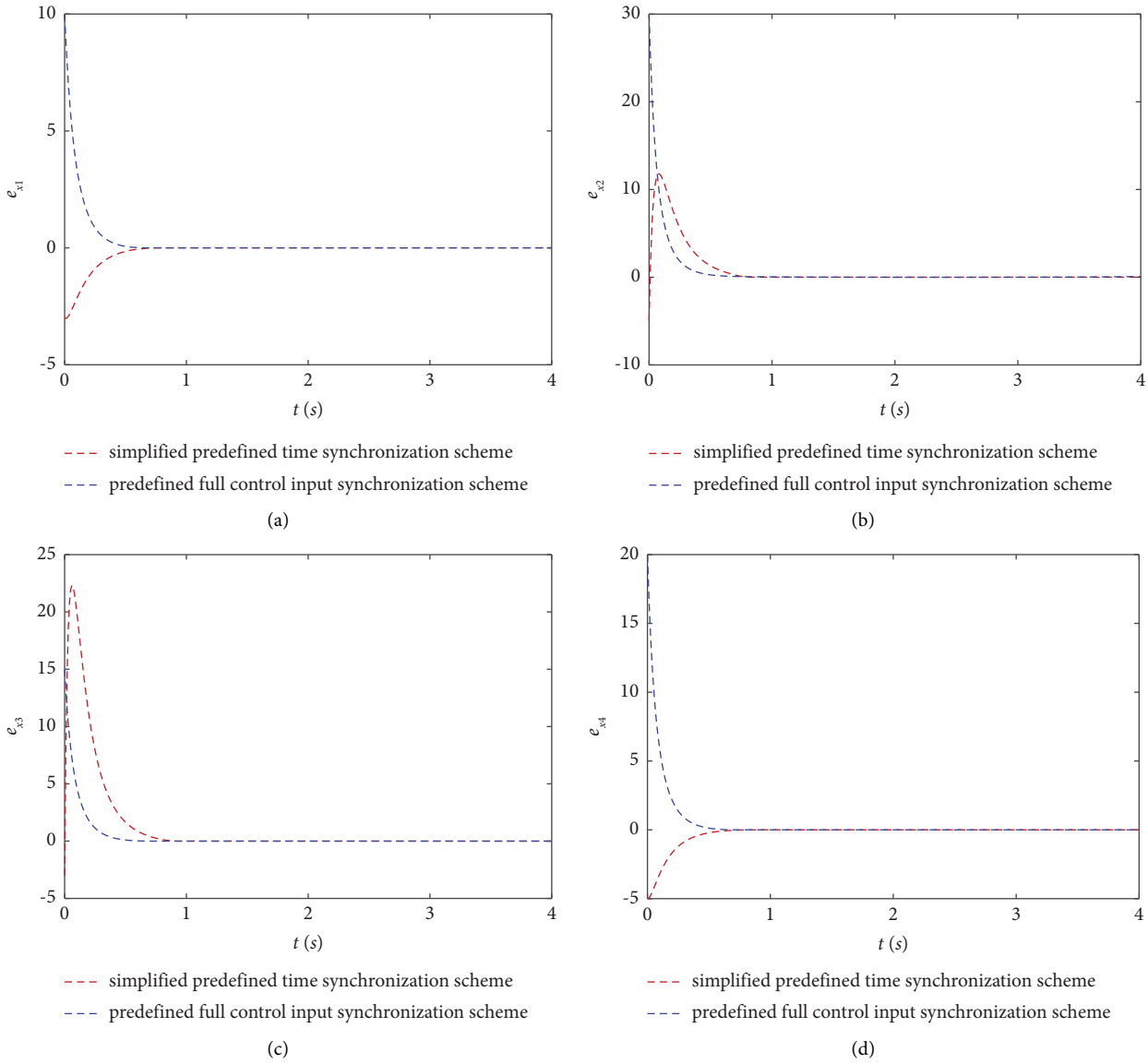

FIGURE 23: The system synchronization error. (a) e_{x_1}; (b) e_{x_2}; (c) e_{x_3}; (d) e_{x_4}.

$$\begin{cases} \overline{e}_{x_2 d} = 0, & \text{if } t \geq \overline{T}_{fx_1}, \\ \overline{e}_{x_3 d} = 0, & \text{if } t \geq \overline{T}_{fx_4}. \end{cases} \tag{40}$$

Combining equation (36) and equation (39) can obtain

$$\begin{cases} \dot{e}_{x_1} = -\dfrac{\pi/2}{T_{fx_1} q_{x_1}} \left(\left| e_{x_1} \right|^{1-q_{x_1}} \operatorname{sign}\left(e_{x_1}\right) + \left| e_{x_1} \right|^{1+q_{x_1}} \operatorname{sign}\left(e_{x_1}\right) \right), & \text{if } t \geq \overline{T}_{fx_1}, \\ \dot{e}_{x_4} = -\dfrac{\pi/2}{T_{fx_4} q_{x_4}} \left(\left| e_{x_4} \right|^{1-q_{x_4}} \operatorname{sign}\left(e_{x_4}\right) + \left| e_{x_4} \right|^{1+q_{x_4}} \operatorname{sign}\left(e_{x_4}\right) \right), & \text{if } t \geq \overline{T}_{fx_4}. \end{cases} \tag{41}$$

Step 1 shows that $e_{x_1}(\overline{T}_{fx_1})$ and $e_{x_4}(\overline{T}_{fx_4})$ are bounded. Therefore, through Lemma 1, it can be known that $e_{x_1} = 0$ and $e_{x_4} = 0$ can converge to zero to achieve synchronization at the predefined time.

$$\begin{cases} \dot{e}_{x_4} = 0, & \text{if } t \geq \overline{T}_{fx_4} + T_{fx_4}, \\ \dot{e}_{x_1} = 0, & \text{if } t \geq \overline{T}_{fx_1} + T_{fx_1}. \end{cases} \tag{42}$$

So, we have

$$\begin{cases} \dot{e}_{x_1} = 0, & \text{if } t \geq \overline{T}_{fx_1} + T_{fx_1}, \\ \dot{e}_{x_4} = 0, & \text{if } t \geq \overline{T}_{fx_4} + T_{fx_4}. \end{cases} \tag{43}$$

According to equation (26) and equation (43), equation (44) is further established.

$$\begin{cases} e_{x_2} = 0, & \text{if } t \geq \overline{T}_{fx_1} + T_{fx_1}, \\ e_{x_3} = 0, & \text{if } t \geq \overline{T}_{fx_4} + T_{fx_4}. \end{cases} \tag{44}$$

Through equation (42) and equation (44), we can get

$$\begin{cases} e_{x_1} = 0, & \text{if } t \geq \overline{T}_{fx_1} + T_{fx_1}, \\ e_{x_2} = 0, & \text{if } t \geq \overline{T}_{fx_1} + T_{fx_1}, \\ e_{x_3} = 0, & \text{if } t \geq \overline{T}_{fx_4} + T_{fx_4}, \\ e_{x_4} = 0, & \text{if } t \geq \overline{T}_{fx_4} + T_{fx_4}. \end{cases} \tag{45}$$

5.3. Numerical Simulation of Predefined Time Synchronization Scheme of the System. The system parameter selection is $a = 0.6$, $b = 1.3$, $\alpha = 1$, $\beta = 0.1$ and initial value is $x_0 = (1, 0, 0, -1)$. Figure 22 shows the controller input of the synchronization scheme. Figure 22 shows the comparison of two different control schemes, where the red line is the simplified predefined time synchronization scheme, and the blue line is the predefined full time control input synchronization scheme.

By comparing the simplified predefined time synchronization scheme with the predefined full control input synchronization scheme, it is obvious that the simplified predefined time synchronization scheme can reduce the controller input. It can be seen from Figure 22 that the simplified predefined time controller input, which only requires the input of two controllers u_{x_2} and u_{x_3}, and the input of the other two controllers u_{x_1} and u_{x_4} are zero. Figure 23 shows the predefined time synchronization error curve.

From Figure 23, it is found that the synchronization error of the system converges to zero and realizes synchronization within the predefined time. Therefore, the rationality and applicability of the predefined time synchronization control scheme are illustrated by numerical simulation.

6. Conclusion

In this paper, a 4D absolute memristor Jerk chaotic system is proposed. Firstly, the memristor characteristics of the hysteresis loop change of absolute memristor are analyzed according to the changes of frequency and amplitude, which are verified by analog circuit and numerical simulation. Secondly, through the phase diagrams, Poincaré section, power spectrum, bifurcation diagram, 0-1 test, and Lyapunov exponent spectrum method of the system, the complex dynamic behavior caused by the change of parameters and initial values of the system is studied. It is found that the system has reverse period doubling bifurcation, chaos degradation, and offset boosting. In addition, through the system analog circuit design and FPGA digital circuit implementation, the phase diagrams of the system are captured in the oscilloscope to illustrate the feasibility of its practical application. Finally, a simplified predefined time synchronization scheme and a predefined full control input synchronization scheme are proposed. Through numerical simulation, it can be found that the proposed simplified predefined time synchronization scheme not only simplified the input of the controllers but also achieves system synchronization in the predefined time. This paper provides a study for the dynamic analysis of a novel Jerk memristor system, and its rich dynamic behaviors are displayed, providing a theoretical basis for the following practical engineering applications. Meanwhile, we hope that in the next work, we can use the symplectic algorithm to recalculate the numerical solution and realize the control circuit of the system expectantly.

Data Availability

All data used to support the findings of this study are available from the corresponding author upon request.

Conflicts of Interest

The authors declare that they have no conflicts of interest.

Acknowledgments

The authors acknowledge the referees and the editor for carefully reading this paper and giving many helpful comments. This work is supported by the National Natural Science Foundation of China (61973249), the Key Research and Development Programs of Shaanxi Province (2021ZDLGY02-06), the Natural Science Basic Research Program of Shaanxi (2021JM-533, 2021JQ-880, 2020JM-646), the Innovation Capability Support Program of Shaanxi (2018GHJD-21), the Qin Chuangyuan Project (2021QCYRC4-49), the Support Plan for Sanqin Scholars Innovation Team in Shaanxi Province of China, the National Defense Science and Technology Key Laboratory Fund Project (6142101210202), the Qinchuangyuan Scientist + Engineer (2022KXJ-169), the Scientific Research Program Funded by Shaanxi Provincial Education Department (21JK0960), the Scientific Research Fund for High-Level Talents of Xijing University (XJ21B01), and the Scientific Research Foundation of Xijing University (XJ210203).

References

[1] J. Luo, X. Xu, Y. Ding et al., "Application of a memristor-based oscillator to weak signal detection," *The European Physical Journal Plus*, vol. 133, no. 6, pp. 239–310, 2018.

[2] Z. Wang, Z. Wei, K. Sun et al., "Chaotic flows with special equilibria," *European Physical Journal: Special Topics*, vol. 229, no. 6-7, pp. 905–919, 2020.

[3] Z. Hua, Y. Zhou, and H. Huang, "Cosine-transform-based chaotic system for image encryption," *Information Sciences*, vol. 480, pp. 403–419, 2019.

[4] A. Sambas, S. Vaidyanathan, X. Zhang et al., "A novel 3d chaotic system with line equilibrium: multistability, integral sliding mode control, electronic circuit, fpga implementation and its image encryption," *IEEE Access*, vol. 10, pp. 68057–68074, 2022.

[5] Z. Wang, R. Ramamoorthy, X. Xi, and H. Namazi, "Synchronization of the neurons coupled with sequential developing electrical and chemical synapses," *Mathematical Biosciences and Engineering*, vol. 19, no. 2, pp. 1877–1890, 2021.

[6] Z. Wang, H. Tian, O. Krejcar, and H. Namazi, "Synchronization in a network of map-based neurons with memristive synapse," *European Physical Journal: Special Topics*, vol. 231, no. 22-23, pp. 4057–4064, 2022.

[7] Z. Wang, F. Parastesh, K. Rajagopal, I. I. Hamarash, and I. Hussain, "Delay-induced synchronization in two coupled chaotic memristive hopfield neural networks," *Chaos, Solitons & Fractals*, vol. 134, Article ID 109702, 2020.

[8] L. Chua, "Memristor-the missing circuit element," *IEEE Transactions on Circuit Theory*, vol. 18, no. 5, pp. 507–519, 1971.

[9] H. Bao, N. Wang, B. Bao, M. Chen, P. Jin, and G. Wang, "Initial condition-dependent dynamics and transient period in memristor-based hypogenetic jerk system with four line equilibria," *Communications in Nonlinear Science and Numerical Simulation*, vol. 57, pp. 264–275, 2018.

[10] J. M. Muñoz-Pacheco, "Infinitely many hidden attractors in a new fractional-order chaotic system based on a fracmemristor," *European Physical Journal: Special Topics*, vol. 228, no. 10, pp. 2185–2196, 2019.

[11] D. Clemente-López, J. M. Munoz-Pacheco, and J. D. J. Rangel-Magdaleno, "A review of the digital implementation of continuous-time fractional-order chaotic systems using fpgas and embedded hardware," *Archives of Computational Methods in Engineering*, vol. 30, no. 2, pp. 951–983, 2022.

[12] J. Liu, Z. Wang, M. Chen, P. Zhang, R. Yang, and B. Yang, "Chaotic system dynamics analysis and synchronization circuit realization of fractional-order memristor," *European Physical Journal: Special Topics*, vol. 231, no. 16-17, pp. 3095–3107, 2022.

[13] J. Ying, Y. Liang, F. Li, G. Wang, and Y. Shen, "Complex oscillations of chua corsage memristor with two symmetrical locally active domains," *Electronics*, vol. 11, no. 4, Article ID 11040665, 2022.

[14] B. Zhang and F. Deng, "Double-compound synchronization of six memristor-based lorenz systems," *Nonlinear Dynamics*, vol. 77, no. 4, pp. 1519–1530, 2014.

[15] W. Dai, X. Xu, X. Song, and G. Li, "Audio encryption algorithm based on chen memristor chaotic system," *Symmetry*, vol. 14, no. 1, Article ID 14010017, 2021.

[16] H. Tian, Z. Wang, P. Zhang, M. Chen, and Y. Wang, "Dynamic analysis and robust control of a chaotic system with hidden attractor," *Complexity*, vol. 2021, Article ID 8865522, 11 pages, 2021.

[17] R. Zhang, X. Xi, H. Tian, and Z. Wang, "Dynamical analysis and finite-time synchronization for a chaotic system with hidden attractor and surface equilibrium," *Axioms*, vol. 11, no. 11, Article ID 11110579, 2022.

[18] H. Tian, Z. Wang, H. Zhang, Z. Cao, and P. Zhang, "Dynamical analysis and fixed-time synchronization of a chaotic system with hidden attractor and a line equilibrium," *European Physical Journal: Special Topics*, vol. 231, no. 11-12, pp. 2455–2466, 2022.

[19] A. Yousefpour, H. Jahanshahi, J. M. Munoz-Pacheco, S. Bekiros, and Z. Wei, "A fractional-order hyper-chaotic economic system with transient chaos," *Chaos, Solitons & Fractals*, vol. 130, Article ID 109400, 2020.

[20] H. Chang, Y. Li, G. Chen, and F. Yuan, "Extreme multistability and complex dynamics of a memristor-based chaotic system," *International Journal of Bifurcation and Chaos*, vol. 30, no. 8, Article ID 2030019, 2020.

[21] M. Chen, M. Sun, B. Bao, H. Wu, Q. Xu, and J. Wang, "Controlling extreme multistability of memristor emulator-based dynamical circuit in flux–charge domain," *Nonlinear Dynamics*, vol. 91, no. 2, pp. 1395–1412, 2018.

[22] Z. Wang, R. Ramamoorthy, X. Xi, K. Rajagopal, P. Zhang, and S. Jafari, "The effects of extreme multistability on the collective dynamics of coupled memristive neurons," *European Physical Journal: Special Topics*, vol. 231, no. 16-17, pp. 3087–3094, 2022.

[23] H. Tian, J. Liu, Z. Wang, F. Xie, and Z. Cao, "Characteristic analysis and circuit implementation of a novel fractional-order memristor-based clamping voltage drift," *Fractal and Fractional*, vol. 7, no. 1, p. 2, 2022.

[24] F. Min, W. Zhang, Z. Ji, and L. Zhang, "Switching dynamics of a non-autonomous FitzHugh-Nagumo circuit with piecewise-linear flux-controlled memristor," *Chaos, Solitons & Fractals*, vol. 152, Article ID 111369, 2021.

[25] L.-L. Huang, S. Liu, J.-H. Xiang, and L.-Y. Wang, "Design and multistability analysis of five-value memristor-based chaotic system with hidden attractors," *Chinese Physics B*, vol. 30, no. 10, Article ID 100506, 2021.

[26] J. Luo, S. Qu, Y. Chen, X. Chen, and Z. Xiong, "Synchronization, circuit and secure communication implementation of a memristor-based hyperchaotic system using single input controller," *Chinese Journal of Physics*, vol. 71, pp. 403–417, 2021.

[27] C. Li and J. C. Sprott, "Variable-boostable chaotic flows," *Optik*, vol. 127, no. 22, pp. 10389–10398, 2016.

[28] Z. Zhang, L. Huang, J. Liu, Q. Guo, and X. Du, "A new method of constructing cyclic symmetric conservative chaotic systems and improved offset boosting control," *Chaos, Solitons & Fractals*, vol. 158, Article ID 112103, 2022.

[29] C. Ma, J. Mou, L. Xiong, S. Banerjee, T. Liu, and X. Han, "Dynamical analysis of a new chaotic system: asymmetric multistability, offset boosting control and circuit realization," *Nonlinear Dynamics*, vol. 103, no. 3, pp. 2867–2880, 2021.

[30] S. Saifullah, A. Ali, and E. Franc Doungmo Goufo, "Investigation of complex behaviour of fractal fractional chaotic attractor with mittag-leffler kernel," *Chaos, Solitons & Fractals*, vol. 152, Article ID 111332, 2021.

[31] S. Gu, S. He, H. Wang, and B. Du, "Analysis of three types of initial offset-boosting behavior for a new fractional-order dynamical system," *Chaos, Solitons & Fractals*, vol. 143, Article ID 110613, 2021.

[32] S. Li and Y.-P. Tian, "Finite time synchronization of chaotic systems," *Chaos, Solitons & Fractals*, vol. 15, no. 2, pp. 303–310, 2003.

[33] L. Wang, T. Dong, and M.-F. Ge, "Finite-time synchronization of memristor chaotic systems and its application in image encryption," *Applied Mathematics and Computation*, vol. 347, pp. 293–305, 2019.

[34] W. Xiong and J. Huang, "Finite-time control and synchronization for memristor-based chaotic system via impulsive adaptive strategy," *Advances in Difference Equations*, vol. 2016, no. 1, pp. 101–9, 2016.

[35] G. Velmurugan, R. Rakkiyappan, and J. Cao, "Finite-time synchronization of fractional-order memristor-based neural networks with time delays," *Neural Networks*, vol. 73, pp. 36–46, 2016.

[36] C. Chen, L. Li, H. Peng, and Y. Yang, "Fixed-time synchronization of memristor-based bam neural networks with time-varying discrete delay," *Neural Networks*, vol. 96, pp. 47–54, 2017.

[37] J. Cao and R. Li, "Fixed-time synchronization of delayed memristor-based recurrent neural networks," *Science China Information Sciences*, vol. 60, no. 3, pp. 032201–032215, 2017.

[38] B. Bao, H. Bao, N. Wang, M. Chen, and Q. Xu, "Hidden extreme multistability in memristive hyperchaotic system," *Chaos, Solitons & Fractals*, vol. 94, pp. 102–111, 2017.

[39] Y. Feng, J. Yang, C. Wu, M. Lu, and X.-J. Zhao, "Solving 0–1 knapsack problems by chaotic monarch butterfly optimization algorithm with Gaussian mutation," *Memetic Computing*, vol. 10, no. 2, pp. 135–150, 2018.

[40] H. Wang, D. Zhan, X. Wu, and S. He, "Dynamics of a fractional-order colpitts oscillator and its fpga implementation," *European Physical Journal: Special Topics*, vol. 231, no. 11-12, pp. 2467–2476, 2022.

[41] Y. Zhang, J. Zhuang, Y. Xia, Y. Bai, J. Cao, and L. Gu, "Fixed-time synchronization of the impulsive memristor-based neural networks," *Communications in Nonlinear Science and Numerical Simulation*, vol. 77, pp. 40–53, 2019.

Hindawi
Complexity
Volume 2023, Article ID 3478719, 20 pages
https://doi.org/10.1155/2023/3478719

Research Article

Supply Chain Management (SCM) Breakdowns and SCM Strategy Selection during the COVID-19 Pandemic Using the Novel Rough MCDM Model

Željko Stević,[1] **Alptekin Ulutaş**,[2] **Selçuk Korucuk**,[3] **Salih Memiş**,[3] **Ezgi Demir**,[4] **Ayşe Topal**,[5] **and Çağlar Karamaşa**[6]

[1]*Faculty of Transport and Traffic Engineering, University of East Sarajevo, Doboj, Republic of Srpska, Bosnia and Herzegovina*
[2]*Department of International Trade and Business, Inonu University, Malatya, Turkey*
[3]*The Department of Logistics Management, Bulancak Kadir Karabaş Vocational School, Giresun University, Giresun, Turkey*
[4]*Department of Management Information Systems, Gebze Technical University, Darıca, Kocaeli, Turkey*
[5]*Department of Business, Nigde Omer Halisdemir University, Nigde, Turkey*
[6]*Anadolu University, Department of Business Administration, Eskişehir, Turkey*

Correspondence should be addressed to Željko Stević; zeljkostevic88@yahoo.com

Received 18 July 2022; Revised 22 November 2022; Accepted 22 March 2023; Published 12 April 2023

Academic Editor: Atila Bueno

Supply chain management (SCM) is deeply affected by the COVID-19 pandemic besides breakdowns occurred in all sectors. Nowadays, managers need techniques for protecting supply chains from serious and costly disruptions, establishing permanent relationships with the customers and partners and preventing breakdowns throughout the process. Each firm needs to determine SCM strategies to be prepared for breakdowns in an intense competitive environment. With COVID-19, the change in business and trade environments has taken a different dimension, and it has revealed a new relationship between the efforts to perpetuate supply chains and strategies for supply chain management and enabled new models. In this study, it is aimed to prioritize the factors that lead to SCM breaks needed in project management and the realization of projects, and to choose the most successful SCM strategy considering COVID-19. For this purpose, rough SWARA was used for weighting factors and rough MARCOS was used for the alternative selection. According to the findings, the transportation capacity factor was found to be the most important factor leading to SCM breakdowns. The most ideal supply chain management strategy has been the "collaborative supply chain management strategy." In the food manufacturing sector, the study can be considered as a roadmap in terms of preventing supply chain management breaks during the COVID-19 process and helping to ensure a sustainable production. As another theoretical and practical importance of the study, it is aimed to propose a robust, powerful, and practical decision-making model that can cope with the current uncertainties.

1. Introduction

Disasters caused by epidemics differ from other disasters due to two factors which are long-term breaks in the sectors and increased spread of the disease. Failure to control these disasters causes serious disruption to supply chains and communities. For this reason, irreparable losses may occur [1]. Breakdowns in supply chain management, especially in developing countries, cause output reduction and increase the unemployment rate [2]. According to Fortune [3], most of the companies on the Fortune 1000 list face disruptions in their supply chain management (SCM) due to COVID-19. WHO stated that in the global supply chain components, there is a great challenge to ensure the smooth supply of food and medical devices, including masks and medicines, which are vital and necessary for the treatment of COVID-19 infection [4].

Outbreaks that affect the whole world are among the reasons that cause the supply chain to break. Unlike most factors that cause supply chain disruptions, outbreaks have a low impact in the beginning. However, with its fast spread

to various geographical areas, it can cause a break in the global supply chain very quickly [5]. In this context, it is obvious that the COVID-19 pandemic creates too much uncertainty and unidentified disruptions in global supply chains [6, 7]. FAO declared that the impact of COVID-19 on agriculture and supply chains occurs in terms of food supply and demand. The issue of food security is closely correlated with the supply and demand of food; thus, it has been said that they increase the risk in global food security [8].

The COVID-19 pandemic that has been characterized as an economic crisis [9], which has affected the whole world since March 2020, has been showing its effects on operations and supply chains around the world in a way that is difficult to model, measure, and predict. To stop the disease from spreading in the absence of vaccines, governments have taken nonpharmacological interventions (such as social distance policies and civil lockdowns) around the world and tried to limit human mobility. These phenomena cause serious damage to economic activities, particularly in the service and agriculture sectors deeply [10]. In other words, the COVID-19 pandemic has had an impact on many facets of global supply chains. It ranges everything from the availability of labour, raw material supply, and worker presence to product transportation and retail channel functioning.

Breakdowns in supply chain management caused by the pandemic vary from sector to sector, but the basic components act with the same phenomena for all sectors. Stank et al. [11] stated that with the measures and practices to be taken against these breaks, businesses will have the chance to compete in changing environments. They will play a key role in overcoming these obstacles. As a contrast to that, supply chain management strategies are also significant for preventing disruptions caused by breaks in supply chain management. According to Waters [12], strategic decisions, which affect the whole business, involve significant resources, carry a high level of risk, and have long-term consequences.

The supply chain strategy of an organization includes decisions, plans, policies, and cultural relationships regarding the management of all processes from procuring the raw material to the delivery of the product to the customer, and if necessary, it also includes reverse supply chain activities. While determining the supply chain strategy, it was emphasized that concepts such as cost, service level, time, quality, and flexibility should be carefully considered. In addition, the supply chain is an interconnected system with both forward and backward activities due to the intertwining of many units and operations. For achieving a competitive advantage, it is significant to select the supply chain strategy that takes customers into account as well as establishes appropriate supply and distribution networks [13]. Small- and medium-sized enterprises operating in the manufacturing industry appear as structures in which tactical activities and operational decisions are generally considered. Especially enterprises that have the goal of institutionalization should first determine their general strategies and organize their processes depending on this strategy. Otherwise, the continuity of the gains created within a certain period is not possible. Thus, it is very significant to determine the general supply chain strategy that will guide procurement decisions, materials management, and distribution planning activities [14].

In this context, there are many reasons that push the authors to investigate the problem discussed. In line with the expertise, experience, and knowledge of the decision makers, breaks in supply chain management during the COVID-19 period emerged as an important concept in terms of the continuation of production, meeting the basic needs of people, and meeting both products and services. With COVID-19, the change in business and trade environments has taken a different dimension, and it has revealed a new relationship between the efforts to perpetuate supply chains and strategies for supply chain management and enabled new models.

In terms of businesses, breaks in supply chain management and supply chain management strategy selection are considered as one of the most promising solutions for manufacturing/production and service businesses to react quickly to market conditions, prevent losses, make product and service levels sustainable, and to reduce reputational loss.

At the same time, the study is seen as a critical component in terms of bringing an effective and applicable solution to the decision-making problem involving the selection of supply chain management break factors and supply chain management strategies in the COVID-19 process in a vital area such as the manufacturing sector.

It is thought that it is valuable to work on determining the supply chain management breakage factors and supply chain management strategy with COVID-19, creating a model that will allow businesses to make self-assessments, and helping businesses to improve the production process, as well as providing businesses with a new perspective.

In the food manufacturing sector, the study can be considered as a roadmap in terms of preventing supply chain management breaks during the COVID-19 process and helping to ensure a sustainable production. It also examines the similarities and differences of the factors that cause the supply chain management break in the enterprises in the relevant sector and to what extent they can be reflected. Thus, the study provides a practical roadmap for the supply chain management breakdown factors and supply chain management strategy selection process for the food manufacturing industry during the COVID-19 era.

As another theoretical and practical importance of the study, it is aimed to propose a robust, powerful, and practical decision-making model that can cope with the current uncertainties. Therefore, in addition to contributing to the permanent solution of the relevant decision-making problem for the food manufacturing sector in the COVID-19 period, it is aimed to provide a strong and robust methodological framework to fill the theoretical gaps in the literature by using the advantages of the methods used in the study.

Thus, it will contribute to the solution of similar problems in different fields. In addition, when the results to be achieved are only related to the food sector and are

evaluated within the scope of its structure suitable for comparison with other sectors, it is thought that the relevant study will make a significant contribution to the business world and literature in general, especially at the point of sustainable supply chain management and sustainable production in the COVID-19 process.

In this study, it has been investigated that COVID-19, which has been on the agenda of the whole world for about a year, causes many deaths, breaks in supply chains, collapses economies, and has many negative effects within the framework of the supply chain management. The food industry in Turkey has been affected greatly by the breaks in the supply chains during COVID-19. It has become one of the issues that needed to be dealt within the country for the effective management of the supply chain. This study's goal is to determine the most ideal supply chain strategy by prioritizing the breakdown factors of supply chain management in food manufacturing enterprises operating, which are corporates, in the Eastern Black Sea Region and have 50 or more employees. Several methodologies are used to solve prioritizing problems in the literature such as optimization models [15] and decision-making methods [16]. In this context, rough MARCOS methods based on SWARA have been used because of the complexity of the decision problem.

This study consists of six parts. SCM breakdowns and the COVID-19 pandemic impact are handled in the first part. Literature review related to SCM breakdowns due to the pandemic and studies based on SWARA and MARCOS are mentioned in the second part. Rough numbers, rough SWARA, and rough MARCOS methods are explained in the methodology section. Case studies of food firms in the East Black Sea Region are examined in the fourth part. Sensitivity and comparison analyses are executed in the fifth part. Results and suggestions are stated in the conclusion part.

2. Literature Review

Studies related to SCM breakdowns due to the pandemic process are limited and can be summarized as mentioned below.

Chou et al. [17] assessed the impact of the SARS epidemic on Taiwan airlines and detected 30 percent suspension related to international flights. Salem and Haouari [18] created a three-stage stochastic optimization model for designing the expected demand and supply based on the supply chain network. Araz et al. [19] highlighted the COVID-19 pandemic as one of the critical suspensions in the world. Queiroz et al. [20] made COVID-19-based mapping related to the impact of the epidemic on supply chains and mentioned six perspectives. These are adaptation, digitalization, preparation, recovery, fluctuation effect, and sustainability, respectively.

Ivanov [21] evaluated the spread of the pandemic on global networks for predicting both the short- and long-term effects of simulating with AnyLogic software. According to the findings factor, namely, the opening and closing dates of the facilities was obtained as the most effective for the spread. Aydın and Güner [22] examined the effect of the pandemic on the agricultural industry and food safety and stated the importance level of food safety risk for Turkey. Govindan et al. [1] utilized a fuzzy inference system (FIS)-based support system for decreasing stress levels in the society with demand management in the health supply chain, thereby breaking the COVID-19 spread chain and thus preventing the health service-related supply chain interruptions. According to the study, the first four groups (very sensitive, sensitive, a little sensitive, and normal) are determined in terms of the risk level of the immune system and past diseases (diabetics, heart disease, high blood pressure, etc.) and then the criteria are classified by using the FIS method.

Ivanov and Dolgui [23] developed a game-based theoretical model by considering the interwoven supply network for simulating the supply chain problem in the COVID-19 process and meeting the food-, communication-, and logistics-related social demand. Biswas and Das [7] detected the effect of the pandemic on the Indian manufacturing sector based on five base points (labour force deficiency, local law enforcement, lack of transportation, raw material shortage, and cash flow inadequacy). Singh et al. [24] proposed a simulation model for considering the effect of COVID-19 on logistics and suspensions that took place in food supply chains.

Wang et al. [25] detected the short-term effect of the pandemic on the supply chain breakdown for the hog market in China. Bhattacharya [26] presented a lot of propositions to cope with the global supply chain breakdowns in Singapore. Kaya [27] investigated the effects of the pandemic on OECD countries' sustainable development and evaluated the sustainability performances with the MAIRCA method.

According to the literature review, no study aims to prioritize factors leading to SCM breakdowns and selecting the most successful SCM strategy for food firms in COVID-19 and that underlined the novelty and importance of the study, especially because the COVID-19 pandemic has ushered in a new age in the world [28].

SWARA and MARCOS studies in the literature are shown in Table 1.

According to Table 1, rough SWARA-based rough MARCOS methodology is not applied for weighting factors leading to SCM breakdowns and for selecting the most successful SCM strategy for food firms during COVID-19, and that shows the originality of the study from the methodology.

3. Methodology

In this study, while determining the weights of the criteria with the rough SWARA method, the strategies will be listed with the rough MARCOS method. The methodology section consists of three parts, and they are as follows: rough set theory, rough SWARA, and rough MARCOS.

3.1. Rough Set Theory. Rough numbers convey expert decision makers' impressions in an impartial manner, and they improve the decision-making process of the decision makers [49]. Assume that D indicates the universe, K is an arbitrary

Table 1: Studies related to SWARA and MARCOS methods.

Author(s)	Methodology	Application
Valipour et al. [29]	SWARA-COPRAS	Identification and assessment of risks in deep excavation and foundation projects for big cities in Iran
Sremac et al. [30]	Rough SWARA-WASPAS	Evaluation of 3PLs
Veskovic et al. [31]	DELPHI-SWARA-MABAC	Evaluation of Bosnia and Herzegovina's railway administration system
Vockic et al. [32]	Rough SWARA-ARAS	Electric forklift selection
Zavadskas et al. [33]	Rough SWARA	Choosing of railroad carriages for local transportation requirements
Aydoğan and Özmen [34]	Rough SWARA-TODIM	Evaluating the competitiveness of countries in terms of travel
Prajapati et al. [35]	Modified SWARA-WASPAS	Weighting the solutions of reverse logistics solutions
Badi and Pamucar [36]	Grey MARCOS	Selection of suppliers for LISCO steel manufacturing firm
Chakraborty et al. [37]	D-MARCOS	Selection of suppliers in iron and steel industry
Stankovic et al. [38]	Fuzzy MARCOS	Risk analysis of traffic
Stevic et al. [39]	MARCOS	Supplier selection for Bosnia and Herzegovina's healthcare sector in terms of sustainability
Ulutaş et al. [40]	CCSD-ITARA-MARCOS	Choice of stackers in logistics
Miskic et al. [41]	SWARA-MARCOS	The classification of products into three groups
Özdağoğlu et al. [42]	Fuzzy SWARA-fuzzy MARCOS	In order to determine the importance of the criteria that airline companies should take into account in the recruitment of cabin crew and to choose the most appropriate one among the cabin crew alternatives
Taş et al. [43]	Fuzzy SWARA-MARCOS	A new combined fuzzy methodology is proposed to handle green supplier selection problem
Matic et al. [44]	IMF SWARA-rough MARCOS	To create a novel integrated multicriteria decision-making (MCDM) model for the selection of pavers for the middle category of roads
Mešić et al. [45]	MARCOS	Evaluation of the Logistics Performance Index of the Western Balkan countries
Stević et al. [46]	Fuzzy SWARA	Seven representative studies (logistics, construction industry, financial performance management, and supply chain) with different parameter structures and decision matrix sizes
Tus and Adalı [47]	Fuzzy SWARA-fuzzy MARCOS	To develop applicable and efficient methodology for green supplier selection
Puška and Stojanović [48]	Fuzzy SWARA-fuzzy MABAC, MARCOS, and CRADIS	Green supplier selection in an agrifood company

object of D, and P presents a set of t classes $\{U_1, U_2, \ldots, U_t\}$ including all the objects in D, $P = \{U_1, U_2, \ldots, U_t\}$. If these classes are sequenced as $U_1 < U_2 < \ldots < U_t$, then $\forall K \in D$, $U_q \in P$, and $1 \le q \le t$, by $P(K)$, we refer the group to which the object belongs, and the upper approximation ($\overline{\text{Apr}}(U_q)$) and lower approximation ($\text{Apr}(U_q)$) of class U_q are explained as follows [50]:

$$\underline{\text{Apr}}\left(U_q\right) = \left\{\frac{K \in D}{P(K)} \le U_q\right\}, \tag{1}$$

$$\overline{\text{Apr}}\left(U_q\right) = \left\{\frac{K \in D}{P(K)} \ge U_q\right\}, \tag{2}$$

where U_q can be demonstrated as a rough number $\text{RN}(U_q)$ and its lower limit ($\text{Lim}\_(U_q)$) and upper limit ($\overline{\text{Lim}}(U_q)$) can be computed as

$$\text{Lim}\left(U_q\right) = \frac{1}{M_L}\sum\left\{K \in \text{Apr}\left(U_q\right)\right\}P(K), \tag{3}$$

$$\overline{\text{Lim}}\left(U_q\right) = \frac{1}{M_U}\sum\left\{K \in \overline{\text{Apr}}\left(U_q\right)\right\}P(K), \tag{4}$$

$$\text{RN}\left(U_q\right) = \left[\text{Lim}\left(U_q\right), \overline{\text{Lim}}\left(U_q\right)\right], \tag{5}$$

where M_L and M_U are the number objects included in $\text{Apr}(U_q)$ and $\overline{\text{Apr}}(U_q)$, respectively. The arithmetic operations of the two rough numbers, that is, ($\text{RN}(D)$ and $\text{RN}(E)$) are as follows:

$$\begin{aligned}
\text{Addition: } \text{RN}(D) + \text{RN}(E) &= \left[\underline{\text{Lim}}(D) + \underline{\text{Lim}}(E), \overline{\text{Lim}}(D) + \overline{\text{Lim}}(E)\right],\\
\text{Subtraction: } \text{RN}(D) - \text{RN}(E) &= \left[\underline{\text{Lim}}(D) - \overline{\text{Lim}}(E), \overline{\text{Lim}}(D) - \underline{\text{Lim}}(E)\right],\\
\text{Multiplication: } \text{RN}(D) \times \text{RN}(E) &= \left[\underline{\text{Lim}}(D) \times \underline{\text{Lim}}(E), \overline{\text{Lim}}(D) \times \overline{\text{Lim}}(E)\right],\\
\text{Division: } \text{RN}(D) \div \text{RN}(E) &= \left[\underline{\text{Lim}}(D) \div \overline{\text{Lim}}(E), \overline{\text{Lim}}(D) \div \underline{\text{Lim}}(E)\right].
\end{aligned} \tag{6}$$

3.2. Rough SWARA. The SWARA method, which was proposed by Keršuliene et al. [51], is frequently used in the literature as it consists of a few steps of calculation, and it needs a few pairwise comparisons. The rough SWARA method was developed by Zavadskas and his colleagues [33]. The subjectivity and uncertainty of decision makers are reduced by the combination of rough numbers with the SWARA method [33]. Simple access creation, simple data collecting, and a few processes step are all traits of rough SWARA [33]. The rough SWARA method is utilized to obtain the weights of the criteria in this study. The phase in this method is outlined as follows [33]:

Phase 1: a set of criteria is explained

Phase 2: decision makers rank the criteria with respect to the importance level

Phase 3: the preferences of experts are consolidated to achieve a group rough matrix c_j, which is represented as

$$\text{RN}\left(C_j\right) = \left[c_j^L, c_j^U\right]_{1\times n}. \tag{7}$$

Phase 4: the group rough matrix is normalized by equation (9) to achieve the normalized rough matrix ($\text{RN}(S_j)$), that is,

$$\text{RN}\left(S_j\right) = \left[s_j^L, s_j^U\right]_{1\times n}, \tag{8}$$

where

$$\text{RN}\left(S_j\right) = \begin{cases} j = 1, & [1,1],\\ j > 1, & \dfrac{\left[c_j^L, c_j^U\right]}{\max_r\left[c_r^L, c_r^U\right]}. \end{cases} \tag{9}$$

Phase 5: $\text{RN}(K_j) = [k_j^L, k_j^U]_{1\times n}$ matrix is computed as

$$\text{RN}\left(K_j\right) = \begin{cases} j = 1, & [1,1],\\ j > 1, & \left[s_j^L + 1, s_j^U + 1\right]. \end{cases} \tag{10}$$

Phase 6: $\text{RN}(Q_j)$ (recalculated weights) matrix is computed as

$$\text{RN}\left(Q_j\right) = \begin{cases} j = 1, & [1,1],\\ j > 1, & \left[\dfrac{q_{j-1}^L}{k_j^U}, \dfrac{q_{j-1}^U}{k_j^L}\right]. \end{cases} \tag{11}$$

Phase 7: the weights of criteria are computed as

$$\text{RN}\left(W_j\right) = \left[w_j^L, w_j^U\right]_{1\times n} = \left[\frac{\left[q_j^L, q_j^U\right]}{\sum\left[q_j^L, q_j^U\right]}\right]. \tag{12}$$

3.3. Rough MARCOS. The foundation of the MARCOS approach is the definition of the relationship between alternatives and reference values (anti-ideal and ideal alternatives). The utility functions of the alternatives are established using the defined relationships, and

a compromise ranking is then created by using anti-ideal and ideal solutions [46]. In this study, the rough MARCOS (R-MARCOS) method is utilized to rank supply chain strategies. The R-MARCOS method is helpful to decrease the uncertainty and subjectivity of the decision-makers. The phases of R-MARCOS are as follows [52]:

Phase 1: rough decision matrix ($\mathrm{RN}(V)$) is organized as follows:

$$\mathrm{RN}(V) = \left[v_{ij}^{L}, v_{ij}^{U}\right]_{m\times n}. \tag{13}$$

Phase 2: extended rough matrix $\mathrm{RN}(EV)$ is arranged by adding anti-idealRN (AID) and ideal RN (ID) solutions to the matrix.

$$\mathrm{RN}(\mathrm{AID}) = \left[v_{\mathrm{aid}}^{L}, v_{\mathrm{aid}}^{U}\right] = \begin{cases} \min\limits_{i}\left[v_{ij}^{L}, v_{ij}^{U}\right], & \text{if } j \in B, \\ \max\limits_{i}\left[v_{ij}^{L}, v_{ij}^{U}\right], & \text{if } j \in C, \end{cases} \tag{14}$$

$$\mathrm{RN}(\mathrm{ID}) = \left[v_{\mathrm{id}}^{L}, v_{\mathrm{id}}^{U}\right] = \begin{cases} \max\limits_{i}\left[v_{ij}^{L}, v_{ij}^{U}\right], & \text{if } j \in B, \\ \min\limits_{i}\left[v_{ij}^{L}, v_{ij}^{U}\right], & \text{if } j \in C. \end{cases} \tag{15}$$

In equations (14) and (15), B and C indicate beneficial and nonbeneficial criteria.

Phase 3: rough normalized matrix $\mathrm{RN}(T)$ is created by using equations (17) and (18).

$$\mathrm{RN}(T) = \left[t_{\mathrm{ij}}^{L}, t_{\mathrm{ij}}^{U}\right]_{m\times n}, \tag{16}$$

$$\left[t_{ij}^{L}, t_{ij}^{U}\right] = \left[\frac{v_{ij}^{L}}{v_{id}^{U}}, \frac{v_{ij}^{U}}{v_{id}^{U}}\right] \text{if } j \in B, \tag{17}$$

$$\left[t_{\mathrm{ij}}^{L}, t_{\mathrm{ij}}^{U}\right] = \left[\frac{v_{id}^{L}}{v_{ij}^{U}}, \frac{v_{id}^{L}}{v_{ij}^{L}}\right] \text{if } \ j \in C. \tag{18}$$

Phase 4: rough weighted normalized matrix $\mathrm{RN}(E)$ is computed by using the following equation:

$$\mathrm{RN}(E) = \left[e_{\mathrm{ij}}^{L}, e_{\mathrm{ij}}^{U}\right] = \left[t_{\mathrm{ij}}^{L} \times w_{j}^{L}, t_{\mathrm{ij}}^{U} \times w_{j}^{U}\right]. \tag{19}$$

Phase 5: $RN(Z)$ is computed by using the equation as follows:

$$\mathrm{RN}(Z) = \left[z_{i}^{L}, z_{i}^{U}\right] = \sum_{j=1}^{n}\left[e_{\mathrm{ij}}^{L}, e_{\mathrm{ij}}^{U}\right]. \tag{20}$$

Phase 6: rough utility degrees of alternatives $\mathrm{RN}(Y_i^-)$ and $\mathrm{RN}(Y_i^+)$ are calculated as

$$\mathrm{RN}\left(Y_{i}^{-}\right) = \left[y_{i}^{-L}, y_{i}^{-U}\right] = \left[\frac{z_{i}^{L}}{z_{\mathrm{aid}}^{U}}, \frac{z_{i}^{U}}{z_{\mathrm{aid}}^{L}}\right], \tag{21}$$

$$\mathrm{RN}\left(Y_{i}^{+}\right) = \left[y_{i}^{+L}, y_{i}^{+U}\right] = \left[\frac{z_{i}^{L}}{z_{id}^{U}}, \frac{z_{i}^{U}}{z_{id}^{L}}\right]. \tag{22}$$

Phase 7: rough utility degrees ($\mathrm{RN}(Y_i^-)$ and $\mathrm{RN}(Y_i^+)$) are then converted into crisp Y_i^- and Y_i^+.

$$Y_{i}^{-} = \frac{y_{i}^{-L} + y_{i}^{-U}}{2}, \tag{23}$$

$$Y_{i}^{+} = \frac{y_{i}^{+L} + y_{i}^{+U}}{2}. \tag{24}$$

Phase 8: the utility functions in relation to the anti-ideal $f(Y_i^-)$ and ideal $f(Y_i^+)$ solutions are computed by using equations (25) and (26), respectively.

$$f\left(Y_{i}\right) = \frac{Y_{i}^{+} + Y_{i}^{-}}{1 + \left(1 - f\left(Y_{i}^{+}\right)/f\left(Y_{i}^{+}\right)\right) + \left(1 - f\left(Y_{i}^{-}\right)/f\left(Y_{i}^{-}\right)\right)}, \tag{25}$$

where

$$f\left(Y_{i}^{-}\right) = \frac{Y_{i}^{+}}{Y_{i}^{+} + Y_{i}^{-}}, \tag{26}$$

$$f\left(Y_{i}^{+}\right) = \frac{Y_{i}^{-}}{Y_{i}^{+} + Y_{i}^{-}}. \tag{27}$$

Phase 9: the alternatives are then ranked from the maximum to the minimum utility function.

4. Application

In this study, it is aimed to prioritize the factors leading to SCM breakdowns and choosing the most successful SCM strategy in the COVID-19 process. The SCM strategies considered in the assessment in this study are as follows: lean supply chain management strategy (LSCMS), agile supply chain management strategy (ASCMS), collaborative supply chain management strategy (CSCMS), vertical integration strategy-based on lean supply chain axis (VIS), and lean supply chain outsourcing axis-based strategy (LSCOAS). These SCM strategies are evaluated with respect to their performance under the criteria leading to SCM breakdowns.

The factors considered in the evaluation of this study are existence of skilled workforce (ESW), business dispute (BD), local laws-related incentives (LLRI), cash flow scarcity in the manufacturing sector (CFSMS), supplier bankruptcy (SB), alternative supplier capacity and flexibility (ASCF), lack of risks related to pandemic (COVID-19), war, terrorism, and force majeure (LRRPWTFM), transportation capacity (TC), and level of raw material procurement (LRMP). Factors and strategies were determined according to the literature review and experts (academicians, managers, and public authorities) decisions. The Eastern Black Sea Region of Turkey provided the data for this study. First, the six major company managers ranked the factors from most important to least important. The decision makers consisted of 6 experts in total, including the operation manager (2), the process manager (2), the purchasing manager (1), and the general manager of the business (1) working in the field of food manufacturing.

The ranking of factors according to the preferences of managers (M) is shown in Table 2.

The weights of the factors are found by using the rough SWARA method and the data in Tables 2 and 3 present the findings of the rough SWARA. Figure 1 shows the weight of the factors. First, the rankings of the factors are consolidated to achieve a group rough matrix by using equations (3) and (4). The ESW factor is as an example to illustrate the calculation as follows:

$$\mathrm{ESW} = \{2, 5, 5, 3, 6, 5\}$$

$$\overline{\mathrm{Lim}}(2) = 2,$$

$$\overline{\mathrm{Lim}}(2) = \frac{(2 + 5 + 5 + 3 + 6 + 5)}{6} = 4.333$$

$$\underline{\mathrm{Lim}}(5) = \frac{(2 + 5 + 5 + 3 + 5)}{5} = 4,$$

$$\overline{\mathrm{Lim}}(5) = \frac{(5 + 5 + 6 + 5)}{4} = 5.25$$

$$\underline{\mathrm{Lim}}(3) = \frac{(2 + 3)}{2} = 2.5,$$

$$\overline{\mathrm{Lim}}(3) = \frac{(5 + 5 + 3 + 6 + 5)}{5} = 4.8$$

$$\underline{\mathrm{Lim}}(6) = \frac{(2 + 5 + 5 + 3 + 5 + 6)}{6} = 4.333,$$

$$\overline{\mathrm{Lim}}(6) = 6$$

$$\mathrm{RN}(\mathrm{ESW}_1) = [2, 4.333]$$

$$\mathrm{RN}(\mathrm{ESW}_2) = [4, 5.25]$$

$$\mathrm{RN}(\mathrm{ESW}_3) = [4, 5.25]$$

$$\mathrm{RN}(\mathrm{ESW}_4) = [2.5, 4.8]$$

$$\mathrm{RN}(\mathrm{ESW}_5) = [4.333, 6]$$

$$\mathrm{RN}(\mathrm{ESW}_6) = [4, 5.25]$$

$$\mathrm{ESW}^L = \frac{2 + 4 + 4 + 2.5 + 4.333 + 4}{6} = 3.472$$

$$\mathrm{ESW}^U = \frac{4.333 + 5.25 + 5.25 + 4.8 + 6 + 5.25}{6} = 5.147. \tag{28}$$

The same operations are performed for other factors. Then, the normalization process is performed with equation (12). The ESW factor is taken as an example to illustrate the calculation as follows:

$$\mathrm{RN}(S_{\mathrm{ESW}}) = \left[\frac{3.472}{7.956}, \frac{5.147}{4.444}\right] = [0.436, 1.158]. \tag{29}$$

The same operation is performed for other factors. After the normalization process, the $\mathrm{RN}(K_j)$ value is found by using equation (13). The ESW factor is taken as an example to illustrate the calculation as follows:

$$\mathrm{RN}(K_{\mathrm{ESW}}) = [1 + 0.436, 1 + 1.158] = [1.436, 2.158]. \tag{30}$$

After these calculations, the $\mathrm{RN}(Q_j)$ value is obtained by using equation (14). The ESW factor is taken as an example to illustrate the calculation that follows:

$$\mathrm{RN}(Q_{\mathrm{ESW}}) = \left[\frac{1.277}{2.158}, \frac{2.216}{1.436}\right] = [0.592, 1.543]. \tag{31}$$

In the final step, the weights of the factors are calculated by using equation (15). The ESW factor is taken as an example to indicate the computation.

$$\mathrm{RN}(w_{\mathrm{ESW}}) = \left[\frac{0.592}{(1 + 0.783 + 1.543 + 1.539 + 1.704 + 1.722 + 1.710 + 1.795 + 1.743)}, \frac{1.543}{(1 + 0.451 + 0.592 + 0.573 + 0.567 + 0.572 + 0.524 + 0.553 + 0.547)}\right] \tag{32}$$

$$= [0.044, 0.287].$$

Table 2: The ranking of factors.

Factors	Managers					
	M1	M2	M3	M4	M5	M6
ESW	2	5	5	3	6	5
BD	6	8	7	4	4	2
LLRI	5	1	6	1	7	3
CFSMS	8	2	3	5	1	1
SB	4	3	9	2	3	8
ASCF	3	7	4	9	2	6
LRRPWTFM	1	6	8	8	9	4
TC	9	4	2	6	8	7
LRMP	7	9	1	7	5	9

Table 3: The rough SWARA findings.

Factors	w_j^L	w_j^U	w_j	Ranking
CFSMS	0.074	0.186	0.130	8
LLRI	0.033	0.146	0.089	9
ESW	0.044	0.287	0.165	6
SB	0.042	0.286	0.164	7
BD	0.042	0.317	0.179	4
ASCF	0.042	0.320	0.181	3
LRRPWTFM	0.039	0.318	0.178	5
TC	0.041	0.334	0.187	1
LRMP	0.040	0.324	0.182	2

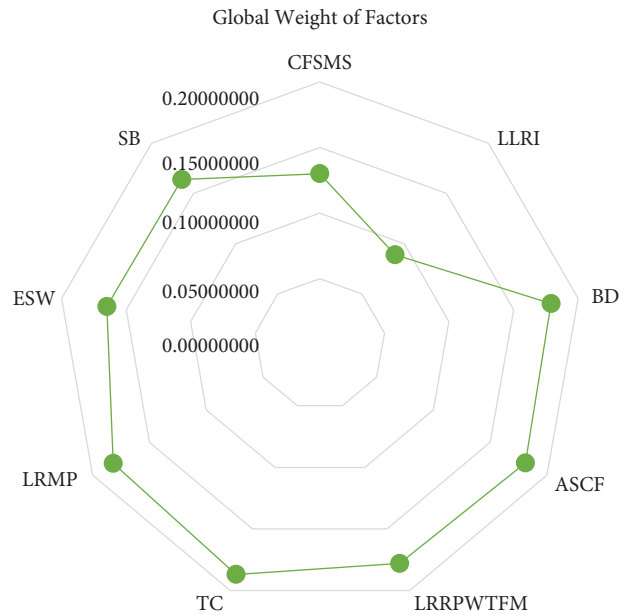

Figure 1: Weight of the factors.

Table 3 shows the weights of the factors.

By taking the arithmetic mean of the w_j^L and w_j^U values, it can be determined which factor is more important by finding the crisp weights of the factors. w_j values have shown that the most significant criterion is TC with the value of 0.187. On the other hand, the criterion of LLRI is determined as the least significant with the value of 0.089. Managers assigned values between 1 (the lowest) and 9 (the highest) to each factor. The preferences of managers are consolidated by using equations (3) and (4) to organize a rough decision matrix. The ESW factor for the LSCMS strategy is taken as an example to indicate these calculations.

$$\begin{aligned}
&\mathrm{LSCMS}_{\mathrm{ESW}} = \{3,5,3,2,3,2\}\\
&\underline{\mathrm{Lim}}(3) = \frac{(3+3+2+3+2)}{5} = 2.6,\\
&\overline{\mathrm{Lim}}(3) = \frac{(3+5+3+3)}{4} = 3.5\\
&\underline{\mathrm{Lim}}(5) = \frac{(3+5+3+2+3+2)}{6} = 3,\\
&\overline{\mathrm{Lim}}(5) = 5\\
&\underline{\mathrm{Lim}}(2) = 2,\\
&\overline{\mathrm{Lim}}(2) = \frac{(3+5+3+2+3+2)}{6} = 3\\
&\mathrm{RN}(\mathrm{LSCMS}_1) = [2.6, 3.5]\\
&\mathrm{RN}(\mathrm{LSCMS}_2) = [3, 5]\\
&\mathrm{RN}(\mathrm{LSCMS}_3) = [2.6, 3.5]\\
&\mathrm{RN}(\mathrm{LSCMS}_4) = [2, 3]\\
&\mathrm{RN}(\mathrm{LSCMS}_5) = [2.6, 3.5]\\
&\mathrm{RN}(\mathrm{LSCMS}_6) = [2, 3]
\end{aligned} \tag{33}$$

$$\mathrm{LSCM}^L = \frac{2.6+3+2.6+2+2.6+2}{6} = 2.467$$

$$\mathrm{LSCM}^U = \frac{3.5+5+3.5+3+3.5+3}{6} = 3.583.$$

The same operations are performed in other strategies and other factors. The rough decision matrix is shown in Table 4.

Anti-ideal and perfect solutions are added to the matrix to create the extended rough matrix. This matrix is shown in Table 5.

The extended rough matrix is transformed into the rough normalized matrix by using equations (17) and (18). Table 6 shows the rough normalized matrix.

The ESW factor for the LSCMS strategy will be taken as an example to illustrate this calculation. This factor is a beneficial factor, so equation (17) will be used.

$$\left[t_{11}^{L}, t_{11}^{U}\right] = \left[\frac{v_{11}^{L}}{v_{11}^{U}}, \frac{v_{11}^{U}}{v_{11}^{U}}\right] = \left[\frac{2.467}{4.881}, \frac{3.583}{4.881}\right] = [0.505, 0.734]. \tag{34}$$

The rough weighted matrix (Table 7) is created by multiplying (equation (19)) the rough normalized values with the rough weights of the factors. The ESW factor for the LSCMS strategy is taken as an example to illustrate this calculation.

$$\mathrm{RN}(E) = \left[e_{11}^{L}, e_{11}^{U}\right] = \left[t_{11}^{L} \times w_{1}^{L}, t_{11}^{U} \times w_{1}^{U}\right] = [0.505 \times 0.044, 0.734 \times 0.287] = [0.022, 0.211]. \tag{35}$$

The findings of the rough MARCOS technique are derived using the equations (20)–(27). Table 8 ranks the strategies based on these findings. The LSCMS strategy is taken as an example to illustrate these calculations.

$$\mathrm{RN}(Z) = \left[z_{1}^{L}, z_{1}^{U}\right] = \sum_{j=1}^{n}\left[e_{ij}^{L}, e_{ij}^{U}\right] = \begin{bmatrix} (0.022 + 0.026 + 0.021 + 0.039 + 0.017 + 0.023 + 0.018 + 0.027 + 0.023), \\ (0.211 + 0.303 + 0.134 + 0.176 + 0.278 + 0.280 + 0.274 + 0.321 + 0.310) \end{bmatrix} = [0.216, 2.287]$$

$$\mathrm{RN}\left(Y_{1}^{-}\right) = \left[y_{1}^{-L}, y_{1}^{-U}\right] = \left[\frac{z_{1}^{L}}{z_{aid}^{U}}, \frac{z_{1}^{U}}{z_{aid}^{L}}\right] = \left[\frac{0.216}{1.929}, \frac{2.287}{0.186}\right] = [0.112, 12.296]$$

$$\mathrm{RN}\left(Y_{1}^{+}\right) = \left[y_{1}^{+L}, y_{1}^{+U}\right] = \left[\frac{z_{1}^{L}}{z_{id}^{U}}, \frac{z_{1}^{U}}{z_{id}^{L}}\right] = \left[\frac{0.216}{2.518}, \frac{2.287}{0.254}\right] = [0.086, 9.004]$$

$$Y_{1}^{-} = \frac{y_{1}^{-L} + y_{1}^{-U}}{2} = \frac{0.112 + 12.296}{2} = 6.204$$

$$Y_{1}^{+} = \frac{y_{1}^{+L} + y_{1}^{+U}}{2} = \frac{0.086 + 9.004}{2} = 4.545$$

$$f\left(Y_{1}^{-}\right) = \frac{Y_{1}^{+}}{Y_{1}^{+} + Y_{1}^{-}} = \frac{4.545}{6.204 + 4.545} = 0.423$$

$$f\left(Y_{1}^{+}\right) = \frac{Y_{1}^{-}}{Y_{1}^{+} + Y_{1}^{-}} = \frac{6.204}{6.204 + 4.545} = 0.577$$

$$f\left(Y_{1}\right) = \frac{Y_{1}^{+} + Y_{1}^{-}}{1 + \left(1 - f\left(Y_{1}^{+}\right)/f\left(Y_{1}^{+}\right)\right) + \left(1 - f\left(Y_{1}^{-}\right)/f\left(Y_{1}^{-}\right)\right)} = \frac{6.204 + 4.545}{1 + (1 - 0.577/0.577) + (1 - 0.423/0.423)} = 3.471. \tag{36}$$

The strategies are ranked as follows according to the findings of the rough MARCOS: CSCMS, LSCMS, LSCOAS, VIS, and ASCMS. By standing first, CSCMS shows its importance in providing cost benefits to businesses that implement it as a strategy, as it allows for the direction of their manpower, capital, and time to their core capabilities and operations while outsourcing the noncore activities and functions to other logistics service providers. The first place in the ranking of the strategy is also attributed to its perceived value, especially during the COVID-19 pandemic, regarding the expansion of the service area of the relevant sector, the expansion of the location served, the reduction

Table 4: The rough decision matrix.

Strategies	Factors								
	ESW	BD	LLRI	CFSMS	SB	ASCF	LRRPWTFM	TC	LRMP
LSCMS	(2.467, 3.583)	(2.611, 4.111)	(3.308, 4.750)	(2.667, 3.583)	(2.656, 6.478)	(2.681, 4.320)	(3.045, 5.822)	(3.681, 5.320)	(3.861, 6.547)
ASCMS	(2.764, 3.939)	(3.117, 3.917)	(2.583, 4.500)	(3.658, 5.722)	(3.295, 6.214)	(3.495, 4.889)	(4.117, 6.417)	(4.061, 5.236)	(2.875, 5.314)
CSCMS	(2.706, 4.872)	(2.500, 3.500)	(3.153, 5.172)	(3.522, 5.278)	(3.761, 6.661)	(2.878, 4.472)	(4.250, 6.750)	(3.495, 4.889)	(4.556, 6.845)
VIS	(2.428, 4.881)	(3.500, 4.500)	(2.569, 4.361)	(2.528, 4.878)	(3.928, 6.556)	(2.928, 4.789)	(4.500, 6.500)	(3.211, 5.072)	(3.811, 6.044)
LSCOAS	(3.111, 4.506)	(4.461, 5.861)	(3.461, 4.861)	(3.478, 5.811)	(2.583, 5.633)	(2.978, 4.944)	(3.334, 6.067)	(4.417, 5.533)	(3.694, 6.017)

Table 5: Extended rough matrix.

Strategies	Factors								
	ESW	BD	LLRI	CFSMS	SB	ASCF	LRRPWTFM	TC	LRMP
Anti-ideal	(2.428, 3.583)	(4.461, 5.861)	(2.569, 4.361)	(3.658, 5.811)	(3.928, 6.661)	(2.681, 4.320)	(3.045, 5.822)	(3.211, 4.889)	(2.875, 5.314)
LSCMS	(2.467, 3.583)	(2.611, 4.111)	(3.308, 4.750)	(2.667, 3.583)	(2.656, 6.478)	(2.681, 4.320)	(3.045, 5.822)	(3.681, 5.320)	(3.861, 6.547)
ASCMS	(2.764, 3.939)	(3.117, 3.917)	(2.583, 4.500)	(3.658, 5.722)	(3.295, 6.214)	(3.495, 4.889)	(4.117, 6.417)	(4.061, 5.236)	(2.875, 5.314)
CSCMS	(2.706, 4.872)	(2.500, 3.500)	(3.153, 5.172)	(3.522, 5.278)	(3.761, 6.661)	(2.878, 4.472)	(4.250, 6.750)	(3.495, 4.889)	(4.556, 6.845)
VIS	(2.428, 4.881)	(3.500, 4.500)	(2.569, 4.361)	(2.528, 4.878)	(3.928, 6.556)	(2.928, 4.789)	(4.500, 6.500)	(3.211, 5.072)	(3.811, 6.044)
LSCOAS	(3.111, 4.506)	(4.461, 5.861)	(3.461, 4.861)	(3.478, 5.811)	(2.583, 5.633)	(2.978, 4.944)	(3.334, 6.067)	(4.417, 5.533)	(3.694, 6.017)
Ideal	(3.111, 4.881)	(2.500, 3.500)	(3.461, 5.172)	(2.528, 4.806)	(2.583, 5.633)	(3.495, 4.944)	(4.500, 6.750)	(4.417, 5.533)	(4.556, 6.845)

Table 6: Rough normalized matrix.

Strategies	Factors								
	ESW	BD	LLRI	CFSMS	SB	ASCF	LRRPWTFM	TC	LRMP
Anti-ideal	(0.497, 0.734)	(0.427, 0.560)	(0.497, 0.843)	(0.435, 0.691)	(0.388, 0.658)	(0.542, 0.874)	(0.451, 0.863)	(0.580, 0.884)	(0.420, 0.776)
LSCMS	(0.505, 0.734)	(0.608, 0.957)	(0.640, 0.918)	(0.526, 0.948)	(0.399, 0.973)	(0.542, 0.874)	(0.451, 0.863)	(0.665, 0.962)	(0.564, 0.956)
ASCMS	(0.566, 0.807)	(0.638, 0.802)	(0.499, 0.870)	(0.442, 0.691)	(0.416, 0.784)	(0.707, 0.989)	(0.610, 0.951)	(0.734, 0.946)	(0.420, 0.776)
CSCMS	(0.554, 0.998)	(0.714, 1.000)	(0.610, 1.000)	(0.479, 0.718)	(0.388, 0.687)	(0.582, 0.905)	(0.630, 1.000)	(0.632, 0.884)	(0.666, 1.000)
VIS	(0.497, 1.000)	(0.556, 0.714)	(0.497, 0.843)	(0.518, 1.000)	(0.394, 0.658)	(0.592, 0.969)	(0.667, 0.963)	(0.580, 0.917)	(0.557, 0.883)
LSCOAS	(0.637, 0.923)	(0.427, 0.560)	(0.669, 0.940)	(0.435, 0.727)	(0.459, 1.000)	(0.602, 1.000)	(0.494, 0.899)	(0.798, 1.000)	(0.540, 0.879)
Ideal	(0.637, 1.000)	(0.714, 1.000)	(0.669, 1.000)	(0.526, 1.000)	(0.459, 1.000)	(0.707, 1.000)	(0.667, 1.000)	(0.798, 1.000)	(0.666, 1.000)

Table 7: Rough weighted normalized matrix.

Strategies	Factors								
	ESW	BD	LLRI	CFSMS	SB	ASCF	LRRPWTFM	TC	LRMP
Anti-ideal	(0.022, 0.211)	(0.018, 0.178)	(0.016, 0.123)	(0.032, 0.129)	(0.016, 0.188)	(0.023, 0.280)	(0.018, 0.274)	(0.024, 0.295)	(0.017, 0.251)
LSCMS	(0.022, 0.211)	(0.026, 0.303)	(0.021, 0.134)	(0.039, 0.176)	(0.017, 0.278)	(0.023, 0.280)	(0.018, 0.274)	(0.027, 0.321)	(0.023, 0.310)
ASCMS	(0.025, 0.232)	(0.027, 0.254)	(0.016, 0.127)	(0.033, 0.129)	(0.017, 0.224)	(0.030, 0.316)	(0.024, 0.302)	(0.030, 0.316)	(0.017, 0.251)
CSCMS	(0.024, 0.286)	(0.030, 0.317)	(0.020, 0.146)	(0.035, 0.134)	(0.016, 0.196)	(0.024, 0.290)	(0.025, 0.318)	(0.026, 0.295)	(0.027, 0.324)
VIS	(0.022, 0.287)	(0.023, 0.226)	(0.016, 0.123)	(0.038, 0.186)	(0.017, 0.188)	(0.025, 0.310)	(0.026, 0.306)	(0.024, 0.306)	(0.022, 0.286)
LSCOAS	(0.028, 0.265)	(0.018, 0.178)	(0.022, 0.137)	(0.032, 0.135)	(0.019, 0.286)	(0.025, 0.320)	(0.019, 0.286)	(0.033, 0.334)	(0.022, 0.285)
Ideal	(0.028, 0.287)	(0.030, 0.317)	(0.022, 0.146)	(0.039, 0.186)	(0.019, 0.286)	(0.030, 0.320)	(0.026, 0.318)	(0.033, 0.334)	(0.027, 0.324)

Table 8: The findings of rough MARCOS.

Strategies	Results								
	RN(Z)	RN(Y_i^-)	RN(Y_i^+)	Y_i^-	Y_i^+	$f(Y_i^-)$	$f(Y_i^+)$	$f(Y_i)$	Rankings
Anti-ideal	(0.186, 1.929)								
LSCMS	(0.216, 2.287)	(0.112, 12.296)	(0.086, 9.004)	6.204	4.545	0.423	0.577	3.471	2
ASCMS	(0.219, 2.151)	(0.114, 11.565)	(0.087, 8.469)	5.840	4.278	0.423	0.577	3.267	5
CSCMS	(0.227, 2.306)	(0.118, 12.398)	(0.090, 9.079)	6.258	4.585	0.423	0.577	3.501	1
VIS	(0.213, 2.218)	(0.110, 11.925)	(0.085, 8.732)	6.018	4.409	0.423	0.577	3.367	4
LSCOAS	(0.218, 2.226)	(0.113, 11.968)	(0.087, 8.764)	6.041	4.426	0.423	0.577	3.380	3
Ideal	(0.254, 2.518)								

and sharing of the total costs, increasing the level and quality of service, as well as creating a common power.

Another important strategy in manufacturing enterprises is LSCMS. This is because enterprises can only minimize waste, reduce stocks, and ensure an effective material flow through LSCMS, especially during the COVID-19 period. In other words, reducing each resource used in all operations as much as possible is the strategic element that creates added value that all businesses focus on.

5. Sensitivity and Comparative Analysis

5.1. Sensitivity Analysis. In this part of the paper, we have analysed the effect of changing the three most important criteria C8-TC, C9-LRMP, and C6-ASCF on the ranks because it is a higher probability that the most essential criteria can have an influence on the ranking alternatives. For the creation of scenarios with simulated criteria weights (Table 9), we have used the following equation:

$$W_{n\beta} = \left(1 - W_{n\alpha}\right)\frac{W_\beta}{\left(1 - W_n\right)}. \tag{37}$$

In equation (37), $W_{n\beta}$ represents the corrected values of all criteria values and $W_{n\alpha}$ indicates the lowered values of the criterion TC in scenarios S1–S10, LRMP in scenarios S11–S20, and ASCF in scenarios S21–S30. W_β is the original value of each considered criterion, and W_n is the initial value of the criterion TC in scenarios S1–S10, LRMP in scenarios S11–S20, and ASCF in scenarios S21–S30.

The value of the criterion TC was lowered by 5% in the first scenario, while the values of the other criteria were modified accordingly using the equation mentioned above. The value of the TC criterion is 10% less in each of the S2–S10 scenarios, so in scenario S10, it has a value of only (0.006, 0.050) (reduced by 95%). The same procedure is followed in scenarios S11–S20 for the LRMP criterion, and in scenarios S21–S30 for the ASCF criterion which means that scenarios S1–10 represent reduction of the most important criterion (TC) in the range 5–95%, and scenarios S11–S20 represent the reduction of LRMP criterion. Scenarios S21–S30 represent the reduction of the ASCF criterion.

The output of the model created from the newly created 30 criterion weight vectors is presented in Figure 2. A sensitivity analysis was formed in terms of 30 scenarios with simulated criteria weights.

According to Figure 2, only the strategies of VIS and LSCOAS changed their position (VIS from third to fourth place) in the total number of 10 scenarios (S4–S10, S27, S29, and S30). Considering such results, we may draw the conclusion that the model is not extremely sensitive to the significance of the criteria and that the shift in the importance of the criteria values does not have a significant effect.

5.2. Comparative Analysis. Rough ARAS [53], rough WASPAS [54], and rough SAW [55] methods were applied to determine whether the rough MARCOS method achieved the correct results. Table 10 shows the results of the rough MCDM methods. Figure 3 refers to rough number values in a comparative analysis with the mentioned methods.

As seen in Table 10, the ranking of the strategies was the same in rough MARCOS and rough WASPAS methods. Likewise, the results of the rough SAW and rough ARAS methods are the same. The Spearman correlation coefficient between the results of the rough MARCOS-rough ARAS methods was determined as 0.9. In addition, the Spearman correlation coefficient between the results of the rough MARCOS and rough SAW methods was determined as 0.9 since the results of the rough SAW method were the same as the results of the rough ARAS method. As can be seen, there is a high correlation between the results of the proposed rough MARCOS method and the results of other rough MCDM methods. Therefore, it has been confirmed that the proposed rough MARCOS method achieved accurate results. As seen in Figure 3, rough MARCOS has the smallest range, while the rough values in rough ARAS have the largest range (0.053–14.380), as can be seen by observing the lower and upper limits of the rough number. The rough numbers and rough WASPAS have a relatively small range (0.496–2.937), and for rough SAW it is (0.213–3.572). The values of rough numbers may vary depending on the methodology itself, but the results obtained using the integrated rough SWARA and rough MARCOS model have been verified, as can be seen from their ranks and the calculated Spearman's coefficient (SCC).

Also, the Spearman correlation coefficient SCC [56] was made between rough MARCOS and the other methods. SCC as 0.90 was calculated between rough MARCOS, rough ARAS, and rough SAW. Finally, the highest coefficient as 1.00 showing the same alternative ranking between rough MARCOS and rough WASPAS was acquired.

Table 9: The weights of new simulated criteria in a sensitivity analysis.

	W1	W2	W3	W4	W5	W6	W7	W8	W9
SN1	(0.045, 0.288)	(0.043, 0.318)	(0.034, 0.146)	(0.076, 0.186)	(0.043, 0.287)	(0.043, 0.321)	(0.040, 0.319)	(0.039, 0.317)	(0.041, 0.325)
SN2	(0.047, 0.289)	(0.045, 0.319)	(0.035, 0.147)	(0.080, 0.187)	(0.045, 0.288)	(0.045, 0.322)	(0.042, 0.320)	(0.035, 0.284)	(0.043, 0.326)
SN3	(0.050, 0.290)	(0.047, 0.320)	(0.037, 0.148)	(0.083, 0.188)	(0.047, 0.289)	(0.047, 0.323)	(0.044, 0.321)	(0.031, 0.251)	(0.045, 0.327)
SN4	(0.052, 0.291)	(0.049, 0.322)	(0.039, 0.148)	(0.087, 0.189)	(0.049, 0.290)	(0.049, 0.325)	(0.046, 0.323)	(0.027, 0.217)	(0.047, 0.329)
SN5	(0.054, 0.293)	(0.051, 0.323)	(0.040, 0.149)	(0.091, 0.190)	(0.051, 0.292)	(0.051, 0.326)	(0.048, 0.324)	(0.023, 0.184)	(0.049, 0.330)
SN6	(0.056, 0.294)	(0.054, 0.324)	(0.042, 0.149)	(0.094, 0.190)	(0.054, 0.293)	(0.054, 0.328)	(0.050, 0.325)	(0.018, 0.150)	(0.051, 0.332)
SN7	(0.058, 0.295)	(0.056, 0.326)	(0.044, 0.150)	(0.098, 0.191)	(0.056, 0.294)	(0.056, 0.329)	(0.052, 0.327)	(0.014, 0.117)	(0.053, 0.333)
SN8	(0.061, 0.296)	(0.058, 0.327)	(0.045, 0.151)	(0.102, 0.192)	(0.058, 0.295)	(0.058, 0.330)	(0.054, 0.328)	(0.010, 0.084)	(0.055, 0.334)
SN9	(0.063, 0.297)	(0.060, 0.0329)	(0.047, 0.151)	(0.106, 0.193)	(0.060, 0.296)	(0.060, 0.332)	(0.056, 0.330)	(0.006, 0.050)	(0.057, 0.336)
SN10	(0.065, 0.299)	(0.062, 0.330)	(0.049, 0.152)	(0.109, 0.194)	(0.062, 0.298)	(0.062, 0.333)	(0.058, 0.331)	(0.002, 0.017)	(0.059, 0.337)
SN11	(0.045, 0.288)	(0.043, 0.318)	(0.034, 0.146)	(0.076, 0.186)	(0.043, 0.287)	(0.043, 0.321)	(0.040, 0.319)	(0.042, 0.335)	(0.038, 0.308)
SN12	(0.047, 0.289)	(0.045, 0.319)	(0.035, 0.147)	(0.079, 0.187)	(0.045, 0.288)	(0.045, 0.322)	(0.042, 0.320)	(0.044, 0.336)	(0.034, 0.275)
SN13	(0.049, 0.290)	(0.047, 0.320)	(0.037, 0.148)	(0.083, 0.188)	(0.047, 0.289)	(0.047, 0.323)	(0.044, 0.321)	(0.046, 0.337)	(0.030, 0.243)
SN14	(0.051, 0.291)	(0.049, 0.322)	(0.039, 0.148)	(0.086, 0.189)	(0.049, 0.290)	(0.049, 0.325)	(0.046, 0.323)	(0.048, 0.339)	(0.026, 0.211)
SN15	(0.053, 0.292)	(0.051, 0.323)	(0.040, 0.149)	(0.090, 0.189)	(0.051, 0.291)	(0.051, 0.326)	(0.047, 0.324)	(0.050, 0.340)	(0.022, 0.178)
SN16	(0.056, 0.294)	(0.053, 0.324)	(0.042, 0.149)	(0.094, 0.190)	(0.053, 0.293)	(0.053, 0.327)	(0.049, 0.325)	(0.052, 0.342)	(0.018, 0.146)
SN17	(0.041, 0.295)	(0.039, 0.326)	(0.030, 0.150)	(0.068, 0.191)	(0.039, 0.294)	(0.039, 0.329)	(0.036, 0.327)	(0.038, 0.343)	(0.014, 0.113)
SN18	(0.060, 0.296)	(0.057, 0.327)	(0.045, 0.151)	(0.101, 0.192)	(0.057, 0.295)	(0.057, 0.330)	(0.053, 0.328)	(0.056, 0.344)	(0.010, 0.081)
SN19	(0.062, 0.297)	(0.059, 0.328)	(0.046, 0.151)	(0.104, 0.193)	(0.059, 0.296)	(0.059, 0.331)	(0.055, 0.329)	(0.058, 0.346)	(0.006, 0.049)
SN20	(0.064, 0.298)	(0.061, 0.330)	(0.048, 0.152)	(0.108, 0.193)	(0.061, 0.297)	(0.061, 0.333)	(0.057, 0.331)	(0.060, 0.347)	(0.002, 0.016)
SN21	(0.045, 0.288)	(0.043, 0.318)	(0.034, 0.146)	(0.076, 0.186)	(0.043, 0.287)	(0.040, 0.304)	(0.040, 0.319)	(0.042, 0.335)	(0.041, 0.325)
SN22	(0.047, 0.289)	(0.045, 0.319)	(0.0035, 0.147)	(0.079, 0.187)	(0.045, 0.288)	(0.036, 0.272)	(0.042, 0.320)	(0.044, 0.336)	(0.043, 0.326)
SN23	(0.049, 0.29)	(0.047, 0.320)	(0.037, 0.148)	(0.083, 0.188)	(0.047, 0.289)	(0.032, 0.240)	(0.044, 0.321)	(0.046, 0.338)	(0.045, 0.328)
SN24	(0.051, 0.291)	(0.049, 0.322)	(0.038, 0.148)	(0.086, 0.189)	(0.049, 0.290)	(0.027, 0.208)	(0.045, 0.323)	(0.048, 0.339)	(0.047, 0.329)
SN25	(0.053, 0.293)	(0.051, 0.323)	(0.040, 0.149)	(0.090, 0.190)	(0.051, 0.292)	(0.023, 0.176)	(0.047, 0.324)	(0.050, 0.341)	(0.048, 0.330)
SN26	(0.055, 0.294)	(0.053, 0.325)	(0.042, 0.150)	(0.093, 0.190)	(0.053, 0.293)	(0.019, 0.144)	(0.049, 0.326)	(0.052, 0.342)	(0.050, 0.332)
SN27	(0.057, 0.295)	(0.055, 0.326)	(0.043, 0.150)	(0.097, 0.191)	(0.055, 0.294)	(0.015, 0.112)	(0.051, 0.327)	(0.054, 0.344)	(0.052, 0.333)
SN28	(0.060, 0.296)	(0.057, 0.327)	(0.045, 0.151)	(0.100, 0.192)	(0.057, 0.295)	(0.011, 0.080)	(0.053, 0.328)	(0.055, 0.345)	(0.054, 0.335)
SN29	(0.062, 0.298)	(0.059, 0.329)	(0.046, 0.151)	(0.104, 0.193)	(0.059, 0.297)	(0.006, 0.048)	(0.055, 0.330)	(0.057, 0.346)	(0.056, 0.336)
SN30	(0.064, 0.299)	(0.061, 0.330)	(0.048, 0.152)	(0.107, 0.194)	(0.061, 0.298)	(0.002, 0.016)	(0.056, 0.331)	(0.059, 0.348)	(0.058, 0.337)

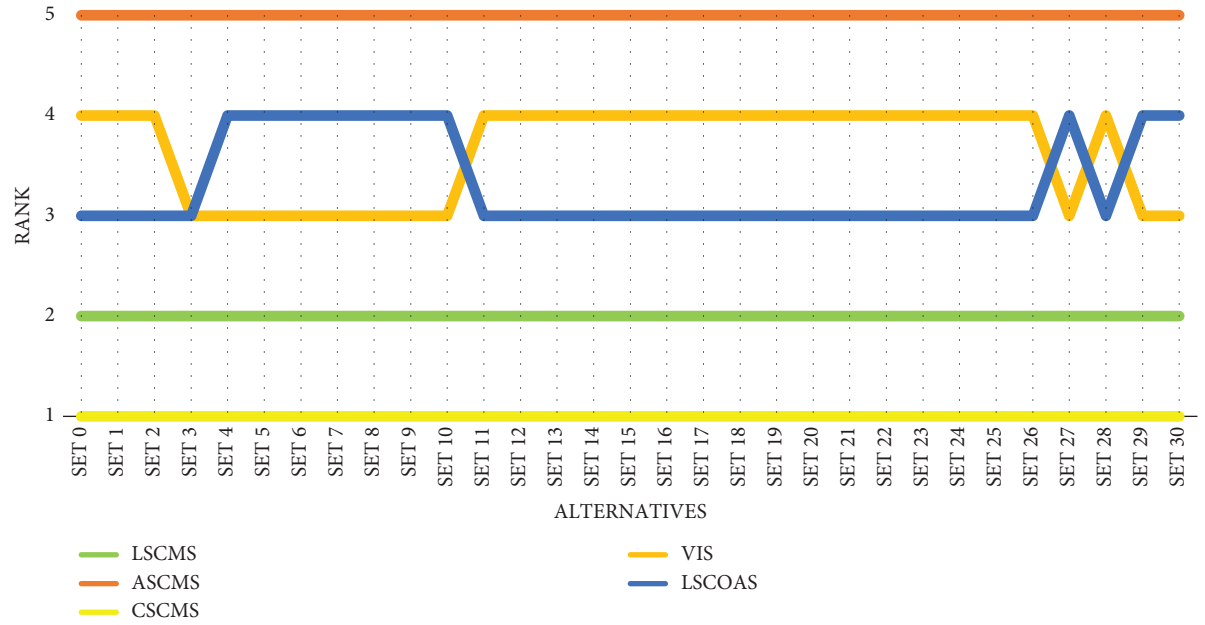

Figure 2: 30 new scenarios in a sensitivity analysis.

Table 10: The results of rough methods.

Strategies	Methods			
	Rough MARCOS	Rough WASPAS	Rough ARAS	Rough SAW
LSCMS	2	2	1	1
ASCMS	5	5	5	5
CSCMS	1	1	2	2
VIS	4	4	4	4
LSCOAS	3	3	3	3

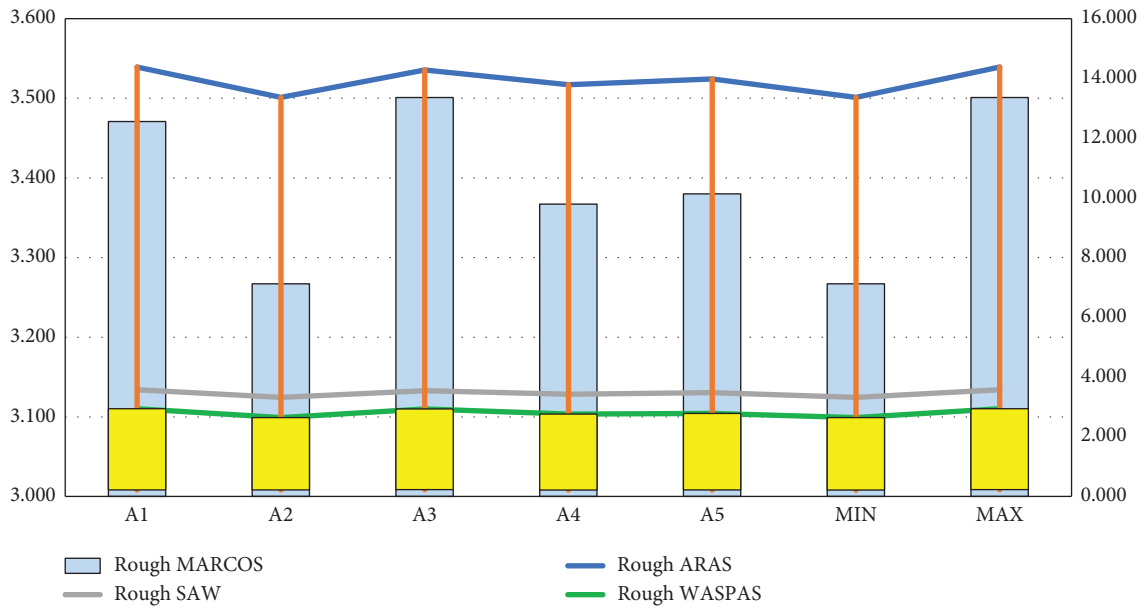

Figure 3: Alternative values in comparative analysis.

6. Conclusion and Suggestions

Companies develop and underline new strategies as alternatives for preventing SCM-related breakdowns during the COVID-19 pandemic because determining alternative supply scenarios and evaluating them with respect to operations has gained importance for coping with breakdowns in SCM during the pandemic process. With this perspective, it is aimed to analyse the factors leading to SCM breakdowns for manufacturing firms. In this study, a rough set-based SWARA-MARCOS methodology was used to prioritize factors leading to SCM breakdowns and to select the most successful SCM strategy in the COVID-19 process for food firms in the East Black Sea Region, respectively. Rough sets were preferred for aggregating the data of group decision making and thus data loss was prevented in this way. This was the advantageous side of rough sets compared with other methods. According to the results of the criteria weights calculated by using the rough SWARA method, the transportation capacity (TC) criterion was obtained as the most important leading to SCM breakdowns, and the local laws-related incentives (LLRI) criterion was found as the least important one. Other criteria ranking was LRMP > ASCF > BD > LRRPWTFM > ESW > SB > CFSMS, respectively.

It was determined that the most important weight was "transportation capacity (TC)." The result is consistent with the studies of Tao [57], Korucuk [58], and Gkiotsalitis and Cats [59] because with COVID-19, processes such as customs clearance level, delivery time, processing activities, especially the carrying capacity, have not been realized at the desired level. Depending on the carrying capacity, disruptions have occurred in production processes with the pandemic. In fact, the supply shock from the COVID-19 process has been impressive.

Another important factor is the "level of raw material procurement (LRMP)." The result is consistent with the studies of Askariazad and Wanous [60] and Xu et al. [61]. The supply level and level of raw materials are important in terms of realizing production levels at the desired level in the supply chain management, including the COVID-19 process.

Another important result reached in terms of supply chain management breaks in the COVID-19 process within the scope of the study is "alternative supplier capacity and flexibility (ASCF)." The obtained result supports the study of Kim and Zhao [62]. In this sense, determining the right suppliers to work with is of great importance in creating an effective supply chain because any negativity in the supply chain flow can make a difference in competition and can cause businesses to face some risks in the supply chain management [63].

Following that the most successful SCM strategy was determined as the collaborative supply chain management strategy (CSCMS) with the rough MARCOS method.

On the other hand, the best alternative in the results of the study was "collaborative supply chain management strategy (CSCMS)." This result supports the study of Maheshwari et al. [64] because this strategy is based on mutual cooperation and solidarity at different levels during the COVID-19 period, within the framework of bilateral principles or multilateral agreements, policies, procedures, plans, new activities, joint decision-making and participation, joint procurement practices, support for joint production, product/goods exchange, distribution management, supply chain management, joint transportation, new service arrangements and sharing, development of new procedures, and determination of appropriate costs, so it allows partnerships to be established between logistics sectors and businesses.

Firms having lean and agility capabilities mostly prefer CSCMS recently. This flexible strategy providing service quality and cost advantage has gained importance to carry out SCM functions for manufacturing firms during the pandemic process. The competitive power of firms is being supported by this strategy as similar to the literature.

In addition to its theoretical contributions, the study has very important implications for decision makers and practitioners in the food sector and those who are interested in the subject. These provide the opportunity to evaluate the factors of supply chain management breaks. It also pioneers a basic model for selecting the optimal alternative for supply chain management breaks and the supply chain strategy selection process. It provides a flexible and structured decision-making environment, that is, a decision-making environment and opportunity that considers different and separate views. Another valuable contribution of the study is that it helps decision makers make a new route in planning that considers the market conditions in the COVID-19 process in eliminating the disruptions in the supply chain by using the proposed model. In addition, the related study presents a new set of criteria suitable for real-worlddecision-making problems encountered in the food industry, addressing a critical area such as ensuring the efficiency of supply chain management in the COVID-19 process.

Finally, the evaluation of the supply chain management breakdown and the selection of the most ideal supply chain management strategy processes in the COVID-19 period, with the methods in the study, provided the opportunity to convey the practical approaches of the decision makers working in the food sector in a scientific perspective, and contributed to the interaction of theoretical and practical applications.

As opposed to that, the least successful SCM strategy was found as the agile supply chain management strategy (ASCMS). Other strategies were ranked as LSCMS > LSCOAS > VIS, respectively. A comparison analysis was executed with other methods (rough ARAS, WASPAS, and SAW) to underline the similarities and differences in terms of SCM strategies. The Spearman correlation coefficient was calculated between rough MARCOS and other methods and was found to be 0.9. As generally said, firms need to focus on alternative SCM strategies to evaluate their role in the operation for preventing breakdowns in supply chains because of the virus spreading in various regions. For future studies, criteria and strategies can be expanded and applied to different industries with hybrid methods. Also, comparison studies can

be executed with respect to industry, region, country, and methodology.

In this study, some managerial implications for the food manufacturing industry were obtained. The aim of this study is to prioritize factors leading to SCM breakdowns and selecting the most successful SCM strategy in the COVID-19 process. According to the results of the rough SWARA method used in determining the weights of the factors in this study, the three most important factors are the following: transportation capacity, level of raw material procurement, and alternative supplier capacity and flexibility. According to these results, the managers of the companies should pay particular attention to the transportation capacity factor as much as possible. In addition, the managers of the companies need to keep the transportation capacity at the optimum level as possible. Besides, the managers of the companies should be careful about the level of raw material procurement and control their raw material stocks as much as possible. In addition, the managers of the companies are required to periodically check the capacity and flexibility of the company's alternative suppliers. This will prevent the companies from remaining without raw materials or semifinished products or products in both pandemic conditions and disaster situations. According to the results of the rough MARCOS method used in ranking the strategies, the best strategies are as follows: collaborative supply chain management strategy and lean supply chain management strategy. If the managers of the companies adopt the supply chain management in a collaborative way, they can cope with the pandemic conditions more easily. In addition, by using the lean supply chain management strategy as a support for the collaborative supply chain management strategy, the company's survival in pandemic and disaster conditions can be ensured. Although the effects of the COVID-19 pandemic have decreased, the results presented in this study will help the managers of the companies to choose the strategy they need to manage their companies against future possible pandemics.

Data Availability

The data used to support the findings of this study are included within this article. However, the reader may contact the corresponding author for more details on the data.

Conflicts of Interest

The authors declare that they have no conflicts of interest.

References

[1] K. Govindan, H. Mina, and B. Alavi, "A decision support system for demand management in healthcare supply chains considering the epidemic outbreaks: a case study of coronavirus disease 2019 (COVID-19)," *Transportation Research Part E: Logistics and Transportation Review*, vol. 138, pp. 101967–102014, 2020.

[2] İ. Arslan and İ. Bayar, "Covid-19 outbreak, economic effects and future of global economy," *Gaziantep University Journal of Social Sciences*, vol. 19, pp. 87–104, 2020.

[3] Fortune, "94% of the Fortune 1000 are seeing coronavirus supply chain disruptions," 2020, https://fortune.com/2020/02/21/fortune-1000-coronavirus-china%20-supply-chain-impact/.

[4] D. Cucinotta and M. Vanelli, "WHO declares COVID-19 a pandemic," *Acta BioMedica*, vol. 91, no. 1, pp. 157–160, 2020.

[5] Y. He and N. Liu, "Methodology of emergency medical logistics for public health emergencies," *Transportation Research Part E: Logistics and Transportation Review*, vol. 79, pp. 178–200, 2015.

[6] A. F. Adedotun, "Hybrid neural network prediction for time series analysis of COVID-19 cases in Nigeria," *International Journal of Management and Decision Making*, vol. 1, no. 1, pp. 46–55, 2022.

[7] T. K. Biswas and M. C. Das, "Selection of the barriers of supply chain management in Indian manufacturing sectors due to covid-19 impacts," *Operational Research in Engineering Sciences: Theory and Applications*, vol. 3, no. 3, pp. 1–12, 2020.

[8] R. Siche, "What is the impact of COVID-19 disease on agriculture?" *Scientia Agropecuaria*, vol. 11, no. 1, pp. 3–6, 2020.

[9] A. Đukić, M. Štaka, and D. Drašković, "The impact of the COVID-19 pandemic on the macroeconomic aggregates of the European union," *Economıcs-Innovative and Economic Research*, vol. 9, no. 2, pp. 91–108, 2021.

[10] R. Barichello, "The COVID-19 pandemic: anticipating its effects on Canada's agricultural trade," *Canadian Journal of Agricultural Economics/Revue Canadienne D'agroeconomie*, vol. 68, no. 2, pp. 219–224, 2020.

[11] T. P. Stank, J. Paul Dittmann, and C. W. Autry, "The new supply chain agenda: a synopsis and directions for future research," *International Journal of Physical Distribution & Logistics Management*, vol. 41, no. 10, pp. 940–955, 2011.

[12] D. Waters, *Logistics: An Introduction to Supply Chain Management*, Palgrave Macmillan, New York, NY, USA, 2003.

[13] D. Bowersox, D. Closs, and M. B. Cooper, *Supply Chain Logistics Management*, McGraw-Hill Higher Education, McGraw-Hill, IA, USA, 3 edition, 2009.

[14] A. Görener, "Supply chain strategy selection: an application in manufacturing industry by fuzzy VIKOR method," *International Journal of Alanya Faculty of Business*, vol. 5, no. 3, pp. 47–62, 2013.

[15] K. T. Atanassov, "New topological operator over intuitionistic fuzzy sets," *Journal of Computational and Cognitive Engineering*, vol. 1, no. 3, pp. 94–102, 2022.

[16] M. Barma and U. M. Modibbo, "Multiobjective mathematical optimization model for municipal solid waste management with economic analysis of reuse/recycling recovered waste materials," *Journal of Computational and Cognitive Engineering*, vol. 1, no. 3, pp. 122–137, 2021.

[17] J. Chou, N. F. Kuo, and S. L. Peng, "Potential impacts of the SARS outbreak on Taiwan's economy," *Asian Economic Papers*, vol. 3, no. 1, pp. 84–99, 2004.

[18] R. W. Salem and M. Haouari, "A simulation-optimisation approach for supply chain network design under supply and demand uncertainties," *International Journal of Production Research*, vol. 55, no. 7, pp. 1845–1861, 2017.

[19] O. M. Araz, T. M. Choi, D. L. Olson, and F. S. Salman, "Data analytics for operational risk management," *Decision Sciences*, vol. 51, no. 6, pp. 1316–1319, 2020.

[20] M. M. Queiroz, D. Ivanov, A. Dolgui, and S. Fosso Wamba, "Impacts of epidemic outbreaks on supply chains: mapping a research agenda amid the COVID-19 pandemic through

a structured literature review," *Annals of Operations Research*, vol. 319, pp. 1159–1196, 2020.

[21] D. Ivanov, "Predicting the impacts of epidemic outbreaks on global supply chains: a simulation-based analysis on the coronavirus outbreak (COVID-19/SARS-CoV-2) case," *Transportation Research Part E: Logistics and Transportation Review*, vol. 136, Article ID 101922, 2020.

[22] A. Aydın and A. Güner, "Impact of covid-19 epidemic on agricultural sector and food security: an evaluation on Turkey," *Artuklu Kaime Internation Journal of Economics and Administrative Researches*, vol. 3, no. 2, pp. 155–171, 2020.

[23] D. Ivanov and A. Dolgui, "Viability of intertwined supply networks: extending the supply chain resilience angles towards survivability. A position paper motivated by COVID-19 outbreak," *International Journal of Production Research*, vol. 58, no. 10, pp. 2904–2915, 2020.

[24] S. Singh, R. Kumar, R. Panchal, and M. K. Tiwari, "Impact of COVID-19 on logistics systems and disruptions in food supply chain," *International Journal of Production Research*, vol. 59, no. 7, pp. 1993–2008, 2021.

[25] Y. Wang, J. Wang, and X. Wang, "COVID-19, supply chain disruption and China's hog market: a dynamic analysis," *China Agricultural Economic Review*, vol. 12, no. 3, pp. 427–443, 2020.

[26] S. Bhattacharya, *Dealing with Global Supply Chain Breaks Business Times (Singapore)*, Research Collection Lee Kong Chian School Of Business, Singapore, 2020, https://ink.library.smu.edu.sg/lkcsb_research/6562.

[27] S. K. Kaya, "Evaluation of the effect of COVID-19 on countries' sustainable development level: a comparative MCDM framework," *Operational Research in Engineering Sciences: Theory and Applications*, vol. 3, no. 3, pp. 101–122, 2020.

[28] M. M. H. Mukit, N. J. Nabila, A. I. Abdel-Razzaq, and K. F. Shaznin, "The economic influence on consumers buying behavior in islamic countries: evidence from the COVID-19 economic crisis," *Economics, Innovative and Economic Research*, vol. 9, no. 1, pp. 179–203, 2021.

[29] A. Valipour, N. Yahaya, N. Md Noor, J. Antuchevičienė, and J. Tamošaitienė, "Hybrid SWARA-COPRAS method for risk assessment in deep foundation excavation project: an Iranian case study," *Journal of Civil Engineering and Management*, vol. 23, no. 4, pp. 524–532, 2017.

[30] S. Sremac, Ž. Stević, D. Pamučar, M. Arsić, and B. Matić, "Evaluation of a third-party logistics (3PL) provider using a rough SWARA–WASPAS model based on a new rough dombi aggregator," *Symmetry*, vol. 10, pp. 1–25, 2018.

[31] S. Veskovic, Ž. Stević, G. Stojić, M. Vasiljević, and S. Milinković, "Evaluation of the railway management model by using a new integrated model DELPHI-SWARA-MABAC," *Decision Making: Applications in Management and Engineering*, vol. 1, no. 2, pp. 34–50, 2018.

[32] M. Vockic, G. Stojic, and B. Stevic, "Integrated rough swara-aras model for selection of electric forklift," in *Proceedings of the 2nd International Conference on Management, Engineering and Environment (ICMNEE 2018)*, pp. 216–227, Obrenovac, Serbia, October 2018.

[33] E. K. Zavadskas, Ž. Stević, I. Tanackov, and O. Prentkovskis, "A novel multicriteria approach–rough step-wise weight assessment ratio analysis method (R-SWARA) and its application in logistics," *Studies in Informatics and Control*, vol. 27, no. 1, pp. 97–106, 2018.

[34] E. K. Aydoğan and M. Özmen, "Travel and tourism competitiveness of economies around the world using rough SWARA and TODIM method," in *Strategic Innovative Marketing And Tourism. Springer Proceedings in Business and Economics*, A. Kavoura, E. Kefallonitis, and P. Theodoridis, Eds., pp. 765–774, Springer, Berlin, Germany, 2020.

[35] H. Prajapati, R. Kant, and R. Shankar, "Prioritizing the solutions of reverse logistics implementation to mitigate its barriers: a hybrid modified SWARA and WASPAS approach," *Journal of Cleaner Production*, vol. 240, pp. 118219–118315, 2019.

[36] I. Badi and D. Pamucar, "Supplier selection for steelmaking company by using combined Grey-MARCOS methods," *Decision Making: Applications in Management and Engineering*, vol. 3, no. 2, pp. 37–48, 2020.

[37] R. Chattopadhyay, S. Chakraborty, and S. Chakraborty, "An integrated D-MARCOS method for supplier selection in an iron and steel industry," *Decision Making: Applications in Management and Engineering*, vol. 3, no. 2, pp. 49–69, 2020.

[38] M. Stankovic, Ž. Stević, D. K. Das, M. Subotić, and D. Pamučar, "A new fuzzy MARCOS method for road traffic risk analysis," *Mathematics*, vol. 8, no. 3, pp. 457–518, 2020.

[39] Z. Stevic, D. K. Das, R. Tesic, M. Vidas, and D. Vojinovic, "Objective criticism and negative conclusions on using the fuzzy SWARA method in multi-criteria decision making," *Mathematics*, vol. 10, no. 4, p. 635, 2022.

[40] A. Ulutaş, D. Karabasevic, G. Popovic, D. Stanujkic, P. T. Nguyen, and Ç. Karaköy, "Development of a novel integrated CCSD-ITARA-MARCOSdecision-making approach for stackers selection in a logistics system," *Mathematics*, vol. 8, no. 10, pp. 1672–1715, 2020.

[41] S. Miskic, Z. Stevic, and I. Tanackov, "A novel integrated SWARA -MARCOS model for inventory classification," *International Journal of Industrial Engineering & Production Research*, vol. 32, no. 4, pp. 1–17, 2021.

[42] A. Özdağoğlu, M. K. Keleş, and B. Işıldak, "Cabin crew selection in civil aviation with fuzzy SWARA and fuzzy MARCOS methods," *Gümüşhane University Journal of Social Sciences Institute*, vol. 12, no. 2, pp. 284–302, 2021.

[43] M. A. Taş, E. Çakır, and Z. Ulukan, "Spherical fuzzy SWARA-MARCOS approach for green supplier selection," *3C Tecnología_Glosas de innovación aplicadas a la pyme*, vol. 10, no. 2021, pp. 115–133, 2021.

[44] B. Matic, M. Marinkovic, S. Jovanović, S. Sremac, and Ž. Stević, "Intelligent novel IMF D-SWARA—rough MARCOS algorithm for selection construction machinery for sustainable construction of road infrastructure," *Buildings*, vol. 12, no. 7, p. 1059, 2022.

[45] A. Mešić, S. Miškić, Ž. Stević, and Z. Mastilo, "Hybrid MCDM solutions for evaluation of the logistics performance index of the western balkan countries," *Economics-Innovative and Research Journal*, vol. 10, no. 1, pp. 13–34, 2022.

[46] Ž. Stević, D. Pamučar, A. Puška, and P. Chatterjee, "Sustainable supplier selection in healthcare industries using a new MCDM method: measurement of alternatives and ranking according to COmpromise solution (MARCOS)," *Computers & Industrial Engineering*, vol. 140, Article ID 106231, 2020.

[47] A. Tus and E. A. Adalı, "Green supplier selection based on the combination of fuzzy SWARA (SWARA-F) and fuzzy MARCOS (MARCOS-F) methods," *Gazi University Journal of Science*, vol. 35, no. 4, pp. 1535–1554, 2022.

[48] A. Puška and I. Stojanović, "Fuzzy multi-criteria analyses on green supplier selection in an agri-food company," *Journal of Intelligent Management Decision*, vol. 1, no. 1, pp. 2–16, 2022.

[49] D. Pamučar, L. Gigović, Z. Bajić, and M. Janošević, "Location selection for wind farms using GIS multi-criteria hybrid model: an approach based on fuzzy and rough numbers," *Sustainability*, vol. 9, no. 8, p. 1315, 2017.

[50] D. Pamučar, Ž. Stević, and E. K. Zavadskas, "Integration of interval rough AHP and interval rough MABAC methods for evaluating university web pages," *Applied Soft Computing*, vol. 67, pp. 141–163, 2018.

[51] V. Keršuliene, E. K. Zavadskas, and Z. Turskis, "Selection of rational dispute resolution method by applying new step-wise weight assessment ratio analysis (SWARA)," *Journal of Business Economics and Management*, vol. 11, no. 2, pp. 243–258, 2010.

[52] N. Vojinović, S. Sremac, and D. Zlatanović, "A Novel Integrated Fuzzy-Rough MCDM Model for Evaluation of Companies for Transport of Dangerous Goods," *Complexity*, vol. 2021, 2021.

[53] D. Radović, Ž. Stević, D. Pamučar et al., "Measuring performance in transportation companies in developing countries: a novel rough ARAS model," *Symmetry*, vol. 10, no. 10, p. 434, 2018.

[54] G. Stojić, Ž. Stević, J. Antuchevičienė, D. Pamučar, and M. Vasiljević, "A novel rough WASPAS approach for supplier selection in a company manufacturing PVC carpentry products," *Information*, vol. 9, no. 5, p. 121, 2018.

[55] E. Durmić, Ž. Stević, P. Chatterjee, M. Vasiljević, and M. Tomašević, "Sustainable supplier selection using combined FUCOM–Rough SAW model," *Reports in Mechanical Engineering*, vol. 1, no. 1, pp. 34–43, 2020.

[56] M. Subotić, B. Stević, B. Ristić, and S. Simić, "The selection of a location for potential roundabout construction–a case study of Doboj," *Operational Research in Engineering Sciences: Theory and Applications*, vol. 3, no. 2, pp. 41–56, 2020.

[57] X. Tao, "Performance evaluation of supply chain based on fuzzy matter-element theory," *International Conference on Information Management, Innovation Management and Industrial Engineering*, pp. 549–552, 2009.

[58] S. Korucuk, "ÇKKV yöntemleri ile imalat işletmelerinde TZY Performans faktörlerinin önem derecelerinin belirlenmesi ve en ideal rekabet stratejisi seçimi: Ordu ili örneği," *Dokuz Eylül Üniversitesi İktisadi İdari Bilimler Fakültesi Dergisi*, vol. 33, no. 2, pp. 569–593, 2019.

[59] K. Gkiotsalitis and O. Cats, "Public transport planning adaption under the COVID-19 pandemic crisis: literature review of research needs and directions," *Transport Reviews*, vol. 41, no. 3, pp. 374–392, 2021.

[60] M. Askariazad and M. Wanous, "A proposed value model for prioritising supply chain performance measures," *International Journal of Business Performance and Supply Chain Modelling*, vol. 1, no. 2/3, pp. 115–128, 2009.

[61] F. Xu, Y. M. Zhang, Y. Su, J. Li, and J. M. Zhu, "Intelligent application of raw material supply chain planning system based on genetic algorithm," *Wireless Communications and Mobile Computing*, vol. 2022, Article ID 5054529, 13 pages, 2022.

[62] K. Kim and L. Zhao, "Filtering facepiece respirator supply chain management framework in a disaster such as COVID-19," *Societies*, vol. 11, no. 4, p. 136, 2021.

[63] S. Korucuk and S. Memiş, "Measurement of risk factors in the supply chain management with AHP: erzurum provincial example," *Journal of Bitlis Eren University Institute of Social Sciences*, vol. 7, no. 2, pp. 1036–1051, 2018.

[64] B. Maheshwari, V. Kumar, and U. Kumar, "Optimizing success in supply chain partnerships," *Journal of Enterprise Information Management*, vol. 19, no. 3, pp. 277–291, 2006.

[65] E. Demir and Ç. Karamaşa, "Analysis of experts' psychological behaviors under risk with pythagorean fuzzy sets and todim method in terms of balanced scorecard: an example of factoring and financial leasing companies," *Journal of Multiple-Valued Logic and Soft Computing*, vol. 35, pp. 125–145, 2020.

Hindawi
Complexity
Volume 2022, Article ID 2274684, 18 pages
https://doi.org/10.1155/2022/2274684

Research Article

Investigation of Blockchain Technology by Using the Innovative Concepts of Complex Pythagorean Fuzzy Soft Information

Naeem Jan,[1] Jeonghwan Gwak ,[1,2,3,4] Younghoon Jeon,[1] and Bushra Akram[5]

[1]*Department of Biomedical Engineering, Korea National University of Transportation, Chungju 27469, Republic of Korea*
[2]*Department of Software, Korea National University of Transportation, Chungju 27469, Republic of Korea*
[3]*Department of AI Robotics Engineering, Korea National University of Transportation, Chungju 27469, Republic of Korea*
[4]*Department of IT & Energy Convergence (BK21 Four), Korea National University of Transportation, Chungju 27469, Republic of Korea*
[5]*Department of Mathematics, Institute of Numerical Sciences, Gomal University, KPK, Dera Ismail Khan 29050, Pakistan*

Correspondence should be addressed to Jeonghwan Gwak; jgwak@ut.ac.kr

Received 5 August 2022; Revised 7 September 2022; Accepted 12 September 2022; Published 17 November 2022

Academic Editor: Zeljko Stevic

A blockchain is a valuable and proficient type of digital ledger technology that involves of expanding list of records, called blocks, that are strongly connected simultaneously using cryptography. Further, complex Pythagorean fuzzy sets (CPFSs) are the generalized form of the intuitionistic fuzzy sets (IFSs), Pythagorean fuzzy sets (PyFSs), and complex intuitionistic fuzzy sets (CIFSs), used for evaluating the awkward and unreliable information in genuine life problems. In this analysis, we aim to diagnose the innovative idea of complex Pythagorean fuzzy soft relations (CPyFSRs) by using the Cartesian product (CP) of two complex Pythagorean fuzzy soft sets (CPyFSSs), which are computed with the help of two different ideas, called complex Pythagorean fuzzy relation and soft sets. Additionally, using the presented approaches, we examined different kinds of relations and also justified them with the help of some suitable examples. The CPyFSRs has a comprehensive structure because it is discussing both degrees of membership and non-membership with multidimensional variable. Further, includes the CPyFSR-based modeling techniques that use the score function to choose the best blockchain technology (BCT) to enhance the worth of the evaluated information. Using a good BCT, the transaction may be simply transferred record between users. Finally, the benefit of this proposed framework is demonstrated by comparing it to other frameworks to show the supremacy and feasibility of the diagnosed approaches.

1. Introduction

The uncertainty involved in any problem-solving situation is a result of some information inadequacy. Uncertainty is a natural part of our life. Many everyday decisions are highly unpredictable. It frequently happens when there is not enough information available regarding the results, the future environment is unpredictable, and everything is unstable. A novel mathematical innovation called fuzzy set (FS) was presented by Zadeh [1] in 1965 for detecting and resolving ambiguity. Each element in this collection is given a membership degree between 0 and 1, which represents the element's quality or effectiveness. The FS is more important in human decision-making. Zimmermann [2] proposed the FS theory and its applications. Maiers and Sherif [3] use of FSs theory apply to a wide range of issues and fuzzy control techniques. Roberts [4] explained ordination based on FS theory. Kahraman [5] used FS in industrial engineering. Mendel [6] proposed the concept of fuzzy relationships (FRs). FRs used the membership degree of every element to indicate the quality of the relationship. If membership is closer to 1 then it indicates a good relationship and if the degree closer to 0 shows poor relationships. The FRs are an extended structure than classical relations. Nemitz [7] goes into much detail about FRs and fuzzy functions. Yang and Shih [8] designated the cluster analysis based on FRs. After

FS, Ramot et al. [9] nominated the new set called complex fuzzy set (CFS) that explains membership ranging between unit circles. It defines membership using two terms: amplitude which describes effectiveness, and phase which describes the duration of effectiveness. It lowers the likelihood of errors and ambiguity. Hu et al. [10] developed the orthogonality relation of CFSs. Li and Tu [11] examined CFSs and their applications in multi-class prediction. Zhang et al. [12] explored the various operating features and δ-equalities of CFSs. Moreover, he also defines complex fuzzy relations (CFRs). Khan et al. [13] established the CFRs in the future commission market.

After all of these advancements in human decision-making, people can become confused while deciding on the best alternative. There are numerous doubts and ambiguities in this situation. Molodtsov [14] examined the idea of the soft set (SS) in 1999, which helps people make better decisions in difficult situations. SS chooses the items based on some parameters. Ali et al. [15] developed some novel SSs operations. Kostek [16] used an SS approach to analyze sound quality. Mushrif et al. [17] suggested a new SS theory-based technique for evaluating natural textures. Maji et al. [18] employed an SS theory to resolve a decision-making difficulty. Babitha and Sunil [19] introduced the soft relations (SRs) between the CP of SSs. Park et al. [20] studied some features of equivalence SRs. Maji et al. [21] created the fuzzy soft set (FSS) by merging the FS and the SS. It helps humans make better decisions by reducing uncertainty in daily life decisions. Kong et al. [22] employed FSS in decision-making issues. Gogoi et al. [23] looked into how FSS theory may be used to solve various difficulties. Borah et al. [24] established the innovative idea of fuzzy soft relations (FSRs) by examining the CP of FSSs. Mockor and Hurtik [25] used image processing to approximate FSSs using FSRs. Thirunavukarasu et al. [26] looked into the novel idea of complex fuzzy soft sets (CFSSs) in which the degree of membership is expressed in complex numbers and sorted out all the problems by using multi-variables. TAmir et al. [27] analyzed an outline of CFS and complex fuzzy logic theory and applications.

Atanassov [28] established the idea of an intuitionistic fuzzy set (IFSs), which is broader than the FSs. An IFSs examined both degrees of membership and non-membership, whereas FSs only discussed the membership degree. Both of these values between the unit interval [0, 1] and sum also lie within this interval. Szmidt and Kacprzyk [29] resolved the distances among IFSs; Gerstenkorn and Manko [30] determined the IFS correlation. Alkouri [31] defined the notion of the complex intuitionistic fuzzy set (CIFS). The CIFS uses a complex number to define both membership and non-membership degrees. It consists of both amplitude term and phase term. Ngan et al. [32] used quaternion numbers to represent CIFS and applied them in decision-making. Xu et al. [33] nominate the intuitionistic fuzzy soft set (IFSS), which combines the SS and IFS. The IFSS is the expansion form of the FSS. Agarwal et al. [34] invented the modified IFSS with applications in decision-making. Dinda and Samanta [35] used the CP of IFSS to recommend the intuitionistic fuzzy soft relation (IFSR). Kumar and Bajaj [36] evaluated the concept of complex intuitionistic fuzzy soft sets (CIFSSs), which are parametric. The CIFSSs are used to apply parametrization tools to explain multicriteria decision-making issues. Yager [37] proposed Pythagorean fuzzy sets (PyFS), which increased the space by imposing new constraints. The constraint of PyFS is that the total of the squares of membership and non-membership degrees must be in the range [0, 1]. Garg [38] applied PyFS in the form of new logarithmic operational laws. Ullah et al. [39] suggested the thought of a complex Pythagorean fuzzy set (CPyFS) with application in pattern recognition. The CPyFS provides membership and non-membership values as a complex number. Dick et al. [40] described the CPyFS operations. Nasir et al. [41] used economic relationships to define the concept of a complex Pythagorean fuzzy relation (CPyFR). Peng et al. [42] presented the Pythagorean fuzzy soft set (PyFSS), by merging the SS with the PyFS and interpreted this notion through various possible applications. Akram et al. [43] introduced the complex Pythagorean fuzzy soft set (CPyFSS) with the application. Gillpatrick et al. [44] evaluated the blockchain contribute to developing country economies.

To expose the significance and proficiency of the evaluated theories by comparing them with other prevailing theories, for this, we demonstrated it with the help of some genuine life examples. Assume an enterprise N decided to purchase some new cars from a carmaker, for this the owner of the enterprise N provided two types of information regarding each car: (a) model of cars; (b) making the date of cars. Very carmaker produced the same model of car with some improvements or upgrading based on some parameters (like improving the quality of the fuel consumption, tire quality, comfort zone, etc.) in every new year. Where the model of the car expressed the amplitude term, and the production date of the car shows the phase term which changes time by time continuously. Traditionally PFS or Pythagorean fuzzy soft sets are not able to deal with it. For this, the theory of CPyFSR is much better than the prevailing theories. Because the theory of CPyFSR deals with two-dimension information at a time and the because of this reason, the IFS, PyFS, and CIFS are special cases of the proposed work. The concept of CPyFSS is a convenient tool in CIFSS theory for dealing with ambiguity and uncertainty. However, the concept of relations has not yet been defined for the CPyFSS. Based on our observation, the main analyses of this analysis are listed below:

(1) To propose the concept of CPFSRs by studying the CP of two CPyFSS.

(2) To describe different types of CPyFSR as well as the CPyFS-reflexive relation, CPyFS-symmetric relation, CPyFS-transitive relation, CPyFS-equivalence relation, CPyFS-partial order relation, CPyFS-linear order relation, CPyFS-strict order relation, CPyFS-converse relation, CPyFS-composite relation and many more. Each CPyFSR definition has been illustrated with examples.

(3) To illustrate numerous results for the type of CPyFSRs.

(4) To derive the innovative idea of CPyFSR is superior to pre-defined structures of SS, FSS, CFSS, IFSS, CIFSS, and PyFSS. The CPyFSS discussed both membership and non-membership degrees with increased space. They can also solve problems with multi-variables due to complex-valued mappings. Additionally, offered an application for selecting the best BCT by using CPyFSRs. The score function has been utilized to choose the best BCT. Experts have recommended a variety of parameters and selected the finest BCT based on those criteria.

(5) To compare the presented work with some prevailing work is to show the reliability of the evaluated work.

The rest of this article is arranged as follows: Section 2 contains all pre-existing structures of fuzzy algebra. Section 3 introduced the newly defined notion of CPyFSRs and CP of two CPyFSSs for example. Section 4 proposed an application of BCT by using the study of CPyFSRs. Section 5 compares the proposed structure with pre-existing structure. Section 6 concludes the results.

2. Preliminaries

The theory of CFS, SS, SR, FSS, CFSS, CIFS, IFSS, CIFSS, CPyFS, and CPyFSS are the part of this section which are very useful for evaluating the proposed ideas in next section.

Definitioni 1 (see [9]). Let $\dot{\Upsilon}$ be a universal set, then a CFS $\mathfrak{T}$ on $\dot{\Upsilon}$ can be defined as:

$$\mathfrak{T} = \left\{\left(\dot{s}, m_{\mathfrak{T}_c}(\dot{s})\right): \dot{s} \in \dot{\Upsilon}\right\}, \tag{1}$$

Where, $m_{\mathfrak{T}}(\dot{s}) = r_{m_{\mathfrak{T}}}(\dot{s})e^{(q_{m_{\mathfrak{T}}}(\dot{s}))2\pi i}$ represented the membership grade with $r_{m_{\mathfrak{T}}}, q_{m_{\mathfrak{T}}}: \dot{\Upsilon} \longrightarrow [0,1]$. Further, the mathematical terms $r_{m_{\mathfrak{T}}}$ and $q_{m_{\mathfrak{T}}}$ are represented the amplitude and phase terms of the membership degree individually.

Definition 2 (see [14].) Let $\dot{\Upsilon}$ be a universal set and $\dot{\xi}$ be the set of parameters, $\mathfrak{p}(\dot{\Upsilon})$ denote the power set of $\dot{\Upsilon}$. Then, a pair $(\mathfrak{T}, \dot{\kappa})$ is called SS on $\dot{\Upsilon}$ with mapping $\mathfrak{T}: \dot{\kappa} \longrightarrow \mathfrak{p}(\dot{\Upsilon})$ is defined as:

$$\mathfrak{T} = \left\{\acute{o}, \mathfrak{T}(\acute{o}), \acute{o} \in \dot{\kappa}, \mathfrak{T}(\acute{o}) \in \mathfrak{p}(\dot{\Upsilon})\right\}. \tag{2}$$

Example 1. Suppose $\dot{\Upsilon}$ is a universal set consisting of the set of five watches $= \{\dot{\alpha}_1, \dot{\alpha}_2, \dot{\alpha}_3, \dot{\alpha}_4, \dot{\alpha}_5\}\dot{\Upsilon}$ under consideration, and $\dot{\xi}$ is the set of parameters $\dot{\xi} = \left\{\acute{o}_1, \acute{o}_2, \acute{o}_3, \acute{o}_4\right\}$ for universal set $\dot{\Upsilon}$, where each parameter stands for beautiful, expensive, very beautiful, and cheap individually. Suppose a SS $(\mathfrak{T}, \dot{\kappa})$ shows the attractiveness of the watches, such that

$$\begin{aligned}\mathfrak{T}\left(\acute{o}_1\right) &= \{\dot{\alpha}_1, \dot{\alpha}_3, \dot{\alpha}_5\}\mathfrak{T}\left(\acute{o}_2\right) = \{\dot{\alpha}_2, \dot{\alpha}_5\}\mathfrak{T}\left(\acute{o}_3\right) = \{\dot{\alpha}_1, \dot{\alpha}_4\}\mathfrak{T}\left(\acute{o}_4\right)\\ &= \{\dot{\alpha}_3, \dot{\alpha}_4, \dot{\alpha}_5\}.\end{aligned} \tag{3}$$

Then, the SS $(\mathfrak{T}, \dot{\kappa})$ is a parameterized family, and $\left\{\mathfrak{T}(\acute{o}_i), i = 1,2,3,4\right\}$.

Definition 3 (see [19]). Let $(\mathfrak{T}, \tilde{A})$ and $(\mathcal{G}, \underline{B})$ be two SSs on $\dot{\Upsilon}$ and $\tilde{A}, \underline{B} \subseteq \dot{\xi}$. Then their CP of $(\mathfrak{T}, \tilde{A}) \times (\mathcal{G}, \underline{B}) = (\mathbb{H}, \mathcal{D})$ with a mapping $\mathbb{H}: \mathcal{D} \longrightarrow \mathfrak{p}(\dot{\Upsilon})$ is defined as:

$$\mathbb{H}(\hat{u}, \acute{u}) = \left\{\left(\acute{o}_{\hat{u}}, \acute{t}_{\acute{u}}\right): \acute{o}_{\hat{u}} \in (\mathfrak{T}, \tilde{A}), \acute{t}_{\acute{u}} \in (\mathcal{J}, \underline{B})\right\}. \tag{4}$$

Any subset of the CP of two SSs is called SR.

Definition 4 (see [21]). Let $\dot{\Upsilon}$ be a universal set and $\dot{\xi}$ be the set of parameters, $\mathfrak{p}^{\dot{\Upsilon}}$ represents the set of fuzzy subsets of $\dot{\Upsilon}$. Then FSS $(\mathfrak{T}, \dot{\kappa})$ with mapping $\mathfrak{T}: \dot{\kappa} \longrightarrow \mathfrak{p}^{\dot{\Upsilon}}$ is defined as:

$$\mathfrak{T} = \left\{\left(\acute{o}, m_{\mathfrak{T}}(\acute{o})\right): \acute{o} \in \dot{\kappa}, m_{\mathfrak{T}}(\acute{o}) \in \mathfrak{p}^{\dot{\Upsilon}}\right\}. \tag{5}$$

Where $m_{\mathfrak{T}}(\acute{o})$ is called the membership degree.

Example 2. Let $\dot{\Upsilon}$ is the set of LED companies and $\dot{\xi}$ be the set of parameters. The FSS $(\mathfrak{T}, \dot{\kappa})$ express the LED characteristics concerning some parameters and each membership degree assigned by the experts. $\dot{\Upsilon} = \{\dot{\alpha}_1, \dot{\alpha}_2, \dot{\alpha}_3, \dot{\alpha}_4\}$ i.e., $\dot{\alpha}_1 =$ Orient, $\dot{\alpha}_2 =$ Samsung, $\dot{\alpha}_3 =$ Haier, and $\dot{\alpha}_4 =$ Sony.

$\dot{\xi} = \left\{\acute{o}_1, \acute{o}_2, \acute{o}_3\right\}$ i.e., $\acute{o}_1 =$ no electromagnetic radiation, $\acute{o}_2 =$ Price, and $\acute{o}_3 =$ higher resolution.

$$\begin{aligned}\mathfrak{T}\left(\acute{o}_1\right) &= \{\dot{\alpha}_1 = 0.7, \dot{\alpha}_2 = 0.2, \dot{\alpha}_3 = 0.4, \dot{\alpha}_4 = 0.1\}\mathfrak{T}\left(\acute{o}_2\right)\\ &= \{\dot{\alpha}_1 = 0.9, \dot{\alpha}_2 = 0.8, \dot{\alpha}_3 = 0.3, \dot{\alpha}_4 = 0.6\}\mathfrak{T}\left(\acute{o}_3\right)\\ &= \{\dot{\alpha}_1 = 0.1, \dot{\alpha}_2 = 0.5, \dot{\alpha}_3 = 0.9, \dot{\alpha}_4 = 0.7\}.\end{aligned} \tag{6}$$

Then $(\mathfrak{T}, \dot{\kappa})$ is a parameterized family $\left\{\mathfrak{T}(\acute{o}_i), i = 1,2,3\right\}$.

Definition 5 (see [26]). Let $\dot{\Upsilon}$ be a universal set and $\dot{\xi}$ be the set of parameters, $C(\mathfrak{p}^{\dot{\Upsilon}})$ express the set of all complex fuzzy subsets of $\dot{\Upsilon}$. Then CFSS $(\mathfrak{T}, \dot{\kappa})$ with mapping $\mathfrak{T}: \dot{\kappa} \longrightarrow C(\mathfrak{p}^{\dot{\Upsilon}})$ is defined as,

$$\mathfrak{T} = \left\{\left(\acute{o}, m_{\mathfrak{T}_c}(\acute{o})\right): \acute{o} \in \dot{\kappa}, m_{\mathfrak{T}}(\acute{o}) \in C\left(\mathfrak{p}^{\dot{\Upsilon}}\right)\right\}. \tag{7}$$

And $m_{\mathfrak{T}_c}(\acute{o}) = r_{m_{\mathfrak{T}}}(\acute{o})e^{(q_{m_{\mathfrak{T}}}(\acute{o}))2\pi i}$ Since $r_{m_{\mathfrak{T}}}, q_{m_{\mathfrak{T}}}: \dot{\Upsilon} \longrightarrow [0,1]$.

Where $r_{m_{\mathfrak{T}}}$ and $q_{m_{\mathfrak{T}}}$ are called amplitude terms and phase terms of the membership degree individually.

Definition 6 (see [31]). Let $\dot{\Upsilon}$ be a universal set. Then CIFS $\mathfrak{T}$ on $\dot{\Upsilon}$ with a mapping $m_{\mathfrak{T}_c}, m_{\mathfrak{T}_c}: \dot{\Upsilon} \longrightarrow [0,1]$ is defined as,

$$\mathfrak{T} = \left\{\left(\acute{o}, m_{\mathfrak{T}_c}(\acute{o}), m_{\mathfrak{T}_c}(\acute{o})\right): \acute{o} \in \dot{\Upsilon}\right\}. \tag{8}$$

Since $m_{\mathfrak{T}_c}(\acute{o}) = r_{m_{\mathfrak{T}}}(\acute{o})e^{q_{m_{\mathfrak{T}}}(\acute{o})2\pi i}$ and $m_{\mathfrak{T}_c}(\acute{o}) = r_{m_{\mathfrak{T}}}(\acute{o})e^{q_{m_{\mathfrak{T}}}(\acute{o})2\pi i}$, on condition that, $r_{m_{\mathfrak{T}}}(\acute{o}) + r_{m_{\mathfrak{T}}}(\acute{o}) \in [0,1]$ and $q_{m_{\mathfrak{T}}}(\acute{o}) + q_{m_{\mathfrak{T}}}(\acute{o}) \in [0,1]$.

Where $r_{m_{\mathfrak{T}}}, r_{m_{\mathfrak{T}}}$ are known as amplitude terms of membership and non-membership degree individually. $q_{m_{\mathfrak{T}}}, q_{m_{\mathfrak{T}}}$ are known as the phase terms of membership and non-membership degree, individually.

Definition 7 (see [33]). Let $\dot{\Upsilon}$ be a universal set and $\dot{\xi}$ be the set of parameters, $\mathfrak{p}\mathfrak{T}^{\dot{\Upsilon}}$ denotes the set of all intuitionistic fuzzy subsets of $\dot{\Upsilon}$. Then an IFSS $(\mathfrak{T}, \dot{\kappa})$ with mapping $\mathfrak{T}: \dot{\kappa} \longrightarrow \mathfrak{p}\mathfrak{T}^{\dot{\Upsilon}}$ is defined as:

$$\mathbb{T} = \left\{(\acute{o}, m_{\mathbb{T}}(\acute{o}), m_{\mathbb{T}}(\acute{o})) : \acute{o} \in \dot{k}, m_{\mathbb{T}}(\acute{o}) m_{\mathbb{T}}(\acute{o}) \in \dot{p}\mathbb{T}^{\dot{Y}}\right\}, \quad (9)$$

Where $m_{\mathbb{T}}(\acute{o}), m_{\mathbb{T}}(\acute{o})$ are called membership and non-membership degrees, individually.

Example 3. From example 2, Assume an IFSS $(\mathbb{T}, \dot{k})$ describe the characteristic of the LED concerning some parameters and each membership and non-membership degree given by experts.

$$\begin{aligned}
\mathbb{T}(\acute{o}_1) &= \{\dot{q}_1 = (0.2, 0.4), \dot{q}_2 = (0.5, 0.3), \dot{q}_3 = (0.1, 0.9), \dot{q}_4 = (0.3, 0.5)\} \\
\mathbb{T}(\acute{o}_2) &= \{\dot{q}_1 = (0.1, 0.3), \dot{q}_2 = (0.2, 0.6), \dot{q}_3 = (0.5, 0.3), \dot{q}_4 = (0.3, 0.2)\} \\
\mathbb{T}(\acute{o}_3) &= \{\dot{q}_1 = (0, 0.6), \dot{q}_2 = (0.4, 0), \dot{q}_3 = (0.7, 0.1), \dot{q}_4 = (0.4, 0.5)\}.
\end{aligned} \quad (10)$$

Then the IFSS $(\mathbb{T}, \dot{k})$ is a parameterized family $\{\mathbb{T}(\acute{o}_i), i = 1, 2, 3\}$.

Definition 8 (see [36]). Let $\dot{Y}$ be a universal set and $\dot{\mathbb{E}}$ be the set of parameters, $C(\dot{p}\mathbb{T}^{\dot{Y}})$ denotes the set of all complex intuitionistic fuzzy subsets of $\dot{Y}$. Then CIFSS $(\mathbb{T}, \dot{k})$ with mapping $\mathbb{T}: \dot{k} \longrightarrow C(\dot{p}\mathbb{T}^{\dot{Y}})$ is defined as,

$$\mathbb{T} = \left\{\left(\acute{o}, m_{\mathbb{T}^c}(\acute{o}), m_{\mathbb{T}^c}(\acute{o})\right) : \acute{o} \in \dot{k}, m_{\mathbb{T}}(\acute{o}), m_{\mathbb{T}}(\acute{o}) \in C\left(\dot{p}\mathbb{T}^{\dot{Y}}\right)\right\}. \quad (11)$$

Since
$m_{\mathbb{T}^c}(\acute{o}) = r_{m_{\mathbb{T}}}(\acute{o}) e^{q_{m_{\mathbb{T}}}(\acute{o})2\pi i}, m_{\mathbb{T}^c}(\acute{o}) = r_{m_{\mathbb{T}}}(\acute{o}) e^{q_{m_{\mathbb{T}}}(\acute{o})2\pi i}$

Definition 9 (see [39]). Let $\dot{Y}$ be a universal set. Then a CPyFS $\mathbb{T}$ on $\dot{Y}$ with mapping $m_{\mathbb{T}^c}, m_{\mathbb{T}^c}: \dot{Y} \longrightarrow [0, 1]$ is defined as,

$$\mathbb{T} = \left\{\left(\acute{o}, m_{\mathbb{T}^c}(\acute{o}), m_{\mathbb{T}^c}(\acute{o})\right) : \acute{o} \in \dot{Y}\right\}. \quad (12)$$

Since $m_{\mathbb{T}^c}(\acute{o}) = r_{m_{\mathbb{T}}}(\acute{o}) e^{q_{m_{\mathbb{T}}}(\acute{o})2\pi i}$ and $m_{\mathbb{T}^c}(\acute{o}) = r_{m_{\mathbb{T}}}(\acute{o}) e^{q_{m_{\mathbb{T}}}(\acute{o})2\pi i}$ on condition that, $(r_{m_{\mathbb{T}}}(\acute{o}))^2 + (r_{m_{\mathbb{T}}}(\acute{o}))^2 \in [0, 1]$ and $(q_{m_{\mathbb{T}}}(\acute{o}))^2 + (q_{m_{\mathbb{T}}}(\acute{o}))^2 \in [0, 1]$.

Where $r_{m_{\mathbb{T}}}, r_{m_{\mathbb{T}}}$ are known as amplitude terms of membership and non-membership degree, individually. $q_{m_{\mathbb{T}}}, q_{m_{\mathbb{T}}}$ is called the phase terms of membership and non-membership degree, individually.

Definition 10 (see [43]). Let $\dot{Y}$ be a universal set and $\dot{\mathbb{E}}$ be the set of parameters, $C(Py\dot{p}^{\dot{Y}})$ denotes the set of all complex Pythagorean fuzzy subsets of $\dot{Y}$. Then CPyFSS $(\mathbb{T}, \dot{k})$ with mapping $\mathbb{T}: \dot{k} \longrightarrow C(Py\dot{p}^{\dot{Y}})$ is defined as:

$$\mathbb{T} = \left\{\left(\left(\acute{o}, m_{\mathbb{T}^c}(\acute{o}), m_{\mathbb{T}^c}(\acute{o})\right) : \acute{o} \in \dot{k}, m_{\mathbb{T}}(\acute{o}), m_{\mathbb{T}}(\acute{o}) \in C\left(Py\dot{p}^{\dot{Y}}\right)\right)\right\}. \quad (13)$$

Since $m_{\mathbb{T}^c}(\acute{o}) = r_{m_{\mathbb{T}}}(\acute{o}) e^{q_{m_{\mathbb{T}}}(\acute{o})2\pi i}$ and $m_{\mathbb{T}^c}(\acute{o}) = r_{m_{\mathbb{T}}}(\acute{o}) e^{q_{m_{\mathbb{T}}}(\acute{o})2\pi i}$.

3. Main Result

In this section, we aim to diagnose the innovative idea of CPyFSRs by using the CP of two CPyFSSs, which are computed with the help of two different ideas, called CPF relation and soft sets. Additionally, using the presented approaches, we examined different kinds of relations and also justified them with the help of some suitable examples. The CPyFSRs has a comprehensive structure because it is discussing both degrees of membership and non-membership with multidimensional variable.

Definition 11. Suppose $(\mathbb{T}, \tilde{A})$ and $(\mathbb{S}, \underline{B})$ be two complex Pythagorean fuzzy soft sets (CPyFSSs) on $\dot{Y}$, $\dot{\mathbb{E}}$ be the set of parameters. Let $(\mathbb{T}, \tilde{A}) \times (\mathbb{S}, \underline{B}) = (\mathbb{H}, \mathbb{D})$ and $\tilde{A}, \underline{B} \subseteq \dot{\mathbb{E}}$ with a mapping $\mathbb{H}: \mathbb{D} \longrightarrow C(Py\mathbb{T}^{\dot{Y}})$ then the CP of CPyFSSs

$$\tilde{A} = \left\{\begin{pmatrix} \acute{o}, r_{m_{\mathbb{T}}}^{\tilde{A}}(\acute{o}) e^{q_{m_{\mathbb{T}}}^{\tilde{A}}(\acute{o})2\pi i}, \\ r_{m_{\mathbb{T}}}^{\tilde{A}}(\acute{o}) e^{q_{m_{\mathbb{T}}}^{\tilde{A}}(\acute{o})2\pi i} \end{pmatrix} : \acute{o} \in \tilde{A}\right\} \quad \text{and}$$

$$\underline{B} = \left\{\begin{pmatrix} \dot{\imath}, r_{m_{\mathbb{T}}}^{\underline{B}}(\dot{\imath}) e^{q_{m_{\mathbb{T}}}^{\underline{B}}(\dot{\imath})2\pi i}, \\ r_{m_{\mathbb{T}}}^{\underline{B}}(\dot{\imath}) e^{q_{m_{\mathbb{T}}}^{\underline{B}}(\dot{\imath})2\pi i} \end{pmatrix} : \dot{\imath} \in \underline{B}\right\}$$

Is denoted and defined as,

$$(\mathbb{H}, \mathbb{D}) = \tilde{A} \times \underline{B} = \left\{\begin{pmatrix} (\acute{o}, \dot{\imath}), r_{m_{\mathbb{T}}}^{\tilde{A}\times\underline{B}}(\acute{o}, \dot{\imath}) e^{q_{m_{\mathbb{T}}}^{\tilde{A}\times\underline{B}}(\acute{o}, \dot{\imath})2\pi i}, \\ r_{m_{\mathbb{T}}}^{\tilde{A}\times\underline{B}}(\acute{o}, \dot{\imath}) e^{q_{m_{\mathbb{T}}}^{\tilde{A}\times\underline{B}}(\acute{o}, \dot{\imath})2\pi i} \end{pmatrix} : \acute{o} \in \tilde{A}, \dot{\imath} \in \underline{B}\right\}, \quad (14)$$

Where $\left\{ r_{m_{\mathbb{T}}}^{\tilde{A}\times\underline{B}}(\acute{o}, \dot{\imath}) = \min\left\{r_{m_{\mathbb{T}}}^{\tilde{A}}(\acute{o}), r_{m_{\mathbb{T}}}^{\underline{B}}(\dot{\imath})\right\} r_{m_{\mathbb{T}}}^{\tilde{A}\times\underline{B}}(\acute{o}, \dot{\imath}) = \max\left\{r_{m_{\mathbb{T}}}^{\tilde{A}}(\acute{o}), r_{m_{\mathbb{T}}}^{\underline{B}}(\dot{\imath})\right\}\right\}$

$$\left\{ q_{m_{\mathbb{T}}}^{\tilde{A}\times\underline{B}}(\acute{o}, \dot{\imath}) = \min\left\{q_{m_{\mathbb{T}}}^{\tilde{A}}(\acute{o}), q_{m_{\mathbb{T}}}^{\underline{B}}(\dot{\imath})\right\} q_{m_{\mathbb{T}}}^{\tilde{A}\times\underline{B}}(\acute{o}, \dot{\imath}) = \max\left\{q_{m_{\mathbb{T}}}^{\tilde{A}}(\acute{o}), q_{m_{\mathbb{T}}}^{\underline{B}}(\dot{\imath})\right\}\right\}. \quad (15)$$

Example 4. Let the universal set $\dot{Y} = \{\dot{\varrho}_1, \dot{\varrho}_2, \dot{\varrho}_3\}$ consist of three types of shoe brands i.e., $\dot{\varrho}_1$ =Bata, $\dot{\varrho}_2$ =Servis, and $\dot{\varrho}_3$ =Metro and there are three parameters $\dot{E} = \{\acute{o}_1, \acute{o}_2, \acute{o}_3\}$ i.e., $\acute{o}_1$ =Good condition, $\acute{o}_2$ =attrictive appearance, and $\acute{o}_3$ =Stable. Then $(\dot{\mathcal{F}}, \tilde{A})$ and $(\dot{\mathcal{G}}, \dot{B})$ be two CPyFSSs on $\dot{Y}$ individually, Their corresponding membership and non-membership are as follows; for $n = 2$.

$$= \left\{ \begin{array}{l} \left(\acute{o}_1, \left(0.4e^{0.6\pi i}, 0.6e^{0.3\pi i} \right), \left(0.5e^{0.2\pi i}, 0.6e^{0.9\pi i} \right), \right. \\ \left. \left(0.4e^{0.1\pi i}, 0.8e^{0.4\pi i} \right), \left(0.8e^{0.8\pi i}, 0.3e^{0.6\pi i} \right) \right), \\ \left(\acute{o}_2, \left(0.7e^{0.8\pi i}, 0.2e^{0.5\pi i} \right), \left(0.9e^{0.7\pi i}, 0.2e^{0.1\pi i} \right), \right. \\ \left. \left(0.3e^{0.7\pi i}, 0.6e^{0.4\pi i} \right), \left(0.6e^{0.7\pi i}, 0.3e^{0.5\pi i} \right) \right), \\ \left(\acute{o}_3, \left(0.8e^{0.7\pi i}, 0.4e^{0.6\pi i} \right), \left(0.1e^{0.5\pi i}, 0.8e^{0.3\pi i} \right), \right. \\ \left. \left(0.7e^{0.4\pi i}, 0.5e^{0.1\pi i} \right), \left(0.5e^{0.2\pi i}, 0.5e^{0.8\pi i} \right) \right), \end{array} \right\} \tag{16}$$

In the above observations, the first three values characterize the membership and non-membership degree of each brand and the fourth value shows the general belongingness of each parameter to the company. Each row represents the parametric observations. Now the CP of $(\dot{\mathcal{F}}, \tilde{A})$ and $(\dot{\mathcal{G}}, \dot{B})$ in Table 1 is:

Definition 12. The complex Pythagorean fuzzy soft relations (CPyFSRs) $\bar{\dot{R}}$ is a subset of the CP of two CPyFSSs.

Example 5. From Table 1, take a subset of the CP. Then the CPyFSR $\bar{\dot{R}}$ are as:

$$\bar{\dot{R}} = \left\{ \begin{array}{l} \left(\left(\acute{o}_1, \acute{o}_2 \right), \begin{pmatrix} 0.6e^{0.7\pi i}, \\ 0.2e^{0.5\pi i} \end{pmatrix}, \begin{pmatrix} 0.6e^{0.7\pi i}, \\ 0.6e^{0.2\pi i} \end{pmatrix}, \begin{pmatrix} 0.2e^{0.3\pi i}, \\ 0.6e^{0.4\pi i} \end{pmatrix}, \begin{pmatrix} 0.4e^{0.1\pi i}, \\ 0.3e^{0.8\pi i} \end{pmatrix} \right), \\ \left(\left(\acute{o}_2, \acute{o}_3 \right), \begin{pmatrix} 0.8e^{0.4\pi i}, \\ 0.4e^{0.8\pi i} \end{pmatrix}, \begin{pmatrix} 0.1e^{0.3\pi i}, \\ 0.8e^{0.6\pi i} \end{pmatrix}, \begin{pmatrix} 0.5e^{0.3\pi i}, \\ 0.5e^{0.9\pi i} \end{pmatrix}, \begin{pmatrix} 0.5e^{0.4\pi i}, \\ 0.7e^{0.8\pi i} \end{pmatrix} \right), \\ \left(\left(\acute{o}_3, \acute{o}_1 \right), \begin{pmatrix} 0.7e^{0.2\pi i}, \\ 0.5e^{0.8\pi i} \end{pmatrix}, \begin{pmatrix} 0.1e^{0.5\pi i}, \\ 0.8e^{0.3\pi i} \end{pmatrix}, \begin{pmatrix} 0.4e^{0.4\pi i}, \\ 0.9e^{0.3\pi i} \end{pmatrix}, \begin{pmatrix} 0.4e^{0.2\pi i}, \\ 0.5e^{0.8\pi i} \end{pmatrix} \right), \\ \left(\left(\acute{o}_3, \acute{o}_3 \right), \begin{pmatrix} 0.7e^{0.2\pi i}, \\ 0.5e^{0.8\pi i} \end{pmatrix}, \begin{pmatrix} 0.1e^{0.5\pi i}, \\ 0.8e^{0.3\pi i} \end{pmatrix}, \begin{pmatrix} 0.4e^{0.4\pi i}, \\ 0.9e^{0.3\pi i} \end{pmatrix}, \begin{pmatrix} 0.4e^{0.2\pi i}, \\ 0.5e^{0.8\pi i} \end{pmatrix} \right) \end{array} \right\}. \tag{17}$$

Definition 13. Suppose that CPyFSR $\bar{\dot{R}}$ on $(\dot{\mathcal{F}}, \dot{k})$ is said to be CPyFS-inverse relation if

$$\begin{aligned} &\forall \left(\left((\acute{o}, \acute{\imath}) \left[r_{\dot{m}} (\acute{o}, \acute{\imath}) \right] e^{q_{\dot{m}} (\acute{o}, \acute{\imath})\pi i}, (\acute{o}, \acute{\imath}) \left[r_{\dot{m}} (\acute{o}, \acute{\imath}) \right] e^{q_{\dot{m}} (\acute{o}, \acute{\imath})\pi i} \right) \right) \\ &\in \bar{\dot{R}} \Leftrightarrow \forall \left(\left((\acute{\imath}, \acute{o}) \left[r_{\dot{m}} (\acute{\imath}, \acute{o}) \right] e^{q_{\dot{m}} (\acute{\imath}, \acute{o})\pi i}, (\acute{\imath}, \acute{o}) \left[r_{\dot{m}} (\acute{\imath}, \acute{o}) \right] e^{q_{\dot{m}} (\acute{\imath}, \acute{o})\pi i} \right) \right) \in \bar{\dot{R}}^{-1}. \end{aligned} \tag{18}$$

Example 6. Take a relation from Table 1 as:

Table 1: Cartesian product.

Ordered pair	$\dot{\mathfrak{q}}_1$	$\dot{\mathfrak{q}}_2$	$\dot{\mathfrak{q}}_3$	λ
$(\acute{\mathfrak{o}}_1, \acute{\mathfrak{o}}_1)$	$\begin{pmatrix} 0.4e^{0.6\pi i}, \\ 0.6e^{0.4\pi i} \end{pmatrix}$	$\begin{pmatrix} 0.5e^{0.2\pi i}, \\ 0.6e^{0.9\pi i} \end{pmatrix}$	$\begin{pmatrix} 0.2e^{0.1\pi i}, \\ 0.8e^{0.4\pi i} \end{pmatrix}$	$\begin{pmatrix} 0.4e^{0.1\pi i}, \\ 0.3e^{0.8\pi i} \end{pmatrix}$
$(\acute{\mathfrak{o}}_1, \acute{\mathfrak{o}}_2)$	$\begin{pmatrix} 0.6e^{0.7\pi i}, \\ 0.2e^{0.5\pi i} \end{pmatrix}$	$\begin{pmatrix} 0.6e^{0.7\pi i}, \\ 0.6e^{0.2\pi i} \end{pmatrix}$	$\begin{pmatrix} 0.2e^{0.3\pi i}, \\ 0.6e^{0.4\pi i} \end{pmatrix}$	$\begin{pmatrix} 0.4e^{0.1\pi i}, \\ 0.3e^{0.8\pi i} \end{pmatrix}$
$(\acute{\mathfrak{o}}_1, \acute{\mathfrak{o}}_3)$	$\begin{pmatrix} 0.6e^{0.7\pi i}, \\ 0.4e^{0.6\pi i} \end{pmatrix}$	$\begin{pmatrix} 0.1e^{0.5\pi i}, \\ 0.8e^{0.3\pi i} \end{pmatrix}$	$\begin{pmatrix} 0.2e^{0.3\pi i}, \\ 0.5e^{0.3\pi i} \end{pmatrix}$	$\begin{pmatrix} 0.4e^{0.1\pi i}, \\ 0.5e^{0.8\pi i} \end{pmatrix}$
$(\acute{\mathfrak{o}}_2, \acute{\mathfrak{o}}_1)$	$\begin{pmatrix} 0.4e^{0.4\pi i}, \\ 0.6e^{0.8\pi i} \end{pmatrix}$	$\begin{pmatrix} 0.3e^{0.2\pi i}, \\ 0.8e^{0.9\pi i} \end{pmatrix}$	$\begin{pmatrix} 0.4e^{0.1\pi i}, \\ 0.8e^{0.9\pi i} \end{pmatrix}$	$\begin{pmatrix} 0.6e^{0.4\pi i}, \\ 0.7e^{0.6\pi i} \end{pmatrix}$
$(\acute{\mathfrak{o}}_2, \acute{\mathfrak{o}}_2)$	$\begin{pmatrix} 0.7e^{0.4\pi i}, \\ 0.4e^{0.8\pi i} \end{pmatrix}$	$\begin{pmatrix} 0.3e^{0.3\pi i}, \\ 0.8e^{0.6\pi i} \end{pmatrix}$	$\begin{pmatrix} 0.3e^{0.3\pi i}, \\ 0.6e^{0.9\pi i} \end{pmatrix}$	$\begin{pmatrix} 0.6e^{0.4\pi i}, \\ 0.7e^{0.5\pi i} \end{pmatrix}$
$(\acute{\mathfrak{o}}_2, \acute{\mathfrak{o}}_3)$	$\begin{pmatrix} 0.8e^{0.4\pi i}, \\ 0.4e^{0.8\pi i} \end{pmatrix}$	$\begin{pmatrix} 0.1e^{0.3\pi i}, \\ 0.8e^{0.6\pi i} \end{pmatrix}$	$\begin{pmatrix} 0.5e^{0.3\pi i}, \\ 0.5e^{0.9\pi i} \end{pmatrix}$	$\begin{pmatrix} 0.5e^{0.4\pi i}, \\ 0.7e^{0.8\pi i} \end{pmatrix}$
$(\acute{\mathfrak{o}}_3, \acute{\mathfrak{o}}_1)$	$\begin{pmatrix} 0.7e^{0.2\pi i}, \\ 0.5e^{0.8\pi i} \end{pmatrix}$	$\begin{pmatrix} 0.1e^{0.5\pi i}, \\ 0.8e^{0.3\pi i} \end{pmatrix}$	$\begin{pmatrix} 0.4e^{0.4\pi i}, \\ 0.9e^{0.3\pi i} \end{pmatrix}$	$\begin{pmatrix} 0.4e^{0.2\pi i}, \\ 0.5e^{0.8\pi i} \end{pmatrix}$
$(\acute{\mathfrak{o}}_3, \acute{\mathfrak{o}}_2)$	$\begin{pmatrix} 0.7e^{0.2\pi i}, \\ 0.5e^{0.8\pi i} \end{pmatrix}$	$\begin{pmatrix} 0.3e^{0.6\pi i}, \\ 0.3e^{0.3\pi i} \end{pmatrix}$	$\begin{pmatrix} 0.3e^{0.5\pi i}, \\ 0.9e^{0.4\pi i} \end{pmatrix}$	$\begin{pmatrix} 0.4e^{0.7\pi i}, \\ 0.3e^{0.5\pi i} \end{pmatrix}$
$(\acute{\mathfrak{o}}_3, \acute{\mathfrak{o}}_3)$	$\begin{pmatrix} 0.7e^{0.2\pi i}, \\ 0.5e^{0.8\pi i} \end{pmatrix}$	$\begin{pmatrix} 0.1e^{0.5\pi i}, \\ 0.8e^{0.3\pi i} \end{pmatrix}$	$\begin{pmatrix} 0.4e^{0.4\pi i}, \\ 0.9e^{0.3\pi i} \end{pmatrix}$	$\begin{pmatrix} 0.4e^{0.2\pi i}, \\ 0.5e^{0.8\pi i} \end{pmatrix}$

$$\dot{\bar{\mathsf{R}}} = \left\{ \begin{array}{l} \left(\left(\acute{\mathfrak{o}}_1, \acute{\mathfrak{o}}_3 \right), \begin{pmatrix} 0.6e^{0.7\pi i}, \\ 0.4e^{0.6\pi i} \end{pmatrix}, \begin{pmatrix} 0.1e^{0.5\pi i}, \\ 0.8e^{0.3\pi i} \end{pmatrix}, \begin{pmatrix} 0.2e^{0.3\pi i}, \\ 0.5e^{0.3\pi i} \end{pmatrix}, \begin{pmatrix} 0.4e^{0.1\pi i}, \\ 0.5e^{0.8\pi i} \end{pmatrix} \right), \\ \left(\left(\acute{\mathfrak{o}}_2, \acute{\mathfrak{o}}_2 \right), \begin{pmatrix} 0.7e^{0.4\pi i}, \\ 0.4e^{0.8\pi i} \end{pmatrix}, \begin{pmatrix} 0.3e^{0.3\pi i}, \\ 0.8e^{0.6\pi i} \end{pmatrix}, \begin{pmatrix} 0.3e^{0.3\pi i}, \\ 0.6e^{0.9\pi i} \end{pmatrix}, \begin{pmatrix} 0.6e^{0.4\pi i}, \\ 0.7e^{0.5\pi i} \end{pmatrix} \right), \\ \left(\left(\acute{\mathfrak{o}}_3, \acute{\mathfrak{o}}_2 \right), \begin{pmatrix} 0.7e^{0.2\pi i}, \\ 0.5e^{0.8\pi i} \end{pmatrix}, \begin{pmatrix} 0.3e^{0.6\pi i}, \\ 0.3e^{0.3\pi i} \end{pmatrix}, \begin{pmatrix} 0.3e^{0.5\pi i}, \\ 0.9e^{0.4\pi i} \end{pmatrix}, \begin{pmatrix} 0.4e^{0.7\pi i}, \\ 0.3e^{0.5\pi i} \end{pmatrix} \right), \\ \left(\left(\acute{\mathfrak{o}}_3, \acute{\mathfrak{o}}_3 \right), \begin{pmatrix} 0.7e^{0.2\pi i}, \\ 0.5e^{0.8\pi i} \end{pmatrix}, \begin{pmatrix} 0.1e^{0.5\pi i}, \\ 0.8e^{0.3\pi i} \end{pmatrix}, \begin{pmatrix} 0.4e^{0.4\pi i}, \\ 0.9e^{0.3\pi i} \end{pmatrix}, \begin{pmatrix} 0.4e^{0.2\pi i}, \\ 0.5e^{0.8\pi i} \end{pmatrix} \right) \end{array} \right\}. \tag{19}$$

Then inverse relation $\dot{\bar{\mathsf{R}}}^{-1}$ of $\dot{\bar{\mathsf{R}}}$ is

$$\dot{\bar{\mathsf{R}}}^{-1} = \left\{ \begin{array}{l} \left(\left(\acute{\mathfrak{o}}_3, \acute{\mathfrak{o}}_1 \right), \begin{pmatrix} 0.7e^{0.2\pi i}, \\ 0.5e^{0.8\pi i} \end{pmatrix}, \begin{pmatrix} 0.1e^{0.5\pi i}, \\ 0.8e^{0.3\pi i} \end{pmatrix}, \begin{pmatrix} 0.4e^{0.4\pi i}, \\ 0.9e^{0.3\pi i} \end{pmatrix}, \begin{pmatrix} 0.4e^{0.2\pi i}, \\ 0.5e^{0.8\pi i} \end{pmatrix} \right), \\ \left(\left(\acute{\mathfrak{o}}_2, \acute{\mathfrak{o}}_2 \right), \begin{pmatrix} 0.7e^{0.4\pi i}, \\ 0.4e^{0.8\pi i} \end{pmatrix}, \begin{pmatrix} 0.3e^{0.3\pi i}, \\ 0.8e^{0.6\pi i} \end{pmatrix}, \begin{pmatrix} 0.3e^{0.3\pi i}, \\ 0.6e^{0.9\pi i} \end{pmatrix}, \begin{pmatrix} 0.6e^{0.4\pi i}, \\ 0.7e^{0.5\pi i} \end{pmatrix} \right), \\ \left(\left(\acute{\mathfrak{o}}_2, \acute{\mathfrak{o}}_3 \right), \begin{pmatrix} 0.8e^{0.4\pi i}, \\ 0.4e^{0.8\pi i} \end{pmatrix}, \begin{pmatrix} 0.1e^{0.3\pi i}, \\ 0.8e^{0.6\pi i} \end{pmatrix}, \begin{pmatrix} 0.5e^{0.3\pi i}, \\ 0.5e^{0.9\pi i} \end{pmatrix}, \begin{pmatrix} 0.5e^{0.4\pi i}, \\ 0.7e^{0.8\pi i} \end{pmatrix} \right), \\ \left(\left(\acute{\mathfrak{o}}_3, \acute{\mathfrak{o}}_3 \right), \begin{pmatrix} 0.7e^{0.2\pi i}, \\ 0.5e^{0.8\pi i} \end{pmatrix}, \begin{pmatrix} 0.1e^{0.5\pi i}, \\ 0.8e^{0.3\pi i} \end{pmatrix}, \begin{pmatrix} 0.4e^{0.4\pi i}, \\ 0.9e^{0.3\pi i} \end{pmatrix}, \begin{pmatrix} 0.4e^{0.2\pi i}, \\ 0.5e^{0.8\pi i} \end{pmatrix} \right) \end{array} \right\}. \tag{20}$$

Definition 14. Suppose that CPyFSR $\dot{\bar{\mathsf{R}}}$ on $(\mathfrak{T}, \dot{\mathfrak{k}})$ is known as CPyFS-reflexive relation if

$$\Leftrightarrow \forall \left(\begin{pmatrix} (\acute{\mathfrak{o}}, \acute{\mathfrak{o}}) \left[r_{\mathfrak{m}_*}(\acute{\mathfrak{o}}, \acute{\mathfrak{o}}) \right] e^{q_{\mathfrak{m}_*}(\acute{\mathfrak{o}}, \acute{\mathfrak{o}})\pi i}, \\ \left[r_{\mathfrak{m}_*}(\acute{\mathfrak{o}}, \acute{\mathfrak{o}}) \right] e^{q_{\mathfrak{m}_*}(\acute{\mathfrak{o}}, \acute{\mathfrak{o}})\pi i} \end{pmatrix} \right) \in \dot{\bar{\mathsf{R}}}. \tag{21}$$

Example 7. Take a relation from Table 1 as:

$$\bar{\dot{\mathrm{R}}} = \left\{ \begin{array}{l} \left(\left(\acute{\mathrm{o}}_1, \acute{\mathrm{o}}_1 \right), \begin{pmatrix} 0.4e^{0.6\pi i}, \\ 0.6e^{0.4\pi i} \end{pmatrix}, \begin{pmatrix} 0.5e^{0.2\pi i}, \\ 0.6e^{0.9\pi i} \end{pmatrix}, \begin{pmatrix} 0.2e^{0.1\pi i}, \\ 0.8e^{0.4\pi i} \end{pmatrix}, \begin{pmatrix} 0.4e^{0.1\pi i}, \\ 0.3e^{0.8\pi i} \end{pmatrix} \right), \\ \left(\left(\acute{\mathrm{o}}_2, \acute{\mathrm{o}}_2 \right), \begin{pmatrix} 0.7e^{0.4\pi i}, \\ 0.4e^{0.8\pi i} \end{pmatrix}, \begin{pmatrix} 0.3e^{0.3\pi i}, \\ 0.8e^{0.6\pi i} \end{pmatrix}, \begin{pmatrix} 0.3e^{0.3\pi i}, \\ 0.6e^{0.9\pi i} \end{pmatrix}, \begin{pmatrix} 0.6e^{0.4\pi i}, \\ 0.7e^{0.5\pi i} \end{pmatrix} \right), \\ \left(\left(\acute{\mathrm{o}}_3, \acute{\mathrm{o}}_3 \right), \begin{pmatrix} 0.7e^{0.2\pi i}, \\ 0.5e^{0.8\pi i} \end{pmatrix}, \begin{pmatrix} 0.1e^{0.5\pi i}, \\ 0.8e^{0.3\pi i} \end{pmatrix}, \begin{pmatrix} 0.4e^{0.4\pi i}, \\ 0.9e^{0.3\pi i} \end{pmatrix}, \begin{pmatrix} 0.4e^{0.2\pi i}, \\ 0.5e^{0.8\pi i} \end{pmatrix} \right) \end{array} \right\}, \tag{22}$$

is a CPyFS-reflexive relation $\bar{\dot{\mathrm{R}}}$.

Definition 15. Suppose that CPyFSR $\bar{\dot{\mathrm{R}}}$ on $(\mathbb{T}, \dot{\mathrm{k}})$ is known as CPyFS-irreflexive relation if

$$\Leftrightarrow \forall \left(\begin{pmatrix} (\acute{\mathrm{o}}, \acute{\mathrm{o}}) \left[r_{\mathrm{m}_*} (\acute{\mathrm{o}}, \acute{\mathrm{o}}) \right] e^{q_{\mathrm{m}_*} (\acute{\mathrm{o}}, \acute{\mathrm{o}}) \pi i}, \\ \left[r_{\mathrm{m}_*} (\acute{\mathrm{o}}, \acute{\mathrm{o}}) \right] e^{q_{\mathrm{m}_*} (\acute{\mathrm{o}}, \acute{\mathrm{o}}) \pi i} \end{pmatrix} \right) \notin \bar{\dot{\mathrm{R}}}. \tag{23}$$

Definition 16. Suppose that CPyFSR $\bar{\dot{\mathrm{R}}}$ on $(\mathbb{T}, \dot{\mathrm{k}})$ is known as CPyFS-symmetric relation if

$$\Leftrightarrow \forall \left(\begin{pmatrix} (\dot{\imath}, \acute{\mathrm{o}}) \left[r_{\mathrm{m}_*} (\dot{\imath}, \acute{\mathrm{o}}) \right] e^{q_{\mathrm{m}_*} (\dot{\imath}, \acute{\mathrm{o}}) \pi i}, \\ (\dot{\imath}, \acute{\mathrm{o}}) \left[r_{\mathrm{m}_*} (\dot{\imath}, \acute{\mathrm{o}}) \right] e^{q_{\mathrm{m}_*} (\dot{\imath}, \acute{\mathrm{o}}) \pi i} \end{pmatrix} \right) \in \bar{\dot{\mathrm{R}}}. \tag{24}$$

Definition 17. Suppose that CPyFSR $\bar{\dot{\mathrm{R}}}$ on $(\mathbb{T}, \dot{\mathrm{k}})$ is known as CPyFS-antisymmetric relation if

$$\forall \left((\acute{\mathrm{o}}, \dot{\imath}), \begin{pmatrix} \left[r_{\mathrm{m}_*} (\acute{\mathrm{o}}, \dot{\imath}) \right] e^{q_{\mathrm{m}_*} (\acute{\mathrm{o}}, \dot{\imath}) \pi i}, \\ \left[r_{\mathrm{m}_*} (\acute{\mathrm{o}}, \dot{\imath}) \right] e^{q_{\mathrm{m}_*} (\acute{\mathrm{o}}, \dot{\imath}) \pi i} \end{pmatrix} \right) \in \bar{\dot{\mathrm{R}}}, \tag{25}$$

and $((\dot{\imath}, \acute{\mathrm{o}}), ([r_{\mathrm{m}_*} (\dot{\imath}, \acute{\mathrm{o}})] e^{q_{\mathrm{m}_*} (\dot{\imath}, \acute{\mathrm{o}}) \pi i}, [r_{\mathrm{m}_*} (\dot{\imath}, \acute{\mathrm{o}})]\ e^{q_{\mathrm{m}_*} (\dot{\imath}, \acute{\mathrm{o}}) \pi i})) \in \bar{\dot{\mathrm{R}}}$

$$\Leftrightarrow \left((\acute{\mathrm{o}}, \dot{\imath}), \begin{pmatrix} \left[r_{\mathrm{m}_*} (\acute{\mathrm{o}}, \dot{\imath}) \right] e^{q_{\mathrm{m}_*} (\acute{\mathrm{o}}, \dot{\imath}) \pi i}, \\ \left[r_{\mathrm{m}_*} (\acute{\mathrm{o}}, \dot{\imath}) \right] e^{q_{\mathrm{m}_*} (\acute{\mathrm{o}}, \dot{\imath}) \pi i} \end{pmatrix} \right) = \left((\dot{\imath}, \acute{\mathrm{o}}), \begin{pmatrix} \left[r_{\mathrm{m}_*} (\dot{\imath}, \acute{\mathrm{o}}) \right] e^{q_{\mathrm{m}_*} (\dot{\imath}, \acute{\mathrm{o}}) \pi i}, \\ \left[r_{\mathrm{m}_*} (\dot{\imath}, \acute{\mathrm{o}}) \right] e^{q_{\mathrm{m}_*} (\dot{\imath}, \acute{\mathrm{o}}) \pi i} \end{pmatrix} \right). \tag{26}$$

Definition 18. Suppose that CPyFSR $\bar{\dot{\mathrm{R}}}$ on $(\mathbb{T}, \dot{\mathrm{k}})$ is known as CPyFS-transitive relation if

$$\forall \left((\acute{\mathrm{o}}, \dot{\imath}), \begin{pmatrix} \left[\mathrm{r}_{\mathrm{m}_*} (\acute{\mathrm{o}}, \dot{\imath}) \right] \mathrm{e}^{q_{\mathrm{m}_*} (\acute{\mathrm{o}}, \dot{\imath}) \pi i}, \\ \left[\mathrm{r}_{\mathrm{m}_*} (\acute{\mathrm{o}}, \dot{\imath}) \right] \mathrm{e}^{q_{\mathrm{m}_*} (\acute{\mathrm{o}}, \dot{\imath}) \pi i} \end{pmatrix} \right) \in \bar{\dot{\mathrm{R}}}, \tag{27}$$

and $((\dot{\imath}, \dot{\mathrm{t}}), ([\mathrm{r}_{\mathrm{m}_*} (\dot{\imath}, \dot{\mathrm{t}})] \mathrm{e}^{q_{\mathrm{m}_*} (\dot{\imath}, \dot{\mathrm{t}}) \pi i}, [\mathrm{r}_{\mathrm{m}_*} (\dot{\imath}, \dot{\mathrm{t}})] \mathrm{e}^{q_{\mathrm{m}_*} (\dot{\imath}, \dot{\mathrm{t}}) \pi i})) \in \bar{\dot{\mathrm{R}}}$

$$\Rightarrow \left((\acute{\mathrm{o}}, \dot{\mathrm{t}}), \begin{pmatrix} \left[\mathrm{r}_{\mathrm{m}_*} (\acute{\mathrm{o}}, \dot{\mathrm{t}}) \right] \mathrm{e}^{q_{\mathrm{m}_*} (\acute{\mathrm{o}}, \dot{\mathrm{t}}) \pi i}, \\ \left[\mathrm{r}_{\mathrm{m}_*} (\acute{\mathrm{o}}, \dot{\mathrm{t}}) \right] \mathrm{e}^{q_{\mathrm{m}_*} (\acute{\mathrm{o}}, \dot{\mathrm{t}}) \pi i} \end{pmatrix} \right) \in \bar{\dot{\mathrm{R}}}. \tag{28}$$

Definition 19. Suppose that CPyFSR $\bar{\dot{\mathrm{R}}}$ on $(\mathbb{T}, \dot{\mathrm{k}})$ is known as CPyFS-equivalence relation if,

(i) Reflexive
(ii) Symmetric
(iii) Transitive

Example 8. Take a relation from Table 1 as:

$$\bar{\dot{R}} = \left\{ \begin{array}{l} \left(\left(\acute{\delta}_1, \acute{\delta}_1 \right), \left(\begin{array}{l} 0.4e^{0.6\pi i}, \\ 0.6e^{0.4\pi i} \end{array} \right), \left(\begin{array}{l} 0.5e^{0.2\pi i}, \\ 0.6e^{0.9\pi i} \end{array} \right), \left(\begin{array}{l} 0.2e^{0.1\pi i}, \\ 0.8e^{0.4\pi i} \end{array} \right), \left(\begin{array}{l} 0.4e^{0.1\pi i}, \\ 0.3e^{0.8\pi i} \end{array} \right) \right), \\ \left(\left(\acute{\delta}_1, \acute{\delta}_2 \right), \left(\begin{array}{l} 0.6e^{0.7\pi i}, \\ 0.2e^{0.5\pi i} \end{array} \right), \left(\begin{array}{l} 0.6e^{0.7\pi i}, \\ 0.6e^{0.2\pi i} \end{array} \right), \left(\begin{array}{l} 0.2e^{0.3\pi i}, \\ 0.6e^{0.4\pi i} \end{array} \right), \left(\begin{array}{l} 0.4e^{0.1\pi i}, \\ 0.3e^{0.8\pi i} \end{array} \right) \right), \\ \left(\left(\acute{\delta}_2, \acute{\delta}_1 \right), \left(\begin{array}{l} 0.4e^{0.4\pi i}, \\ 0.6e^{0.8\pi i} \end{array} \right), \left(\begin{array}{l} 0.3e^{0.2\pi i}, \\ 0.8e^{0.9\pi i} \end{array} \right), \left(\begin{array}{l} 0.4e^{0.1\pi i}, \\ 0.8e^{0.9\pi i} \end{array} \right), \left(\begin{array}{l} 0.6e^{0.4\pi i}, \\ 0.7e^{0.6\pi i} \end{array} \right) \right), \\ \left(\left(\acute{\delta}_2, \acute{\delta}_2 \right), \left(\begin{array}{l} 0.7e^{0.4\pi i}, \\ 0.4e^{0.8\pi i} \end{array} \right), \left(\begin{array}{l} 0.3e^{0.3\pi i}, \\ 0.8e^{0.6\pi i} \end{array} \right), \left(\begin{array}{l} 0.3e^{0.3\pi i}, \\ 0.6e^{0.9\pi i} \end{array} \right), \left(\begin{array}{l} 0.6e^{0.4\pi i}, \\ 0.7e^{0.5\pi i} \end{array} \right) \right), \\ \left(\left(\acute{\delta}_2, \acute{\delta}_3 \right), \left(\begin{array}{l} 0.8e^{0.4\pi i}, \\ 0.4e^{0.8\pi i} \end{array} \right), \left(\begin{array}{l} 0.1e^{0.3\pi i}, \\ 0.8e^{0.6\pi i} \end{array} \right), \left(\begin{array}{l} 0.5e^{0.3\pi i}, \\ 0.5e^{0.9\pi i} \end{array} \right), \left(\begin{array}{l} 0.5e^{0.4\pi i}, \\ 0.7e^{0.8\pi i} \end{array} \right) \right), \\ \left(\left(\acute{\delta}_3, \acute{\delta}_2 \right), \left(\begin{array}{l} 0.7e^{0.2\pi i}, \\ 0.5e^{0.8\pi i} \end{array} \right), \left(\begin{array}{l} 0.3e^{0.6\pi i}, \\ 0.3e^{0.3\pi i} \end{array} \right), \left(\begin{array}{l} 0.3e^{0.5\pi i}, \\ 0.9e^{0.4\pi i} \end{array} \right), \left(\begin{array}{l} 0.4e^{0.7\pi i}, \\ 0.3e^{0.5\pi i} \end{array} \right) \right), \\ \left(\left(\acute{\delta}_3, \acute{\delta}_3 \right), \left(\begin{array}{l} 0.7e^{0.2\pi i}, \\ 0.5e^{0.8\pi i} \end{array} \right), \left(\begin{array}{l} 0.1e^{0.5\pi i}, \\ 0.8e^{0.3\pi i} \end{array} \right), \left(\begin{array}{l} 0.4e^{0.4\pi i}, \\ 0.9e^{0.3\pi i} \end{array} \right), \left(\begin{array}{l} 0.4e^{0.2\pi i}, \\ 0.5e^{0.8\pi i} \end{array} \right) \right) \end{array} \right\}, \tag{29}$$

is a CPyFS-equivalence relation $\bar{\dot{R}}$.

Definition 20. Suppose that CPyFSR $\bar{\dot{R}}$ on $(\mathbb{T}, \dot{k})$ is known as CPyFS-partial order relation if;

(i) Reflexive

(ii) Antisymmetric

(iii) Transitive

Example 9. Take a relation from Table 1 as:

$$\bar{\dot{R}} = \left\{ \begin{array}{l} \left(\left(\acute{\delta}_1, \acute{\delta}_1 \right), \left(\begin{array}{l} 0.4e^{0.6\pi i}, \\ 0.6e^{0.4\pi i} \end{array} \right), \left(\begin{array}{l} 0.5e^{0.2\pi i}, \\ 0.6e^{0.9\pi i} \end{array} \right), \left(\begin{array}{l} 0.2e^{0.1\pi i}, \\ 0.8e^{0.4\pi i} \end{array} \right), \left(\begin{array}{l} 0.4e^{0.1\pi i}, \\ 0.3e^{0.8\pi i} \end{array} \right) \right), \\ \left(\left(\acute{\delta}_1, \acute{\delta}_2 \right), \left(\begin{array}{l} 0.6e^{0.7\pi i}, \\ 0.2e^{0.5\pi i} \end{array} \right), \left(\begin{array}{l} 0.6e^{0.7\pi i}, \\ 0.6e^{0.2\pi i} \end{array} \right), \left(\begin{array}{l} 0.2e^{0.3\pi i}, \\ 0.6e^{0.4\pi i} \end{array} \right), \left(\begin{array}{l} 0.4e^{0.1\pi i}, \\ 0.3e^{0.8\pi i} \end{array} \right) \right), \\ \left(\left(\acute{\delta}_2, \acute{\delta}_2 \right), \left(\begin{array}{l} 0.7e^{0.4\pi i}, \\ 0.4e^{0.8\pi i} \end{array} \right), \left(\begin{array}{l} 0.3e^{0.3\pi i}, \\ 0.8e^{0.6\pi i} \end{array} \right), \left(\begin{array}{l} 0.3e^{0.3\pi i}, \\ 0.6e^{0.9\pi i} \end{array} \right), \left(\begin{array}{l} 0.6e^{0.4\pi i}, \\ 0.7e^{0.5\pi i} \end{array} \right) \right), \\ \left(\left(\acute{\delta}_2, \acute{\delta}_3 \right), \left(\begin{array}{l} 0.8e^{0.4\pi i}, \\ 0.4e^{0.8\pi i} \end{array} \right), \left(\begin{array}{l} 0.1e^{0.3\pi i}, \\ 0.8e^{0.6\pi i} \end{array} \right), \left(\begin{array}{l} 0.5e^{0.3\pi i}, \\ 0.5e^{0.9\pi i} \end{array} \right), \left(\begin{array}{l} 0.5e^{0.4\pi i}, \\ 0.7e^{0.8\pi i} \end{array} \right) \right), \\ \left(\left(\acute{\delta}_1, \acute{\delta}_3 \right), \left(\begin{array}{l} 0.6e^{0.7\pi i}, \\ 0.4e^{0.6\pi i} \end{array} \right), \left(\begin{array}{l} 0.1e^{0.5\pi i}, \\ 0.8e^{0.3\pi i} \end{array} \right), \left(\begin{array}{l} 0.2e^{0.3\pi i}, \\ 0.5e^{0.3\pi i} \end{array} \right), \left(\begin{array}{l} 0.4e^{0.1\pi i}, \\ 0.5e^{0.8\pi i} \end{array} \right) \right), \\ \left(\left(\acute{\delta}_3, \acute{\delta}_3 \right), \left(\begin{array}{l} 0.7e^{0.2\pi i}, \\ 0.5e^{0.8\pi i} \end{array} \right), \left(\begin{array}{l} 0.1e^{0.5\pi i}, \\ 0.8e^{0.3\pi i} \end{array} \right), \left(\begin{array}{l} 0.4e^{0.4\pi i}, \\ 0.9e^{0.3\pi i} \end{array} \right), \left(\begin{array}{l} 0.4e^{0.2\pi i}, \\ 0.5e^{0.8\pi i} \end{array} \right) \right) \end{array} \right\}, \tag{30}$$

is a CPyFS-partial order relation $\bar{\dot{R}}$.

Definition 21. Suppose that CPyFSR $\bar{\dot{R}}$ on $(\mathbb{T}, \dot{k})$ is known as CPyFS-pre order relation if;

(i) Reflexive

(ii) Transitive

Definition 22. Suppose that CPyFSR $\bar{\dot{R}}$ on $(\mathbb{T}, \dot{k})$ is known as CPyFS-complete relation if;

$$\forall\left((\acute{o}),\begin{pmatrix}\left[r_{m_*}(\acute{o})\right]e^{q_{m_*}(\acute{o})\pi i},\\ \left[r_{m_*}(\acute{o})\right]e^{q_{m_*}(\acute{o})\pi i}\end{pmatrix}\right),\left((\dot{\imath}),\begin{pmatrix}\left[r_{m_*}(\dot{\imath})\right]e^{q_{m_*}(\dot{\imath})\pi i},\\ \left[r_{m_*}(\dot{\imath})\right]e^{q_{m_*}(\dot{\imath})\pi i}\end{pmatrix}\right)\in\bar{\dot{R}},$$
$$\Rightarrow\left((\acute{o},\dot{\imath}),\begin{pmatrix}\left[r_{m_*}(\acute{o},\dot{\imath})\right]e^{q_{m_*}(\acute{o},\dot{\imath})\pi i},\\ \left[r_{m_*}(\acute{o},\dot{\imath})\right]e^{q_{m_*}(\acute{o},\dot{\imath})\pi i}\end{pmatrix}\right)\in\bar{\dot{R}}\text{ or}\left((\dot{\imath},\acute{o}),\begin{pmatrix}\left[r_{m_*}(\dot{\imath},\acute{o})\right]e^{q_{m_*}(\dot{\imath},\acute{o})\pi i},\\ \left[r_{m_*}(\dot{\imath},\acute{o})\right]e^{q_{m_*}(\dot{\imath},\acute{o})\pi i}\end{pmatrix}\right)\in\bar{\dot{R}}. \tag{31}$$

Definition 23. Suppose that CPyFSR $\bar{\dot{R}}$ on $(\mathbb{T}, \dot{k})$ is known as CPyFS-linear order relation if;

(i) Reflexive

(ii) Antisymmetric

(iii) Transitive

(iv) Complete

Definition 24. Suppose that CPyFSR $\bar{\dot{R}}$ on $(\mathbb{T}, \dot{k})$ is known as CPyFS-strict order relation if;

(i) Irreflexive

(ii) Transitive

Example 10. Take a relation from Table 1 as:

$$\bar{\dot{R}}=\left\{\begin{array}{l}\left(\left(\acute{o}_1,\acute{o}_2\right),\begin{pmatrix}0.6e^{0.7\pi i},\\ 0.2e^{0.5\pi i}\end{pmatrix},\begin{pmatrix}0.6e^{0.7\pi i},\\ 0.6e^{0.2\pi i}\end{pmatrix},\begin{pmatrix}0.2e^{0.3\pi i},\\ 0.6e^{0.4\pi i}\end{pmatrix},\begin{pmatrix}0.4e^{0.1\pi i},\\ 0.3e^{0.8\pi i}\end{pmatrix}\right),\\ \left(\left(\acute{o}_1,\acute{o}_3\right),\begin{pmatrix}0.6e^{0.7\pi i},\\ 0.4e^{0.6\pi i}\end{pmatrix},\begin{pmatrix}0.1e^{0.5\pi i},\\ 0.8e^{0.3\pi i}\end{pmatrix},\begin{pmatrix}0.2e^{0.3\pi i},\\ 0.5e^{0.3\pi i}\end{pmatrix},\begin{pmatrix}0.4e^{0.1\pi i},\\ 0.5e^{0.8\pi i}\end{pmatrix}\right),\\ \left(\left(\acute{o}_2,\acute{o}_3\right),\begin{pmatrix}0.8e^{0.4\pi i},\\ 0.4e^{0.8\pi i}\end{pmatrix},\begin{pmatrix}0.1e^{0.3\pi i},\\ 0.8e^{0.6\pi i}\end{pmatrix},\begin{pmatrix}0.5e^{0.3\pi i},\\ 0.5e^{0.9\pi i}\end{pmatrix},\begin{pmatrix}0.5e^{0.4\pi i},\\ 0.7e^{0.8\pi i}\end{pmatrix}\right)\end{array}\right\}, \tag{32}$$

is a CPyFS-strict order relation $\bar{\dot{R}}$.

Definition 25. Let $\bar{\dot{R}}$ be a CPyFSR on $(\mathbb{T}, \dot{k})$ is known as CPyFS equivalence class of $\acute{o}$ mod $\bar{\dot{R}}$ is defined as:

$$\bar{\dot{R}}[\acute{o}]=\left\{\begin{array}{c}\left(\acute{o},\left(\left[r_{m_*}(\acute{o})\right]e^{q_{m_*}(\acute{o})\pi i},\left[r_{m_*}(\acute{o})\right]e^{q_{m_*}(\acute{o})\pi i}\right)\right):\\ \left((\dot{\imath},\acute{o}),\left(\left[r_{m_*}(\dot{\imath},\acute{o})\right]e^{q_{m_*}(\dot{\imath},\acute{o})\pi i},\left[r_{m_*}(\dot{\imath},\acute{o})\right]e^{q_{m_*}(\dot{\imath},\acute{o})\pi i}\right)\in\bar{\dot{R}}\end{array}\right\}. \tag{33}$$

Example 11. Take an equivalence relation from example 8 as:

$$\bar{\dot{R}} = \left\{ \begin{array}{l} \left(\left(\acute{\delta}_1, \acute{\delta}_1 \right), \left(\begin{matrix} 0.4e^{0.6\pi i}, \\ 0.6e^{0.4\pi i} \end{matrix} \right), \left(\begin{matrix} 0.5e^{0.2\pi i}, \\ 0.6e^{0.9\pi i} \end{matrix} \right), \left(\begin{matrix} 0.2e^{0.1\pi i}, \\ 0.8e^{0.4\pi i} \end{matrix} \right), \left(\begin{matrix} 0.4e^{0.1\pi i}, \\ 0.3e^{0.8\pi i} \end{matrix} \right) \right), \\ \left(\left(\acute{\delta}_1, \acute{\delta}_2 \right), \left(\begin{matrix} 0.6e^{0.7\pi i}, \\ 0.2e^{0.5\pi i} \end{matrix} \right), \left(\begin{matrix} 0.6e^{0.7\pi i}, \\ 0.6e^{0.2\pi i} \end{matrix} \right), \left(\begin{matrix} 0.2e^{0.3\pi i}, \\ 0.6e^{0.4\pi i} \end{matrix} \right), \left(\begin{matrix} 0.4e^{0.1\pi i}, \\ 0.3e^{0.8\pi i} \end{matrix} \right) \right), \\ \left(\left(\acute{\delta}_2, \acute{\delta}_1 \right), \left(\begin{matrix} 0.4e^{0.4\pi i}, \\ 0.6e^{0.8\pi i} \end{matrix} \right), \left(\begin{matrix} 0.3e^{0.2\pi i}, \\ 0.8e^{0.9\pi i} \end{matrix} \right), \left(\begin{matrix} 0.4e^{0.1\pi i}, \\ 0.8e^{0.9\pi i} \end{matrix} \right), \left(\begin{matrix} 0.6e^{0.4\pi i}, \\ 0.7e^{0.6\pi i} \end{matrix} \right) \right), \\ \left(\left(\acute{\delta}_2, \acute{\delta}_2 \right), \left(\begin{matrix} 0.7e^{0.4\pi i}, \\ 0.4e^{0.8\pi i} \end{matrix} \right), \left(\begin{matrix} 0.3e^{0.3\pi i}, \\ 0.8e^{0.6\pi i} \end{matrix} \right), \left(\begin{matrix} 0.3e^{0.3\pi i}, \\ 0.6e^{0.9\pi i} \end{matrix} \right), \left(\begin{matrix} 0.6e^{0.4\pi i}, \\ 0.7e^{0.5\pi i} \end{matrix} \right) \right), \\ \left(\left(\acute{\delta}_2, \acute{\delta}_3 \right), \left(\begin{matrix} 0.8e^{0.4\pi i}, \\ 0.4e^{0.8\pi i} \end{matrix} \right), \left(\begin{matrix} 0.1e^{0.3\pi i}, \\ 0.8e^{0.6\pi i} \end{matrix} \right), \left(\begin{matrix} 0.5e^{0.3\pi i}, \\ 0.5e^{0.9\pi i} \end{matrix} \right), \left(\begin{matrix} 0.5e^{0.4\pi i}, \\ 0.7e^{0.8\pi i} \end{matrix} \right) \right), \\ \left(\left(\acute{\delta}_3, \acute{\delta}_2 \right), \left(\begin{matrix} 0.7e^{0.2\pi i}, \\ 0.5e^{0.8\pi i} \end{matrix} \right), \left(\begin{matrix} 0.3e^{0.6\pi i}, \\ 0.3e^{0.3\pi i} \end{matrix} \right), \left(\begin{matrix} 0.3e^{0.5\pi i}, \\ 0.9e^{0.4\pi i} \end{matrix} \right), \left(\begin{matrix} 0.4e^{0.7\pi i}, \\ 0.3e^{0.5\pi i} \end{matrix} \right) \right), \\ \left(\left(\acute{\delta}_3, \acute{\delta}_3 \right), \left(\begin{matrix} 0.7e^{0.2\pi i}, \\ 0.5e^{0.8\pi i} \end{matrix} \right), \left(\begin{matrix} 0.1e^{0.5\pi i}, \\ 0.8e^{0.3\pi i} \end{matrix} \right), \left(\begin{matrix} 0.4e^{0.4\pi i}, \\ 0.9e^{0.3\pi i} \end{matrix} \right), \left(\begin{matrix} 0.4e^{0.2\pi i}, \\ 0.5e^{0.8\pi i} \end{matrix} \right) \right) \end{array} \right\}. \tag{34}$$

Now, the equivalence class of.

(i) $\acute{\delta}_1 \bmod \bar{\dot{R}}$

$$\bar{\dot{R}}\left[\acute{\delta}_1\right] = \left\{ \begin{array}{l} \left(\acute{\delta}_1, \left(\begin{matrix} 0.4e^{0.6\pi i}, \\ 0.6e^{0.4\pi i} \end{matrix} \right), \left(\begin{matrix} 0.5e^{0.2\pi i}, \\ 0.6e^{0.9\pi i} \end{matrix} \right), \left(\begin{matrix} 0.2e^{0.1\pi i}, \\ 0.8e^{0.4\pi i} \end{matrix} \right), \left(\begin{matrix} 0.4e^{0.1\pi i}, \\ 0.3e^{0.8\pi i} \end{matrix} \right) \right), \\ \left(\acute{\delta}_2, \left(\begin{matrix} 0.7e^{0.4\pi i}, \\ 0.4e^{0.8\pi i} \end{matrix} \right), \left(\begin{matrix} 0.3e^{0.3\pi i}, \\ 0.8e^{0.6\pi i} \end{matrix} \right), \left(\begin{matrix} 0.3e^{0.3\pi i}, \\ 0.6e^{0.9\pi i} \end{matrix} \right), \left(\begin{matrix} 0.6e^{0.4\pi i}, \\ 0.7e^{0.5\pi i} \end{matrix} \right) \right) \end{array} \right\}. \tag{35}$$

(ii) $\acute{\delta}_2 \bmod \bar{\dot{R}}$

$$\bar{\dot{R}}\left[\acute{\delta}_2\right] = \left\{ \begin{array}{l} \left(\acute{\delta}_1, \left(\begin{matrix} 0.4e^{0.6\pi i}, \\ 0.6e^{0.4\pi i} \end{matrix} \right), \left(\begin{matrix} 0.5e^{0.2\pi i}, \\ 0.6e^{0.9\pi i} \end{matrix} \right), \left(\begin{matrix} 0.2e^{0.1\pi i}, \\ 0.8e^{0.4\pi i} \end{matrix} \right), \left(\begin{matrix} 0.4e^{0.1\pi i}, \\ 0.3e^{0.8\pi i} \end{matrix} \right) \right), \\ \left(\acute{\delta}_2, \left(\begin{matrix} 0.7e^{0.4\pi i}, \\ 0.4e^{0.8\pi i} \end{matrix} \right), \left(\begin{matrix} 0.3e^{0.3\pi i}, \\ 0.8e^{0.6\pi i} \end{matrix} \right), \left(\begin{matrix} 0.3e^{0.3\pi i}, \\ 0.6e^{0.9\pi i} \end{matrix} \right), \left(\begin{matrix} 0.6e^{0.4\pi i}, \\ 0.7e^{0.5\pi i} \end{matrix} \right) \right), \\ \left(\acute{\delta}_3, \left(\begin{matrix} 0.7e^{0.2\pi i}, \\ 0.5e^{0.8\pi i} \end{matrix} \right), \left(\begin{matrix} 0.1e^{0.5\pi i}, \\ 0.8e^{0.3\pi i} \end{matrix} \right), \left(\begin{matrix} 0.4e^{0.4\pi i}, \\ 0.9e^{0.3\pi i} \end{matrix} \right), \left(\begin{matrix} 0.4e^{0.2\pi i}, \\ 0.5e^{0.8\pi i} \end{matrix} \right) \right) \end{array} \right\}. \tag{36}$$

(iii) $\acute{\delta}_3 \bmod \bar{\dot{R}}$

$$\bar{\dot{R}}\left[\acute{\delta}_3\right] = \left\{ \begin{array}{l} \left(\acute{\delta}_2, \left(\begin{matrix} 0.7e^{0.4\pi i}, \\ 0.4e^{0.8\pi i} \end{matrix} \right), \left(\begin{matrix} 0.3e^{0.3\pi i}, \\ 0.8e^{0.6\pi i} \end{matrix} \right), \left(\begin{matrix} 0.3e^{0.3\pi i}, \\ 0.6e^{0.9\pi i} \end{matrix} \right), \left(\begin{matrix} 0.6e^{0.4\pi i}, \\ 0.7e^{0.5\pi i} \end{matrix} \right) \right), \\ \left(\acute{\delta}_3, \left(\begin{matrix} 0.7e^{0.2\pi i}, \\ 0.5e^{0.8\pi i} \end{matrix} \right), \left(\begin{matrix} 0.1e^{0.5\pi i}, \\ 0.8e^{0.3\pi i} \end{matrix} \right), \left(\begin{matrix} 0.4e^{0.4\pi i}, \\ 0.9e^{0.3\pi i} \end{matrix} \right), \left(\begin{matrix} 0.4e^{0.2\pi i}, \\ 0.5e^{0.8\pi i} \end{matrix} \right) \right) \end{array} \right\}. \tag{37}$$

Definition 26. Let $\dot{\bar{R}}$ be a CPyFSR on $(\dot{T}, \dot{k})$ is said to be CPyFS composite relation $\dot{\bar{R}}_1 \circ \dot{\bar{R}}_2$ is defined as:

$$\left((\acute{o}, \dot{\imath}), \begin{pmatrix} \left[r_{m_r}(\acute{o}, \dot{\imath})\right] e^{q_{m_r}(\acute{o}, \dot{\imath})\pi i}, \\ \left[r_{m_r}(\acute{o}, \dot{\imath})\right] e^{q_{m_r}(\acute{o}, \dot{\imath})\pi i} \end{pmatrix}\right) \in \dot{\bar{R}}_1, \tag{38}$$

and $((\dot{\imath}, \dot{t}), ([r_{m_r}(\dot{\imath}, \dot{t})] e^{q_{m_r}(\dot{\imath}, \dot{t})\pi i}, [r_{m_r}(\dot{\imath}, \dot{t})] e^{q_{m_r}(\dot{\imath}, \dot{t})\pi i})) \in \dot{\bar{R}}_2$

$$\Rightarrow \left((\acute{o}, \dot{t}), \begin{pmatrix} \left[r_{m_r}(\acute{o}, \dot{t})\right] e^{q_{m_r}(\acute{o}, \dot{t})\pi i}, \\ \left[r_{m_r}(\acute{o}, \dot{t})\right] e^{q_{m_r}(\acute{o}, \dot{t})\pi i} \end{pmatrix}\right) \dot{\bar{R}}_1 \circ \dot{\bar{R}}_2. \tag{39}$$

Theorem 1. *A CPyFSR $\dot{\bar{R}}$ is CPyFS symmetric relation on a CPyFSS $\dot{T}$ iff $\dot{\bar{R}} = \dot{\bar{R}}^c$.*

Proof 1. Suppose that$\dot{\bar{R}} = \dot{\bar{R}}^c$, then $((\acute{o}, \dot{\imath}), (m_{r_c}(\acute{o}, \dot{\imath})), (m_{r_c}(\acute{o}, \dot{\imath}))) \in \dot{\bar{R}}$

$$\begin{aligned} &\Longrightarrow \left((\dot{\imath}, \acute{o}), \left(m_{r_c}(\dot{\imath}, \acute{o})\right), \left(m_{r_c}(\dot{\imath}, \acute{o})\right)\right) \in \dot{\bar{R}}^c \\ &\Longrightarrow \left((\dot{\imath}, \acute{o}), \left(m_{r_c}(\dot{\imath}, \acute{o})\right), \left(m_{r_c}(\dot{\imath}, \acute{o})\right)\right) \in \dot{\bar{R}}. \end{aligned} \tag{40}$$

Thus, $\dot{\bar{R}}$ is CPyFS symmetric relation on a CPyFSS$\dot{T}$.

Conversely, assume that $\dot{\bar{R}}$ is CPyFS symmetric relation on CPyFSS$\dot{T}$ then

$$\begin{aligned} &\left((\acute{o}, \dot{\imath}), \left(m_{r_c}(\acute{o}, \dot{\imath})\right), \left(m_{r_c}(\acute{o}, \dot{\imath})\right)\right) \in \dot{\bar{R}} \\ &\Longrightarrow \left((\dot{\imath}, \acute{o}), \left(m_{r_c}(\dot{\imath}, \acute{o})\right), \left(m_{r_c}(\dot{\imath}, \acute{o})\right)\right) \in \dot{\bar{R}}. \end{aligned} \tag{41}$$

However, $((\dot{\imath}, \acute{o}), (m_{r_c}(\dot{\imath}, \acute{o})), (m_{r_c}(\dot{\imath}, \acute{o}))) \in \dot{\bar{R}}^c$

$$\Longrightarrow \dot{\bar{R}} = \dot{\bar{R}}^c. \tag{42}$$

□

Theorem 2. *A CPyFSR $\dot{\bar{R}}$ is CPyFS transitive relation on CPyFSS $\dot{T}$ iff $\dot{\bar{R}} \circ \dot{\bar{R}} \subseteq \dot{\bar{R}}^c$.*

Proof 2. Suppose that $\dot{\bar{R}}$ is CPyFS transitive relation on CPyFSS$\dot{T}$.

Let $((\acute{o}, \dot{t}), (m_{r_c}(\acute{o}, \dot{t}), (m_{r_c}(\acute{o}, \dot{t}))) \in \dot{\bar{R}} \circ \dot{\bar{R}}$,

Then by the definition of CPyFS transitive relation, $((\acute{o}, \dot{\imath}), (m_{r_c}(\acute{o}, \dot{\imath})), (m_{r_c}(\acute{o}, \dot{\imath}))) \in \dot{\bar{R}}$ And $((\dot{\imath}, \dot{t}), (m_{r_c}(\dot{\imath}, \dot{t})), (m_{r_c}(\dot{\imath}, \dot{t}))) \in \dot{\bar{R}}$

$$\Longrightarrow \dot{\bar{R}} \circ \dot{\bar{R}} \subseteq \dot{\bar{R}}. \tag{43}$$

Conversely suppose that $\dot{\bar{R}} \circ \dot{\bar{R}} \subseteq \dot{\bar{R}}$, then.

For $((\acute{o}, \dot{\imath}), (m_{r_c}(\acute{o}, \dot{\imath}), (m_{r_c}(\acute{o}, \dot{\imath}))) \in \dot{\bar{R}}$ and $((\dot{\imath}, \dot{t}), (m_{r_c}(\dot{\imath}, \dot{t})), (m_{r_c}(\dot{\imath}, \dot{t}))) \in \dot{\bar{R}}$

$$\left((\acute{o}, \dot{t}), \left(m_{r_c}(\acute{o}, \dot{t})\right), \left(m_{r_c}(\acute{o}, \dot{t})\right)\right) \in \dot{\bar{R}}. \tag{44}$$

Thus $\dot{\bar{R}}$ is a CPyFS transitive relation on CPyFSS$\dot{T}$. □

Theorem 3. *A CPyFSR $\dot{\bar{R}}$ is CPyFS equivalence relation on a CPyFSS $\dot{T}$ iff $\dot{\bar{R}} \circ \dot{\bar{R}} = \dot{\bar{R}}$.*

Proof 3. Suppose that $((\acute{o}, \dot{\imath}), (m_{r_c}(\acute{o}, \dot{\imath}), (m_{r_c}(\acute{o}, \dot{\imath}))) \in \dot{\bar{R}}$,

Then by the definition of CPyFS symmetric relation,

$$\left((\dot{\imath}, \acute{o}), \left(m_{r_c}(\dot{\imath}, \acute{o})\right), \left(m_{r_c}(\dot{\imath}, \acute{o})\right)\right) \in \dot{\bar{R}}. \tag{45}$$

Now by the definition of CPyFS transitive relation,

$$\left((\acute{o}, \acute{o})\left[r_{m_r}(\acute{o}, \acute{o})\right] e^{q_{m_r}(\acute{o}, \acute{o})\pi i}, \left[r_{m_r}(\acute{o}, \acute{o})\right] e^{q_{m_r}(\acute{o}, \acute{o})\pi i}\right) \in \dot{\bar{R}}. \tag{46}$$

However, by the definition of CPyFS composite relation,

$$\left((\acute{o}, \acute{o})\left[r_{m_r}(\acute{o}, \acute{o})\right] e^{q_{m_r}(\acute{o}, \acute{o})\pi i}, \left[r_{m_r}(\acute{o}, \acute{o})\right] e^{q_{m_r}(\acute{o}, \acute{o})\pi i}\right) \in \dot{\bar{R}} \circ \dot{\bar{R}}. \tag{47}$$

Hence,

$$\dot{\bar{R}} \subseteq \dot{\bar{R}} \circ \dot{\bar{R}}. \tag{48}$$

Conversely, assume that

$$\left((\acute{o}, \dot{\imath}), (m_{r_c}(\acute{o}, \dot{\imath}), \left(m_{r_c}(\acute{o}, \dot{\imath})\right)\right) \in \dot{\bar{R}} \circ \dot{\bar{R}}. \tag{49}$$

Then there exist $\dot{t} \in \dot{T} \ni ((\acute{o}, \dot{t}), ([r_{m_r}(\acute{o}, \dot{t})] e^{q_{m_r}(\acute{o}, \dot{t})\pi i}, [r_{m_r}(\acute{o}, \dot{t})] e^{q_{m_r}(\acute{o}, \dot{t})\pi i})) \in \dot{\bar{R}}$ and

$$\left((\dot{t}, \dot{\imath}), \left(\left[r_{m_r}(\dot{t}, \dot{\imath})\right] e^{q_{m_r}(\dot{t}, \dot{\imath})\pi i}, \left[r_{m_r}(\dot{t}, \dot{\imath})\right] e^{q_{m_r}(\dot{t}, \dot{\imath})\pi i}\right)\right) \in \dot{\bar{R}}. \tag{50}$$

However, □ is a CPyFS equivalence relation on CPyFSS $\dot{T}$, so $\dot{\bar{R}}$ is also CPyFS transitive relation. Therefore,

$$\Rightarrow \dot{\bar{R}} \circ \dot{\bar{R}} \subseteq \dot{\bar{R}}. \tag{51}$$

Henceforth, (48) and (51),

$$\dot{\bar{R}} \circ \dot{\bar{R}} = \dot{\bar{R}}. \tag{52}$$

□

4. Applications

Here, is an application of the proposed concepts to select the best blockchain technology (BCT) by applying the idea of complex Pythagorean fuzzy soft relation (CPyFSR) and their types.

4.1. Blockchain Technology (BCT). Blockchain is one of the most talked-about technologies in business right now. BCT has the potential to drive major changes and create new opportunities across industries from banking and cybersecurity to intellectual property and healthcare. BCT is a database system that preserves and stores data in a way that enables various organizations and people to reliably share access to the same data in real time while alleviating concerns about security, privacy, and control. The technology provides a reliable technique for individuals to contract directly with each other, without an intermediary like a government, bank, or other third parties. Figure 1 shows the algorithm of the application.

Firstly, express the universal set that consists of three types of BCT. The universal set consists of three types of BCT i.e., $\dot{\alpha}_1$ = Public blockchains, $\dot{\alpha}_2$ = Private blockchain and $\dot{\alpha}_3$ = Consortium blockchains. Figure 2 discusses the types of BCT.

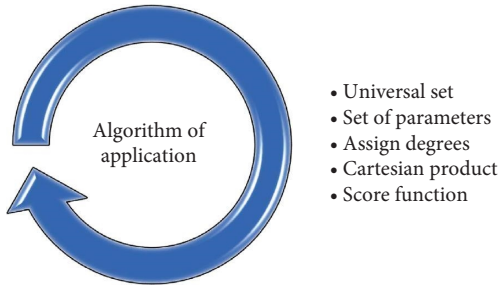

Figure 1: Algorithm of application.

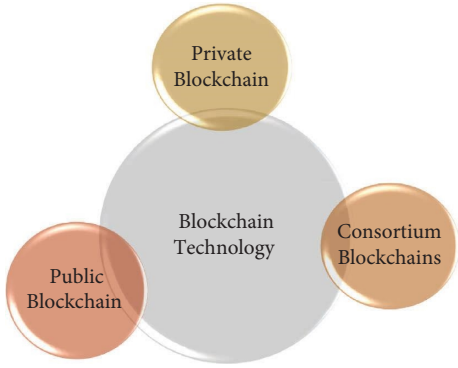

Figure 2: Summary of BCT.

4.1.1. Public Blockchains. Public blockchains are non-restrictive, permissionless distributed ledger systems. They are open networks that allow anyone to participate in the network. Public blockchains are generally secure if the users rigidly follow security guidelines and procedures.

4.1.2. Private (or Managed) Blockchains. Private blockchains are frequently used within an association or enterprise where only nominated members are applicants of a blockchain network. The level of security, authorizations, permissions, and availability is in the hands of the monitoring organizations.

4.1.3. Consortium Blockchains. Consortium blockchains are a semi-decentralized form where more than one association accomplishes a blockchain network. More than one association can act as a node in this nature of blockchains and exchange information. Consortium blockchains are classically used by banks, government organizations, etc.

Secondly, describe the parameter of the BCT. Figure 3 shows the summary of BCT parameters.

(1) Increased Capacity. The most amazing thing about this BCT is that it increases the capacity of the entire network. The average number of transactions successfully recorded per second in the BCT.

(2) Better Security. BCT produces a structure of data with inherent security qualities. BCT is considered more secure than its contemporaries because of the lack of a single point of failure.

(3) Faster Settlement. It can explain this problem by employing blockchains as they can allow money transfer at certainly fast speeds. This eventually saves a lot of time and money from these establishments and provides accessibility to the consumer also.

(4) Decentralized System. Decentralized technology gives the power to store resources in a network without the oversight and control of a single person organization or entity. BCT shows to be an operative tool for decentralizing the web so it is a small revolt in the Internet's world.

(5) Distributed Ledger. The distributed ledger allows anyone with the required access to view the ledger and makes the process transparent and reliable. This distributed computational power across the computer to ensure a better outcome.

The expert examines the BCT in which characteristic of all parameters. Let observations $(\mathscr{F}, \mathscr{A})$ by experts individually. They give the value of membership and non-membership on the base of parameters.

Assume that their corresponding membership and non-membership matrices are as follows.

$$(\mathscr{F}, \mathscr{A}) = \begin{pmatrix} \begin{pmatrix} 0.6e^{0.5\pi i}, \\ 0.5e^{0.6\pi i} \end{pmatrix} & \begin{pmatrix} 0.5e^{0.3\pi i}, \\ 0.4e^{0.8\pi i} \end{pmatrix} & \begin{pmatrix} 0.4e^{0.7\pi i}, \\ 0.2e^{0.5\pi i} \end{pmatrix} & \begin{pmatrix} 0.7e^{0.7\pi i}, \\ 0.2e^{0.3\pi i} \end{pmatrix} \\ \begin{pmatrix} 0.7e^{0.7\pi i}, \\ 0.2e^{0.3\pi i} \end{pmatrix} & \begin{pmatrix} 0.3e^{0.4\pi i}, \\ 0.6e^{0.7\pi i} \end{pmatrix} & \begin{pmatrix} 0.5e^{0.9\pi i}, \\ 0.3e^{0.1\pi i} \end{pmatrix} & \begin{pmatrix} 0.9e^{0.4\pi i}, \\ 0.3e^{0.2\pi i} \end{pmatrix} \\ \begin{pmatrix} 0.8e^{0.4\pi i}, \\ 0.3e^{0.3\pi i} \end{pmatrix} & \begin{pmatrix} 0.6e^{0.9\pi i}, \\ 0.1e^{0.2\pi i} \end{pmatrix} & \begin{pmatrix} 0.8e^{0.6\pi i}, \\ 0.3e^{0.5\pi i} \end{pmatrix} & \begin{pmatrix} 0.5e^{0.8\pi i}, \\ 0.6e^{0.3\pi i} \end{pmatrix} \\ \begin{pmatrix} 0.9e^{0.6\pi i}, \\ 0.4e^{0.2\pi i} \end{pmatrix} & \begin{pmatrix} 0.7e^{0.6\pi i}, \\ 0.4e^{0.4\pi i} \end{pmatrix} & \begin{pmatrix} 0.6e^{0.4\pi i}, \\ 0.3e^{0.3\pi i} \end{pmatrix} & \begin{pmatrix} 0.9e^{0.6\pi i}, \\ 0.1e^{0.4\pi i} \end{pmatrix} \\ \begin{pmatrix} 0.5e^{0.5\pi i}, \\ 0.2e^{0.7\pi i} \end{pmatrix} & \begin{pmatrix} 0.8e^{0.6\pi i}, \\ 0.3e^{0.4\pi i} \end{pmatrix} & \begin{pmatrix} 0.7e^{0.8\pi i}, \\ 0e^{0.2\pi i} \end{pmatrix} & \begin{pmatrix} 0.7e^{0.4\pi i}, \\ 0.6e^{0.7\pi i} \end{pmatrix} \end{pmatrix}. \tag{53}$$

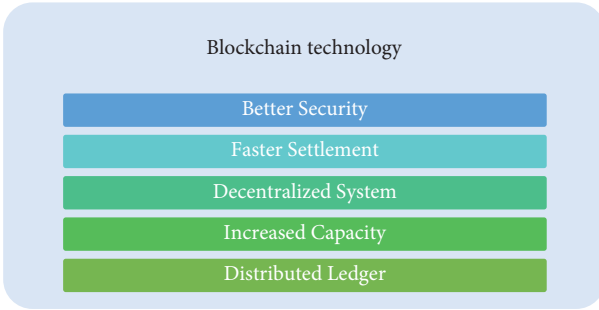

Figure 3: Summary of Blockchain technology parameters.

The first value of each parameter indicates the degrees of membership and non-membership assigned by experts to the $\dot{\alpha}_1$, the second value of each parameter indicates the degree of membership and non-membership assigned by experts to the $\dot{\alpha}_2$, the third value of each parameter shows the degree of membership and non-membership assigned by experts to the $\dot{\alpha}_3$ and the last value of each parameter shows the general belongingness of each parameter to the BCT and is denoted by λ.

Then, the CP of $(\mathscr{F}, \mathscr{A})$ shown in Table 2.

Now to calculate the score function, convert the complex values into real values to calculate the score values. Firstly, given values in complex polar form, i.e., $e^{\pi\vartheta i} = \cos\pi\vartheta + i\sin\pi\vartheta$. To convert the all-exponential values to the form of $a + ib$. i.e., $a + ib = re^{\pi i\theta}$, as $r = \sqrt{a^2 + b^2}$ and $e^{\pi i\theta} = \cos\pi(\theta) + i \quad \sin\pi(\theta)$. Then $a = r\cos\pi(\theta), b = \sin\pi(\theta)$. Here, π is just a notion and shows the cycle of the circle. Make polar form into standard form and then take modulus. After all, this process, apply to membership and non-membership score formula to $1/2\,(m_{\dot{\alpha}}^2 + q_{m_{\dot{\alpha}}}^2 - m_{\dot{\alpha}}^2 - q_{m_{\dot{\alpha}}}^2)$, as shown in Table 3.

Now, to determine the best BCT, take the largest value from each row and ignore the last column. The last column is the general belongingness of each BCT parameter. Now every BCT score is calculated by adding the product of these numerical degrees with the corresponding value of λ. The best BCT preferred by any user is the one that gets a greater numerical value than others. We do not study the numerical degree of the same parametric ordered pair's BCT because it is not a unique work to compare with itself. Now, estimate the score function in Table 4.

$$\begin{aligned} S(\dot{\alpha}_3) = {} & (0.155 \times 0.235) + (0.09 \times 0.145) + (0.18 \times -0.1) + (0.155 \times 0.235) + (0.38 \times -0.1) + (0.09 \times 0.145) \\ & + (0.255 \times -0.22) + (0.18 \times -0.1) + (0.38 \times -0.1) + (0.255 \times -0.22) = -0.125. \end{aligned} \tag{54}$$

Thus, public blockchains are the best BCT as compared to other blockchain technology.

5. Comparative Analysis

In this section, the innovative framework of CPyFSRs is compared to the numerous pre-existing structures in FSS theory, such as FSRs, CFSRs, IFSRs, CIFSRs, and PyFSRs.

5.1. Comparison of FSRs, CFSRs with CPyFSRs. The structure of FSS and CFSSs is explained by a membership degree which is a fuzzy number, and the associated relations are known as FSRs and CFSRs. FSRs and CFSRs are defined only by the membership degree. The FSRs in an ordered pair show only the effectiveness of the first parameter over the second. The FSRs have only one dimension and provide limited information. The CFSRs analyzed only the membership degree with the complex number. The CFSRs are basic two components, i.e., amplitude terms and phase terms. An amplitude term describes the strength of the different BCT, and the phase term is used to define the period over specified situations. Therefore, the CPyFSRs defined both the membership and non-membership degrees with complex numbers.

Assume that their corresponding membership of CFSRs matrices is as follows.

$$(\mathscr{F}, \mathscr{A}) = \begin{pmatrix} (0.6e^{0.5\pi i}) & (0.5e^{0.3\pi i}) & (0.4e^{0.7\pi i}) & (0.7e^{0.7\pi i}) \\ (0.7e^{0.7\pi i}) & (0.3e^{0.4\pi i}) & (0.5e^{0.9\pi i}) & (0.9e^{0.4\pi i}) \\ (0.8e^{0.4\pi i}) & (0.6e^{0.9\pi i}) & (0.8e^{0.6\pi i}) & (0.5e^{0.8\pi i}) \end{pmatrix}. \tag{55}$$

The first three values of each parameter indicate the degrees of membership assigned by experts, and the last value of each parameter shows the general belongingness of each parameter to the BCT and is denoted by λ. Then, its self CP is shown in Table 5:

5.2. IFSR and Cifsr with CPyFSRS. The IFSSs and CIFSSs are defined as membership and non-membership degrees. The related relations are known as IFSRs and CIFSRs. The IFSRs indicate the effectiveness and ineffectiveness of the first parameter over the second in an ordered pair. An IFSRs

Table 2: Cartesian product.

Ordered pair	$\dot{\alpha}_1$	$\dot{\alpha}_2$	$\dot{\alpha}_3$	λ
$(\acute{\alpha}_1, \acute{\alpha}_1)$	$\begin{pmatrix} 0.6e^{0.5\pi i}, \\ 0.5e^{0.6\pi i} \end{pmatrix}$	$\begin{pmatrix} 0.5e^{0.3\pi i}, \\ 0.4e^{0.8\pi i} \end{pmatrix}$	$\begin{pmatrix} 0.4e^{0.7\pi i}, \\ 0.2e^{0.5\pi i} \end{pmatrix}$	$\begin{pmatrix} 0.7e^{0.7\pi i}, \\ 0.2e^{0.3\pi i} \end{pmatrix}$
$(\acute{\alpha}_1, \acute{\alpha}_2)$	$\begin{pmatrix} 0.6e^{0.5\pi i}, \\ 0.5e^{0.6\pi i} \end{pmatrix}$	$\begin{pmatrix} 0.3e^{0.3\pi i}, \\ 0.6e^{0.8\pi i} \end{pmatrix}$	$\begin{pmatrix} 0.4e^{0.7\pi i}, \\ 0.3e^{0.5\pi i} \end{pmatrix}$	$\begin{pmatrix} 0.7e^{0.4\pi i}, \\ 0.3e^{0.3\pi i} \end{pmatrix}$
$(\acute{\alpha}_1, \acute{\alpha}_3)$	$\begin{pmatrix} 0.6e^{0.4\pi i}, \\ 0.5e^{0.6\pi i} \end{pmatrix}$	$\begin{pmatrix} 0.5e^{0.3\pi i}, \\ 0.4e^{0.8\pi i} \end{pmatrix}$	$\begin{pmatrix} 0.4e^{0.6\pi i}, \\ 0.3e^{0.5\pi i} \end{pmatrix}$	$\begin{pmatrix} 0.5e^{0.7\pi i}, \\ 0.6e^{0.3\pi i} \end{pmatrix}$
$(\acute{\alpha}_1, \acute{\alpha}_4)$	$\begin{pmatrix} 0.6e^{0.5\pi i}, \\ 0.5e^{0.6\pi i} \end{pmatrix}$	$\begin{pmatrix} 0.5e^{0.3\pi i}, \\ 0.4e^{0.8\pi i} \end{pmatrix}$	$\begin{pmatrix} 0.4e^{0.4\pi i}, \\ 0.3e^{0.5\pi i} \end{pmatrix}$	$\begin{pmatrix} 0.7e^{0.6\pi i}, \\ 0.2e^{0.4\pi i} \end{pmatrix}$
$(\acute{\alpha}_1, \acute{\alpha}_5)$	$\begin{pmatrix} 0.5e^{0.5\pi i}, \\ 0.5e^{0.7\pi i} \end{pmatrix}$	$\begin{pmatrix} 0.5e^{0.3\pi i}, \\ 0.4e^{0.8\pi i} \end{pmatrix}$	$\begin{pmatrix} 0.4e^{0.7\pi i}, \\ 0.2e^{0.5\pi i} \end{pmatrix}$	$\begin{pmatrix} 0.7e^{0.4\pi i}, \\ 0.6e^{0.7\pi i} \end{pmatrix}$
$(\acute{\alpha}_2, \acute{\alpha}_1)$	$\begin{pmatrix} 0.6e^{0.5\pi i}, \\ 0.5e^{0.6\pi i} \end{pmatrix}$	$\begin{pmatrix} 0.3e^{0.3\pi i}, \\ 0.6e^{0.8\pi i} \end{pmatrix}$	$\begin{pmatrix} 0.4e^{0.7\pi i}, \\ 0.3e^{0.5\pi i} \end{pmatrix}$	$\begin{pmatrix} 0.7e^{0.4\pi i}, \\ 0.3e^{0.3\pi i} \end{pmatrix}$
$(\acute{\alpha}_2, \acute{\alpha}_2)$	$\begin{pmatrix} 0.7e^{0.7\pi i}, \\ 0.2e^{0.3\pi i} \end{pmatrix}$	$\begin{pmatrix} 0.3e^{0.4\pi i}, \\ 0.6e^{0.7\pi i} \end{pmatrix}$	$\begin{pmatrix} 0.5e^{0.9\pi i}, \\ 0.3e^{0.1\pi i} \end{pmatrix}$	$\begin{pmatrix} 0.9e^{0.4\pi i}, \\ 0.3e^{0.2\pi i} \end{pmatrix}$
$(\acute{\alpha}_2, \acute{\alpha}_3)$	$\begin{pmatrix} 0.7e^{0.4\pi i}, \\ 0.3e^{0.3\pi i} \end{pmatrix}$	$\begin{pmatrix} 0.3e^{0.4\pi i}, \\ 0.6e^{0.7\pi i} \end{pmatrix}$	$\begin{pmatrix} 0.5e^{0.6\pi i}, \\ 0.3e^{0.5\pi i} \end{pmatrix}$	$\begin{pmatrix} 0.5e^{0.4\pi i}, \\ 0.6e^{0.3\pi i} \end{pmatrix}$
$(\acute{\alpha}_2, \acute{\alpha}_4)$	$\begin{pmatrix} 0.7e^{0.6\pi i}, \\ 0.4e^{0.3\pi i} \end{pmatrix}$	$\begin{pmatrix} 0.3e^{0.4\pi i}, \\ 0.6e^{0.7\pi i} \end{pmatrix}$	$\begin{pmatrix} 0.5e^{0.4\pi i}, \\ 0.3e^{0.3\pi i} \end{pmatrix}$	$\begin{pmatrix} 0.9e^{0.4\pi i}, \\ 0.3e^{0.4\pi i} \end{pmatrix}$
$(\acute{\alpha}_2, \acute{\alpha}_5)$	$\begin{pmatrix} 0.5e^{0.5\pi i}, \\ 0.2e^{0.7\pi i} \end{pmatrix}$	$\begin{pmatrix} 0.3e^{0.4\pi i}, \\ 0.6e^{0.7\pi i} \end{pmatrix}$	$\begin{pmatrix} 0.5e^{0.8\pi i}, \\ 0.3e^{0.2\pi i} \end{pmatrix}$	$\begin{pmatrix} 0.7e^{0.4\pi i}, \\ 0.6e^{0.7\pi i} \end{pmatrix}$
$(\acute{\alpha}_3, \acute{\alpha}_1)$	$\begin{pmatrix} 0.6e^{0.4\pi i}, \\ 0.5e^{0.6\pi i} \end{pmatrix}$	$\begin{pmatrix} 0.5e^{0.3\pi i}, \\ 0.4e^{0.8\pi i} \end{pmatrix}$	$\begin{pmatrix} 0.4e^{0.6\pi i}, \\ 0.3e^{0.5\pi i} \end{pmatrix}$	$\begin{pmatrix} 0.5e^{0.7\pi i}, \\ 0.6e^{0.3\pi i} \end{pmatrix}$
$(\acute{\alpha}_3, \acute{\alpha}_2)$	$\begin{pmatrix} 0.7e^{0.4\pi i}, \\ 0.3e^{0.3\pi i} \end{pmatrix}$	$\begin{pmatrix} 0.3e^{0.4\pi i}, \\ 0.6e^{0.7\pi i} \end{pmatrix}$	$\begin{pmatrix} 0.5e^{0.6\pi i}, \\ 0.3e^{0.5\pi i} \end{pmatrix}$	$\begin{pmatrix} 0.5e^{0.4\pi i}, \\ 0.6e^{0.3\pi i} \end{pmatrix}$
$(\acute{\alpha}_3, \acute{\alpha}_3)$	$\begin{pmatrix} 0.8e^{0.4\pi i}, \\ 0.3e^{0.3\pi i} \end{pmatrix}$	$\begin{pmatrix} 0.6e^{0.9\pi i}, \\ 0.1e^{0.2\pi i} \end{pmatrix}$	$\begin{pmatrix} 0.8e^{0.6\pi i}, \\ 0.3e^{0.5\pi i} \end{pmatrix}$	$\begin{pmatrix} 0.5e^{0.8\pi i}, \\ 0.6e^{0.3\pi i} \end{pmatrix}$
$(\acute{\alpha}_3, \acute{\alpha}_4)$	$\begin{pmatrix} 0.8e^{0.4\pi i}, \\ 0.4e^{0.3\pi i} \end{pmatrix}$	$\begin{pmatrix} 0.6e^{0.6\pi i}, \\ 0.4e^{0.4\pi i} \end{pmatrix}$	$\begin{pmatrix} 0.6e^{0.4\pi i}, \\ 0.3e^{0.5\pi i} \end{pmatrix}$	$\begin{pmatrix} 0.5e^{0.6\pi i}, \\ 0.6e^{0.4\pi i} \end{pmatrix}$
$(\acute{\alpha}_3, \acute{\alpha}_5)$	$\begin{pmatrix} 0.5e^{0.4\pi i}, \\ 0.3e^{0.7\pi i} \end{pmatrix}$	$\begin{pmatrix} 0.6e^{0.6\pi i}, \\ 0.3e^{0.4\pi i} \end{pmatrix}$	$\begin{pmatrix} 0.7e^{0.6\pi i}, \\ 0.3e^{0.5\pi i} \end{pmatrix}$	$\begin{pmatrix} 0.5e^{0.4\pi i}, \\ 0.6e^{0.7\pi i} \end{pmatrix}$
$(\acute{\alpha}_4, \acute{\alpha}_1)$	$\begin{pmatrix} 0.6e^{0.5\pi i}, \\ 0.5e^{0.6\pi i} \end{pmatrix}$	$\begin{pmatrix} 0.5e^{0.3\pi i}, \\ 0.4e^{0.8\pi i} \end{pmatrix}$	$\begin{pmatrix} 0.4e^{0.4\pi i}, \\ 0.3e^{0.5\pi i} \end{pmatrix}$	$\begin{pmatrix} 0.7e^{0.6\pi i}, \\ 0.2e^{0.4\pi i} \end{pmatrix}$
$(\acute{\alpha}_4, \acute{\alpha}_2)$	$\begin{pmatrix} 0.7e^{0.6\pi i}, \\ 0.4e^{0.3\pi i} \end{pmatrix}$	$\begin{pmatrix} 0.3e^{0.4\pi i}, \\ 0.6e^{0.7\pi i} \end{pmatrix}$	$\begin{pmatrix} 0.5e^{0.4\pi i}, \\ 0.3e^{0.3\pi i} \end{pmatrix}$	$\begin{pmatrix} 0.9e^{0.4\pi i}, \\ 0.3e^{0.4\pi i} \end{pmatrix}$
$(\acute{\alpha}_4, \acute{\alpha}_3)$	$\begin{pmatrix} 0.8e^{0.4\pi i}, \\ 0.4e^{0.3\pi i} \end{pmatrix}$	$\begin{pmatrix} 0.6e^{0.6\pi i}, \\ 0.4e^{0.4\pi i} \end{pmatrix}$	$\begin{pmatrix} 0.6e^{0.4\pi i}, \\ 0.3e^{0.5\pi i} \end{pmatrix}$	$\begin{pmatrix} 0.5e^{0.6\pi i}, \\ 0.6e^{0.4\pi i} \end{pmatrix}$
$(\acute{\alpha}_4, \acute{\alpha}_4)$	$\begin{pmatrix} 0.9e^{0.6\pi i}, \\ 0.4e^{0.2\pi i} \end{pmatrix}$	$\begin{pmatrix} 0.7e^{0.6\pi i}, \\ 0.4e^{0.4\pi i} \end{pmatrix}$	$\begin{pmatrix} 0.6e^{0.4\pi i}, \\ 0.3e^{0.3\pi i} \end{pmatrix}$	$\begin{pmatrix} 0.9e^{0.6\pi i}, \\ 0.1e^{0.4\pi i} \end{pmatrix}$
$(\acute{\alpha}_4, \acute{\alpha}_5)$	$\begin{pmatrix} 0.5e^{0.5\pi i}, \\ 0.4e^{0.7\pi i} \end{pmatrix}$	$\begin{pmatrix} 0.7e^{0.6\pi i}, \\ 0.4e^{0.4\pi i} \end{pmatrix}$	$\begin{pmatrix} 0.6e^{0.4\pi i}, \\ 0.3e^{0.3\pi i} \end{pmatrix}$	$\begin{pmatrix} 0.7e^{0.4\pi i}, \\ 0.6e^{0.7\pi i} \end{pmatrix}$
$(\acute{\alpha}_5, \acute{\alpha}_1)$	$\begin{pmatrix} 0.5e^{0.5\pi i}, \\ 0.5e^{0.7\pi i} \end{pmatrix}$	$\begin{pmatrix} 0.5e^{0.3\pi i}, \\ 0.4e^{0.8\pi i} \end{pmatrix}$	$\begin{pmatrix} 0.4e^{0.7\pi i}, \\ 0.2e^{0.5\pi i} \end{pmatrix}$	$\begin{pmatrix} 0.7e^{0.4\pi i}, \\ 0.6e^{0.7\pi i} \end{pmatrix}$
$(\acute{\alpha}_5, \acute{\alpha}_2)$	$\begin{pmatrix} 0.5e^{0.5\pi i}, \\ 0.2e^{0.7\pi i} \end{pmatrix}$	$\begin{pmatrix} 0.3e^{0.4\pi i}, \\ 0.6e^{0.7\pi i} \end{pmatrix}$	$\begin{pmatrix} 0.5e^{0.8\pi i}, \\ 0.3e^{0.2\pi i} \end{pmatrix}$	$\begin{pmatrix} 0.7e^{0.4\pi i}, \\ 0.6e^{0.7\pi i} \end{pmatrix}$
$(\acute{\alpha}_5, \acute{\alpha}_3)$	$\begin{pmatrix} 0.5e^{0.4\pi i}, \\ 0.3e^{0.7\pi i} \end{pmatrix}$	$\begin{pmatrix} 0.6e^{0.6\pi i}, \\ 0.3e^{0.4\pi i} \end{pmatrix}$	$\begin{pmatrix} 0.7e^{0.6\pi i}, \\ 0.3e^{0.5\pi i} \end{pmatrix}$	$\begin{pmatrix} 0.5e^{0.4\pi i}, \\ 0.6e^{0.7\pi i} \end{pmatrix}$
$(\acute{\alpha}_5, \acute{\alpha}_4)$	$\begin{pmatrix} 0.5e^{0.5\pi i}, \\ 0.4e^{0.7\pi i} \end{pmatrix}$	$\begin{pmatrix} 0.7e^{0.6\pi i}, \\ 0.4e^{0.4\pi i} \end{pmatrix}$	$\begin{pmatrix} 0.6e^{0.4\pi i}, \\ 0.3e^{0.3\pi i} \end{pmatrix}$	$\begin{pmatrix} 0.7e^{0.4\pi i}, \\ 0.6e^{0.7\pi i} \end{pmatrix}$
$(\acute{\alpha}_5, \acute{\alpha}_5)$	$\begin{pmatrix} 0.5e^{0.5\pi i}, \\ 0.2e^{0.7\pi i} \end{pmatrix}$	$\begin{pmatrix} 0.8e^{0.6\pi i}, \\ 0.3e^{0.4\pi i} \end{pmatrix}$	$\begin{pmatrix} 0.7e^{0.8\pi i}, \\ 0e^{0.2\pi i} \end{pmatrix}$	$\begin{pmatrix} 0.7e^{0.4\pi i}, \\ 0.6e^{0.7\pi i} \end{pmatrix}$

Table 3: Modulus of each complex number.

Ordered pair	$\dot{\varrho}_1$	$\dot{\varrho}_2$	$\dot{\varrho}_3$	λ
$(\acute{\sigma}_1, \acute{\sigma}_1)$	0	−0.23	0.18	0.425
$(\acute{\sigma}_1, \acute{\sigma}_2)$	0	−0.41	0.155	0.235
$(\acute{\sigma}_1, \acute{\sigma}_3)$	−0.045	−0.23	0.09	0.145
$(\acute{\sigma}_1, \acute{\sigma}_4)$	0	−0.23	−0.01	0.325
$(\acute{\sigma}_1, \acute{\sigma}_5)$	−0.12	−0.23	0.18	−0.1
$(\acute{\sigma}_2, \acute{\sigma}_1)$	0	−0.41	0.155	0.235
$(\acute{\sigma}_2, \acute{\sigma}_2)$	0.425	−0.3	0.48	0.42
$(\acute{\sigma}_2, \acute{\sigma}_3)$	0.235	−0.3	0.135	−0.02
$(\acute{\sigma}_2, \acute{\sigma}_4)$	0.3	−0.3	0.115	0.36
$(\acute{\sigma}_2, \acute{\sigma}_5)$	−0.015	−0.3	0.38	−0.1
$(\acute{\sigma}_3, \acute{\sigma}_1)$	−0.045	−0.23	0.09	0.145
$(\acute{\sigma}_3, \acute{\sigma}_2)$	0.235	−0.3	0.135	−0.02
$(\acute{\sigma}_3, \acute{\sigma}_3)$	0.31	0.56	0.33	0.22
$(\acute{\sigma}_3, \acute{\sigma}_4)$	0.275	0.2	0.09	0.045
$(\acute{\sigma}_3, \acute{\sigma}_5)$	−0.085	0.235	0.255	−0.22
$(\acute{\sigma}_4, \acute{\sigma}_1)$	0	−0.23	−0.01	0.325
$(\acute{\sigma}_4, \acute{\sigma}_2)$	0.3	−0.3	0.115	0.36
$(\acute{\sigma}_4, \acute{\sigma}_3)$	0.275	0.2	0.09	0.045
$(\acute{\sigma}_4, \acute{\sigma}_4)$	0.485	0.265	0.17	0.5
$(\acute{\sigma}_4, \acute{\sigma}_5)$	−0.075	0.265	0.17	−0.1
$(\acute{\sigma}_5, \acute{\sigma}_1)$	−0.12	−0.23	0.18	−0.1
$(\acute{\sigma}_5, \acute{\sigma}_2)$	−0.015	−0.3	0.38	−0.1
$(\acute{\sigma}_5, \acute{\sigma}_3)$	−0.085	0.235	0.255	−0.22
$(\acute{\sigma}_5, \acute{\sigma}_4)$	−0.075	0.265	0.17	−0.1
$(\acute{\sigma}_5, \acute{\sigma}_5)$	−0.015	0.375	0.545	−0.1

Table 4: Score function.

$\bar{\dot{R}}$	$(\acute{\sigma}_1, \acute{\sigma}_1)$	$(\acute{\sigma}_1, \acute{\sigma}_2)$	$(\acute{\sigma}_1, \acute{\sigma}_3)$	$(\acute{\sigma}_1, \acute{\sigma}_4)$	$(\acute{\sigma}_1, \acute{\sigma}_5)$	$(\acute{\sigma}_2, \acute{\sigma}_1)$	$(\acute{\sigma}_2, \acute{\sigma}_2)$	$(\acute{\sigma}_2, \acute{\sigma}_3)$	$(\acute{\sigma}_2, \acute{\sigma}_4)$
$\dot{\varrho}_i$	$\dot{\varrho}_3$	$\dot{\varrho}_3$	$\dot{\varrho}_3$	$\dot{\varrho}_1$	$\dot{\varrho}_3$	$\dot{\varrho}_3$	$\dot{\varrho}_3$	$\dot{\varrho}_1$	$\dot{\varrho}_1$
Highest degree	×	0.155	0.09	0	0.18	0.155	×	0.235	0.3
λ	×	0.235	0.145	0.325	−0.1	0.235	×	−0.02	0.36
$\bar{\dot{R}}$	$(\acute{\sigma}_2, \acute{\sigma}_5)$	$(\acute{\sigma}_3, \acute{\sigma}_1)$	$(\acute{\sigma}_3, \acute{\sigma}_2)$	$(\acute{\sigma}_3, \acute{\sigma}_3)$	$(\acute{\sigma}_3, \acute{\sigma}_4)$	$(\acute{\sigma}_3, \acute{\sigma}_5)$	$(\acute{\sigma}_4, \acute{\sigma}_1)$	$(\acute{\sigma}_4, \acute{\sigma}_2)$	$(\acute{\sigma}_4, \acute{\sigma}_3)$
$\dot{\varrho}_i$	$\dot{\varrho}_3$	$\dot{\varrho}_3$	$\dot{\varrho}_1$	$\dot{\varrho}_2$	$\dot{\varrho}_1$	$\dot{\varrho}_3$	$\dot{\varrho}_1$	$\dot{\varrho}_1$	$\dot{\varrho}_1$
Highest degree	0.38	0.09	0.235	×	0.275	0.255	0	0.3	0.275
λ	−0.1	0.145	−0.02	×	0.045	−0.22	0.325	0.36	0.045
$\bar{\dot{R}}$	$(\acute{\sigma}_4, \acute{\sigma}_4)$	$(\acute{\sigma}_4, \acute{\sigma}_5)$	$(\acute{\sigma}_5, \acute{\sigma}_1)$	$(\acute{\sigma}_5, \acute{\sigma}_2)$	$(\acute{\sigma}_5, \acute{\sigma}_3)$	$(\acute{\sigma}_5, \acute{\sigma}_4)$	$(\acute{\sigma}_5, \acute{\sigma}_5)$		
$\dot{\varrho}_i$	$\dot{\varrho}_1$	$\dot{\varrho}_2$	$\dot{\varrho}_3$	$\dot{\varrho}_3$	$\dot{\varrho}_3$	$\dot{\varrho}_2$	$\dot{\varrho}_3$		
Highest degree	×	0.265	0.18	0.38	0.255	0.265	×		
λ	×	−0.1	−0.1	−0.1	−0.22	−0.1	×		

cannot characterize such problems that include time, so they are provided incomplete information. The CIFSRs are examined the degrees of membership and non-membership with complex numbers. They explain both the amplitude term and phase term. The innovative structure of CPyFSRs discusses the degree of membership and non-membership with complex numbers and increases the space of CIFSRs. So, it provides comprehensive information on any problem.

Assume that their corresponding membership and non-membership of CIFSRs matrices are as follows.

$$(\mathscr{F}, \mathscr{A}) = \begin{pmatrix} \begin{pmatrix} 0.3e^{0.5\pi i}, \\ 0.5e^{0.4\pi i} \end{pmatrix} & \begin{pmatrix} 0.5e^{0.1\pi i}, \\ 0.4e^{0.8\pi i} \end{pmatrix} & \begin{pmatrix} 0.4e^{0.3\pi i}, \\ 0.2e^{0.5\pi i} \end{pmatrix} & \begin{pmatrix} 0.7e^{0.7\pi i}, \\ 0.2e^{0.3\pi i} \end{pmatrix} \\ \begin{pmatrix} 0.7e^{0.7\pi i}, \\ 0.2e^{0.3\pi i} \end{pmatrix} & \begin{pmatrix} 0.3e^{0.4\pi i}, \\ 0.6e^{0.5\pi i} \end{pmatrix} & \begin{pmatrix} 0.5e^{0.9\pi i}, \\ 0.3e^{0.1\pi i} \end{pmatrix} & \begin{pmatrix} 0.6e^{0.4\pi i}, \\ 0.3e^{0.2\pi i} \end{pmatrix} \\ \begin{pmatrix} 0.5e^{0.4\pi i}, \\ 0.3e^{0.3\pi i} \end{pmatrix} & \begin{pmatrix} 0.6e^{0.6\pi i}, \\ 0.1e^{0.2\pi i} \end{pmatrix} & \begin{pmatrix} 0.5e^{0.3\pi i}, \\ 0.3e^{0.5\pi i} \end{pmatrix} & \begin{pmatrix} 0.5e^{0.5\pi i}, \\ 0.4e^{0.3\pi i} \end{pmatrix} \end{pmatrix} \tag{56}$$

Table 5: Cartesian product.

Ordered pair	$\dot{\varrho}_1$	$\dot{\varrho}_2$	$\dot{\varrho}_3$	λ
$(\acute{\varrho}_1, \acute{\varrho}_1)$	$\left(0.6e^{0.5\pi i}\right)$	$\left(0.5e^{0.3\pi i}\right)$	$\left(0.4e^{0.7\pi i}\right)$	$\left(0.7e^{0.7\pi i}\right)$
$(\acute{\varrho}_1, \acute{\varrho}_2)$	$\left(0.6e^{0.5\pi i}\right)$	$\left(0.3e^{0.3\pi i}\right)$	$\left(0.4e^{0.7\pi i}\right)$	$\left(0.7e^{0.4\pi i}\right)$
$(\acute{\varrho}_1, \acute{\varrho}_3)$	$\left(0.6e^{0.4\pi i}\right)$	$\left(0.5e^{0.3\pi i}\right)$	$\left(0.4e^{0.6\pi i}\right)$	$\left(0.5e^{0.7\pi i}\right)$
$(\acute{\varrho}_2, \acute{\varrho}_1)$	$\left(0.6e^{0.5\pi i}\right)$	$\left(0.3e^{0.3\pi i}\right)$	$\left(0.4e^{0.7\pi i}\right)$	$\left(0.7e^{0.4\pi i}\right)$
$(\acute{\varrho}_2, \acute{\varrho}_2)$	$\left(0.7e^{0.7\pi i}\right)$	$\left(0.3e^{0.4\pi i}\right)$	$\left(0.5e^{0.9\pi i}\right)$	$\left(0.9e^{0.4\pi i}\right)$
$(\acute{\varrho}_2, \acute{\varrho}_3)$	$\left(0.7e^{0.4\pi i}\right)$	$\left(0.3e^{0.4\pi i}\right)$	$\left(0.5e^{0.6\pi i}\right)$	$\left(0.5e^{0.4\pi i}\right)$
$(\acute{\varrho}_3, \acute{\varrho}_1)$	$\left(0.6e^{0.4\pi i}\right)$	$\left(0.5e^{0.3\pi i}\right)$	$\left(0.4e^{0.6\pi i}\right)$	$\left(0.5e^{0.7\pi i}\right)$
$(\acute{\varrho}_3, \acute{\varrho}_2)$	$\left(0.7e^{0.4\pi i}\right)$	$\left(0.3e^{0.4\pi i}\right)$	$\left(0.5e^{0.6\pi i}\right)$	$\left(0.5e^{0.4\pi i}\right)$
$(\acute{\varrho}_3, \acute{\varrho}_3)$	$\left(0.8e^{0.4\pi i}\right)$	$\left(0.6e^{0.9\pi i}\right)$	$\left(0.8e^{0.6\pi i}\right)$	$\left(0.5e^{0.8\pi i}\right)$

Table 6: Cartesian product.

Ordered pair	$\dot{\varrho}_1$	$\dot{\varrho}_2$	$\dot{\varrho}_3$	λ
$(\acute{\varrho}_1, \acute{\varrho}_1)$	$\begin{pmatrix}0.3e^{0.5\pi i},\\0.5e^{0.4\pi i}\end{pmatrix}$	$\begin{pmatrix}0.5e^{0.1\pi i},\\0.4e^{0.8\pi i}\end{pmatrix}$	$\begin{pmatrix}0.4e^{0.3\pi i},\\0.2e^{0.5\pi i}\end{pmatrix}$	$\begin{pmatrix}0.7e^{0.7\pi i},\\0.2e^{0.3\pi i}\end{pmatrix}$
$(\acute{\varrho}_1, \acute{\varrho}_2)$	$\begin{pmatrix}0.3e^{0.5\pi i},\\0.5e^{0.4\pi i}\end{pmatrix}$	$\begin{pmatrix}0.3e^{0.1\pi i},\\0.6e^{0.8\pi i}\end{pmatrix}$	$\begin{pmatrix}0.4e^{0.3\pi i},\\0.3e^{0.5\pi i}\end{pmatrix}$	$\begin{pmatrix}0.6e^{0.4\pi i},\\0.3e^{0.3\pi i}\end{pmatrix}$
$(\acute{\varrho}_1, \acute{\varrho}_3)$	$\begin{pmatrix}0.3e^{0.4\pi i},\\0.5e^{0.4\pi i}\end{pmatrix}$	$\begin{pmatrix}0.5e^{0.1\pi i},\\0.4e^{0.8\pi i}\end{pmatrix}$	$\begin{pmatrix}0.4e^{0.3\pi i},\\0.3e^{0.5\pi i}\end{pmatrix}$	$\begin{pmatrix}0.5e^{0.5\pi i},\\0.4e^{0.3\pi i}\end{pmatrix}$
$(\acute{\varrho}_2, \acute{\varrho}_1)$	$\begin{pmatrix}0.3e^{0.5\pi i},\\0.5e^{0.4\pi i}\end{pmatrix}$	$\begin{pmatrix}0.3e^{0.1\pi i},\\0.6e^{0.8\pi i}\end{pmatrix}$	$\begin{pmatrix}0.4e^{0.3\pi i},\\0.3e^{0.5\pi i}\end{pmatrix}$	$\begin{pmatrix}0.6e^{0.4\pi i},\\0.3e^{0.3\pi i}\end{pmatrix}$
$(\acute{\varrho}_2, \acute{\varrho}_2)$	$\begin{pmatrix}0.7e^{0.7\pi i},\\0.2e^{0.3\pi i}\end{pmatrix}$	$\begin{pmatrix}0.3e^{0.4\pi i},\\0.6e^{0.5\pi i}\end{pmatrix}$	$\begin{pmatrix}0.5e^{0.9\pi i},\\0.3e^{0.1\pi i}\end{pmatrix}$	$\begin{pmatrix}0.6e^{0.4\pi i},\\0.3e^{0.2\pi i}\end{pmatrix}$
$(\acute{\varrho}_2, \acute{\varrho}_3)$	$\begin{pmatrix}0.5e^{0.4\pi i},\\0.3e^{0.3\pi i}\end{pmatrix}$	$\begin{pmatrix}0.3e^{0.4\pi i},\\0.6e^{0.5\pi i}\end{pmatrix}$	$\begin{pmatrix}0.5e^{0.3\pi i},\\0.3e^{0.5\pi i}\end{pmatrix}$	$\begin{pmatrix}0.5e^{0.4\pi i},\\0.4e^{0.3\pi i}\end{pmatrix}$
$(\acute{\varrho}_3, \acute{\varrho}_1)$	$\begin{pmatrix}0.3e^{0.4\pi i},\\0.5e^{0.4\pi i}\end{pmatrix}$	$\begin{pmatrix}0.5e^{0.1\pi i},\\0.4e^{0.8\pi i}\end{pmatrix}$	$\begin{pmatrix}0.4e^{0.3\pi i},\\0.3e^{0.5\pi i}\end{pmatrix}$	$\begin{pmatrix}0.5e^{0.5\pi i},\\0.4e^{0.3\pi i}\end{pmatrix}$
$(\acute{\varrho}_3, \acute{\varrho}_2)$	$\begin{pmatrix}0.5e^{0.4\pi i},\\0.3e^{0.3\pi i}\end{pmatrix}$	$\begin{pmatrix}0.3e^{0.4\pi i},\\0.6e^{0.5\pi i}\end{pmatrix}$	$\begin{pmatrix}0.5e^{0.3\pi i},\\0.3e^{0.5\pi i}\end{pmatrix}$	$\begin{pmatrix}0.5e^{0.4\pi i},\\0.4e^{0.3\pi i}\end{pmatrix}$
$(\acute{\varrho}_3, \acute{\varrho}_3)$	$\begin{pmatrix}0.5e^{0.4\pi i},\\0.3e^{0.3\pi i}\end{pmatrix}$	$\begin{pmatrix}0.6e^{0.6\pi i},\\0.1e^{0.2\pi i}\end{pmatrix}$	$\begin{pmatrix}0.5e^{0.3\pi i},\\0.3e^{0.5\pi i}\end{pmatrix}$	$\begin{pmatrix}0.5e^{0.5\pi i},\\0.4e^{0.3\pi i}\end{pmatrix}$

The first three value of each parameter indicates the degrees of membership and non-membership assigned by experts, and the last value of each parameter shows the general belongingness of each parameter to the BCT and is denoted by λ. Then, its CP is shown in Table 6:

5.3. PyFSRs with CPyFSRS. The structure of PyFSS is explained by membership and non-membership degrees and the associated relations are known as PyFSRs. The structure of PyFSRs is improved by the limitation of FSRs and IFSRs, but they do not provide the time duration. The innovative structure of CPyFSRs discusses the degree of membership and non-membership with complex numbers and increases the space of CIFSRs. So, it provides comprehensive information on any problem. Table 7 summarizes the comparative study of CPyFSRs with a pre-defined structure.

Table 7: Summary of comparative analysis based on the structure.

Structure	Membership	Non-membership	Multi-dimension	Space
SR	No	No	No	No
FSR	Yes	No	No	n = 1
CFSR	Yes	No	Yes	n = 1
IFSR	Yes	Yes	No	n = 1
CIFSR	Yes	Yes	Yes	n = 1
PyFSR	Yes	Yes	No	n = 1
CPyFSR	Yes	Yes	Yes	n = 2

6. Conclusion

This paper defined the novel concept of CPyFSRs by using the CP of two CPyFSS. Furthermore, various types of CPyFSRs are also discussed, such as CPyFS-converse relation, CPyFS-reflexive relation, CPyFS-irreflexive relation, CPyFS symmetric relation, CPyFS anti-symmetric relation, CPyFS asymmetric relation, CPyFS-complete relation, CPyFS transitive relation, CPyFS equivalence relation, CPyFS-partial order relation, CPyFS-strict order relation, CPyFS preorder relation, and CPyFS equivalence classes. Some outcomes were proved with appropriate examples. Moreover, this novel concept of CPyFSRs has used the application of BCT. The goal of this application is to find the most effective BCT. The BCT represents the different parameters. The expert gives the membership and non-membership values of each BCT parameter. Then, using the score function, they choose the best BCT based on a set of parameters. The score function is used in this article to choose the best object, or anything based on some parameters. Finally, the innovative framework of the CPyFSRs is the more generalization form of all the pre-determined structures. Because it discusses both the degrees of membership and non-membership with complex numbers. The CPyFSRs can solve periodicity.The proposed work is more generalized then the bundle of exiting ideas, for instance, fuzzy relations, soft relations, complex fuzzy relations, fuzzy soft relations, complex fuzzy soft relations, intuitionistic fuzzy relations, intuitionistic fuzzy soft relations, complex intuitionistic fuzzy relations, complex intuitionistic fuzzy soft relations, Pythagorean fuzzy soft relations, and complex Pythagorean fuzzy soft relations, they all are the special cases of the pioneered relations.For better approach in the future, we aim to utilize different types of aggregation operators, hybrid aggregation operators, similarity measures, distance measures, TOPSIS technique, VIKOR technique, AHP technique, and MARCOS technique in the environment of CPyFSR and justified their application with the help of medical diagnosis, pattern recognition, network signals, artificial intelligence, risk analysis, and game theory are to enhance the quality of the presented information.

Data Availability

All the data used is given in the paper.

Conflicts of Interest

The authors do not have any conflicts.

Acknowledgments

This work was supported in part by the "Regional Innovation Strategy (RIS)" through the National Research Foundation of Korea (NRF) funded by the Ministry of Education (MOE) (2021RIS-001 (1345341783)) and the Brain Pool program funded by the Ministry of Science and ICT through the National Research Foundation of Korea (2022H1D3A2A02060097).

References

[1] L. A. Zadeh, "Fuzzy sets," *Information and Control*, vol. 8, no. 3, pp. 338–353, 1965.
[2] H. J. Zimmermann, *Fuzzy Set Theory—And its Applications*, Springer Science & Business Media, Berlin, 2011.
[3] J. Maiers and Y. S. Sherif, "Applications of fuzzy set theory," *IEEE Transactions on Systems, Man, and Cybernetics*, no. 1, pp. 175–189, 1985.
[4] D. W. Roberts, "Ordination on the basis of fuzzy set theory," *Vegetatio*, vol. 66, no. 3, pp. 123–131, 1986.
[5] C. Kahraman, *Fuzzy Applications in Industrial Engineering*, vol. 201, Springer, Heidelberg, 2006..
[6] J. M. Mendel, "Fuzzy logic systems for engineering: a tutorial," *Proceedings of the IEEE*, vol. 83, no. 3, pp. 345–377, 1995.
[7] W. C. Nemitz, "Fuzzy relations and fuzzy functions," *Fuzzy Sets and Systems*, vol. 19, no. 2, pp. 177–191, 1986.
[8] M. S. Yang and H. M. Shih, "Cluster analysis based on fuzzy relations," *Fuzzy Sets and Systems*, vol. 120, no. 2, pp. 197–212, 2001.
[9] D. Ramot, R. Milo, M. Friedman, and A. Kandel, "Complex fuzzy sets," *IEEE Transactions on Fuzzy Systems*, vol. 10, no. 2, pp. 171–186, 2002.
[10] B. Hu, L. Bi, and S. Dai, "The orthogonality between complex fuzzy sets and its application to signal detection," *Symmetry*, vol. 9, no. 9, 175 pages, 2017.
[11] C. Li and C. H. Tu, "Complex neural fuzzy system and its application on multi-class prediction—a novel approach using complex fuzzy sets, IIM and multi-swarm learning," *Applied Soft Computing*, vol. 84, Article ID 105735, 2019.
[12] G. Zhang, T. S. Dillon, K. Y. Cai, J. Ma, and J. Lu, "Operation properties and δ-equalities of complex fuzzy sets," *International Journal of Approximate Reasoning*, vol. 50, no. 8, pp. 1227–1249, 2009.
[13] M. Khan, M. Zeeshan, S. Z. Song, and S. Iqbal, "Types of complex fuzzy relations with applications in future commission market," *Journal of Mathematics*, vol. 2021, Article ID 6685977, 14 pages, 2021.
[14] D. Molodtsov, "Soft set theory—first results," *Computers & Mathematics with Applications*, vol. 37, no. 4-5, pp. 19–31, 1999.
[15] M. I. Ali, F. Feng, X. Liu, W. K. Min, and M. Shabir, "On some new operations in soft set theory," *Computers & Mathematics with Applications*, vol. 57, no. 9, pp. 1547–1553, 2009.
[16] B. Kostek, "Soft set approach to the subjective assessment of sound quality," in *Proceedings of the IEEE International Conference on Fuzzy Systems Proceedings. IEEE World Congress on Computational Intelligence (Cat. No. 98CH36228)*, vol. 1, pp. 669–674, IEEE, Anchorage, AK, USA, May 1998.
[17] M. M. Mushrif, S. Sengupta, and A. K. Ray, "Texture classification using a novel, soft-set theory based classification algorithm," in *Asian Conference on Computer Vision*, pp. 246–254, Springer, Berlin, Heidelberg, 2006.
[18] P. K. Maji, A. R. Roy, and R. Biswas, "An application of soft sets in a decision making problem," *Computers & Mathematics with Applications*, vol. 44, no. 8-9, pp. 1077–1083, 2002.
[19] K. V. Babitha and J. Sunil, "Soft set relations and functions," *Computers & Mathematics with Applications*, vol. 60, no. 7, pp. 1840–1849, 2010.
[20] J. H. Park, O. H. Kim, and Y. C. Kwun, "Some properties of equivalence soft set relations," *Computers & Mathematics with Applications*, vol. 63, no. 6, pp. 1079–1088, 2012.
[21] P. K. Maji, R. K. Biswas, and A. Roy, *Fuzzy Soft Sets*, 2001.

[22] Z. Kong, L. Wang, and Z. Wu, "Application of fuzzy soft set in decision making problems based on grey theory," *Journal of Computational and Applied Mathematics*, vol. 236, no. 6, pp. 1521–1530, 2011.

[23] K. Gogoi, A. Kr Dutta, and C. Chutia, "Application of fuzzy soft set theory in day to day problems," *International journal of computer Applications*, vol. 85, no. 7, pp. 27–31, 2014.

[24] M. J. Borah, T. J. Neog, and D. K. Sut, "Relations on fuzzy soft sets," *Journal of Fuzzy Mathematics*, vol. 2, no. 3, pp. 515–534, 2012.

[25] J. Močkoř and P. Hurtík, "Approximations of fuzzy soft sets by fuzzy soft relations with image processing application," *Soft Computing*, vol. 25, no. 10, pp. 6915–6925, 2021.

[26] P. Thirunavukarasu, R. Suresh, and V. Ashokkumar, "Theory of complex fuzzy soft set and its applications," *Int J Innov Res Sci Technol*, vol. 3, no. 10, pp. 13–18, 2017.

[27] D. E. Tamir, N. D. Rishe, and A. Kandel, "Complex fuzzy sets and complex fuzzy logic an overview of theory and applications," *Fifty years of fuzzy logic and its applications*, vol. 326, pp. 661–681, 2015.

[28] K. T. Atanassov, "Intuitionistic fuzzy sets," *Fuzzy Sets and Systems*, vol. 20, no. 1, pp. 87–96, 1986.

[29] E. Szmidt and J. Kacprzyk, "Distances between intuitionistic fuzzy sets," *Fuzzy Sets and Systems*, vol. 114, no. 3, pp. 505–518, 2000.

[30] T. Gerstenkorn and J. Mańko, "Correlation of intuitionistic fuzzy sets," *Fuzzy Sets and Systems*, vol. 44, no. 1, pp. 39–43, 1991.

[31] A. M. J. S. Alkouri and A. R. Salleh, "Complex intuitionistic fuzzy sets," *AIP Conference Proceedings*, vol. 1482, p. 464, 2012.

[32] R. T. Ngan, L. H. Son, M. Ali, D. E. Tamir, N. D. Rishe, and A. Kandel, "Representing complex intuitionistic fuzzy set by quaternion numbers and applications to decision making," *Applied Soft Computing*, vol. 87, Article ID 105961, 2020.

[33] Y. J. Xu, Y. K. Sun, and D. F. Li, "Intuitionistic fuzzy soft set," in *Proceedings of the 2010 2nd International Workshop on Intelligent Systems and Applications*, pp. 1–4, IEEE, Wuhan, China, May 2010.

[34] M. Agarwal, K. K. Biswas, and M. Hanmandlu, "Generalized intuitionistic fuzzy soft sets with applications in decision-making," *Applied Soft Computing*, vol. 13, no. 8, pp. 3552–3566, 2013.

[35] B. Dinda and T. K. Samanta, "Relations on intuitionistic fuzzy soft sets," 2012, https://arxiv.org/.

[36] T. Kumar and R. K. Bajaj, "On complex intuitionistic fuzzy soft sets with distance measures and entropies," *Journal of Mathematics*, vol. 2014, Article ID 972198, 12 pages, 2014.

[37] R. R. Yager, "Properties and applications of Pythagorean fuzzy sets," in *Imprecision and Uncertainty in Information Representation and Processing*, pp. 119–136, Springer, Cham, 2016.

[38] H. Garg, "New logarithmic operational laws and their aggregation operators for Pythagorean fuzzy set and their applications," *International Journal of Intelligent Systems*, vol. 34, no. 1, pp. 82–106, 2019.

[39] K. Ullah, T. Mahmood, Z. Ali, and N. Jan, "On some distance measures of complex Pythagorean fuzzy sets and their applications in pattern recognition," *Complex & Intelligent Systems*, vol. 6, no. 1, pp. 15–27, 2020.

[40] S. Dick, R. R. Yager, and O. Yazdanbakhsh, "On Pythagorean and complex fuzzy set operations," *IEEE Transactions on Fuzzy Systems*, vol. 24, no. 5, pp. 1009–1021, 2016.

[41] N. Jan, S. U. Rehman, A. Nasir, H. Aydi, and S. U. Khan, "Analysis of economic relationship using the concept of complex pythagorean fuzzy information," *Security and Communication Networks*, vol. 2021, 2021.

[42] X. D. Peng, Y. Yang, J. Song, and Y. Jiang, "Pythagorean fuzzy soft set and its application," *Computer Engineering*, vol. 41, no. 7, pp. 224–229, 2015.

[43] M. Akram, F. Wasim, and F. Karaaslan, "MCGDM with complex Pythagorean fuzzy-soft model," *Expert Systems*, vol. 38, no. 8, Article ID e12783, 2021.

[44] T. Gillpatric, S. Boğa, and O. Aldanmaz, "How can blockchain contribute to developing country economies? A literature review on application areas," *ECONOMICS-INNOVATIVE AND ECONOMICS RESEARCH JOURNAL*, vol. 10, no. 1, pp. 105–128, 2022.

Hindawi
Complexity
Volume 2022, Article ID 2691804, 26 pages
https://doi.org/10.1155/2022/2691804

Research Article

A Large-Scale Group Decision-Making Consensus Model considering the Experts' Adjustment Willingness Based on the Interactive Weights' Determination

Shizhen Bai,[1] **Hao He**,[1] **Dan Luo**,[1] **Mengke Ge**,[2] **Ruobing Yang**,[1] **and Xinrui Bi**[1]

[1]*School of Management, Harbin University of Commerce, Harbin 150028, China*
[2]*School of Mathematical Sciences, Mudanjiang Normal University, Mudanjiang 157012, China*

Correspondence should be addressed to Hao He; he156958505@163.com

Received 4 July 2022; Revised 20 August 2022; Accepted 3 September 2022; Published 17 November 2022

Academic Editor: Zeljko Stevic

This study proposes a large-scale group decision-making (LSGDM) consensus model considering the experts' adjustment willingness based on the interactive weights' determination, which can be applied to an LSGDM problem through a case of earthquake shelters. The main contributions of our research are of three aspects as follows. First, the determination method of the interactive weight, which obtains the DMs' attitude towards the decision-making results, is presented. The subgroups' weights are calculated, and the unit adjustment cost for each DM is defined. Second, we introduce an objective consensus threshold by the mean and variance of the consensus level for each subgroup. Subsequently, an identification rule is performed to determine the DM to be adjusted with the large difference and the low adjustment cost. And we developed a novel consensus adjustment method that takes the DMs' adjustment willingness into account to retain as much original information as possible. Thirdly, in order to reduce the subjectivity of the preset consensus threshold and the maximum number of iterations, an objective consensus termination condition that combines the current group consensus level and the consensus adjustment rate is put forward. Finally, the proposed model has demonstrated its effectiveness and superiority based on the comparative and sensitive analysis through a practical example.

1. Introduction

Group decision-making (GDM) is a process in which, under certain constraints, some experts or decision-makers (DMs) obtain the optimal from several feasible alternatives by expressing their opinions or preferences [1]. With the development of social, science, and technology, the complexity of decision-making events has becoming increasingly high [1], the ambiguity and uncertainty of the decision-making environment and context have become increasingly high, and the number and diversity of DMs participating in decision-making issues have increased rapidly. GDM has developed into large-scale group decision-making (LSGDM) [2–6], multiattribute LSGDM [7–10] and so on. Compared with GDM, the number of experts and DMs involved in LSGDM is larger, usually more than 20 [4, 9, 11, 12]. The differences in DMs' backgrounds and knowledge are greater, and thereby the consensus level among DMs is lower.

In recent years, LSGDM and fuzzy mathematics, game theory, computers, information technology, and other theories are being integrated and developed. The research of multiattribute LSGDM mainly focuses on the expression of DMs' or experts' preference information [13, 14], clustering [12], aggregation of group preference information [2, 13–16], determination of weight [3, 17, 18], and consensus reaching process (CRP) [2, 3, 9, 14, 19]. Many methods of expression of experts' preference information have proposed, such as fuzzy preference information, linguistic preference information, and random preference information. Liu et al. [20] transformed interval-valued intuitionistic fuzzy numbers into single-valued numbers and then proposed a two-stage regularized generalized canonical

correlation analysis decision-making method based on multiblock analysis to address the MALSGDM problem in the interval-valued intuitionistic fuzzy environment. Bai et al. [11] developed an LSGDM model with cooperative behavior based on social network analysis, considering the propagation of decision-makers' preferences by considering the propagation of DMs' preferences. Zhen et al. [21] proposed a computational model based on the use of extended linguistic hierarchies and used multigranularity linguistic distribution to provide interpretable aggregate linguistic results to experts in order to maximize information retention.

To reduce the dimension and complexity of the decision-making process, many clustering methods have been proposed and applied, such as the k-means clustering method [4, 12], fuzzy c-means clustering method [22], vector space-based clustering method [23], the and transitive closure clustering method [5]. Several researchers have proposed some novel clustering methods that can be used in LSGDM problems from different perspectives. For instance, Du et al. [6] developed a new clustering method considering both trust relationships and opinion similarity in a social network context. In this study, the k-means clustering method is utilized to reduce the dimension of the LSGDM problem.

However, despite a number of LSGDM methods having been proposed, these methods are used in specific situations. For instance, in Liu et al. [24]'s research, DMs cannot give complete and accurate evaluation information at once, and it is therefore difficult for decision-making groups to reach a consensus at once. In addition, some proposed LSGDM models include the determination process of the DMs' weight, but the weight of the DM is relatively simple, that is, the dynamics of the decision-making process are not taken into account. Next, CRP, a rather critical and essential process, reduces and even eliminates the conflicts of group and further improves the effectiveness and rationality of decision results. But in the existing literature, the threshold determination of many CRP is very subjective, which is not conducive to the objectivity of decision-making results. Therefore, our research intends to answer the following questions:

(a) How can we not only ensure that more DMs participate in the decision-making process but also make the results represent the opinions and attitudes of more DMs?

(b) How to obtain a more scientific and accurate consensus threshold?

(c) Under what conditions can the consensus adjustment process terminate automatically?

Based on the above analysis, an LSGDM consensus model considering the experts' adjustment willingness based on the interactive weights is proposed in this study. Its innovations and contributions are shown as follows:

(1) A novel method of weight determination has been developed, which considers the DMs' attitude towards the decision-making results, thereby ensuring the effective participation of DMs. Moreover, to improve the rationality of LSGDM, a harmonious degree is taken into account in the calculation of subgroups' weight.

(2) In the consensus measure process, a more reasonable consensus measure method is introduced, which considers both the differences between the DMs' opinion and the group opinion and the harmonious degree. In the consensus feedback process, an identification process is presented, which considers the unit adjustment cost for each DM. Then, a new adjustment process is constructed, which the evaluation information is less distorted or lost by considering the experts' adjustment willingness.

(3) An objective calculation method of the consensus threshold is presented from the perspective of the mean and variance of the consensus level, and then a termination condition that considers both the current consensus level and the consensus adjustment rate is designed to objectively terminate the CRP. It not only compares the current consensus level with the consensus threshold but also compares the consensus adjustment rate. As a result, this method can address the subjectivity and unreasonableness of the preset consensus threshold and the maximum number of iterations to a certain extent.

The remainder of this paper is organized as follows: In Section 2, we briefly summarize the recent literature review from the following four aspects: the aggregation of group preference information, the interactive process, the weight determination method, and the CRP. Section 3 introduces the multiattribute LSGDM problems, and then the k-means clustering method is used to classify the DMs into several subgroups. The determination methods of the DMs, the attributes, the subgroups, and the unit adjustment cost are shown in Section 4. Section 5 presents the proposed consensus model, which includes the consensus measurement process and the consensus feedback process and explains how its framework is conducted. In Section 6, the proposed model is applied to a case study to illustrate its effectiveness and rationality. The comparative analysis and the sensitivity analysis are performed in Sections 7 and 8, respectively, to further validate the proposed model. We draw the conclusions of this research in Section 9.

2. Literature Review

In this study, we summarize the existing literature from the following four perspectives: the aggregation of group preference information, the interactive process, the weight determination method, and the CRP.

2.1. Research on the Aggregation of Group Preference Information. Many scholars are interested in the aggregation of group preference information, which is mainly to obtain the results of group clustering. Xu et al. [19] presented

a two-stage method to support the CRP. The first stage classifies and obtains several subgroups by utilizing the self-organizing maps, and then an iterative algorithm is proposed to obtain the group preference for each subgroup. The second stage treats the group preference of each subcluster as the representative preference and collapses each subcluster to form a smaller and more manageable group. Liu et al. [25, 26] utilized the idea of principal component analysis (PCA), regarded attributes and decision makers as interval-valued intuitionistic fuzzy variables, transformed them into several independent variables, and then combined them with the traditional preference aggregation operator to obtain a decision-making method to solve the complex multi-attribute LSGDM problems. Chen et al. [27] developed a two-tier collective opinion generation framework integrating professional knowledge structure and risk preference to generate collective preference assessment, and thereby to obtain an accurate and reliable alternative ranking. In this paper, we utilize weighted arithmetic averaging (WAA) to aggregate each DM's opinion.

2.2. Studies about the Interactive Process. In reality, DMs often cannot give complete and accurate evaluation information at once, it is difficult for decision-making groups to reach a consensus at once, and thereby, the evaluation information needs to be continuously supplemented and adjusted. Therefore, the interactive process is not only necessary but significant to avoid the limitations of the DMs' opinions, improve the effectiveness of the DMs' participation, and ensure the rationality of the decision-making results.

Zeng et al. [28] developed an interactive procedure for GDM based on intuitionistic fuzzy preference relations, in which the similarity measures between the collective preference relation and the intuitionistic fuzzy ideal solution are used to rank the alternatives. Liao and Xu [29] established an optimization model for determining the weight and an interactive model of a multiattribute decision-making problem with hesitant fuzzy information to make the decision more reasonable. Ding et al. [30] proposed an interactive method to deal with the probability hesitation fuzzy multiattribute GDM problem with incomplete attribute weight information, which can reflect the DMs' subjective desirability and reduce the effect of unfair arguments on the decision results. Therefore, in our research, the interactive process is utilized for the experts' weights determination to improve the rationality of the decision-making results.

2.3. The Aspects of the Weight Determination. The determination of weight is a hot issue in LSGDM problems, which includes mainly the weights of experts' or DMs', the weights of the attributes of the alternatives, and the weights of the subgroups. For the determination method of experts or DMs, Meng et al. [14] integrated objectively cooperation networks and references network of DMs to construct a directed and weighted social network, and then obtained the DMs' relative weights. Wan et al. [31] show that DM's weight can be obtained through a programming model by minimizing the distance between individual semantics and collective. Liu et al. [17] proposed a double weight determination method of experts by utilizing mathematical programming and information entropy for multiattribute LSGDM in an interval-valued intuitionistic fuzzy environment. Wan et al. [32] developed a similarity determination method to calculate the weight for each DM and constructed two programming models to obtain the optimal weight for each attribute.

Related to the studies of the attributes' weight, Zhong et al. [4] developed an approach to determine the attributes and their weights based on the social media data relevant to decision-making problems by using the term frequency-inverse document frequency (TF-IDF) method. It considers both the experts' opinions and the views of stakeholders. In this study, the interactive process is introduced in the determination process of the DMs' weights. For the subgroups' weights, Liu et al. [8] set an equal weight for different subgroups, while Xu et al.[1] determine the subgroups' weights according to the size of the subgroup.

In this study, by considering the DMs' attitude towards the decision-making results (i.e., satisfaction degree), the DMs' weights are updated and obtained, and then the attributes' weights are obtained within the subgroups. The weights of the subgroups are calculated and updated by considering the number within the subgroup and the level of the subgroup's satisfaction degree (i.e., harmonious degree).

2.4. CRP Studies. CRP is a rather critical and essential segment in LSGDM problems [33, 34], which is reducing and eliminating the conflict of a group and improving the effectiveness and rationality of decision results. Zhong et al. [4] presented a multistage hybrid consensus-achieving model by integrating both cardinal consensus and ordinal consensus and applied it in the scene of the selection of a hotel for the centralized isolation of entry personnel during the COVID-19 epidemic. For the consensus feedback process in the CRP, experts may not tolerate their opinions being modified unrestricted during the CRP. Hence, all experts have an accepted modification for their opinions, which can be presented as the adjustment willingness. However, few studies have focused on the experts' adjustment willingness. Zhong et al. [5] proposed a nonthreshold consensus model, which includes an objective termination condition for CRP. It can reduce the subjectivity of the predefined consensus threshold and the maximum number of iterations to a certain extent. In addition, Wan et al. [35] developed a novel two-stage CRP method considering DM's willingness to modify preference information.

Therefore, our research presents an objective calculation method of the consensus threshold from the perspective of the mean and variance of the consensus level and then develops a termination condition that considers both the current consensus level and the consensus adjustment rate to objectively terminate the CRP.

2.5. Research on the Case Application. Many scholars have proposed many LSGDM approaches from the perspective of practice and application. Xiao et al. [36] established the civil engineering construction contractor selection framework in

the LSGDM environment by considering the interaction within and between the management layers of the consensus model. Chen et al. [37] determined passenger demands and evaluated their satisfaction by using a combination of online review analysis and LSGDM based on a case study of a high-speed rail system in China.

3. Preliminaries

3.1. The Multiattribute LSGDM Problems Description. LSGDM is the process of selecting the best option from the opinion of many DMs, who express their opinion based on the decision-making information provided for alternatives [11]. Accordingly, let $X = \{x1, \ldots, xp, \ldots, xP\}(P \geq 2)$ be the set of alternatives, $E = \{e1, \ldots, em, \ldots, eM\}(M \geq 20)$ be the set of experts and DMs, and $F = \{f1, \ldots, fn, \ldots, fN\}(N \geq 2)$ be the set of attributes for each alternative.

First, the DM em provides his or her evaluation information $Qm = (q_{pn}^m)P \times N(m = 1, \ldots, M)$, where q_{pn}^m represents the evaluation value of the attribute fn on the alternative xp for the DM em. Then, the DM em provides his or her allowed modification values θ_m^+ and θ_m^-, which represents, respectively, the DM em is allowed to modify the positive and negative range of the evaluation information q_{pn}^m they provide. It is noting that the allowed modification values represent the DMs' adjustment willingness and the values of θ_m^+ and θ_m^- are both positive. For instance, a DM em provides the values of q_{pn}^m, θ_m^+ and θ_m^-, the modification value of $q_{pn}^{m'}$ can be more acceptable in the interval $[\max(q_{pn}^m - \theta_m^-, 0), \min(q_{pn}^m + \theta_m^+, 1)]$. Note that the value of q_{pn}^m should be in the range [0, 1] before and after adjustment. The greater the value of $\theta_m^+ + \theta_m^-$, the lower the difficulty of adjusting the evaluation information, and the higher the concession degree of the DM em in order to reach group consensus. However, if the adjustment value exceeds the allowed modification range of the DM, it will pay an enormous adjustment cost, and the evaluation information of the DM will be forced to change, resulting in information distortion. Therefore, this situation is not considered in this paper.

In this paper, the weight vectors of attribute for each alternative are denoted as $wm = [w_1^m, \ldots, w_n^m, \ldots, w_N^m]$, where w_n^m represents a weight value of the attribute fn that the DM em provided according to his or her knowledge and experience, $0 \leq w_n^m \leq 1$, and $\sum_{n=1}^N w_n^m = 1$. The set of the DMs' weights is denoted as $Wt = \{\omega_t^{m,G_k} | m = 1, \ldots, M\}$, where ω_t^m means the weight value of the DM em participating in the subgroup G_k given at the t-th stage. Clearly, $W1$ is the initial set of the DMs' weights.

Generally, the LSGDM process usually involves the following four stages:

Stage 1. Clustering. In order to reduce the complexity of the LSGDM problem and the calculation process, a clustering method is generally utilized to divide all DMs to several subgroups according to some rules. In this study, the k-means clustering method is utilized according to the opinion similarity. The details are shown in Section 3.2.

Stage 2. Aggregate the opinion. The weighted arithmetic averaging (WAA) operator is usually used to aggregate each DM's evaluation information to a subgroup's decision matrix and each subgroup's decision matrix into the collective decision matrix [38]. For a LSGDM problem, suppose that ω^{m,G_k} is the em's weight in the subgroup Gk, ω^{G_k} is the Gk's weight. Then, the aggregation process can be derived as

$$q_{pm}^{G_k} = WAA\left(q_{pn}^m\right) \sum_{e_m \in G_k} \omega^{m,G_k} q_{pn}^m, e_m \in G_k; p = 1, \ldots, P; n = 1, \ldots, N, \tag{1}$$

where ω^{m,G_k} meets $0 \leq \omega^{m,G_k} \leq 1$ and $\sum_{e_m \in G_k} \omega^{m,G_k} = 1$.

$$q_{pn} = WAA\left(q_{pn}^{G_k}\right) \sum_{k=1}^K \omega^{G_k} q_{pn}^{G_k}, k = 1, \ldots K; p = 1, \ldots, P; n = 1, \ldots N, \tag{2}$$

where ω^{G_k} meets $0 \leq \omega^{G_k} \leq 1$ and $\sum_{k=1}^K \omega^{G_k} = 1$.

Stage 3. The CRP. Due to the large number and the complex background of DMs in the subgroup, the consensus level is lower. It aims to obtain an acceptable consensus level. If the consensus is not reached, then the consensus feedback process should be executed. The details are shown in Section 5.

Stage 4. Selection process. After obtaining the collective decision matrix by equation (2), the collective opinion score $s(xp)$ for each alternative xp is derived as

$$s(xp) = \sum_{n=1}^N w_n q_{pn}, p = 1, \ldots, P, \tag{3}$$

where $w_n \in [0, 1]$ is the weight of attribute fn for the group, and $\sum_{n=1}^N w_n = 1$. w_n's calculation equation is shown in Section 4.2 by equation (22).

3.2. The DMs Clustering Process. In this study, all DMs are classified as K subgroups by using k-means clustering method. The algorithm is given as Algorithm 1.

Input: The value of Qm for each DM and the number of subgroups K.
Output: The clustering results $G1, G2, \ldots, GK$.
Step 1. Each evaluation information matrix Qm $(m = 1, \ldots, M)$ is transformed into one-dimensional vector. For instance, the transformed vectors are denoted as $\overline{Q^m}$ $(m = 1, \ldots, M)$, $\overline{Q^m} = (q_{11}^m, \ldots, q_{1N}^m, \ldots, q_{PN}^m)$
Step 2. Set or Choose randomly K vectors as the initial cluster centers $\{\mu^1, \ldots, \mu^K\}$, where $\mu^k = (q_1^k, q_2^k, \ldots, q_{P.N}^k)$
Step 3. Let each DM enter to the subgroup closest to him or her. In other words, calculate the distance $d(ei, \mu^k)$ between the DM ei and the k-th cluster center. $d(ei, \mu^k)$ can use the Euclidean distance given by $d(ei, \mu^k) = \sum_{j=1}^{P.N} (q_j^m - q_j^k)^2$
Then, we can obtain $\alpha_j = argmin_{i=1}^{K} d(ei, \mu^k)$, and the DM ei therefore should enter to the subgroup G_{α_j}.
Step 4. Recompute the cluster results by using the member information of the current subgroups. Suppose that the new cluster centers are $\{\mu^{1'}, \ldots, \mu^{K'}\}$, where $\mu^{k'} = (q_1^k, q_2^k, \ldots, q_{P.N}^k)$
Step 5. Set the boundary conditions of clustering process. Setting $\delta > 0$, and the total differences before and after adjusting clustering are called TD, where $TD = \sum_{k=1}^{K} \sum_{j=1}^{P.N} (q_j^k - q_j^k)^2$
Step 6. The judgment process. If the condition $TD < \delta$ is satisfied, the clustering process is over, and then go to the next step; Otherwise, go to Step 4.
Step 7. Output the cluster results $G1, G2, \ldots, GK$. End.

Algorithm 1: The k-means clustering method.

In this paper, K meets the condition $2 \le K \le M/3$. The number of the DMs is denoted as n_k in the subgroup Gk.

4. Several Important Concepts in This Study

4.1. The Determination of the DMs' Weights and the Attributes' Weights. There are many factors that affect the determination of the DMs' weights, such as the subjective degree of the DMs' opinion, DMs' attitude towards the overall or intragroup opinion, and so on. Apparently, the higher the subjective degree of the DM's opinion or preference, the lower the objectivity of the DM's decision results, the smaller the influence of the DM on the final results of decision-making, and the DM's weight value therefore should be decreased to some extent. Again, the higher the DM's attitude towards the overall or intragroup opinion or preference, the more satisfied the DM is with the clustering results, the greater the DM's recognition of the results of group decision-making, and the DM's weight value therefore should be enhanced to a certain extent. In this study, the determination methods of the DMs' weights and the attributes' weights are developed in Algorithm 2.

It is noted that the purpose of the Step 10 is to obtain the attitude of DMs, i.e., the satisfaction degree, and then to adjust the weights of DMs according to it. The decision information is fed back to the DMs, and then their attitude towards the decision result is obtained. The step, which is necessary and significant, cannot only improve the participation of DMs in the decision-making process and better reflect the attitude of DMs, but make the decision-making results more scientific and reasonable.

4.2. The Weight Determination for Each SubGroup. There are several factors that affect the weight value of the subgroup, such as the number of the subgroup and the harmonious degree of the subgroup. If the subgroup has more DMs, the higher weight value should be given to the subgroup. Conversely, the fewer xDMs in the subgroup, the lower the weight value of the subgroup. Moreover, the greater the harmonious degree of the subgroup, the higher the support of the DMs in the subgroup for the decision results, the larger the satisfaction degree of the DMs in the subgroup with the clustering, and the weight value of the subgroup should be increased appropriately. The algorithm for the weight determination of the subgroup has been developed in Algorithm 3.

According to the weight ω^{G_k} of each subgroup and the weight $w_n^{G_k}$ of the attribute for each subgroup, the collective attribute weight vector $wG = [w_1^G, \ldots, w_N^G]$ is derived as

$$w_n^G = \sum_{k=1}^{K} \omega^{G_k} w_n^{G_k}, k = 1 \ldots K. \quad (4)$$

4.3. The Determination Method of the Unit Adjustment Cost. In the existing studies, the unit adjustment cost for each DM sometimes is given in advance [39–41], while others is calculated according to some rules [42]. For instance, Labella et al. [42] developed an objective metric based on the cost of modifying experts' opinions to evaluate CRPs in GDM problems, which is based on two novel minimum cost consensus (MCC) models that consider the distance of the DMs to the collective opinion and also ensure the minimum consistency among DMs.

However, in reality, the unit adjustment cost for each DM is many factors involved. DM may have different perspective for the same problem under the different context. Moreover, DM may have different expectation for the LSGDM result, and then have different attitude. Therefore, the unit adjustment cost must be related to the DMs' individual characteristics. In this study, we determine the unit adjustment cost of each DM according to two factors: the DMs' adjustment willingness θ_m^+ and θ_m^- and the satisfaction degree ρ_m. For the θ_m^+ and θ_m^-, the larger the value of $\theta_m^+ + \theta_m^-$, the higher the concession degree of the DM em in order to reach group consensus, the lower the difficulty of adjusting the evaluation information, the unit adjustment cost of em should be smaller. On the contrary, if the lower the value of $\theta_m^+ + \theta_m^-$, the unit adjustment cost of em should be larger. For

Input: The values of q_{pn}^{m}, θ_{m}^{+}, θ_{m}^{-}, and w^{m}, and the subgroups $G1$, $G2$, …, GK.
Output: The final values of the DMs' weights and the attributes' weights.
Step 1. Calculate the evaluation information Q^{G_k} for each subgroup, $k=1, \ldots, K$, where $Q^{G_k} = 1/n_k \sum_{e_m \in G_k} Q^m$
Step 2. Compute the evaluation information differences between each DM and his or her subgroup by using equation (4). For instance, the difference between the DM em and the subgroup Gk is $d(en, Gk) = \sqrt[2]{N \sum_{j=1}^{N} \sum_{i=1}^{P} ((q_{ij}^{m} - q_{ij}^{G_k})^2}$
Step 3. The initial weight values for each DM are given. Note that the evaluation difference of the DM and his or her subgroup is an important basis for determining the initial value of the DM's weight. The higher the difference between them, the lower the initial value of the DM's weight. Conversely, if the DM's opinion or preference are closer his or her subgroup, a higher weight should be given initially. Therefore, the determination of the initial weight value is given as follows.
$\omega_1^{m,G_k} = (1/d(e_m, G_k))/(1/\sum_{e_m \in G_k} d(e_m, G_k))$, $k = 1, \ldots, K$
Step 4. Calculate the weighted attributes' weight values for each subgroup. The calculation formula is $w_n^{G_k} = \sum_{e_m \in G_k} \omega_1^{m,G_k} w_n^m, k = 1, \ldots K, n = 1, \ldots, N$
Step 5. Calculate the distances of weight value between each DM and his or her subgroup. For instance, if the distance $dH(em, Gk)$ between the DM em and the subgroup Gk is larger, the weight value of the DM em in the subgroup Gk should be decreased to a certain extent. On the contrary, the value of $dH(em, Gk)$ is lower, it indicates that the subjective attitude of the DM em is closer to the collective attitude of the subgroup Gk, the weight value of the DM em in the subgroup Gk should be improved to some extent. d$H(em, Gk)$ can utilize the Hamming distance given by $dH(em, Gk) = \sum_{n=1}^{N} |w_n^m - w_n^{G_k}|, em \in Gk, k = 1, \ldots, K$
Step 6. Updating the weight value for each DM. The updating formula is: $\omega_2^{m,G_k} = \omega_1^{m,G_k} + \gamma_1 \beta_{m,G_k} / \sum (\omega_1^{m,G_k} + \gamma_1 \beta_{m,G_k}) em \in Gk$, $k = 1, \ldots, K$
where γ_i represents the importance of adjusting DMs' weight for each time, the higher the value of γ_i, the larger the importance of updating DMs' weight in this time, and β_{m,G_k} is the deviation proportion of the DM em in the subgroup Gk, and the compute formula is shown as follows. $\beta_{m,G_k} = d_H(e_m, G_k) / \sum_{e_m \in G_k} d_H(e_m, G_k), m = 1, \ldots M, k = 1, \ldots K$
Step 7. Computing the proportion of the allowed modification range, and update the weight value for each DM. The greater the proportion of the allowed modification range $\theta_m^+ + \theta_m^-$, the more concessions the DM makes in order to obtain the subgroup consensus, and the larger the proportion should be given when adjusting the DMs' weight. The calculation and modification equations are performed so that $\tau_{m,G_k} = \theta_m^+ + \theta_m^- / \sum_{e_m \in G_k} (\theta_m^+ + \theta_m^-)$, $k = 1, \ldots K$
where τ_{m,G_k} represents the proportion of the allowed modification value of the DM em in the subgroup Gk, and meets condition $0 \le \tau_{m,G_k} \le 1$. The normalization process should be then carried out.
$\omega_3^{m,G_k} = \omega_2^{m,G_k} + \gamma_2 \tau_{m,G_k} / \sum (\omega_2^{m,G_k} + \gamma_2 \tau_{m,G_k}) em \in Gk$, $k = 1, \ldots, K$
Step 8. Recalculate the weighted attributes' weight values for each subgroup by using equation (9), and the calculation results are presented that $w_n^{G_k'} = \sum_{e_m \in G_k} \omega_3^{m,G_k} w_n^m, k = 1, \ldots, K, n = 1, \ldots, N$
Step 9. Show the weight values $w_n^{G_k}$ of the aggregated attributes in this time to each DM, and then obtain the satisfaction degree ρ_m provided by em. The values of ρ_m provided by em are chosen from the set {0.1, 0.2, 0.3, 0.4, 0.5, 0.6, 0.7, 0.8, 0.9}, which means {extremely dissatisfied, very dissatisfied, dissatisfied, slightly dissatisfied, average, slightly satisfied, satisfied, very satisfied, extremely satisfied}.
Step 10. Re-update the weight value for each DM through the satisfaction degree ρ_m. The greater the values of ρ_m, the more satisfied the DM em is with the current weight value, the higher the enthusiasm for the current decision results, and the weight value of the DM em in the subgroup Gk should be improved to some extent. Conversely, if the value of ρ_m is smaller, the weight value of the DM em in the subgroup Gk should be reduced appropriately. The updating formula of the DMs' weights is that:
$\omega_4^{m,G_k} = \omega_3^{m,G_k} + \gamma_3 \rho_m / \sum (\omega_3^{m,G_k} + \gamma_3 \rho_m)$, $em \in Gk$, $k = 1, \ldots K$
The weight value in this time is the final weights for each DM. The final weight value of the DM em in the subgroup Gk is denoted as ω^{m,G_k}, that is, $\omega^{m,G_k} = \omega_4^{m,G_k}, em \in Gk, k = 1, \ldots, K$
Step 11. Compute the aggregated attributes' weight values for each subgroup according to the DMs' final weight values by using equation (9), that is, $w_n^{G_k''} \sum_{e_m \in G_k} \omega^{m,G_k} w_n^m, k = 1 \ldots K, n = 1, \ldots, N$
The weight value in this time is the final attributes' weights. The final weight value for each attribute in the subgroup Gk is denoted as $w_n^{G_k}$, that is, $w_n^{G_k} = w_n^{G_k''}, k = 1 \ldots K, n = 1, \ldots, N$
Step 12. Output the values of ω^{m,G_k} and $w_n^{G_k}$. End.

Algorithm 2: The determination method of the DMs' weights and the attributes' weights.

the ρ_m, the larger the value of ρ_m, the more satisfied the DM em is with the current decision-making result, the less the difficulty of adjusting the em's evaluation information to the subgroup collective decision result, and the unit adjustment cost of em should be smaller. Conversely, if the value of ρ_m is smaller, the unit adjustment cost of em should be higher.

As aforementioned, in this paper, we define the unit adjustment cost for each DM as follows.

Definition 1. Suppose that the unit adjustment cost of em is cm, the allowed modification values of em are θ_m^+ and θ_m^-, and the satisfaction degree of em is ρ_m.

$$cm = \vartheta \cdot cos \frac{\pi \cdot (\theta_m^+ + \theta_m^-)}{4} + (1 - \vartheta) \cdot \left(1 - sin \frac{\pi \cdot \rho_m}{2}\right), \quad (5)$$

where ϑ is a scale factor and represents the proportion of the allowed modification range. Apparently, cm increases

Input: The cluster results $G1$, $G2$, ..., GK, and the satisfaction degree ρ_m for each DM.
Output: The final weight value for each subgroup.
Step 1. Calculate the initial weight for each subgroup according to the number of the DMs in the subgroup. Obviously, the larger the number of the subgroup, the higher the weight value. The calculation equation is that: $\overline{\omega^{G_k}} = (n_k)^2 / \sum (n_k)^2 k = 1 \ldots K$ where $\overline{\omega^{G_k}}$ represents the initial weight value of the subgroup Gk, and satisfies $0 \le \overline{\omega^{G_k}} \le 1$, and $\sum_{k=1}^{K} \overline{\omega^{G_k}} = 1$.
Step 2. Compute the mean value and variance of satisfaction degree for each subgroup. The mean value and variance of satisfaction degree ρ_m of the subgroup is denoted as ρ_{G_k} and $v_{G_k}^2$, respectively, and the calculation formulas are shown as follows.
$\rho_{G_k} = 1/n_k \sum_{e_m \in G_k} \rho_m k = 1 \ldots K$, $v_{G_k}^2 = 1/n_k \sum_{e_m \in G_k} (\rho_m - \rho_{G_k})^2 k = 1 \ldots K$
Step 3. Define and calculate the harmonious degree for each subgroup. Apparently, the harmonious degree is related not only to the mean value of the satisfaction degree but also to the variance in a subgroup. The calculation equation of the harmonious degree h_{G_k} of the subgroup Gk is presented as follows. $h_{G_k} = \rho_{G_k}(1 - -v_{G_k}) k = 1 \ldots K$
The properties of the harmonious degree h_{G_k} is introduced as follows for the subgroup Gk:
(a) The value of h_{G_k} meets condition $0 \le h_{G_k} \le 1$.
(b) $h_{G_k} = \rho_{G_k}$ when $v_{G_k} = 0$.
(c) $h_{G_k} \le \rho_{G_k}$ at any time.
(d) It increases monotonically for ρ_{G_k}, and decreases for v_{G_k}.
Step 4. Update the weight for each subgroup according to the harmonious degree. Obviously, the greater the harmonious degree, and the weight of the subgroup should be improved to some extent. The updating formula is performed as follows.
$\omega^{G_k} = \overline{\omega^{G_k}} + \gamma h_{G_k} / \sum_{k=1}^{K} (\overline{\omega^{G_k}} + t\gamma n h_{G_k}), k = 1 \ldots K$
where γ represents the importance of harmonious degree in the updating weight process. The value of ω^{G_k} is considered as the final weight value for each subgroup.
Step 5. Output $\omega^{G_1}, \ldots, \omega^{G_K}$. End.

Algorithm 3: The weight determination for each subgroup.

Input: the values of q_{pn}^{m*}, θ_{m*}^{+}, θ_{m*}^{-}, and $q_{pn}^{G_{k*}}$.
Output: the adjustment values of $\overline{q_{pn}^{m*}}$, and $\overline{q_{pn}^{G_{k*}}}$.
Step 1. Obtain the evaluation values q_{pn}^{m*} to be modified of em^* for the attribute fn of the alternative xp. Hence, the difference matrix $\Delta Qm^* = (\triangle q_{pn}^{m*}) P \times N$ is defined as: $\Delta Qh^* = Qm^* - Q^{G_{k*}} = (\triangle q_{pn}^{m*}) p \times n$
Step 2. If $\triangle q_{pn}^{m*} = 0$, it means that the evaluation values q_{pn}^{m*} is same as the subgroup Gk's opinion, and the em^*'s evaluation value q_{pn}^{m*} for the attribute fn of the alternative xp does not need to be modified. Then, turn to the Step 5; otherwise, go to the next step.
Step 3. $\overline{q_{pn}^{m*}}$ is denoted as the modified value. Considering both the subgroup Gk^*'s opinion and the DM em^*s allowed modification range, the modification calculation is given as follows.
(a) If $\triangle q_{pn}^{m*} > 0$, it means that the evaluation values q_{pn}^{m*} is higher than the subgroup Gk's opinion. The evaluation values q_{pn}^{m*} therefore should be reduced appropriately. Then, $\overline{q_{pn}^{m*}} = \begin{cases} \max(q_{pn}^{m*} - \theta_{m*}^{-}, 0), \max(q_{pn}^{m*} - \theta_{m*}^{-}, 0) > q_{pn}^{G_{k*}} \\ q_{pn}^{G_{k*}}, \max(q_{pn}^{m*} - \theta_{m*}^{-}, 0) \le q_{pn}^{G_{k*}} \end{cases} p = 1 \ldots P, n = 1 \ldots N$
(b) $\triangle q_{pn}^{m*} < 0$, it means that the evaluation values q_{pn}^{m*} is lower than the subgroup Gk's opinion. The evaluation values q_{pn}^{m*} therefore should be increased to a certain extent. Thus, $\overline{q_{pn}^{m*}} = \begin{cases} \min(q_{pn}^{m*} + \theta_{m*}^{+}, 1), \min(q_{pn}^{m*} + \theta_{m*}^{+}, 1) < q_{pn}^{G_{k*}} \\ q_{pn}^{G_{k*}}, \min(q_{pn}^{m*} + \theta_{m*}^{+}, 1) \ge q_{pn}^{G_{k*}} \end{cases} p = 1 \ldots P, n = 1 \ldots N$
Step 4. Repeat Step 3 until the values cannot be modified.
Step 5. End. Let q_{pn}^{m*} is equal to $\overline{q_{pn}^{m*}}$, and calculate the value of $q_{pn}^{G_{k*}}$ by equation (1). Output $\overline{q_{pn}^{m*}}$ and $\overline{q_{pn}^{G_{k*}}}$.

Algorithm 4: The modified method for the DM em^* in the subgroup Gk^*.

monotonically with respect to $(\theta_m^+ + \theta_m^-)$, and decreases with respect to ρ_m.

Theorem 1. *The value of cm is in the interval of [0, 1].*
The proof of Theorem 1 is shown in Appendix A.

5. The Proposed Consensus Model

The CRP mainly includes two parts: consensus measure and consensus feedback. The details of the method of consensus measure are shown in Section 5.1, and Section 5.2 presents the consensus feedback process.

5.1. Consensus Measure. This procedure aims to judge whether an acceptable consensus level among group is reached or not. Clearly, in reality, the collective consensus level is related not only to the differences between the DMs' and the subgroups' opinion but to the attitude for each DM in a subgroup, i.e. the harmonious degree of a subgroup. Therefore, we define the consensus measure method as follows.

Definition 2. Suppose that $Qm = (q_{pn}^{m}) P \times N$ is the evaluation information of the DM em, $Q^{G_k} = (q_{pn}^{G_k}) P \times N$ is the evaluation information of the subgroup Gk obtained by equation (1), and h_{G_k} represents the harmonious degree for the

subgroup Gk by equation (19). The differences d^{m,G_k} between the DM em's and the subgroup Gk's opinion can be derived as

$$d^{m,G_k} = \frac{1}{P}\sum_{n=1}^{N} w_n^{G_k} \sum_{p=1}^{P} \left| q_{pn}^{m} - q_{pn}^{G_k} \right| em \in Gk, k = 1 \ldots K, \quad (6)$$

where the greater the value of $d^{m,G_k} \in [0, 1]$, the larger the deviation between em and Gk. And, the differences d^{G_k} within the subgroup Gk's opinion can be presented as

$$d^{G_k} = \sum_{e_m \in G_k} \omega^{m,G_k} d^{m,G_k}, em \in Gk, k = 1 \ldots K, \quad (7)$$

where the larger the value of $d^{G_k} \in [0, 1]$, the lower the opinion similarity in the subgroup Gk. The consensus level CLk in a subgroup Gk is derived as

$$CLk = a\left(1 - -d^{G_k}\right) + (1 - a)h_{G_k} \ldots K. \quad (8)$$

Accordingly, the group consensus level GCL can be calculated by

$$GCL = \sum_{k=1}^{K} \omega^{G_k} CL_k, \quad (9)$$

where GCL meets $0 \le \mathrm{GCL} \le 1$. Obviously, the greater the value of GCL, the higher the consensus level between the group. If $\mathrm{GCL} = 1$, it means that a complete consensus has been reached, however, is almost impossible. Hence, soft consensus is generally a rule for LSGDM problems [43–45].

$\delta \in [0, 1]$ is usually a preset consensus threshold. If $\mathrm{GCL} \ge \delta$, then it means that an acceptable consensus level has been reached among the group. Otherwise, consensus feedback is an imperative process to improve the consensus level, and let $\mathrm{GCL0} = \mathrm{GCL}$. Consequently, the determination method of δ is important for consensus process. Generally speaking, the consensus threshold is composed of the level of each individual, which indicates that the overall threshold must reflect the willingness of the individual. Therefore, without losing generality, the value of δ is obtained from the perspective of mean and variance.

Definition 3. Suppose that δ^1 and δ^2 are the reasonable thresholds, the calculation process is shown as

$$\delta^1 = CL_G\left(1 - v_{CL_G}\right), \quad (10)$$

$$\delta^2 = \frac{CL_G}{CL_G + v_{CL_G}}, \quad (11)$$

where $CL_G = 1/K$ CLk and $v_{CL_G} = \sqrt{1/K \sum_{k=1}^{K} (CL_k - CL_G)^2}$ represent the mean and standard deviation of the consensus level CLk($k = 1, \ldots, K$), respectively. We define that the consensus threshold δ is the average value of δ^1 and δ^2, namely,

$$\delta = \frac{\delta^1 + \delta^2}{2}. \quad (12)$$

The determination method of the consensus threshold is to make the setting of the consensus threshold more objective from the perspective of the current consensus level. In reality, the consensus level is related to the experts' evaluation information, which means the consensus level is uncertainty in the group. Therefore, to reduce the chance, the calculation of the consensus threshold is by weighting two reasonable thresholds in this study, which can reduce the subjectivity of the pre-defined it to a certain extent.

5.2. Consensus Feedback. Consensus feedback aims to obtain a high-consensus level in the group. Generally, the feedback process includes two parts: identification and adjustment.

5.2.1. Identification Process. It aims to determine the subgroup and the DM to be adjusted, which have the maximum differences. First, the determination of the subgroup to be adjusted is necessary. Due to the consensus level involves the difference between opinions and harmonious degree and harmonious degree does not change, the determination method of the adjusted subgroup focus on the difference between opinions, and the equation is $d^{G_{k*}} = \max\{d^{G_k}\}(k = 1, \ldots, K)$. Then, the DM em^* to be modified is obtained in the subgroup Gk^* by the $cm^* = \min\{cm | em \in Gk^*\}$. Therefore, the DM em^* of the subgroup Gk^* should be modified in the adjustment process. It should be noted that a DM can be adjusted at most once in the feedback process.

5.2.2. Adjustment Process. This process goals to modified the DMs' evaluation information according to some advices. Most of existing studies generally are given on adjustment strategies based on mathematical analysis. In this study, the DMs' evaluation information is modified according to both the subgroup's opinion and the DM's adjustment willingness. Detailed procedure is given in Algorithm 4.

The CRP is an iterative process that should be terminated by a condition. For the existing consensus model, a consensus threshold and the maximum iterative number generally should be set subjectively in advance [2, 4, 9, 39–42, 44–46]. In this study, we refer to the concept of consensus improvement rate proposed by Zhong et al. [5], the consensus adjustment rate is defined to judge whether the adjustment process is terminated. The detailed procedure is performed as follows.

We suppose that in the t-th stage, the consensus adjustment cost ACt is defined as

$$ACt = cm * \sum_{p=1}^{P}\sum_{n=1}^{N} \left| \overline{q_{pn}^{m*}} - q_{pn}^{m*} \right|. \quad (13)$$

Then, the total adjustment cost TACt before the t-th stage can be derived as

$$TACt = \sum_{i=1}^{t} AC_t. \quad (14)$$

Definition 4. (see [5]).Suppose that consensus adjustment rate is denoted as CARt before the t-th stage, which considers both the adjustment cost and the consensus improvement rate. The equation can be given as follows:

$$\mathrm{CAR}t = \frac{\mathrm{TAC}_t}{\mathrm{GCL}_t - \mathrm{GCL}}, \quad (15)$$

Input: The expert original evaluation matrices Qm, the number of subgroups K, the initial subject weight vector wm, and the allowed modification values θ_m^+ and θ_m^-.
Output: The expert adjusted evaluation matrices, the number of iterations of CRP T, the final group consensus level GCLT and the optimal alternative xp^*.
Stage 1. Expert clustering.
Step 1. The DMs participated the LSGDM problem are divided into K subgroups by using Algorithm 1. Then, the subgroups $G1,\ldots, GK$ are obtained.
Stage 2. The weight determination.
Step 2. Calculate the DMs' weights and the attributes' weights for each subgroup through Algorithm 2. Then, the final weights of DMs and attributes for each subgroup can be derived. For the subgroup $G1$, ω^{m,G_1} $(em \in Gk)$ and $w_n^{G_1}$ $(n = 1, \ldots, N)$ are obtained. It should be noted that there is an interactive process with DMs to improve the participation of DMs and better reflect the attitude of DMs. The details are shown in Step 10 of Algorithm 2.
Step 3. Compute the weights of the subgroups and the collective attributes by utilizing the Algorithm 3.
Stage 3. Obtain the unit adjustment cost cm by equation (22).
Stage 4. The CRP.
Step 4. Calculate the value of δ through equation (12), and let $t = 0$,
Step 5. Calculate the current consensus level GCLt, and judge whether the consensus level is acceptable. If GCLt $\geq \delta$, it means that an acceptable consensus level has been reached and go to Step 11; otherwise, let $t = t + 1$, and go to the Step 6.
Step 6. Determine which the subgroup and DM should be adjusted in the t-th round. The details are shown in Section 5.2.1.
Step 7. Modify the DM's evaluation information matrix and obtain the adjusted evaluation matrix through Algorithm 4.
Step 8. Compute the consensus adjustment cost ACt in the t-th round by using equation (12).
Step 9. Compute the total adjustment cost TACt and consensus adjustment rate CARt before the t-th round by equations (13) and (14), respectively.
Step 10. Determinate whether the CRP should be terminated. If CARt-1 $\leq$ CARt, it should go to the Step 5; otherwise, the CRP should be terminated, let $T = t - 1$, and go to the Step 11.
Step 11. Output the final evaluation matrices of the DMs, the number of iterations of CRP T, and the final group consensus level GCLT. Then, go to the Step 13.
Stage 5. Selection process.
Step 12. Calculate the score $s(xp)$for each alternative by equation (3) and obtain the ranking of the alternative.
Step 13. Output the optimal alternative xp^*. End.

Algorithm 5

where GCLt represents the group consensus level after adjusting the t-th round. If CARt $\leq$ CARt + 1, it means the consensus adjustment rate is well, and then the CRP can be proceed; otherwise, the CRP should be terminated, and the $(t+1)$-th adjustment should be restored. Thus, the t-th adjustment is the last adjustment. To compare the termination condition, i.e., consensus adjustment rate CARt, the consensus feedback process for at least one round.

5.3. The Framework of the Proposed Consensus Model. As the above aforementioned, the procedure of the proposed consensus model can be summarized as follows, and the framework can be shown in Figure 1 (Algorithm 5).

6. Case Study

6.1. Case Background. Earthquake is a natural phenomenon. According to statistics, the number of earthquakes in China from 2010 to 2020 was 6029, of which 48 were above magnitude 6.0. The earthquake will not only cause huge losses to the regional economy, but also cause huge casualties. Therefore, it is very critical to prepare before the earthquake to reduce casualties.

Tangshan, in Hebei Province of China, is an earthquake prone area. A county in this city plans to build several earthquake shelters. However, due to limited conditions, only one earthquake shelter can be built according to the existing resources. There are four feasible alternatives to choose from: (1) $x1$: near the station; (2) $x2$: near a school; (3) $x3$: near the residential area; (4) $x4$: near the hospital. The 20 experts participated in the building of the project, including government officials, construction builders, emergency management experts and many other fields. These experts need to evaluate the feasible alternatives from the following five factors: (1) $f1$: cost; (2) $f2$: capacity; (3) $f3$: construction difficulty; (4) $f4$: individual preference; (5) $f5$: time constraint. For example, when building a large capacity shelter, its manufacturing cost, construction difficulty and construction time will usually increase, so everyone has different attitude on these factors. Due to each alternative has its own advantages and disadvantages, it is necessary to select a satisfactory alternative through group decision-making. The information provided by experts is reported in Appendix B.

6.2. Decision-Making Process. The proposed consensus model is applied to increase the consensus level and to obtain the optimal alternative, the steps of which are shown as follows. Noting that $\gamma_1 = \gamma_2 = \gamma_3 = \gamma = 0.2$, $\vartheta = 0.5$, and $a = 0.8$ in this case:

Step 1. The 20 DMs are divided into 5 subgroups by using the Algorithm 1 as shown in Table 1.

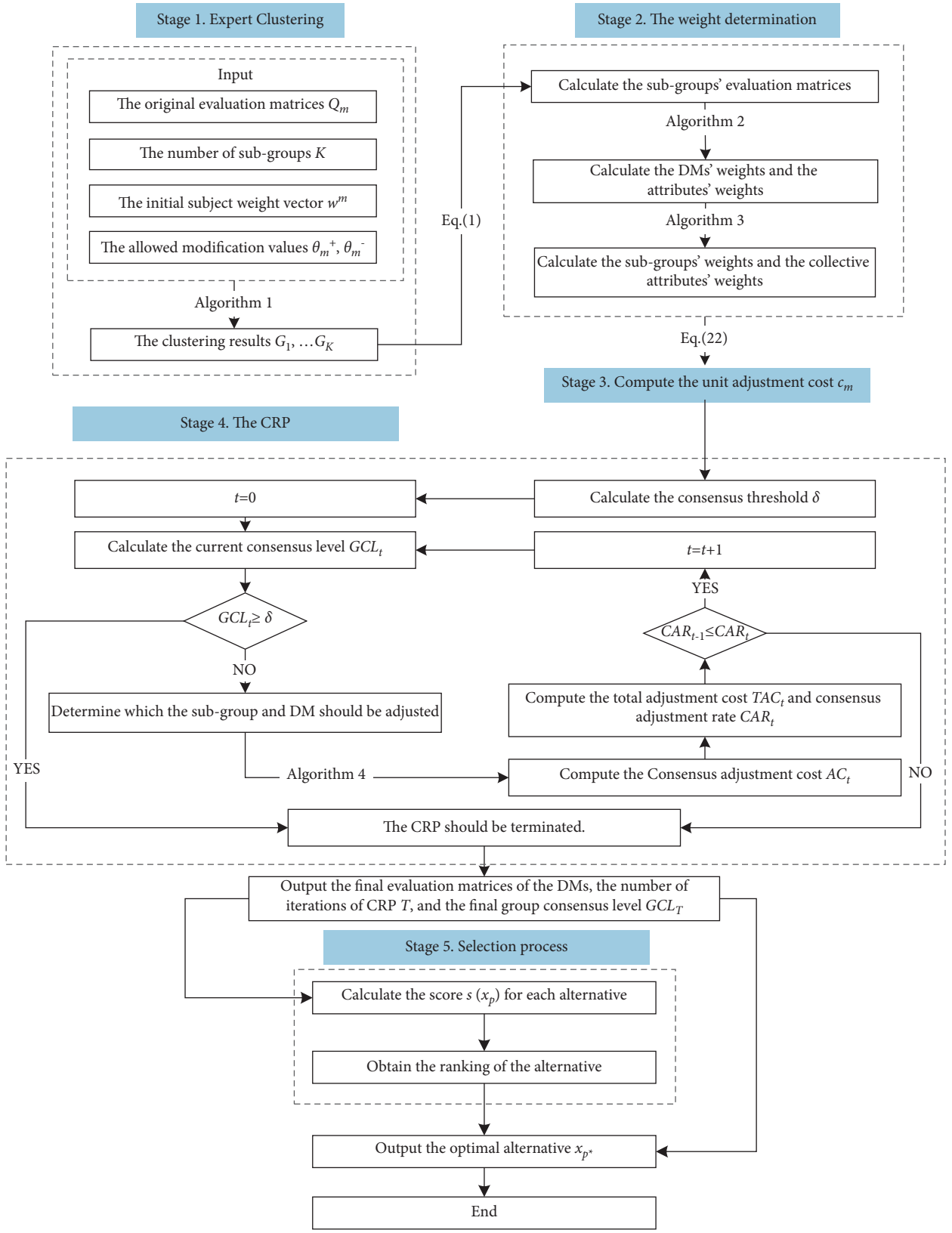

Figure 1: The process of the proposed consensus model.

Table 1: The clustering results.

Subgroups Gk	$G1$	$G2$	$G3$	$G4$	$G5$
Nk	5	4	1	5	5
Member em	$e1$, $e12$, $e15$, $e16$, $e19$	$e2$, $e6$, $e13$, $e14$	$e17$	$e4$, $e5$, $e7$, $e11$, $e18$	$e3$, $e8$, $e9$, $e10$, $e20$

Step 2. Calculate the subgroups' original evaluation matrices through equation (1), that is,

$$Q^{G_1} = \begin{bmatrix} 0.32 & 0.50 & 0.46 & 0.44 & 0.54 \\ 0.48 & 0.74 & 0.52 & 0.82 & 0.54 \\ 0.52 & 0.54 & 0.70 & 0.74 & 0.42 \\ 0.38 & 0.74 & 0.64 & 0.58 & 0.32 \end{bmatrix},$$

$$Q^{G_2} = \begin{bmatrix} 0.60 & 0.35 & 0.40 & 0.40 & 0.45 \\ 0.70 & 0.30 & 0.40 & 0.625 & 0.35 \\ 0.775 & 0.60 & 0.40 & 0.625 & 0.375 \\ 0.40 & 0.30 & 0.525 & 0.20 & 0.700 \end{bmatrix},$$

$$Q^{G_3} = \begin{bmatrix} 0.70 & 0.30 & 0.10 & 0.60 & 0.80 \\ 1.00 & 0.40 & 0.30 & 0.90 & 0 \\ 0.80 & 0 & 0.60 & 0.80 & 1.00 \\ 0.50 & 0.20 & 0.20 & 0.80 & 1.00 \end{bmatrix}, \quad (16)$$

$$Q^{G_4} = \begin{bmatrix} 0.44 & 0.48 & 0.48 & 0.48 & 0.50 \\ 0.84 & 0.38 & 0.50 & 0.36 & 0.66 \\ 0.70 & 0.62 & 0.70 & 0.74 & 0.62 \\ 0.58 & 0.50 & 0.46 & 0.34 & 0.12 \end{bmatrix},$$

$$Q^{G_5} = \begin{bmatrix} 0.46 & 0.28 & 0.66 & 0.68 & 0.40 \\ 0.22 & 0.54 & 0.56 & 0.36 & 0.50 \\ 0.62 & 0.34 & 0.74 & 0.60 & 0.70 \\ 0.72 & 0.22 & 0.88 & 0.56 & 0.34 \end{bmatrix}.$$

Then, calculate the DMs' weights and the attributes' weights in Gk($k = 1,2, \ldots, 5$) by using Algorithm 2. And compute the subgroups' weights and the collective attributes' weights through Algorithm 3. The calculation results are shown in Table 2.

Noting that in this step the computation results of the harmonious degree h_{G_k} of the subgroups are shown in Table 3.

Step 3. Based on equation (22), the unit adjustment cost for each DM can be calculated and then obtained, and the results are reported in Table 4.

Step 4. The CRP.

First, the computation results of the current consensus level and other information and the consensus threshold are recorded in Tables 5 and 6, respectively.

Apparently, $\mathrm{GCL0} = \mathrm{GCL} = 0.8302 < \delta = 0.8590$, the consensus feedback then should be executed.

The opinion of the DM e8 in G5 is first modified through adjustment process, and then obtain the adjustment result, i.e. $\mathrm{GCL1} = 0.8362 < \delta = 0.8590$. The consensus adjustment process therefore should be executed again. The DM e19 in G1 is identified and adjusted, and then obtain the adjustment result, i.e. $\mathrm{GCL2} = 0.8410 < \delta = 0.8590$. In this time, $\mathrm{CAR1} = 2.4717 < \mathrm{CAR2} = 2.6229$, so the CRP should not be terminated. Subsequently, the evaluation information of the DM e20 in G5 need to be modified, then the adjustment result is $\mathrm{GCL3} = 0.8446 < \delta = 0.8590$, and $\mathrm{CAR2} = 2.6229 < \mathrm{CAR3} = 3.0673$. The consensus feedback should be executed again. The opinion of the DM e4 in G4 is modified. The adjustment result is $\mathrm{GCL4} = 0.8489 < \delta = 0.8590$, and $\mathrm{CAR3} = 3.0673 > \mathrm{CAR4} = 2.7436$. The consensus feedback process should be terminated and $T = 3$. In addition, the fourth iteration result should be restored, and the final group consensus level is $\mathrm{GCLT} = 0.8446$. The adjustment process of the consensus level and the change process of CARt are shown in Tables 7 and 8, respectively.

The expert adjusted evaluation matrices are obtained and reported in Appendix B. And the subgroups' adjusted evaluation matrices can be derived by equation (1), that is,

$$Q^{G_1} = \begin{bmatrix} 0.3056 & 0.4870 & 0.4899 & 0.4828 & 0.5030 \\ 0.4978 & 0.7417 & 0.5666 & 0.8713 & 0.5621 \\ 0.5136 & 0.5209 & 0.7307 & 0.7771 & 0.4506 \\ 0.3921 & 0.7295 & 0.6719 & 0.5839 & 0.3138 \end{bmatrix},$$

$$Q^{G_2} = \begin{bmatrix} 0.6189 & 0.3333 & 0.4000 & 0.3912 & 0.4418 \\ 0.6610 & 0.3112 & 0.4112 & 0.6264 & 0.3686 \\ 0.7817 & 0.6024 & 0.3936 & 0.6186 & 0.4173 \\ 0.4112 & 0.3112 & 0.5234 & 0.2039 & 0.6671 \end{bmatrix},$$

$$Q^{G_3} = \begin{bmatrix} 0.70 & 0.30 & 0.10 & 0.60 & 0.80 \\ 1.00 & 0.40 & 0.30 & 0.90 & 0 \\ 0.80 & 0 & 0.60 & 0.80 & 1.00 \\ 0.50 & 0.20 & 0.20 & 0.80 & 1.00 \end{bmatrix},$$

$$Q^{G_4} = \begin{bmatrix} 0.4446 & 0.4822 & 0.4827 & 0.4902 & 0.4860 \\ 0.8557 & 0.3449 & 0.4984 & 0.3658 & 0.6767 \\ 0.7061 & 0.6372 & 0.7042 & 0.7637 & 0.6265 \\ 0.5610 & 0.4993 & 0.4546 & 0.3396 & 0.1152 \end{bmatrix},$$

$$Q^{G_5} = \begin{bmatrix} 0.4476 & 0.2714 & 0.5770 & 0.7352 & 0.4086 \\ 0.1622 & 0.5543 & 0.5900 & 0.3986 & 0.4822 \\ 0.6704 & 0.2874 & 0.7890 & 0.5843 & 0.8022 \\ 0.7004 & 0.2080 & 0.8174 & 0.5285 & 0.3466 \end{bmatrix}. \quad (17)$$

Table 2: The final weight results.

k	DMs' weights within a subgroup ω^{m,G_k}	Weight for each subgroup ω^{G_k}	Attributes' weight vectors of the subgroups w^{G_k}	The collective attributes' weights wG
1	$\omega^{1,G_1} = 0.1572$, $\omega^{12,G_1} = 0.2222$, $\omega^{15,G_1} = 0.1664$, $\omega^{16,G_1} = 0.2274$ $\omega^{19,G_1} = 0.2268$	$\omega^{G_1} = 0.2314$	$w^{G_1} = [0.2796, 0.1444, 0.1791, 0.2190, 0.1778]$.	$w^G = [0.2517, 0.1807, 0.2239, 0.1871, 0.1567]$.
2	$\omega^{2,G_2} = 0.2340$, $\omega^{6,G_2} = 0.2605$ $\omega^{13,G_2} = 0.1837$, $\omega^{14,G_2} = 0.3219$	$\omega^{G_2} = 0.1821$	$w^{G_2} = [0.3338, 0.1556, 0.1418, 0.1817, 0.1873]$.	
3	$\omega^{17,G_3} = 1.0000$	$\omega^{G_3} = 0.1075$	$w^{G_3} = [0.1000, 0.2000, 0.3000, 0.3000, 0.1000]$.	
4	$\omega^{4,G_4} = 0.2108$, $\omega^{5,G_4} = 0.2070$ $\omega^{7,G_4} = 0.1787$, $\omega^{11,G_4} = 0.2410$ $\omega^{18,G_4} = 0.1625$	$\omega^{G_4} = 0.2548$	$w^{G_4} = [0.2805, 0.2037, 0.2565, 0.1207, 0.1386]$.	
5	$\omega^{3,G_5} = 0.1469$, $\omega^{8,G_5} = 0.2673$ $\omega^{9,G_5} = 0.2108$, $\omega^{10,G_5} = 0.1764$ $\omega^{20,G_5} = 0.1985$	$\omega^{G_5} = 0.2243$	$w^{G_5} = [0.1962, 0.2029, 0.2632, 0.1799, 0.1576]$.	

Table 3: The computation results of the harmonious degree h_{G_k} ($k = 1, \ldots, 5$).

k	1	2	3	4	5
ρ_{G_k}	0.5800	0.6500	0.8000	0.7200	0.4800
v_{G_k}	0.1720	0.1118	0	0.0748	0.1166
h_{G_k}	0.4802	0.5773	0.8000	0.6661	0.4240

Step 5. Based on the above calculation results, the group's evaluation information is obtained, that is,

$$Q^G = \begin{bmatrix} 0.4724 & 0.3894 & 0.4494 & 0.5373 & 0.4983 \\ 0.5975 & 0.4835 & 0.4976 & 0.5950 & 0.4778 \\ 0.6775 & 0.4570 & 0.6617 & 0.7041 & 0.6273 \\ 0.5194 & 0.4209 & 0.5715 & 0.4633 & 0.4087 \end{bmatrix}, \tag{18}$$

and the score value for each alternative can be derived by equation (3), that is $s(x1) = 0.4739$, $s(x2) = 0.5413$, $s(x3) = 6383$, and $s(x4) = 0.4901$. Furthermore, the ranking of the alternative is $x3 \succ x2 \succ x4 \succ x1$, and the optimal alternative is x3.

6.3. Discussion. In this case, the consensus level is changed from 0.8302 to 0.8446. Although the consensus threshold $\delta = 0.8590$ has not been reached, and the consensus level has also been greatly improved. Also, the original information has been retained as much as possible in the consensus feedback process. Therefore, the proposed consensus model considering the interactive weights and the experts' adjustment willingness is verified to be effective.

7. Comparative Analysis

In this section, to demonstrate that the characteristics of the proposed consensus method is imperative, comparative analyses that without the interactive and without the experts' adjustment willingness, respectively, are implemented in Section 7.1 and Section 7.2.

7.1. The Proposed Model without considering the Interactive Weights. Continuing the case that given in Section 5, the proposed consensus model is executed without considering the determination of the interactive weight. Therefore, from Step 10 to Step 12 of Algorithm 2 and from Step 2 to Step 4 of Algorithm 3 are missing. The analyses process is performed as follows:

Step 1-A. The content of this part is the same as the Step 1 of Section 6.2.

Step 2-A. The subgroups' original evaluation matrices do not change. But the weight determination process and results are changed and shown in Table 9.

Step 3-A. Due to the interactive process is missing, the unit adjustment cost is not affected by harmonious degree. Thus, the determination method of the unit adjustment cost is simplified, that is,

$$cm = \cos\frac{\pi \cdot \left(\theta_m^+ + \theta_m^-\right)}{4}. \tag{19}$$

The unit adjustment cost without considering the interactive weights can be derived and shown in Table 10.

Step 4-A. The computation results of the current consensus level and other information and the consensus threshold are reported in Tables 11 and 12, respectively.

Apparently, $GCL'0 = GCL' = 0.8976 < \delta = 0.9068$, the consensus feedback then should be executed. The adjustment process of the consensus level is shown in Table 13. It should be noted that in the identification process the DM who have a higher weight is adjusted if there are several DMs who have the same unit adjustment.

Table 4: The unit adjustment cost cm ($m = 1,2, \ldots, 20$).

	$e1$	$e2$	$e3$	$e4$	$e5$	$e6$	$e7$	$e8$	$e9$	$e10$	$e11$	$e12$	$e13$	$e14$	$e15$	$e16$	$e17$	$e18$	$e19$	$e20$
cm	0.5919	0.5300	0.7485	0.2780	0.4808	0.6084	0.5574	0.4490	0.6220	0.6923	0.5183	0.5574	0.5955	0.5000	0.6775	0.5000	0.5183	0.4347	0.4590	0.5710

Table 5: The initial consensus levels.

	$G1$	$G2$	$G3$	$G4$	$G5$	The collective
The differences of subgroup	0.1209	0.0953	0	0.1052	0.1426	—
Consensus level	0.7993	0.8392	0.9600	0.8491	0.7707	0.8302

Table 6: The consensus threshold.

	$\delta 1$	$\delta 2$	δ
Value	0.7892	0.9289	0.8590

Table 7: The adjustment process of the consensus level.

Gk	d^{G_k} (0)	CL_k (0)	d^{G_k} (1)	CL_k (1)	d^{G_k} (2)	CL_k (2)	d^{G_k} (3)	CL_k (3)	d^{G_k} (4)	CL_k (4)
1	0.1209	0.7993	0.1209*	0.7993	0.0953	0.8193	0.0953	0.8198	0.0953	0.8198
2	0.0953	0.8392	0.0953	0.8392	0.0953	0.8392	0.0953	0.8392	0.0953	0.8392
3	0	0.9600	0	0.9600	0	0.9600	0	0.9600	0	0.9600
4	0.1052	0.8491	0.1052	0.8491	0.1052	0.8461	0.1052*	0.8491	0.0842	0.8659
5	0.1426*	0.7707	0.1090	0.7976	0.1090*	0.7969	0.0887	0.8138	0.0887	0.8138
Group		0.8302		0.8362		0.8410		0.8446		0.8489

Note. For example, *represents that this subgroup should be adjusted in the next stage.

Table 8: The termination condition judgment.

t	1	2	3	4
AC_t	1.4830	1.3497	1.5842	0.7136
TAC_t	1.4830	2.8327	4.4169	5.1305
CAR_t ($\times 10^2$)	2.4717	2.6229	3.0673	2.7436

Table 9: The final weights without considering the interactive weights.

k	DMs' weights within a subgroup ω^{m,G_k}	Weight for each subgroup ω^{G_k}	Attributes' weight vectors of the subgroups w^{G_k}	The collective attributes' weights w^G
1	$\omega^{1,G_1} = 0.1484$, $\omega^{12,G_1} = 0.2310$, $\omega^{15,G_1} = 0.2029$, $\omega^{16,G_1} = 0.1993$ $\omega^{19,G_1} = 0.2184$	$\omega^{G_1} = 0.2717$	$w^{G_1} = [0.2897, 0.1462, 0.1760, 0.2131, 0.1750]$.	$w^G = [0.2707, 0.1779, 0.2168, 0.1747, 0.1598]$.
2	$\omega^{2,G_2} = 0.2156$, $\omega^{6,G_2} = 0.2959$ $\omega^{13,G_2} = 0.1592$, $\omega^{14,G_2} = 0.3293$	$\omega^{G_2} = 0.1739$	$w^{G_2} = [0.3433, 0.1545, 0.1375, 0.1841, 0.1807]$.	
3	$\omega^{17,G_3} = 1.0000$	$\omega^{G_3} = 0.0109$	$w^{G_3} = [0.1000, 0.2000, 0.3000, 0.3000, 0.1000]$.	
4	$\omega^{4,G_4} = 0.2026$, $\omega^{5,G_4} = 0.2160$ $\omega^{7,G_4} = 0.1874$, $\omega^{11,G_4} = 0.2545$ $\omega^{18,G_4} = 0.1395$	$\omega^{G_4} = 0.2717$	$w^{G_4} = [0.2845, 0.1993, 0.2542, 0.1216, 0.1403]$.	
5	$\omega^{3,G_5} = 0.1574$, $\omega^{8,G_5} = 0.2756$ $\omega^{9,G_5} = 0.2120$, $\omega^{10,G_5} = 0.1811$ $\omega^{20,G_5} = 0.1738$	$\omega^{G_5} = 0.2717$	$w^{G_5} = [0.1984, 0.2024, 0.2676, 0.1783, 0.1533]$.	

Step 5-A. Based on the above calculation results, the group's evaluation information is obtained, that is,

$$Q^G = \begin{bmatrix} 0.4566 & 0.4052 & 0.4940 & 0.5161 & 0.4659 \\ 0.5470 & 0.5081 & 0.5050 & 0.5411 & 0.5376 \\ 0.6629 & 0.5062 & 0.6584 & 0.6819 & 0.5818 \\ 0.5034 & 0.4427 & 0.6219 & 0.4453 & 0.3323 \end{bmatrix}, \tag{20}$$

and the score value for each alternative can be derived by equation (3), that is $s(x1) = 0.4674$, $s(x2) = 0.5284$, $s(x3) = 0.6243$, and $s(x4) = 0.4808$. Furthermore, the ranking of the alternative is $x3 \succ x2 \succ x4 \succ x1$, and the optimal alternative is $x3$.

7.2. The Consensus Feedback without considering the Adjustment Willingness. Similar to Section 7.1, the proposed consensus model is executed without considering the adjustment willingness. Therefore, Step 8 and Step 9 of

Table 10: The unit adjustment cost without considering the interactive weights.

	$e1$	$e2$	$e3$	$e4$	$e5$	$e6$	$e7$	$e8$	$e9$	$e10$	$e11$	$e12$	$e13$	$e14$	$e15$	$e16$	$e17$	$e18$	$e19$	$e20$
c_m	0.8910	0.9511	0.9511	0.7071	0.8526	0.9239	0.9239	0.7071	0.9511	0.9724	0.9877	0.9239	1.000	0.9511	0.8090	0.9511	0.9877	0.7604	0.8090	0.9511

Table 11: The consensus level without considering the interactive weights.

	$G1$	$G2$	$G3$	$G4$	$G5$	The collective
The differences of subgroup	0.1197	0.0925	0	0.1030	0.1416	—
Consensus level	0.8803	0.9075	1.0000	0.8970	0.8584	0.8976

Table 12: The consensus threshold without considering the interactive weights.

	$\delta 1$	$\delta 2$	δ
Value	0.8645	0.9492	0.9068

Table 13: The adjustment process without considering the interactive weights.

Gk	d^{G_k} (0)	CL_k (0)	d^{G_k} (1)	CL_k (1)	d^{G_k} (2)	CL_k (2)
1	0.1197	0.8803	0.1197	0.8803	0.0952	0.9048
2	0.0925	0.9075	0.0925	0.9075	0.0925	0.9075
3	0	1	0	1	0	1
4	0.1030	0.8970	0.1030	0.8970	0.1030	0.8970
5	0.1416*	0.8584	0.1076	0.8924	0.1076	0.8924
Group		0.8976		0.9052		0.9108

Table 14: The final weights without considering the adjustment willingness.

k	DMs' weights within a subgroup ω^{m,G_k}	Weight for each subgroup ω^{G_k}	Attributes' weight vectors of the subgroups w^{G_k}	The collective attributes' weights w^G
1	$\omega^{1,G_1} = 0.1515$, $\omega^{12,G_1} = 0.2310$, $\omega^{15,G_1} = 0.1594$, $\omega^{16,G_1} = 0.2363$ $\omega^{19,G_1} = 0.2218$	$\omega^{G_1} = 0.2314$	$w^{G_1} = [0.2770, 0.1462, 0.1792, 0.2193, 0.1784]$.	$w^G = [0.2513, 0.1805, 0.2239, 0.1867, 0.1577]$.
2	$\omega^{2,G_2} = 0.2219$, $\omega^{6,G_2} = 0.2488$ $\omega^{13,G_2} = 0.2046$, $\omega^{14,G_2} = 0.3247$	$\omega^{G_2} = 0.1821$	$w^{G_2} = [0.3293, 0.1547, 0.1426, 0.1795, 0.1939]$.	
3	$\omega^{17,G_3} = 1.0000$	$\omega^{G_3} = 0.1075$	$w^{G_3} = [0.1000, 0.2000, 0.3000, 0.3000, 0.1000]$.	
4	$\omega^{4,G_4} = 0.1991$, $\omega^{5,G_4} = 0.2074$ $\omega^{7,G_4} = 0.1829$, $\omega^{11,G_4} = 0.2635$ $\omega^{18,G_4} = 0.1470$	$\omega^{G_4} = 0.2548$	$w^{G_4} = [0.2837, 0.2013, 0.2552, 0.1207, 0.1390]$.	
5	$\omega^{3,G_5} = 0.1465$, $\omega^{8,G_5} = 0.2505$ $\omega^{9,G_5} = 0.2179$, $\omega^{10,G_5} = 0.1847$ $\omega^{20,G_5} = 0.2004$	$\omega^{G_5} = 0.2243$	$w^{G_5} = [0.1971, 0.2038, 0.2637, 0.1794, 0.1559]$.	

Algorithm 2 are missing, and Algorithm 4 is no longer available. The analyses process is shown as follows:

Step 1-B. The content of this part is the same as the Step 1 of Section 6.2.

Step 2-B. The subgroups' original evaluation matrices do not change. But the weight determination process and results are changed and shown in Table 14.

Step 3-B. Due to the adjustment willingness of the DM is missing, the unit adjustment cost is not affected by the allowed modification range. Thus, the determination method of the unit adjustment cost is simplified, that is,

$$cm = 1 - \sin\frac{\pi \cdot \rho_m}{2}. \tag{21}$$

The unit adjustment cost without considering the adjustment willingness can be derived and shown in Table 15.

Step 4-B. The computation results of the current consensus level and other information and the consensus threshold are reported in Tables 16 and 17, respectively.

Apparently, $GCL'0 = GCL' = 0.8306 < \delta = 0.8592$, the consensus feedback then should be executed. In this subsection, a novel adjustment rule is used, and the details are carried out as follows.

Table 15: The unit adjustment cost without considering the adjustment willingness.

	$e1$	$e2$	$e3$	$e4$	$e5$	$e6$	$e7$	$e8$	$e9$	$e10$	$e11$	$e12$	$e13$	$e14$	$e15$	$e16$	$e17$	$e18$	$e19$	$e20$
c_m	0.2929	0.1090	0.5460	0.0489	0.1090	0.2929	0.1910	0.1910	0.2929	0.4122	0.0489	0.1910	0.1910	0.0489	0.5460	0.0489	0.0489	0.1090	0.1090	0.1910

Table 16: The consensus level without considering the adjustment willingness.

	$G1$	$G2$	$G3$	$G4$	$G5$	The collective
The differences of subgroup	0.1205	0.0957	0	0.1031	0.1426	—
Consensus level	0.7996	0.8389	0.9600	0.8507	0.7707	0.8306

Table 17: The consensus threshold without considering the adjustment willingness.

	$\delta 1$	$\delta 2$	δ
Value	0.7895	0.9289	0.8592

Table 18: The adjustment process without considering the interactive weights.

Gk	d^{G_k} (0)	CL_k (0)	d^{G_k} (1)	CL_k (1)	d^{G_k} (2)	CL_k (2)	d^{G_k} (3)	CL_k (3)
1	0.1205	0.7996	0.1205	0.7996	0.1205*	0.7996	0.1069	0.8105
2	0.0957	0.8389	0.0957	0.8389	0.0957	0.8389	0.0957	0.8389
3	0	0.9600	0	0.9600	0	0.9600	0	0.9600
4	0.1031	0.8507	0.1031	0.8507	0.1031	0.8507	0.1031	0.8507
5	0.1426*	0.7707	0.1260*	0.7840	0.1101	0.7967	0.1101*	0.7967
Group		0.8306		0.8336		0.8365		0.8389

Table 19: The termination condition judgment without considering the interactive weights.

t	1	2	3
AC_t	0.3218	0.3761	0.0677
TAC_t	0.3218	0.6979	0.7656
CAR_t ($\times 10^2$)	1.0727	2.3859	3.1900

Suppose that the evaluation matrices of the DM and the subgroup to be adjusted are QM^* and $Q^{G_{k*}}$, then the adjusted evaluation matrix of the DM is $QM^{*'} = 1/2\,QM^* + 1/2Q^{G_{k*}}$. The adjustment process of the consensus level is shown in Tables 18 and 19, respectively.

In this consensus feedback process, the maximum adjustment round T is 2.

Step 5-B. Based on the above calculation results, the group's evaluation information is obtained, that is,

$$Q^G = \begin{bmatrix} 0.4778 & 0.3980 & 0.4514 & 0.5245 & 0.5098 \\ 0.6044 & 0.4873 & 0.4753 & 0.5670 & 0.4702 \\ 0.6664 & 0.4722 & 0.6385 & 0.7044 & 0.6031 \\ 0.5074 & 0.4328 & 0.5677 & 0.4655 & 0.4097 \end{bmatrix}, \tag{22}$$

and the score value for each alternative can be derived by equation (3), that is $s(x1) = 0.4713$, $s(x2) = 0.5263$, $s(x3) = 0.6223$, and $s(x4) = 0.4843$. Furthermore, the ranking of the alternative is $x3 \succ x2 \succ x4 \succ x1$, and the optimal alternative is $x3$.

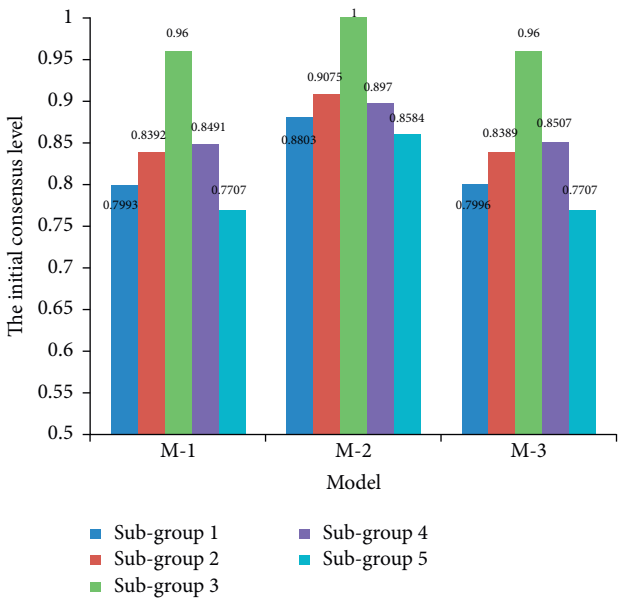

Figure 2: The changes of the subgroups' consensus level. Note: M-1: the proposed consensus model, M-2: without considering the interactive weights, and M-3: without the experts' adjustment.

7.3. Discussion. Based on the above introduction, the differences between the proposed model and without considering the interactive weights, the proposed model and without the experts' adjustment willingness are shown as follows.

Table 20: The change of GCL_t and adjustment cost.

Iteration (t)	The proposed model (M-1)		Without considering the interactive weights (M-2)		Without considering the experts' adjustment willingness (M-3)	
	Group consensus level	Adjustment cost	Group consensus level	Adjustment cost	Group consensus level	Adjustment cost
$t=0$	0.8302	0	0.8976	0	0.8306	0
$t=1$	0.8362	1.4830	0.9052	2.2941	0.8336	0.3218
$t=2$	0.8410	2.8327	0.9108^{T}		0.8365^{T}	0.6979
$t=3$	0.8446^{T}	4.4169			0.8389	0.7656
$t=4$	0.8489	5.1305				

Note. For example, 0.8446^{T} represents that the consensus level is 0.8446 at the third round of the iteration process and this stage is the last stage.

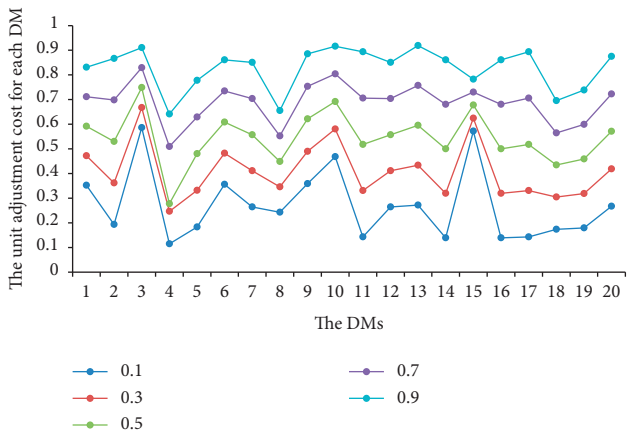

Figure 3: The unit adjustment cost with different ϑ for each DM.

7.3.1. The Subgroups' Consensus Level. The proposed model, without considering the interactive weights, and without the experts' adjustment willingness of the subgroups' consensus levels are shown in Figure 2. Specifically, the ranking of the initial consensus level is $CL_3 > CL_4 > CL_2 > CL_1 > CL_5$ in the models M-1 and M-3 while model M-2 is $CL_3 > CL_2 > CL_4 > CL_1 > CL_5$. The consensus levels of the subgroups $G3$ and $G5$ of the M-1 and M-3 are 0.9600 and 0.7707, respectively, while the M-2 are 1.0000 and 0.8584.

For the model M-2, the stage showing the decision results to experts is omitted in the process of weight determination. Hence, the decision information is not fed back to DM in time, and the decision-maker's attitude towards the decision information is not obtained. Although the consensus level of the M-2 is higher than the M-1 (i.e. the proposed model), the calculation of consensus level is inaccurate and partial. Therefore, the decision-making result cannot fully represent the wishes and attitudes of the DMs.

For the model M-3, the stage reflecting the DMs' adjustment willingness information is removed. Thus, the adjustment attitude of DMs to their own evaluation information cannot be known, and the lack and distortion of the DMs' evaluation information may lead. Although the consensus level for each subgroup of the M-3 is very similar with the M-1, the DMs' adjustment willingness (i.e. the stubborn degree to their own opinion) is omitted, and the acquisition of consensus level is not scientific and reasonable. Therefore, it may lead to the unreasonable decision-making result due to the DMs' opinion is distorted or ignored.

7.3.2. The Changes of the Group Consensus Level GCL_t and the Adjustment Cost. The proposed model, without considering the interactive weights, and without the experts' adjustment willingness of the group consensus level GCL_t and the adjustment cost are record in Table 20.

For the model M-2, after 2 rounds of the consensus feedback process, the consensus threshold and an acceptable consensus level has been reached. Due to the lack of timely attitude of DMs towards decision-making information, the satisfaction degree for each DM is not obtained. Also, the consensus level of the subgroup does not involve the harmonious degree, namely the recognition of the subgroup is not presented. Therefore, the consensus level of the M-2 improves faster than the M-1 because it does not consider the harmonious degree of the subgroup. Meanwhile, the calculation method of the unit adjustment cost is partial, and the adjustment cost of the M-2 increases faster than the M-1 and then is inaccurate and unscientific. Therefore, the decision-making result of the M-1 is more reasonable than M-2.

For the model M-3, after 2 rounds of the consensus feedback process, the termination condition is satisfied and the final consensus level can be obtained. Due to the lack of the DMs' adjustment willingness information, the distortion of the DMs' opinion may lead. And, the consensus level of the M-3 increases slower than the M-1. For instance, after 2 rounds of the iteration process the group consensus level of the M-3 is 0.8365 while the M-1 is 0.8410. And t after one round the group consensus level of the M-1 is 0.8362. It is obvious that the result of the M-3 adjustment twice is similar to that of the M-1 adjustment once. Meanwhile, the computation process of the unit adjustment cost is also partial, and the adjustment cost of the M-3 is lower than the M-1

Table 21: The group consensus levels for the different ϑ.

Iteration (t)	$\vartheta = 0.1$		$\vartheta = 0.3$		$\vartheta = 0.5$		$\vartheta = 0.7$		$\vartheta = 0.9$	
	(1)	(2)	(1)	(2)	(1)	(2)	(1)	(2)	(1)	(2)
0	0.8302	0	0.8302	0	0.8302	0	0.8302	0	0.8302	0
1	0.8362^{T}	0.8176	0.8362^{T}	1.1848	0.8362	1.4830	0.8362	1.8242	0.8362	2.1651
2	0.8401	1.1272	0.8410	2.1228	0.8410	2.8327	0.8410	3.5855	0.8410	4.3381
3					0.8446^{T}	4.4169	0.8446^{T}	5.5913	0.8446^{T}	6.7656
4					0.8489	5.1305	0.8489	6.8996	0.8489	8.4117

Note. (1) and (2) represent the group consensus level and the adjustment cost, respectively. 0.8362^{T} represents that the consensus level is 0.8362 at the first round of the iteration process and this stage is the last stage.

Table 22: The score for each alternative with different ϑ.

	$x1$	$x2$	$x3$	$x4$	Ranking
$\vartheta = 0.1$	0.4741	0.5361	0.6293	0.4871	$x3 \succ x2 \succ x4 \succ x1$
$\vartheta = 0.3$	0.4743	0.5362	0.6291	0.4872	$x3 \succ x2 \succ x4 \succ x1$
$\vartheta = 0.5$	0.4739	0.5413	0.6383	0.4901	$x3 \succ x2 \succ x4 \succ x1$
$\vartheta = 0.7$	0.4743	0.5362	0.6291	0.4872	$x3 \succ x2 \succ x4 \succ x1$
$\vartheta = 0.9$	0.4738	0.5413	0.6383	0.4901	$x3 \succ x2 \succ x4 \succ x1$

Table 23: The consensus thresholds of the different a.

Consensus thresholds	$a = 0.6$	$a = 0.7$	$a = 0.8$	$a = 0.9$	$a = 1.0$
$\delta 1$	0.7167	0.7527	0.7892	0.8259	0.8629
$\delta 2$	0.9056	0.9177	0.9289	0.9392	0.9487
δ	0.8112	0.8352	0.8590	0.8825	0.9057

Table 24: The group consensus levels and the adjustment costs of the different a.

Iteration (t)	$a = 0.6$		$a = 0.7$		$a = 0.8$		$a = 0.9$		$a = 1.0$	
	(1)	(2)	(1)	(2)	(1)	(2)	(1)	(2)	(1)	(2)
0	0.7644	0	0.7973	0	0.8302	0	0.8631	0	0.8960	0
1	0.7689	1.4830	0.8026	1.4830	0.8362	1.4830	0.8699	1.4830	0.9035	1.4830
2	0.7725^{T}	2.8327	0.8067	2.8327	0.8410	2.8327	0.8752	2.8327	0.9094^{T}	
3	0.7860	4.4169	0.8099^{T}	4.4169	0.8446^{T}	4.4169	0.8793	4.4169		
4			0.8137	5.1305	0.8489	5.1305	0.8841^{T}			

Note. (1) and (2) represent the group consensus level and the adjustment cost, respectively. 0.7725^{T} represents that the consensus level is 0.7725 at the second round of the iteration process and this stage is the last stage.

Table 25: The score for each alternative with the difference value of a.

	$x1$	$x2$	$x3$	$x4$	Ranking
$a = 0.6$	0.4736	0.5423	0.6341	0.4895	$x3 \succ x2 \succ x4 \succ x1$
$a = 0.7$	0.4739	0.5413	0.6383	0.4901	$x3 \succ x2 \succ x4 \succ x1$
$a = 0.8$	0.4739	0.5413	0.6383	0.4901	$x3 \succ x2 \succ x4 \succ x1$
$a = 0.9$	0.4726	0.5384	0.6373	0.4918	$x3 \succ x2 \succ x4 \succ x1$
$a = 1.0$	0.4736	0.5423	0.6341	0.4895	$x3 \succ x2 \succ x4 \succ x1$

and then is inaccurate and unreasonable. From the perspective of the experts' adjustment willingness, the decision-making result of the M-1 is more scientific than M-3.

In summary, it is apparent that both considering the interactive weights and the experts' adjustment willingness for the CRP is not only very reasonable but imperative.

Table 26: The original evaluation information $Qm = (q_{pn}^{m})P \times N$ ($m = 1, \ldots, 20$) for each DM.

		$f1$	$f2$	$f3$	$f4$	$f5$		$f1$	$f2$	$f3$	$f4$	$f5$		$f1$	$f2$	$f3$	$f4$	$f5$		$f1$	$f2$	$f3$	$f4$	$f5$
$x1$		0.2	0.3	0.4	0.6	0.4		0.7	0.2	0.4	0.5	0.5		0.8	0.3	0.6	0.4	0.6		0.4	0.4	0.7	0.4	0.6
$x2$	$e1$	0.1	0.4	0.5	0.9	0.6	$e2$	0.9	0.4	0.5	0.3	0.2	$e3$	0	0.6	0.4	0.9	0.6	$e4$	0.9	0.1	0.5	1.0	0.6
$x3$		0.5	0.2	0.8	0.8	0.7		0.8	0.8	0.7	1.0	0.1		1.0	0.4	0.8	0.7	0.8		0.7	0.8	0.6	0.7	0.8
$x4$		0.9	0.9	0.5	0.8	0.2		0.5	0.4	0.6	0.4	0.9		1.0	0	0.9	0.3	0.3		0.5	0.6	0.2	0.3	0.3
$x1$		0.6	0.5	0.4	0.4	0.4		0.6	0.5	0.4	0.4	0.4		0.6	0.7	0.6	0.5	0.1		0.3	0.4	0.9	0.7	0.5
$x2$	$e5$	1.0	0.2	0.5	0.1	0.7	$e6$	0.6	0.2	0.3	0.9	0.6	$e7$	0.9	0.9	0.4	0.3	0.6	$e8$	0.4	0.5	0.5	0.2	0.3
$x3$		0.8	0.5	0.8	0.8	0.4		0.8	0.5	0.3	0.7	0.7		0.8	0.6	0.5	0.9	0.7		0.2	0.7	0.6	0.8	0.2
$x4$		0.3	0.2	0.5	0.6	0		0.3	0.2	0.5	0.3	0.5		0.8	0.5	0.6	0.4	0.2		0.9	0.5	1.0	0.5	0.4
$x1$		0.4	0.3	0.3	1.0	0.4		0.2	0.2	0.6	0.8	0.4		0.4	0.5	0.4	0.7	0.4		0.4	0.5	0.6	0.6	0.6
$x2$	$e9$	0	0.6	0.6	0.5	0.2	$e10$	0.1	0.5	0.8	0	0.3	$e11$	0.9	0.1	0.5	0.2	0.9	$e12$	0.7	1.0	0.4	0.9	0.6
$x3$		0.7	0.2	0.8	0.5	1.0		0.5	0.2	0.9	1.0	0.8		0.7	0.8	0.8	1.0	0.7		0.4	0.5	0.5	0.8	0.6
$x4$		0.5	0.4	0.5	0.1	0.2		0.9	0.1	1.0	1.0	0.6		0.5	0.6	0.5	0.2	0		0	0.9	0.6	0.8	0.3
$x1$		0.4	0.5	0.4	0.4	0.5		0.7	0.2	0.4	0.3	0.4		0.4	0.6	0.3	0.4	0.4		0.2	0.5	0.6	0.4	0.5
$x2$	$e13$	0.9	0.2	0.3	0.7	0.2	$e14$	0.4	0.4	0.5	0.6	0.4	$e15$	0.6	0.6	0.6	1.0	0.9	$e16$	0.5	0.8	0.8	0.9	0.3
$x3$		0.7	0.5	0.3	0.4	0.1		0.8	0.6	0.3	0.4	0.6		0.7	0.4	0.8	0.9	0.7		0.5	0.8	0.9	0.7	0.1
$x4$		0.3	0.2	0.5	0	0.9		0.5	0.4	0.5	0.1	0.5		0.2	0.5	0.5	0.5	0.3		0.6	0.6	1.0	0.3	0.4
$x1$		0.7	0.3	0.1	0.6	0.8		0.2	0.3	0.3	0.4	1.0		0.4	0.6	0.4	0.2	0.8		0.6	0.2	0.9	0.5	0.1
$x2$	$e17$	1.0	0.4	0.3	0.9	0	$e18$	0.5	0.6	0.6	0.2	0.5	$e19$	0.5	0.9	0.3	0.4	0.3	$e20$	0.6	0.5	0.5	0.2	0.8
$x3$		0.8	0	0.6	0.8	1.0		0.5	0.4	0.8	0.3	0.5		0.5	0.8	0.5	0.5	0.0		0.7	0.2	0.6	0	0.7
$x4$		0.5	0.2	0.2	0.8	1.0		0.8	0.6	0.5	0.2	0.1		0.2	0.8	0.6	0.5	0.4		0.3	0.1	1.0	0.9	0.2

Table 27: The values of θ_m^+ and θ_m^- for each DM provided.

	$e1$	$e2$	$e3$	$e4$	$e5$	$e6$	$e7$	$e8$	$e9$	$e10$	$e11$	$e12$	$e13$	$e14$	$e15$	$e16$	$e17$	$e18$	$e19$	$e20$
θ_m^+	0.3	0.2	0.3	0.5	0.6	0.3	0.2	0.5	0.2	0.3	0.1	0.2	0	0.1	0.5	0.1	0.1	0.6	0.3	0.2
θ_m^-	0.3	0.2	0.1	0.5	0.1	0.2	0.3	0.5	0.2	0	0.1	0.3	0	0.3	0.3	0.3	0.1	0.3	0.5	0.2

Table 28: The initial subject weight vector w^m of the DM em ($m = 1, \ldots, 20$).

	$e1$	$e2$	$e3$	$e4$	$e5$	$e6$	$e7$	$e8$	$e9$	$e10$	$e11$	$e12$	$e13$	$e14$	$e15$	$e16$	$e17$	$e18$	$e19$	$e20$
$f1$	0.1	0.3	0.5	0.2	0.3	0.5	0.4	0.1	0.1	0.2	0.3	0.2	0.2	0.3	0.5	0.2	0.1	0.2	0.4	0.2
$f2$	0.1	0.2	0.1	0.2	0.1	0.1	0.2	0.2	0.2	0.3	0.2	0.3	0.1	0.2	0.1	0.1	0.2	0.35	0.1	0.2
$f3$	0.3	0.2	0.2	0.4	0.2	0.1	0.1	0.3	0.3	0.4	0.3	0.25	0.2	0.1	0.05	0.1	0.3	0.25	0.2	0.1
$f4$	0.3	0.2	0.1	0.1	0.2	0.2	0.1	0.2	0.3	0.05	0.1	0.15	0.1	0.2	0.15	0.3	0.3	0.1	0.2	0.2
$f5$	0.2	0.1	0.1	0.3	0.2	0.1	0.2	0.2	0.1	0.05	0.1	0.1	0.4	0.1	0.2	0.3	0.1	0.1	0.1	0.3

Table 29: The values of ρ_m for each DM provided.

	$e1$	$e2$	$e3$	$e4$	$e5$	$e6$	$e7$	$e8$	$e9$	$e10$	$e11$	$e12$	$e13$	$e14$	$e15$	$e16$	$e17$	$e18$	$e19$	$e20$
ρ_m	0.5	0.7	0.3	0.8	0.7	0.5	0.6	0.6	0.5	0.4	0.8	0.6	0.6	0.8	0.3	0.8	0.8	0.7	0.7	0.6

8. Sensitivity Analysis

In this section, sensitivity analyses that the unit adjustment cost and the harmonious degree in the CRP, respectively, are presented in Section 8.1 and Section 8.2.

8.1. The Effect of the Unit Adjustment Cost cm in Consensus Feedback Process. In Section 6, the unit adjustment cost cm for each DM is obtain based on equation (22) and the value of ϑ is 0.5. In this subsection, a discussion based on the different unit adjustment cost is introduced. To further prove the rationality of the proposed consensus model, a sensitivity analysis is conducted with different values of $\vartheta = \{0.1, 0.3, 0.5, 0.7, 0.9\}$. The unit adjustment cost for each DM, the group consensus levels, and the score of the alternatives with different ϑ are recorded in Figure 3, Tables 21, and 22, respectively.

According to Figure 3, it is apparent that the unit adjustment cost cm increases with respect to the value of ϑ for each DM. For the different value of ϑ, the unit adjustment cost between two decision makers may be different. For

Table 30: The adjusted evaluation information $Q^m = (q_{pn}^m)P \times N$ $(m = 1, \ldots, 20)$ for each DM.

		$f1$	$f2$	$f3$	$f4$	$f5$		$f1$	$f2$	$f3$	$f4$	$f5$		$f1$	$f2$	$f3$	$f4$	$f5$		$f1$	$f2$	$f3$	$f4$	$f5$
$x1$		0.2	0.3	0.4	0.6	0.4		0.7	0.2	0.4	0.5	0.5		0.8	0.3	0.6	0.4	0.6		0.4	0.4	0.7	0.4	0.6
$x2$	$e1$	0.1	0.4	0.5	0.9	0.6	$e2$	0.9	0.4	0.5	0.3	0.2	$e3$	0	0.6	0.4	0.9	0.6	$e4$	0.9	0.1	0.5	1.0	0.6
$x3$		0.5	0.2	0.8	0.8	0.7		0.8	0.8	0.7	1.0	0.1		1.0	0.4	0.8	0.7	0.8		0.7	0.8	0.6	0.7	0.8
$x4$		0.9	0.9	0.5	0.8	0.2		0.5	0.4	0.6	0.4	0.9		1.0	0	0.9	0.3	0.3		0.5	0.6	0.2	0.3	0.3
$x1$		0.6	0.5	0.4	0.4	0.4		0.6	0.5	0.4	0.4	0.4		0.6	0.7	0.6	0.5	0.1		0.4364	0.2892	0.6764	0.6970	0.3965
$x2$	$e5$	1.0	0.2	0.5	0.1	0.7	$e6$	0.6	0.2	0.3	0.9	0.6	$e7$	0.9	0.9	0.4	0.3	0.6	$e8$	0.2437	0.5357	0.5593	0.3308	0.4751
$x3$		0.8	0.5	0.8	0.8	0.4		0.8	0.5	0.3	0.7	0.7		0.8	0.6	0.5	0.9	0.7		0.5751	0.3630	0.7244	0.5985	0.6619
$x4$		0.3	0.2	0.5	0.6	0		0.3	0.2	0.5	0.3	0.5		0.8	0.5	0.6	0.4	0.2		0.7112	0.2555	0.8798	0.5538	0.3387
$x1$		0.4	0.3	0.3	1.0	0.4		0.2	0.2	0.6	0.8	0.4		0.4	0.5	0.4	0.7	0.4		0.4	0.5	0.6	0.6	0.6
$x2$	$e9$	0	0.6	0.6	0.5	0.2	$e10$	0.1	0.5	0.8	0	0.3	$e11$	0.9	0.1	0.5	0.2	0.9	$e12$	0.7	1.0	0.4	0.9	0.6
$x3$		0.7	0.2	0.8	0.5	1.0		0.5	0.2	0.9	1.0	0.8		0.7	0.8	0.8	1.0	0.7		0.4	0.5	0.5	0.8	0.6
$x4$		0.5	0.4	0.5	0.1	0.2		0.9	0.1	1.0	1.0	0.6		0.5	0.6	0.5	0.2	0		0	0.9	0.6	0.8	0.3
$x1$		0.4	0.5	0.4	0.4	0.5		0.7	0.2	0.4	0.3	0.4		0.4	0.6	0.3	0.4	0.4		0.2	0.5	0.6	0.4	0.5
$x2$	$e13$	0.9	0.2	0.3	0.7	0.2	$e14$	0.4	0.4	0.5	0.6	0.4	$e15$	0.6	0.6	0.6	1.0	0.9	$e16$	0.5	0.8	0.8	0.9	0.3
$x3$		0.7	0.5	0.3	0.4	0.1		0.8	0.6	0.3	0.4	0.6		0.7	0.4	0.8	0.9	0.7		0.5	0.8	0.9	0.7	0.1
$x4$		0.3	0.2	0.5	0	0.9		0.5	0.4	0.5	0.1	0.5		0.2	0.5	0.5	0.5	0.3		0.6	0.6	1.0	0.3	0.4
$x1$		0.7	0.3	0.1	0.6	0.8		0.2	0.3	0.3	0.4	1.0		0.3231	0.5079	0.4733	0.4305	0.5579		0.4729	0.2596	0.7000	0.6962	0.3000
$x2$	$e17$	1.0	0.4	0.3	0.9	0	$e18$	0.5	0.6	0.6	0.2	0.5	$e19$	0.4982	0.7710	0.5173	0.7000	0.5137	$e20$	0.4000	0.5453	0.5751	0.3657	0.6000
$x3$		0.8	0	0.6	0.8	1.0		0.5	0.4	0.8	0.3	0.5		0.5111	0.5725	0.6880	0.7259	0.3000		0.6753	0.2729	0.7577	0.2000	0.7853
$x4$		0.5	0.2	0.2	0.8	1.0		0.8	0.6	0.5	0.2	0.1		0.3566	0.7425	0.6586	0.5686	0.3297		0.5000	0.1901	0.8477	0.7000	0.3223

example, the unit adjustment costs of e14 and e15 are 0.5000 and 0.6775 when $\vartheta = 0.5$, respectively, while they are 0.8608 and 0.7827 when $\vartheta = 0.9$. In other words, $c14 < c15$ when $\vartheta = 0.5$ while $c14 > c15$ when $\vartheta = 0.9$. Therefore, we set a moderate value (i.e. $\vartheta = 0.5$) in the case study due to we cannot accurately obtain the importance of the experts' adjustment willingness or the satisfaction degree. For Table 21, the termination round is the first stage when $\vartheta = 0.1$ and 0.3, while the termination round is the third stage when $\vartheta = 0.5$, 0.7, and 0.9. This is because with the increase of adjustment cost, there are more opportunities, however, if the adjustment cost is too high, it is unfavorable for the consensus feedback process. Therefore, setting $\vartheta = 0.5$ is reasonable in the case study.

Based on Table 22, we found that the scores for each alternative are very similar. Due to the different unit adjustment cost, the different value of ϑ may lead to different DM to be adjusted in the same stage. Therefore, it will be a small difference in the score of the alternative with the different ϑ. However, the ranking of the alternatives is the same with the different ϑ. Therefore, it means that setting $\vartheta = 0.5$ is reasonable in the case study, and the proposed consensus model considering both the interactive weights and the experts' adjustment willingness is stability and rationality.

8.2. The Effect of Harmonious Degree in the Consensus Level Calculation. In Section 6, the consensus level for each subgroup is computed based on equation (14) and the value of a is 0.8. To further prove the rationality and stability of the proposed consensus model, a sensitivity analysis is introduced with different values of $a = \{0.6, 0.7, 0.8, 0.9, 1.0\}$. The consensus thresholds, the group consensus levels and the adjustment costs, and the score of the alternatives with different values of a are reported in Tables 23–25, respectively.

For Tables 23 and 24, it is apparent that the consensus thresholds and the initial group consensus levels increases with respect to a. Although the increase of the importance of the subgroups' harmonious degree will lead to the decrease of the subgroups' and the collective consensus level, it is very critical for the decision-making results. The consensus level of the subgroup not only represents the consistency of the opinion within subgroup, but also represents the DMs' attitude towards the decision-making results and the stability of the sub group's opinion. Therefore, it is reasonable and imperative that the consensus level considers both the opinion's consistency and the DMs' attitude. Meanwhile, the final group consensus levels satisfies the equation $CAR_T \leq CAR_{T+1}$ when $a = 0.6$, 0.7 and 0.8, while that meets the equation $GCL_T \geq \delta$ when $a = 0.9$ and 1.0. This is because with the increase of a, the differences between the consensus threshold δ and the initial consensus level GCL0 decreases, the consensus termination conditions are easy to meet than before. For example, the difference between the consensus threshold δ and the initial consensus level $GCL0$ is 0.0468 when $a = 0.6$ while 0.0097 when $a = 1.0$. Hence, with the increase of a, the difference between the current $GCLt$ and δ is less and less. Also, the constraint condition $CAR_T \leq CAR_{T+1}$ can obtain the $GCLT$ faster. Therefore, it is reasonable that the importance of the harmonious degree is 0.2 (i.e. $a = 0.8$) in the case study, and the termination condition is necessary and rationality.

According to Table 25, we found that the scores of alternatives are the same when a is 0.6 and 1.0, 0.7 and 0.8, respectively. This is because the iteration round is the same. Interestingly, the ranking of alternatives is the same when a is different. It shows that the proposed consensus model is more stable and the decision-making result is more scientific.

9. Conclusion

In this study, we propose a consensus model of LSGDM considering the interactive weights' determination and the experts' adjustment willingness, and apply it to select the building of an earthquake shelter. The main contributions and innovations of this research are shown as follows:

(1) We develop a novel method of weight determination, which considers the DMs' attitude towards the decision-making results, thereby ensuring the effective participation of DMs. Moreover, to improve the rationality of LSGDM, the harmonious degree is conducted in the calculation of subgroups' weight. It is of significance for the DMs more involved in the decision-making process and the decision-making result more reflect the willingness of DMs.

(2) By considering the experts' adjustment willingness, it is ensured that the evaluation information is less distorted or lost. Moreover, the unit adjustment cost is designed. Subsequently, to improve the efficiency of CRP, an identification rule combines the unit adjustment cost and the consensus level is presented to retain as much original information as possible in consensus feedback process, which can easily reach an acceptable level of consensus.

(3) An objective calculation method of the consensus threshold is conducted, and then a termination condition that considers both the current consensus level and the consensus adjustment rate is designed to objectively terminate the CRP. It not only compares the current consensus level with consensus threshold but compares the consensus adjustment rate. As a result, this method can address the subjectivity and unreasonableness of the preset consensus threshold and the maximum number of iterations to a certain extent.

Despite several valuable findings obtained by our research, there remain some limitations that should be further dealt with in the future. In this study, in addition to the interactive weights of the proposed model, the professional knowledge background and decision-making experience and other individual attributes of DMs should be considered. Moreover, with the development of social networks, the relationship between DMs that become complex should be considered in LSGDM. Also, the behavioral factors (i.e.

non-cooperation) [47] and psychological factor (i.e. self-confident) [48] of DMs should also be conducted, it will be a meaningful research for the LSGDM problems.

Appendix

A: The Proof of Theorem 1

Proof. First, the values of θ_m^+ and θ_m^- are both positive and in the interval [0, 1], so we have $0 \le \theta_m^+ + \theta_m^- \le 2$ and $0 \le \pi \cdot (\theta_m^+ + \theta_m^-)/4 \le \pi/2$. For the function $y = \cos(x)$, y is monotone decreasing when x is in the interval $[0, \pi/2]$. Thus, we can obtain that the value of $\cos\pi \cdot (\theta_m^+ + \theta_m^-)/4$ is in the interval of [0, 1]. Then, the value of ρ_m is positive and in the interval [0, 1]. The function $z = \sin(\pi \cdot x/2)$ is monotone increasing when x is in the interval [0, 1], so the value of z is in the interval [0, 1]. Therefore, the value of cm is in the interval of [0, 1]. □

B: The Information Provided by Experts

The information provided by experts are reported in Tables 26–28. In this paper, the value range of q_{pn}^m is from 0 to 1 (Tables 29 and 30).

Data Availability

The data used to support the findings of this paper are included within the article (Case Study section and Appendix).

Conflicts of Interest

The authors declare that they have no conflicts of interest.

Acknowledgments

The authors appreciate the financial support of the National Key Research and Development Program of China (Grant no. 2018YFB1402500) and the Natural Science Foundation of Heilongjiang Province (Grant no. JJ2021LH1530). The Reform and Develop High-Level Talent Projects in Local Universities Supported by the Central Government (2020GSP13)

References

[1] X.-H. Xu, Z.-J. Du, and X.-H. Chen, "Consensus model for multi-criteria large-group emergency decision making considering non-cooperative behaviors and minority opinions," *Decision Support Systems*, vol. 79, pp. 150–160, 2015.

[2] L. Li and W. Wei, "Two-stage consensus model based on opinion dynamics and evolution of social power in large-scale group decision making," *Applied Soft Computing*, vol. 111, Article ID 107615, 2021.

[3] Z. Shi, X. Wang, I. Palomares, S. Guo, and R.-X. Ding, "A novel consensus model for multi-attribute large-scale group decision making based on comprehensive behavior classification and adaptive weight updating," *Knowledge-Based Systems*, vol. 158, pp. 196–208, 2018.

[4] Z. Zhong, X. Xu, and Y. Yin, "A multi-stage hybrid consensus reaching model for multi-attribute large group decision-making: integrating cardinal consensus and ordinal consensus," *Computers & Industrial Engineering*, vol. 158, Article ID 107443, 2021.

[5] Z. Zhong, X. Xu, and P. Pan, "A non-threshold consensus model based on the minimum cost and maximum consensus-increasing for multi-attribute large group decision-making," *Information Fusion*, vol. 77, no. 77, pp. 90–106, 2022.

[6] Z.-j. Du, H.-y. Luo, X.-d. Lin, and S.-m. Yu, "A trust-similarity analysis-based clustering method for large-scale group decision-making under a social network," *Information Fusion*, vol. 63, pp. 13–29, 2020.

[7] S.-P. Wan and J.-Y. Dong, "Interval-valued intuitionistic fuzzy mathematical programming method for hybrid multi-criteria group decision making with interval-valued intuitionistic fuzzy truth degrees," *Information Fusion*, vol. 26, pp. 49–65, 2015.

[8] L. Liu, X. Xu, G. Gong, and H. Herrera, "Democratic consensus reaching process for multi-person multi-criteria large scale decision making considering participants' individual attributes and concerns," *Information Fusion*, vol. 77, pp. 220–232, 2022.

[9] X.-h. Xu, Z.-j. Du, and X.-h. Chen, "Consensus model for multi-criteria large-group emergency decision making considering non-cooperative behaviors and minority opinions," *Decision Support Systems*, vol. 79, pp. 150–160, 2015.

[10] Z.-S. Chen, L.-L. Yang, K.-S. Chin et al., "Sustainable building material selection: an integrated multi-criteria large group decision making framework," *Applied Soft Computing*, vol. 113, Article ID 107903, 2021.

[11] S. Bai, H. He, M. Ge, R. Yang, D. Luo, and X. Bi, "Large-scale group decision-making model with cooperative behavior based on social network analysis considering propagation of decision-makers' preference," *Journal of Mathematics*, vol. 2022, 2022.

[12] Z. Wu and J. Xu, "A consensus model for large-scale group decision making with hesitant fuzzy information and changeable clusters," *Information Fusion*, vol. 41, pp. 217–231, 2018.

[13] L. Huchang, L. Xiaofang, and T. Ming, "How to process local and global consensus? A large-scale group decision making model based on social network analysis with probabilistic linguistic information," *Information Sciences*, vol. 579, pp. 368–387, 2021.

[14] Z. Meng, G. Mei, and L. Zichao, "A consensus model for large-scale multi-attribute group decision making with collaboration-reference network under uncertain linguistic environment," *Journal of Intelligent and Fuzzy Systems*, vol. 37, no. 3, pp. 4133–4156, 2019.

[15] G. Luis, F. Pérez, F. Mata, and M. Chiclana, "Social network decision making with linguistic trustworthiness-based induced OWA operators," *International Journal of Intelligent Systems*, vol. 29, no. 12, pp. 1117–1137, 2014.

[16] B. Liu, Y. Shen, X. Chen, Y. Chen, and X. Wang, "A partial binary tree DEA-DA cyclic classification model for decision makers in complex multi-attribute large-group interval-valued intuitionistic fuzzy decision-making problems," *Information Fusion*, vol. 18, pp. 119–130, 2014.

[17] B. Liu, S. Guo, K. Yan, L. Li, and X. Wang, "Double weight determination method for experts of complex multi-attribute large-group decision-making in interval-valued intuitionistic

fuzzy environment," *Journal of Systems Engineering and Electronics*, vol. 28, no. 01, pp. 88–96, 2017.

[18] W. Qifeng, X. Xuanhua, Z. Jun, and P. Bin, "A sentiment analysis-based expert weight determination method for large-scale group decision-making driven by social media data," *Expert Systems with Applications*, vol. 185, Article ID 115629, 2021.

[19] Y. Xu, X. Wen, and W. Zhang, "A two-stage consensus method for large-scale multi-attribute group decision making with an application to earthquake shelter selection," *Computers & Industrial Engineering*, vol. 116, 2018.

[20] B. Liu, L. Yu, R.-X. Ding, B. Yang, and Z. Li, "A decision-making method based on a two-stage regularized generalized canonical correlation analysis for complex multi-attribute large-group decision making problems," *Journal of Intelligent and Fuzzy Systems*, vol. 34, no. 6, pp. 3941–3953, 2018.

[21] Z. Zhen, C. Guo, and L. Martínez, "Managing multi-granular linguistic distribution assessments in large-scale multi-attribute group decision making," *IEEE Transactions on Systems Man & Cybernetics Systems*, vol. 47, no. 11, pp. 3063–3076, 2017.

[22] I. Palomares, L. Martinez, and F. Herrera, "A consensus model to detect and manage noncooperative behaviors in large-scale group decision making," *IEEE Transactions on Fuzzy Systems*, vol. 22, no. 3, pp. 516–530, 2014.

[23] X. H. Xu, X. Y. Zhong, X. H. Chen, and Y. J. Zhou, "A dynamical consensus method based on exit–delegation mechanism for large group emergency decision making," *Knowledge-Based Systems*, vol. 86, pp. 237–249, 2015.

[24] B. Liu, Q. Zhou, R.-X. Ding, I. Palomares, and F. Herrera, "Large-scale group decision making model based on social network analysis: trust relationship-based conflict detection and elimination," *European Journal of Operational Research*, vol. 275, no. 2, pp. 737–754, 2018.

[25] B. Liu, Y. Chen, Y. Shen, H. Sun, and X. Xu, "A complex multi-attribute large-group decision making method based on the interval-valued intuitionistic fuzzy principal component analysis model," *Soft Computing*, vol. 18, no. 11, pp. 2149–2160, 2014.

[26] B. Liu, Y. Shen, W. Zhang, X. Chen, and X. Wang, "An interval-valued intuitionistic fuzzy principal component analysis model-based method for complex multi-attribute large-group decision-making," *European Journal of Operational Research*, vol. 245, no. 1, pp. 209–225, 2015.

[27] Z.-S. Chen, X. Zhang, R. M. Rodriguez, W. Pedrycz, L. Martinez, and M. J. Skibniewski, "Expertise-structure and risk-appetite-integrated two-tiered collective opinion generation framework for large scale group decision making," *IEEE Transactions on Fuzzy Systems*, 2022.

[28] S. Zeng, W. Su, and L. Sun, "A method based on similarity measures for interactive group decision-making with intuitionistic fuzzy preference relations," *Applied Mathematical Modelling*, vol. 37, no. 10-11, pp. 6909–6917, 2013.

[29] H. Liao and Z. Xu, "Satisfaction degree based interactive decision making under hesitant fuzzy environment with incomplete weights," *International Journal of Uncertainty, Fuzziness and Knowledge-Based Systems: IJUFKS*, vol. 22, no. 4, pp. 553–572, 2014.

[30] J. Ding, Z. Xu, and N. Zhao, "An interactive approach to probabilistic hesitant fuzzy multi-attribute group decision making with incomplete weight information," *Journal of Intelligent and Fuzzy Systems*, vol. 32, no. 3, pp. 2523–2536, 2017.

[31] S.-P. Wan, J. Yan, and J.-Y. Dong, "Personalized individual semantics based consensus reaching process for large-scale group decision making with probabilistic linguistic preference relations and application to COVID-19 surveillance," *Expert Systems with Applications*, vol. 191, Article ID 116328, 2022.

[32] S.-P. Wan, W.-C. Zou, J.-Y. Dong, and L. Martínez, "A probabilistic linguistic dominance score method considering individual semantics and psychological behavior of decision makers," *Expert Systems with Applications*, vol. 184, Article ID 115372, 2021.

[33] Z. Zhang, Y. Gao, and Z. Li, "Consensus reaching for social network group decision making by considering leadership and bounded confidence," *Knowledge-Based Systems*, vol. 204, Article ID 106240, 2020.

[34] Z. Zhang, Z. Li, and Y. Gao, "Consensus reaching for group decision making with multi-granular unbalanced linguistic information: a bounded confidence and minimum adjustment-based approach," *Information Fusion*, vol. 74, pp. 96–110, 2021.

[35] S.-P. Wan, W.-C. Zou, J.-Y. Dong, and L. Martínez, "A consensual method for multi-criteria group decision-making with linguistic intuitionistic information," *Information Sciences*, vol. 582, pp. 797–832, 2022.

[36] L. Xiao, Z.-S. Chen, X. Zhang, J.-P. Chang, W. Pedrycz, and K.-S. Chin, "Bid evaluation for major construction projects under large-scale group decision-making environment and characterized expertise levels," *International Journal of Computational Intelligence Systems*, vol. 13, no. 1, pp. 1227–1242, 2020.

[37] Z.-S. Chen, X.-L. Liu, K.-S. Chin, W. Pedrycz, K.-L. Tsui, and M. J. Skibniewski, "Online-review analysis based large-scale group decision-making for determining passenger demands and evaluating passenger satisfaction: case study of high-speed rail system in China," *Information Fusion*, vol. 69, pp. 22–39, 2021.

[38] Y. Dong, Y. Liu, H. Liang, F. Chiclana, and E. Herrera-Viedma, "Strategic weight manipulation in multiple attribute decision making," *Omega*, vol. 75, pp. 154–164, 2018.

[39] L. Yanling, X. Yejun, H. V. Enrique, and H. Yefan, "Consensus of large-scale group decision making in social network: the minimum cost model based on robust optimization," *Information Sciences*, vol. 547, pp. 910–930, 2021.

[40] N. Zhang, Z. Gong, and F. Chiclana, "Minimum cost consensus models based on random opinions," *Expert Systems with Applications*, vol. 89, pp. 149–159, 2017.

[41] D. Cheng, Z. Zhou, F. Cheng, Y. Zhou, and Y. Xie, "Modeling the minimum cost consensus problem in an asymmetric costs context," *European Journal of Operational Research*, vol. 270, no. 3, pp. 1122–1137, 2018.

[42] Á. Labella, H. Liu, R. M. Rodríguez, and L. Martínez, "A cost consensus metric for consensus reaching processes based on a comprehensive minimum cost model," *European Journal of Operational Research*, vol. 281, no. 2, pp. 316–331, 2020.

[43] T. Wu, X. Liu, J. Qin, and F. Herrera, "Balance dynamic clustering analysis and consensus reaching process with consensus evolution networks in large-scale group decision making," *IEEE Transactions on Fuzzy Systems*, vol. 29, no. 2, pp. 357–371, 2021.

[44] H. Liang, Y. Dong, Z. Ding, R. Urena, and E. Herrera-Viedma, "Consensus reaching with time constraints and minimum adjustments in group with bounded confidence effects," *IEEE Transactions on Fuzzy Systems*, vol. 28, no. 10, pp. 2466–2479, 2019.

[45] H. Zhang, G. Kou, and Y. Peng, "Soft consensus cost models for group decision making and economic interpretations," *European Journal of Operational Research*, vol. 277, no. 3, pp. 964–980, 2019.

[46] W. Zelin, W. Y. Ming, and M. Luis, "A two-stage minimum adjustment consensus model for large scale decision making based on reliability modeled by two-dimension 2-tuple linguistic information," *Computers & Industrial Engineering*, vol. 151, Article ID 106973, 2020.

[47] Y. Gao and Z. Zhang, "Consensus reaching with non-cooperative behavior management for personalized individual semantics-based social network group decision making," *Journal of the Operational Research Society*, pp. 1–18, 2021.

[48] Z. Zhang, X. Kou, W. Yu, and Y. Gao, "Consistency improvement for fuzzy preference relations with self-confidence: an application in two-sided matching decision making," *Journal of the Operational Research Society*, pp. 1–14, 2020.

Hindawi
Complexity
Volume 2022, Article ID 9198737, 14 pages
https://doi.org/10.1155/2022/9198737

Research Article

Performance Analysis in Production Systems with Uncertain Data: A Stochastic Data Envelopment Analysis Approach

Seyedeh Fatemeh Bagheri,[1] Alireza Amirteimoori,[1] Sohrab Kordrostami,[2] and Mansour Soufi[3]

[1]*Department of Applied Mathematics, Rasht Branch, Islamic Azad University, Rasht, Iran*
[2]*Department of Applied Mathematics, Lahijan Branch, Islamic Azad University, Lahijan, Iran*
[3]*Department of Industrial Management, Rasht branch, Islamic Azad University, Rasht, Iran*

Correspondence should be addressed to Alireza Amirteimoori; aamirteimoori@gmail.com

Received 6 August 2022; Revised 13 September 2022; Accepted 5 October 2022; Published 12 October 2022

Academic Editor: Zeljko Stevic

The problem of determining an optimal benchmark to inefficient decision-making units (DMUs) is an important issue in the field of performance analysis. Previous methods for determining the projection points of inefficient DMUs have only focused on one objective and other features have been ignored. This paper attempts to determine the best projection point for each DMU when the inputs and outputs data are in stochastic form and presents an alternative definition for the best projection by considering three main aspects: technical efficient, minimal cost, and maximal revenue as much as possible. Considering the important role of the electricity industry in the economic growth of each country, a practical example has been implemented on 16 regional electricity companies in Iran in 9 consecutive periods. The efficiency score along with the projection points of the three technical models (BCC model of Banker et al. (1984)), cost, and stochastic revenue are compared with the projection point obtained from the model presented in this article, which simultaneously meets these three objectives, showing the improvement of companies' performance.

1. Introduction

Data envelopment analysis (DEA) was first introduced by Charnes et al. [1] (CCR model) to calculate the relative efficiency of a set of homogeneous decision-making units (DMU) and extended by Banker et al. [2] (BCC model). Traditional DEA models (BCC and CCR models) rely on past information and they are developed in deterministic case, and hence the uncertainty and stochasticity of the data are ignored. In the real world, we are faced with many decisions, most of which are associated with uncertainty. Stochastic data envelopment analysis models to address these shortcomings were proposed by Charnes and Cooper [3]. In the last two decades, performance analysis in an uncertain environment has been studied frequently. See for instances Hossain et al. [4], Mo et al. [5], Rong et al. [6], Amirteimoori et al. [7], and Ghasemi et al. [8].

Some of the differences between DEA and stochastic DEA (SDEA) models have been presented in Table 1. SDEA method is based on stochastic programming methods, which is one of the branches of mathematical programming. Stochastic programming models are divided into E-model and P-model in terms of the type of objective function. E-model based stochastic programming models are used to obtain the expected value or mathematical expectation that the objective function of such models does not include a random variable. To obtain the highest probability of an event occurring, stochastic programming models based on P-model are used so that in the objective function of such models, a random variable is used possibly. Charnes and Cooper [9] proposed a stochastic programming model with potential constraints. They were then introduced by Land et al. [10] E-model-based stochastic programming model. Programming models based on E-model are used to obtain

Table 1: Differences between models.

DEA model	SDEA model
The values of inputs and outputs are definite.	The values of inputs and outputs are random.
No accidental error is entered in the model	Random error enters the model in the form of a random component
The model offers only past performance	Allows you to predict performance in the future
The efficiency frontier is very sensitive to small changes in inputs and outputs.	The efficiency frontier is less sensitive to changes in inputs and outputs.
The error level in such models is considered zero.	Efficiency is defined according to the level of error in the model.
In the final model, the correlation between inputs and outputs is not considered.	The correlation between inputs and outputs is considered in such models.

the expected value. The objective function of these models does not include random variables.

The efficiency measure in which, in addition to input and output data, the price of the input of the DMUs is also required and its goal is cost minimization, called cost efficiency, was introduced by Farrell [11]. Färe et al. [12] developed cost efficiency. By studying data envelopment analysis and stochastic cost functions, Cooper and Ton [13] identified some specific problems in stochastic frontier analysis (SFA). Stochastic frontier analysis method is a parametric method. Shiraz et al. [14] formulated the stochastic cost model in a nonlinear form.

Färe et al. [12] have played a key role in the development of revenue efficiency. In addition to input and output data, they have also paid attention to the output of the decision-making unit aiming at maximizing revenue. Lin [15] proposed a method to set revenue targets at the efficient frontier. Shiraz et al. [14] also presented a random income model that is nonlinear.

In data envelopment analysis, DMUs are divided into two categories: efficient and inefficient units. Inefficient units can be efficient by decreasing their inputs level and increasing their outputs level.

Achieving optimal scale size (OSS) has always been of interest to researchers. Cesaroni and Giovannola [16] introduced a new definition of optimal scale size based on minimizing the cost of each unit so that average cost productivity combines scale productivity and allocation and generalizes economic scale size in productivity analysis. In the following, Haghighatpisheh et al. [17] proposed a new definition of optimal scale size that uses both of the cost of inputs and the revenue of outputs. This measure of average cost-revenue efficiency (ACRE) shows the ratio of profitability efficiency to average productivity.

The process of industrialization of developed countries shows proper planning, optimal use of resources, and determining the appropriate pattern as the main goal in the development process of these countries. The electricity industry has an infrastructural and influential role on the economic growth of any country. In recent years, per capita electricity consumption in Iran has increased significantly in parallel with its production rate. Accordingly, efficiency and determining the appropriate model for companies has always been the concern of managers in the electricity industry. In this article, a real and useful example has been done on Iran's regional electricity distribution companies and it has used random data that can play an important role as a vision in the electricity industry and solving future challenges.

Most studies to find the projection point of each inefficient unit have focused on only one goal. For example, the projection point obtained from the cost model finds an efficient point on efficient frontier with the cost minimization approach. The projection point obtained from the revenue model moves towards the frontier with the revenue maximization approach. Bagheri et al. [18] presented a method that simultaneously tried to meet the projection point of each unit from three perspectives, cost minimization, revenue maximization, and the shortest distance to the efficient frontier as much as possible and it was proved that the efficiency of the model obtained for inefficient units is higher than the unit under evaluation. The results of solving this method for managers to make decisions were based on past information, so we tried to use stochastic programming. In this paper, for each inefficient unit, a projection point is obtained, which is very important in two stages. First, the resulting projection for each unit meets as many as possible the three technical, cost, and revenue concepts. Secondly, random data and stochastic programming in linear form are used in it. Therefore, it will greatly help managers to make better decisions in the future and improve the performance of units.

This paper has been organized as follows: technical, cost, and revenue efficiency with deterministic and random data are examined in Sections 2 and 3, respectively. The random models of the linearly shaped models have been presented in Section 3. In Section 4, the method proposed by Bagheri et al. [18] to determine the ideal projection point has been implemented this time in stochastic programming. In Section 5, we will provide a real and practical example, and finally in Section 6, the conclusion of the article is presented.

2. Deterministic DEA Models

In this section, we briefly review some basic DEA models in deterministic environment. Technical efficiency measure was first introduced by Debreu [19] and Farrell [11]. The traditional DEA-based models CCR model of Charnes et al. [1] and its subsequent extension BCC model of Banker et al. [2] was developed on classical efficiency analysis model of Farrell [11]. The BCC model for evaluating a specific DMU_p

is formulated in the input-oriented deterministic environment as follows:

$$\begin{aligned}
&\text{Min}\theta \\
&\sum_{j=1}^{n}\lambda_j x_{ij} \le \theta x_{ip}, \quad i = 1,\ldots,m, \\
&\sum_{j=1}^{n}\lambda_j y_{rj} \ge y_{rp}, \quad r = 1,\ldots,s, \\
&\sum_{j=1}^{n}\lambda_j = 1, \quad \lambda_j \ge 0,\ j = 1,\ldots,n, \\
&\theta_p \text{free variable.}
\end{aligned} \tag{1}$$

In the above model, θ is the input abatement factor. DMU_p is said to be technically efficient if and only $\theta = 1$ and all slack variables are equal to zero. Corresponding to each inefficient point, a frontier point is determined by reducing inputs. Removing the third convexity constraint $\sum_{j=1}^{n}\lambda_j = 1$ leads to CCR model.

For each inefficient unit, there is one or more efficient units on the efficient frontier that is called the reference set. The reference set of a specific inefficient DMU (denoted by E_o) is defined as follows:

$$E_o = \left\{ j \mid \lambda_j^* > 0 \right\} (j \in \{1,\ldots,n\}). \tag{2}$$

In technical efficiency models we have less information on inputs and outputs of DMUs. In other words, all we know the quantitative values of inputs and outputs and there is no information on inputs and outputs prices. More information will be available if we also have the costs of the inputs and the prices of the outputs. In this case, we are motivated to calculate the allocative efficiency of the DMUs. We first introduce cost allocative model. Suppose that $C = (c_1, c_2, \ldots, c_m)^t$ is the vector of input prices and $\overline{X} = (\overline{x}_1, \overline{x}_2, \ldots, \overline{x}_m)^t$ is cost minimizing vector of input quantities. Farrell (1957) proposed a measure of cost efficiency. The cost efficiency model in VRS environment is formulated as follows:

$$\begin{aligned}
&\text{Min}\sum_{i=1}^{m} c_i \overline{x}_i, \\
&\sum_{j=1}^{n}\lambda_j x_{ij} \le \overline{x}_i, \quad i = 1,\ldots,m, \\
&\sum_{j=1}^{n}\lambda_j y_{rj} \ge y_{rp}, \quad r = 1,\ldots,s, \\
&\sum_{j=1}^{n}\lambda_j = 1 \quad \lambda_j \ge 0, \quad j = 1,\ldots,n,
\end{aligned} \tag{3}$$

The cost efficiency of DMU_p is defined as the ratio of the optimal cost to the actual cost as follows:

$$CE_p = \frac{\sum_{i=1}^{m} c_i \overline{x}_i}{\sum_{i=1}^{m} c_i x_{ip}}. \tag{4}$$

Clearly, $CE_p \le 1$ and when this score is equal to one, then DMU_p is called cost efficient, otherwise we say DMU_p is cost inefficient.

Now suppose that we are given information on the price of the outputs. In this case, the revenue efficiency model in VRS environment is formulated as follows:

$$\begin{aligned}
&\text{Max}\sum_{r=1}^{s} p_r \overline{y}_r, \\
&\sum_{j=1}^{n}\lambda_j x_{ij} \le x_{ip}, \quad i = 1,\ldots,m, \\
&\sum_{j=1}^{n}\lambda_j y_{rj} \ge \overline{y}_r, \quad r = 1,\ldots,s, \\
&\sum_{j=1}^{n}\lambda_j = 1 \quad \lambda_j \ge 0,\ j = 1,\ldots,n.
\end{aligned} \tag{5}$$

In the above equation, $P = (p_1, p_2, \ldots, p_s)^t$ is vector of output prices and $\overline{Y} = (\overline{y}_1, \overline{y}_2, \ldots, \overline{y}_s)^t$ is revenue maximizing vector of output quantities.

The revenue efficiency of $DM\ U_p$ is defined as the ratio of optimal revenue to the actual revenue, i.e., $RE_p = \sum_{r=1}^{s} p_r \overline{y}_r / \sum_{r=1}^{s} p_r y_{rp}$.

It is easy to see that $RE_p \ge 1$. If this score is equal to one, then DMU_p is called revenue efficient, otherwise we say DMU_p is revenue inefficient.

3. Basic DEA Models in Stochastic Environment

As we stated before, in many real applications, we often encounter uncertainty, so it is necessary to generalize the models to the uncertainty mode, especially the random mode. SDEA models were first proposed by Charnes and Cooper (1959). Land et al. (1993) introduced the CCR model in the stochastic mode considering the inputs and outputs and estimating the probability distribution prevailing over them, after estimating the efficiency in the future, that by considering the convexity condition, the BCC model is obtained randomly in the nature of the input. In this model, we show the random input and output values by $\widetilde{x}_{ij}$ and $\widetilde{y}_{rj}$, respectively. These values show the mathematical expectations of random inputs and outputs. Also, a_{ij} and b_{rj} are the standard deviations of random inputs and outputs, respectively. Using a random variable error structure, Cooper et al. [20] proposed the following input-oriented DEA model:

$$
\begin{aligned}
&\text{Min}\theta\\
&\sum_{j=1}^{n}\lambda_j x_{ij} - \varnothing^{-1}(\propto)\sigma\left(p_i^+ + p_i^-\right) \le \theta x_{ip}, \quad i = 1,\ldots,m,\\
&\sum_{j=1}^{n}\lambda_j a_{ij} - \theta a_{ip} = p_i^+ - p_i^-, \quad i = 1,\ldots,m,\\
&\sum_{j=1}^{n}\lambda_j y_{rj} + \varnothing^{-1}(\propto)\sigma\left(q_r^+ + q_r^-\right) \ge y_{rp}, \quad r = 1,\ldots,s,\\
&\sum_{j=1}^{n}\lambda_j b_{rj} - \theta b_{rp} = q_r^+ - q_r^-, \quad r = 1,\ldots,s,\\
&\sum_{j=1}^{n}\lambda_j = 1\lambda_j, \quad \ge 0,\ j = 1,\ldots,n,\\
&p_i^+, p_i^- \ge 0, \quad i = 1,\ldots,m,\ q_r^+, q_r^- \ge 0,\ r = 1,\ldots,s.
\end{aligned}
\tag{6}
$$

The first two constraints in model (4) are related to input variables and the next two constraints are related to output variables. The goal is to minimize the level of inputs by the abatement factor θ. σ has a standard normal distribution and $\varnothing^{-1}$ shows the inverse of the standard normal distribution function. The positive deviation variables $p_i^+, p_i^-, q_r^+, q_r^-$ have been used to transform the model into a linear form.

Corresponding to each inefficient DMU, the projection point was obtained from the above stochastic model through the formula $(\sum_{j=1}^{n}\lambda_j x_{ij}, \sum_{j=1}^{n}\lambda_j y_{rj})$.

Producing a certain level of outputs from the least cost of inputs is called cost efficiency, in which information about the price of inputs is considered. In the following, we present the cost efficiency model in stochastic environment. Inspired by the deterministic form of a stochastic model, we assume that c_i is the *i-th* input price whose value is constant for all units. Also, $\overline{x_i}$ is considered to be the ideal input whose value is unknown.

Suppose that x_{ij} and y_{rj} are the mathematical expectations of the inputs and outputs of $\widetilde{x}_{ij}$ and $\widetilde{y}_{rj}$, respectively. Moreover, suppose a_{ij} and b_{rj} are their corresponding standard deviations. The cost efficiency model is formulated as follows:

$$
\begin{aligned}
&\text{Min}\sum_{i=1}^{m} c_i\overline{x}_i,\\
&\sum_{j=1}^{n}\lambda_j x_{ij} - \varnothing^{-1}(\propto)\sigma\left(p_i^+ + p_i^-\right) \le \overline{x}_i, \quad i = 1,\ldots,m,\\
&\sum_{j=1}^{n}\lambda_j a_{ij} - \theta a_{ip} = p_i^+ - p_i^-, \quad i = 1,\ldots,m,\\
&\sum_{j=1}^{n}\lambda_j y_{rj} + \varnothing^{-1}(\propto)\sigma\left(q_r^+ + q_r^-\right) \ge y_{rp}, \quad r = 1,\ldots,s,\\
&\sum_{j=1}^{n}\lambda_j b_{rj} - b_{rp} = q_r^+ - q_r^-, \quad r = 1,\ldots,s,\\
&\sum_{j=1}^{n}\lambda_j = 1, \quad \lambda_j, \ge 0, \quad j = 1,\ldots,n,\\
&p_i^+, p_i^- \ge 0, \quad i = 1,\ldots,m, q_r^+, q_r^- \ge 0,\ r = 1,\ldots,s.
\end{aligned}
\tag{7}
$$

In this model, the objective is to minimize the total cost of inputs. This model is formulated under variable returns to scale and the cost efficiency of DMU_p is defined as follows:

$$
CE_p = \frac{\sum_{i=1}^{m} c_i\overline{x}_i}{\sum_{i=1}^{m} c_i x_{ip}}. \tag{8}
$$

Corresponding to each inefficient point, the efficient projection point is obtained from the above stochastic model through the formula $(\sum_{j=1}^{n}\lambda_j x_{ij}, \sum_{j=1}^{n}\lambda_j y_{rj})$. It can be easily shown that the obtained projection point is efficient at the desired confidence level. σ has a standard normal distribution and $\varnothing^{-1}$ shows the inverse of the standard normal distribution function in the above linear model.

Now, we propose the revenue efficiency model. As it is known in DEA literature, producing the highest level of outputs from a certain level of inputs is called revenue efficiency. Assume that w_r is the *r-th* output price whose value is constant for all units. Also, $\overline{y_{\text{r}}}$ is considered to be the *r-th* optimal output value whose value is unknown. Suppose that x_{ij} and y_{rj} are the mathematical expectations of the inputs and outputs of $\widetilde{x}_{ij}$ and $\widetilde{y}_{rj}$, respectively. Also, a_{ij} and b_{rj} are the standard deviations of the inputs and outputs $\widetilde{x}_{ij}$ and $\widetilde{y}_{rj}$, respectively. The revenue efficiency model is formulated in a linear form in a random environment as follows:

$$
\begin{aligned}
&\text{Max}\sum_{r=1}^{s} w_r\overline{y_{\text{r}}},\\
&s.t:\ \sum_{j=1}^{n}\lambda_j x_{ij} - \varnothing^{-1}(\propto)\sigma\left(p_i^+ + p_i^-\right) \le x_{ip}, \quad i = 1,\ldots,m,\\
&\sum_{j=1}^{n}\lambda_j a_{ij} - \theta a_{ip} = p_i^+ - p_i^-, \quad i = 1,\ldots,m,\\
&\sum_{j=1}^{n}\lambda_j y_{rj} + \varnothing^{-1}(\propto)\sigma\left(q_r^+ + q_r^-\right) \ge \overline{y_{\text{r}}}, \quad r = 1,\ldots,s,\\
&\sum_{j=1}^{n}\lambda_j b_{rj} - b_{rp} = q_r^+ - q_r^-, \quad r = 1,\ldots,s,\\
&\sum_{j=1}^{n}\lambda_j = 1 \quad \lambda_j, \ge 0, \quad j = 1,\ldots,n,\\
&p_i^+, p_i^- \ge 0, \quad i = 1,\ldots,m\, q_r^+, q_r^- \ge 0,\ r = 1,\ldots,s.
\end{aligned}
\tag{9}
$$

The first two constraints in the above model are related to input variables and the next two constraints are related to output variables. In this model, the goal is to maximize the revenue of outputs. This model is formulated under variable returns to scale and its efficiency score is obtained from the following formula.

$$RE_p = \frac{\sum_{r=1}^{s} w_r \overline{y}_r}{\sum_{r=1}^{s} w_r y_{rp}}. \quad (10)$$

The projection point is obtained from the above linearized random revenue model through the formula $(\sum_{j=1}^{n} \lambda_j x_{ij}, \sum_{j=1}^{n} \lambda_j y_{rj})$. It can be easily proved that the obtained projection point is efficient at the desired confidence level. σ has a standard normal distribution and $\varnothing^{-1}$ shows the inverse of the standard normal distribution function in the above linear model.

4. The Best Projection Point

In this section, the best projection point in a random environment is determined. As you know, there is an ideal pattern for any inefficient unit. The ideal pattern means the projection point obtained as each decision unit. Bagheri et al. [18] presented a method in which an ideal model was obtained for each unit, which first dominates the unit under evaluation. Therefore, it will be much more efficient. Secondly, in the convex combination of projection points obtained from cost, revenue, and technical models, this projection point is simultaneously examined from three technical, minimum cost, and maximum revenue perspectives. One of the defects of such models is that they rely on past information, so they cannot provide the desired result. One way to solve this problem is to use random data envelopment analysis. In such models, a random error is added to the model in the form of a random component, in which the efficiency is defined according to the error level ($\propto$.)and the correlation between the input and output variables is taken into account in the model. Toward this end, we proceed as follows:

Step 1: First, we obtain the projection points of the technical, cost, and random revenue models in linear form under the variable returns to scale (models (4)–(6)), which were described in the previous section, naming (x_{ip}^T, y_{rp}^T), (x_{ip}^C, y_{rp}^C), and (x_{ip}^R, y_{rp}^R), such that random cost and revenue models in linear form are an innovation of this article.

Step 2: Then, using the proposed model, we introduce the point distance $(\overline{x}_i, \overline{y}_r)$ from each of the projection points of the BCC, cost, and revenue linearized random models (models (4)–(6)), which are represented by d_1, d_2, d_3, respectively, and minimized under norm 2 in the objective function of the model (8) so that this point of the new projection is located in the convex shell of these points and at the same time overcome the unit under its evaluation. Therefore, the obtained model will be more efficient for each inefficient unit and also more efficient than the unit under evaluation.

$$\begin{aligned}
&\text{Min} d_1 + d_2 + d_3 \\
&\sqrt{\sum_{i=1}^{m} \left(\overline{x}_i - x_{ip}^T\right)^2 + \sum_{r=1}^{s} \left(\overline{y}_r - y_{rp}^T\right)^2} = d_1, \quad j = 1, \ldots, n, \\
&\sqrt{\sum_{i=1}^{m} \left(\overline{x}_i - x_{ip}^C\right)^2 + \sum_{r=1}^{s} \left(\overline{y}_r - y_{rp}^C\right)^2} = d_2, \quad j = 1, \ldots, n, \\
&\sqrt{\sum_{i=1}^{m} \left(\overline{x}_i - x_{ip}^R\right)^2 + \sum_{r=1}^{s} \left(\overline{y}_r - y_{rp}^R\right)^2} = d_3, \quad j = 1, \ldots, n, \\
&\lambda_1 x_{ip}^T + \lambda_2 x_{ip}^C + \lambda_3 x_{ip}^R = \overline{x}_i, \quad i = 1, \ldots, m \; j = 1, \ldots, n, \\
&\lambda_1 y_{rp}^T + \lambda_2 y_{rp}^C + \lambda_3 y_{rp}^R = \overline{y}_r, \quad r = 1, \ldots, s \; j = 1, \ldots, n, \\
&\sum_{k=1}^{3} \lambda_k = 1, \\
&d_1 \geq 0, d_2 \geq 0, \; d_3 \geq 0 \\
&\overline{x}_i \geq 0 \,, \; \overline{y}_r \geq 0 \,, \lambda_k \geq 0
\end{aligned} \quad (11)$$

Table 2: Input and output variables.

Input variables	Output variables
(1) Fuel consumption in terms of million liters (2) Nominal power (3) Length of transmission lines (4) Capacity of transfer posts (5) The length of the above distribution lines (6) Capacity of the above distribution posts	(1) Sending energy to neighboring and overseas power companies at the transmission voltage level (2) Selling energy to electricity distribution companies and industrial companies and the above distribution voltage level

Table 3: The mean value inputs and outputs.

DMUs	Electricity distribution companies	The mean value of the first input	The mean value of the second input	The mean value of the third input	The mean value of the fourth input	The mean value of the fifth input	The mean value of the sixth input	The mean value of the first output	The mean value of the second output
1	Azerbaijan	2921	2776	3723	5808	4234	4574	7420	12211
2	Esfahan	3526	2204	3200	8406	5545	6700	6708	20752
3	Kermanshah	2898	2360	3975	7767	5562	5446	7849	13818
4	Tehran	7994	7682	4214	21400	4679	13864	9751	390100
5	Khorasan	3570	3538	1883	4166	8400	6913	2591	16434
6	Khuzestan	2906	2286	3691	12983	3874	8716	7274	28195
7	Zanjan	177	324	1170	3231	2382	2989	2270	6695
8	Semnan	109	269	1002	2401	859	1066	1527	2629
9	Sistan and Baluchestan	1127	1002	3716	2046	2935	2077	411	4468
10	The west	1609	1481	2958	4682	4369	3330	5012	6182
11	Fars	3144	3496	5321	10982	7933	8349	7729	16456
12	Kerman	1756	1858	4371	4967	4302	3490	3399	9577
13	Guilan	1628	1433	1115	3267	1348	2101	6110	4368
14	Mazandaran	2992	2212	2460	6449	3236	4523	5894	9501
15	Hormozgan	3126	2444	2110	6555	3522	4010	3678	9983
16	Yazd	818	930	1561	2514	1659	1868	1851	5294

Table 4: Standard deviation of inputs.

DMUs	Electricity distribution companies	Deviation of the first input criterion	Deviation of the second input criterion	Deviation of the third input criterion	Deviation of the fourth input criterion	Deviation of the fifth input criterion	Deviation of the sixth input criterion	Deviation of the first output criterion	Deviation of the second output criterion
1	Azerbaijan	1089.883	1237.542	215.0558	1070.038	270.2961	775.2903	831.979	1673.598
2	Esfahan	1498.915	705.8272	319.7671	1188.98	428.8438	995.109	933.7435	2313.444
3	Kermanshah	322.6686	0	289.0778	1296.611	561.172	693.5971	678.1084	1340.566
4	Tehran	2489.094	2504.389	83.29466	1720.807	249.0723	1123.076	1623.369	3402.231
5	Khorasan	881.8044	908.9224	431.5762	771.0019	502.0667	926.4356	1356.391	1607.083
6	Khuzestan	297.5013	217.1843	366.632	2131.656	276.4489	1200.906	2192.867	2713.754
7	Zanjan	237.1139	313.7117	335.8794	695.6687	375.4917	513.3965	681.8732	918.4726
8	Semnan	134.3652	264.0417	280.8594	654.7603	106.6865	160.7389	812.4838	315.395
9	Sistan and Baluchestan	196.5782	197.9394	496.7202	603.1526	300.5495	327.6523	185.0081	685.6501
10	The west	371.9556	476.3024	396.2865	1144.02	255.3703	425.3939	1682.792	763.4743
11	Fars	1379.946	1118.915	634.9756	2660.342	739.18	1423.841	4040.326	2041.423
12	Kerman	224.6264	256.3416	285.8916	713.4466	312.9601	314.8651	626.4647	1252.81
13	Guilan	632.6855	562.7966	150.9967	497.6073	109.0138	286.4961	697.3034	606.6424
14	Mazandaran	251.6188	6.63325	53.64699	924.1342	529.2353	893.8775	472.1165	1412.197
15	Hormozgan	118.1397	216	377.599	1084.704	1882.73	824.2087	667.4624	2207.234
16	Yazd	185.1756	195.287	315.0286	648.9068	73.67496	224.0982	903.4788	1074.818

Table 5: Technical efficiency numbers, cost and random revenue in three error levels.

DMUs	Electricity distribution companies	The stochastic efficiency of companies		
		$\propto = 0.05$	$\propto = 0.3$	$\propto = 0.5$
1	Azerbaijan	TE = 1 CE = 1 RE = 3.29	TE = 1 CE = 1 RE = 3.49	TE = 1 CE = 1 RE = 3.54
2	Esfahan	TE = 0.91 CE = 0/62 RE = 3.46	TE = 0.88 CE = 0.59 RE = 3.55	TE = 0.86 CE = 0.57 RE = 3.60
3	Kermanshah	TE = 1 CE = 1 RE = 3.79	TE = 1 CE = 1 RE = 4.34	TE = 1 CE = 1 RE = 4.60
4	Tehran	TE = 1 CE = 1 RE = 1	TE = 1 CE = 1 RE = 1	TE = 1 CE = 1 RE = 1
5	Khorasan	TE = 0.78 CE = 0.39 RE = 2.08	TE = 0.77 CE = 0.36 RE = 2.13	TE = 0.76 CE = 0.35 RE = 2.15
6	Khuzestan	TE = 1 CE = 0.81 RE = 2.49	TE = 1 CE = 0.70 RE = 2.79	TE = 1 CE = 0.62 RE = 2.95
7	Zanjan	TE = 1 CE = 0.73 RE = 1	TE = 1 CE = 0.70 RE = 1	TE = 1 CE = 0.69 RE = 1
8	Semnan	TE = 1 CE = 1 RE = 1	TE = 1 CE = 1 RE = 1	TE = 1 CE = 1 RE = 1
9	Sistan and Baluchestan	TE = 1 CE = 0.55 RE = 1	TE = 1 CE = 0.53 RE = 1	TE = 1 CE = 0.52 RE = 1
10	The west	TE = 0.94 CE = 0.59 RE = 3.74	TE = 0.81 CE0.55 RE = 3.97	TE = 0.76 CE = 0.52 RE = 4.7
11	Fars	TE = 1 CE = 1 RE = 5.3	TE = 1 CE = 0.89 RE = 5.58	TE = 0.90 CE = 0.68 RE = 5.70
12	Kerman	TE = 0.63 CE = 0.44 RE = 4.15	TE = 0.61 CE = 0.43 RE = 4.24	TE = 0.60 CE = 0.42 RE = 4.27
13	Guilan	TE = 1 CE = 1 RE = 1	TE = 1 CE = 1 RE = 1.21	TE = 1 CE = 1 RE = 1.40
14	Mazandaran	TE = 0.80 CE = 0.56 RE = 4.84	TE = 0.70 CE = 0.53 RE = 5.01	TE = 0.65 CE = 0.51 RE = 5.03
15	Hormozgan	TE = 0.53 CE = 0.51 RE = 5.72	TE = 0.53 CE = 0.45 RE = 5.93	TE = 0.52 CE = 0.42 RE = 6.1
16	Yazd	TE = 1 CE = 0.77 RE = 1.02	TE = 1 CE = 0.75 RE = 1.07	TE = 1 CE = 0.75 RE = 1.09

TE: technical efficiency, CE: cost efficiency, and RE: revenue efficiency.

Table 12: Comparing ideal cost and revenue with observed one.

DMU	Electricity distribution companies	Observed cost	Observed revenue	$\propto = 0.05$		$\propto = 0.3$		$\propto = 0.5$	
				Ideal cost	Ideal revenue	Ideal cost	Ideal revenue	Ideal cost	Ideal revenue
1	Azerbaijan	64869	46682	64869	46682	64869	46682	64869	46682
2	Esfahan	82515	61628	49525.05	63197.13	48718.95	62461.3	47259.5	61873.59
3	Kermanshah	78727	51183	78731	51183	78731	51183	78731	51183
4	Tehran	163677	809453	163689	809453	163689	809453	163689	809453
5	Khorasan	72017	40641	25976.57	42635.91	26570.28	41505.5	26915.9	41074.78
6	Khuzestan	100157	78212	86018.87	81868.52	82519.32	82819.31	64110.27	82608.58
7	Zanjan	30236	20200	30236	20200	30236	20200	30236	20200
8	Semnan	17806	9839	17806	9839	17806	9839	17806	9839
9	Sistan and Baluchestan	35547	10169	35547	10169	35547	10169	35547	10169
10	The west	52068	27400	31034.99	29389.36	28884.55	28146.23	28863.41	27739.03
11	Fars	110172	56099	110172	56099	96631.43	210432.8	75343.34	56320.16
12	Kerman	58237	29351	24871.5	30382.8	25958.79	29965.9	26578.33	29753.85
13	Guilan	29348	27066	29348	27066	29348	27066	29348	27066
14	Mazandaran	60126	36684	35456.75	38660.06	30563.11	37062.47	30816.2	36767.75
15	Hormozgan	59832	31000	25772.51	32923.34	25486.15	31614.52	25352.1	31000
16	Yazd	26018	5553	22159.96	16913.13	22411.55	16627.34	22567.87	16509.86

Considering that the expression under the radical of the first three constraints is greater than or equal to zero, therefore, the model can be rewritten as follows:

$$
\begin{aligned}
&\text{Min} d_1 + d_2 + d_3 \\
&s.t. \sum_{i=1}^{m} \left(\overline{x}_i - x_{ip}^{T}\right)^2 + \sum_{r=1}^{s} \left(\overline{y}_r - y_{rp}^{T}\right)^2 = d_1^2, \quad j = 1, \ldots, n, \\
&\sum_{i=1}^{m} \left(\overline{x}_i - x_{ip}^{C}\right)^2 + \sum_{r=1}^{s} \left(\overline{y}_r - y_{rp}^{C}\right)^2 = d_2^2, \quad j = 1, \ldots, n, \\
&\sum_{i=1}^{m} \left(\overline{x}_i - x_{ip}^{R}\right)^2 + \sum_{r=1}^{s} \left(\overline{y}_r - y_{rp}^{R}\right)^2 = d_3^2, \quad j = 1, \ldots, n, \\
&\lambda_1 x_{ip}^{T} + \lambda_2 x_{ip}^{C} + \lambda_3 x_{ip}^{R} = \overline{x}_i \quad i = 1, \ldots, m \; j = 1, \ldots, n, \\
&\lambda_1 y_{rp}^{T} + \lambda_2 y_{rp}^{C} + \lambda_3 y_{rp}^{R} = \overline{y}_r, \quad r = 1, \ldots, s \; j = 1, \ldots, n, \\
&\sum_{k=1}^{3} \lambda_k = 1, \\
&d_1 \geq 0, d_2 \geq 0, \; d_3 \geq 0, \\
&\overline{x}_i \geq 0 \,, \; \overline{y}_r \geq 0 \,, \lambda_k \geq 0.
\end{aligned}
\tag{12}
$$

In the above model, we intend to minimize the total sum of the distance between projection points and ideal points from each of the projection points obtained from the BCC random, cost, and revenue models under norm 2 (L2) in the objective function of the proposed model so that the ideal point are in the convex combination of these points and at the same time dominate the unit under evaluation. This projection point obtained for each unit simultaneously meets the three technical, cost, and revenue objectives as much as possible. Secondly, random data and technical, cost, and revenue stochastic models are used in a linear form that has not been addressed so far, so obtaining such a pattern with these scores is very important.

5. Practical Example

The electricity industry has an infrastructural and influential role on the economic growth of any country. Iran Regional Electricity Company is one of the most important companies in the field of electricity industry, whose main task is to

Table 6: Projection points obtained from different models at the error level of 0.05.

DMUs	Companies	0.05 Projection points of random models
1	Azerbaijan	TE = (2921, 2776, 3723, 5808, 4234, 4574, 7420, 12211) CE = (2921, 2776, 3723, 5808, 4234, 4574, 7420, 12211) RE = (2337.70, 2197.15, 3625.07, 5676.51, 3119.44, 4204.98, 2226.99, 76203.28)
2	Esfahan	TE = (2223.96, 1915.04, 2056.28, 5657.61, 2589.11, 3770.64, 6708, 21300.80) CE = (2315.68, 21547.78, 2201.58, 5054.89, 2640.87, 3564.31, 6708, 21380.93) RE = (2094.71, 2129.11, 1916.77, 7688.32, 2945.51, 5656.92, 4105.28, 100754.13)
3	Kermanshah	TE = (2898, 2360, 3975, 7767, 5562, 5446, 7849, 13818) CE = (2898, 2360, 3975, 7767, 5562, 5446, 7849, 13818) RE = (1903.34, 1948.97, 1842.25, 7243.52, 2889.28, 5390.68, 3922.14, 91367.89)
4	Tehran	TE = (7994, 7682, 4214, 21400, 4679, 3864, 9751, 390100) CE = (7994, 7682, 4214, 21400, 4679, 3864, 9751, 390100) RE = (7994, 7682, 4214, 21400, 4679, 3864, 9751, 390100)
5	Khorasan	TE = (987.19, 1050.11, 1429.09, 3200.08, 1497.03, 2074.81, 2684.91, 16624.70) CE = (740.23, 802.17,1143.70, 3284.25, 1108.46, 1764.05, 2869.79, 17008.05) RE = (1054.04, 1115.63, 1816.35, 4153.73, 1612.42, 2480.12, 2105.98, 40070.06)
6	Khuzestan	TE = (2906, 2286, 3691,12983,3874, 8716, 7274, 28195) CE = (2867.07, 2911.31, 3663.17, 7969.76, 4984.47, 5876.36, 7274, 28770.86) RE = (1938.28, 1981.86, 1855.86, 7324.73, 2899.55, 5439.29, 3955.57, 93081.56)
7	Zanjan	TE = (177, 324, 1170, 3231, 2382, 2989, 2270, 6695) CE = (430.05, 529.39, 1053.42, 2736.14, 975.79, 1362.63, 2332.38, 6965.58) RE = (177, 324,1170, 3231, 2382, 2989, 2270, 6695)
8	Semnan	TE = (109, 269, 1002, 2401, 859, 1066, 1527, 2629) CE = (109, 269, 1002, 2401, 859, 1066, 1527, 2629) RE = (109, 269, 1002, 2401, 859, 1066, 1527, 2629)
9	Sistan and Baluchestan	TE = (1127, 1002, 3716, 2046,2935, 2077, 411, 4468) CE = (150.14, 307.68, 1018.76, 2500.12, 878.93, 1132.77, 1569.91, 4650.52) RE = (1127, 1002, 3716, 2046, 2935, 2077, 411, 4468)
10	The west	TE = (1418.26, 1265.45, 1276.62, 3828.85, 1698.70, 2662.49, 5425.06, 6219.54) CE = (1457.53, 1309.99, 1116.90, 3250.39, 1300.24, 2026.10, 5509.21, 6275.16) RE = (1492.03, 1469.44, 2589.53, 4482.77, 2234.03, 3025.13, 1999.49, 49129.09)
11	Fars	TE = (3144, 3496, 5321,10982, 7933, 8349, 7729, 16456) CE = (3144, 3496, 5321,10982, 7933, 8349, 7729, 16456) RE = (2969.64, 2952.66, 2257.48, 9721.92, 3202.61, 6874.12, 4942.60, 143667.32)
12	Kerman	TE = (976.84, 952.22, 1314.61, 3054.18, 1295.44, 1800.64, 3569.72, 9715.72) CE = (844.49, 856.15, 1101.82, 3069.52, 1117.79, 1694.73, 3478.60, 9973.50) RE = (1619.31, 1600.36, 2525.83, 4930.55, 2216.15, 3263.94, 2241.68, 57804.96)
13	Guilan	TE = (1628, 1433,1115, 3267, 1348, 2101, 6110, 4368) CE = (1628, 1433,1115, 3267, 1348, 2101, 6110, 4368) RE = (1628, 1433,1115, 3267, 1348, 2101, 6110, 4368)
14	Mazandaran	TE = (1788.77, 1555.52, 1816.97, 4450.99, 2494.05, 3084.56, 6059.26, 9649.62) CE = (1672.51, 1486.96, 1156.34, 3502.43, 1380.89, 2238.87, 6018.83, 9900.02) RE = (1774.99, 1835.11, 1683.03, 6426.53, 1691.42, 3800.82, 3276.03, 84508.40)
15	Hormozgan	TE = (984.32, 963.99, 1113.55, 3156.53, 1163.45, 1793.73, 3892.66, 10323.81) CE = (939.82, 932.02, 1114.31, 3153.67, 1151.12, 1774.94, 3734.24, 10860.31) RE = (1776.79, 1836.96, 1681.38, 6419.56, 1666.99, 3772.96, 3266.50, 84584.74)
16	Yazd	TE = (818., 930,1561, 2514,1659, 1868, 1851, 5294) CE = (271.05, 403.50, 1033.82, 2602.57, 920.82, 1232.31, 1898.77, 5663.27) RE = (380.40, 480.75, 1558.01, 2510.97, 1297.13, 1382.27, 1388.16, 6630.61)

produce, distribute, and transmit electricity. In this practical example, fuel consumption and nominal power are used in the power generation process. The nominal power of a propulsion device has been written by the manufacturer on its specifications plate for certain conditions in terms of horsepower or megawatts. In small machines, the nominal power is specified in kilowatts. The power transmission section is done by posts and lines of the transmission network. The substation is part of a network, which has been concentrated in a given location and is used to selectively connect and disconnect electrical circuits within a network. Power distribution is also used to send and sell energy to

Table 7: Projection point obtained from different models and revenue at the error level of 0.3.

DMUs	Companies	0.3 Projection points of random models
1	Azerbaijan	TE = (2921,2776,3723,5808,4234,4574,7420,12211) CE = (2921,2776,3723,5808,4234,4574,7420,12211) RE = (2396.61,2248.41,3691.32,5766.85,3177.07,4288.80,2248.41,78212.43)
2	Esfahan	TE = (2215.49,1910.07,2044.56,5532.79,2595.41,3689.31,6708, 20920.39) CE = (2340.91,2160.66,2208.97,4866.56,2555.11,3449.95, 6733.10, 20949.90) RE = (2146.40, 2177.76,1936.90,7808.47,2960.70,5728.83,4154.75,103289.41)
3	Kermanshah	TE = (2898,2360,3975,7767,5562,5446,7849,13818) CE = (2898,2360,3975,7767,5562,5446,7849,13818) RE = (2185.89,2217.48,1912.23,7710.10,2547, 5266.38,4000.71,105019.24)
4	Tehran	TE = (7994, 7682, 4214,21400,4679,3864, 9751, 390100) CE = (7994, 7682, 4214,21400,4679,3864, 9751, 390100) RE = (7994, 7682, 4214,21400,4679,3864, 9751, 390100)
5	Khorasan	TE = (971.93,1039.61,1434.32,3181.68,1499.94,2066.24,2618.40,16491.39) CE = (672.80,749.37,1136.52,3233.86,1085.69,1711.99,2679.17,16619.22) RE = (1076.22,1132.88,1862.31,4162.08,1648.58,2505.82,2094.15,40386.29)
6	Khuzestan	TE = (2906, 2286, 3691,12983,3874, 8716, 7274, 28195) CE = (3112.07,2958.78, 3687.80, 6426.26,4190.80,4921.63,7492.31, 28357.32) RE = (2148.19,2179.45,1937.60, 7812.63,2961.23,5731.32,4156.47,103377.29)
7	Zanjan	TE = (177, 324,1170, 3231, 2382, 2989,2270, 6695) CE = (413.74, 516.30,1051.06,2720.52, 969.99,1348.28, 2289.98,6781.83) RE = (177, 324,1170, 3231, 2382, 2989,2270, 6695)
8	Semnan	TE = (109, 269,1002, 2401, 859,1066,1527, 2629) CE = (109, 269,1002, 2401, 859,1066,1527, 2629) RE = (109, 269,1002, 2401, 859,1066,1527, 2629)
9	Sistan and Baluchestan	TE = (1127, 1002, 3716,2046,2935, 2077, 411, 4468) CE = (147.61,305.30,1017.73,2494.03,877.71,1128.67,1567.27,4526.31) RE = (1127, 1002, 3716,2046,2935, 2077, 411, 4468)
10	The west	TE = (1270.64,1164.25,1139.12,3315.03,1627.56,2369.27, 5122.45, 6194.40) CE = (1345.69,1224.53,1109.06,3189.23,1264.47,1951.23,5168.97, 6215.15) RE = (1484.06,1474.44,2458.10,4620.08,2141.94,3047.94, 2112.58,51423.40)
11	Fars	TE = (3144, 3496, 5321,10982, 7933, 8349,7729,16456) CE = (3968.25,3477.71,4025.19,10630.16,5376.55,7213.93,8248.45,92843.70) RE = (3094.35,3070.05,2306.04,10011.78,3239.25,7047.62, 5061.95,149784.07)
12	Kerman	TE = (1031.86,990.28,1503.94,3011.20,1436.16,1856.41,3448.12, 9613.69) CE = (823.21,838.96,1098.54,3048,1110.11,1675.42, 3424.48,9704.16) RE = (1710.73,1670.73,2723.01,4955.52,2370.54,3367.72, 2185.55,58945.75)
13	Guilan	TE = (1628, 1433,1115, 3267,1348, 2101, 6110,4368) CE = (1628, 1433,1115, 3267,1348, 2101, 6110,4368) RE = (336.35,482.74,1094.61,2948.81,969.14,1435.01,1764.13,13801.11)
14	Mazandaran	TE = (1635.34,1456.78,1158.58,3503.21,1446.07,2302.12, 5956.02, 9555.20) CE = (1641.19,1462.11,1152.38,3475.58,1370.01,2212.92, 5934.02,9629.27) RE = (2094.46, 2076.21,2420.36,6440.61,2240.50,4118.56,3020.48, 87420.82)
15	Hormozgan	TE = (933.79,924.64,1108.58,3121.04,1146.59,1755.89, 3747.37,10091.75) CE = (919.27,914.20,1108.81,3119.98,1142.56,1749.69,3695.82,10263.53) RE = (1908.51,1943.64,1911.08,6521.97,1851.98,3937.66,3237.15, 87368.43)
16	Yazd	TE = (818., 930,1561, 2514,1659,1868,1851, 5294) CE = (257.05,391.92,1031.15,2585.58,915.51,1218.16,1866.19, 5412.24) RE = (381.96,482.07,1560.03,2513.02,1298.84,1384.40,1388.47,6677.91)

companies. Iranian electricity distribution companies are responsible for managing and coordinating subsidiary units and supplying the production, transmission and sale of electricity and are subsidiaries of Tavanir specialized parent company.

Considering the importance of this industry in the economic growth and development of the country, the model is evaluated based on data related to 16 regional electricity companies in Iran, in a 9-year period (from 2005 to 2014) derived from the statistical yearbook of the Ministry

Table 8: Projection point obtained from different models at the error level of 0.5.

DMUs	Companies	0.5 Projection points of random models
1	Azerbaijan	TE = (2921,2776,3723,5808,4234,4574,7420,12211) CE = (2921,2776,3723,5808,4234,4574,7420,12211) RE = (2424.07,2272.24,3723,5808,3204.48,4327.67,2257.65,79132.64)
2	Esfahan	TE = (2197.77,1906.40,1994.79,5127.10,2599.98,3422.09, 6708,20752) CE = (2315.77,2134.59,2159.53,4816.42,2500.41,3401.92,6708,20752) RE = (2174.28,2204,1947.75,7873.26,2968.89,5767.61,4181.43,104656.59)
3	Kermanshah	TE = (2898,2360,3975,7767,5562,5446,7849,13818) CE = (2898,2360,3975,7767,5562,5446,7849,13818) RE = (2333.23,2360,1909.46,7767,1951.51,4694.30,3853.60,111935.69)
4	Tehran	TE = (7994, 7682, 4214,21400,4679,3864, 9751, 390100) CE = (7994, 7682, 4214,21400,4679,3864, 9751, 390100) RE = (7994, 7682, 4214,21400,4679,3864, 9751, 390100)
5	Khorasan	TE = (963.76,1033.47,1434.71,3174.20,1498.68,2060.50, 2591,16434) CE = (641.54,724.88,1133.16,3210.31,1075.12,1687.76,2591,16434) RE = (1086.26,1140.70,1883,4166,1664.87,2517.49,2088.89,40531.70)
6	Khuzestan	TE = (2906, 2286, 3691,12983,3874, 8716, 7274, 28195) CE = (2905.31,2742.88,3240.12,6037.62,3695.09,4524.88,7274,28195) RE = (2261.39, 2286,1981.68,8075.74,2994.49,5888.80,4264.80,108929.39)
7	Zanjan	TE = (177, 324,1170, 3231, 2382, 2989,2270, 6695) CE = (406.06,510.13,1049.95,2713.15,967.25,1341.51,2270,6695) RE = (177, 324,1170, 3231, 2382, 2989,2270, 6695)
8	Semnan	TE = (109, 269,1002, 2401, 859,1066,1527, 2629) CE = (109, 269,1002, 2401, 859,1066,1527, 2629) RE = (109, 269,1002, 2401, 859,1066,1527, 2629)
9	Sistan and Baluchestan	TE = (1127, 1002, 3716,2046,2935, 2077, 411, 4468) CE = (146.42,304.18,1017.24,2491.17,877.13,1126.74,1566.03,4468) RE = (1127, 1002, 3716,2046,2935, 2077, 411, 4468)
10	The west	TE = (1227.88,1131.28,1140.06,3310.29,1656.42,2392.23,5012,6182) CE = (1294.02,1185.03,1105.39,3160.77,1247.92,1916.53,5012, 6182) RE = (1486.23,1481,2412.56,4682,2111.03,3064.41,2158.81,52502.82)
11	Fars	TE = (2843.69,2334.76,3751.67,7534.80,5221.84,5257.97,7729,16456) CE = (2947.91,2536.30,3897.17,7260.41,5133.90,5240.15,7729,16456) RE = (3144,3116.78,2325.37,10127.18,3253.84,7116.69,5109.47,152219.20)
12	Kerman	TE = (1058.23,1008.68,1588.66,2993.30,1499.59,1882.68, 3399,9577) CE = (813.19,830.86,1096.99,3037.85,1106.49,1666.32,3399,9577) RE = (1756.,1705.50,2821.36,4967,2447.49,3418.90,2157.07,59495.45)
13	Guilan	TE = (1628, 1433,1115, 3267,1348, 2101, 6110,4368) CE = (1628, 1433,1115, 3267,1348, 2101, 6110,4368) RE = (386.40,529.79,1115,3069.40,993.39,1516.24,1816.33,16260.45)
14	Mazandaran	TE = (1610.73,1437.64,1158.72,3498.34,1461.75,2313.48,5894,9501) CE = (1626.41,1450.38,1150.50,3462.88,1364.88,2200.67, 5894,9501) RE = (2114.01,2091.50,2460,6449,2271.78,4141.44,3010.85,87717.07)
15	Hormozgan	TE = (909.69,905.88,1106.22,3104.19,1138.56,1737.87,3678, 9983) CE = (909.69,905.88,1106.22,3104.19,1138.56,1737.87,3678,9983) RE = (1968.92,1991.45,2027.82,6555,1944.67,4010.,3212.88,88405.76)
16	Yazd	TE = (818., 930,1561, 2514,1659,1868,1851, 5294) CE = (250.51,386.50,1029.89,2577.60,913.03,1211.53,1851, 5294)

of Energy (https://www.moe.gov.ir) according to Jafari et al. [21]. Therefore, for each company, six inputs and two outputs have been considered, which are defined as follows. The selection of these indicators is based on a study of research conducted in the electricity industry.

Input and output variables have been organized in Table 2.

Input and output indices have a normal distribution, the mean value and standard deviation for each of which have been shown in Tables 3 and 4, respectively.

Table 5 shows the efficiency number obtained from technical, stochastic cost, and revenue models at three error levels ($\alpha = 0.05$, 0.3, and 0.5). According to the results obtained from this table, units 1, 3, 4, 6, 7, 8, 9, 10, 13, and 16

Table 9: The best projection point at the error level 0.05.

DMUs	Electricity distribution companies	$\propto = 0.05$
1	Azerbaijan	(2921,2776,3723,5808,4234,4574,7420,12211)
2	Esfahan	(2.3E + 3,2053.44,2138.45,5320.41, 2619.40,3658.21, 6701.45,21546.39)
3	Kermanshah	(2.9E + 3,2360, 3975, 7767, 5562, 5446,7849,13818)
4	Tehran	(8.0E + 3,7682,4214,21400,4679,13864,9751,390100)
5	Khorasan	(761.10,823.11,1168.64,3279.76,1141.32,1791.17, 2852.75,17038.83)
6	Khuzestan	(2.9E + 3,2655.77,3628.85,9818.35,4519.93,6921.68, 7191.98,30146.29)
7	Zanjan	(177, 324,1170,3231,2382,2989,2270,6695)
8	Semnan	(109,269,1002,2401,859,1066,1527,2629)
9	Sistan and Baluchestan	(1.1E + 3,1002,3716,2046,2935,2077,411,4468)
10	The west	(1.4E + 3,1289.45,1203.82,3538.60,1499.32,2340.86, 5445.68,6526.16)
11	Fars	(3.1E + 3,3496,5321,10982,7933,8349,7729,16456)
12	Kerman	(844.49,856.15,1101.82,3069.52,1117.79,1694.73, 3478.60,9973.50)
13	Guilan	(1.6E + 3,1433,1115,3267,1348,2101,6110,4368)
14	Mazandaran	(1.7E + 3,1516.75,1424.20,3901.72,1828.32,2587.78, 6016.42,10305.40)
15	Hormozgan	(939.82,932.02,1114.31,3153.67,1151.12,1774.94,3734.24,10860.31)
16	Yazd	(443.18,561.08,1321.06,2553.29,1219.40,1438.99, 1738.57,5848.71)

Table 10: The best projection point at the error level 0.3.

DMUs	Electricity distribution companies	$\propto = 0.3$
1	Azerbaijan	(2921,2776,3723,5808,4234,4574,7420,12211)
2	Esfahan	(2.3E + 3,2036.03,2126.43,5206.07,2576.27,3575.27, 6713.56, 21160.31)
3	Kermanshah	(2.9E + 3,2360, 3975, 7767, 5562, 5446,7849,13818)
4	Tehran	(8.0E + 3,7682,4214,21400,4679,13864,9751,390100)
5	Khorasan	(791.66, 864.63,1257.68,3221.82,1250.33,1855.51,2650.64, 16776.79)
6	Khuzestan	(3.0E + 3,2634.24,3638.40,9408.85,4012.92,6647.86, 7297.45,30463.48)
7	Zanjan	(177, 324,1170,3231,2382,2989,2270,6695)
8	Semnan	(109,269,1002,2401,859,1066,1527,2629)
9	Sistan and Baluchestan	(1.1E + 3,1002,3716,2046,2935,2077,411,4468)
10	The west	(1.3E + 3,1195.40,1129.01,3257.20,1448.68,2163.64, 5134.53, 6371.32)
11	Fars	(4.0E + 3,3477.71,4025.19,10630.16,5376.55,7213.93, 8248.45,92843.70)
12	Kerman	(912.28,904.21,1271.26,3039.47,1248.86,1755.89,3429.92,9838.07)
13	Guilan	(1.6E + 3,1433,1115,3267,1348,2101,6110,4368)
14	Mazandaran	(1.6E + 3,1462.07,1152.46,3475.91,1370.78,2213.84, 5934.19,9629.95)
15	Hormozgan	(919.27,914.20,1108.81, 3119.98,1142.56,1749.69, 3695.82,10263.53)
16	Yazd	(467.82,586.17,1340.05,2543.55,1253.07,1468.09, 1733.72,5713.09)

are technical efficiencies. Units 1, 3, 4, 8, and 13 are cost efficient. Revenue efficiency includes units 4, 7, 8, and 9. Therefore, among the companies, only two electricity distribution companies (units 4 and 8) in Tehran and Semnan provinces are efficient at all three levels of error in technical, stochastic cost, and revenue models.

The projections obtained from the technical, stochastic cost, and revenue models can be seen at three levels of error in Tables 6–8. For each company, the projection points of the technical, cost, and revenue models have been shown in three rows with TE, CE, and RE, respectively. The results have been set in separate tables for three error levels. These tables have been presented in the appendix.

Also, the projection point of the proposed model for each of the electricity distribution companies with three levels of error has been shown in Tables 9–11, which is attached to the article. According to the results obtained for most units, the projection point of the proposed dominant model of the unit under evaluation has been obtained. Dominance means having fewer inputs and more outputs than the unit under evaluation. For example, consider the electricity distribution company of Khorasan province (unit 5) at the error level of 0.05. The model point of the model presented in this paper shows that all inputs have decreased and all outputs have increased compared to the unit under evaluation of this unit. These results can also be generalized to units 10, 12, 14, and 15. The projection point obtained from the model presented in this paper for units 1, 3, 4, 7, 8, 9, 11, and 13 equals to the unit under evaluation is obtained at an error level of 0.05. These results can be analyzed for other error levels.

In Table 12, the ideal cost and revenue are compared with the observed cost and revenue at three levels of error for all companies. The results in this table show that for all companies in all three levels of error, the ideal cost is not more than the observed cost and the ideal revenue is not less than the observed revenue as per unit, which indicates an improvement in performance of all companies. For example, consider the Electricity Distribution Company of Khuzestan Province (DMU 6) at the error level of 0.05. Although in the proposed model, the second and fifth inputs have been increased, but the ideal cost of this unit is less than the

Table 11: The best projection point at error level 0.5.

DMUs	Electricity distribution companies	$\propto = 0.5$
1	Azerbaijan	(2921, 2776, 3723, 5808, 4234, 4574, 7420, 12211)
2	Esfahan	(2.3E + 3, 2015.65, 2073.26, 4983.18, 2553.07, 3416.07, 6704.13, 20880.60)
3	Kermanshah	(2.9E + 3, 2360, 3975, 7767, 5562, 5446, 7849, 13818)
4	Tehran	(8.0E + 3, 7682, 4214, 21400, 4679, 13864, 9751, 390100)
5	Khorasan	(815.53, 891.41, 1299.09, 3200.15, 1303.88, 1891.96, 2586.34, 16657.88)
6	Khuzestan	(2.7E + 3, 2285.41, 2873.81, 6748.02, 3872.99, 4596.19, 7274, 30393.29)
7	Zanjan	(177, 324, 1170, 3231, 2382, 2989, 2270, 6695)
8	Semnan	(109, 269, 1002, 2401, 859, 1066,1527,2629)
9	Sistan and Baluchestan	(1.1E + 3, 1002, 3716, 2046, 2935, 2077, 411, 4468)
10	The west	(1.3E + 3, 1158.05, 1128.84, 3245.29, 1465.54, 2170.53, 5000.49, 6368.78)
11	Fars	(2.9E + 3, 2433.94, 3821.60, 7402.84, 5177.20, 5250.82, 7726.8, 16569.88)
12	Kerman	(949.33, 930.45, 1369.45, 3021.90, 1324.17, 1790.38, 3393.79, 9786.24)
13	Guilan	(1.6E + 3, 1433, 1115, 3267, 1348, 2101, 6110, 4368)
14	Mazandaran	(1.6E + 3, 1444.02, 1155.58, 3483.29, 1416.54, 2261.33, 5892.37, 9545.32)
15	Hormozgan	(909.69, 905.88, 1106.22, 3104.19, 1138.56, 1737.87, 3678, 9983)
16	Yazd	(482.43, 600.76, 1352.32, 2538.99, 1272.95, 1485.24, 1731.40, 5657.83)

observed cost. Also, despite the decrease in the first output of the proposed model for this province, its ideal income has been obtained more than its observed income. This analysis can be generalized to other units.

The input price vector and the output price vector for all units are given a fixed value as follows:

$$(c_1 = 2, c_2 = 1,\ c_3 = 3,\ c_4 = 4,\ c_5 = 3,\ c_6 = 2,\ p_1 = 3,\ p_2 = 2). \tag{13}$$

For example, the ideal cost and the observed cost along with the ideal revenue and the observed revenue for DMU11 at the error level of 0.03 are obtained from the following formula, which can be generalized to all units.

$$\begin{aligned}
\text{Observed Cost} &= c_1x_1 + c_2x_2 + c_3x_3 + c_4x_4 + c_5x_5 + c_6x_6 \\
&= (2 * 3144) + (3496 * 1) + (5321 * 3) + (10982 * 4) + (7933 * 3) + (8349 * 2) = 110172, \\
\text{Ideal Cost} &= c_1x_1^* + c_2x_2^* + c_3x_3^* + c_4x_4^* + c_5x_5^* + c_6x_6^* \\
&= (2 * 4.00\text{E} + 03 * 2) + (3477.71 * 1) + (4025.19 * 3) + (10630.16 * 4) + (5376.55 * 3) + (7213.93 * 2) \\
&= 966314, \\
\text{Observed Cost} &= p_1y_1 + p_2y_2 = (7729 * 3) + (16456 * 2) = 56099, \\
\text{Ideal Cost} &= p_1y_1^* + p_2y_2^* = (8248.45 * 3) + (92843.7 * 2) = 210433.
\end{aligned} \tag{14}$$

6. Conclusions

Decision-making units are divided into two categories: efficient and inefficient units. For each inefficient DMU, there is a projection point on the efficient frontier so that the inefficient unit moves towards the efficient frontier with different approaches and becomes efficient.

In this paper, in the first step, by technical efficiency models, linear stochastic cost, and revenue under variable returns to scale, we identify projection points such as each DMU. Then, through the presented model, a projection point is obtained that the distance from each of the projection points obtained in the first step under norm 2 is the least. The projection point obtained for each inefficient DMU is very important in two ways. First, the projection obtained for each DMU simultaneously meets the three main aspects of technical efficient, minimal cost, and maximal revenue as much as possible. Secondly, random data and stochastic programming in linear form are used in it. Therefore, it will help managers to make better decisions in the future and will enjoy the benefits of random planning. Considering the importance of the electricity industry in the economic growth and development of each country, a practical example has been implemented on 16 regional electricity companies in Iran in 9 periods. Comparison between cost efficiency and ideal income with observed cost and revenue efficiency showed that the ideal cost of each unit is less than or equal to its observed cost and the ideal revenue of each unit is greater than or equal to the observed revenue of that unit at three levels of error. According to the obtained results, the managers of Iranian electricity distribution companies can plan by identifying inefficient companies,

identifying the projection point of the units and setting goals in order to increase their efficiency before the actual performance of the companies. For further studies, the method presented in this paper can be applied to other types of uncertain data such as fuzzy or interval data and can also be focused on other aspects.

Appendix

Projection points obtained from different models along with the best projection points in three levels of error are given in this section.

Data Availability

All the data used in the application of the model were collected by the authors and they are available per request.

Conflicts of Interest

The authors declare that there are no conflicts of interest regarding the publication of this paper.

References

[1] A. Charnes, W. W. Cooper, and E. Rhodes, "Measuring the efficiency of decision-making units," *European Journal of Operational Research*, vol. 2, no. 6, pp. 429–444, 1978.

[2] R. D. Banker, A. Charnes, and W. W. Cooper, "Some models for estimating technical and scale inefficiencies in data envelopment analysis," *Management Science*, vol. 30, no. 9, pp. 1078–1092, 1984.

[3] A. Charnes and W. W. Cooper, "Chance-constrained programming," *Management Science*, vol. 6, no. 1, pp. 73–79, 1959.

[4] N. U. I. Hossain, F. Nur, R. Jaradat et al., "Metrics for assessing overall performance of inland waterway ports: a bayesian network based approach," *Complexity*, vol. 2019, pp. 1–17, Article ID 3518705, 2019.

[5] R. Mo, H. Huang, and L. Yang, "An interval efficiency measurement in DEA when considering undesirable outputs," *Complexity*, vol. 2020, pp. 1–12, Article ID 7161628, 2020.

[6] R. Hu, X. Wu, B. Qian, J. Mao, and H. Jin, "Differential evolution algorithm combined with uncertainty handling techniques for stochastic reentrant job shop scheduling problem," *Complexity*, vol. 2022, pp. 1–11, Article ID 9924163, 2022.

[7] A. Amirteimoori, S. Mehdizadeh, and S. Kordrostami, "Stochastic performance measurement in two-stage network processes: a data envelopment analysis approach," *Kybernetika*, vol. 58, pp. 200–217, 2022.

[8] M. Ghasemi, M. R. Mozaffari, and F. Hosseinzadeh Lotfi, M. Rostamy malkhalifeh, M. Rostamy malkhalifeh, and M. H. Behzadi, New approach in fixed resource allocation and target setting using data envelopment analysis with common set of weights," *Complexity*, vol. 2022, pp. 1–11, Article ID 2149093.

[9] A. Charnes and W. W. Cooper, "Deterministic equivalents for optimizing and satisficing under chance constraints," *Operations Research*, vol. 11, no. 1, pp. 18–39, 1963.

[10] K. C. Land, C. A. K. Lovell, and S. Thore, "Chance constrained data envelopment analysis," *Managerial and Decision Economics*, vol. 14, no. 6, pp. 541–554, 1993.

[11] M. J. Farrell, "The measurement of productive efficiency," *Journal of the Royal Statistical Society: Series A*, vol. 120, no. 3, pp. 253–281, 1957.

[12] R. Färe, S. F. Grosskopf, and C. A. K. Lovell, *The Measurement of Efficiency of Production*, Kluwer Academic Publisher, Dordrecht MA, 1985.

[13] W. W. Cooper and K. Tone, "Measures of inefficiency in data envelopment analysis and stochastic Frontier estimation," *European Journal of Operational Research*, vol. 99, no. 1, pp. 72–88, 1997.

[14] R. K. Shiraz, A. Hatami-Marbini, A. Emrouznejad, and H. Fukuyama, "Chance-constrained cost efficiency in data envelopment analysis model with random inputs and outputs," *Operational Research*, vol. 20, no. 3, pp. 1863–1898, 2020.

[15] H. T. Lin, "An efficiency-driven approach for setting revenue target," *Decision Support Systems*, vol. 49, no. 3, pp. 311–317, 2010.

[16] G. Cesaroni and D. Giovannola, "Average-cost efficiency and optimal scale sizes in non-parametric analysis," *European Journal of Operational Research*, vol. 242, no. 1, pp. 121–133, 2015.

[17] H. Haghighatpisheh, S. Kordrostami, A. Amirteimoori, and F. H. Lotfi, "Optimal scale sizes in input–output allocative data envelopment analysis models," *Annals of Operations Research*, vol. 315, no. 2, pp. 1455–1476, 2019.

[18] F. Bagheri, A. Amirteimoori, S. Kordrostami, and M. Soufi, "Determining the ideal pattern of units by simultaneously examining the lowest cost, highest revenue and closest distance," *Modern research in decision making*, vol. 6, pp. 214–234, 2022.

[19] G. Debreu, "The coefficient of resource utilization," *Econometrica*, vol. 19, no. 3, pp. 273–292, 1951.

[20] W. W. Cooper, Z. M. Huang, V. Lelas, S. X. Li, and O. B. Olesen, "Chance constrained programming formulations for stochastic characterizations of efficiency and dominance in DEA," *Journal of Productivity Analysis*, vol. 9, pp. 530–579, 1998.

Hindawi
Complexity
Volume 2022, Article ID 2394472, 18 pages
https://doi.org/10.1155/2022/2394472

Research Article

Novel EDAS Methodology Based on Single-Valued Neutrosophic Aczel-Alsina Aggregation Information and Their Application in Complex Decision-Making

Shahzaib Ashraf,[1] **Shakoor Ahmad**,[2] **Muhammad Naeem**,[3] **Muhammad Riaz**,[4] **and Md. Ashraful Alam**[5]

[1]*Institute of Mathematics, Khwaja Fareed University of Engineering & Information Technology, Rahim Yar Khan, Pakistan*
[2]*Department of Mathematics, COMSATS University Islamabad, Islamabad Campus, Park Road, Chak Shahzad, Islamabad 45550, Pakistan*
[3]*Deanship of Combined First Year, Umm Al-Qura University, Makkah, Saudi Arabia*
[4]*Department of Mathematics, University of the Punjab, Lahore 54590, Pakistan*
[5]*Department of Mathematics, Jahangirnagar University, Savar, Dhaka, Bangladesh*

Correspondence should be addressed to Md. Ashraful Alam; ashraf_math20@juniv.edu

Received 27 June 2022; Revised 24 July 2022; Accepted 1 September 2022; Published 10 October 2022

Academic Editor: Zeljko Stevic

In this article, we proposed an extended EDAS (Evaluation based on Distance from Average Solution) method based on the single-valued neutrosophic (SVN) Aczel-Alsina aggregation information. The fundamental concept of a single-valued neutrosophic (SVN) set is a universal mathematical tool for effectively managing uncertain and imprecise information. To accomplish our goal, we first extend the Aczel-Alsina t-norm and t-conorm to SVN scenarios and introduce a few new SVN operations on which we construct novel SVN aggregation operators. Furthermore, a decision support strategy is built in the SVN framework using the EDAS methodology and the suggested Aczel-Alsina aggregation operators. This method computes the aggregated outcomes of each investigated alternative, as well as their score values. Finally, to demonstrate the functionality of the developed SVN- EDAS, an application has been made related to the role of commercial banks in providing loans to their customers, which has recently affected our world, and the results are compared with other existing methods. The results suggest that the proposed method may overcome the inadequacies of the existing decision method's lack of decision flexibility by using SVN aggregation operators.

1. Introduction

Multi-attribute group decision making (MAGDM) is the practice of utilizing expert evaluation information to analyze, rank and pick the best solutions using a given decision-making (DM) approach. Making a decision entails providing relevant information and making a choice amongst several DM approaches. Enhancing the MADM approach has become a hot topic in today's DM area since it is difficult to predict the future and because experts' expertise is limited. In the DM procedure, there is vagueness and uncertainty, and Zadeh's theory [1] of fuzzy sets gives an extremely effective technique to cope with these challenges. Atanasov [2] devised the concept of intuitionistic fuzzy sets to reflect uncertainty in DM (IFS). IFS comprise membership functions and non-membership functions. Some decision-makers started using intuitionistic fuzzy numbers to express their preferences for alternatives in the DM dilemma [3–5]. Because of this, intuitionistic fuzzy information is becoming more popular among academics.

Following the acquisition of the expert data, we must integrate it using various aggregating operators (Agop). Several Agops, such as the IF averaging operator, were created by Xu [6]. Jana and Pal [7] introduced the decision

making EDAS method to tackle the uncertainty in decision support problems. Several Einstein Agops, such as IFE averaging/geometric operators (Aveg/GAOs), were introduced by Liu and Liu [8]. Xu and Xu [9] created a prioritized list of Agops and explained how they could be used to solve DM challenges (Dcmp). Under the linguistic IF strategy, Wang and Wang [10] produced various unique Agops and proposed an algorithm to address the difficult uncertain Dcmp. Jana et al. [11] presented the multi-attribute decision making method using power Dombi operators and MABAC method to tackle the uncertain information in decision support problems. IF Bonferroni means Agop, Xu and Yager [12] established the DM technique (DMA). The Group DMA was created by Arora and Garg [13] built on the prioritized IF Agop under the linguistic set of data. Zhao et al. [14] examined the uses of generalized IF Agops, such as the generalized IF averaging/geometric operators, to deal with uncertainty in Dcmp. Yu [15] demonstrated certain IF Agops depending on levels of confidence and handled challenging real-world Dcmps. Yu [16] created the IF Agop and discussed its usefulness in DM using Heronian mean. Jiang et al. [17] devised a DM strategy depends on the IF power Agop and the entropy measurement. Senapati et al. [18] developed various IF Aczel-Alsina (Acz-Als) Agops depending on the Acz-Als norm and used them in the IF multi-attribute DM process. Khan et al. [19] created the unique generalized IF soft evidence Agops and investigated their use in DM.

Even though all of these approaches are beneficial for representing incomplete data, they are unable to deal with indeterminate (neutral) data and inconsistent data in actual practice. Cuong [20] consider the three type of uncertain situation at a time to developed the picture fuzzy set (PFS). It is clear that PFS interpretations of ambiguous data are more rational and accurate than those provided by the FS and IFS models. Many researchers began researching on PFS after its development. The synthesis of the achievement degree of criterion necessitates the collection of information. To understand the various uncertain data in Dcmp, Ashraf et al. [21] proposed the list of novel picture fuzzy (PF) algebraic Agop and decision support (D-S) strategy. Riaz et al. [22] introduced the decision making method under bipolar picture fuzzy operators and distance measures. Some Agops, such as PF geometic operators, were created by Garg [23]. Wei [24] compiled a list of PF Agops and discussed their use in DM challenges. Ashraf et al. [25] presented decision based application for Internet finance soft power evaluation under fuzzy information. Khan et al. [26] proposed and investigated the use of generalized PF soft details Agops in DM. Some Einstein Agops, such as PF Einstein (Aveg/GAOs), were introduced by Khan et al. [27]. Under algebraic norm and linguistic deta set, Qiyas et al. [28] created some PF averaging/geometric Agop. Jana et al. [29] investigated certain Dombi Agops in PF situations, such as PF Dombi averaging/geometric operators. Jana and Pal [30] presented the dynamical hybrid method using GRA technique to tackle decision support problems. PF Hamacher averaging/geometric operators employing Hamacher t-norm and s-norm were presented by Wei [31]. In a cubic PF setting, Ashraf et al. [32] devised a novel distance measure dependent on algebraic Agops. Khan et al. [33] created some logarithmic PF Agops and discussed how to use them in DM. Qiyas et al. [34] introduced the linguistic approach to tackle the decision problems using picture fuzzy Dombi information.

The portrayal of fuzzy sets and their extensions allow greater flexibility for DM, although there are still certain limitations. Data discontinuity and inconsistency cannot be solved such that the NS emerges as required by time. In this study, the degree of truth, uncertainty, and falsity are all taken into account. This theory can assist decision-makers in expressing their ideas more accurately and in detail and addresses issues that the fuzzy sets are unable to address. The concept of neutrosophic sets was first introduced by Smarandache [35]. This epistemology is a mathematical model that describes not only the origins, nature, and scope of impartiality, but also the interactions between their many conceptualization ranges. In order to overcome DM difficulties in unclear contexts, such enhancements have been developed. Smarandache [36] presented the plithogeny, plithogenic set, logic as a novel neutrosophic information. Ye [37] developed an AgOs-depends strategy for DM, while Peng et al. [38] highlighted the power of AgOs in dealing with uncertainty in NS data and examined their usefulness in the context of uncertainty in data management. In order to deal with uncertain data in the form of neutrosophic numbers, Chen and Ye [39] defined the SVN information depends Dombi AgOs, while Liu et al. [40] established the generalized Hamacher AgOs. Al-Hamido [41] described the novel algebraic structure of neutrosophic set. Garg and Nancy [42] presented the novel methodology depends on SVNSs with linguistic terms. Ashraf et al. [43] proposed novel decision model for hydrogen power plant selection using SVN sine trigonometric AgOs. The flexible DM correlating to favoured rankings of alternatives was not studied thoroughly in the MADM process, despite the fact that these operators provide some motivation for solving MADM difficulties.

The EDAS approach was initially defined by Keshavarz Ghorabaee et al. [44] and used it to multi-criteria inventory categorization issues. Kahraman et al. [45] developed a novel EDAS model for solid waste disposal site selection. Batool et al. [46] proposed the EDAS method with Pythagorean probabilistic hesitant information and discussed their applicability in decision making. Peng and Liu [47] proposed approaches for neutrosophic soft decision making depends on the EDAS algorithm using similarity measure. Karasan and Kahraman [48] developed the novel interval-valued neutrosophic EDAS approach. The EDAS method was used to develop the dynamic fuzzy approach for multi-criteria evaluation of subcontractors by Keshavarz-Ghorabaee et al. [49]. For more study, we refer to.

In fuzzy sets and their extended fuzzy architectures, the t-norms and t-conorms are commonly acknowledged as important operations. The Acz-Als t-norm and t-conorm procedures, created by Aczel and Alsina, have the advantage of changeability by modifying a parameter [50]. Under the single valued neutrosophic framework, the Acz-Als t-norm and t-conorm procedures, [51–57] as well as a number of

additional aggregation operators [58–60] (AOs), are proposed. In addition, to deal with uncertain data in complex real-life decision scenarios, an expanded EDAS (Evaluation based on Distance from Average Solution) method depends on the SVN Acz-Als aggregation operations is described.

Our technique's objectives are represented as follows:

(1) We devised certain Acz-Als operations for SVNNs in order to overcome the lack of algebraic, Einstein, and Hamacher processes and represent the relationship between the various SVNNs.

(2) In support of SVN data, we extended Acz-Als operators to SVN Acz-Als operators: SVN Aczel-Alsina weighted geometric (SV-NAWG) operator and SVN Aczel-Alsina order weighted geometric (SV-NAOWG) operator, which overcome the present operator's drawbacks.

(3) Based on the suggested SVN Aczel-Alsina aggregation technique, we developed an expanded EDAS approach.

(4) Using SVN data, we developed an approach to deal with MAGDM difficulties.

(5) The suggested Aczel-Alsina aggregate operators and the EDAS technique are applied to the MAGDM issue in order to demonstrate their usability and reliability.

(6) The results suggest that the proposed process is more powerful and generates more authentic results when compared to existing methodologies.

The remaining sections of the document are formatted in the following order: Under SVN information, Section 2 provides some basic information on t-norms, SVNSs, and a few functional rules. Section 3 discusses the Aczel-Alsina working guidelines as well as the characteristics of SVNNs. In Section 4, we look at the various desirable qualities of several SVN Aczel-Alsina AOs. The next section develops an expanded EDAS method depends decision making algorithm using SVN Aczel-Alsina aggregation operations. In Section 6, we use an example to demonstrate the applicability of the suggested hybrid method. In Section 7, we examine at how a factor effects DM results. The comparison study for new and existing aggregating operators was developed in Section 8. Section 8 concludes the research work and elaborates future directions.

2. Preliminaries

We will look at some key topics in this section that will be significant in the creation of this article.

Definition 1 (see [50]). A mapping $(\widehat{W}_a^{\wp})_{\wp\in[0,\infty]}$ is a Acz-Als t-norm if

$$\widehat{W}_a^{\wp}(\Delta,\hbar)=\begin{cases}\widehat{W}_{\mathscr{D}}(\Delta,\hbar) & \text{if} \quad \wp=0\\ \min(\Delta,) & \text{if} \quad \wp=\infty,\\ e^{-((-\ell n'\Delta)^{\wp}+(-\ell n')^{\wp})^{1/\wp}} & \text{otherwise}\end{cases} \tag{1}$$

where $\Delta, \in [0,1]$, $\wp$ is $+ve$ fixed and $\widehat{W}_{\mathscr{D}}$ is extreme t-norm defined as

$$\widehat{W}_{\mathscr{D}}(\Delta,)=\begin{cases}\Delta & \text{if} \quad \Delta=1\\ \text{if} \quad \Delta=1 & \\ 0 & \text{otherwise.}\end{cases} \tag{2}$$

Definition 2 (see [50]). A mapping $(\beta_a^{\wp})_{\wp\in[0,\infty]}$ is a Acz-Als s-norm if

$$\beta_a^{\wp}(\Delta,)=\begin{cases}\beta_{\mathscr{D}}(\Delta,) & \text{if} \quad \wp=0\\ \max(\Delta,) & \text{if} \quad \wp=\infty\\ 1-e^{-\left((-\ell n_{\prime}(1-\Delta))^{\wp}+(-\ell n_{\prime}(1-))^{\wp}\right)^{1/\wp}} & \text{otherwise}\end{cases}, \tag{3}$$

where $\Delta, \in [0,1]$, $\wp$ is positive constant and $\beta_{\mathscr{D}}$ is drastic s-norm defined as

$$\beta_{\mathscr{D}}(\Delta,)=\begin{cases}\Delta & \text{if} \quad \Delta=0\\ \text{if} \quad \Delta=0 & \\ 0 & \text{otherwise.}\end{cases} \tag{4}$$

For every $\wp\in[0,\infty]$, the t-norm $\widehat{W}_a^{\wp}$ and s-norm $\beta_a^{\wp}$ are dual to each other.

Definition 3 (see [35]). A neutrosophic set Ξ in a fixed set $\Bbbk$ is defined as

$$\Xi=\{\overline{O}_{\Xi}(\flat),\Delta_{\Xi}(\flat),\mathscr{G}_{\Xi}(\flat)\in\,]0^{-},1^{+}[|\flat\in\Bbbk\}, \tag{5}$$

where $\overline{O}_{\Xi}$ positive grade, Δ_{Ξ} neutral grade and $\mathscr{G}_{\Xi}$ negative grade of the value $\flat$ to neutrosophic set Ξ, satisfying $0^{-}\le\overline{O}_{\Xi}+\Delta_{\Xi}+\mathscr{G}_{\Xi}\le 3^{+}$, for each $\flat\in\Bbbk$.

Definition 4 (see [35]). A single valued neutrosophic set (SV-NS) Ξ in $\Bbbk$ is defined as

$$\Xi=\{\overline{O}_{\Xi}(\flat),\Delta_{\Xi}(\flat),\mathscr{G}_{\Xi}(\flat)\in[0,1]|\flat\in\Bbbk\}, \tag{6}$$

where $\overline{O}_{\Xi}$ positive grade, Δ_{Ξ} neutral grade and $\mathscr{G}_{\Xi}$ negative grade of the element $\flat$ to SV-NS Ξ, satisfying $0\le\overline{O}_{\Xi}+\Delta_{\Xi}+\mathscr{G}_{\Xi}\le 3$, for each $\flat\in\Bbbk$.

Definition 5 (see [35]). Let $\Xi_{\mathfrak{J}}=\left\{\overline{O}_{\Xi_{\mathfrak{J}}},\Delta_{\Xi_{\mathfrak{J}}},\mathscr{G}_{\Xi_{\mathfrak{J}}}\right\}$ be two single valued neutrosophic numbers (SVNNs), where ($\mathfrak{J}=1,2$). Then:

(1) $\Xi_1\subseteq\Xi_2$ iff $\overline{O}_{\Xi_1}\le\overline{O}_{\Xi_2},\Delta_{\Xi_1}\le\Delta_{\Xi_2}$ and $\mathscr{G}_{\Xi_1}\ge\mathscr{G}_{\Xi_2}$ for all $\flat\in\Bbbk$;

(2) $\Xi_1=\Xi_2$ if $\Xi_1\subseteq\Xi_2$ and $\Xi_2\subseteq\Xi_1$;

(3) $\Xi_1=\Xi_2=\left\{\min(\overline{O}_{\Xi_1},\overline{O}_{\Xi_2}),\max(\Delta_{\Xi_1},\Delta_{\Xi_2}),\max(\mathscr{G}_{\Xi_1},\mathscr{G}_{\Xi_2})\right\}$;

(4) $\Xi_1=\Xi_2=\left\{\max(\overline{O}_{\Xi_1},\overline{O}_{\Xi_2}),\min(\Delta_{\Xi_1},\Delta_{\Xi_2}),\min(\mathscr{G}_{\Xi_1},\mathscr{G}_{\Xi_2})\right\}$;

(5) $(\Xi_1)^{c}=\left\{\mathscr{G}_{\Xi_1},\Delta_{\Xi_1},\overline{O}_{\Xi_1}\right\}$.

Definition 6 (see [35]). Let $\Xi_{\mathfrak{F}} = \left\{\overline{O}_{\Xi_{\mathfrak{F}}}, \Delta_{\Xi_{\mathfrak{F}}}, \mathscr{G}_{\Xi_{\mathfrak{F}}}\right\}$ be two SVNNs, where $(\mathfrak{F} = 1, 2)$. Then the operations about any two SVNNs are defined as follows:

(1) $\Xi_1 \oplus \Xi_2 = \left\{\overline{O}_{\Xi_1} + \overline{O}_{\Xi_2} - \overline{O}_{\Xi_1}\overline{O}_{\Xi_2}, \Delta_{\Xi_1}\Delta_{\Xi_2}, \mathscr{G}_{\Xi_1}\mathscr{G}_{\Xi_2}\right\}$;
(2) $\Xi_1 \otimes \Xi_2 = \left\{\overline{O}_{\Xi_1}\overline{O}_{\Xi_2}, \Delta_{\Xi_1} + \Delta_{\Xi_2} - \Delta_{\Xi_1}.\Delta_{\Xi_2}, \mathscr{G}_{\Xi_1} + \mathscr{G}_{\Xi_2} - \mathscr{G}_{\Xi_1}.\mathscr{G}_{\Xi_2}\right\}$;
(3) $\eta \cdot \Xi_1 = \left\{1 - (1 - \overline{O}_{\Xi_1})^{\eta}, (\Delta_{\Xi_1})^{\eta}, (\mathscr{G}_{\Xi_1})^{\eta}\right\},, \eta > 0$;
(4) $(\Xi_1)^{\eta} = \left\{(\overline{O}_{\Xi_1})^{\eta}, 1 - (1 - \Delta_{\Xi_1})^{\eta}, 1 - (1 - \mathscr{G}_{\Xi_1})^{\eta}\right\}, \eta > 0$.

On the basis of Definition 6, Ashraf [6] derived several operations in the following ways:

Definition 7 (see [51]). Let $\Xi_{\mathfrak{F}} = \left\{\overline{O}_{\Xi_{\mathfrak{F}}}, \Delta_{\Xi_{\mathfrak{F}}}, \mathscr{G}_{\Xi_{\mathfrak{F}}}\right\}$ be a collection of SVNNs, where $(\mathfrak{F} = 1, 2, ..., n)$ and $\eta_1, \eta_1 > 0$. Then

(1) $\Xi_1 \oplus \Xi_2 = \Xi_2 \oplus \Xi_1$;
(2) $\Xi_1 \otimes \Xi_2 = \Xi_2 \otimes \Xi_1$;
(3) $\eta_1(\Xi_1 \oplus \Xi_2) = \eta_1\Xi_1 \oplus \eta_1\Xi_2$;
(4) $(\Xi_1 \otimes \Xi_2)^{\eta_1} = \Xi_1^{\eta_1} \otimes \Xi_2^{\eta_1}$;
(5) $\eta_1\Xi_1 \oplus \eta_2\Xi_1 = (\eta_1 + \eta_2)\Xi_1$;
(6) $\Xi_1^{\eta_1} \otimes \Xi_1^{\eta_2} = \Xi_1^{(\eta_1 + \eta_2)}$;
(7) $(\Xi_1^{\eta_1})^{\eta_2} = \Xi_1^{\eta_1\eta_2}$.

Definition 8 (see [43]). Let $\Xi = \left\{\overline{O}_{\Xi}, \Delta_{\Xi}, \mathscr{G}_{\Xi}\right\}$ be SV-NN. Then the score $\mathscr{Q}(\Xi)$ and accuracy $a(\Xi)$ are given as follows:

(1) $\mathscr{Q}(\Xi) = (\overline{O}_{\Xi} - \Delta_{\Xi} - \mathscr{G}_{\Xi})$;
(2) $a(\Xi) = (\overline{O}_{\Xi} + \Delta_{\Xi} + \mathscr{G}_{\Xi})$.

Definition 9 (see [43]). Let $\Xi_{\mathfrak{F}} = \left\{\overline{O}_{\Xi_{\mathfrak{F}}}, \Delta_{\Xi_{\mathfrak{F}}}, \mathscr{G}_{\Xi_{\mathfrak{F}}}\right\}$ be two SVNNs, where $(\mathfrak{F} = 1, 2)$. Then the comparison technique of SVNNs can be defined as:

(1) $\mathscr{Q}(\Xi_1) > \mathscr{Q}(\Xi_2)$ implies that $\Xi_1 > \Xi_2$;
(2) $\mathscr{Q}(\Xi_1) = \mathscr{Q}(\Xi_2)$ and $a(\Xi_1) > a(\Xi_2)$ implies that $\Xi_1 > \Xi_2$;
(3) $\mathscr{Q}(\Xi_1) = \mathscr{Q}(\Xi_2)$ and $a(\Xi_1) = a(\Xi_2)$ implies that $\Xi_1 = \Xi_2$.

Ashraf et al. [6] developed the algebraic AO under SVNNs illustrate in the superseding definition.

Definition 10 (see [52]). Let $\Xi_{\mathfrak{F}} = \left\{\overline{O}_{\Xi_{\mathfrak{F}}}, \Delta_{\Xi_{\mathfrak{F}}}, \mathscr{G}_{\Xi_{\mathfrak{F}}}\right\}$ be a collection of SVNNs, where $(\mathfrak{F} = 1, 2, ..., \ell)$. A single valued neutrosophic weighted geometric (SV-NWG) AO of dimention ℓ is a mapping $\mathfrak{F}^{\ell} \longrightarrow \mathfrak{F}$ with weight vector $\varpi = (\varpi_1, \varpi_1, ..., \varpi_{\ell})^T$ such that $\varpi_{\mathfrak{F}} > 0$ and as

$$
\begin{aligned}
&SV - NWG(\Xi_1, \Xi_2, \ldots, \Xi_{\ell}) \\
&= \prod_{\mathfrak{F}=1}^{\ell} (\Xi_{\mathfrak{F}})^{\varpi_{\mathfrak{F}}} \\
&= \left\{ \begin{array}{c} \prod_{\mathfrak{F}=1}^{\ell} \left(\overline{O}_{\Xi_{\mathfrak{F}}}\right)^{\varpi_{\mathfrak{F}}}, 1 - \prod_{\mathfrak{F}=1}^{\ell} \left(1 - \Delta_{\Xi_{\mathfrak{F}}}\right)^{\varpi_{\mathfrak{F}}}, \\ 1 - \prod_{\mathfrak{F}=1}^{\ell} \left(1 - \mathscr{G}_{\Xi_{\mathfrak{F}}}\right)^{\varpi_{\mathfrak{F}}} \end{array} \right\}.
\end{aligned} \tag{7}
$$

3. Aczel–Alsina Operation for SVNNs

We discussed Acz-Als operations in relation to SVNNs, taking into account the Acz-Als t-norm and Acz-Als t-conorm.

Definition 11. Let $\Xi_{\mathfrak{F}} = \left\{\overline{O}_{\Xi_{\mathfrak{F}}}, \Delta_{\Xi_{\mathfrak{F}}}, \mathscr{G}_{\Xi_{\mathfrak{F}}}\right\}$ be two SVNNs, where $(\mathfrak{F} = 1, 2)$ and $\wp$ is $+ve$ fixed. Then Acz-Als norms depends operations for SVNNs are defined as follows:

(1) $\Xi_1 \oplus \Xi_2 = \left\{1 - e^{-((-\ell n'(1-\overline{O}_{\Xi_1}))^{\wp} + (-\ell n'(1-\overline{O}_{\Xi_2}))^{\wp})^{1/\wp}}, e^{-((-\ell n'\Delta_{\Xi_1})^{\wp} + (-\ell n'\Delta_{\Xi_2})^{\wp})^{1/\wp}}, e^{-((-\ell n'\mathscr{G}_{\Xi_1})^{\wp} + (-\ell n'\mathscr{G}_{\Xi_2})^{\wp})^{1/\wp}}\right\}$;
(2) $\Xi_1 \otimes \Xi_2 = \left\{e^{-((-\ell n'\overline{O}_{\Xi_1})^{\wp} + (-\ell n'\overline{O}_{\Xi_2})^{\wp})^{1/\wp}}, 1 - e^{-((-\ell n'(1-\Delta_{\Xi_1}))^{\wp} + (-\ell n'(1-\Delta_{\Xi_2}))^{\wp})^{1/\wp}}, 1 - e^{-((-\ell n'(1-\mathscr{G}_{\Xi_1}))^{\wp} + (-\ell n'(1-\mathscr{G}_{\Xi_2}))^{\wp})^{1/\wp}}\right\}$;
(3) $\eta \cdot \Xi_1 = \left\{1 - e^{-(\eta(-\ell n'(1-\overline{O}_{\Xi_1}))^{\wp})^{1/\wp}}, e^{-(\eta(-\ell n'\Delta_{\Xi_1})^{\wp})^{1/\wp}}, e^{-(\eta(-\ell n'\mathscr{G}_{\Xi_1})^{\wp})^{1/\wp}}\right\},, \eta > 0$;
(4) $(\Xi_1)^{\eta} = \left\{e^{-(\eta(-\ell n'\overline{O}_{\Xi_1})^{\wp})^{1/\wp}}, 1 - e^{-(\eta(-\ell n'(1-\Delta_{\Xi_1}))^{\wp})^{1/\wp}}, 1 - e^{-(\eta(-\ell n'(1-\mathscr{G}_{\Xi_1}))^{\wp})^{1/\wp}}\right\}, \eta > 0$.

Theorem 1. *Let $\Xi_{\mathfrak{F}} = \left\{\overline{O}_{\Xi_{\mathfrak{F}}}, \Delta_{\Xi_{\mathfrak{F}}}, \mathscr{G}_{\Xi_{\mathfrak{F}}}\right\}$ be a collection of SVNNs, where $(\mathfrak{F} = 1, 2, ..., n)$ and $\eta_1, \eta_1 > 0$. Then:*

(1) $\Gamma_1 \oplus \Gamma_2 = \Gamma_2 \oplus \Gamma_1$;
(2) $\Gamma_1 \otimes \Gamma_2 = \Gamma_2 \otimes \Gamma_1$;
(3) $\eta_1(\Gamma_1 \oplus \Gamma_2) = \eta_1\Gamma_1 \oplus \eta_1\Gamma_2$;
(4) $(\Gamma_1 \otimes \Gamma_2)^{\eta_1} = \Gamma_1^{\eta_1} \otimes \Gamma_2^{\eta_1}$;
(5) $\eta_1\Gamma_1 \oplus \eta_2\Gamma_1 = (\eta_1 + \eta_2)\Gamma_1$;
(6) $\Gamma_1^{\eta_1} \otimes \Gamma_1^{\eta_2} = \Gamma_1^{(\eta_1 + \eta_2)}$;
(7) $(\Gamma_1^{\eta_1})^{\eta_2} = \Gamma_1^{\eta_1\eta_2}$.

Proof.

(1) Let $\Xi_{\mathfrak{F}} = \left\{\overline{O}_{\Xi_{\mathfrak{F}}}, \Delta_{\Xi_{\mathfrak{F}}}, \mathcal{G}_{\Xi_{\mathfrak{F}}}\right\}$ be collection of SVNNs, where $(\mathfrak{F} = 1, 2, ..., n)$ and $\eta_1, \eta_1 > 0$. Then by the Definition 11, it follows that

$$\begin{aligned}\Xi_1 \oplus \Xi_2 &= \left\{ \begin{array}{c} 1 - e^{-\left(\left(-\ell n'\left(1-\overline{O}_{\Xi_1}\right)\right)^{\wp} + \left(-\ell n'\left(1-\overline{O}_{\Xi_2}\right)\right)^{\wp}\right)^{1/\wp}}, e^{-\left(\left(-\ell n'\Delta_{\Xi_1}\right)^{\wp} + \left(-\ell n'\Delta_{\Xi_2}\right)^{\wp}\right)^{1/\wp}}, \\ e^{-\left(\left(-\ell n'\mathcal{G}_{\Xi_1}\right)^{\wp} + \left(-\ell n'\mathcal{G}_{\Xi_2}\right)^{\wp}\right)^{1/\wp}} \end{array} \right\} \\ &= \left\{ \begin{array}{c} 1 - e^{-\left(\left(-\ell n'\left(1-\overline{O}_{\Xi_2}\right)\right)^{\wp} + \left(-\ell n'\left(1-\overline{O}_{\Xi_1}\right)\right)^{\wp}\right)^{1/\wp}}, e^{-\left(\left(-\ell n'\Delta_{\Xi_2}\right)^{\wp} + \left(-\ell n'\Delta_{\Xi_1}\right)^{\wp}\right)^{1/\wp}}, \\ e^{-\left(\left(-\ell n'\mathcal{G}_{\Xi_2}\right)^{\wp} + \left(-\ell n'\mathcal{G}_{\Xi_1}\right)^{\wp}\right)^{1/\wp}} \end{array} \right\} \\ &= \Xi_2 \oplus \Xi_1. \end{aligned} \tag{8}$$

(2) Utilizing the Definition 11, it follows that

$$\begin{aligned}\Xi_1 \otimes \Xi_2 &= \left\{ \begin{array}{c} e^{-\left(\left(-\ell n'\overline{O}_{\Xi_1}\right)^{\wp} + \left(-\ell n'\overline{O}_{\Xi_2}\right)^{\wp}\right)^{1/\wp}}, 1 - e^{-\left(\left(-\ell n'\left(1-\Delta_{\Xi_1}\right)\right)^{\wp} + \left(-\ell n'\left(1-\Delta_{\Xi_2}\right)\right)^{\wp}\right)^{1/\wp}}, \\ 1 - e^{-\left(\left(-\ell n'\left(1-\mathcal{G}_{\Xi_1}\right)\right)^{\wp} + \left(-\ell n'\left(1-\mathcal{G}_{\Xi_2}\right)\right)^{\wp}\right)^{1/\wp}} \end{array} \right\} \\ &= \left\{ \begin{array}{c} e^{-\left(\left(-\ell n'\overline{O}_{\Xi_2}\right)^{\wp} + \left(-\ell n'\overline{O}_{\Xi_1}\right)^{\wp}\right)^{1/\wp}}, 1 - e^{-\left(\left(-\ell n'\left(1-\Delta_{\Xi_2}\right)\right)^{\wp} + \left(-\ell n'\left(1-\Delta_{\Xi_1}\right)\right)^{\wp}\right)^{1/\wp}}, \\ 1 - e^{-\left(\left(-\ell n'\left(1-\mathcal{G}_{\Xi_2}\right)\right)^{\wp} + \left(-\ell n'\left(1-\mathcal{G}_{\Xi_1}\right)\right)^{\wp}\right)^{1/\wp}} \end{array} \right\} \\ &= \Xi_2 \otimes \Xi_1. \end{aligned} \tag{9}$$

(3) Utilizing the Definition 11, it follows that

$$\begin{aligned}\eta_1\left(\Xi_1 \oplus \Xi_2\right) &= \eta_1 \left\{ \begin{array}{c} 1 - e^{-\left(\left(-\ell n'\left(1-\overline{O}_{\Xi_1}\right)\right)^{\wp} + \left(-\ell n'\left(1-\overline{O}_{\Xi_2}\right)\right)^{\wp}\right)^{1/\wp}}, e^{-\left(\left(-\ell n'\Delta_{\Xi_1}\right)^{\wp} + \left(-\ell n'\Delta_{\Xi_2}\right)^{\wp}\right)^{1/\wp}}, \\ e^{-\left(\left(-\ell n'\mathcal{G}_{\Xi_1}\right)^{\wp} + \left(-\ell n'\mathcal{G}_{\Xi_2}\right)^{\wp}\right)^{1/\wp}} \end{array} \right\} \\ &= \left\{ \begin{array}{c} 1 - e^{-\left(\eta_1\left(-\ell n'\left(1-\overline{O}_{\Xi_1}\right)\right)^{\wp} + \eta_1\left(-\ell n'\left(1-\overline{O}_{\Xi_2}\right)\right)^{\wp}\right)^{1/\wp}}, e^{-\left(\eta_1\left(-\ell n'\Delta_{\Xi_1}\right)^{\wp} + \eta_1\left(-\ell n'\Delta_{\Xi_2}\right)^{\wp}\right)^{1/\wp}}, \\ e^{-\left(\eta_1\left(-\ell n'\mathcal{G}_{\Xi_1}\right)^{\wp} + \eta_1\left(-\ell n'\mathcal{G}_{\Xi_2}\right)^{\wp}\right)^{1/\wp}} \end{array} \right\} \\ &= \left\{ \begin{array}{c} 1 - e^{-\left(\eta_1\left(-\ell n'\left(1-\overline{O}_{\Xi_1}\right)\right)^{\wp}\right)^{1/\wp}}, \\ e^{-\left(\eta_1\left(-\ell n'\Delta_{\Xi_1}\right)^{\wp}\right)^{1/\wp}}, \\ e^{-\left(\eta_1\left(-\ell n'\mathcal{G}_{\Xi_1}\right)^{\wp}\right)^{1/\wp}} \end{array} \right\} \oplus \left\{ \begin{array}{c} 1 - e^{-\left(\eta_1\left(-\ell n'\left(1-\overline{O}_{\Xi_1}\right)\right)^{\wp}\right)^{1/\wp}}, \\ e^{-\left(\eta_1\left(-\ell n'\Delta_{\Xi_1}\right)^{\wp}\right)^{1/\wp}}, \\ e^{-\left(\eta_1\left(-\ell n'\mathcal{G}_{\Xi_1}\right)^{\wp}\right)^{1/\wp}} \end{array} \right\} \\ &= \eta_1 \Xi_1 \oplus \eta_1 \Xi_2. \end{aligned} \tag{10}$$

(4) It is similar of the proof of (3).

(5) Utilizing the Definition 11, it follows that

$$\begin{aligned}\eta_1\Xi_1 \oplus \eta_2\Xi_1 &= \left\{\begin{array}{c} 1-e^{-\left(\eta_1\left(-\ell n'\left(1-\overline{O}_{\Xi_1}\right)\right)^{\wp}\right)^{1/\wp}}, \\ e^{-\left(\eta_1\left(-\ell n'\Delta_{\Xi_1}\right)^{\wp}\right)^{1/\wp}}, \\ e^{-\left(\eta_1\left(-\ell n'\mathcal{G}_{\Xi_1}\right)^{\wp}\right)^{1/\wp}} \end{array}\right\} \oplus \left\{\begin{array}{c} 1-e^{-\left(\eta_2\left(-\ell n'\left(1-\overline{O}_{\Xi_1}\right)\right)^{\wp}\right)^{1/\wp}}, \\ e^{-\left(\eta_2\left(-\ell n'\Delta_{\Xi_1}\right)^{\wp}\right)^{1/\wp}}, \\ e^{-\left(\eta_2\left(-\ell n'\mathcal{G}_{\Xi_1}\right)^{\wp}\right)^{1/\wp}} \end{array}\right\} \\ &= \left\{\begin{array}{c} 1-e^{-\left(\eta_1\left(-\ell n'\left(1-\overline{O}_{\Xi_1}\right)\right)^{\wp}+\eta_2\left(-\ell n'\left(1-\overline{O}_{\Xi_1}\right)\right)^{\wp}\right)^{1/\wp}}, e^{-\left(\eta_1\left(-\ell n'\Delta_{\Xi_1}\right)^{\wp}+\eta_2\left(-\ell n'\Delta_{\Xi_1}\right)^{\wp}\right)^{1/\wp}}, \\ e^{-\left(\eta_1\left(-\ell n'\mathcal{G}_{\Xi_1}\right)^{\wp}+\eta_2\left(-\ell n'\mathcal{G}_{\Xi_1}\right)^{\wp}\right)^{1/\wp}} \end{array}\right\} \\ &= \left\{\begin{array}{c} 1-e^{-\left(\eta_1+\eta_2\left(-\ell n'\left(1-\overline{O}_{\Xi_1}\right)\right)^{\wp}\right)^{1/\wp}}, e^{-\left(\eta_1+\eta_2\left(-\ell n'\Delta_{\Xi_1}\right)^{\wp}\right)^{1/\wp}}, \\ e^{-\left(\eta_1+\eta_2\left(-\ell n'\mathcal{G}_{\Xi_1}\right)^{\wp}\right)^{1/\wp}} \end{array}\right\} \\ &= (\eta_1+\eta_2)\Xi_1. \end{aligned} \tag{11}$$

(6) and (7) are similar to the proof of (5). □

4. Aczel–Alsina Geometric Aggregation Operators for SVNNs

Acz-Als norms depends list of novel AOs under single valued neutrosophic settings are construct in this section.

Definition 12. Let $\Xi_{\mathfrak{J}} = \left\{\overline{O}_{\Xi_{\mathfrak{J}}}, \Delta_{\Xi_{\mathfrak{J}}}, \mathcal{G}_{\Xi_{\mathfrak{J}}}\right\}$ be collection of SVNNs, where $(\mathfrak{J} = 1, 2, ..., \ell)$. A SVN Acz-Als weighted geometric (SVNAWG) AO of dimention ℓ is a mapping with weight vector $\varpi = (\varpi_1, \varpi_1, ..., \varpi_\ell)^T$ such that $\varpi_{\mathfrak{J}} > 0$ and $\sum_{\mathfrak{J}=1}^{\ell} \varpi_{\mathfrak{J}}$ = as

$$SV - NAWG(\Xi_1, \Xi_2, \ldots, \Xi_\ell) = \prod_{\mathfrak{J}=1}^{\ell} (\Xi_{\mathfrak{J}})^{\varpi_{\mathfrak{J}}}. \tag{12}$$

Theorem 2. *Suppose* $\Xi_{\mathfrak{J}} = \left\{\overline{O}_{\Xi_{\mathfrak{J}}}, \Delta_{\Xi_{\mathfrak{J}}}, \mathcal{G}_{\Xi_{\mathfrak{J}}}\right\}$ *be collection of SVNNs, where* $(\mathfrak{J} = 1, 2, ..., \ell)$. *A SVN Acz-Als weighted geometric (SVNAWG) AO of dimention* ℓ *is a mapping with weight vector* $\varpi = (\varpi_1, \varpi_1, ..., \varpi_\ell)^T$ *such that* $\varpi_{\mathfrak{J}} > 0$ *and* $\sum_{\mathfrak{J}=1}^{\ell} \varpi_{\mathfrak{J}}$ = *is defined as:*

$$SV - NAWG(\Xi_1, \Xi_2, \ldots, \Xi_\ell) = \prod_{\mathfrak{J}=1}^{\ell} (\Xi_{\mathfrak{J}})^{\varpi_{\mathfrak{J}}} = \left\{\begin{array}{c} e^{-\left(\sum_{\mathfrak{J}=1}^{\ell} \varpi_{\mathfrak{J}}\left(-\ell n'\overline{O}_{\Xi_{\mathfrak{J}}}\right)^{\wp}\right)^{1/\wp}}, 1-e^{-\left(\sum_{\mathfrak{J}=1}^{\ell} \varpi_{\mathfrak{J}}\left(-\ell n'\left(1-\Delta_{\Xi\mathfrak{J}}\right)\right)^{\wp}\right)^{1/\wp}}, \\ 1-e^{-\left(\sum_{\mathfrak{J}=1}^{\ell} \varpi_{\mathfrak{J}}\left(-\ell n'\left(1-\mathcal{G}_{\Xi_{\mathfrak{J}}}\right)\right)^{\wp}\right)^{1/\wp}} \end{array}\right\}. \tag{13}$$

Proof. Theorem's 2 proof is derived by implemention of induction method as follows: □

Step 1. for $\ell = 2$, we have

$$SV - NAWG(\Xi_1, \Xi_2) = (\Xi_1)^{\varpi_1} \otimes (\Xi_2)^{\varpi_2}. \tag{14}$$

Utilizing the Definition 11, it follows that

$$(\Xi_1)^{\varpi_1} = \left\{e^{-\left(\varpi_1\left(-\ell n'\overline{O}_{\Xi_1}\right)^{\wp}\right)^{1/\wp}}, 1-e^{-\left(\varpi_1\left(-\ell n'\left(1-\Delta_{\Xi_1}\right)\right)^{\wp}\right)^{1/\wp}}, 1-e^{-\left(\varpi_1\left(-\ell n'\left(1-\mathcal{G}_{\Xi_1}\right)\right)^{\wp}\right)^{1/\wp}}\right\}, \tag{15}$$

and

$$(\Xi_2)^{\varpi_2} = \left\{e^{-\left(\varpi_2\left(-\ell n'\overline{O}_{\Xi_2}\right)^{\wp}\right)^{1/\wp}}, 1-e^{-\left(\varpi_2\left(-\ell n'\left(1-\Delta_{\Xi_2}\right)\right)^{\wp}\right)^{1/\wp}}, 1-e^{-\left(\varpi_2\left(-\ell n'\left(1-\mathcal{G}_{\Xi_2}\right)\right)^{\wp}\right)^{1/\wp}}\right\}. \tag{16}$$

Therefore

$$SV-NAWG(\Xi_1,\Xi_2)=\left\{\begin{array}{c} e^{-\left(\omega_1\left(-\ell n'\overline{O}_{\Xi_1}\right)^{\wp}\right)^{1/\wp}}, \\ 1-e^{-\left(\omega_1\left(-\ell n'\left(1-\Delta_{\Xi_1}\right)\right)^{\wp}\right)^{1/\wp}}, \\ 1-e^{-\left(\omega_1\left(-\ell n'\left(1-\mathcal{G}_{\Xi_1}\right)\right)^{\wp}\right)^{1/\wp}} \end{array}\right\}\otimes\left\{\begin{array}{c} e^{-\left(\omega_2\left(-\ell n'\overline{O}_{\Xi_2}\right)^{\wp}\right)^{1/\wp}}, \\ 1-e^{-\left(\omega_2\left(-\ell n'\left(1-\Delta_{\Xi_2}\right)\right)^{\wp}\right)^{1/\wp}}, \\ 1-e^{-\left(\omega_2\left(-\ell n'\left(1-\mathcal{G}_{\Xi_2}\right)\right)^{\wp}\right)^{1/\wp}} \end{array}\right\}$$
$$=\left\{\begin{array}{cc} e^{-\left(\omega_1\left(-\ell n'\overline{O}_{\Xi_1}\right)^{\wp}+\omega_2\left(-\ell n'\overline{O}_{\Xi_2}\right)^{\wp}\right)^{1/\wp}}, & 1-e^{-\left(\omega_1\left(-\ell n'\left(1-\Delta_{\Xi_1}\right)\right)^{\wp}+\omega_2\left(-\ell n'\left(1-\Delta_{\Xi_2}\right)\right)^{\wp}\right)^{1/\wp}}, \\ 1-e^{-\left(\omega_1\left(-\ell n'\left(1-\mathcal{G}_{\Xi_1}\right)\right)^{\wp}+\omega_2\left(-\ell n'\left(1-\mathcal{G}_{\Xi_2}\right)\right)^{\wp}\right)^{1/\wp}} & \end{array}\right\} \tag{17}$$
$$=\left\{\begin{array}{cc} e^{-\left(\sum_{\mathfrak{J}=1}^{2}\omega_{\mathfrak{J}}\left(-\ell n'\overline{O}_{\Xi_{\mathfrak{J}}}\right)^{\wp}\right)^{1/\wp}}, & 1-e^{-\left(\sum_{\mathfrak{J}=1}^{2}\omega_{\mathfrak{J}}\left(-\ell n'\left(1-\Delta_{\Xi_{\mathfrak{J}}}\right)\right)^{\wp}\right)^{1/\wp}}, \\ 1-e^{-\left(\sum_{\mathfrak{J}=1}^{2}\omega_{\mathfrak{J}}\left(-\ell n'\left(1-\mathcal{G}_{\Xi_{\mathfrak{J}}}\right)\right)^{\wp}\right)^{1/\wp}} & \end{array}\right\}.$$

Thus, Theorem 2 is valid. $\ell=2$.

Now, we assume that, Theorem 2 is valid for $\ell=d$, that is

$$SV-NAWG(\Xi_1,\Xi_2,\ldots,\Xi_d)$$
$$=\left\{\begin{array}{cc} e^{-\left(\sum_{\mathfrak{J}=1}^{d}\omega_{\mathfrak{J}}\left(-\ell n'\overline{O}_{\Xi_{\mathfrak{J}}}\right)^{\wp}\right)^{1/\wp}}, & 1-e^{-\left(\sum_{\mathfrak{J}=1}^{d}\omega_{\mathfrak{J}}\left(-\ell n'\left(1-\Delta_{\Xi_{\mathfrak{J}}}\right)\right)^{\wp}\right)^{1/\wp}}, \\ 1-e^{-\left(\sum_{\mathfrak{J}=1}^{d}\omega_{\mathfrak{J}}\left(-\ell n'\left(1-\mathcal{G}_{\Xi_{\mathfrak{J}}}\right)\right)^{\wp}\right)^{1/\wp}} & \end{array}\right\}. \tag{18}$$

Now we prove that Theorem 2 is valid for $\ell=d+1$. That is, we prove

$$SV-NAWG(\Xi_1,\Xi_2,\ldots,\Xi_d,\Xi_{d+1})=\prod_{\mathfrak{J}=1}^{\ell}\left(\Xi_{\mathfrak{J}}\right)^{\omega_{\mathfrak{J}}}\otimes\left(\Xi_{d+1}\right)^{\omega_{d+1}}$$
$$\prod_{\mathfrak{J}=1}^{\ell}\left(\Xi_{\mathfrak{J}}\right)^{\omega_{\mathfrak{J}}}\otimes\left(\Xi_{d+1}\right)^{\omega_{d+1}}=\left\{\begin{array}{c} e^{-\left(\sum_{\mathfrak{J}=1}^{d}\omega_{\mathfrak{J}}\left(-\ell n'\overline{O}_{\Xi_{\mathfrak{J}}}\right)^{\wp}\right)^{1/\wp}}, \\ 1-e^{-\left(\sum_{\mathfrak{J}=1}^{d}\omega_{\mathfrak{J}}\left(-\ell n'\left(1-\Delta_{\Xi_{\mathfrak{J}}}\right)\right)^{\wp}\right)^{1/\wp}}, \\ 1-e^{-\left(\sum_{\mathfrak{J}=1}^{d}\omega_{\mathfrak{J}}\left(-\ell n'\left(1-\mathcal{G}_{\Xi_{\mathfrak{J}}}\right)\right)^{\wp}\right)^{1/\wp}} \end{array}\right\}\otimes\left\{\begin{array}{c} e^{-\left(\omega_{d+1}\left(-\ell n'\overline{O}_{\Xi_{d+1}}\right)^{\wp}\right)^{1/\wp}}, \\ 1-e^{-\left(\omega_{d+1}\left(-\ell n'\left(1-\Delta_{\Xi_{d+1}}\right)\right)^{\wp}\right)^{1/\wp}}, \\ 1-e^{-\left(\omega_{d+1}\left(-\ell n'\left(1-\mathcal{G}_{\Xi_{d+1}}\right)\right)^{\wp}\right)^{1/\wp}} \end{array}\right\}$$

$$= \left\{ \begin{array}{c} e^{-\left(\sum_{\mathfrak{z}=1}^{d} \omega_{\mathfrak{Z}}\left(-\ell n' \overline{O}_{\Xi_{\mathfrak{Z}}}\right)^{\wp} + \omega_{d+1}\left(-\ell n' \overline{O}_{\Xi d+1}\right)^{\wp}\right)^{1/\wp}}, \\ 1 - e^{-\left(\sum_{\mathfrak{z}=1}^{d} \omega_{\mathfrak{Z}}\left(-\ell n'\left(1 - \Delta_{\Xi_{\mathfrak{Z}}}\right)\right)^{\wp} + \omega_{d+1}\left(-\ell n'\left(1 - \Delta_{\Xi d+1}\right)\right)^{\wp}\right)^{1/\wp}}, \\ 1 - e^{-\left(\sum_{\mathfrak{z}=1}^{d} \omega_{\mathfrak{Z}}\left(-\ell n'\left(1 - \mathcal{G}_{\Xi_{\mathfrak{Z}}}\right)\right)^{\wp} + \omega_{d+1}\left(-\ell n'\left(1 - \mathcal{G}_{\Xi d+1}\right)\right)^{\wp}\right)^{1/\wp}} \end{array} \right\}$$

$$= \left\{ \begin{array}{cc} e^{-\left(\sum_{\mathfrak{z}=1}^{d+1} \omega_{\mathfrak{Z}}\left(-\ell n' \overline{O}_{\Xi_{\mathfrak{Z}}}\right)^{\wp}\right)^{1/\wp}}, & 1 - e^{-\left(\sum_{\mathfrak{z}=1}^{d+1} \omega_{\mathfrak{Z}}\left(-\ell n'\left(1 - \Delta_{\Xi_{\mathfrak{Z}}}\right)\right)^{\wp}\right)^{1/\wp}}, \\ 1 - e^{-\left(\sum_{\mathfrak{z}=1}^{d+1} \omega_{\mathfrak{Z}}\left(-\ell n'\left(1 - \mathcal{G}_{\Xi_{\mathfrak{Z}}}\right)\right)^{\wp}\right)^{1/\wp}} & \end{array} \right\}. \tag{19}$$

Prove that, Theorem 2 is valid for all ℓ.

Using the operator SVNAWG, we can efficiently illustrate the following characteristics.

Theorem 3. *(Idempotency) Let* $\Xi_{\mathfrak{Z}} = \left\{\overline{O}_{\Xi_{\mathfrak{Z}}}, \Delta_{\Xi_{\mathfrak{Z}}}, \mathcal{G}_{\Xi_{\mathfrak{Z}}}\right\} (\mathfrak{Z} = 1, 2, ..., \ell)$ *be a collection of equivalent SVNNs,* $\Xi_{\mathfrak{Z}} = \Xi$ *for each* $(\mathfrak{Z} = 1, 2, ..., \ell)$*. Then*

$$SV - NAWG\left(\Xi_1, \Xi_2, \ldots, \Xi_\ell\right) = \Xi. \tag{20}$$

Proof. Since

$$SV - NAWG\left(\Xi_1, \Xi_2, \ldots, \Xi_\ell\right) = \left\{ \begin{array}{cc} e^{-\left(\sum_{\mathfrak{z}=1}^{\ell} \omega_{\mathfrak{Z}}\left(-\ell n' \overline{O}_{\Xi_{\mathfrak{Z}}}\right)^{\wp}\right)^{1/\wp}}, & 1 - e^{-\left(\sum_{\mathfrak{z}=1}^{\ell} \omega_{\mathfrak{Z}}\left(-\ell n'\left(1 - \Delta_{\Xi_{\mathfrak{Z}}}\right)\right)^{\wp}\right)^{1/\wp}}, \\ 1 - e^{-\left(\sum_{\mathfrak{z}=1}^{\ell} \omega_{\mathfrak{Z}}\left(-\ell n'\left(1 - \mathcal{G}_{\Xi_{\mathfrak{Z}}}\right)\right)^{\wp}\right)^{1/\wp}} & \end{array} \right\}. \tag{21}$$

Put

$$\Xi_{\mathfrak{Z}} = \left\{\overline{O}_{\Xi_{\mathfrak{Z}}}, \Delta_{\Xi_{\mathfrak{Z}}}, \mathcal{G}_{\Xi_{\mathfrak{Z}}}\right\} = \Xi (\mathfrak{Z} = 1, 2, ..., \ell), \tag{22}$$

we have

$$\begin{aligned} SV - NAWG\left(\Xi_1, \Xi_2, \ldots, \Xi_\ell\right) &= \left\{ \begin{array}{cc} e^{-\left(\sum_{\mathfrak{z}=1}^{\ell} \omega_{\mathfrak{Z}}\left(-\ell n' \overline{O}_{\Xi}\right)^{\wp}\right)^{1/\wp}}, & 1 - e^{-\left(\sum_{\mathfrak{z}=1}^{\ell} \omega_{\mathfrak{Z}}\left(-\ell n'\left(1 - \Delta_{\Xi}\right)\right)^{\wp}\right)^{1/\wp}}, \\ 1 - e^{-\left(\sum_{\mathfrak{z}=1}^{\ell} \omega_{\mathfrak{Z}}\left(-\ell n'\left(1 - \mathcal{G}_{\Xi}\right)\right)^{\wp}\right)^{1/\wp}} & \end{array} \right\} \\ &= \left\{ \begin{array}{cc} e^{-\left(\left(-\ell n' \overline{O}_{\Xi}\right)^{\wp}\right)^{1/\wp}}, & 1 - e^{-\left(\left(-\ell n'\left(1 - \Delta_{\Xi}\right)\right)^{\wp}\right)^{1/\wp}}, \\ 1 - e^{-\left(\left(-\ell n'\left(1 - \mathcal{G}_{\Xi}\right)\right)^{\wp}\right)^{1/\wp}} & \end{array} \right\} \\ &= \left(\overline{O}_{\Xi}, \Delta_{\Xi}, \mathcal{G}_{\Xi}\right) = \Xi. \end{aligned} \tag{23}$$

Thus, $SV - NAWG\left(\Xi_1, \Xi_2, ..., \Xi_\ell\right) = \Xi$ holds. □

Theorem 4. *(Boundedness) Let* $\Xi_{\mathfrak{J}} = \left\{\overline{O}_{\Xi_{\mathfrak{J}}}, \Delta_{\Xi_{\mathfrak{J}}}, \mathcal{G}_{\Xi_{\mathfrak{J}}}\right\} (\mathfrak{J} = 1, 2, ..., \ell)$ *be collection of SVNNs. Let* $\Xi_{\mathfrak{J}}^{-} = \left(min_{\mathfrak{J}}\left\{\overline{O}_{\Xi_{\mathfrak{J}}}\right\}, max_{\mathfrak{J}}\left\{\Delta_{\Xi_{\mathfrak{J}}}\right\}, max_{\mathfrak{J}}\left\{\mathcal{G}_{\Xi_{\mathfrak{J}}}\right\}\right)$ *and* $\Xi_{\mathfrak{J}}^{+} = \left(max_{\mathfrak{J}}\left\{\overline{O}_{\Xi_{\mathfrak{J}}}\right\}, min_{\mathfrak{J}}\left\{\Delta_{\Xi_{\mathfrak{J}}}\right\}, min_{\mathfrak{J}}\left\{\mathcal{G}_{\Xi_{\mathfrak{J}}}\right\}\right) (\mathfrak{J} = 1, 2, ..., \ell)$. *Then,*

$$\Xi_{\mathfrak{J}}^{-} \le SV - NAWG\left(\Xi_1, \Xi_2, \ldots, \Xi_\ell\right) \le \Xi_{\mathfrak{J}}^{+}. \tag{24}$$

Proof. Since $\min_{\mathfrak{J}}\left\{\overline{O}_{\Xi_{\mathfrak{J}}}\right\} \le \overline{O}_{\Xi_{\mathfrak{J}}} \le \max_{\mathfrak{J}}\left\{\overline{O}_{\Xi_{\mathfrak{J}}}\right\}$, it follows that

$$e^{-\left(\sum_{\mathfrak{J}=1}^{\ell} \omega_{\mathfrak{J}}\left(-\ell n'\left(\min\overline{O}_{\Xi_{\mathfrak{J}}}\right)\right)^{\wp}\right)^{1/\wp}} \le e^{-\left(\sum_{\mathfrak{J}=1}^{\ell} \omega_{\mathfrak{J}}\left(-\ell n'\overline{O}_{\Xi_{\mathfrak{J}}}\right)^{\wp}\right)^{1/\wp}} \le e^{-\left(\sum_{\mathfrak{J}=1}^{\ell} \omega_{\mathfrak{J}}\left(-\ell n'\left(\max\overline{O}_{\Xi_{\mathfrak{J}}}\right)\right)^{\wp}\right)^{1/\wp}}. \tag{25}$$

Similarly

$$\begin{aligned} 1 - e^{-\left(\sum_{\mathfrak{J}=1}^{\ell} \omega_{\mathfrak{J}}\left(-\ell n'\left(\max\left(1-\Delta_{\Xi_{\mathfrak{J}}}\right)\right)\right)^{\wp}\right)^{1/\wp}} &\le 1 - e^{-\left(\sum_{\mathfrak{J}=1}^{\ell} \omega_{\mathfrak{J}}\left(-\ell n'\left(1-\Delta_{\Xi_{\mathfrak{J}}}\right)\right)^{\wp}\right)^{1/\wp}} \\ &\le 1 - e^{-\left(\sum_{\mathfrak{J}=1}^{\ell} \omega_{\mathfrak{J}}\left(-\ell n'\left(\min\left(1-\Delta_{\Xi_{\mathfrak{J}}}\right)\right)\right)^{\wp}\right)^{1/\wp}}. \end{aligned} \tag{26}$$

Now we have

$$\begin{aligned} 1 - e^{-\left(\sum_{\mathfrak{J}=1}^{d} \omega_{\mathfrak{J}}\left(-\ell n'\left(\max\left(1-\mathcal{G}_{\Xi_{\mathfrak{J}}}\right)\right)\right)^{\wp}\right)^{1/\wp}} &\le 1 - e^{-\left(\sum_{\mathfrak{J}=1}^{d} \omega_{\mathfrak{J}}\left(-\ell n'\left(1-\mathcal{G}_{\Xi_{\mathfrak{J}}}\right)\right)^{\wp}\right)^{1/\wp}} \\ &\le 1 - e^{-\left(\sum_{\mathfrak{J}=1}^{d} \omega_{\mathfrak{J}}\left(-\ell n'\left(\min\left(1-\mathcal{G}_{\Xi_{\mathfrak{J}}}\right)\right)\right)^{\wp}\right)^{1/\wp}}. \end{aligned} \tag{27}$$

Therefore

$$\Xi_{\mathfrak{J}}^{-} \le SV - NAWG\left(\Xi_1, \Xi_2, \ldots, \Xi_\ell\right) \le \Xi_{\mathfrak{J}}^{+}. \tag{28}$$

□

Theorem 5. *Let* $\Xi_{\mathfrak{J}} = \left\{\overline{O}_{\Xi_{\mathfrak{J}}}, \Delta_{\Xi_{\mathfrak{J}}}, \mathcal{G}_{\Xi_{\mathfrak{J}}}\right\}$ *and* $\Xi_{\mathfrak{J}}^{*} = \left\{\overline{O}_{\Xi_{\mathfrak{J}}}^{*}, \Delta_{\Xi_{\mathfrak{J}}}^{*}, \mathcal{G}_{\Xi_{\mathfrak{J}}}^{*}\right\} (\mathfrak{J} = 1, 2, ..., \ell)$ *be two collections of SVNNs. If* $\Xi_{\mathfrak{J}} \le \Xi_{\mathfrak{J}}^{*}$ *for* $(\mathfrak{J} = 1, 2, ..., \ell)$. *Then,*

$$SV - NAWG\left(\Xi_1, \Xi_2, \ldots, \Xi_\ell\right) \le SV - NAWG\left(\Xi_1^{*}, \Xi_2^{*}, \ldots, \Xi_\ell^{*}\right). \tag{29}$$

Proof. The proof is straightforward. □

Definition 13. Let $\Xi_{\mathfrak{J}} = \left\{\overline{O}_{\Xi_{\mathfrak{J}}}, \Delta_{\Xi_{\mathfrak{J}}}, \mathcal{G}_{\Xi_{\mathfrak{J}}}\right\}$ be a collection of SVNNs, where $(\mathfrak{J} = 1, 2, ..., \ell)$. An SVN Acz-Als ordered weighted geometric (SV-NAOWG) AO of dimention ℓ is a mapping $\mathfrak{J}^{\ell} \longrightarrow \mathfrak{J}$ with $\varpi = (\varpi_1, \varpi_1, ..., \varpi_\ell)^T$ such that $\omega_{\mathfrak{J}} > 0$ and $\sum_{\mathfrak{J}=1}^{\ell} \omega_{\mathfrak{J}}$ = as

$$SV - NAOWG\left(\Xi_1, \Xi_2, \ldots, \Xi_\ell\right) = \prod_{\mathfrak{J}=1}^{\ell} \left(\Xi_{\tau(\mathfrak{J})}\right)^{\omega_{\mathfrak{J}}}, \tag{30}$$

where $(\tau(1), \tau(2), ..., \tau(\ell))$ are the permutation in such a way that. $\Xi_{\tau(\mathfrak{J})} \le \Xi_{\tau(\mathfrak{J}-1)}$.

Theorem 6. *Suppose* $\Xi_{\mathfrak{J}} = \left\{\overline{O}_{\Xi_{\mathfrak{J}}}, \Delta_{\Xi_{\mathfrak{J}}}, \mathcal{G}_{\Xi_{\mathfrak{J}}}\right\}$ *be a collection of SVNNs, where* $(\mathfrak{J} = 1, 2, ..., \ell)$. *An SVN Acz-Als ordered weighted geometric (SV-NAOWG) AO of dimention* ℓ *is a mapping* $\mathfrak{J}^{\ell} \longrightarrow \mathfrak{J}$ *with weight vector* $\varpi = (\varpi_1, \varpi_1, ..., \varpi_\ell)^T$ *such that* $\omega_{\mathfrak{J}} > 0$ *and* $\sum_{\mathfrak{J}=1}^{\ell} \omega_{\mathfrak{J}}$ = *is defined as:*

$$SV-NAOWG\left(\Xi_1,\Xi_2,\ldots,\Xi_\ell\right)=\prod_{\mathfrak{J}=1}^{\ell}\left(\Xi_{\tau(\mathfrak{J})}\right)^{\varpi_{\mathfrak{J}}}$$

$$=\left\{\begin{array}{cc} e^{-\left(\sum_{\mathfrak{J}=1}^{\ell}\varpi_{\mathfrak{J}}\left(-\ell n'\overline{O}_{\Xi_{\tau(\mathfrak{J})}}\right)^{\wp}\right)^{1/\wp}}, & 1-e^{-\left(\sum_{\mathfrak{J}=1}^{\ell}\varpi_{\mathfrak{J}}\left(-\ell n'\left(1-\Delta_{\Xi_{\tau(\mathfrak{J})}}\right)\right)^{\wp}\right)^{1/\wp}}, \\ & 1-e^{-\left(\sum_{\mathfrak{J}=1}^{\ell}\varpi_{\mathfrak{J}}\left(-\ell n'\left(1-\mathscr{G}_{\Xi_{\tau(\mathfrak{J})}}\right)\right)^{\wp}\right)^{1/\wp}} \end{array}\right\}, \tag{31}$$

where $(\tau(1),\tau(2),...,\tau(\ell))$ *are the permutation in such a way as.* $\Gamma_{\tau(\mathfrak{J})}\le\Gamma_{\tau(\mathfrak{J}-1)}$.

Using the operator SV-NAOWG, we can efficiently illustrate the following characteristics.

Theorem 7.

(1) (Idempotency) Let $\Xi_{\mathfrak{J}}=\left\{\overline{O}_{\Xi_{\mathfrak{J}}},\Delta_{\Xi_{\mathfrak{J}}},\mathscr{G}_{\Xi_{\mathfrak{J}}}\right\}(\mathfrak{J}=1,2,...,\ell)$ *be collection of equivalent SVNNs,* $\Xi_{\mathfrak{J}}=\Xi$ *for each* $(\mathfrak{J}=1,2,...,\ell)$. *Then*

$$SV-NAOWG\left(\Xi_1,\Xi_2,\ldots,\Xi_\ell\right)=\Xi. \tag{32}$$

(2) (Boundedness) Let $\Gamma_{\mathfrak{J}}=\left\{\overline{O}_{\Gamma_{\mathfrak{J}}},\Delta_{\Gamma_{\mathfrak{J}}},\mathscr{G}_{\Gamma_{\mathfrak{J}}}\right\}(\mathfrak{J}=1,2,...,\ell)$ *be a collection of SVNNs. Let* $\Gamma_{\mathfrak{J}}^{-}=\left(min_{\mathfrak{J}}\left\{\overline{O}_{\Gamma_{\mathfrak{J}}}\right\},max_{\mathfrak{J}}\left\{\Delta_{\Gamma_{\mathfrak{J}}}\right\},max_{\mathfrak{J}}\left\{\mathscr{G}_{\Gamma_{\mathfrak{J}}}\right\}\right)$ *and* $\Gamma_{\mathfrak{J}}^{+}=\left(\underset{\mathfrak{J}}{max}\left\{\overline{O}_{\Gamma_{\mathfrak{J}}}\right\},\underset{\mathfrak{J}}{min}\left\{\Delta_{\Gamma_{\mathfrak{J}}}\right\},\underset{\mathfrak{J}}{min}\left\{\mathscr{G}_{\Gamma_{\mathfrak{J}}}\right\}\right)(\mathfrak{J}=1,2,...,\ell)$. *Then*

$$\Xi_{\mathfrak{J}}^{-}\le SV-NAOWG\left(\Xi_1,\Xi_2,\ldots,\Xi_\ell\right)\le\Xi_{\mathfrak{J}}^{+}. \tag{33}$$

(3) Let $\Gamma_{\mathfrak{J}}=\left\{\overline{O}_{\Gamma_{\mathfrak{J}}},\Delta_{\Gamma_{\mathfrak{J}}},\mathscr{G}_{\Gamma_{\mathfrak{J}}}\right\}$ *and* $\Gamma_{\mathfrak{J}}^{*}=\left\{\overline{O}_{\Gamma_{\mathfrak{J}}}^{*},\Delta_{\Gamma_{\mathfrak{J}}}^{*},\mathscr{G}_{\Gamma_{\mathfrak{J}}}^{*}\right\}(\mathfrak{J}=1,2,...,\ell)$ *be two collection of SVNNs. If* $\Gamma_{\mathfrak{J}}\le\Gamma_{\mathfrak{J}}^{*}$ *for* $(\mathfrak{J}=1,2,...,\ell)$. *Then*

$$\begin{aligned} &SV-NAOWG\left(\Xi_1,\Xi_2,\ldots,\Xi_\ell\right)\\ &\le SV-NAOWG\left(\Xi_1^{*},\Xi_2^{*},\ldots,\Xi_\ell^{*}\right). \end{aligned} \tag{34}$$

Proof. Using Theorem 2, 3 and 4, the proof is straightforward. □

5. EDAS Method Based on SVN Aczel–Alsina Aggregation Information

A novel extended EDAS approach is built here to handle the complex uncertain data in real-life D-S issues in order to validate the effectiveness of the SVN Acz-Als geometric AOs. The following are the particular measures to take.

Assume, that there is a set of ℓ alternatives, and an acceptable rating by the attributes $\{\mathbb{R}_1,\mathbb{R}_2,...,\mathbb{R}_m\}$. Then, the usefulness of different attributes $\mathbb{R}_\imath(\imath=1,2,...,\mathrm{m})$ is specified by $\varpi=(\varpi_1,\varpi_1,...,\varpi_m)^T$ such that $\varpi_\imath>0$ and $\sum_{\imath=1}^{m}\varpi_\imath=$.

Let $\Xi_{\mathfrak{J}\imath}=\left\{\overline{O}_{\Xi_{\mathfrak{J}\imath}},\Delta_{\Xi_{\mathfrak{J}\imath}},\mathscr{G}_{\Xi_{\mathfrak{J}\imath}}\right\}$ for $\overline{O}_{\Xi_{\mathfrak{J}\imath}},\Delta_{\Xi_{\mathfrak{J}\imath}},\mathscr{G}_{\Xi_{\mathfrak{J}\imath}}\in[0,1]$ be the acceptable rating of every attribute for each alternative, where $\overline{O}_{\Xi_{\ell m}}$ depicts the $+ve$ grade function the alternative $(\mathfrak{J}=1,2,\ldots,\ell)$ satisfies $\mathbb{R}_\imath(\imath=1,2,...,\mathrm{m})$. $\Delta_{\Xi_{\ell m}}$ and $\mathscr{G}_{\Xi_{\ell m}}$ designate the nutral grade function and $-ve$ grade function, respectively. The decision matrix of SVNNs can be obtained based from assessment data: $\Xi=(\Xi_{\mathfrak{J}\imath})_{\ell m}$.

The procedure for determining the best alternative using EDAS methodology depends on SVN Acz-Als aggregation information is prsented as the following steps: Step-1: Select a series of attributes that are suitable for use in evaluating the problem under consideration:

The prospective assessment characteristics are gathered via a study of the literature, and an expert DM committee is created to screen the attributes in order to develop an acceptable collection of evaluation attributes $\mathbb{R}_\imath(\imath=1,2,...,\mathrm{m})$.

$$D_{\mathfrak{J}\times\imath}=\begin{array}{c} \\ R_1\\ R_2\\ \vdots\\ R_\ell \end{array}\begin{array}{c} \begin{array}{cccc} \mathbb{R}_1 & \mathbb{R}_2 & & \mathbb{R}_m \end{array}\\ \begin{pmatrix} \left(\overline{O}_{\Xi_{11}},\Delta_{\Xi_{11}},\mathscr{G}_{\Xi_{11}}\right) & \left(\overline{O}_{\Xi_{12}},\Delta_{\Xi_{12}},\mathscr{G}_{\Xi_{12}}\right) & \ldots & \left(\overline{O}_{\Xi_{1m}},\Delta_{\Xi_{1m}},\mathscr{G}_{\Xi_{1m}}\right)\\ \left(\overline{O}_{\Xi_{21}},\Delta_{\Xi_{21}},\mathscr{G}_{\Xi_{21}}\right) & \left(\overline{O}_{\Xi_{22}},\Delta_{\Xi_{22}},\mathscr{G}_{\Xi_{22}}\right) & \ldots & \left(\overline{O}_{\Xi_{2m}},\Delta_{\Xi_{2m}},\mathscr{G}_{\Xi_{2m}}\right)\\ \vdots & \vdots & \ddots & \vdots\\ \left(\overline{O}_{\Xi_{\ell1}},\Delta_{\Xi_{\ell1}},\mathscr{G}_{\Xi_{\ell1}}\right) & \left(\overline{O}_{\Xi_{\ell2}},\Delta_{\Xi_{\ell2}},\mathscr{G}_{\Xi_{\ell2}}\right) & \ldots & \left(\overline{O}_{\Xi_{\ell m}},\Delta_{\Xi_{\ell m}},\mathscr{G}_{\Xi_{\ell m}}\right) \end{pmatrix} \end{array}. \tag{35}$$

Step 2. Normalization is used to obtain the normalised decision matrix as:

$$\mathcal{N}_{\mathfrak{J}\times 1}=\begin{cases}\left(\overline{O}_{\Xi_{\mathfrak{J}_1}},\Delta_{\Xi_{\mathfrak{J}_1}},\mathcal{G}_{\Xi_{\mathfrak{J}_1}}\right) & if \quad C_I\\ \left(\mathcal{G}_{\Xi_{\mathfrak{J}_1}},\Delta_{\Xi_{\mathfrak{J}_1}},\overline{O}_{\Xi_{\mathfrak{J}_1}}\right) & if \quad C_{II}\end{cases}, \tag{36}$$

where C_I refers to "if $\mathbb{R}_1(1=1,2,\ldots,m)$ is a benefit criterion" and C_{II} refers to "if $\mathbb{R}_1(1=1,2,\ldots,m)$ is a cost criterion".

Step 3. Aggregated Data: Established SVN Acz-Als operators are utilized to aggregate the specialists uncertain data of D-S problems.

$$SV-NAWG(\Xi_1,\Xi_2,\ldots,\Xi_\ell)=\prod_{\mathfrak{J}=1}^{\ell}(\Xi_{\mathfrak{J}})^{\omega_{\mathfrak{J}}}=\left\{\begin{matrix}e^{-\left(\sum_{\mathfrak{J}=1}^{\ell}\omega_{\mathfrak{J}}\left(-\ell n'\overline{O}_{\Xi_{\mathfrak{J}}}\right)^{\wp}\right)^{1/\wp}}, 1-e^{-\left(\sum_{\mathfrak{J}=1}^{\ell}\omega_{\mathfrak{J}}\left(-\ell n'\left(1-\Delta_{\Xi_{\mathfrak{J}}}\right)\right)^{\wp}\right)^{1/\wp}},\\ 1-e^{-\left(\sum_{\mathfrak{J}=1}^{\ell}\omega_{\mathfrak{J}}\left(-\ell n'\left(1-\mathcal{G}_{\Xi_{\mathfrak{J}}}\right)\right)^{\wp}\right)^{1/\wp}}\end{matrix}\right\}. \tag{37}$$

Step 4. Determine the average solution (A_VS) depends on all provided characteristics:

$$A_VS=\left[A_VS_1\right]_{1\times m}=\left[\frac{\sum_{\mathfrak{J}=1}^{\ell}\left(\Xi_{\mathfrak{J}_1}\right)}{\ell}\right]_{1\times m} \tag{38}$$

Based on Definition 11, we get

$$A_VS=\left[A_VS_1\right]_{1\times m}=\left[\frac{\sum_{\mathfrak{J}=1}^{\ell}\left(\Xi_{\mathfrak{J}_1}\right)}{\ell}\right]_{1\times m}=\left\{\begin{matrix}1-e^{-\left(\sum_{\mathfrak{J}=1}^{\ell}1/\ell\left(-\ell n'\left(1-\overline{O}_{\Xi_{\mathfrak{J}_1}}\right)\right)^{\wp}\right)^{1/\wp}}, e^{-\left(\sum_{\mathfrak{J}=1}^{\ell}1/\ell\left(-\ell n'\Delta_{\Xi\mathfrak{J}_1}\right)^{\wp}\right)^{1/\wp}},\\ e^{-\left(\sum_{\mathfrak{J}=1}^{\ell}1/\ell\left(-\ell n'\mathcal{G}_{\Xi_{\mathfrak{J}_1}}\right)^{\wp}\right)^{1/\wp}}\end{matrix}\right\}. \tag{39}$$

Step 5. According to the results of A_VS, we can compute the positive distance from average (PDA_v) and negative distance from average (NDA_v) by using the following formula:

$$\begin{aligned}PDA_{v_{\mathfrak{J}_1}}&=\frac{\max\left(0,\left(\Xi_{\mathfrak{J}_1}-A_VS_1\right)\right)}{A_VS_1},\\ NDA_{v_{\mathfrak{J}_1}}&=\frac{\max\left(0,\left(A_VS_1-\Xi_{\mathfrak{J}_1}\right)\right)}{A_VS_1}.\end{aligned} \tag{40}$$

We may adopt the score function of SVNNs described in Definition 8 to compute the PDA and NDA as follows:

$$\begin{aligned}PDA_{v_{\mathfrak{J}_1}}&=\frac{\max\left(0,\left(\mathcal{Q}\left(\Xi_{\mathfrak{J}_1}\right)-\mathcal{Q}\left(A_VS_1\right)\right)\right)}{\mathcal{Q}\left(A_VS_1\right)},\\ NDA_{v_{\mathfrak{J}_1}}&=\frac{\max\left(0,\left(\mathcal{Q}\left(A_VS_1\right)-\mathcal{Q}\left(\Xi_{\mathfrak{J}_1}\right)\right)\right)}{\mathcal{Q}\left(A_VS_1\right)},\end{aligned} \tag{41}$$

where $\mathcal{Q}$ represented the score value.

Step 6. Determine SPDA and SNDA, which represent the weighted average of PDA and NDA as follows:

$$\begin{aligned}SPDA_{\mathfrak{J}}&=\sum_{1=1}^{m}\omega_1PDA_{v_{\mathfrak{J}_1}},\\ SNDA_{\mathfrak{J}}&=\sum_{1=1}^{m}\omega_1NDA_{v\mathfrak{J}_1},\end{aligned} \tag{42}$$

Where $\omega_1\in[0,1],\sum_{1=1}^{m}\omega_1=1$.

Step 7. Normalize weighted sum of PDA and NDA is denoted and defined as respectively:

$$\begin{aligned}NSPDA_{\mathfrak{J}}&=\frac{SPDA_{\mathfrak{J}}}{\max\left(SP\ DA_{\mathfrak{J}}\right)},\\ NSNDA_{\mathfrak{J}}&=\frac{SNDA_{\mathfrak{J}}}{\max\left(SNDA_{\mathfrak{J}}\right)}.\end{aligned} \tag{43}$$

Step 8. Compute the values of appraisal score (ASC) depends on each alternative's as:

$$ASC_{\mathfrak{J}}=\frac{1}{2}\left(NSPDA_{\mathfrak{J}}+1-NSNDA_{\mathfrak{J}}\right). \tag{44}$$

Step 9. Depending on the calculating values of *ASC*,alternatives are ranked in a decreasing order, and the bigger value of $ASC_{\mathfrak{J}}$ is the best alternative selected will be.

6. Numerical Illustration of EDAS Method

In order to authenticate the effectiveness and appropriate of the developed technique, We call on Akram and Khan [53]'s example related to the role of commercial banks in providing loans to their customers to validate the MAGDM method, and perform a sensitivity analysis and comparative analysis with other existing methods. The problem is described below.

6.1. Case Study. Low pricing are offered to clients by commercial banks. Like wholesale corporations, clients purchase large quantities and then resell them at a lower price to other customers. Discounts include free checking, no fees for creating accounts, and reduced interest rates for real estate loans. A debit card, credit card, or both are all options available at commercial banks, as are investment accounts, commercial real estate loans, and mortgage plans. In addition to managing their checking and savings accounts, customers may use Internet banking to pay bills, move money between accounts, apply for short- and long-term loans, and more. Using a 24-hour ATM, a client may maintain control of their accounts even if their bank is closed. Long and short-term loans are both available from commercial banks. Long-term loans are available to help a variety of businesses get their start-up capital. Suppose a customer is looking for financing for his food business. He had a list of five banks and wanted to check out. He called a DM specialist to help him choose a bank that could lend him money, and the expert looked at the following criteria:

(1) Markup and penalty ($\mathbb{R}_1$);

(2) Customers' guarantee requirements and regulations ($\mathbb{R}_2$);

(3) Paperwork costs and customer packages ($\mathbb{R}_3$);

(4) Procedural time and credit time ($\mathbb{R}_4$);

(5) safe and secure banking ($\mathbb{R}_5$).

In this evaluation, experts were requested to utilize SV neutrosophic information to determine the best bank for business loans.

Table 1 summarizes the expert assessment data for SVNNs:

Cost type SVN information is given in I_2 and I_4. Therefore the normalised expert evaluation decision information matrix is enclosed in Table 2:

Because there is just one expert in this case study, we do not need to calculate the cumulative decision matrix.

As per Table 2, we may use formula (3) to get the A_VS depends on all provided characteristics.

$$A_VS_2 = \left\{ \begin{pmatrix} 1 - e^{-\left(\begin{matrix} 1/5 * (-\ell og(1-0.5))^5 + 1/5 * (-\ell og(1-0.7))^5 + 1/5 * (-\ell og(1-0.6))^5 + \\ 1/5 * (-\ell og(1-0.7))^5 + 1/5 * (-\ell og(1-0.5))^5 \end{matrix} \right)^{1/5}} \\ \\ \left(e^{-\left(1/5 * (-\ell og(0.2))^5 + 1/5 * (-\ell og(0.2))^5 + 1/5 * (-\ell og(0.2))^5 + 1/5 * (-\ell og(0.2))^5 + 1/5 * (-\ell og(0.1))^5\right)^{1/5}}\right) \\ \left(e^{-\left(1/5 * (-\ell og(0.3))^5 + 1/5 * (-\ell og(0.3))^5 + 1/5 * (-\ell og(0.4))^5 + 1/5 * (-\ell og(0.2))^5 + 1/5 * (-\ell og(0.2))^5\right)^{1/5}}\right) \end{pmatrix} \right\}$$

$$= (0.447278, 0.157468, 0.245549).$$

$$A_VS_3 = \left\{ \begin{pmatrix} 1 - e^{-\left(\begin{matrix} 1/5 * (-\ell og(1-0.2))^5 + 1/5 * (-\ell og(1-0.6))^5 + 1/5 * (-\ell og(1-0.6))^5 + \\ 1/5 * (-\ell og(1-0.4))^5 + 1/5 * (-\ell og(1-0.4))^5 \end{matrix} \right)^{1/5}} \\ \\ \left(e^{-\left(1/5 * (-\ell og(0.2))^5 + 1/5 * (-\ell og(0.3))^5 + 1/5 * (-\ell og(0.1))^5 + 1/5 * (-\ell og(0.5))^5 + 1/5 * (-\ell og(0.1))^5\right)^{1/5}}\right) \\ \left(e^{-\left(1/5 * (-\ell og(0.6))^5 + 1/5 * (-\ell og(0.2))^5 + 1/5 * (-\ell og(0.2))^5 + 1/5 * (-\ell og(0.2))^5 + 1/5 * (-\ell og(0.5))^5\right)^{1/5}}\right) \end{pmatrix} \right\}$$

$$= (0.69715, 0.141507, 0.23343).$$

$$A_V S_4 = \left\{ \begin{pmatrix} 1 - e^{-\left(\begin{matrix} 1/5 * (-\ell og(1-0.3))^5 + 1/5 * (-\ell og(1-0.6))^5 + 1/5 * (-\ell og(1-0.5))^5 + \\ 1/5 * (-\ell og(1-0.5))^5 + 1/5 * (-\ell og(1-0.4))^5 \end{matrix} \right)^{1/5}} \\ \left(e^{-\left(1/5 * (-\ell og(0.2))^5 + 1/5 * (-\ell og(0.4))^5 + 1/5 * (-\ell og(0.1))^5 + 1/5 * (-\ell og(0.2))^5 + 1/5 * (-\ell og(0.3))^5\right)^{1/5}} \right) \\ \left(e^{-\left(1/5 * (-\ell og(0.4))^5 + 1/5 * (-\ell og(0.2))^5 + 1/5 * (-\ell og(0.3))^5 + 1/5 * (-\ell og(0.2))^5 + 1/5 * (-\ell og(0.6))^5\right)^{1/5}} \right) \end{pmatrix} \right\}$$
$$= (0.606536, 0.168535, 0.252183).$$
$$A_V S_5 = \left\{ \begin{pmatrix} 1 - e^{-\left(\begin{matrix} 1/5 * (-\ell og(1-0.3))^5 + 1/5 * (-\ell og(1-0.7))^5 + 1/5 * (-\ell og(1-0.6))^5 + \\ 1/5 * (-\ell og(1-0.4))^5 + 1/5 * (-\ell og(1-0.3))^5 \end{matrix} \right)^{1/5}} \\ \left(e^{-\left(1/5 * (-\ell og(0.3))^5 + 1/5 * (-\ell og(0.1))^5 + 1/5 * (-\ell og(0.4))^5 + 1/5 * (-\ell og(0.5))^5 + 1/5 * (-\ell og(0.2))^5\right)^{1/5}} \right) \\ \left(e^{-\left(1/5 * (-\ell og(0.4))^5 + 1/5 * (-\ell og(0.2))^5 + 1/5 * (-\ell og(0.3))^5 + 1/5 * (-\ell og(0.4))^5 + 1/5 * (-\ell og(0.4))^5\right)^{1/5}} \right) \end{pmatrix} \right\}$$
$$= (0.642351, 0.176204, 0.28647). \tag{45}$$

Then we can get the value of $A_V S_1$ as

$$A_V S_1 = \left\{ \begin{matrix} (0.513968, 0.143849, 0.278161),\ (0.447278, 0.157468, 0.245549), \\ (0.69715, 0.141507, 0.23343),\ (0.606536, 0.168535, 0.252183), \\ (0.642351, 0.176204, 0.28647) \end{matrix} \right\}. \tag{46}$$

According to the results of average solution $A_V S_1$, we can compute the positive distance from average (PDA ν) and negative distance from average (NDA ν) by using formula (5) which are listed in Tables 3–5.

Calculate the values of $SP\ DA_{\mathfrak{F}}$ and $SN\ DA_{\mathfrak{F}}$ by (6) and attributes weighting vector $\varpi = (0.15, 0.28, 0.20, 0.22, 0.15)$, we can obtain the results as:

$$\begin{aligned} SPDA_1 &= 0.00\, SP\ DA_2 = 1.50\, SP\ DA_3 = 0.00\, SP\ DA_4 = 1.79\, SP\ DA_5 = 0.98 \\ SNDA_1 &= 2.38\, SN\ DA_1 = 0.35\, SN\ DA_1 = 1.10\, SN\ DA_1 = 1.05\, SN\ DA_1 = 1.68 \\ NSNDA_1 &= 2.16\, NSN\ DA_2 = 0.323\, NSND_3 = 1.00 \\ NSNDA_4 &= 0.95\, NSN\ DA_5 = 1.526. \end{aligned} \tag{47}$$

Normalize weighted sum of PDA and NDA are evaluated by (7) as follows:

$$\begin{aligned} NSP\ DA_1 &= 0.00\, NSP\ DA_2 = 1.53\, NSP\ DA_3 = 0.00 \\ NSP\ DA_4 &= 1.82\, NSP\ DA_5 = 1.00. \end{aligned} \tag{48}$$

Compute the values of appraisal score (ASC) depends on each alternative's NSPDA and NSNDA as:

$$\begin{aligned} ASC_1 &= -0.580\, ASC_2 = 1.103\, ASC_3 = 0.000 \\ ASC_4 &= 0.933\, ASC_5 = 0.236. \end{aligned} \tag{49}$$

Based on ASC results, we may rate all of the possibilities; the greater ASC, the better the alternative selected. Obviously, ranking results are and is the best alternative.

7. Comparison of EDAS Method with Some Aggregation Operators under SVNNs

In order to evaluate the established EDAS approach's potential and effectiveness and to compare it with new discoveries, we've included some applicable instances below.

Table 1: Expert evaluation information.

	R_1	R_2	R_3	R_4	R_5
$\varnothing_1$	(0.5, 0.3, 0.4)	(0.3, 0.2, 0.5)	(0.2, 0.2, 0.6)	(0.4, 0.2, 0.3)	(0.3, 0.3, 0.4)
$\varnothing_2$	(0.7, 0.1, 0.3)	(0.3, 0.2, 0.7)	(0.6, 0.3, 0.2)	(0.2, 0.4, 0.6)	(0.7, 0.1, 0.2)
$\varnothing_3$	(0.5, 0.3, 0.4)	(0.4, 0.2, 0.6)	(0.6, 0.1, 0.2)	(0.3, 0.1, 0.5)	(0.6, 0.4, 0.3)
$\varnothing_4$	(0.7, 0.3, 0.2)	(0.2, 0.2, 0.7)	(0.4, 0.5, 0.2)	(0.2, 0.2, 0.5)	(0.4, 0.5, 0.4)
$\varnothing_5$	(0.4, 0.1, 0.3)	(0.2, 0.1, 0.5)	(0.4, 0.1, 0.5)	(0.6, 0.3, 0.4)	(0.3, 0.2, 0.4)

Table 2: Normalized expert data.

	R_1	R_2	R_3	R_4	R_5
$\varnothing_1$	(0.5, 0.3, 0.4)	(0.5, 0.2, 0.3)	(0.2, 0.2, 0.6)	(0.3, 0.2, 0.4)	(0.3, 0.3, 0.4)
$\varnothing_2$	(0.7, 0.1, 0.3)	(0.7, 0.2, 0.3)	(0.6, 0.3, 0.2)	(0.6, 0.4, 0.2)	(0.7, 0.1, 0.2)
$\varnothing_3$	(0.5, 0.3, 0.4)	(0.6, 0.2, 0.4)	(0.6, 0.1, 0.2)	(0.5, 0.1, 0.3)	(0.6, 0.4, 0.3)
$\varnothing_4$	(0.7, 0.3, 0.2)	(0.7, 0.2, 0.2)	(0.4, 0.5, 0.2)	(0.5, 0.2, 0.2)	(0.4, 0.5, 0.4)
$\varnothing_5$	(0.4, 0.1, 0.3)	(0.5, 0.1, 0.2)	(0.4, 0.1, 0.5)	(0.4, 0.3, 0.6)	(0.3, 0.2, 0.4)

Table 4: The valus of $P\ DA_v$.

	R_1	R_2	R_3	R_4	R_5
$\varnothing_1$	0.0	0.0	0.0	0.0	0.0
$\varnothing_2$	2.262	3.518	0.0	0.0	1.226
$\varnothing_3$	0.0	0.0	0.0	0.0	0.0
$\varnothing_4$	1.174	5.777	0.0	0.0	0.0
$\varnothing_5$	0.0	3.518	0.0	0.0	0.0

Table 3: Score value of $Z_{\Im_i}$ and $A_V S_i$.

	R_1	R_2	R_3	R_4	R_5
$\varnothing_1$	0.2	0	−0.6	−0.3	−0.4
$\varnothing_2$	0.3	0.2	0.1	0	0.4
$\varnothing_3$	−0.2	0	0.3	0.1	−0.1
$\varnothing_4$	0.2	0.3	−0.3	0.1	−0.5
$\varnothing_5$	0	0.2	−0.2	−0.5	−0.3
$A_V S_1$	0.0919	0.0442	0.3222	0.1858	0.1796

Table 5: The valus of NDA_v.

	R_1	R_2	R_3	R_4	R_5
$\varnothing_1$	3.174	1.00	2.862	2.614	3.226
$\varnothing_2$	0.00	0.00	0.689	1.00	0.00
$\varnothing_3$	3.174	1.00	0.068	0.461	3.782
$\varnothing_4$	0.00	0.00	1.931	0.461	3.782
$\varnothing_5$	1.00	0.00	1.620	3.690	2.669

Table 6: *SVN* Acz-A1s geometric *AOSVNAWG*.

$\varnothing_1$	(0.354965, 0.228894, 0.413376)
$\varnothing_2$	(0.658326, 0.226143, 0.24175)
$\varnothing_3$	(0.562678, 0.194736, 0.321488)
$\varnothing_4$	(0.54847, 0.316751, 0.228029)
$\varnothing_5$	(0.410712, 0.152477, 0.392657)

Table 7: Exisiting Aggregated SVN information.

	$SVNWA$ [54]	$SVNOWA$ [54]	NWA [55]	$SVNFWA$ [42]
$\varnothing_1$	(0.37, 0.22, 0.40)	(0.38, 0.24, 0.40)	(0.37, 0.23, 0.42)	(0.37, 0.22, 0.40)
$\varnothing_2$	(0.66, 0.20, 0.23)	(0.66, 0.18, 0.24)	(0.66, 0.24, 0.24)	(0.66, 0.20, 0.23)
$\varnothing_3$	(0.56, 0.17, 0.31)	(0.55, 0.18, 0.31)	(0.56, 0.21, 0.32)	(0.56, 0.17, 0.31)
$\varnothing_4$	(0.57, 0.29, 0.22)	(0.57, 0.31, 0.22)	(0.57, 0.33, 0.23)	(0.56, 0.29, 0.22)
$\varnothing_5$	(0.41, 0.14, 0.36)	(0.39, 0.13, 0.36)	(0.41, 0.16, 0.41)	(0.41, 0.14, 0.36)

Table 8: Existing aggregated SVN information.

	$SVNHWA$ [40]	$SVNHWA$ [40]	$L-SVNWA$ [55]	$L-SVNOWA$ [55]
$\varnothing_1$	(0.37, 0.22, 0.40)	(0.36, 0.22, 0.40)	(0.31, 0.17, 0.35)	(0.32, 0.19, 0.36)
$\varnothing_2$	(0.66, 0.20, 0.23)	(0.66, 0.20, 0.23)	(0.64, 0.19, 0.23)	(0.65, 0.17, 0.23)
$\varnothing_3$	(0.56, 0.17, 0.31)	(0.56, 0.30, 0.22)	(0.49, 0.17, 0.33)	(0.48, 0.18, 0.33)
$\varnothing_4$	(0.56, 0.29, 0.22)	(0.56, 0.30, 0.22)	(0.55, 0.27, 0.19)	(0.55, 0.29, 0.19)
$\varnothing_5$	(0.41, 0.14, 0.36)	(0.41, 0.14, 0.37)	(0.28, 0.12, 0.37)	(0.24, 0.12, 0.38)

Table 9: Existing aggregated SVN information.

	$ST-SVNWA$ [43]	$ST-SVNWG$ [43]	$ST-SVNOWA$ [43]	$ST-SVNOWG$ [43]
$\varnothing_1$	(0.56, 0.02, 0.07)	(0.50, 0.02, 0.08)	(0.56, 0.02, 0.08)	(0.51, 0.03, 0.08)
$\varnothing_2$	(0.86, 0.02, 0.02)	(0.85, 0.03, 0.03)	(0.86, 0.01, 0.02)	(0.85, 0.02, 0.03)
$\varnothing_3$	(0.77, 0.01, 0.04)	(0.76, 0.02, 0.05)	(0.77, 0.01, 0.04)	(0.76, 0.03, 0.05)
$\varnothing_4$	(0.78, 0.04, 0.02)	(0.73, 0.06, 0.02)	(0.78, 0.04, 0.02)	(0.72, 0.06, 0.02)
$\varnothing_5$	(0.60, 0.09, 0.06)	(0.59, 0.01, 0.08)	(0.58, 0.09, 0.06)	(0.57, 0.01, 0.08)

Table 10: Overall ranking of the alternatives.

Exsisting operations	Ranking	Best alternative
NWA [55]	$\mathcal{Q}(\varnothing_2) > \mathcal{Q}(\varnothing_3) > \mathcal{Q}(\varnothing_1) > \mathcal{Q}(\varnothing_5) > \mathcal{Q}(\varnothing_4)$	$\varnothing_2$
$SVNWA$ [54]	$\mathcal{Q}(\varnothing_2) > \mathcal{Q}(\varnothing_3) > \mathcal{Q}(\varnothing_1) > \mathcal{Q}(\varnothing_5) > \mathcal{Q}(\varnothing_4)$	$\varnothing_2$
$SVNOWA$ [54]	$\mathcal{Q}(\varnothing_2) > \mathcal{Q}(\varnothing_3) > \mathcal{Q}(\varnothing_1) > \mathcal{Q}(\varnothing_5) > \mathcal{Q}(\varnothing_4)$	$\varnothing_2$
$SVNFWA$ [42]	$\mathcal{Q}(\varnothing_2) > \mathcal{Q}(\varnothing_3) > \mathcal{Q}(\varnothing_1) > \mathcal{Q}(\varnothing_5) > \mathcal{Q}(\varnothing_4)$	$\varnothing_2$
$SVNHWA$ for $\gamma = 2$ [40]	$\mathcal{Q}(\varnothing_2) > \mathcal{Q}(\varnothing_3) > \mathcal{Q}(\varnothing_1) > \mathcal{Q}(\varnothing_5) > \mathcal{Q}(\varnothing_4)$	$\varnothing_2$
$SVNHWA$ for $\gamma = 3$ [40]	$\mathcal{Q}(\varnothing_2) > \mathcal{Q}(\varnothing_3) > \mathcal{Q}(\varnothing_1) > \mathcal{Q}(\varnothing_5) > \mathcal{Q}(\varnothing_4)$	$\varnothing_2$
$L-SVNWA$ [55]	$\mathcal{Q}(\varnothing_2) > \mathcal{Q}(\varnothing_3) > \mathcal{Q}(\varnothing_1) > \mathcal{Q}(\varnothing_5) > \mathcal{Q}(\varnothing_4)$	$\varnothing_2$
$L-SVNOWA$ [55]	$\mathcal{Q}(\varnothing_2) > \mathcal{Q}(\varnothing_3) > \mathcal{Q}(\varnothing_1) > \mathcal{Q}(\varnothing_5) > \mathcal{Q}(\varnothing_4)$	$\varnothing_2$
$ST-SVNWA$ [43]	$\mathcal{Q}(\varnothing_2) > \mathcal{Q}(\varnothing_3) > \mathcal{Q}(\varnothing_1) > \mathcal{Q}(\varnothing_5) > \mathcal{Q}(\varnothing_4)$	$\varnothing_2$
$ST-SVNWG$ [43]	$\mathcal{Q}(\varnothing_2) > \mathcal{Q}(\varnothing_3) > \mathcal{Q}(\varnothing_1) > \mathcal{Q}(\varnothing_5) > \mathcal{Q}(\varnothing_4)$	$\varnothing_2$
$ST-SVNOWA$ [43]	$\mathcal{Q}(\varnothing_2) > \mathcal{Q}(\varnothing_3) > \mathcal{Q}(\varnothing_1) > \mathcal{Q}(\varnothing_5) > \mathcal{Q}(\varnothing_4)$	$\varnothing_2$
$ST-SVNOWG$ [43]	$\mathcal{Q}(\varnothing_2) > \mathcal{Q}(\varnothing_3) > \mathcal{Q}(\varnothing_1) > \mathcal{Q}(\varnothing_5) > \mathcal{Q}(\varnothing_4)$	$\varnothing_2$
SVNAWG (proposed)	$\mathcal{Q}(\varnothing_2) > \mathcal{Q}(\varnothing_3) > \mathcal{Q}(\varnothing_1) > \mathcal{Q}(\varnothing_5) > \mathcal{Q}(\varnothing_4)$	$\varnothing_2$

Table 11: Sensitivity analysis of parameter $\wp$.

Υ	Operators	Score					Ranking best alternative
		$\mathcal{Q}(\varnothing_1)$	$\mathcal{Q}(\varnothing_2)$	$\mathcal{Q}(\varnothing_3)$	$\mathcal{Q}(\varnothing_4)$	$\mathcal{Q}(\varnothing_5)$	
$\longrightarrow 0.2$	$SVNAWG$	−0.274	0.203	0.060	0.025	−0.113	$\varnothing_2$
$\longrightarrow 1$	$SVNAWG$	−0.309	0.168	0.022	−0.034	−0.168	$\varnothing_2$
$\longrightarrow 2$	$SVNAWG$	−0.352	0.129	−0.022	−0.107	−0.232	$\varnothing_2$
$\longrightarrow 5$	$SVNAWG$	−0.464	0.051	−0.116	−0.265	−0.357	$\varnothing_2$
$\longrightarrow 10$	$SVNAWG$	−0.562	−0.010	−0.189	−0.372	−0.450	$\varnothing_2$
$\longrightarrow 15$	$SVNAWG$	−0.606	−0.038	−0.223	−0.413	−0.494	$\varnothing_2$
$\longrightarrow 30$	$SVNAWG$	−0.652	−0.068	−0.260	−0.456	−0.546	$\varnothing_2$

Table 12: Comparision.

Techniques	Whether utilized fuzzy data	Whether make a data aggregationthrough parameter
Peng et al. [54]	Yes	No
Nancy and Gar [55]	Yes	No
Developed method	Yes	Yes

The expert evaluation information under SVNNs is given in Table 1.

Now we apply proposed single valued neutrosophic Acz-Als geometric AOs to adrress the uncertainty and chose the best alternative as follows in Table 6:

Tables 7–9 illustrate how existing techniques of AOs are used to aggregate the ambiguous information.

Now, according to collective data, the overall ranking of alternative is in the following Table 10.

Based on the outcomes of the recommended operators and the previously employed methodologies, we may deduce that the ranking lists are identical. Based on Acz-Als aggregation operations depends EDAS technique is generalized and new way to dealing with uncertainty in DM situations. It is more flexible and economical in real-world issues to use Acz-Als norm-depends aggregate operators in a single valued NS context.

7.1. Sensitivity Analysis. Using the given SVN Acz-Als aggregation approaches, we change the parameter $\wp$ value from 0 to 30 in this section to investigate the different patterns of scores and ranking of the alternatives. The findings from suggested SVNAWG operator is listed in Table 11. The obtained results illustrate to decision-makers that they can obtain the best option depends on their preferences.

Attribute analysis within a few previous techniques are as follows in Table 12.

8. Conclusion

In this study, we extended Acz-Als t-norm and t-conorm to single-valued neutrosophic scenarios, suggested a few novel working rules for SVNNs, and studied their properties and linkages in this research. This led to the development of an additional set of aggregate operators, including an Acz-Als depends approach for dealing with conflicts in SVNNs, which were introduced at that time. Various attractive qualities and special circumstances of these operators, as well as the connections between these operators, have recently been investigated in more depth. The suggested operators and decision making methodology, along with SVN data, were placed on MAGDM problems, and to demonstrate the DM procedure, a mathematical formulation was offered. The influence of parameter $\wp$ on the results of DM has been investigated. Operators may be used to find the best solution by adjusting a parameter $\wp$. This means that decision-makers now have a more flexible way for addressing the problems of SVN-MAGDM. The aggregation process is more clearly observable when a parameter is provided, making it easier to represent ambiguous information than other existing methodologies. The existing AOs [54, 55], on the other hand, do not make data aggregation more flexible. It is because of this that our suggested AOs in SVN data DM are more complex and trustworthy.

We will investigate the use of Acz-Als weighted AOs of SVNNs in additional domains, such as intelligent manufacturing, machine learning, and data mining, in future research.

Data Availability

The data utilized in this article is hypothetical any one can be use just citing this article.

Ethical Approval

This article does not contain any studies with human participants or animals performed by any of the authors.

Conflicts of Interest

The authors declare that they have no conflicts of interest to report regarding the present study.

Acknowledgments

The author (Muhammad Naeem) would like to thank the Deanship of Scientific Research at Umm Al-Qura University for supporting this work by Grant Code: 22UQU4310396DSR26.

References

[1] L. A. Zadeh, "Fuzzy sets," *Information and Control*, vol. 8, no. 3, pp. 338–353, 1965.

[2] K. T. Atanassov, "Intuitionistic fuzzy sets," *Fuzzy Sets and Systems*, vol. 20, no. 1, pp. 87–96, 1986.

[3] F. Shen, X. Ma, Z. Li, and D. Cai, "An extended intuitionistic fuzzy TOPSIS method based on a new distance measure with an application to credit risk evaluation," *Information Sciences*, vol. 428, pp. 105–119, 2018.

[4] M. C. Wu and T. Y. Chen, "The ELECTRE multicriteria analysis approach based on Atanassov's intuitionistic fuzzy sets," *Expert Systems with Applications*, vol. 38, no. 10, pp. 12318–12327, 2011.

[5] Y. X. Xue, J. X. You, X. D. Liu, and H. C. Liu, "An interval-valued intuitionistic fuzzy MABAC approach for material selection with incomplete weight information," *Applied Soft Computing*, vol. 38, pp. 703–713, 2016.

[6] Z. Xu, "Intuitionistic fuzzy aggregation operators," *IEEE Transactions on Fuzzy Systems*, vol. 15, no. 6, pp. 1179–1187, 2007.

[7] C. Jana and M. Pal, "Extended bipolar fuzzy EDAS approach for multi-criteria group decision-making process," *Computational and Applied Mathematics*, vol. 40, no. 1, pp. 1–15, 2021.

[8] W. Liu and X. Liu, "Intuitionistic fuzzy information aggregation using Einstein operations," *IEEE Transactions on Fuzzy Systems*, vol. 20, no. 5, pp. 923–938, 2012.
[9] X. Xu and Z. Xu, "Prioritized intuitionistic fuzzy aggregation operators," *Information Fusion*, vol. 14, no. 1, pp. 108–116, 2013.
[10] P. Wang and P. Wang, "Some improved linguistic intuitionistic fuzzy aggregation operators and their applications to multiple-attribute decision making," *International Journal of Information Technology and Decision Making*, vol. 16, no. 03, pp. 817–850, 2017.
[11] C. Jana, H. Garg, and M. Pal, "Multi-attribute decision making for power Dombi operators under Pythagorean fuzzy information with MABAC method," *Journal of Ambient Intelligence and Humanized Computing*, pp. 1–18, 2022.
[12] Z. Xu and R. R. Yager, "Intuitionistic fuzzy Bonferroni means," *IEEE Transactions on Systems, Man, and Cybernetics*, vol. 41, no. 2, pp. 568–578, 2010.
[13] R. Arora and H. Garg, "Group decision-making method based on prioritized linguistic intuitionistic fuzzy AOs and its fundamental properties," *Computational and Applied Mathematics*, vol. 38, no. 2, pp. 1–32, 2019.
[14] H. Zhao, Z. Xu, M. Ni, and S. Liu, "Generalized aggregation operators for intuitionistic fuzzy sets," *International Journal of Intelligent Systems*, vol. 25, no. 1, pp. 1–30, 2010.
[15] D. Yu, "Intuitionistic fuzzy information aggregation under confidence levels," *Applied Soft Computing*, vol. 19, pp. 147–160, 2014.
[16] D. Yu, "Intuitionistic fuzzy geometric Heronian mean aggregation operators," *Applied Soft Computing*, vol. 13, no. 2, pp. 1235–1246, 2013.
[17] W. Jiang, B. Wei, X. Liu, X. Zheng, and H. Zheng, "Intuitionistic fuzzy power aggregation operator based on entropy and its application in decision making," *International Journal of Intelligent Systems*, vol. 33, no. 1, pp. 49–67, 2018.
[18] T. Senapati, G. Chen, and R. R. Yager, "Aczel–Alsina aggregation operators and their application to intuitionistic fuzzy multiple attribute decision making," *International Journal of Intelligent Systems*, vol. 324, p. 83, 2021.
[19] M. J. Khan, P. Kumam, P. Liu, W. Ashraf, and S. Ashraf, "A novel approach to generalized intuitionistic fuzzy soft sets and its application in decision support system," *Mathematics*, vol. 7, no. 8, p. 742, 2019.
[20] B. C. Cuong, *Picture Fuzzy Sets-First Results. Part 1, Seminar Neuro-Fuzzy Systems with Applications*, Institute of Mathematics, Hanoi, 2013.
[21] S. Ashraf, T. Mahmood, S. Khan, and Q. Khan, "Different approaches to multi-criteria group decision making problems for picture fuzzy environment," *Bulletin of the Brazilian Mathematical Society, New Series*, vol. 50, no. 2, pp. 373–397, 2019.
[22] M. Riaz, H. Garg, H. M. A. Chinram, and R. Chinram, "Multi-criteria decision making based on bipolar picture fuzzy operators and new distance measures," *Computer Modeling in Engineering and Sciences*, vol. 127, no. 2, pp. 771–800, 2021.
[23] H. Garg, "Some picture fuzzy aggregation operators and their applications to multicriteria decision-making," *Arabian Journal for Science and Engineering*, vol. 42, no. 12, pp. 5275–5290, 2017.
[24] G. Wei, "Picture fuzzy aggregation operators and their application to multiple attribute decision making," *Journal of Intelligent and Fuzzy Systems*, vol. 33, no. 2, pp. 713–724, 2017.
[25] S. Ashraf, S. Khan, and S. Khan, "Fuzzy decision support modeling for internet finance soft power evaluation based on sine trigonometric Pythagorean fuzzy information," *Journal of Ambient Intelligence and Humanized Computing*, vol. 12, no. 2, pp. 3101–3119, 2021.
[26] M. J. Khan, P. Kumam, S. Kumam, and W. Kumam, "Generalized picture fuzzy soft sets and their application in decision support systems," *Symmetry*, vol. 11, no. 3, p. 415, 2019.
[27] S. Khan and S. Ashraf, "Picture fuzzy aggregation information based on Einstein operations and their application in decision making," *Mathematical Sciences*, vol. 13, no. 3, pp. 213–229, 2019.
[28] M. Qiyas, S. Abdullah, S. Aslam, and M. Aslam, "Utilizing linguistic picture fuzzy aggregation operators for multiple-attribute decision-making problems," *International Journal of Fuzzy Systems*, vol. 22, no. 1, pp. 310–320, 2020.
[29] C. Jana, T. Senapati, M. Yager, and R. R. Yager, "Picture fuzzy Dombi aggregation operators: application to MADM process," *Applied Soft Computing*, vol. 74, pp. 99–109, 2019.
[30] C. Jana and M. Pal, "A dynamical hybrid method to design decision making process based on GRA approach for multiple attributes problem," *Engineering Applications of Artificial Intelligence*, vol. 100, p. 104203, 2021.
[31] G. Wei, "Picture fuzzy Hamacher aggregation operators and their application to multiple attribute decision making," *Fundamenta Informaticae*, vol. 157, no. 3, pp. 271–320, 2018.
[32] S. Ashraf, S. Abdullah, and M. Aslam, "Cleaner production evaluation in gold mines using novel distance measure method with cubic picture fuzzy numbers," *International Journal of Fuzzy Systems*, vol. 21, no. 8, pp. 2448–2461, 2019.
[33] S. Khan, S. Abdullah, L. Ashraf, and S. Ashraf, "Logarithmic aggregation operators of picture fuzzy numbers for multi-attribute decision making problems," *Mathematics*, vol. 7, no. 7, p. 608, 2019.
[34] M. Qiyas, S. Abdullah, S. Abdullah, and L. Abdullah, "Linguistic picture fuzzy Dombi aggregation operators and their application in multiple attribute group decision making problem," *Mathematics*, vol. 7, no. 8, p. 764, 2019.
[35] F. Smarandache, *Neutrosophy. Neutrosophic Probability, Set, and Logic*, ProQuest Information & Learning, Ann Arbor, MI, USA, 1998.
[36] F. Smarandache, "Plithogeny, plithogenic set, logic, probability and statistics: a short review," *Journal of Computational and Cognitive Engineering*, pp. 47–50, 2022.
[37] J. Ye, "A multicriteria decision-making method using aggregation operators for simplified neutrosophic sets," *Journal of Intelligent and Fuzzy Systems*, vol. 26, no. 5, pp. 2459–2466, 2014.
[38] J. J. Peng, J. Q. Wang, X. H. Wu, J. Chen, and X. H. Chen, "Multi-valued neutrosophic sets and power aggregation operators with their applications in multi-criteria group decision-making problems," *International Journal of Computational Intelligence Systems*, vol. 8, no. 2, pp. 345–363, 2015.
[39] J. Chen and J. Ye, "Some single-valued neutrosophic Dombi weighted aggregation operators for multiple attribute decision-making," *Symmetry*, vol. 9, no. 6, p. 82, 2017.
[40] P. Liu, Y. Chu, Y. Li, and Y. Chen, "Some generalized neutrosophic number Hamacher aggregation operators and their application to group decision making," *International Journal of Fuzzy Systems*, vol. 16, no. 2, pp. 242–255, 2014.
[41] R. K. Al-Hamido, "A new neutrosophic algebraic structures," *Journal of Computational and Cognitive Engineering*, p. 5, 2022.
[42] H. Garg and S. Nancy, "Linguistic single-valued neutrosophic prioritized aggregation operators and their applications to multiple-attribute group decision-making," *Journal of*

Ambient Intelligence and Humanized Computing, vol. 9, no. 6, pp. 1975–1997, 2018.

[43] S. Ashraf, S. Abdullah, S. Zeng, H. Ghani, and F. Ghani, "Fuzzy decision support modeling for hydrogen power plant selection based on single valued neutrosophic sine trigonometric aggregation operators," *Symmetry*, vol. 12, no. 2, p. 298, 2020.

[44] M. Keshavarz Ghorabaee, E. K. Zavadskas, L. Turskis, and Z. Turskis, "Multi-criteria inventory classification using a new method of evaluation based on distance from average solution (EDAS)," *Informatica*, vol. 26, no. 3, pp. 435–451, 2015.

[45] C. Kahraman, M. Keshavarz Ghorabaee, E. K. Zavadskas, S. C. Cevik Onar, and B. Oztaysi, "Intuitionistic fuzzy EDAS method: an application to solid waste disposal site selection," *Journal of Environmental Engineering and Landscape Management*, vol. 25, no. 1, pp. 1–12, 2017.

[46] B. Batool, S. S. Abosuliman, S. Abdullah, and S. Ashraf, "EDAS method for decision support modeling under the Pythagorean probabilistic hesitant fuzzy aggregation information," *Journal of Ambient Intelligence and Humanized Computing*, pp. 1–14, 2021.

[47] X. D. Peng and C. Liu, "Algorithms for neutrosophic soft decision making based on EDAS, new similarity measure and level soft set," *Journal of Intelligent and Fuzzy Systems*, vol. 32, no. 1, pp. 955–968, 2017.

[48] A. Karasan and C. Kahraman, "A novel interval-valued neutrosophic EDAS method: prioritization of the United Nations national sustainable development goals," *Soft Computing*, vol. 22, pp. 4891–4906, 2018.

[49] M. Keshavarz-Ghorabaee, M. Amiri, E. K. Zavadskas, Z. Antucheviciene, and J. Antucheviciene, "A dynamic fuzzy approach based on the EDAS method for multi-criteria subcontractor evaluation," *Information*, vol. 9, no. 3, p. 68, 2018.

[50] J. Aczél and C. Alsina, "Characterizations of some classes of quasilinear functions with applications to triangular norms and to synthesizing judgements," *Aequationes Mathematicae*, vol. 25, no. 1, pp. 313–315, 1982.

[51] J. Ye, "Subtraction and division operations of simplified neutrosophic sets," *Information*, vol. 8, no. 2, p. 51, 2017.

[52] G. Wei and Z. Zhang, "Some single-valued neutrosophic Bonferroni power aggregation operators in multiple attribute decision making," *Journal of Ambient Intelligence and Humanized Computing*, vol. 10, no. 3, pp. 863–882, 2019.

[53] M. Akram and A. Khan, "Complex Pythagorean Dombi fuzzy graphs for decision making," *Granular Computing*, p. 34, 2020.

[54] J. J. Peng, J. Q. Wang, and J. Wang, "Simplified neutrosophic sets and their applications in multi-criteria group decision-making problems," *International Journal of Systems Science*, vol. 47, no. 10, pp. 2342–2358, 2016.

[55] D. Nancy and H. Garg, "Novel single-valued neutrosophic aggregated operators under Frank norm operation and its application to decision-making process," *International Journal for Uncertainty Quantification*, vol. 6, no. 4, pp. 361–375, 2016.

[56] X. Li, Y. Ju, D. Ju, W. Zhang, P. Wang, and A. Wang, "Multi-attribute group decision making method based on EDAS under picture fuzzy environment," *IEEE Access*, vol. 7, pp. 141179–141192, 2019.

[57] P. Liu, T. Khan, and Q. Khan, "Group decision making based on power Heronian aggregation operators under linguistic neutrosophic environment," *International Journal of Fuzzy Systems*, vol. 20, no. 3, pp. 970–985, 2018.

[58] S. Ashraf, S. Khan, and S. Khan, "Fuzzy decision support modeling for internet finance soft power evaluation based on sine trigonometric Pythagorean fuzzy information," *Journal of Ambient Intelligence and Humanized Computing*, vol. 12, no. 2, pp. 3101–3119, 2021.

[59] A. O. Almagrabi, S. Abdullah, M. Shams, Y. D. Al-Otaibi, and S. Ashraf, "A new approach to q-linear Diophantine fuzzy emergency decision support system for COVID19," *Journal of Ambient Intelligence and Humanized Computing*, vol. 13, no. 4, pp. 1687–1713, 2022.

[60] S. Ashraf, S. Abdullah, and F. Muneeza, "Some novel aggregation operators for cubic picture fuzzy information: application in multi-attribute decision support problem," *Granular Computing*, vol. 6, no. 3, pp. 603–618, 2021.

Hindawi
Complexity
Volume 2022, Article ID 2832175, 13 pages
https://doi.org/10.1155/2022/2832175

Research Article

Models of Analysis of Credible Deviation from Speed Limits on Two-Lane Roads of Bosnia and Herzegovina

Marko Subotić,[1] Nemanja Stepanović,[2] Vladan Tubić,[2] Edis Softić,[3] and Mouhamed Bayane Bouraima[4]

[1]*Faculty of Transport and Traffic Engineering Doboj, University of East Sarajevo, Vojvode Mišića 52, Bosnia and Herzegovina*
[2]*Faculty of Transport and Traffic Engineering Belgrade, University of Belgrade, Vojvode Stepe 305, Belgrade, Serbia*
[3]*Technical Faculty Bihać, University of Bihać, Irfana Ljubijankića Bb, Bihać, Bosnia and Herzegovina*
[4]*Organization of African Academic Doctors (OAAD), Off Kamiti Road, P. O. Box 25305-00100, Nairobi, Kenya*

Correspondence should be addressed to Mouhamed Bayane Bouraima; mouba121286@yahoo.fr

Received 6 July 2022; Revised 9 September 2022; Accepted 23 September 2022; Published 7 October 2022

Academic Editor: Dan Selişteanu

Any deviation of speed in a traffic flow from a speed limit represents a potential risk of traffic accidents, so speed management appears as an imperative. However, an inadequately set speed limit often causes drivers' noncompliance to it in the conditions of real traffic flow. By determining the value of exceeding the speed limit according to vehicle classes, it is possible to recommend a credible speeding value that can be considered credible up to a value above the speed limit. In this paper, deterministic multistep mathematical models of speed deviation from the speed limit as a function of longitudinal gradient for the proposed vehicle classes were developed. A total of 11 measuring sections with different traffic flow types were analyzed. Based on a detailed analysis of speeding, models for the deviation of the 15th, 50th, and 85th percentiles were obtained, with the aim of adjusting the credible deviation to control measures. The results obtained in this study were compared with a survey of traffic flow speeding on two-lane roads conducted in Serbia.

1. Introduction

Roads represent significant resources and the most important public investments of a country, with significant funds allocated for the construction and maintenance with two fundamental tasks, to be efficient and to be safe. In real traffic flow, almost all functional dependencies are based on the relationship between flow, speed, density, number of traffic accidents, etc. as traffic parameters, and longitudinal gradient, road condition, minimum radius of horizontal curvature, etc. as road characteristics. Special attention in the analysis of the functional dependence of traffic and road parameters is expressed for two-lane roads since a large percentage of these roads make up the largest part of the road network of a country. By analyzing traffic parameters, it is evident that the speed of traffic flow is one of the main parameters, and, at the same time, a main indicator for sizing and functional and economic evaluation of project solutions. Any speeding in a traffic management system implies the application of an adequate speed management policy in order to ensure a harmonized traffic flow.

Deviation from a speed limit is mainly connected with the increased probability of traffic accidents. Additionally, determining a credible deviation from a speed limit of a real traffic flow is an imperative in the analysis of speeding, and thus reducing a potential occurrence of incidents. Commonly, the number of traffic accidents and the increase in risk are related to operating speeds. Operating speeds have been shown to be higher than design speeds for a speed limit of about 55 mph or less. Therefore, it is very important to analyze speed through five specific indicators of the dependence of speed on the geometric characteristics of the road. These are relationships between road geometry and operating speeds, influence of road geometry on operating

speeds, influence of safety and security on road geometry, potential impacts on large vehicles, and nature of the speed-safety trade-off [1].

Analysis and determination of the value of appropriate speed limit exceeding represent the power in decision making in traffic engineering, which is often neglected. Any deviation from the speed limit is related to technical and exploitation characteristics of the road, driving and dynamic characteristics of vehicles in a flow, as well as to the psychophysical abilities of drivers. It was shown that after the 20 mph intervention, control of confounding variables for driver speeds declined [2, 3]. For example, on the slope ranging from −5.50% to 4.50% on the measuring plateau or terrain, it was found that the speed decreases with increasing the slope (ascent and descent), but the stress during driving increases on the descent and ascent [4]. Also, within this research, measuring sections on the ascent were identified as potential places with a high percentage of traffic accidents. According to the research [5], about 40% of drivers drive at free speed over the allowed speed limit, and this percentage of speeding varies from location to location. It was concluded that the 60 km/h limit was not appropriate for most of the locations selected. In traffic and operational analyzes conducted on two-lane roads, unadjusted speed is one of key indicators of traffic accidents. The importance of the 85th percentile of speed is especially emphasized in the scientific literature since it is a representative speed for design analyses in a traffic flow of road network users [5–9].

Modern HCM (Highway Capacity Manual) methodology [10], depending on the speed limit, can classify all two-lane suburban roads into three classes. Based on the recommendations from HCM, in this research, it has been analyzed two-lane class II roads in Bosnia and Herzegovina, where the speed limit does not exceed 80 km/h. The assessment of the qualitative measure of the Level of Service (LOS) has not been analyzed as it is based on the determination of the percentage of time losses and not on the mean value of speed or deviation from the speed limit [10]. The German methodology HBS 2001 [11] mainly expresses the problem of the functional dependence of travel speed on traffic lane width. This method defines a minimum lane width of 2.75 m, while on some sections in Bosnia and Herzegovina, the lane width can be 2.50 m.

The main contribution of this paper is reflected in the formation of deterministic models for predicting the deviation of real speeds of different vehicle classes from speed limits as a function of longitudinal gradients (ascent and descent). This enables the consideration of speed limit credibility in local conditions on specific segments of sections, i.e., the adoption of adequate engineering measures in terms of setting a credible limit in order to harmonize speeds in traffic flow and improve traffic efficiency and safety.

Further in the paper, a review of relevant literature is presented. Subsequently, Section 2 presents the methodology required for data analysis and synthesis, with the limitation and selection of adequate sites for empirical research. In Section 3, the results are provided with multistep empirical models, deterministic graphical models, and comparison of research results with surveys in Serbia. In Sections 4 and 5, the discussion and conclusion of the paper are given.

2. Literature Review

Studies based on an analysis of individual drivers' attitudes and behaviors while driving can predict the level of compliance with speed limits including the perception of speed limit credibility and the perception of road risks [12]. The harmonization of the geometrical characteristics of the road with the expectations of drivers is performed according to their own perception of the road, and not according to the designer's perception (projected speed) [7]. In general, the geometry of the road, the characteristics of drivers, and weather conditions are important factors that influence the drivers' decision to adhere to the existing speed limit. However, the establishment of credible restrictions is possible only if the factors that affect drivers' compliance are identified [2, 13, 14]. Additionally, some studies show that a deviation from a speed limit for drivers is realistically acceptable if it is 10% higher than the speed limit on the roads [15, 16]. Lee et al. analyzed the average speed and standard deviation according to the speed limit using driving record data and confirmed the effect of reducing the average speed [17].

The main reason for exceeding speed limits, by some authors, refers to the credibility of set speed limits because drivers do not consider them realistic [18–20]. However, some authors have investigated the functional dependence of speed, length of individual geometric elements of the road, radius of curvature, transverse/longitudinal gradient, and traffic accidents [21–24]. Also, the research presents the problem of reducing speed due to the geometric characteristics of the road. The reduction in the speed of heavy-duty vehicles was specifically analyzed in the study [25], where a longitudinal gradient of 9.0% at 1.20 km of the road was taken into account, which significantly reduced the speed of heavy vehicles. According to this study, in order to increase speed due to influential road factors, the mass/power ratio must be improved [25]. Based on a report conducted in Texas [26], regression analysis identified that the following variables affect the prediction of traffic accidents: AADT (Annual Average Daily Traffic), lane width, shoulder width, and section length. The use of wider longitudinal markings on the road leads to a reduction in the speed of vehicles, and thus a reduction in the number of traffic accidents. The analysis of speed reduction in day and night driving conditions at average traffic load resulted in the following reduction of vehicle speed: by 2.24% in the day and by 1.96% at night for light vehicles, and 2.46% in the day and 2.15% at night for heavy vehicles [27]. In the analysis of the Bayesian network for predicting the probability of the influence of traffic and road factors on the occurrence of traffic accidents, the following are especially emphasized: vehicle speed, horizontal curve radius, vehicle type, adhesion coefficient, and longitudinal slope [23]. Also, the results of a study [24] show that the continuous use of several limit indexes and the excessive average slope of long and steep sections of roads were one of the major causes of frequent

accidents on a section of HeXi road in China. In their study, Silvano et al. assessed the impact of technical and exploitation characteristics of the road and changes in speed limits on the speed of free traffic flow using an extensive dataset of urban roads [28]. Based on a survey conducted in Poland, it was found that for a speed limit of 90 km/h in free traffic conditions, 38% of light vehicles exceed the speed limit during the day and 42% at night. For heavy vehicles with a limit of 70 km/h, speed limit exceeding of this class of vehicles in same traffic flow conditions is 83.5% in the day and 86% at night [29]. Research focused on the credibility of the 80 km/h speed limit of two-lane rural roads, where drivers verified the proposed speed for each of 27 road situations, which shows that there were large differences in drivers' attitudes for different road and environmental characteristics related to (non) compliance with the limits in given situations [16]. In addition, based on research in Malaysia, two experiments were conducted where photographs of a situation were presented to drivers, without a speed limit, based on which drivers chose speeds. The second experiment was based on the assessment of appropriate speed of drivers created according to a subjective attitude for a given situation. Experiments have concluded that there are limits within which drivers can modify their estimates of appropriate driving speed, based on speed limits [30]. According to a study [31] conducted in the UK, 30 mph (Urban Road) and 70 mph (Rural Motorway) limits were characterized as credible, 40 mph (Urban Motorway) as too slow, and 60 mph for a measuring rural location (Rural single carriageway) as a too high-speed limit. In our region, a study [32] was conducted in Serbia based on the examination of the value of speeds on highways and two-lane roads in a function of longitudinal gradient. Within this research, models of free traffic flow speeds as a function of longitudinal gradient were developed.

The research in Bogotá reduced the speed limit from 60 km/h to 50 km/h for 3 different periods starting from 2017 to 2019. The average speed reduction in the corridors with speed management was 1.48 km/h during daytime and 3.04 km/h during nighttime, and without speed management, the average speed reduction was 0.7 km/h during daytime and 2.2 km/h during nighttime. By reducing the speed limit, the average number of driving accidents was reduced by 10% [14]. Similar research was conducted in Boston where the speed limit was reduced from 30 mph to 25 mph. It was concluded that setting a speed limit of the 85th percentile of free flow speed can be a hurdle for local communities looking to lower speed limits [9]. By analyzing studies of posted speed limit (PSL) from 50 to 40 or 60 km = h, the results showed that a reduced PSL to 40 km/h was a significant reduction in the mean free-flow speed and speed variance, while an increased PSL to 60 km/h resulted in an increase in the mean free-flow speed, but without a change in speed variability. [33].

Also, the analysis of transport networks has established that during early morning hours with very light traffic, the impact of lowering speed limit was significant. During congested time periods, the travel speed reduction from lowering speed limit was not significant. [20].

Based on variable speed limit (VSL) research, it was shown that under medium and lower traffic density conditions, different VSL values can always reduce the mean traffic speeds and under similar traffic conditions, most VSL values reduced the speed differences between consecutive vehicles, thereby reducing the speed discretions in the traffic stream [34].

3. Research Methodology

Monitoring speeding is an integral part of speed management policy. However, setting speed limits on a road network does not mean compliance with it by drivers who exploit the road. The main goal of the research, which is based on the examination of speeding on sections of two-lane roads, is given in this section of the paper. Within the methodology, measuring sections were selected, the values of speed deviations from speed limits were determined, and then the necessary analysis and synthesis of collected data were carried out. The hypothetical framework of this research is based on the assumption that with increasing the longitudinal gradient (ascent/descent) in real conditions, the deviation of traffic flow speed values from the speed limit increases. This statement is based on all classes of vehicles, Passenger Vehicles (PV), Light Duty Vehicles (LDV), Heavy Duty Vehicles (HDV), Buses (BUS), and depends on a large number of influencing environmental factors. Also, in accordance with the hypothetical framework, the research [4] has shown that with increasing a slope (ascent/descent) increases the deviation of speeds beyond the speed limits, which also applies to the level of stress. Credible speed deviation from the speed limit implies a credible deviation if it corresponds to road and environmental conditions and if most drivers comply with it as a deviation. If road and environment conditions are not in accordance with the speed limit (favorable technical and exploitation characteristics of the road, and low speed limit), it cannot be considered credible. Relevant literature for the analysis of the values of credible speed deviation from the speed limit provides quite contradictory views, so that the deviation values are verified from values where there is no deviation from the speed limit to extreme values of deviation [5, 28, 35].

In this paper, we conducted a survey on eight measuring sections (11 cross-sections–S_1–S_{11}) in order to define the values of credible deviation from the speed limit on two-lane class I roads on the basis of a reference sample, and in a form of a recommendation. The use of the model for calculating a credible deviation from the speed limit is based on deterministic mathematical modeling, with the aim of adapting the model to real road conditions in Bosnia and Herzegovina. Research methodology and techniques, site selection, and data processing methods are given in Table 1 and were used by the following criteria:

Determining a credible deviation involves classifying vehicles (PV, BUS, LDV, and HDV) on 11 sections as a function of longitudinal gradient (ascent/descent). At each measuring section given in Table 2, it was determined by empirical research that more than 65% of vehicles exceed the

Table 1: Criteria for obtaining the values of a credible deviation from the speed limit.

Applied methodology	The basic method of defining credible speed deviation from the speed limit ($\Delta V = V_{real} - V_{lim}$), observation of four classes of vehicles and their grouping (PV, BUS, LDV, and HDV)
Recording technique	Using a special measuring device (handheld radar) bushnell NSN 5840-01-620–6670
Site selection	Road class: Standard two-lane roads (class I highway)—two-lane class II roads (according to HCM-2016) [10] Traffic lane width: from 2.75 m to 3.5 m Distance from side disturbances: <2.50 m Access density (on one side): <13 access points/km Terrain: flat or hilly suburban road Speed limit: 50–80 km/h Free flow speed: speed limit + 10–20 km/h Overtaking lane length (if any): location specific Road condition: good condition Longitudinal gradient: $-5.70 \le G \le 7.00$ Length of measuring section from a cross section: min 1000 m Traffic light intersection: none There is no impact of pedestrian flows
General information on traffic requirements	Traffic criteria: medium traffic load; higher percentage of commercial vehicles (15 and more); relevant flow according to the 200th hour criterion ≤12% AADT; percentage of traffic requests by directions: 60/40; lack of influence of parking or bus stops, recording in a peak and nonpeak period
Data processing	Based on the average values of individual locations and the summary average values, the values of speeds that do not exceed the speed limit are ignored in the analysis.

Table 2: Percentage of speeding as a function of difference between free and speed limit.

Two-lane road section		Section mark	Section length	Ascent/descent at 1000 m in %	AADT 2017 (veh/day)	V_{fr} (km/h)	Speed limit vlim (km/h)	% Speeding
S_1	Klupe–Teslić	M-I-108	16.734	−5.700	6498	**63**	**50**	90.12
S_2	Klupe–Teslić	M-I-108	16.734	−4.060	6498	**66**	**50**	89.42
S_3	Klupe–Teslić	M-I-108	16.734	−3.000	6498	**61**	**50**	80.91
S_4	Maglaj–Ozimica	M-I-110	10.520	−2.760	10086	**82**	**70**	87.00
S_5	Maglaj–Ozimica	M-I-110	10.520	−1.700	10086	**90**	**80**	67.42
S_6	Maglaj–Ozimica	M-I-110	10.520	−1.350	10086	**79**	**70**	75.37
S_7	Šepak–Karakaj 3	M-I-115	20.950	1.000	6408	**69**	**50**	65.28
S_8	Teslić–Klupe	M-I-108	16.734	3.000	6498	**60**	**50**	75.98
S_9	Teslić–Klupe	M-I-108	16.734	4.060	6498	**71**	**50**	93.40
S_{10}	Teslić–Klupe	M-I-108	16.734	5.700	6498	**64**	**50**	86.34
S_{11}	Border (RS/FBIH)–Donje Caparede	M-I-110	3.140	7.000	4305	**64**	**50**	73.22

speed limit on selected measuring sections of two-lane roads. Also, based on the insight into the database on traffic flows of PE "Roads of RS" and PE "Roads of BiH" for 2017, the section of the two-lane road M-I-108 shows a representative value of hourly load $q_{m200} = 545$ (veh/h), which is 8.38% of AADT. The shortest section M-110 Border (RS/BIH)—Donje Caparde has a low value of hourly load $q_{m200} = 346$ (veh/h), which is 8.03% of AADT.

Determining the deviation from the speed limit selected according to vehicle classes appearing on the measuring sections implies the calculation according to the following equation:

$$\Delta V = V - V_{\lim}\left(\frac{\text{km}}{\text{h}}\right), \tag{1}$$

where V is the measured vehicle speed, $V_{\lim}$ is the speed limit on a measuring section.

The speed limits that were analyzed are also the most common limits set on class I highways in Bosnia and Herzegovina (50 km/h, 70 km/h, and 80 km/h). It is assumed that the values of the speed deviation from the speed limit on an ascent/descent range from 10 km/h to 20 km/h, so a speed class range of 2 km/h was adopted for data synthesis.

Also, when measuring speeds and determining speed deviations from the limited value, it is necessary to identify the characteristics of the basic population based on the sample. The probability that the sample represents the basic population depends on the errors made during data collection and the size of the sample. Errors most often occur due to imperfections in the measuring equipment, sampling methods, or accidently. Sampling errors increase due to recording only a part of a traffic flow (unrepresentative). Using a larger sample reduces the possibility that the characteristics of the sample may differ from the characteristics of the population. By analyzing the deviation of real speeds from the speed limit, the distribution was approximated by a Gaussian distribution, which is symmetric with respect to the mean and asymptotically approaches the ordinate axis.

Table 3: K and U values for a certain level of reliability.

Level of reliability (%)	K	ΔV values in percentage	U
90.0	1.65	50%	0.00
95.0	1.96	15% or 85%	1.04

Table 4: Necessary and sufficient sample size.

The sample size for the acceptable deviation value $e = 1$ (km/h)								
Reliability level (%)	K	U	Standard deviation σ (km/h)					
			2	4	6	8	10	12
90	1.65	0.00	11	44	98	174	272	392
95	1.96	1.04	24	95	213	379	592	852

By analyzing the sample size for the required level of accuracy and reliability, its values from a general form were determined:

$$n = \frac{K^2 \cdot \sigma^2 \cdot \left(2 + U^2\right)}{2 \cdot e^2} (-), \quad (2)$$

where σ is the standard deviation of the sample, K is the number of standard deviations around the mean of normal distribution, $e$is the acceptable deviation limit, and U is the coefficient for a certain level of reliability.

The coefficient U for the percentage speed is given in Table 3 for 15%, 50%, and 85%.

If the standard deviation value of $\sigma = 2$, 4, 6, 8, 10, and 12 km/h is specified, and the limit value of acceptable error $e = 1$ km/h, the value of the sample size given in the following Table 4 is determined for the reliability levels.

3.1. Limits and Research Site Selection. In this paper, measurements were performed in real road and environmental conditions, using a speed measuring device (Bushnell NSN 5840-01-620–6670). Measurement of speeds in free traffic flow was performed by the "local measurement method," on the basis of which the synthesis of the mentioned data was started. The local measurement method implies that the free flow speed of the vehicle is measured on the cross section of the observed section of road over a length of 1000 m. On the observed cross section of the measuring section of the road, the free flow speeds of the vehicles moving towards the cross section were measured. The measured speed values were entered into the database. The research was conducted in daily driving conditions, under optimum weather conditions (there was no snow, rain, fog, or reduced visibility). The research excludes public transport vehicles, special vehicles, fire trucks, and similar vehicles for other purposes. The research was conducted in May, June, and July, 2021 on selected measuring sections, and the empirical measurement was performed on relevant working days from 8 a.m. to 8 p.m. A longitudinal gradient (ascent/descent) on measuring section length of 1000 m was identified by determining the arithmetic mean (based on the database of public enterprises Roads of Republic of Srpska and Roads of Bosnia and Herzegovina) of values of longitudinal gradients of a given section, which were measured every 200 m. The measuring

Figure 1: Position of measuring sections (S_1–S_{11}).

cross section is placed at the end of the measuring section with a length of 1000 m, and with a determined ascent/decent. These locations can be considered representative in order to obtain adequate data. It is also important that when doing measurements on measuring sections of two-lane roads, on all longitudinal gradients (ascent/descent) and on flat terrain, there is no lane for slow driving. Figure 1 shows the locations of the marked measuring sections (S_1–S_{11}) on the road map in Bosnia and Herzegovina.

Measuring points on two-lane roads were selected on the sections of the main roads Klupe–Teslić M-I-108, Border (RS/BiH)–Donje Caparde M-I-110, Šepak–Karakaj M-I-115, and on the section of the main road M-I-110, Maglaj–Ozimica.

Before starting the analysis of the credible speed deviation from the speed limit, it is necessary to determine the structure of the traffic flow on the mentioned measuring sections. The analysis includes four classes of vehicles, with Table 5 showing commercial vehicles (CV), i.e. vehicles other than passenger vehicles (BUS + LDV + HDV).

This structure of traffic flow on the analyzed road network S_1–S_{11} makes approximately 80% of passenger vehicles and 20% of commercial vehicles. From Table 3, it can be concluded that this heterogeneous structure of traffic flow has a relatively low value of AADT on section S_{11}, and over 10,000 veh/day on sections S_4, S_5, and S_6.

4. Synthesis and Analysis of the Research Results

Empirical measurement on the measuring sections was performed using a handheld radar Bushnell NSN 5840-01-620–6670, and data entry and processing was performed on a notebook computer Intel Pentium Dual CPU 2.16 GHz 2 GB. Based on empirically measured values of speeds classified in 5 classes, the values of deviations were obtained from speed limits, which were further processed in Microsoft Office Excel

Table 5: Determined value of measuring sample according to vehicle classes.

Two-lane road section		Section mark	Section length (km)	Ascent/descent at 1000 m in %	Size of measuring sample by speed deviation classes (% error ± 2.0%)					
					PV	BUS	LDV	HDV	CV	Σ all vehicles
S_1	Klupe–Teslić	M-I-108	16.734	−5.70	1805	100	145	75	320	2125
S_2	Klupe–Teslić	M-I-108	16.734	−4.06	1763	47	53	87	187	1950
S_3	Klupe–Teslić	M-I-108	16.734	−3.00	1497	75	98	108	281	1778
S_4	Maglaj–Ozimica	M-I-110	10.520	−2.76	588	84	133	105	322	910
S_5	Maglaj–Ozimica	M-I-110	10.520	−1.70	530	171	121	89	381	911
S_6	Maglaj–Ozimica	M-I-110	10.520	−1.35	415	97	141	105	343	758
S_7	Šepak–Karakaj 3	M-I-115	20.950	1.00	735	106	171	103	380	1115
S_8	Teslić–Klupe	M-I-108	16.734	3.00	1428	58	92	91	241	1669
S_9	Teslić–Klupe	M-I-108	16.734	4.06	1746	79	98	137	314	2060
S_{10}	Teslić–Klupe	M-I-108	16.734	5.70	1691	77	105	92	274	1965
S_{11}	Border (RS/FBIH)–Donje Caparede	M-I-110	3.140	7.00	782	84	104	77	265	1047
TOTAL					12980	978	1261	1069	3308	16288

in accordance with (1), after which further statistical processing was performed.

In the conducted empirical research, the values of speeds for 4 classes of vehicles were measured, and the measured speed values where there is no exceeding of the allowed speed were rejected from the research. By extracting only the exceeded speeds in relation to the traffic flow, it was analyzed the sample size of exceeded speeds, which is greater than 65% of the measured speeds on all measuring sections (Table 2). For each category of vehicles, the values of the arithmetic mean (AM) of speed value deviation from the speed limit, standard deviation (SD), and the coefficient of variation (Cv) were determined on the measuring sections of two-lane roads. The classification of obtained values was performed with a class width of 2 km/h. By classifying, it was obtained the distribution of speed deviation values for each vehicle category (PV, BUS, LDV, and HDV). Tabular data were used for further statistical analysis and definition of adequate distribution of obtained values. Also, tabular data were used to determine $\Delta V_{15\%}$, $\Delta V_{50\%}$, and $\Delta V_{85\%}$ percentile values, using statistical software Table Curve 2D v5.01. Empirically and tabularly obtained values of AM, SD, and Cv were used for the purpose of developing deterministic mathematical models for determining the deviation of free flow speed from the speed limit as a function of longitudinal gradient (ascent/descent). The research in this study was conducted during periods of low traffic (up to a two-way flow of 200 km/h), and the speed measurement of all vehicles was carried out in free-flow conditions on every tenth vehicle, arbitrarily.

Statistical research of the obtained values at the cross sections of the measuring sections was tested by the Gaussian (normal) distribution. Based on statistical analysis, tabularly obtained values of the deviation from the speed limit according to the class layout shows the distribution by Gaussian distribution with an adequate correlation coefficient ($R2 > 0.50$), which is given in Figure 2. The assumption is that the empirical distribution of speed deviation values in the case of a sufficiently large statistical sample for given vehicle classes can be theoretically approximated by the normal distribution (although this was not relevant to the scope of this study). Also, it was determined the values of cumulative relative frequency, which in all cases can be approximated by the cumulative Gaussian distribution (Figure 3).

By obtaining the values of the empirical arithmetic mean (AM) for each cross section of measuring sections for all predicted vehicle classes, it was started the development of multistep mathematical models. Also, the values of standard deviation (SD) were determined, where it was shown that all coefficients of variation (Cv) for the given cross-sections were less than 0.50. The models were developed with the aim of obtaining the functional dependence of the credible speed deviation of certain vehicle classes (PV, LDV, HDV, and BUS) on the longitudinal gradient (ascent/descent) of two-lane roads.

The general form of the multistep model is given in the following form:

$$\Delta V = A + B \cdot G^{\pm 1} + C \cdot G^{\pm 2} + \cdots + X \cdot G^{\pm n}, \tag{3}$$

where A, B, C, …. X is the regression curve coefficients rounded to three decimal places, G is the longitudinal gradient [%] (ascent/descent).

Based on the previously given equation, empirical mathematical models have been developed to determine the functional dependence of the credible speed deviation on the longitudinal gradient. The models are given in a form of higher degree polynomials in Table 6. The precision and high accuracy of the models according to vehicle classes (PV, LDV, HDV, and BUS) processed are confirmed by high coefficients of correlated speed dependence on a longitudinal gradient ($R^2 > 0.8$).

It is especially important to point out that for the PV class for empirically measured speeds, deviations from the speed limit range from the lowest value of the deviation from the speed limit for $G = +3.00\%$, which is 9.743 km/h, to the deviation value for $G = +1.00\%$, which is 22.490 km/h. The

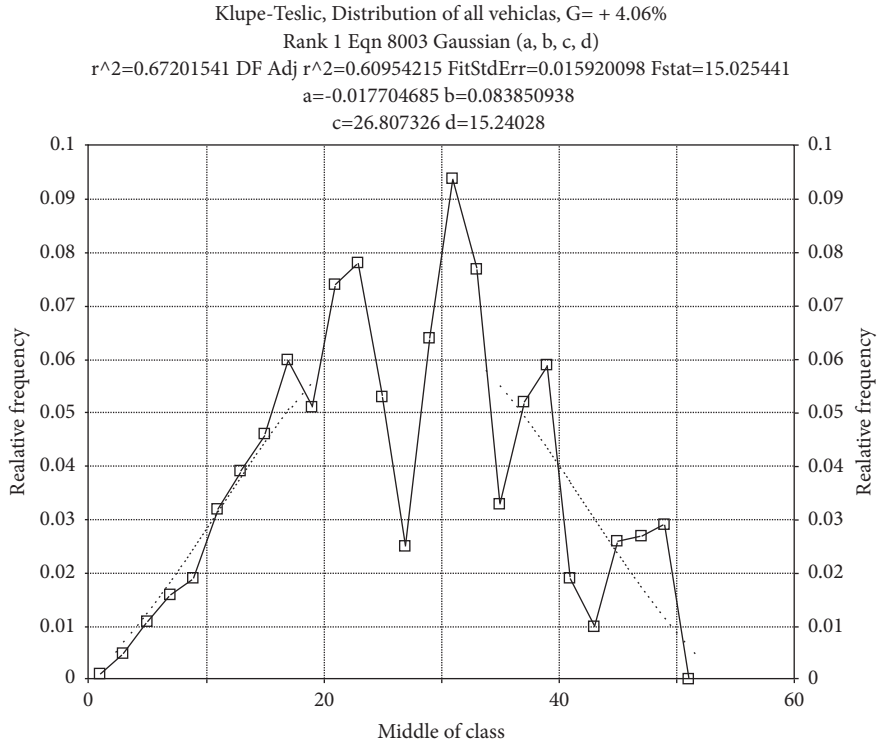

Figure 2: Example of relative frequency of obtained values of speed deviation from the speed limit for all vehicles in traffic flow.

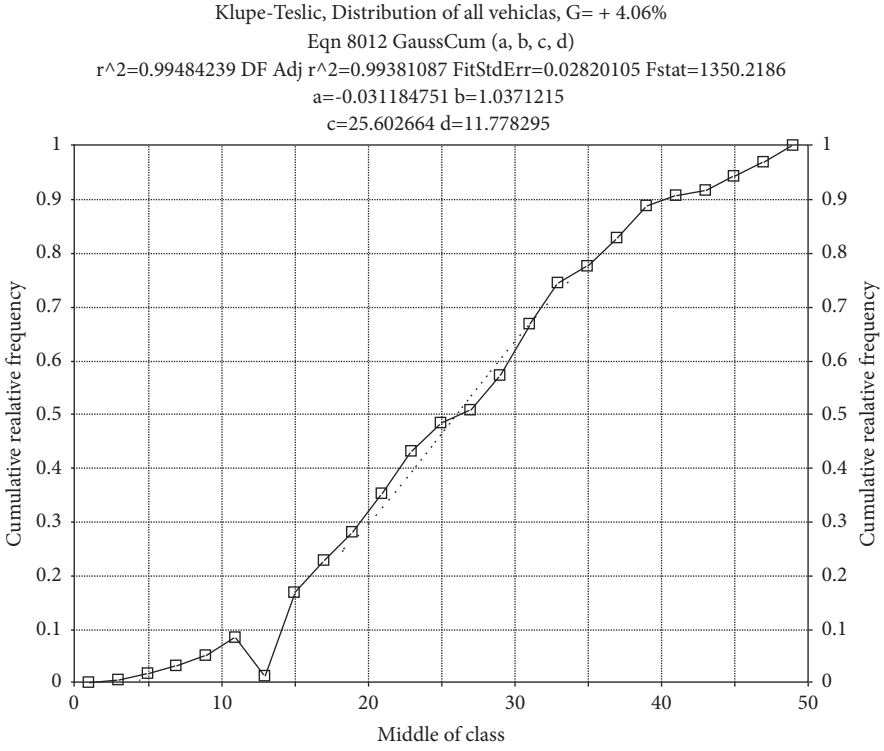

Figure 3: Example of cumulative relative frequency of obtained values of speed deviation from the speed limit for all vehicles in traffic flow.

deviation for PV is balanced on flat terrain, but progressively increasing on the descent. This shows a large dispersion of speeds on individual measuring sections for PV. For LDV, the dispersion of speed deviations towards the longitudinal gradient is slightly lower than that for PV and ranges from $7.417\ \text{km/h} \leq \Delta V \leq 15.316\ \text{km/h}$. The highest deviation from the speed limit on the ascent for PV occurs on the measuring section of a gradient $G = +4.06\%$. Significantly lower

Table 6: Empirical mathematical models of functional speed deviation dependence on a longitudinal gradient.

Vehicle category: PV $\Delta V = 14.845 + 18.524.G - 119.496.G^{-1} + 1.16.G^{2} - 124.945.G^{-2} - 0.866.G^{3} + 104.888.G^{-3} - 0.03.G^{4} + 128.398.G^{-4} + 0.012.G^{5}$ (km/h)	Correlation coefficient: $R^2 = 0.997$
Vehicle category: BUS $\Delta V = 28.118 + 7.292.G - 47.413.G^{-1} - 0.602.G^{2} - 127.083.G^{-2} - 0.325.G^{3} + 29.764.G^{-3} + 0.005.G^{4} + 119.38.G^{-4} + 0.004.G^{5}$ (km/h)	Correlation coefficient: $R^2 = 0.995$
Vehicle category: LDV $\Delta V = 29.12 + 22.622.G^{2} + 7.664.G^{4} - 1.053.G^{6} + 0.064.G^{8} - 0.002.G^{10}$ (km/h)	Correlation coefficient: $R^2 = 0.834$
Vehicle category: HDV $\Delta V = 7.515 + 3.472.G + 1.784.G^{2} - 1.571.G^{3} - 0.513.G^{4} + 0.202.G^{5} + 0.038.G^{6} - 0.01.G^{7} - 0.001.G^{8}$ (km/h)	Correlation coefficient: $R^2 = 0.928$

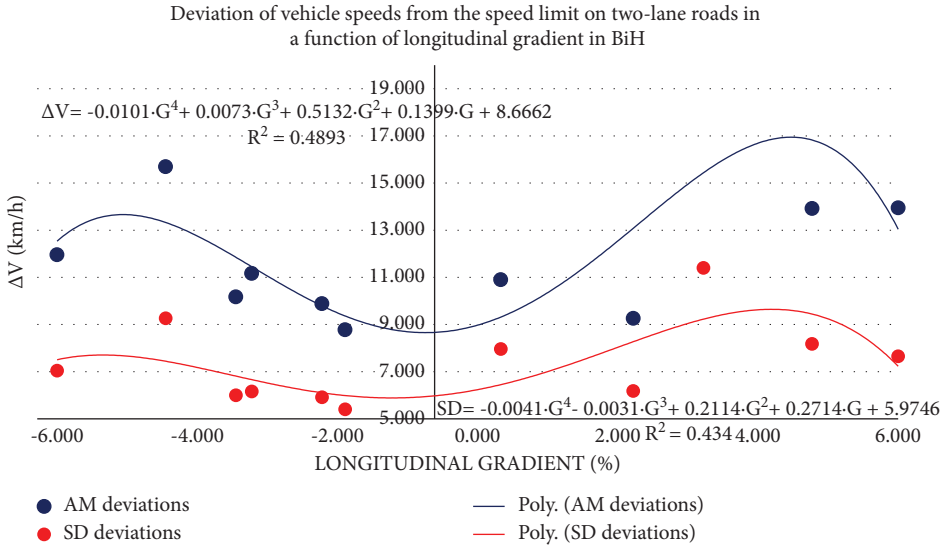

Figure 4: Deviation of traffic flow speeds as a function of longitudinal gradient.

dispersion occurs for BUS and in the functional dependence on the longitudinal gradient, it ranges from 7.143 km/h ≤ ΔV ≤ 13.250 km/h. Also, for BUS, the largest scattering of speed deviations from the speed limit is for $G = +4.06\%$. If it is taken the deviation for HDV, the smallest deviation is with the largest longitudinal gradient $G = +7.00\%$ and it is 3.467, and deviations over 10 km/h occur on flat terrain and downhill for this class of vehicles. Such an unbalanced trend of scattering of speeds that deviate from the speed limit on selected measuring sections can be justified by the characteristics of the terrain, driving and dynamic characteristics of vehicles, psychophysical abilities of drivers, and technical and exploitation characteristics of the two-lane roads. Due to these influencing factors, AM and SD values of speed deviations were identified for the mentioned measuring sections, with the aim of obtaining adequate statistical regressivity.

Figure 4 shows a graphical generalization of the model for determining a credible speed deviation from the speed limit in a form of a fourth-degree polynomial, but for all vehicle classes on the measuring sections of two-lane roads. By calibrating the model for all vehicle classes, two extreme values of speed deviation from the speed limit can be noticed, one lower on the descent and one higher on the ascent. The correlation coefficient $R^2 \approx 0.50$ shows that the arithmetic means of speed value deviation from the speed limit vary from one measuring section to another measuring section, so the fourth-degree polynomial was used as an instrument to simplify the model.

Considering that in the previous model in Figure 4, only speeds deviating from the speed limit were analyzed and that the AM and SD of the stated deviations on the measuring sections are shown; based on the proposed model, there is the smallest speed deviation for all classes of vehicles on flat terrain $G = 0 \pm 1.00\%$, where this value does not exceed 10 km/h. The analysis of the model on class I roads in Bosnia and Herzegovina, and the review of the previously calibrated model shows the apparent conclusion that the deviation of the flow speed from the speed limit increases on the ascent and descent for all classes of vehicles, but it must be taken into account all 4 previously mentioned vehicle classes (PV, LDV, HDV, and BUS).

Also, in order to obtain more precise values of the previously mentioned model, it was further developed a calibrated model for $\Delta V_{15\%}$, $\Delta V_{50\%}$, and $\Delta V_{85\%}$, as a function of longitudinal gradient. Deviations of values on measuring sections by 15%, 50%, and 85% of speed deviations from the limit value are more than 10 km/h, which can be seen according to the model in Figure 5. For analytical generalization of the model for the values of speed deviation from the speed limit for all vehicle classes by 15%, 50%, and 85%, analytically developed mathematical models given in Table 7 were obtained.

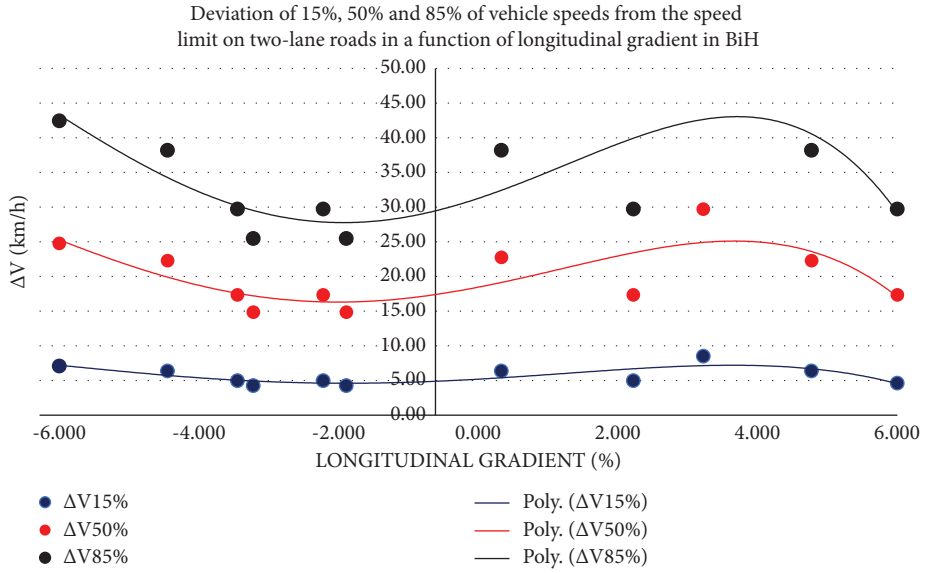

Figure 5: ΔV 15%, 50%, and 85% as a function of longitudinal gradient.

Table 7: Analytical model of 15%, 50%, and 85% speed deviations from the speed limit on two-lane roads in BiH.

15% deviation of values ΔV $\Delta V_{15\%} = -0.002.G^4 - 0.014.G^3 + 0.126.G^2 + 0.397.G + 4.884$ (km/h)	Correlation coefficient: $R^2 = 0.614$
50% deviation of values ΔV $\Delta V_{50\%} = -0.006.G^4 - 0.048.G^3 + 0.394.G^2 + 1.403.G + 17.391$ (km/h)	Correlation coefficient: $R^2 = 0.586$
85% deviation of values ΔV $\Delta V_{85\%} = -0.010.G^4 - 0.079.G^3 + 0.712.G^2 + 2.341.G + 29.462$ (km/h)	Correlation coefficient: $R^2 = 0.596$

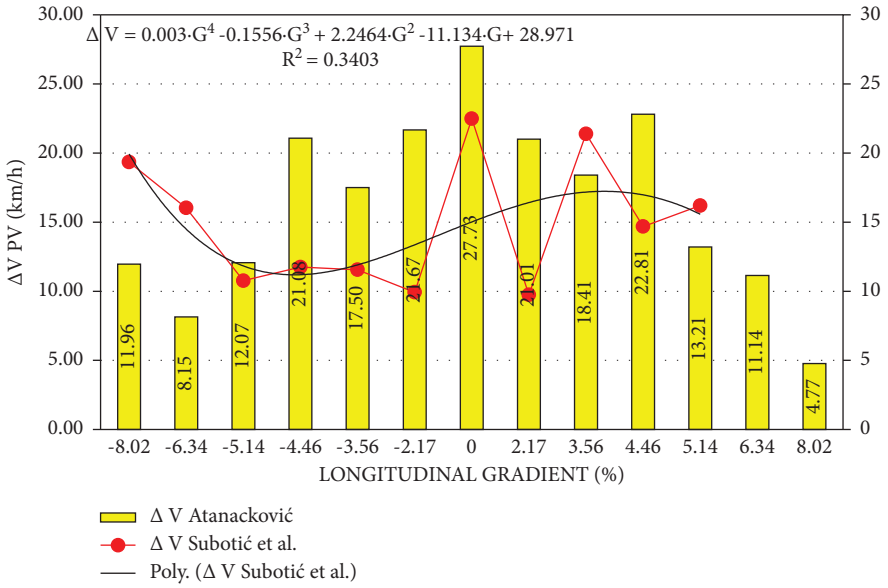

Figure 6: Comparative overview of ΔV for PV in Serbia (ΔV Atanacković) and BiH (ΔV Subotić et al.).

Since analytically developed mathematical models are given in Table 7, Figure 5 shows deterministic models for the deviation of traffic flow speed from the speed limit by ΔV 15, 50, and 85 percentiles as a function of longitudinal gradient. These values show a significant scattering of the deviation values by 85 percentiles and minimum by 15 percentiles.

Figures 6 and 7 compare the empirically obtained ΔV values for passenger vehicles and commercial vehicles obtained on the basis of research conducted in Bosnia and Herzegovina (Subotić et al.) and Serbia (Atanacković). Also, the research conducted in Serbia [32] was given with a speed limit, so that on the suburban sections of two-lane roads, where a speed limit of 70 km/h is provided, the value of AM

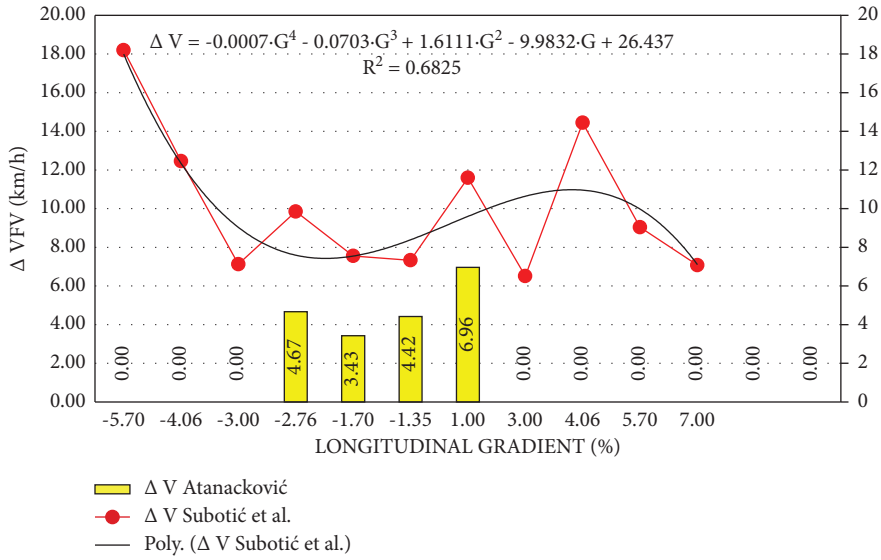

Figure 7: Comparative overview of ΔV for freight vehicles in Serbia (ΔV Atanacković) and BiH (ΔV Subotić et al.).

speed for the specified measuring sections was determined. Based on (1), the values of speed deviations from speed limits for the entire free traffic flow on two-lane roads in Serbia were determined. In this case, not only the speeds that deviated from the limited value were singled out, as is the case with this research, but also the focus of the observation refers to the entire flow. Considering that both surveys were conducted in the conditions of free traffic flow, it is possible to compare the obtained values and give an adequate conclusion in accordance with the speed limits provided.

Research studies with deviations from the speed limit in Serbia (ΔV Atanacković) were measured on cross sections of measuring sections Rudnik II–Ljig (±8.02%), Rudnik I–Gornji Milanovac (±6.34%), Borova Glava–Uvac (±5.14%), Rušanj III (±4.46%), Rušanj II (±3.56), Orlovača (±2.17), and Pančevo–Vršac (0.00%). Research studies with deviation from the speed limit in Bosnia and Herzegovina (ΔV Subotić et al.) were measured on cross sections of measuring sections Granica (RS/FBIH)–Donje Caparede (+7.00%), Klupe–Teslić (±5.70%, ±4.06%, ±3.00%), Maglaj –Ozimica (−2.76%, −1.70% *i* −1.35%), and Šepak–Karakaj 3 (+1.00%).

Figure 6 shows the values of AM speed deviations from the speed limit, towards the longitudinal gradients for PV for studies conducted in Serbia and Bosnia and Herzegovina. For PV, it is evident that the values of ΔV deviate significantly in Serbia, compared to BiH, if the values of $-5.0\% \geq G \geq 5.0\%$ are observed. These deviations would be significantly higher if only the speed values of vehicles that were speeding were taken into account in Serbia, which was the case with the research in BiH. Also, the largest deviation from the speed limit in Serbia for PV is given for a gradient of 0% and it is over 25 km/h. Also, for the research conducted in BiH, there is a large scattering of ΔV values, which shows a low correlation coefficient, $R^2 = 0.34$.

However, Figure 7 shows the values of speed deviation from the speed limit, for the conditions of free flow in Serbia and BiH for all freight vehicles in a function of gradient. In this case, based on the research conducted in Serbia on the sample of measured speeds, it can be concluded that freight vehicles exceed the speed only on flat terrain and a slight descent. If we compare speeding in Serbia and BiH, for all measuring sections of the longitudinal gradient, ΔV is significantly higher in Bosnia and Herzegovina than in the survey conducted in Serbia. Also, on greater ascents and descents, in Serbia, no speeding was recorded in the category of freight vehicles, which is not the case in BiH. In this case, with the development of the fourth-grade model for freight vehicles in Bosnia and Herzegovina, there is a good correlation, $R^2 = 0.6825$, which is not the case with PV.

The deviations recorded in this way in Serbia, which do not exceed 7 km/h, deviate a lot from the results in BiH, but the fact that a small percentage of vehicles on the ascent and descent that exceed the speed limit must be taken into account. For the research conducted in Serbia, freight vehicles that do not exceed the speed limit were not eliminated from the sample, which is a significant limitation compared to this research.

5. Research Results and Discussion

A large number of studies of speed credibility refer to the analysis of meritorious influencing factors that contribute to the increase/decrease of exceeding the speed limit in real road and environmental conditions. In the previous literature review, it was noticed that one part of them is mainly based on the influential factors of road geometry, which includes the longitudinal gradient, and radii of curves. In order to determine the credible value of speed deviation from the speed limit, it is necessary to observe each measuring section separately because there are a large number of road factors, psychophysical abilities of drivers, and driving dynamics characteristics of vehicles that can be representatively influential.

In this paper, 11 measuring sections of main two-lane roads (S1-11) were analyzed, with the aim of determining a credible speed deviation of vehicles that exceed the speed limit as a function of longitudinal gradient. At the given measuring sections, it was determined that the speed limit is exceeded by over 65% of vehicles, and at certain sections ≈95%. By analyzing the speeding, on the basis of empirical measurements, it was determined that the highest speeding occurs for PV, where the average value of AM for ΔV in all measuring sections is 14.898 km/h (≈15 km/h). The lowest value of AM for ΔV on all measuring sections was measured for HDV and is 8.585 km/h (≈9 km/h), while this value for BUS (9.785 km/h) and LDV (10.201 km/h) is ≈10 km/*h*.

Since a credible limit is also an eligible speed limit, it can be represented by the perception of drivers according to road and traffic conditions prevailing on homogeneous road sections, which allow drivers to move at higher speeds. It is the reason why it would be necessary to reconsider the set speed limit on certain measuring sections. By analyzing the previous values of speed deviations from the speed limit on 11 measuring sections (S1-11), it is obtained the values that can be recommended for a credible speed deviation of 10 km/h on two-lane roads in BiH, regardless of the longitudinal gradient.

Based on the synthesis of the obtained data, multistep deterministic mathematical models of the functional dependence on the longitudinal gradient have been developed. Furthermore, in order to generalize the model, a general model was developed for all vehicles, where deviations of ΔV values are shown as two extremes, which occur at the value of $G = \pm 5\%$. Based on the general multistep model calibrated by the fourth-degree polynomial, ΔV 15%, 50%, and 85% models were developed. The deviations between these three models for ΔV are greater than 10 km/h for all measuring sections, and with increasing a percentile value, the scattering of deviations for ΔV increases. Also, at 85% of the percentile value ΔV, the largest scattering of the deviation value was obtained.

Studies [15, 16] have concluded that the credible deviation of real from limited speeds is 10%. Comparing these conclusions with the obtained research results, which determined a deviation of 10 km/h, it can be seen that the threshold of credible deviation obtained in this paper is much more tolerant.

Also, based on the research [5], where it was found that 40% of drivers exceed the speed limit; in this study, this percentage is significantly higher (>65%), but both studies have in common that the percentage of speeding varies on measuring sections. However, it is not possible to have equal limits of deviation, comparing both studies because the exploitation characteristics of sections in the conducted research are specific in relation to the mentioned research [5]. Also, the applied methodology in the research includes sections with ideal characteristics, and with a speed limit of 60 km/h. This is a significant methodological deviation in comparison with the research conducted in this paper.

By comparative analysis of the results obtained in this research and in Serbia [32], the deviation values of PV for ΔV in the Republic of Serbia are higher than in BiH. In Serbia, the analysis also includes PVs that do not exceed the limited speed. These deviations would be even bigger, if only speeding vehicles were singled out in Serbia. Contrary to the deviation for PV, significantly higher values of exceeding ΔV are obtained in BiH than in Serbia.

There are some other factors that influence the deviation from the speed limit. Shoulder width has a larger effect on speed when lanes are narrow, but the effect of shoulder width decreases as lane width increases. A plausible explanation is that a wider lane could be expected to allow a higher traveling speed. It is known that with the increase in the number of access points and no-passing zones, the speed of free flow decreases. However, these parameters were not investigated in this study.

6. Conclusion

The paper presents a detailed analysis of operating speed deviation of different vehicle classes from the speed limit, in a function of longitudinal gradient on two-lane roads of Bosnia and Herzegovina. Based on empirical research conducted on 11 cross sections of representative sections, it has been shown that the deviation depends on a number of factors. In most of the sections, a great compliance of all analyzed speeds has been determined, which indicates that these are measuring sections where the geometric characteristics and the environment of the road correspond to the class of the road.

The conducted research confirmed the hypothetical assumption that with an increase of the longitudinal gradient in real conditions, there is an increase in the deviation of the values of traffic flow speeds from the speed limit. Certainly, if it is taken into account the analysis of individual classes of vehicles in real traffic flow, it can be concluded that the increase in speed deviation increases with increasing the longitudinal descent, while the value of speed varies continuously with increasing the ascent.

Based on the developed models for the prediction of the deviation of operating speeds from the limited speeds as a function of longitudinal gradient, the values of credible deviation by 10 km/h from set limit values were obtained. The obtained values of exceeding the speed limit are closer to the values of the 85th percentile of deviations on the measuring sections, which confirms the validity of using the 85th percentile of measured speeds when determining speed limits in many countries [36] (TRB, 1998). Given the high deviations of speeds from set speed limits, the need for their review was detected. Namely, the highest deviations were recorded on sections with a limit of 50 km/h, where by increasing the speed limit by determined 10 km/h, the percentage of exceeding the speed limit would decrease significantly. This provided a greater degree of harmonization of vehicle speeds of different classes in traffic flow, which would increase efficiency and safety. The obtained results are in accordance with the results of a study [37] conducted by Solomon (1964), which has shown that exceeding the speed limit of 10 km/h leads to the lowest rate of traffic accidents.

Since the focus of the analysis in this paper was on longitudinal gradients, in future research, it is necessary to examine additional factors that have not been considered, such as the influence of transverse profile characteristics, horizontal curvature, vehicle characteristics, meteorological influences, and driver characteristics. Additionally, in order to obtain the most accurate data, in the coming period, it is necessary to conduct a detailed analysis of an even larger number of measuring sections. Continuous research of the values of speed deviations from the speed limit will provide representative criteria for project procedures for determining credible speed limits, with the aim of improving traffic conditions.

Data Availability

All data used to support the findings of the study are included within the paper..

Conflicts of Interest

The authors declare that they have no conflicts of interest.

References

[1] R. J. Porter, E. T. Donnell, and J. M. Mason, "Geometric design, speed, and safety," *Transportation Research Record: Journal of the Transportation Research Board*, vol. 2309, no. 1, pp. 39–47, 2012.

[2] A. Bornioli, I. Bray, P. Pilkington, and E. L. Bird, "The effectiveness of a 20 mph speed limit intervention on vehicle speeds in Bristol, UK: a non-randomised stepped wedge design," *Journal of Transport & Health*, vol. 11, pp. 47–55, 2018.

[3] G. F. Nightingale, A. J. Williams, R. F. Hunter et al., "Evaluating the citywide Edinburgh 20mph speed limit intervention effects on traffic speed and volume: a pre-post observational evaluation," *PLoS One*, vol. 16, no. 12, Article ID e0261383, 2021.

[4] J. Qiao, Y. Wen, N. Yang, and J. Song, "The research of two-lane highway longitudinal slope based on the running speed in the plateau areas," in *Proceedings of the International Conference on Consumer Electronics, Communications and Networks (CECNet)*, pp. 1827–1830, Xianning, China, April 2011.

[5] I. H. Hashim, "Analysis of speed characteristics for rural two-lane roads: a field study from Minoufiya Governorate, Egypt," *Ain Shams Engineering Journal*, vol. 2, no. 1, pp. 43–52, 2011.

[6] A. D'Andrea, F. Carbone, S. Salviera, and O. Pellegrino, "The most influential variables in the determination of V85 speed," *Procedia - Social and Behavioral Sciences*, vol. 53, pp. 633–644, 2012.

[7] P. Misaghi and Y. Hassan, "Modeling operating speed and speed differential on two-lane rural roads," *Journal of Transportation Engineering*, vol. 131, no. 6, pp. 408–418, 2005.

[8] J. McFadden and L. Elefteriadou, "Evaluating horizontal alignment design consistency of two-lane rural highways: development of new procedure," *Transportation Research Record: Journal of the Transportation Research Board*, vol. 1737, no. 1, pp. 9–17, 2000.

[9] W. Hu and J. B. Cicchino, "Lowering the speed limit from 30 mph to 25 mph in Boston: effects on vehicle speeds," *Injury Prevention*, vol. 26, Article ID 043025, 2019.

[10] Trb National Research Council, *Highway Capacity Manual 2016 (HCM 2016)*, TRB. National Research Council, Washington, DC, USA, 2016.

[11] Forschungsgesellschaft für Straßen- und Verkehrswesen, *Handbuch für die Bemessung von Straßenverkehrsanlagen (HBS) (German Highway Capacity Manual)*, Forschungsgesellschaft für Straßen- und Verkehrswesen, Köln, 2005.

[12] Y. Yao, O. Carsten, and D. Hibberd, "Predicting compliance with speed limits using speed limit credibility perception and risk perception data," *Transportation Research Record: Journal of the Transportation Research Board*, vol. 2674, no. 9, pp. 450–461, 2020.

[13] S. A. Gargoum, K. El-Basyouny, and A. Kim, "Towards setting credible speed limits: i," *Accident Analysis & Prevention*, vol. 95, pp. 138–148, 2016.

[14] J. S. López, D. Perez-Barbosa, N. Lleras, D. Hidalgo, and C. Adriazola-Steil, "Effects of reducing and enforcing speed limits in selected arterial roads in Bogota," *International Journal of Engineering, Social Justice, and Peace*, vol. 8, no. 2, pp. 50–71, 2021.

[15] J. Fleiter and B. Watson, "The speed paradox: the misalignment between driver attitudes and speeding behaviour," in *Proceedings of the Australasian Road Safety Research, Policing & Education Conference*, pp. 187–192, 2005.

[16] C. Goldenbeld and I. van Schagen, "The credibility of speed limits on 80km/h rural roads: the effects of road and person(ality) characteristics," *Accident Analysis & Prevention*, vol. 39, no. 6, pp. 1121–1130, 2007.

[17] W. Lee, N. Seong, and G. Park, "Analysis of Regulatory Speed Limit and Its' Effect," *Journal of the Korean Society of Safety Education*, vol. 5, pp. 5–16, 2002.

[18] B. N. Fildes and S. J. Lee, "The speed review: road environment, behaviour, speed limits, enforcement and crashes," Report CR127, Federal Office of Road Safety, Department of Transport and Communications, Canberra, Australia, 1993.

[19] I. N. L. G. Van Schagen, F. C. M. Wegman, and R. Roszbach, *Safe and Credible Speed Limits: A Strategical Exploration. R2004-12*, SWOV Institute for Road Safety Research, Leidschendam, 2004.

[20] S. Jang, S. Wu, D. Kim, K.-H. Song, S. M. Lee, and W. Suh, "Impact of lowering speed limit on urban transportation network," *Applied Sciences*, vol. 12, no. 11, 2022.

[21] L. Aarts and I. van Schagen, "Driving speed and the risk of road crashes: a review," *Accident Analysis & Prevention*, vol. 38, no. 2, pp. 215–224, 2006.

[22] I. Cruzado and E. T. Donnell, "Factors affecting driver speed choice along two-lane rural highway transition zones," *Journal of Transportation Engineering*, vol. 136, no. 8, pp. 755–764, 2010.

[23] G. Cheng, R. Cheng, Y. Pei, and L. Xu, "Probability of roadside accidents for curved sections on highways," *Mathematical Problems in Engineering*, vol. 2020, Article ID 9656434, 18 pages, 2020.

[24] Y. Zheng, H. Guo, and X. Wei, "The evaluation analysis of design code about the road design of longitudinal gradient in the mountain road," in *Proceedings of the 7th International Conference on Education, Management, Computer and Society (EMCS 2017)*, pp. 693–699, 2017.

[25] B. Srnová, "A case of road design in mountainous terrain with an evaluation of heavy vehicles performance," Technical University of Madrid, Spain, Degree of Master - Civil and Architectural Engineering, 2017.

[26] K. Fitzpatrick, H. William, I. Schneider, and E. S. Park, "Comparisons of crashes on rural two-lane and four-lane highways in Texas," FHWA/TX-06/0-4618-1, Report 0-4618-1, Texas Transportation Institute, Texas, TX, USA, 2005.

[27] F. Calvo-Poyo, J. de Oña, L. Garach Morcillo, and J. Navarro-Moreno, "Influence of wider longitudinal road markings on vehicle speeds in two-lane rural highways," *Sustainability*, vol. 12, no. 20, 2020.

[28] A. P. Silvano, H. N. Koutsopoulos, and H. Farah, "Free flow speed estimation: a probabilistic, latent approach. Impact of speed limit changes and road characteristics," *Transportation Research Part A: Policy and Practice*, vol. 138, pp. 283–298, 2020.

[29] A. Maczyński, K. Brzozowski, and A. Ryguła, "Analysis and prediction of vehicles speed in free-flow traffic," *Transport and Telecommunication Journal*, vol. 22, no. 3, pp. 266–277, 2021.

[30] Y. M. Lee, S. Y. Chong, K. Goonting, and E. Sheppard, "The effect of speed limit credibility on drivers' speed choice," *Transportation Research Part F: Traffic Psychology and Behaviour*, vol. 45, pp. 43–53, 2017.

[31] Y. Yao, O. Carsten, and D. Hibberd, "A close examination of speed limit credibility and compliance on UK roads," *IATSS Research*, vol. 44, 2019.

[32] Ž. Atanacković, *Prilog Utvrđivanju Slobodnih Brzina I Reprezentativnih Vozila U Saobraćajnom Toku U Procedurama Vrednovanja, Doktorska Disertacija*, Saobraćajni Fakultet Beograd, Serbia, 2008.

[33] A. P. Silvano and K. L. Bang, "Impact of speed limits and road characteristics on free-flow speed in urban areas," *Journal of Transportation Engineering*, vol. 142, no. 2, Article ID 04015039, 2016.

[34] X. Qu, M. Yang, J. Ji, L. Li, and B. Ran, "Analyzing the safety impacts of variable speed limit control on aggregated driving behavior based on traffic big data," *Journal of Advanced Transportation*, vol. 2021, Article ID 8823292, 9 pages, 2021.

[35] N. Van Nes, M. Houtenbos, and I. Van Schagen, "Improving speed behaviour: the potential of in-car speed assistance and speed limit credibility," *IET Intelligent Transport Systems*, vol. 2, no. 4, p. 323, 2008.

[36] Transportation Research Board National Research Council, *Managing Speed: Review of Current Practice for Setting and Enforcing Speed Limits*, Transportation Research Board. National Research Council, Washington, D.C., USA, 1998.

[37] D. Solomon, *Crashes on Main Rural Highways Related to Speed, Driver and Vehicle*, Bureau of Public Roads. U.S. Department of Commerce. United States Government Printing Office, Washington, D.C., USA, 1964.

Hindawi
Complexity
Volume 2022, Article ID 2961999, 13 pages
https://doi.org/10.1155/2022/2961999

WILEY | Hindawi

Research Article

Applications of Uncertainty Models as Support in Smart Buildings and Ethical Computing in Edge Computing of Smart Cities

Ying Li[1] **and Trip Huwan**[2]

[1]*Shanghai Urban Construction Vocational College, Shanghai 200438, China*
[2]*Research Center of Environmental Science and Engineering, Bishkek, Kyrgyzstan*

Correspondence should be addressed to Trip Huwan; dr.tribhuwan@mail.cu.edu.kg

Received 20 July 2022; Revised 15 September 2022; Accepted 21 September 2022; Published 3 October 2022

Academic Editor: Zeljko Stevic

In order to improve the effect of smart city construction, this paper combines smart buildings and ethical computing to conduct research on smart city edge computing. The new smart city architecture based on the flexible deployment of edge computing and data slicing capabilities provides support for the transformation of smart city construction from hardware embedded technology, access means, and software data processing. Moreover, this paper uses information technology to collect, process, analyze, use the information to achieve intelligence, and integrate resources and information of cities and people to build a smart city functional architecture. Moreover, this paper combines simulation technology for experimental research. Through experimental analysis, it can be seen that the smart city edge computing method based on smart buildings and ethical computing proposed in this paper has good results.

1. Introduction

The goal of the smart city is to link, integrate, and improve the internal systems and various services offered by the city, as well as to integrate these efforts with the city's building plans. It increases the pace at which different resources are allocated in the city, optimizes urban services and urban administration, advances the city to a higher level, and raises the standard of living and productivity for city residents [1]. The newest addition to the digital city is the smart city. The Internet of Things, cloud computing, and wireless mobility are the key representations of the new information technology generation that gives rise to the digital city. Based on digital cities, smart cities have the potential to connect things to other things, perceive each other, and use high-level information in ways that benefit both people and people. People, the Internet, and Things are widely and profoundly interconnected, coexisting, and interacting thanks to the network's ubiquity, the vast processing of information and data (cloud storage, cloud computing), and the integration of the Internet of Things and the Internet [2].

This allows all aspects of the world to achieve a more thorough perception, wider interconnection, and deeper intelligence. Different angles can be taken to examine the growth of smart cities. Technology-wise, smart cities should build their infrastructure using cutting-edge information technologies like the Internet, cloud computing, and big data in order to achieve urban connectedness and coverage. From the standpoint of social development, smart cities use social networks, mass media, and other modern tools and applications to facilitate communication between residents and the city, realize innovative development, and foster the sustainable and creative growth of the economic, cultural, technological, and spiritual societies. A smart city encompasses technology, industry, application, service, government, humanities, living, etc. as its content. The application of wisdom, which addresses the four major facets of food, clothing, housing, and transportation, is most closely related to people's lives and primarily reflects changes in agriculture, food, medical care, transportation, schools, communities, agriculture, enterprises, and governments [3].

The creation of smart cities has emerged as a new model and choice for contemporary city construction thanks to the advancement and support of cutting-edge technologies like big data, the Internet of Things, and artificial intelligence. Governments at all levels, businesses, and individuals have adopted the idea of smart cities and tried to integrate new Internet-based technology in order to improve living conditions and preserve the environment in the face of increasingly serious urban problems. The need for a new model of contemporary urban development has prompted the emergence of smart cities. One of the key trends and features of urban development is the improvement of urban governance and innovation. It is also a cutting-edge theory and area of research for furthering the optimization of urban organizational structure and the urban informatization process. In the modern day, improving urban intelligence is essential for urban growth since it improves people's quality of life and positions oneself to take advantage of fresh prospects for urban development.

This article combines smart buildings and ethical computing to study the edge computing of smart cities, which provides a theoretical reference for the construction and development of smart cities.

2. Related Work

Kocakaya [4] believes that smart urban management is a new urban management model supported by a new generation of information technology and a knowledge society innovation 2.0 environment. Through the support of a new generation of information technology, it can achieve comprehensive and thorough perception, broadband ubiquitous interconnection, intelligent integration applications, and promote people-oriented sustainable innovation characterized by user innovation, open innovation, mass innovation, and collaborative innovation. Smart urban management is an evolution of digital urban management to deal with increasingly complex urban governance issues [5]. To realize the intelligent transformation from digital urban management, Ustinovičius et al. [6] propose to establish a complete urban information database, based on 5G, Internet of Things, City Information Model (CIM), and other technologies, combined with the already relatively complete urban management in digital urban management Component information, urban management industry data, related industry applications, and public appeal data form a city information database that can comprehensively portray city portraits. Fadeyi [7] summarized a set of methodologies that can process urban information data. A complete city information database must have the characteristics of big data, that is, the amount of data is huge, the types are various, the value density is low, and the data speed is fast. Mandičák et al. [8] pointed out: should pay attention to the overall data thinking, tolerate the confounding of data, pay more attention to correlation rather than causality, and so on. The ideal big data methodology should be able to complete the analysis and processing of massive data in accordance with established requirements and also provide reference data support for unspecified requirements. Ustinovichius et al. [9] construct an information framework that can be iteratively upgraded. Data only provides evidence to solve the problem, but cannot really solve the actual problem. The treatment of urban issues should also be under an information framework. This requires a standardized deconstruction of the problems that the city urgently needs to solve and the resources of all parties involved in urban governance and provides optimal solutions through algorithms. Then what we need to do is to continuously optimize iteratively. Wei and Chen [10] created a set of management systems to reduce internal management consumption so that different subjects are no longer single vertical command management, but horizontal multidimensional cooperation, coordination, and information exchange.

Smart cities are considered to be a complex ecosystem with the potential to improve the livability, workability, and sustainability of cities through human, process, and data networks [11]. Clarifying the meaning of "smart" in the urban context, determining the main dimensions and elements of smart cities, and comparing different measurement standards of smart cities are the basic conditions for the development of smart cities [12]. Smart city construction currently necessitates technological advancement and demand stimulation. On the one hand, tremendous technological advancement has resulted in a thriving smart city product. On the other hand, cities must urgently address efficiency and sustainability challenges in order for smart cities to become a fruitful ground for economic development [13–15]. The sustainability of resources is an important component in fostering the growth of cities and regions. Smart cities are characterized as cities that are sustainable and efficient in their use of resources to provide a high quality of life [16, 17]. Smart resource cities have emerged as Europe's most recent urban development plan. Several smart energy city projects have been established using advancements in information and communication technology. Research has found that the key components of smart energy city projects are strategically sustainable and consistent [18–20]. Chen et al. [21] study how to promote and realize the sustainability of urban resources through smart city initiatives. The study found that although sustainability is not always the main goal of local implementation of smart city projects, smart city construction projects have increased the ambition to achieve resource sustainability goals. Furthermore, smart cities are built on the advancement of new technologies. However, modern technology is rarely used to drive smart city sustainability initiatives [22]. Simultaneously, smart cities have enormous promise in terms of urban mobility, development, and resource (and related greenhouse gas) conservation [23].

The importance of urban sustainability analysis has been extended to the construction of smart cities [24].

The idea of smart, sustainable cities has gained popularity recently. Smart cities have gained widespread attention as a viable solution to urban sustainability issues [25]. In light of this, the idea of a smart sustainable city is put out using studies on urban sustainability and smart cities. This idea focuses on how programs for smart, sustainable cities merge technology and the natural world. It identifies three

components of such cities: The creation of spatially advanced, environmentally friendly communities; the digitalization of city infrastructure; and the joint experimentation of digital and low-carbon technology. Smart, sustainable cities are now the new standard for constructing and growing cities. According to studies, the growth of the green economy will have a significant impact on how European smart cities develop in the future [26]. Future smart cities will need to take into account topics like how smart cities support urban sustainability and how sustainability in smart cities supports the growth of smart cities sustainably. Existing research demonstrates that smart cities are directly linked to innovation, technology, and the economy, but that they do nothing to advance sustainability.

3. Intelligent Building and Ethical Decision-Making Feature Calculation

The steps in this paper to calculate the decision features are as follows:

(1) This article first classifies the data according to different scene characteristics, and scenes with the same characteristics are classified into the same type of calculation data.

(2) Secondly, this paper calculates the value of decision risk and moral strength under different choices according to the above calculation formula on the classified scene data.

(3) Finally, this paper uses two decision-making features as coordinates to obtain the distribution map of decision-making features for each type of scene. The following first mainly introduces the specific meaning and calculation formula of the two decision-making characteristics of decision-making risk and moral strength.

The main features used in this paper are decision risk and moral strength β_m. Among them, decision risk can also be understood as construction risk in the road construction area, which is represented by decision risk β_d here. First, the calculation of decision-making risk is explained, which is mainly divided into three aspects to consider

People: the above research shows that there are more protected element attributes such as female, young, few people, healthy, low social value, and human beings in the scene selection, which will increase the risk of decision-making. It can also be understood that the presence of certain types of characteristic elements in the scene will increase the risk of construction decision-making in the building area, and the decision should be made cautiously.

Construction equipment: if there are people in the automatic control of construction equipment, it will increase the risk of decision-making; Building area: The existence of obstacles in the building area and intelligent building construction will also increase the risk of building construction decision-making for construction equipment. The presence of obstacles will make the decision more complicated. Intelligent building construction will increase the possibility of movement of elements in the scene, and complex behavior will increase the risk of decision-making.

According to the above description, the performance indicators in the decision risk degree β_d are linearly combined, as shown in the following formula:

$$\beta_d = \beta_7 + a_2\beta_8 + a_3\beta_1 + a_4\beta_2 + a_5\beta_3 + a_6\beta_4 + a_7\beta_5 + a_8\beta_6. \tag{1}$$

In the formula, β_7: represents the degree of decision-making risk brought by the construction of a smart city. β_8: represents the decision-making risk caused by obstacles in the construction area. Specifically, it characterizes the decision-making conflicts between the construction personnel and the protection of pedestrians in the protection of the construction equipment in the data set, so the construction equipment will increase the decision risk. β_1: represents the decision-making risks caused by different genders in the scene, and women are more likely to bring decision-making risks. β_2: represents the decision-making risks brought by the healthy elements in the scene, and high health is more likely to bring decision-making risks. β_3: represents the decision-making risk brought by the social value of the elements in the scene, and high social value will increase the decision-making risk. β_4: represents the decision-making risk brought by the age of the elements in the scene, and a low age will increase the decision-making risk. β_5: represents the decision-making risk brought by the ethnic category of the elements in the scene, and humans will increase the decision-making risk compared to animals. β_6: represents the decision-making risk brought by the number of elements in the scene, and the larger the number of people, the higher the decision-making risk.

Among them, $\mu = [a_1, a_2, a_3, a_4, a_5, a_6, a_7, a_8], \mu$ is the coefficient group of each characteristic index.

The meanings of the above indicators are set according to the aforementioned research and are in line with the moral decision-making judgments of most decision-makers. The specific quantitative values are expressed in the number of attributes. The calculation formula of each indicator is expressed as follows:

$$\begin{aligned}
\beta_7 &= \text{crosignal},\\
\beta_8 &= \text{PedPed} * \text{barrier} * \text{numbercharacter},\\
\beta_1 &= \text{numberfemale},\\
\beta_2 &= \text{numberfintness},\\
\beta_3 &= \text{numbersocialstatus},\\
\beta_4 &= \text{numberyoung},\\
\beta_5 &= \text{numberhuman},\\
\beta_6 &= \text{numbercharacter}.
\end{aligned} \tag{2}$$

In the formula, each indicator is quantified by the number of elements in the data set. Among them, PedPed

and barrier are 1 means that the construction equipment vehicle carries passengers and obstacles increase the risk of decision-making, otherwise, there is no passenger. When the crosignal is 1, it means that there is intelligent building construction in the building area, which increases the decision-making risk.

According to the research, the coefficient of each decision index is defined as the selection frequency difference ΔP of each index.

Through calculation, $\mu = (0.1, 0.15, 0.18, 0.2, 0.35, 0.49, 0.58, 0.65)$ can be obtained. When it is substituted into formula (1), we can get the following formula:

$$\begin{aligned}\beta_d = {} & 0.1\beta_7 + 0.15\beta_8 + 0.18\beta_1 + 0.2\beta_2 + 0.35\beta_3 \\ & + 0.49\beta_4 + 0.58\beta_5 + 0.65\beta_6.\end{aligned} \tag{3}$$

In the formula, β_7 is the decision-making risk brought by the construction of intelligent buildings, and there is no correlation coefficient.

The calculation of moral strength is explained below. Moral strength β_m is mainly from six aspects result size β_{c1}, social theory β_{c2}, effect possibility β_{p1}, instantaneity β_t, intimacy β_{p2}, and affect concentration β_{c3}.

$$\beta_m = \beta_{c1} + \beta_{c2} + \beta_{p1} + \beta_t + \beta_{p2} + \beta_{c3}. \tag{4}$$

Among them, β_{c1}: represents the total harm of the ethical decision-making results to the victim, and represents the total number of elements of the victim in this paper. β_{c2}: represents the impact of ethical decision-making results on society or the degree of social comment on ethical decision-making results. This article uses legal effects to characterize social commentary, and smart building construction will increase the legal effects brought about. β_{p1}: represents the possible harm caused by the result of ethical decision-making. In this paper, the injury possibility of the most protected element is used to express it, and the injury value of the young, adult, and elderly among the elements is estimated, respectively. β_t: represents the time interval between making a decision and causing injury, where changing lanes will increase the duration. β_{p2}: represents the degree of relationship between decision-makers and potential victims. In this paper, the masses are more intimate with construction personnel and automatic control construction equipment. β_{c3}: represents the degree of concentration of injury caused by the decision-making result. The proportion of people in the total number of people in this paper indicates a high degree of concentration of injury.

The above description has corresponding changes according to the element form of the data set. The injury of the decision result is serious injury or death, that is, the degree of injury is high. The specific quantitative value is expressed by the number of attributes, and the specific calculation formula for the six indicators of moral strength is as follows:

$$\beta_{c1} = \text{numbercharacter}, \tag{5}$$

$$\beta_{c2} = \frac{\text{crosignal}}{2} \times \text{number\_character}, \tag{6}$$

$$\begin{aligned}\beta_{p1} = {} & \phi_1 \text{number\_young} \\ & + \phi_2 \text{number\_adult} + \phi_3 \text{number\_old},\end{aligned} \tag{7}$$

$$\beta_t = 1, \tag{8}$$

$$\beta_{p2} = \text{PedPed}, \tag{9}$$

$$\beta_{c3} = \frac{\text{number\_human}}{\text{number\_character}}. \tag{10}$$

In formula (7), $P = [\phi 1, \phi 2, \phi 3]$. According to the failure research of construction equipment, people of different ages have a different probability of being seriously injured. The specific P can be calculated according to the following formula. If it is assumed that the automatic control of the brake failure is constructed in the urban road construction area.

$$\begin{aligned}\phi_{\text{children}} &= 1 - \frac{\exp^{8.85-0.12v}}{1+\exp^{8.85-0.12v}}, \\ \phi_{\text{adults}} &= 1 - \frac{\exp^{8.87-0.13v}}{1+\exp^{9.87-0.13v}}, \\ \phi_{\text{elderly}} &= 1 - \frac{\exp^{9.73-0.20v}}{1+\exp^{9.73-0.20v}}.\end{aligned} \tag{11}$$

We can get $P = [\phi_{\text{children}}, \phi_{\text{adults}}, \phi_{\text{elderly}}] = [0.0171, 0.0248, 0.1506]$. When it is substituted into formula (7), we can get the following formula:

$$\begin{aligned}\beta_{p1} = {} & 0.017\text{number\_young} + 0.0248\text{number\_adult} \\ & + 0.1506\text{number\_old}.\end{aligned} \tag{12}$$

The parameters in the above formula are mainly derived from the moral machine test data set. The final parameters are two decision feature values β_d and β_m.

The following uses the obtained feature formulas to process and calculate the data set, and, respectively, use the decision feature values to coordinate plots for analysis. After classifying and processing the result of feature value calculation, the decision feature distribution of each type of scene is obtained as shown in Figures 1(a)–1(f).

The distribution of decision feature values in each feature scene is shown in Figures 1(a)–1(f). The red point set in the figure represents the distribution of decision-making features under the default selection, and the blue point set represents the distribution of decision-making features under the nondefault selection. It can be seen from the figure that there are central effects and hierarchical effects in the distribution of different decision-making and decision-making features. That is, the area of specific decision-making feature values tends to have the same decision-making choice, and each layer has a clear boundary.

Therefore, this paper draws the following conclusions on the regular characteristics of the decision feature distribution map:

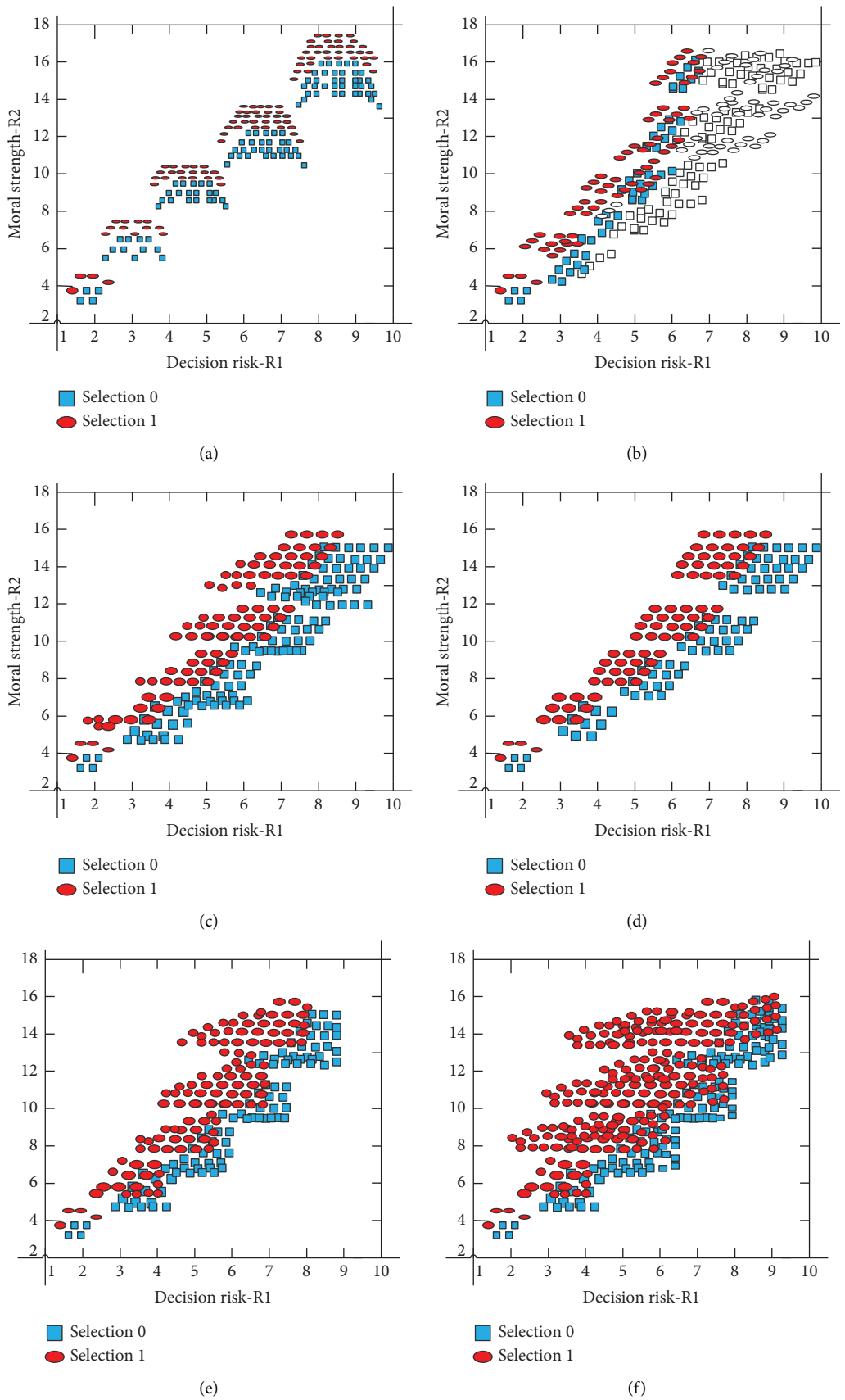

Figure 1: Distribution of decision-making features in six feature scenarios. (a) Distribution map of ethical decision characteristics in fitness feature scenarios. (b) Distribution map of ethical decision characteristics in age feature scenarios. (c) Distribution map of ethical decision characteristics in gender feature scenarios. (d) Distribution map of ethical decision characteristics in social status feature scenarios. (e) Distribution map of ethical decision characteristics in species feature scenarios. (f) Distribution map of ethical decision characteristics in utilitarian feature scenarios.

(1) Decision-making dilemmas with different characteristics have different distributions of decision-making characteristics, that is, different decision-making laws

(2) In the same feature decision scenario, different feature value areas have different decisions; that is, the decision rules can be explained

(3) In the same feature decision scenario, the distribution of decision feature values under the same decision is discontinuous and has the characteristics of discrete stratification

The analysis of the data processing results shows that the decision results under the six dilemma scenarios are distributed in different decision features. The following characteristics can be summarized from the analysis results and the decision feature map:

(1) In the same type of ethical decision-making dilemma scenario, the decision-making results in the specific environment characterized by different decision-making characteristics show a regular and hierarchical distribution

(2) The distribution of each type of hierarchical decision feature in the decision feature map has a relatively regular shape as a whole and presents a central effect

(3) The decision features of each layer in the decision feature map show a nonlinear distribution

Generally, the following basic concepts are included in the pattern recognition classification problem:

3.1. Features. In the classification problem, the feature is the description of the event or problem to be classified. The characteristics of the event are the common attributes of the event, and the model classifies the event by identifying the characteristics of the event. In ethical decision-making problems, the characteristic attributes of the problem can be represented by the $R = (R_1, R_2)$ characteristic vector group, where R_1, R_2 is the characteristic attribute of the model to the current environmental conditions in the corresponding type of environment.

3.2. Class Label. Class is a limited set of categories of classification problems, which represents the result of event classification, which can be represented by $w = \{w_1, w_2, w_3, \ldots w_n\} (n > 1)$. In ethical decision-making problems, the set of classes can be $w = \{w_1, w_2\}$.

3.3. Training Data Set. The training data set of the classification problem is composed of events with known class labels and the characteristic attributes of each event. Therefore, the training data set is a collection of event samples of known categories, which are generally determined by experimental data or empirical data.

3.4. Test Data Set. The main function of the test data set in the classification problem is to verify the feasibility of the classification model. Through the composition of randomly selected samples, the test data set is also a collection of event samples of known categories.

3.5. Classification Decision Model. The classification model is obtained through the learning or training of the training data set through the pattern recognition method, and then the optimized model is verified through the test data set. Generally, the form of classification model includes classification rules, mathematical expressions, or decision trees. The classification model is also the implicit classification law in the data.

The Bayesian classification method is mainly based on the Bayes theorem, which is the Bayes criterion proposed by Bayes. The theorem mainly describes the relationship between the prior probability, posterior probability, and conditional probability of an event through the Bayesian formula. When it is applied to classification problems, the theorem characterizes the relationship between the prior probability, posterior probability, and conditional probability of the category. In practice, two basic premises should be met before applying Bayes' theorem to solve problems such as decision-making classification.

(1) The probability distribution of each category is known; that is, the prior probability of each category and the probability distribution of the event itself

(2) The number of classified categories is limited

We assume that we are studying an m-class classification problem, the sample category space is $w = \{w_1, w_2, w_3, \ldots w_m\} (m > 1)$, the sample feature space is $X = (x_1, x_2 \ldots x_m)$, and the number of samples in each category space is $N = (N_1, N_2 \ldots N_m)$. If a sample x_0 belongs to the class w_0, then $P(w_0)$ represents the prior probability of class w_0. It is the subjective determination of the probability of belonging to a class w_0 according to the number of samples, reflecting the knowledge of the possibility of this class. The prior probability of category w_0 can be estimated from sample data, such as $P(w_0) = N_0/N$. $P(x_0, w_0)$ represents the conditional probability of the sample x_0, that is, the probability distribution of samples in a category w, which can generally be expressed by a probability density function. The posterior probability $P(w_0 \mid x_0)$ represents the probability that a given sample x_0 is determined to be a class w_0. Combining the observed information, the prior probability is modified to obtain a more reasonable probability. It also reflects a kind of observational learning ability, which can be calculated by the Bayesian formula.

Thus, according to Bayes' theorem, the following relationship can be obtained:

$$P(w_i \mid x) = \frac{P(x \mid w_i) \times P(w_i)}{P(x)}. \tag{13}$$

Among them, $P(x)$ represents the probability density function of the sample feature.

In specific classification problems, the Bayesian learning classification method needs to adopt appropriate decision

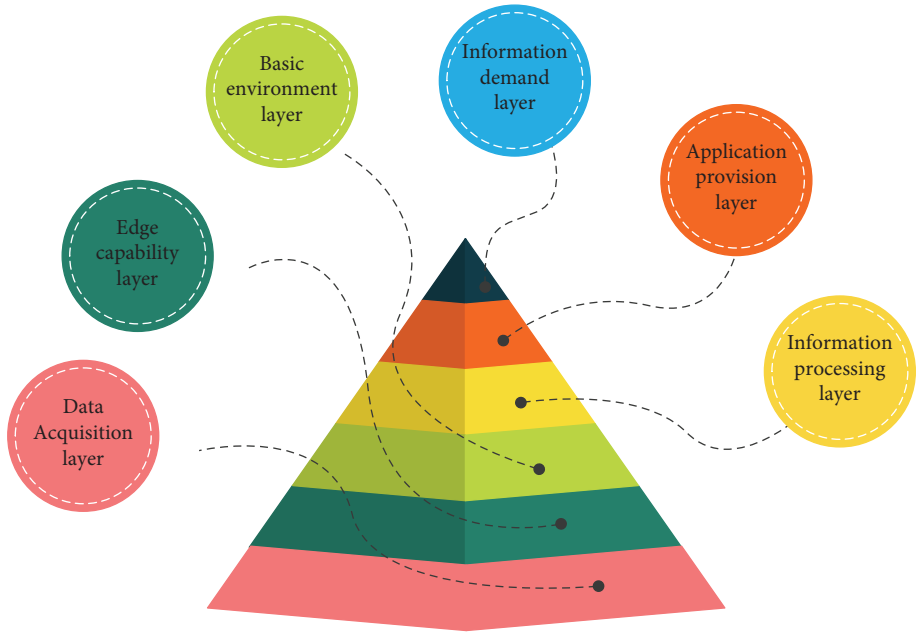

Figure 2: The new smart city system architecture based on edge computing.

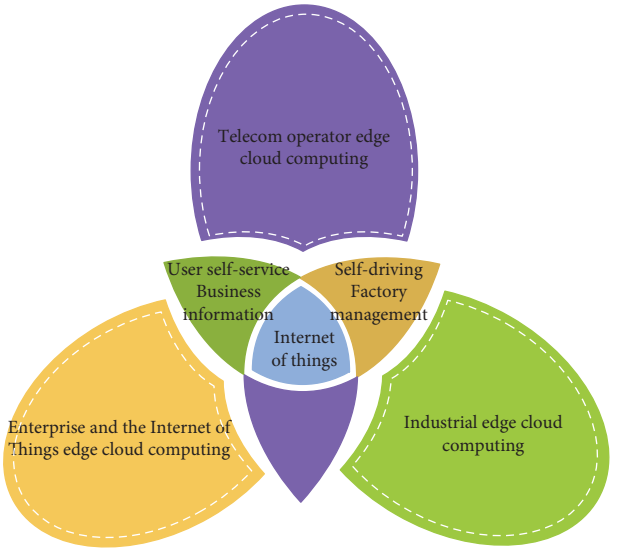

Figure 3: Schematic diagram of edge cloud computing classification and interrelationship.

criteria according to different objectives. Common decision criteria include the minimum error rate criterion and the minimum risk criterion.

3.5.1. Minimum Error Rate Criterion. Misclassification is inevitable in the actual classification. If a sample originally belongs to a class $w_0$but is classified into a class w_1, there will be a phenomenon of misclassification. Therefore, in order to make the classification optimal, it is necessary to minimize the error rate of the classification, that is, to meet the minimum error rate criterion. It can be expressed as

$$\hat{y} = \text{argmax}_{l\in Y} P(l \mid x). \tag{14}$$

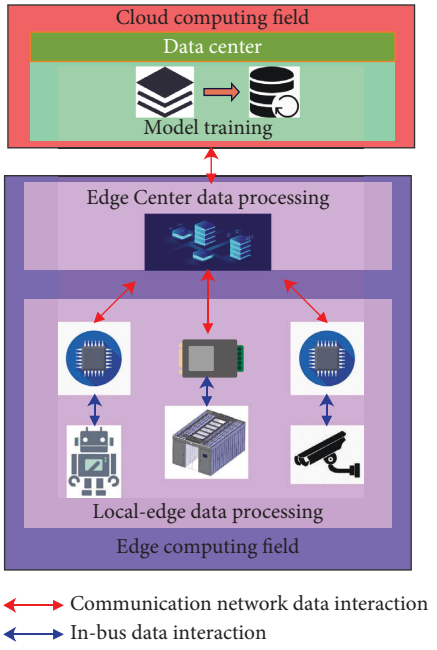

Figure 4: Schematic diagram of the process of edge computing in the industrial Internet application field.

In the formula, $P(l \mid x)$ is the probability of dividing sample x into class 1.

In fact, the error rate can be minimized by maximizing the posterior probability, and the minimum error rate can also be expressed as follows:

$$P(e) = \int_{x\in X} P(e \mid x)P(x)\mathrm{d}x. \tag{15}$$

Among them, $P(e \mid x)$ is expressed as the probability of dividing sample x by mistake.

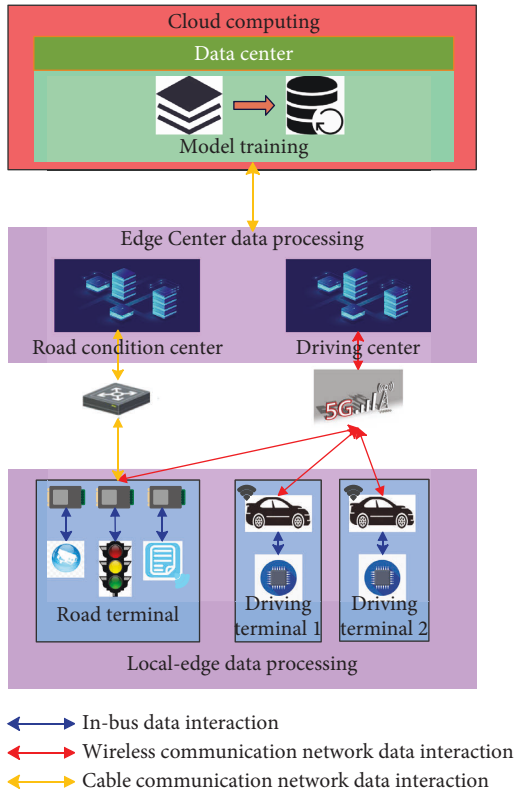

Figure 5: Schematic diagram of the process of edge computing in the field of smart transportation applications.

For sample point x, if it is classified into class 1, the error rate is $P(e \mid x)(x) = P(x)(1 - P(x))$.

Thus, the formula for minimizing the error rate can be obtained

$$\begin{aligned} \hat{y} &= \operatorname{argmin}_{le} P(l \mid x) \\ &= \operatorname{argmin}_{leY} P(x)(1 - P(l \mid x)) \\ &= \operatorname{argmax}_{le} Y P(l \mid x). \end{aligned} \tag{16}$$

Because the posterior probability can be calculated by Bayes' theorem, the above formula can be transformed to

$$\begin{aligned} \hat{y} &= \operatorname{argmax}_{\text{leY}} P(l \mid x) \\ &= \operatorname{argmax}_{\text{leY}} \frac{P(x \mid l)}{P(x)} P(l) \\ &= \operatorname{argmax}_{\text{leY}} (x \mid l) P(l). \end{aligned} \tag{17}$$

Therefore, minimizing the error rate can be seen as maximizing the posterior probability, and can also be seen as maximizing the prior probability and conditional probability.

3.5.2. Minimum Risk Criterion. In classification, not only the error rate of classification should be considered but also the risks brought by classification should be considered. Different classifications or decisions will bring different risks. When a penalty is added to the minimum error rate it

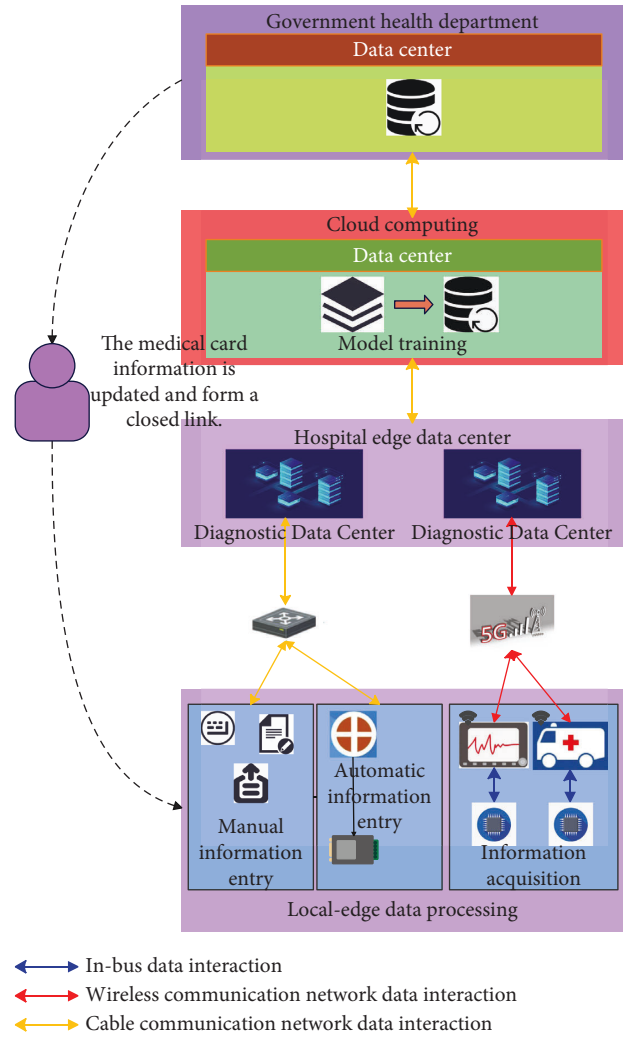

Figure 6: Schematic diagram of the process of edge computing in the field of smart medical applications.

indicates that the impact of classification errors is also a risk. When applying the minimum risk criterion, a loss matrix or loss function is required to represent the penalty coefficient for misclassification.

For example, for an m-class problem, there are m classifications in the decision space Y to classify the samples into different classes. We assume that the loss of a certain w_i-type sample into a w_j class by the j-th classification Y_j is $\lambda(Y_j \mid w_j)$. Then, the risk of misclassification of sample x is expressed as follows:

$$R(Y_i \mid x) = \sum_{j=1}^{m} \lambda(Y_i \mid w_j) P(w_j \mid x). \tag{18}$$

For a given sample x to minimize the risk, it can be expressed as follows:

$$\begin{aligned} \hat{y} &= \operatorname{argmax}_{\text{leY}} R(l \mid x) \\ &= \operatorname{argmax}_{\text{leY}} \sum_{j=1}^{m} \lambda(l \mid w_j) P(x \mid w_j) P(w_j). \end{aligned} \tag{19}$$

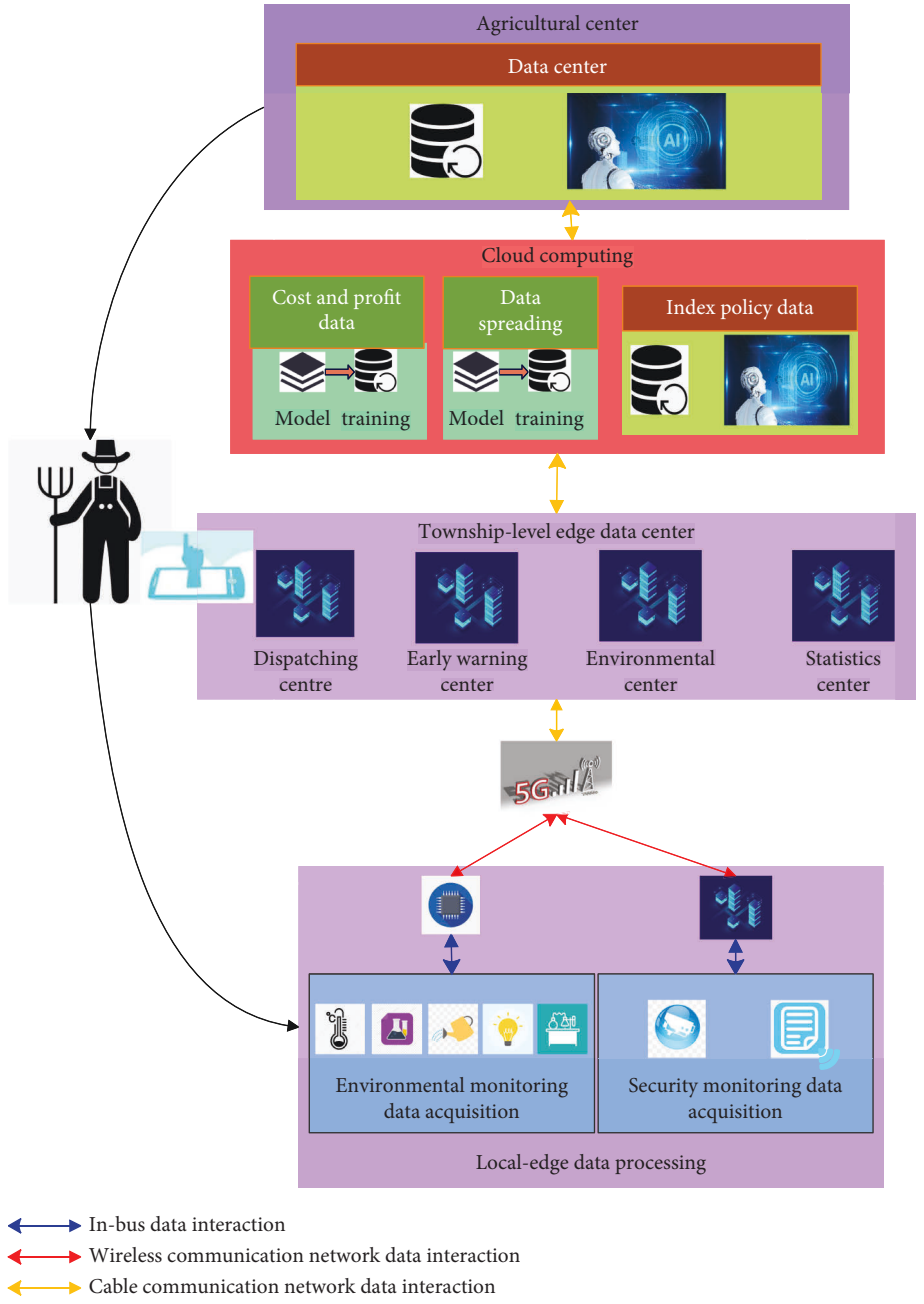

Figure 7: Schematic diagram of the process of edge computing in the application of smart agriculture.

Among them, $\lambda(l \mid w_j)$ is the loss function, and the commonly used loss functions have 0–1 loss functions, that is, the correct classification loss is 0, and the misclassification loss is 1, as expressed by the following formula:

$$\lambda\left(Y_i \mid w_j\right) = \begin{cases} 0, & i = j, \\ 1, & i \neq j, i = 1, \ldots, m. \end{cases} \tag{20}$$

Generally, when the prior probability and conditional probability of the sample are known, both the minimum error rate criterion and the minimum risk criterion can be used to perform Bayesian optimal classification.

4. Smart City Edge Computing Based on Smart Buildings and Ethical Computing

Based on the policy, technology, and market support of the development of the government and the global information application market for the construction of smart cities, as well as the data explosion brought about by 5G technology, the existing technical architecture has become more and more difficult for the processing and interaction of massive real-time data. The new smart city architecture based on the flexible deployment of edge

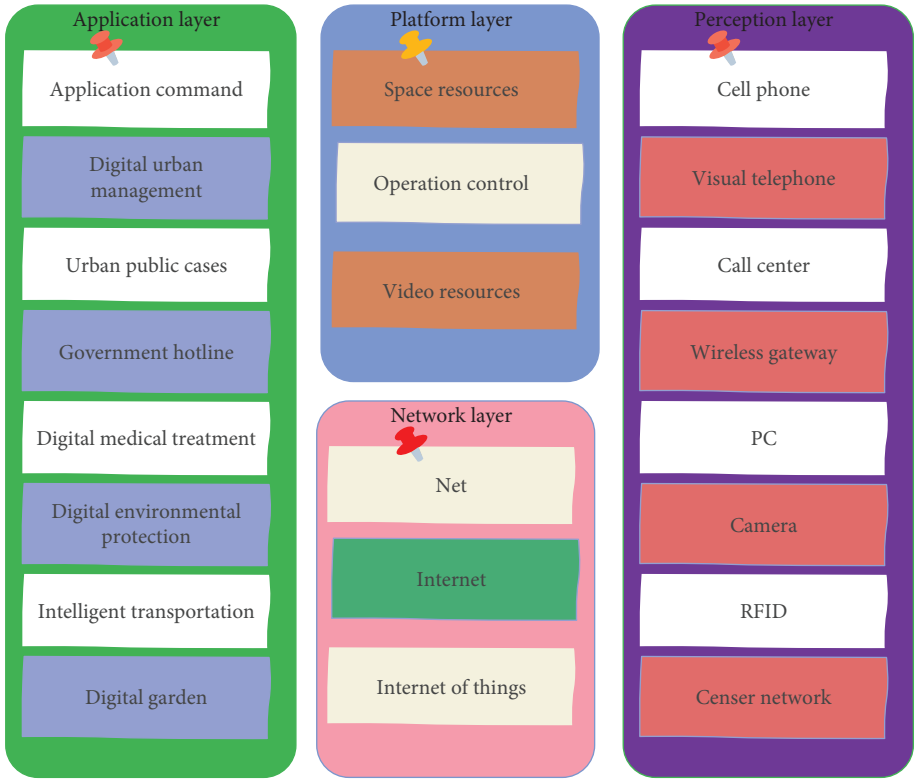

Figure 8: Smart city management platform.

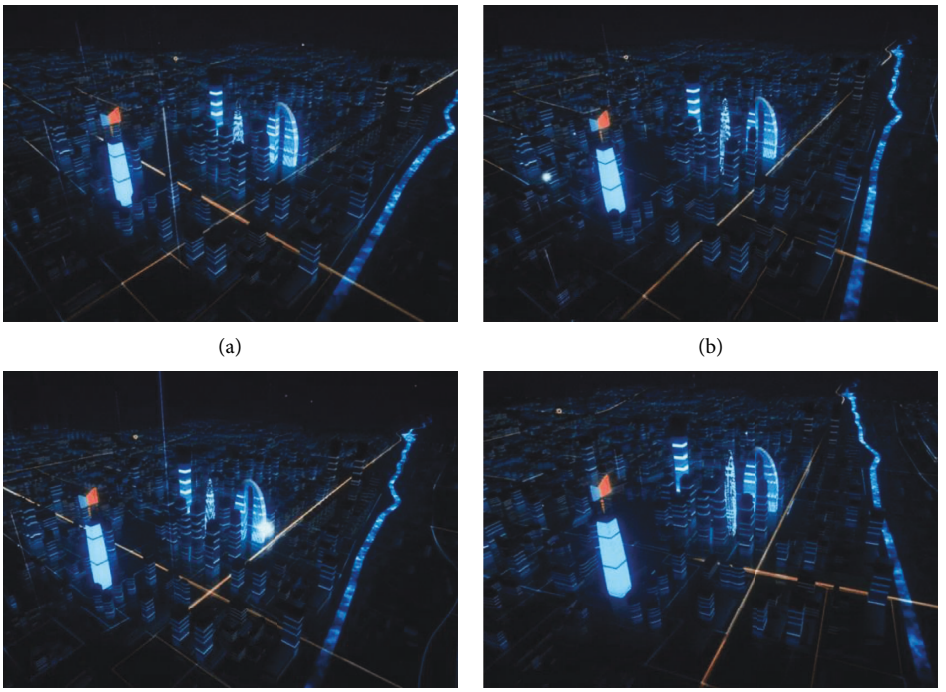

Figure 9: Smart city simulation image.

computing and data slicing capabilities provides strong support for the transformation of smart city construction in terms of hardware-embedded technology, access means, and software data processing. The new smart city system architecture based on edge computing is divided into 6 levels, as shown in Figure 2.

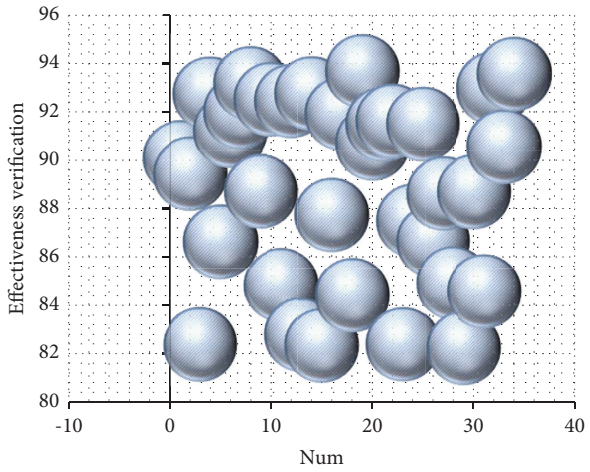

Figure 10: Statistical diagram of the effect of smart city construction.

Table 1: Verification of the effect of smart city construction.

Num	Effectiveness verification	Num	Effectiveness verification
1	90.12	18	84.43
2	89.44	19	93.67
3	82.38	20	90.70
4	92.74	21	91.48
5	86.64	22	91.61
6	91.20	23	82.40
7	91.99	24	87.51
8	93.16	25	91.49
9	88.71	26	86.66
10	92.51	27	88.62
11	84.83	28	84.91
12	92.44	29	82.25
13	82.79	30	88.69
14	92.75	31	84.59
15	82.35	32	92.95
16	87.75	33	90.54
17	91.91	34	93.55

From the perspective of common application scenarios in smart cities, edge computing business types have diversified characteristics, such as industrial operations, smart driving, business orchestration, business data push, online marketing, factory supervision, and video collection. According to implementation methods and business scenarios, the edge computing of smart cities mainly includes three types telecom operators' edge cloud computing, enterprise and IoT edge cloud computing, and industrial edge cloud computing. The three types of edge cloud computing are not mutually exclusive. The specific situation is shown in Figure 3.

In industrial Internet application scenarios, edge computing mainly processes critical business data and improves real-time response speed by installing edge computing chips or small industrial computers on terminal equipment or original data recording nodes, as shown in Figure 4.

With the cooperation of edge computing, cloud computing, and 5G communication, we can extend the existing intelligence from the terminal side of the driving tool to the road environment, as shown in Figure 5.

The schematic diagram of the process of edge computing in the field of smart medical applications and the schematic diagram of the process of edge computing in the field of smart agricultural applications are shown in Figures 6 and 7, respectively.

The smart city management platform designed on the aforementioned basis is shown in Figure 8.

The simulation research of a smart city is carried out through the above system. Figure 9 shows the smart city model proposed in this paper.

On the basis of the above research, the system of this paper is verified by a simulation test of the smart city effect, and multiple sets of data are counted, and the results are shown in Figure 10 and Table 1.

From the above research, it can be seen that the smart city edge computing method based on smart building-ethical computing proposed in this paper has good results. All the effectiveness verification of the smart city effect are >80.25, and half of them are >90.12, which demonstrates that the Applications of uncertainty models as support in smart buildings and ethical computing in edge computing of smart cities that were proposed in this work have a positive effect on the information extraction process.

5. Conclusion

As a new model of urban development, smart cities have swept the world as soon as they were proposed, and have become an important way for the government to respond to reforms and innovations in all aspects of society. China has advanced the construction of smart cities to a strategic height and strives to develop them as an important way to build a new type of urbanization. Building a smart city has many advantages to urban development. Through the means of information technology, information is collected, processed, analyzed, and used to achieve intelligence, integrate resources and information between cities and people, to promote urban development, speed up information exchange, simplify work procedures, and improve work efficiency. Moreover, the development goal of smart cities is to use advanced information technology to promote the adjustment and upgrading of industrial structure, accelerate economic development, optimize the economic structure, realize new social resource allocation, realize industrial innovation and upgrade, and increase economic development. This paper combines smart buildings-ethical computing to conduct research on smart city edge computing and provides a theoretical reference for the construction and development of smart cities. The research shows that the smart city edge computing method based on smart buildings and ethical computing proposed in this paper has good results.

Based on edge computing, smart city buildings are expected to be intelligent and humanized, and the data generated by buildings can be well processed and utilized. Based on mobile edge computing and assisted by autonomous driving technology with deep learning and big data analysis, driverless services can achieve real-time positioning of

vehicles that are not visible in the line of sight, collaborative hazard prediction of urban areas, and 3D map generation of autonomous driving. Edge computing-based multienergy networks can improve the overall efficiency and effectiveness of energy systems in areas of different sizes, such as parks, islands, and towns, including large buildings. Multienergy networks based on edge computing technology can integrate smart grid, heat supply and gas network, and network flow, and realize unified energy management in smart cities. As a new technology, the development of edge computing will also go through the process from scratch, from the beginning to maturity, and will also be affected by social needs and traditional rules. Although edge computing will bring great opportunities to the construction of smart cities from both technical and application levels, its development process will also face challenges from a technical, application, and even legal and ethical levels.

Data Availability

The data used to support the findings of this study are included within the article.

Conflicts of Interest

The authors declare that they have no conflicts of interest.

References

[1] R. R. Dong, "The application of BIM technology in building construction quality management and talent training," *Eurasia Journal of Mathematics, Science and Technology Education*, vol. 13, no. 7, pp. 4311–4317, 2017.

[2] X. Qin, Y. Shi, K. Lyu, and Y. Mo, "Using a TAM-TOE model to explore factors of Building Information Modelling (BIM) adoption in the construction industry," *Journal of Civil Engineering and Management*, vol. 26, no. 3, pp. 259–277, 2020.

[3] Y. C. Kim, W. H. Hong, J. W. Park, and G. W. Cha, "An estimation framework for building information modeling (BIM)-based demolition waste by type," *Waste Management & Research: The Journal for a Sustainable Circular Economy*, vol. 35, no. 12, pp. 1285–1295, 2017.

[4] M. N. Kocakaya and U. NamlıIşıkdağ, "Building information management (BIM), a new approach to project management," *Journal of sustainable construction materials and technologies*, vol. 4, no. 1, pp. 323–332, 2019.

[5] A. Okakpu, H. A. Ghaffarian, J. Tookey, J. Haar, A. Ghaffarianhoseini, and A. Rehman, "A proposed framework to investigate effective BIM adoption for refurbishment of building projects," *Architectural Science Review*, vol. 61, no. 6, pp. 467–479, 2018.

[6] L. Ustinovičius, A. Puzinas, J. Starynina, M. Vaišnoras, O. Černiavskaja, and R. Kontrimovičius, "Challenges of BIM technology application in project planning," *Engineering Management in Production and Services*, vol. 10, no. 2, pp. 15–28, 2018.

[7] M. O. Fadeyi, "The role of building information modeling (BIM) in delivering the sustainable building value," *International Journal of Sustainable Built Environment*, vol. 6, no. 2, pp. 711–722, 2017.

[8] T. Mandičák, P. Mesároš, and M. Tkáč, "Impact of management decisions based on managerial competencies and skills developed trough BIM technology on performance of construction enterprises," *Pollack Periodica*, vol. 13, no. 3, pp. 131–140, 2018.

[9] L. Ustinovichius, V. Popov, J. Cepurnaite, T. Vilutienė, M. Samofalov, and C. Miedziałowski, "BIM-based process management model for building design and refurbishment," *Archives of Civil and Mechanical Engineering*, vol. 18, no. 4, pp. 1136–1149, 2018.

[10] T. Wei and Y. Chen, "Green building design based on BIM and value engineering," *Journal of Ambient Intelligence and Humanized Computing*, vol. 11, no. 9, pp. 3699–3706, 2020.

[11] S. M. Noor, S. R. Junaidi, and M. K. A. Ramly, "Adoption of building information modelling (bim): factors contribution and benefits," *Journal of Information System and Technology Management*, vol. 3, no. 10, pp. 47–63, 2018.

[12] E. Papadonikolaki, C. van Oel, and M. Kagioglou, "Organising and managing boundaries: a structurational view of collaboration with building information modelling (bim)," *International Journal of Project Management*, vol. 37, no. 3, pp. 378–394, 2019.

[13] Y. Liu, C. Yang, L. Jiang, S. Xie, and Y. Zhang, "Intelligent edge computing for IoT-based energy management in smart cities," *IEEE network*, vol. 33, no. 2, pp. 111–117, 2019.

[14] D. Wang, B. Bai, K. Lei, W. Zhao, Y. Yang, and Z. Han, "Enhancing information security via physical layer approaches in heterogeneous IoT with multiple access mobile edge computing in smart city," *IEEE Access*, vol. 7, pp. 54508–54521, 2019.

[15] A. Rejeb, K. Rejeb, S. Simske, H. Treiblmaier, and S. Zailani, "The big picture on the internet of things and the smart city: a review of what we know and what we need to know," *Internet of Things*, vol. 19, Article ID 100565, 2022.

[16] Y. Y. Al-Ashmori, I. Othman, Y. Rahmawati et al., "BIM benefits and its influence on the BIM implementation in Malaysia," *Ain Shams Engineering Journal*, vol. 11, no. 4, pp. 1013–1019, 2020.

[17] A. Koutamanis, J. Heuer, and K. D. Könings, "A visual information tool for user participation during the lifecycle of school building design: bim," *European Journal of Education*, vol. 52, no. 3, pp. 295–305, 2017.

[18] S. Alamgir Hossain, M. Anisur Rahman, and M. A. Hossain, "Edge computing framework for enabling situation awareness in IoT based smart city," *Journal of Parallel and Distributed Computing*, vol. 122, pp. 226–237, 2018.

[19] S. M. Luo, J. Xu, and B. K. Li, "Practice and exploration on teaching reform of engineering project management course in universities based on BIM simulation technology," *Eurasia Journal of Mathematics, Science and Technology Education*, vol. 14, no. 5, pp. 1827–1835, 2018.

[20] Y. Jararweh, S. Otoum, and I. A. Ridhawi, "Trustworthy and sustainable smart city services at the edge," *Sustainable Cities and Society*, vol. 62, Article ID 102394, 2020.

[21] C. J. Chen, S. Y. Chen, S. H. Li, and H. T. Chiu, "Green BIM-based building energy performance analysis," *Computer-Aided Design and Applications*, vol. 14, no. 5, pp. 650–660, 2017.

[22] H. R. Abed, W. A. Hatem, and N. A. Jasim, "Adopting BIM technology in fall prevention plans," *Civil Engineering Journal*, vol. 5, no. 10, pp. 2270–2281, 2019.

[23] L. Joblot, T. Paviot, D. Deneux, and S. Lamouri, "Literature review of Building Information Modeling (BIM) intended for the purpose of renovation projects," *IFAC-PapersOnLine*, vol. 50, no. 1, pp. 10518–10525, 2017.

[24] P. Wu, R. Jin, Y. Xu, F. Lin, Y. Dong, and Z. Pan, "The analysis of barriers to bim implementation for industrialized building construction: a China study," *Journal of Civil Engineering and Management*, vol. 27, no. 1, pp. 1–13, 2021.

[25] I. Kim, J. Choi, E. A. L. Teo, and H. Sun, "Development of K-BIM e-Submission prototypical system for the openBIM-based building permit framework," *Journal of Civil Engineering and Management*, vol. 26, no. 8, pp. 744–756, 2020.

[26] A. Dainty, R. Leiringer, S. Fernie, and C. Harty, "BIM and the small construction firm: a critical perspective," *Building Research & Information*, vol. 45, no. 6, pp. 696–709, 2017.

Hindawi
Complexity
Volume 2022, Article ID 3828370, 16 pages
https://doi.org/10.1155/2022/3828370

Research Article

Novel Development to the Theory of Dombi Exponential Aggregation Operators in Neutrosophic Cubic Hesitant Fuzzy Sets: Applications to Solid Waste Disposal Site Selection

Ateeq Ur Rehman,[1] Muhammad Gulistan,[1] Nasreen Kausar,[2] Sajida Kousar,[3] Mohammed M. Al-Shamiri,[4,5] and Rashad Ismail[4,5]

[1]*Department of Mathematics and Statistics, Hazara University, Mansehra 21130, Pakistan*
[2]*Department of Mathematics, Faculty of Arts and Sciences, Yildiz Technical University, Esenler 34210, Istanbul, Turkey*
[3]*Department of Mathematics and Statistics, International Islamic University, Islamabad, Pakistan*
[4]*Department of Mathematics, Faculty of Science and Arts, Muhayl, Asser, King Khalid University, Saudi Arabia*
[5]*Department of Mathematics and Computer, Faculty of Science, IBB University, IBB, Yemen*

Correspondence should be addressed to Muhammad Gulistan; gulistanm21@yahoo.com

Received 5 July 2022; Revised 1 August 2022; Accepted 10 August 2022; Published 26 September 2022

Academic Editor: Ning Cai

The neutrosophic cubic hesitant fuzzy set can efficiently handle the complex information in a decision-making problem because it combines the advantages of the neutrosophic cubic set and the hesitant fuzzy set. The algebraic operations based on Dombi norms and co-norms are more flexible than the usual algebraic operations as they involve an operational parameter. First, this paper establishes Dombi algebraic operational laws, score functions, and similarity measures in neutrosophic cubic hesitant fuzzy sets. Then, we proposed Dombi exponential operational laws in which the exponents are neutrosophic cubic hesitant fuzzy values and bases are positive real numbers. To use neutrosophic cubic hesitant fuzzy sets in decision-making, we are developing Dombi exponential aggregation operators in the current study. In the end, we present applications of exponential aggregation operators in multiattribute decision-making problems.

1. Introduction

Decision-making (DM) is one of the crucial problems in real life. Due to population increase and urbanization, the proper disposal of waste is a challenging problem nowadays. The proper disposal of waste is necessary for prevention of viral diseases like typhoid, dengue, and tuberculosis. Aggregation operators are fundamental tools in DM. Different sets and their generalizations like fuzzy set (FS), interval-valued fuzzy set (IVFS), intuitionistic fuzzy set (IFS), hesitant fuzzy set (HFS), neutrosophic set (NS), neutrosophic cubic set (NCS), and several aggregation operators have been defined so far [1–4]. Different researchers [5–8] established similarity measures and other important concepts and successfully applied their models to medical diagnosis and selection criteria. Krohling et al. established different useful techniques to sort out MADM problems [9–11]. Jun et al. combined IVFS and FS to form a cubic set (CS). The CS is a combination of FS and IVFS. CS has become a vital tool to deal with vague data. Several researchers explored algebraic aspects and apparently defined ideal theory in CS [12–15]. Smarandache initiated the concept of indeterminacy and described the notion of the neutrosophic set (NS) [16]. NS consist of three independent components, truth, indeterminacy, and falsehood. This characteristic of NS enables researchers to deal smoothly with inconsistent and vague data. For engineering purposes, the neutrosophic set is strict to [0, 1] and is called the single-valued neutrosophic set (SVNS) [17] presented by Wang et al. The NS was further extended to the interval neutrosophic set (INS) [18]. After

the appearance of NS, researchers put their contributions to theoretical as well as technological developments of the set [19–22]. Several researchers use these sets to construct multiattribute decision-making MADM [23–27]. Zhan et al. define aggregation operators and furnished some applications in MADM [28]. Torra defines a hesitant fuzzy set (HFS) [29]. An HFS is basically a function set on X that, when applied to X, returns a subset of [0, 1]. Jun et al. introduced the concept of neutrosophic cubic set (NCS) [30] which consists of both interval-valued neutrosophic and neutrosophic set. These characteristics of neutrosophic cubic sets make it a powerful tool to deal the vague and inconsistent data more efficiently. Soon after its exploration, it attracted researchers to work in many fields like medicine, algebra, engineering, and decision-making theory. Later, the idea of a cubic hesitant fuzzy set was introduced by Mehmood et al. [31]. Ye [32] proposed the concept of the single-valued neutrosophic hesitant fuzzy set (SVNHFS) by combining the advantages of the NS and HFS, which permits its membership functions to have sets of possible values, known as truth, indeterminacy, and falsity membership hesitant functions. Liu and Shi [33] proposed hybrid geometric aggregation operators in INHFS and discuss its presentations in MADM. Zhu et al. [34] proposed the method of β-normalization to add some elements to an HFE, which is a useful technique in case of different cardinalities. Lu and Ye [35] introduced exponential laws in single-valued neutrosophic numbers. Later, the exponential aggregation operators were introduced and applied in typhoon disaster evaluation by Tan et al. [36]. Wang and Li proposed some aggregation operators in pictures hesitant fuzzy sets and compared these operators with some existing decision-making methods [37, 38]. Tan and Zhang introduced trapezoidal fuzzy neutrosophic number arithmetic averaging and hybrid arithmetic averaging for multicriteria decision-making [39]. Feng et al. define type-2 hesitant fuzzy sets and explore some important properties of these sets [40]. Turkarslan et al. proposed the similarity measures in fuzzy multiset with application in medical diagnosis [41].

Dombi [42] established a general class of fuzzy operators. The Dombi T-operators are based on an operational parameter, and hence, the operations based on Dombi operators are more flexible than the other algebraic operations. Shi and Ye [43] established Dombi arithmetic and geometric aggregation operators in neutrosophic cubic sets. Liu et al. [44] established Dombi Bonferroni mean operators of intuitionistic fuzzy sets and discuss their applications in MADM problems. Chen and Ye [45] proposed the Dombi weighted aggregation operators in SVNSs and discuss their applications in MADM problems. Bhattacharya et al. [46] proposed the machine learning model-based approach to discussing the demographic influence of risk behavior of urban investors. Biswas et al. [47] establish an ensemble approach for portfolio selection in a multicriteria decision-making framework. Shi and Ye [43] proposed Dombi aggregation operators in the neutrosophic cubic environments for MADM. Rehman et al. [48] established neutrosophic cubic hesitant fuzzy geometric aggregation operators for MADM problems. Ashraf et al. [49] proposed interval-valued the picture fuzzy Maclaurin symmetric mean operators for MADM problems. Riaz and Farid [50] established picture fuzzy aggregation approach and applied it to the third-party logistic provider selection process. Several researchers [51–54], proposed useful techniques and successfully applied their models to solve decision-making problems.

Motivation: the Dombi exponential laws and Dombi exponential aggregation operators are not defined in the intuitionistic fuzzy set, neutrosophic set, and their extensions. The Dombi T-operators are more flexible than the usual T-operators, and exponential operators are an essential family of aggregation operators. This motivates the researchers to define Dombi exponential aggregation operators so that the inconsistent, hesitant, and vague data can be efficiently handled in the complex work frame where the base is crisp value.

Organization: the rest of this paper is organized as follows: Section 2 deals with some basic definitions used later on. Section 3 discusses Dombi algebraic operational laws and score functions in NCHFSs. In Section 4, we introduced distance and similarity measures in NCHFSs. Exponential operating rules and some useful results in NCHFSs. Section 5 deals with establishing Dombi exponential aggregation operators as NCHFSs. In Section 6, we demonstrate a MADM method based on NCHFDEA operators and use this method in the MADM problem. Section 7 presents the conclusion of the proposed study.

2. Preliminaries

Definition 1 (see [1]). Let $E \neq \varnothing$ be a set. An FS on E is a function $\mathring{\lambda} : E \longrightarrow [0, 1]$.

Definition 2 (see [55]). Let $E \neq \varnothing$ be a set. The CS on E is defined by $\Psi = \{\langle \wp; I(\wp), \mathring{\lambda}(\wp)a\rangle | \wp \in E\}$, where $I(\wp)$ is an IVFS on E and $\mathring{\lambda}(\wp)$ is a FS on E.

Definition 3 (see [17]). An NS on nonempty set E is a set of the form $\{\wp; \langle \Gamma_T(\wp), \Gamma_I(\wp), \Gamma_F(\wp)\rangle | \wp \in E\}$, where $\Gamma_T, \Gamma_I, \Gamma_F$ are mappings from set E to closed interval [0, 1].

Definition 4 (see [30]). An NCS in $E \neq \varnothing$ is a pair $\beta = (B, \hbar)$ where $B = \{\langle \wp; B_T(\wp), B_I(\wp), B_F(\wp)\rangle / \wp \in E\}$ is an INS in E and $\hbar = \{\langle \wp; \hbar_T(\wp), \hbar_I(\wp), \hbar_F(\wp)\rangle / \wp \in E\}$ is an NS in E.

Definition 5 (see [32]). A neutrosophic hesitant fuzzy set (NHFS) on nonempty set E is described by $\hbar = \{\langle \wp; \hbar_T(\wp), \hbar_I(\wp), \hbar_F(\wp)\rangle / \wp \in E\}$, where $\hbar_T(\wp), \hbar_I(\wp), \hbar_F(\wp)$ are three hesitant fuzzy sets such that $\hbar_T(\wp) + \hbar_I(\wp), +\hbar_F(\wp) \leq 3$.

Definition 6 (see [33]). Consider a nonempty set E. An interval neutrosophic hesitant fuzzy set (INHFS) on E is given by the object $B = \{\langle \wp; B_T(\wp), B_I(\wp), B_F(\wp)\rangle / \wp \in E\}$, where $B_T(\wp), B_I(\wp), B_F(\wp)$ are intervalued hesitant fuzzy sets.

The following technique of β-normalization proposed by Zhu et al. is a useful technique in case of different cardinalities of two hesitant fuzzy sets.

Definition 7 (see [34]). Let ϖ^+ and ϖ^- be respectively the maximum and minimum values in a hesitant fuzzy set H and $\Theta(0 \le \Theta \le 1)$ be an optimized parameter; then, an element can be added to H as $\varpi = \varpi^+ + (1-\Theta)\varpi$.

Definition 8 (see [42]). The Dombi norms and dual conorms are given, respectively, as

$$D(s,t) = \frac{1}{1+\left((1-s/s)^{\delta} + (1-t/t)^{\delta}\right)^{(1/\delta)}},$$
$$D^*(s,t) = 1 - \frac{1}{1+\left((s/1-t)^{\delta} + (t/1-t)^{\delta}\right)^{(1/\delta)}}, \tag{1}$$

where $(a,b) \in (0,1)\times(0,1)$ and $\delta \in R$ is an operational parameter. Furthermore, the values of D and D^* for boundaries are defined as $D(1,0) = D(0,1) = D(0,0) = 0, D(1,1) = 1, D^*(1,1) = D^*(1,0) = D^*(0,1) = 1$ and $D^*(0,0) = 0$.

In the next section, first, we define Dombi algebraic operational laws by using Dombi T-norms and T-conorms in NCHFSs. Second, the score functions are defined for the comparison of two NCHFSs.

3. Dombi Operational Laws in Neutrosophic Cubic Hesitant Fuzzy Set

Definition 9. A neutrosophic cubic hesitant fuzzy set (NCHFS) on a nonempty set E is a pair $\alpha = (A, \hbar)$, where $A = \langle e; A_T(e), A_I(e), A_F(e)\rangle$ is an INHFS in E and $\hbar = \langle e; \hbar_T(e), \hbar_I(e), \hbar_F(e)\rangle$ is an NHFS in E. Furthermore ${}_T(e) = \left\{[{}^L_{j_T}(e), {}^U_{j_T}(e)]; j = 1, \ldots, l_e\right\}, {}_I(e) = \left\{[{}^L_{j_T}(e), {}^U_{j_T}(e)]; j = 1, \ldots, m_e\right\}$, and $A_F(e) = \left\{[{}^L_{j_T}(e), {}^U_{j_F}(e)]; i = 1, \ldots, n_e\right\}$ are some interval values in [0, 1] with the property that for each $j0 \le {}^U_{j_T}(x) + {}^U_{j_I}(x) + {}^U_{j_F}(x) \le 3$, and ${}_T(e) = \left\{{}_{j_T}(e); j = 1, \ldots, r_e\right\}, {}_I(e) = \left\{{}_{j_I}(e); j = 1, \ldots, s_e\right\}, {}_F(e) = \left\{{}_{j_F}(e); j = 1, \ldots, t_e\right\}$ are some values in [0, 1] satisfying $0 \le (e) + {}_{j_I}(e) + {}_{j_F}(e) \le 3$.

Example 1. Let $E = \{e_1, e_2, e_3\}$. The pair $\alpha = (A, \lambda)$ with

$$\begin{aligned}
&A_T(e_1) = \{[0.1, 0.5], [0.2, 0.7]\}, \hbar_T(e_1) = \{0.3, 0.5, 0.7\},\\
&A_I(e_1) = \{[0.2, 0.4], [0.3, 0.6]\}, \hbar_I(e_1) = \{0.1, 0.4, 0.7\},\\
&A_F(e_1) = \{[0.1, 0.4], [0, 0.3], [0.6, 0.8]\}, \hbar_F(e_1) = \{0.4, 0.6\},\\
&A_T(e_2) = \{[0.1, 0.5], [0.2, 0.7]\}, \hbar_T(e_2) = \{0.3, 0.5\},\\
&A_I(e_2) = \{[0.2, 0.3], [0.1, 0.6]\}, \hbar_I(e_2) = \{0.7, 0.8\},\\
&A_F(e_2) = \{[0.1, 0.4], [0, 0.3]\}, \hbar_F(e_2) = \{0.4, 0.6\},\\
&A_T(e_3) = \{[0.1, 0.5], [0.2, 0.7]\}, \hbar_T(e_3) = \{0.3, 0.5\},\\
&A_I(e_3) = \{[0.2, 0.3], [0.1, 0.6]\}, \hbar_I(e_3) = \{0.7, 0.8\},\\
&A_F(e_3) = \{[0.1, 0.4], [0, 0.3]\}, \hbar_F(e_3) = \{0.4, 0.6\},
\end{aligned} \tag{2}$$

is a NCHFS.

Definition 10. For two NCHF values $\alpha = (A, \lambda), \beta = (B, \mu)$ and scalars $q, \sigma > 0$, we define, respectively, the Dombi sum, Dombi product, Dombi scalar multiplication, and the Dombi qth power of α as

$$\alpha \oplus \beta = \left(\begin{array}{c}
\left\{\left[1 - \left(1 + \left(\left(\frac{A^L_{j_T}}{1 - A^L_{j_T}}\right)^{\sigma} + \left(\frac{B^L_{j_T}}{1 - B^L_{j_T}}\right)^{\sigma}\right)^{1/\sigma}\right)^{-1}, 1 - \left(1 + \left(\left(\frac{A^U_{j_T}}{1 - A^U_{j_T}}\right)^{\sigma} + \left(\frac{B^U_{j_T}}{1 - B^U_{j_T}}\right)^{\sigma}\right)1/\sigma\right)^{-1}\right]\right\},\\
\left\{\left[1 - \left(1 + \left(\left(\frac{A^L_{j_I}}{1 - A^L_{j_I}}\right)^{\sigma} + \left(\frac{B^L_{j_I}}{1 - B^L_{j_I}}\right)^{\sigma}\right)1/\sigma\right)^{-1}, 1 - \left(1 + \left(\left(\frac{A^U_{j_T}}{1 - A^U_{j_T}}\right)^{\sigma} + \left(\frac{B^U_{j_T}}{1 - B^U_{j_T}}\right)^{\sigma}\right)1/\sigma\right)^{-1}\right]\right\},\\
\left\{\left[\left(1 + \left(\left(\frac{1 - A^L_{j_F}}{A^L_{j_F}}\right)^{\sigma} + \left(\frac{1 - B^L_{j_F}}{B^L_{j_F}}\right)^{\sigma}\right)1/\sigma\right)^{-1}, \left(1 + \left(\left(\frac{1 - A^U_{j_F}}{A^U_{j_F}}\right)^{\sigma} + \left(\frac{1 - B^U_{j_F}}{B^U_{j_F}}\right)^{\sigma}\right)^{1/\sigma}\right)^{-1}\right]\right\},\\
\left\{1 - \left(1 + \left(\left(\frac{\lambda_{j_T}}{1 - \lambda_{j_T}}\right)^{\sigma} + \left(\frac{\mu_{j_T}}{1 - \mu_{j_T}}\right)^{\sigma}\right)^{1/\sigma}\right)^{-1}\right\},\\
\left\{1 - \left(1 + \left(\left(\frac{\lambda_{j_I}}{1 - \lambda_{j_I}}\right)^{\sigma} + \left(\frac{\mu_{j_I}}{1 - \mu_{j_I}}\right)^{\sigma}\right)^{1/\sigma}\right)^{-1}\right\}, \left\{\left(1 + \left(\left(\frac{1 - \lambda_{j_F}}{\lambda_{j_F}}\right)^{\sigma} + \left(\frac{1 - \mu_{j_F}}{\mu_{j_F}}\right)^{\sigma}\right)^{1/\sigma}\right)^{-1}\right\}
\end{array} \right),$$

$$q\alpha = \left(\begin{array}{c} \left\{ \left[1 - \left(1 + \left(q \left(\frac{A^L_{j_T}}{1 - A^L_{j_T}} \right)^{\sigma} \right)^{1/\sigma} \right)^{-1}, 1 - \left(1 + \left(q \left(\frac{A^U_{j_T}}{1 - A^U_{j_T}} \right)^{\sigma} \right)^{1/\sigma} \right)^{-1} \right] \right\}, \\ \left\{ \left[1 - \left(1 + \left(q \left(\frac{A^L_{j_I}}{1 - A^L_{j_I}} \right)^{\sigma} \right)^{1/\sigma} \right)^{-1}, 1 - \left(1 + \left(q \left(\frac{A^U_{j_T}}{1 - A^U_{j_T}} \right)^{\sigma} \right)^{1/\sigma} \right)^{-1} \right] \right\}, \\ \left\{ \left[\left(1 + \left(q \left(\frac{1 - A^L_{j_F}}{A^L_{j_F}} \right)^{\sigma} \right)^{1/\sigma} \right)^{-1}, \left(1 + \left(q \left(\frac{1 - A^U_{j_F}}{A^U_{j_F}} \right)^{\sigma} \right)^{1/\sigma} \right)^{-1} \right] \right\}, \\ \left\{ 1 - \left(1 + \left(q \left(\frac{\lambda_{j_T}}{1 - \lambda_{j_T}} \right)^{\sigma} \right)^{1/\sigma} \right)^{-1} \right\}, \left\{ 1 - \left(1 + \left(q \left(\frac{\lambda_{j_I}}{1 - \lambda_{j_I}} \right)^{\sigma} \right)^{1/\sigma} \right)^{-1} \right\}, \left\{ \left(1 + \left(q \left(\frac{1 - \lambda_{j_F}}{\lambda_{j_F}} \right)^{\sigma} \right)^{1/\sigma} \right)^{-1} \right\} \end{array} \right),$$

$$\alpha^q = \left(\begin{array}{c} \left\{ \left[\left(1 + \left(q \left(\frac{1 - A^L_{j_T}}{A^L_{j_T}} \right)^{\sigma} \right)^{1/\sigma} \right)^{-1}, \left(1 + \left(q \left(\frac{1 - A^U_{j_T}}{A^U_{j_T}} \right)^{\sigma} \right)^{1/\sigma} \right)^{-1} \right] \right\}, \\ \left\{ \left[\left(1 + \left(q \left(\frac{1 - A^L_{j_I}}{A^L_{j_I}} \right)^{\sigma} \right)^{1/\sigma} \right)^{-1}, \left(1 + \left(q \left(\frac{1 - A^U_{j_T}}{A^U_{j_T}} \right)^{\sigma} \right)^{1/\sigma} \right)^{-1} \right] \right\}, \\ \left\{ \left[1 - \left(1 + \left(q \left(\frac{A^L_{j_F}}{1 - A^L_{j_F}} \right)^{\sigma} \right)^{1/\sigma} \right)^{-1}, 1 - \left(1 + \left(q \left(\frac{A^U_{j_F}}{1 - A^U_{j_F}} \right)^{\sigma} \right)^{1/\sigma} \right)^{-1} \right] \right\}, \\ \left\{ \left(1 + \left(q \left(\frac{1 - \lambda_{j_T}}{\lambda_{j_T}} \right)^{\sigma} \right)^{1/\sigma} \right)^{-1} \right\}, \left\{ \left(1 + \left(q \left(\frac{1 - \lambda_{j_I}}{\lambda_{j_I}} \right)^{\sigma} \right)^{1/\sigma} \right)^{-1} \right\}, \left\{ 1 - \left(1 + \left(q \left(\frac{\lambda_{j_F}}{1 - \lambda_{j_F}} \right)^{\sigma} \right)^{1/\sigma} \right)^{-1} \right\} \end{array} \right). \tag{3}$$

Moreover, the β-normalization is used in case of different cardinalities.

Example 11. If $\alpha = (\{[0.1, 0.2], [0.3, 0.4]\}, \{[0, .1, 0.3], [0, 0.2]\}, \{[0.6, 0.7], [0.3, 0.5]\}, \{0.1, 0.2\}, \{0.2, 0.3\}, \{0.6, 0.7\})$ and $\beta = (\{[0.6, 0.8], [0.5, 0.7]\}, \{[0.5, 0.6], [0.6, 0.7]\}, \{[0.1, 0.2], [0, 0.2]\}, \{0.6, 0.7\}, \{0.5, 0.6\}, \{0.2, 0.3\})$, then for $\sigma = 2$,

$$\begin{aligned} \alpha \oplus \beta &= \left(\begin{array}{c} \{[0.600656, 0.800312], [0.521065, 0.708174]\}, \{[0.501534, 0.609379], [0.6, 0.701197]\}, \\ \{[0.099754, 0.199088], [0, 0.296528]\}, \\ \{0.600656, 0.701197\}, \{0.507577, 0.609379\}, \{0.197817, 0.296528\} \end{array} \right), \\ \alpha \otimes \beta &= \left(\begin{array}{c} \{[0.099754, 0.199688], [0.282598, 0.390621]\}, \{[0.099449, 0.291826], [0, 0.199088]\}, \\ \{[0.600656, 0.701197], [0.3, 0.507577]\}, \\ \{0.099754, 0.199088\}, \{0.195194, 0.291826\}, \{0.603283, 0.703472\}, \end{array} \right), \\ 3\alpha &= \left(\begin{array}{c} \{[0.16139, 0.302169], [0.426048, 0.535898]\}, \{[0.16139, 0.426048], [0, 0.302169]\}, \\ \{[0.464102, 0.573952], [0.198356, 0.366025]\}, \\ \{0.16139, 0.302169\}, \{0.302169, 0.426048\}, \{0.464102, 0.573952\} \end{array} \right), \\ \alpha^3 &= \left(\begin{array}{c} \{[0.060283, 0.126132], [0.198356, 0.277926]\}, \{[0.060283, 0.198356], [0, 0.126132]\}, \\ \{[0.722074, 0.801644], [0.426048, 0.633975]\}, \\ \{0.060283, 0.126132\}, \{0.126132, 0.198356\}, \{0.722074, 0.801644\} \end{array} \right). \end{aligned} \tag{4}$$

It is very important to discuss the comparison of NCHF values. For comparison of NCHF values, we propose score functions in next section.

Definition 12. Score, accuracy, and certainty.

The score, accuracy, and certainty of a NCHF value $\alpha = (A, \lambda)$, where $A = A_T, A_I, A_F, A_T = \left\{[A^L_{j_T}, A^U_{j_T}]; \quad j = 1, \ldots, l\right\}, A_I = \left\{[A^L_{j_I}, A^U_{j_I}]; j = 1, \ldots, m\right\}, A_F = \left\{[A^L_{j_F}, \quad A^U_{j_F}]; i = 1, \ldots, n\right\}$ and $\lambda = \lambda_T, \lambda_I, \lambda_F, \lambda_T = \left\{\lambda_{j_T}; j = 1, \ldots, r\right\}, \lambda_I = \left\{\lambda_{j_I}; j = 1, \ldots, s\right\}, \lambda_F = \left\{\lambda_{j_F}; j = 1, \ldots, t\right\}$ are defined as

$$S(\alpha) = \frac{1}{2}\left\{\begin{array}{c} \frac{1}{6}\left(\frac{1}{l}\sum_{j=1}^{l}\left(A^L_{j_T} + A^U_{j_T}\right) + \frac{1}{m}\sum_{j=1}^{m}\left(A^L_{j_I} + A^U_{j_I}\right) + \frac{1}{n}\sum_{j=1}^{n}\left(2 - \left(A^L_{j_F} + A^U_{j_F}\right)\right)\right) \\ + \frac{1}{3}\left(\frac{1}{r}\sum_{j=1}^{r}\lambda_{j_T} + \frac{1}{s}\sum_{j=1}^{s}\lambda_{j_I} + \frac{1}{t}\sum_{j=1}^{t}\left(1 - \lambda_{j_F}\right)\right) \end{array}\right\},$$

$$H(\alpha) = \frac{1}{9}\left\{\frac{1}{l}\sum_{j=1}^{l}\left(A^L_{j_T} + A^U_{j_T}\right) - \frac{1}{n}\sum_{j=1}^{n}\left(A^L_{j_F} + A^U_{j_F}\right) + \frac{1}{r}\sum_{j=1}^{r}\lambda_{j_T} - \frac{1}{t}\sum_{j=1}^{t}\lambda_{j_F}\right\}, \tag{5}$$

$$C(\alpha) = \frac{1}{3}\left\{\frac{1}{l}\sum_{j=1}^{l}\left(A^L_{j_T} + A^U_{j_T}\right) + \frac{1}{r}\sum_{j=1}^{r}\lambda_{j_T}\right\}.$$

The score function is a useful tool for ranking the NCHF values. An NCHF value is greater if the interval hesitant and hesitant degrees of truth and indeterminacy membership grades are bigger and the interval hesitant and hesitant degrees of falsity membership grades are smaller. The greater the difference between truth and falsity memberships, the accuracy is higher and the corresponding NCHF value becomes greater. The certainty of an NCHF value depends on the interval hesitant and hesitant degrees of truth membership grades. The bigger the interval between hesitant and hesitant degrees of truth and indeterminacy membership grades, the greater the NCHF value is.

The following technique is use for ranking the values.

If $\alpha = (A, \lambda)$, $\beta = (B, \mu)$ be two NCHF values then we say that $\alpha \succ \beta$ if and only if $S(\alpha) \succ S(\beta)$.

If $S(\alpha) = S(\beta)$, we compare them on the basis of accuracy. If they have same accuracies too, we define the above comparison on the basis of certainty.

Example 2. If $\alpha = (\{[0.1, 0.2], [0.3, 0.4]\}, \{[0, .1, 0.3], [0, 0.2]\}, \{[0.6, 0.7], [0.3, 0.5]\}, \{0.1, 0.2\}, \{0.2, 0.3\}, \{0.6, 0.7\})$ and $\beta = (\{[0.6, 0.8], [0.5, 0.7]\}, \{[0.5, 0.6], [0.6, 0.7]\}, \{[0.1, 0.2], [0, 0.2]\}, \{0.6, 0.7\}, \{0.5, 0.6\}, \{0.2, 0.3\})$, then

$$S(\alpha) = 0.270833, S(\beta) = 0.679167, H(\alpha) = 0.322222, H(\beta) = 0.466667, C(\alpha) = 0.216667, C(\beta) = 0.65. \tag{6}$$

The distances and similarities are important notions in theory of sets. These two concepts are important tools to describe the degree of closeness in sets. Keeping in mind the importance of these two notions, we define these in the neutrosophic cubic hesitant fuzzy structure.

4. Distance and Similarity Measures in Neutrosophic Cubic Hesitant Fuzzy Sets

Definition 13. A distance measure is a mapping such that

$$\begin{aligned} &(i)\ 0 \le d(\alpha, \beta) \le 1, \\ &(ii)\ d(\alpha, \beta) = 0 \Leftrightarrow \alpha = \beta, \\ &(iii)\ d(\beta, \alpha) = d(\alpha, \beta), \\ &(\text{iv})\ \text{If } \alpha \subseteq \beta \subset \gamma, \text{then } d(\alpha, \gamma) \\ &\quad \ge d(\alpha, \beta) \text{ and } d(\alpha, \gamma) \ge d(\beta, \gamma). \end{aligned} \tag{7}$$

If $\alpha = (A, \lambda)$, $\beta = (B, \mu)$ are two NCHFS on a set $X = \{x_1, \ldots, x_t\}$, then we define the following.

Normalized Hamming Distance:

$$d_H(\alpha,\beta)=\frac{1}{9t}\left\{\sum_{i=1}^{t}\left(\begin{array}{c}\frac{1}{l_i}\sum_{j=1}^{l_i}\left(\left|A_{j_T}^U(x_i)-B_{j_T}^U(x_i)\right|+\left|A_{j_T}^L(x_i)-B_{j_T}^L(x_i)\right|\right)\\+\frac{1}{m_i}\sum_{j=1}^{m_i}\left(\left|A_{j_I}^U(x_i)-B_{j_I}^U(x_i)\right|+\left|A_{j_I}^L(x_i)-B_{j_I}^L(x_i)\right|\right)\\+\frac{1}{n_i}\sum_{j=1}^{n_i}\left(\left|A_{j_F}^U(x_i)-B_{j_F}^U(x_i)\right|+\left|A_{j_F}^L(x_i)-B_{j_F}^L(x_i)\right|\right)\\+\frac{1}{p_i}\sum_{j=1}^{p_i}\left|\lambda_{j_T}(x_i)-\mu_{j_T}(x_i)\right|+\frac{1}{q_i}\sum_{j=1}^{q_i}\left|\lambda_{j_I}(x_i)-\mu_{j_I}(x_i)\right|+\frac{1}{r_i}\sum_{j=1}^{r_i}\left|\lambda_{j_F}(x_i)-\mu_{j_F}(x_i)\right|\end{array}\right)\right\}. \tag{8}$$

Normalized Euclidean Distance:

$$d_E(\alpha,\beta)=\left(\frac{1}{9t}\left\{\sum_{i=1}^{t}\left(\begin{array}{c}\frac{1}{l_i}\sum_{j=1}^{l_i}\left(\left|A_{j_T}^U(x_i)-B_{j_T}^U(x_i)\right|^2+\left|A_{j_T}^L(x_i)-B_{j_T}^L(x_i)\right|^2\right)\\+\frac{1}{m_i}\sum_{j=1}^{m_i}\left(\left|A_{j_I}^U(x_i)-B_{j_I}^U(x_i)\right|^2+\left|A_{j_I}^L(x_i)-B_{j_I}^L(x_i)\right|^2\right)\\+\frac{1}{n_i}\sum_{j=1}^{n_i}\left(\left|A_{j_F}^U(x_i)-B_{j_F}^U(x_i)\right|^2+\left|A_{j_F}^L(x_i)-B_{j_F}^L(x_i)\right|^2\right)\\+\frac{1}{p_i}\sum_{j=1}^{p_i}\left|\lambda_{j_T}(x_i)-\mu_{j_T}(x_i)\right|^2+\frac{1}{q_i}\sum_{j=1}^{q_i}\left|\lambda_{j_I}(x_i)-\mu_{j_I}(x_i)\right|^2+\frac{1}{r_i}\sum_{j=1}^{r_i}\left|\lambda_{j_F}(x_i)-\mu_{j_F}(x_i)\right|^2\end{array}\right)\right\}\right)^{1/2}. \tag{9}$$

Normalized Generalized Distance:

$$d_G(\alpha,\beta)=\left(\frac{1}{9t}\left\{\sum_{i=1}^{t}\left(\begin{array}{c}\frac{1}{l_i}\sum_{j=1}^{l_i}\left(\left|A_{j_T}^U(x_i)-B_{j_T}^U(x_i)\right|^q+\left|A_{j_T}^L(x_i)-B_{j_T}^L(x_i)\right|^q\right)\\+\frac{1}{m_i}\sum_{j=1}^{m_i}\left(\left|A_{j_I}^U(x_i)-B_{j_I}^U(x_i)\right|^q+\left|A_{j_I}^L(x_i)-B_{j_I}^L(x_i)\right|^q\right)\\+\frac{1}{n_i}\sum_{j=1}^{n_i}\left(\left|A_{j_F}^U(x_i)-B_{j_F}^U(x_i)\right|^q+\left|A_{j_F}^L(x_i)-B_{j_F}^L(x_i)\right|^q\right)\\+\frac{1}{p_i}\sum_{j=1}^{p_i}\left|\lambda_{j_T}(x_i)-\mu_{j_T}(x_i)\right|^q+\frac{1}{q_i}\sum_{j=1}^{q_i}\left|\lambda_{j_I}(x_i)-\mu_{j_I}(x_i)\right|^q+\frac{1}{r_i}\sum_{j=1}^{r_i}\left|\lambda_{j_F}(x_i)-\mu_{j_F}(x_i)\right|^q\end{array}\right)\right\}\right)^{1/q},\ q>0. \tag{10}$$

Definition 14. A similarity measure is mapping sm: $NCHFS \times NCHFS \longrightarrow [0,1]$, such that

$$\begin{aligned}&\text{(i) } 0 \le sm(\alpha,\beta) \le 1,\\ &\text{(ii) } sm(\alpha,\beta) = 1 \Leftrightarrow \alpha = \beta,\\ &\text{(iii) } sm(\alpha,\beta) = sm(\beta,\alpha),\\ &\text{(iv) If } \alpha \subseteq \beta \subset \gamma, \text{then } sm(\alpha,\gamma)\\ &\le sm(\alpha,\beta) \text{ and } sm(\alpha,\gamma) \le sm(\beta,\gamma).\end{aligned} \tag{11}$$

Theorem 1. *If $d(\alpha,\beta)$ is a distance measure, then $sm(\alpha,\beta) = 1 - d(\alpha,\beta)$ is a similarity measure.*

Using the above theorem, the similarity measures based on distance measures defined in section 3.5.1 section 3.5.1 are as follows:

$$\begin{aligned}&sm_H(\alpha,\beta) = 1 - d_H(\alpha,\beta),\\ &sm_E(\alpha,\beta) = 1 - d_E(\alpha,\beta), sm_G(\alpha,\beta) = 1 - d_G(\alpha,\beta).\end{aligned} \tag{12}$$

Remark 1. We can order the NCHF values by using similarity measures as follows:

Consider the NCHF values $\alpha = (A,\lambda)$, $\beta = (B,\mu)$ and corresponding maximum ideal NCHF value $\Omega = (\{[1,1]\}, \{1,1\}\{0,0\}, \{1\}, \{1\}, \{0\})$.

$$\begin{aligned}&\text{If } sm(\alpha,\Omega) \succ sm(\beta,\Omega), \text{ then } \alpha \succ \beta,\\ &\text{If } sm(\alpha,\Omega) = sm(\beta,\Omega), \text{ then } \alpha = \beta.\end{aligned} \tag{13}$$

In the next section, we define novel Dombi exponential laws in which bases are crisp values and Table 1 exponents are NCHF values. Using these Dombi exponential laws, we define Dombi exponential aggregation operators in NCHFSs.

Example 3. If $\alpha = (\{[0.1,0.2],[0.3,0.4]\},\{[0,.1,0.3],[0,0.2]\},\{[0.6,0.7],[0.3,0.5]\},\{0.1,0.2\},\{0.2,0.3\},\{0.6,0.7\})$ and $\beta = (\{[0.6,0.8],[0.5,0.7]\},\{[0.5,0.6],[0.6,0.7]\},\{[0.1,0.2],[0,0.2]\},\{0.6,0.7\},\{0.5,0.6\},\{0.2,0.3\})$, then using (10) and (12), we have Table 1 of similarities:

5. Dombi Exponential Laws and Aggregation Operators

Definition 15. For an NCHFS $\alpha = (A,\lambda)$, scalar $q \in (0,1)$ and $\sigma > 0$, we define

$$q^{\alpha} = \left(\begin{array}{c} \left\{\left[\left(1+\left(\left(1-A^L_{j_T}\right)\left(\frac{1-q}{q}\right)^{\sigma}\right)^{1/\sigma}\right)^{-1}, \left(1+\left(\left(1-A^U_{j_T}\right)\left(\frac{1-q}{q}\right)^{\sigma}\right)^{1/\sigma}\right)^{-1}\right]\right\}, \\ \left\{\left[\left(1+\left(\left(1-A^L_{j_I}\right)\left(\frac{1-q}{q}\right)^{\sigma}\right)^{1/\sigma}\right)^{-1}, \left(1+\left(\left(1-A^U_{j_T}\right)\left(\frac{1-q}{q}\right)^{\sigma}\right)^{1/\sigma}\right)^{-1}\right]\right\}, \\ \left\{\left[1-\left(1+\left(A^L_{j_F}\left(\frac{1-q}{q}\right)^{\sigma}\right)^{1/\sigma}\right)^{-1}, 1-\left(1+\left(A^U_{j_F}\left(\frac{1-q}{q}\right)^{\sigma}\right)^{1/\sigma}\right)^{-1}\right]\right\}, \\ \left\{\left(1+\left(\left(1-\lambda_{j_T}\right)\left(\frac{1-q}{q}\right)^{\sigma}\right)^{1/\sigma}\right)^{-1}\right\}, \left\{\left(1+\left(\left(1-\lambda_{j_I}\right)\left(\frac{1-q}{q}\right)^{\sigma}\right)^{1/\sigma}\right)^{-1}\right\}, \\ \left\{1-\left(1+\left(\lambda_{j_F}\left(\frac{1-q}{q}\right)^{\sigma}\right)^{1/\sigma}\right)^{-1}\right\} \end{array} \right). \tag{14}$$

Note that if $\alpha > \beta$, then $q^{\alpha} > q^{\beta}$.

Table 1: Similarities of given values with maximum ideal.

	$sm_G(\alpha, \Omega)$	$sm_G(\beta, \Omega)$	Ranking (using Equation (12))
$q = 1$	0.277778 0	688889	$\beta > \alpha$
$q = 2$	0.25988	0.660065	$\beta > \alpha$
$q = 3$	0.244891	0.640545	$\beta > \alpha$
$q = 4$	**0.231861**	0.625411	$\beta > \alpha$
$q = 5$	0.220223	0.613145	$\beta > \alpha$

Theorem 2. *For an NCHFN $\alpha = (A, \lambda)$ and a scalar $q > 0$, q^{α} is a NCHFN.*

Theorem 3. *For two NCHFNs $\alpha = (A, \lambda)$, $\beta = (B, \mu)$ and a scalar $\varpi \in (0, 1)$, the following commutative laws hold:*

$$\begin{aligned} &\text{(i) } \varpi^{\alpha} \oplus \varpi^{\beta} = \varpi^{\beta} \oplus \varpi^{\alpha}, \\ &\text{(ii) } \varpi^{\alpha} \otimes \varpi^{\beta} = \varpi^{\beta} \otimes \varpi^{\alpha}, \end{aligned} \tag{15}$$

Theorem 4. *For three NCHFNs $\alpha = (A, \lambda)$, $\beta = (B, \mu)$, $\gamma = (C, \nu)$ and a scalar $\varpi \in (0, 1)$, the following associative laws hold:*

$$\begin{aligned} &\text{(i) } \left(\varpi^{\alpha} \oplus \varpi^{\beta}\right) \oplus \varpi^{\gamma} = \varpi^{\beta} \oplus \left(\varpi^{\alpha} \oplus \varpi^{\gamma}\right), \\ &\text{(ii) } \left(\varpi^{\alpha} \otimes \varpi^{\beta}\right) \otimes \varpi^{\gamma} = \varpi^{\beta} \otimes \left(\varpi^{\alpha} \otimes \varpi^{\gamma}\right). \end{aligned} \tag{16}$$

Definition 16. Dombi exponential aggregation operators

Let $\left\{\alpha_{(k)} = (A_{(k)}, \lambda_{(k)})\right\}$ be a collection of NCHFNs and $q_k \in (0, 1)$ be real numbers, then neutrosophic cubic hesitant fuzzy Dombi weighted exponential operator is defined as

$$NCHDWE(\alpha_1, \ldots, \alpha_n) = \bigotimes_{j=1}^{n} q^{\alpha}, \tag{17}$$

where $\alpha_{(k)} = \langle A_{(k)}, \lambda_{(k)} \rangle$ is the exponential weight of attribute values $q_k \in (0, 1)$.

Theorem 5. *Let $\left\{\alpha_{(k)} = (A_{(k)}, \lambda_{(k)})\right\}$ be a collection of NCHFS and $q_k \in (0, 1)$ be real numbers, then neutrosophic cubic hesitant fuzzy Dombi weighted exponential operator is*

$$NCHFDWE(\alpha_1, \alpha_2, \ldots, \alpha_n) = \left(\begin{array}{l} \left\{\left[\left(1 + \left(\sum_{r=1}^{n}\left(1 - A^{L}_{j_{T_{(r)}}}\right)\left(\frac{1-q_r}{q_r}\right)^{\sigma}\right)^{1/\sigma}\right)^{-1}, \left(1 + \left(\sum_{r=1}^{n}\left(1 - A^{U}_{j_{T_{(r)}}}\right)\left(\frac{1-q_r}{q_r}\right)^{\sigma}\right)^{1/\sigma}\right)^{-1}\right]\right\}, \\ \left\{\left[\left(1 + \left(\sum_{r=1}^{n}\left(1 - A^{L}_{j_{I_{(r)}}}\right)\left(\frac{1-q_r}{q_r}\right)^{\sigma}\right)^{1/\sigma}\right)^{-1}, \left(1 + \left(\sum_{r=1}^{n}\left(1 - A^{U}_{j_{I_{(r)}}}\right)\left(\frac{1-q_r}{q_r}\right)^{\sigma}\right)^{1/\sigma}\right)^{-1}\right]\right\}, \\ \left\{\left[1 - \left(1 + \left(\sum_{r=1}^{n} A^{L}_{j_{F_{(r)}}}\left(\frac{1-q_r}{q_r}\right)^{\sigma}\right)^{1/\sigma}\right)^{-1}, 1 - \left(1 + \left(\sum_{r=1}^{n} A^{U}_{j_{F_{(r)}}}\left(\frac{1-q_r}{q_r}\right)^{\sigma}\right)^{1/\sigma}\right)^{-1}\right]\right\}, \\ \left\{\left(1 + \left(\sum_{r=1}^{n}\left(1 - \lambda_{j_{T_{(r)}}}\right)\left(\frac{1-q_r}{q_r}\right)^{\sigma}\right)^{1/\sigma}\right)^{-1}\right\}, \left\{\left(1 + \left(\sum_{r=1}^{n}\left(1 - \lambda_{j_{I_{(r)}}}\right)\left(\frac{1-q_r}{q_r}\right)^{\sigma}\right)^{1/\sigma}\right)^{-1}\right\}, \\ \left\{1 - \left(1 + \left(\sum_{r=1}^{n} \lambda_{j_{F_{(r)}}}\left(\frac{1-q_r}{q_r}\right)^{\sigma}\right)^{1/\sigma}\right)^{-1}\right\} \end{array} \right), \tag{18}$$

and $\left\{\alpha_{(k)} = \langle A_{(k)}, \lambda_{(k)} \rangle\right\}$ are the exponential weights of $q_k \in (0, 1)$. Furthermore, NCHF DW $E(\alpha_1, \alpha_2, \ldots, \alpha_m)$ is also a neutrosophic cubic hesitant fuzzy value.

Proof. We use induction. For $n=2$, we have

$$NCHFDWE(\alpha_1,\alpha_2)$$

$$=\left(\begin{array}{c}\left\{\left[\left(1+\left(\left(1-A^L_{j_{T_{(1)}}}\right)\left(\frac{1-q_1}{q_1}\right)^{\sigma}+\left(1-A^L_{j_{T_{(2)}}}\right)\left(\frac{1-q_2}{q_2}\right)^{\sigma}\right)^{1/\sigma}\right)^{-1},\left(1+\left(\left(1-A^U_{j_{T_{(1)}}}\right)\left(\frac{1-q_1}{q_1}\right)^{\sigma}+\left(1-A^U_{j_{T_{(2)}}}\right)\left(\frac{1-q_2}{q_2}\right)^{\sigma}\right)^{1/\sigma}\right)^{-1}\right]\right\},\\ \left\{\left[\left(1+\left(\left(1-A^L_{j_{I_{(1)}}}\right)\left(\frac{1-q_1}{q_1}\right)^{\sigma}+\left(1-A^L_{j_{I_{(2)}}}\right)\left(\frac{1-q_2}{q_2}\right)^{\sigma}\right)^{1/\sigma}\right)^{-1},\left(1+\left(\left(1-A^U_{j_{I_{(1)}}}\right)\left(\frac{1-q_1}{q_1}\right)^{\sigma}+\left(1-A^U_{j_{I_{(2)}}}\right)\left(\frac{1-q_2}{q_2}\right)^{\sigma}\right)^{1/\sigma}\right)^{-1}\right]\right\},\\ \left\{\left[1-\left(1+\left(A^L_{j_{F_{(1)}}}\left(\frac{1-q_1}{q_1}\right)^{\sigma}+A^L_{j_{F_{(2)}}}\left(\frac{1-q_2}{q_2}\right)^{\sigma}\right)^{1/\sigma}\right)^{-1},1-\left(1+\left(A^L_{j_{F_{(1)}}}\left(\frac{1-q_1}{q_1}\right)^{\sigma}+A^L_{j_{F_{(2)}}}\left(\frac{1-q_2}{q_2}\right)^{\sigma}\right)^{1/\sigma}\right)^{-1}\right]\right\},\\ \left\{\left(1+\left(\left(1-\lambda_{j_{T_{(1)}}}\right)\left(\frac{1-q_1}{q_1}\right)^{\sigma}+\left(1-\lambda_{j_{T_{(2)}}}\right)\left(\frac{1-q_2}{q_2}\right)^{\sigma}\right)^{1/\sigma}\right)^{-1}\right\},\\ \left\{\left(1+\left(\left(1-\lambda_{j_{I_{(1)}}}\right)\left(\frac{1-q_1}{q_1}\right)^{\sigma}+\left(1-\lambda_{j_{I_{(2)}}}\right)\left(\frac{1-q_2}{q_2}\right)^{\sigma}\right)^{1/\sigma}\right)^{-1}\right\},\left\{1-\left(1+\left(\lambda_{j_{F_{(1)}}}\left(\frac{1-q_1}{q_1}\right)^{\sigma}+\lambda_{j_{F_{(2)}}}\left(\frac{1-q_2}{q_2}\right)^{\sigma}\right)^{1/\sigma}\right)^{-1}\right\}\end{array}\right). \tag{19}$$

Considering the result to be true for $n=m$ we prove it for $n=m+1$ as follows:

$$NCHDWE(\alpha_1,\ldots,\alpha_{m+1})=\bigotimes_{j=1}^{m}q^{\alpha_j}\otimes q^{\alpha}. \tag{20}$$

Using (2) and (14), we have

$$NCHFDWE(\alpha_1,\alpha_2,\ldots,\alpha_{m+1})$$

$$=\left(\begin{array}{c}\left\{\left[\left(1+\left(\sum_{r=1}^{m+1}\left(1-A^L_{j_{T_{(r)}}}\right)\left(\frac{1-q_r}{q_r}\right)^{\sigma}\right)^{1/\sigma}\right)^{-1},\left(1+\left(\sum_{r=1}^{m+1}\left(1-A^U_{j_{T_{(r)}}}\right)\left(\frac{1-q_r}{q_r}\right)^{\sigma}\right)^{1/\sigma}\right)^{-1}\right]\right\},\\ \left\{\left[\left(1+\left(\sum_{r=1}^{m+1}\left(1-A^L_{j_{I_{(r)}}}\right)\left(\frac{1-q_r}{q_r}\right)^{\sigma}\right)^{1/\sigma}\right)^{-1},\left(1+\left(\sum_{r=1}^{m+1}\left(1-A^U_{j_{I_{(r)}}}\right)\left(\frac{1-q_r}{q_r}\right)^{\sigma}\right)^{1/\sigma}\right)^{-1}\right]\right\},\\ \left\{\left[1-\left(1+\left(\sum_{r=1}^{m+1}A^L_{j_{F_{(r)}}}\left(\frac{1-q_r}{q_r}\right)^{\sigma}\right)^{1/\sigma}\right)^{-1},1-\left(1+\left(\sum_{r=1}^{m+1}A^U_{j_{F_{(r)}}}\left(\frac{1-q_r}{q_r}\right)^{\sigma}\right)^{1/\sigma}\right)^{-1}\right]\right\},\\ \left\{\left(1+\left(\sum_{r=1}^{m+1}\left(1-\lambda_{j_{T_{(r)}}}\right)\left(\frac{1-q_r}{q_r}\right)^{\sigma}\right)^{1/\sigma}\right)^{-1}\right\},\left\{\left(1+\left(\sum_{r=1}^{m+1}\left(1-\lambda_{j_{T_{(r)}}}\right)\left(\frac{1-q_r}{q_r}\right)^{\sigma}\right)^{1/\sigma}\right)^{-1}\right\},\\ \left\{1-\left(1+\left(\sum_{r=1}^{m+1}\lambda_{j_{F_{(r)}}}\left(\frac{1-q_r}{q_r}\right)^{\sigma}\right)^{1/\sigma}\right)^{-1}\right\}\end{array}\right). \tag{21}$$

□

6. Applications of Neutrosophic Cubic Hesitant Fuzzy Dombi Weighted Exponential Aggregation Operators to MADM Problems

Many methods in MADM ignore the uncertainty and hence yield the results that are unreliable. In this section, we construct algorithm using the Dombi exponential aggregation operators (NCHFDWEs) for MADM problems.

6.1. Solid Waste Disposal Site Selection. Due to population increase and urbanization, the proper disposal of waste is a challenging problem nowadays. The proper disposal of waste is necessary for the prevention of viral diseases like typhoid, dengue, and tuberculosis. Using the above algorithm to select the best alternative (solid waste disposal site) among the given alternatives (sites) $K_1, \ldots, K_5$ on the basis of attributes (i) F_1 water pollution; (ii) F_2 slope; (iii) F_3 distance from the residential area.

The decision matrix $D = (d_{ij})_{5\times 3}$, where entry d_{ij} represents the preference of alternative $K_i\,(i = 1, \ldots, 5)$ corresponding to attribute $F_j\,(j = 1, 2, 3)$, is constructed using fuzzy values with the help of the following scale.

Equal preference: 0.1, moderate preference: 0.3, strong preference: 0.5, demonstrated preference: 0.7, and extreme preference: 0.9. The mean values between the two assessments: 0.2, 0.4, 0.6, and 0.8.

$$D = \begin{bmatrix} 0.2 & 0.2 & 0.4 \\ 0.8 & 0.8 & 0.7 \\ 0.3 & 0.3 & 0.2 \\ 0.8 & 0.5 & 0.6 \\ 0.6 & 0.7 & 0.6 \end{bmatrix}. \tag{22}$$

The weights of the attributes are given as

$$w_1 = \begin{pmatrix} \{[0.3, 0.7], [0.2, 0.4]\}, \\ \{[0.2, 0.5], [0.1, 0.6]\}, \\ \{[0.2, 0.4], [0, 0.1]\}, \\ \{0.5, 0.6\}, \{0.2, 0.4\}, \{0.2, 0.3\} \end{pmatrix},$$

$$w_2 = \begin{pmatrix} \{[0.5, 0.7], [0.2, 0.5]\}, \\ \{[0.2, 0.3], [0.1, 0.6]\}, \\ \{[0.1, 0.4], [0, 0.3]\}, \\ \{0.4, 0.5\}, \{0.3, 0.4\}, \{0.2, 0.4\} \end{pmatrix}, \tag{23}$$

$$w_3 = \begin{pmatrix} \{[0.4, 0.5], [0.6, 0.7]\}, \\ \{[0.1, 0.3], [0.2, 0.5]\}, \\ \{[0.1, 0.2], [0.3, 0.4]\}, \\ \{0.3, 0.5\}, \{0.4, 0.6\}, \{0.3, 0.4\} \end{pmatrix}.$$

The explanation of weights is elaborated as follows.

In the case of w_1, {[0.3, 0.7], [0.2, 0.4]} is the interval hesitant degree of preference for attribute F_1, {[0.2, 0.5], [0.1, 0.6]} is the interval hesitant degree of indeterminacy (preference/nonpreference) for attribute F_1, {[0.2, 0.4], [0, 0.1]} is the interval hesitant degree of nonpreference for an attribute F_1, {0.1, 0.6}} is hesitant degree of preference for attribute F_1, {0.2, 0.4} is hesitant degree of indeterminacy (preference/nonpreference) for an attribute F_1, and {0.4, 0.6} is the hesitant degree of nonpreference for attribute F_1.

Aggregated values of alternatives using NCHFDWE operators ((17)) with $\sigma = 1$:

$$d_1 = \begin{pmatrix} \{[0.149254, 0.240964], [0.125, 0.17094]\}, \\ \{[0.114286, 0.145985], [0.106383, 0.20202]\}, \\ \{[0.574468, 0.777778], [0.310345, 0.6875]\}, \\ \{0.155039, 0.186916\}, \{0.126582, 0.15625\}, \\ \{0.672131, 0.75\} \end{pmatrix},$$

$$d_2 = \begin{pmatrix} \{[0.642202, 0.732984], [0.636364, 0.712468]\}, \\ \{[0.56, 0.625], [0.557769, 0.707071]\}, \\ \{[0.105431, 0.222222], [0.113924, 0.213483]\}, \\ \{0.634921, 0.694789\}, \{0.612691, 0.679612\}, \\ \{0.186047, 0.243243\} \end{pmatrix},$$

$$d_3 = \begin{pmatrix} \{[0.16129, 0.227273], [0.157895, 0.20979]\}, \\ \{[0.12, 0.151515], [0.119048, 0.205479]\}, \\ \{[0.52381, 0.727273], [0.545455, 0.716981]\}, \\ \{0.157068, 0.196078\}, \{0.144928, 0.185185\}, \\ \{0.680851, 0.75\} \end{pmatrix},$$

$$d_4 = \begin{pmatrix} \{[0.481928, 0.585366], [0.441176, 0.540541]\}, \\ \{[0.384615, 0.436364], [0.376176, 0.545455]\}, \\ \{[0.178082, 0.387755], [0.166667, 0.371728]\}, \\ \{0.456274, 0.517241\}, \{0.434783, 0.495868\}, \\ \{0.310345, 0.390863\} \end{pmatrix},$$

$$d_5 = \begin{pmatrix} \{[0.480549, 0.601719], [0.466667, 0.551181]\}, \\ \{[0.403846, 0.47619], [0.396975, 0.564516]\}, \\ \{[0.195402, 0.363636], [0.166667, 0.315961]\}, \\ \{0.486111, 0.551181\}, \{0.447761, 0.519802\}, \\ \{0.295302, 0.373134\} \end{pmatrix}. \tag{24}$$

Scores $S(d_i)$are given using equation (5).

$$\begin{aligned} &S(d_1) = 0.2213, S(d_2) = 0.7043, S(d_3) = 0.2226, \\ &S(d_4) = 0.5456, S(d_5) = 0.5655. \end{aligned} \tag{25}$$

So $K_2 > K_5 > K_4 > K_3 > K_1$.

Similarity measures $sm_G(d_i)$ are given using (10) and (12).

Figure 1 is the graphical representation of score and similarity measures of aggregated values obtained in Table 2.

Aggregated values of alternatives using the NCHFDWE operators (equation (15)) with $\sigma = 2$:

$$d_1 = \begin{pmatrix} \{[0.180727, 0.233923], [0.162659, 0.189576]\}, \\ \{[0.159848, 0.179922], [0.153099, 0.211344]\}, \\ \{[0.691515, 0.784485], [0.451027, 0.729865]\}, \\ \{0.185911, 0.202422\}, \{0.165703, 0.182372\}, \\ \{0.726768, 0.764172\} \end{pmatrix},$$

$$d_2 = \begin{pmatrix} \{[0.699128, 0.735492], [0.705967, 0.739685]\}, \\ \{[0.660032, 0.68909], [0.662536, 0.726421]\}, \\ \{[0.161537, 0.227505], [0.190112, 0.238848]\}, \\ \{0.692421, 0.722115\}, \{0.688889, 0.721856\}, \\ \{0.220591, 0.24988\} \end{pmatrix},$$

$$d_3 = \begin{pmatrix} \{[0.199337, 0.229538], [0.204612, 0.233392]\}, \\ \{[0.172194, 0.191898], [0.173794, 0.221482]\}, \\ \{[0.406748, 0.764784], [0.382966, 0.688361]\}, \\ \{0.194328, 0.217786\}, \{0.191753, 0.217567\}, \\ \{0.648489, 0.799751\} \end{pmatrix},$$

$$d_4 = \begin{pmatrix} \{[0.526252, 0.5762], [0.496575, 0.549739]\}, \\ \{[0.472136, 0.494814], [0.466126, 0.55417]\}, \\ \{[0.283751, 0.417541], [0.267479, 0.41028]\}, \\ \{0.50742, 0.53636\}, \{0.497934, 0.525506\}, \\ \{0.370307, 0.413368\} \end{pmatrix},$$

$$d_5 = \begin{pmatrix} \{[0.549964, 0.609449], [0.548009, 0.587782]\}, \\ \{[0.512821, 0.551397], [0.510304, 0.592385]\}, \\ \{[0.28031, 0.368373], [0.267479, 0.344956]\}, \\ \{0.554875, 0.587782\}, \{0.535767, 0.573149\}, \\ \{0.337256, 0.377007\} \end{pmatrix}. \tag{26}$$

Scores $S(d_i)$ are given using equation (5):

$$\begin{aligned} &S(d_1) = 0.2210, S(d_2) = 0.7296, \\ &S(d_3) = 0.2290, S(d_4) = 0.5590, S(d_5) = 0.5948, \\ &K_2 > K_5 > K_4 > K_3 > K_1. \end{aligned} \tag{27}$$

Similarity measures $sm_G(d_i)$ are given using (10) and (12).

Figure 2 is the graphical representation of score and similarity measures of aggregated values obtained in Table 3.

Aggregated values of alternatives using NCHFDWE operators (equation (15)) with $\sigma = 3$:

Step 1: Identification of alternatives and attributes.
Let $\{K_1, K_2, \ldots, K_r\}$, be the set of r alternatives, $\{F_1, F_2, \ldots, F_s\}$ be s attributes. The NCHFS α_j is used as weight for the attribute F_j. A decision matrix is $D = (d_{ij})$ consisting fuzzy values, where d_{ij} represent the preference of alternative K_i corresponding to attribute F_j.
Step 2. Allocation of weights to attributes
The NCHF value α_j is used as weight assigned to attribute F_j.
Step 3. Computation of weighted aggregated values
Using NCHFDWE operators (equation (18)), we compute the aggregated values $d_j's$ $(j = 1, \ldots, r)$ of alternatives $K_j's$.
Step 4. Ranking of Alternatives
We calculate the scores and similarity measures $S(d_j), sm(d_j, \Omega)$; $j = 1, \ldots, r$ of the alternatives $K_j; i = 1, \ldots, r$ using equations (5), (10) and (14). Using scores and similarity measures, we rank the alternatives $K_i; i = 1, \ldots, n$. If scores of two alternatives are equal, then, we use accuracy function for ranking and if they have same accuracy, we use certainty.

Algorithm 1: Algorithm using the dombi exponential aggregation operators (NCHFDWE) for MADM problems.

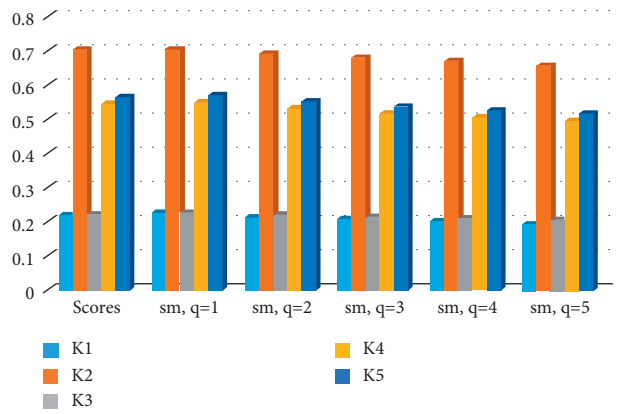

Figure 1: Graphical representation of scores and similarity measures with $\boldsymbol{\sigma} = 1$.

Table 2: Similarity measures of aggregated values using the NCHFDWE operators with $\boldsymbol{\sigma} = 1$.

	$sm_G(d_1, \Omega)$	$sm_G(d_2, \Omega)$	$sm_G(d_3, \Omega)$	$sm_G(d_3, \Omega)$	$sm_G(d_4, \Omega)$	Ranking
$q = 1$	0.228189	0.706196	0.227288	0.549464	0.568689	$K_2 > K_5 > K_4 > K_3 > K_1$
$q = 2$	0.215779	0.690722	0.220804	0.531238	0.551364	$K_2 > K_5 > K_4 > K_3 > K_1$
$q = 3$	0.206874	0.678439	0.21519	0.517484	0.537774	$K_2 > K_5 > K_4 > K_3 > K_1$
$q = 4$	0.200116	0.668399	0.210311	0.506618	0.526813	$K_2 > K_5 > K_4 > K_3 > K_1$
$q = 5$	0.19473	0.659948	0.206046	0.49767	0.51771	$K_2 > K_5 > K_4 > K_3 > K_1$

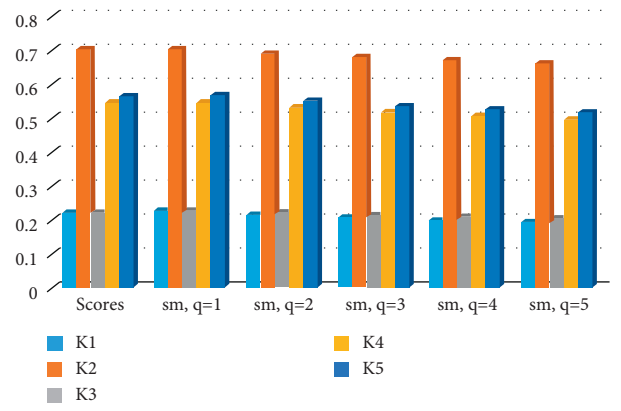

Figure 2: Graphical representation of scores and similarity measures with $\boldsymbol{\sigma} = 2$.

Table 3: Similarity measures of aggregated values using the NCHFDWE operators with $\boldsymbol{\sigma} = 2$.

	$sm_G(d_1, \Omega)$	$sm_G(d_2, \Omega)$	$sm_G(d_3, \Omega)$	$sm_G(d_3, \Omega)$	$sm_G(d_4, \Omega)$	Ranking
$q = 1$	0.246277	0.730842	0.230984	0.557806	0.596572	$K_2 > K_5 > K_4 > K_3 > K_1$
$q = 2$	0.236448	0.726767	0.229542	0.551832	0.591733	$K_2 > K_5 > K_4 > K_3 > K_1$
$q = 3$	0.228268	0.723121	0.228174	0.546761	0.587395	$K_2 > K_5 > K_4 > K_3 > K_1$
$q = 4$	0.209457	0.719847	0.226876	0.542419	0.583509	$K_2 > K_5 > K_4 > K_3 > K_1$
$q = 5$	0.217899	0.716883	0.225643	0.538656	0.58002	$K_2 > K_5 > K_4 > K_3 > K_1$

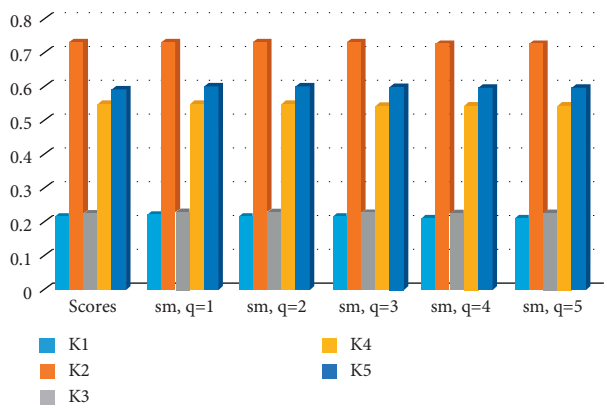

Figure 3: Graphical representation of scores and similarity measures with $\boldsymbol{\sigma} = 3$.

$$d_1 = \begin{pmatrix} \{[0.189119, 0.226119], [0.175473, 0.194219]\}, \\ \{[0.174696, 0.188901], [0.169392, 0.0.174524]\}, \\ \{[0.729242, 0.788562], [0.501035, 0.749884]\}, \\ \{0.193244, 0.20411\}, \{0.178227, 0.189559\}, \\ \{0.749095, 0.773387\} \end{pmatrix},$$

$$d_2 = \begin{pmatrix} \{[0.712208, 0.732458], [0.722704, 0.743899]\}, \\ \{[0.68604, 0.704447], [0.689676, 0.728379]\}, \\ \{[0.188605, 0.233444], [0.222939, 0.251172]\}, \\ \{0.705929, 0.726416\}, \{0.707496, 0.730469\}, \\ \{0.236791, 0.256193\} \end{pmatrix},$$

$$d_3 = \begin{pmatrix} \{[0.20958, 0.226801], [0.218287, 0.237351]\}, \\ \{[0.189706, 0.203424], [0.192323, 0.223189]\}, \\ \{[0.406748, 0.764784], [0.382966, 0.688361]\}, \\ \{0.204582, 0.221478\}, \{0.205815, 0.22503\}, \\ \{0.648489, 0.799751\} \end{pmatrix},$$

$$d_4 = \begin{pmatrix} \{[0.445183, 0.588428], [0.391659, 0.530621]\}, \\ \{[0.303378, 0.385061], [0.291323, 0.536908]\}, \\ \{[0.152128, 0.374173], [0.142083, 0.352469]\}, \\ \{0.412698, 0.500953\}, \{0.379002, 0.470432\}, \\ \{0.285738, 0.422203\} \end{pmatrix},$$

$$d_5 = \begin{pmatrix} \{[0.430671, 0.597105], [0.407249, 0.528306]\}, \\ \{[0.315454, 0.422037], [0.304401, 0.547489]\}, \\ \{[0.172143, 0.361839], [0.142083, 0.304007]\}, \\ \{0.437361, 0.528306\}, \{0.381049, 0.484407\}, \\ \{0.278734, 0.39362\} \end{pmatrix}. \tag{28}$$

Scores $S(d_i)$ are given using equation (5):

$$S(d_1) = 0.2185, S(d_2) = 0.7324, S(d_3) = 0.2288,$$
$$S(d_4) = 0.5497, S(d_5) = 0.5922, \tag{29}$$
$$K_2 > K_5 > K_4 > K_3 > K_1.$$

Similarity measures $sm_G(d_i)$ are given using (10) and (12):

Figure 3 is the graphical representation of score and similarity measures of aggregated values obtained in Table 4.

It can be seen from Figures 1–3, that we obtain the same ranking with respect to different choices of parameters q and σ. Hence the most desirable alternative is K_2.

6.2. Comparative Analysis. To check the validity of results, the above problem is solved by different existing techniques proposed in [36, 46]. The results obtained by these existing methods are similar to those obtained from this study in Tables 2–4.

7. Conclusion

First, the Dombi algebraic operations distance and similarity measures in neutrosophic cubic hesitant fuzzy sets are defined. Then the properties of these notions are discussed. Furthermore, the novel Dombi exponential laws and Dombi exponential aggregation operators are proposed. The Dombi exponential laws are more flexible than the usual exponential laws as they involve an operational parameter. Using these aggregation operators, we established a MADM method. The proper disposal of waste is necessary for the prevention of viral diseases like typhoid, dengue, and tuberculosis. The solid waste disposal site selection problem is solved using the proposed MADM method. To discuss the effectiveness of the

Table 4: Similarity measures of aggregated values using the NCHFDWE operators with $\boldsymbol{\sigma} = 3$.

	$sm_G(d_1, \Omega)$	$sm_G(d_2, \Omega)$	$sm_G(d_3, \Omega)$	$sm_G(d_3, \Omega)$	$sm_G(d_4, \Omega)$	Ranking
$q = 1$	0.222346	0.733388	0.230072	0.551843	0.602963	$K_2 > K_5 > K_4 > K_3 > K_1$
$q = 2$	0.218951	0.731571	0.229472	0.548685	0.600807	$K_2 > K_5 > K_4 > K_3 > K_1$
$q = 3$	0.216225	0.729881	0.228891	0.545899	0.598787	$K_2 > K_5 > K_4 > K_3 > K_1$
$q = 4$	0.214005	0.728307	0.228328	0.543433	0.5969	$K_2 > K_5 > K_4 > K_3 > K_1$
$q = 5$	0.212168	0.726835	0.227783	0.541232	0.595128	$K_2 > K_5 > K_4 > K_3 > K_1$

proposed method, different values of parameters are considered to check the efficiency of the proposed method. At last, the comparative analysis is presented for validation of proposed operators and methods.

For further research, the neutrosophic cubic hesitant fuzzy Dombi arithmetic and geometric aggregation operators and multiexpert decision-making methods using these aggregation operators will be developed. The Dombi Bonferroni mean operators of neutrosophic cubic hesitant fuzzy sets will be established. The Dombi exponential laws and Dombi exponential aggregation operators for Pythagorean fuzzy sets and picture hesitant fuzzy sets will be established [51–54, 56–60].

7.1. Limitations of the Proposed Study. As Dombi operations and generalized similarity measures involve operational parameters, the manual calculation is very complicated and time-consuming. Hence there is a need to develop a software program for such computations. Furthermore, for MADM problems involving more alternatives and attributes handled by Dombi exponential aggregation operators, software programming is needed. We are trying to develop such programming using PYTHON.

Data Availability

No data were used to support the study.

Conflicts of Interest

The authors declare that they have no conflicts of interest.

Acknowledgments

The authors express their appreciation to the Deanship of Scientific Research at King Khalid University for funding this work through the public research project (R.G.P.1/277/43).

References

[1] L. A. Zadeh, "Fuzzy sets," *Information and Control*, no. 3, pp. 338–353, 1965.

[2] L. A. Zadeh, "Outlines of New Approach to the Analysis of Complex System and Dicision Processes Interval Valued Fuzzy Sets," *IEEE Trans*, vol. 3, 1968.

[3] I. B. Turksen and T. Bilgic, "Interval valued strict preference with Zadeh triples," *Fuzzy Sets and Systems*, no. 2, pp. 183–195, 1996.

[4] S. J. Chen and C. L. Hwang, *Fuzzy multiple attribute decision-making, methods and applications Lecture Notes in Economics and Mathematical Systems*, Springer-, Berlin/Heidelberg, 1992.

[5] T. H. Chang and T. C. Wang, "Using the fuzzy multi-criteria decision making approach for measuring the possibility of successful knowledge management," *Information Sciences*, no. 4, pp. 355–370, 2009.

[6] S. P. Kalyan Mondal and K. Mondal, "Weighted fuzzy similarity measure based on tangent function and its application to medical diagnosis," *International Journal of Innovative Research in Science, Engineering and Technology*, vol. 04, no. 02, pp. 158–164, 2015.

[7] C. T. Chen, "Extensions of the TOPSIS for group decision-making under fuzzy environment," *Fuzzy Sets and Systems*, no. 1, pp. 1–9, 2000.

[8] G. Zhang and J. Lu, "An integrated group decision-making method dealing with fuzzy preferences for alternatives and individual judgments for selection criteria," *Group Decision and Negotiation*, no. 6, pp. 501–515, 2003.

[9] R. A. Krohling and V. C. Campanharo, "Fuzzy TOPSIS for group decision making: a case study for accidents with oil spill in the sea," *Expert Systems with Applications*, no. 4, pp. 4190–4197, 2011.

[10] M. Xia and Z. Xu, "A novel method for fuzzy multi-criteria decision making," *International Journal of Information Technology and Decision Making*, no. 03, pp. 497–519, 2014.

[11] M. K. Mehlawat and P. Gupta, "A new fuzzy group multi-criteria decision making method with an application to the critical path selection," *International Journal of Advanced Manufacturing Technology*, no. 5-8, pp. 1281–1296, 2016.

[12] Y. B. Jun, C. S. Kim, and K. O. Yang, "Cubic sets," *Ann. Fuzzy Math. Inform*, no. 1, pp. 83–98, 2012.

[13] Y. B. Jun, C. S. Kim, and M. S. Kang, "Cubic sub algebras and ideals of BCK/BCI-algebras, Far East," *Journal of Mathematical Sciences*, no. 44, pp. 239–250, 2010.

[14] Y. B. Jun, C. S. Kim, and J. G. Kang, "Cubic q-ideals of BCI-algebras," *Ann. Fuzzy Math. Inform.*, no. 1, pp. 25–34, 2011.

[15] Y. B. Jun, K. J. Lee, and M. S. Kang, "Cubic structures applied to ideals of BCI-algebras," *Computers & Mathematics with Applications*, no. 9, pp. 3334–3342, 2011.

[16] F. Smarandache, *A Unifying Field in Logics Neutrosophy: Neutrosophic Probability, Set and Logic*, American Research Press, Rehoboth, 1999.

[17] H. Wang, F. Smarandache, Y. Q. Zhang, and R. Sunderraman, *Single Valued Neutrosophic Sets*, pp. 410–413, Multispace Multistructure, 2010.

[18] H. Wang, F. Smarandache, Y. Q. Zhang, and R. Sunderraman, *Interval Neutrosophic Sets and Logics*, Hexis, Phoenix, USA, 2005.

[19] A. Kharal, "A neutrosophic multi-criteria decision making method," *New Mathematics and Natural Computation*, no. 02, pp. 143–162, 2014.

[20] J. Ye, "Similarity measures between interval neutrosophic sets and their applications in multicriteria decision-making,"

Journal of Intelligent and Fuzzy Systems, no. 1, pp. 165–172, 2014.

[21] J. Ye, "Multiple attribute group decision-making method with completely unknown weights based on similarity measures under single valued neutrosophic environment," *Journal of Intelligent and Fuzzy Systems*, no. 6, pp. 2927–2935, 2014.

[22] K. Mondal and S. Pramanik, "Multi-criteria group decision making approach for teacher recruitment in higher education under simplified neutrosophic environment," *Neutrosophic Sets Syst*, no. 6, pp. 28–34, 2014.

[23] P. Biswas, S. Pramanik, and B. C. Giri, "Entropy based grey relational analysis method for multi-attribute decision making under single valued neutrosophic assessments," *Neutrosophic Sets Syst*, no. 2, pp. 102–110, 2014.

[24] P. Biswas, S. Pramanik, and B. C. Giri, "A new methodology for neutrosophic multi-attribute decision-making with unknown weight information," *Neutrosophic Sets Syst*, no. 3, pp. 44–54, 2014.

[25] P. Biswas, S. Pramanik, and B. C. Giri, "Cosine similarity measure based multi-attribute decision-making with trapezoidal fuzzy neutrosophic numbers," *Neutrosophic Sets Syst*, no. 8, pp. 46–56, 2014.

[26] K. Mondal and S. Pramanik, "Neutrosophic decision making model for clay-brick selection in construction field based on grey relational analysis," *Neutrosophic Sets Syst*, no. 9, pp. 64–71, 2015.

[27] B. Li, J. Wang, L. Yang, and X. Li, "A novel generalized simplified neutrosophic number einstein aggregation operator," *International Journal of Applied mathematics*, no. 48, pp. 67–72, 2018.

[28] J. Zhan, M. Khan, M. Gulistan, and A. Ali, "Applications of neutrosophic cubic sets in multi-criteria decision-making," *International Journal for Uncertainty Quantification*, no. 5, pp. 377–394, 2017.

[29] V. Torra, "Hesitant fuzzy sets," *International Journal of Intelligent Systems*, vol. 25, pp. 529–539, 2010.

[30] Y. B. Jun, F. Smarandache, and C. S. Kim, "Neutrosophic cubic sets," *New Mathematics and Natural Computation*, 2015.

[31] F. Mehmood, T. Mahmood, and Q. Khan, "Cubic hesitant fuzzy sets and their applications to multi criteria decision making," *International Journal of Algebra and Statistics*, vol. 5, pp. 19–51, 2016.

[32] J. Ye, "Multiple-attribute decision-making method under a single-valued neutrosophic hesitant fuzzy environment," *Journal of Intelligent Systems*, vol. 24, no. 1, pp. 23–36, 2015.

[33] P. Liu and L. Shi, "The generalized hybrid weighted average operator based on interval neutrosophic hesitant set and its application to multiple attribute decision making," *Neural Computing & Applications*, vol. 26, no. 2, pp. 457–471, 2015.

[34] B. Zhu, Z. S. Xu, and J. P. Xu, "Deriving a ranking from hesitant fuzzy preference relations under group decision making," *IEEE Transactions on Cybernetics*, vol. 44, no. 8, pp. 1328–1337, 2014.

[35] Z. Lu and J. Ye, "Exponential Operations and an Aggregation Method for Single-Valued Neutrosophic Numbers in Decision Making," *Information*, 2017.

[36] R. Tan, W. Zhang, and S. Chen, "Exponential aggregation operator of interval neutrosophic numbers and its application in typhoon disaster evaluation," *Symmetry*, 2018.

[37] R. Wang, Y. Li, and C. Chen, *Picture Hesitant Fuzzy Set and Its Application to Multiple Criteria Decision-Making, Symmetry*, vol. 10, 2018.

[38] N. H. Shah, K. Rabari, and E. Patel, "A deteriorating inventory model under overtime production and credit policy for stock- and price sensitive demand function Operational Research in Engineering Sciences: Theory and Applications," 2022.

[39] R. Tan and W. Zhang, "Multiple attribute group decision making methods based on trapezoidal fuzzy neutrosophic numbers," *Journal of Intelligent and Fuzzy Systems*, vol. 33, no. 4, pp. 2547–2564, 2017.

[40] L. Feng, F. Chuan-qiang, and X. Wei-he, "Type-2 hesitant fuzzy sets," *Fuzzy Information and Engineering*, vol. 10, no. 2, pp. 249–259, 2018.

[41] E. Turkarslan, J. Ye, M. Unver, and M. Olgun, "Consistency fuzzy sets and a cosine similarity measure in fuzzy multiset setting and application to medical diagnosis," *Mathematical Problems in Engineering*, vol. 2021, p. 1, 2021.

[42] J. Dombi, "A general class of fuzzy operators, the demorgan class of fuzzy operators and fuzziness measures induced by fuzzy operators," *Fuzzy Sets and Systems*, vol. 8, no. 2, pp. 149–163, 1982.

[43] L. Shi and J. Ye, "Dombi Aggregation Operators of Neutrosophic Cubic Sets for Multiple Attribute Decision Making," *algorithms*, vol. 11, 2018.

[44] P. D Liu, J. L. Liu, and S. M. Chen, "Some intuitionistic fuzzy Dombi Bonferroni mean operators and their application to multi-attribute group decision making," *Journal of the Operational Research Society*, 2017.

[45] J. Q. Chen and J. Ye, "Some single-valued neutrosophic Dombi weighted aggregation operators for multiple attribute decision-making," *Symmetry*, vol. 9, no. 6, p. 82, 2017.

[46] A. Bhattacharya, A. Dutta, and S. Kar, "Does demographics influence the risk behaviour of urban investors? A machine learning model based approach," *Operational Research in Engineering Sciences: Theory and Applications*, 2022.

[47] S. Biswas, G. Bandyopadhyay, B. Guha, and M. Bhattacharjee, "An ensemble approach for portfolio selection in a multi-criteria decision making framework," *Decision Making: Applications in Management and Engineering*, vol. 2, no. 2, pp. 138–158, 2019.

[48] A. Rehman, M. Guistan, Z. Khan, and F. S. Al-Duas, "A study of neutrosophic cubic hesitant fuzzy hybrid geometric aggregation operators and its application to multi expert decision making system," *Neutrosophic Sets Syst*, vol. 50, pp. 83–110, 2022.

[49] A. Ashraf, K. Ullah, A. Hussain, and M. Bari, "Interval-valued picture fuzzy Maclaurin symmetric mean operator with application in multiple attribute decision-making," *Reports in Mechanical Engineering*, vol. 3, no. 1, pp. 301–317, 2022.

[50] M. Riaz and H. M. A. Farid, "Picture fuzzy aggregation approach with application to third-party logistic provider selection process," *Reports in Mechanical Engineering*, vol. 3, no. 1, pp. 318–327, 2022.

[51] M. I. Youssef and B. Webster, "A multi-criteria decision making approach to the new product development process in industry," *Reports in Mechanical Engineering*, vol. 3, no. 1, pp. 83–93.

[52] A. Mešić, S. Miškić, Ž. Stević, and Z. Mastilo, "Hybrid MCDM solutions for evaluation of the logistics performance

index of the western Balkan countries," *Economics - Innovative and Research Journal*, vol. 10, no. 1, pp. 13–34, 2022.

[53] B. F. Yildirim and S. K. Yıldırım, "Evaluating the satisfaction level of citizens in municipality services by using picture fuzzy VIKOR method: 2014-2019 period analysis," *Decision Making: Applications in Management and Engineering*, vol. 5, no. 1, pp. 50–66, 2022.

[54] S. Kumar, S. R. Maity, and L. Patnaik, "Optimization of wear parameters for duplex-tiain coated MDC-K tool steel using fuzzy MCDM techniques," *Operational Research in Engineering Sciences: Theory and Applications*, 2022.

[55] K. T. Atanassov, "Intuitionistic fuzzy sets," *Fuzzy Sets and Systems*, no. 1, pp. 87–96, 1986.

[56] K. Atanassov and G. Gargov, "Interval valued intuitionistic fuzzy sets," *Fuzzy Sets and Systems*, no. 3, pp. 343–349, 1989.

[57] Z. Xu, "Some similarity measures of intuitionistic fuzzy sets and their applications to multiple attribute decision making," *Fuzzy Optimization and Decision Making*, no. 2, pp. 109–121, 2007.

[58] K. Mondal and S. Pramanik, "Intuitionistic fuzzy multi criteria group decision making approach to quality-brick selection problem," *J. Appl. Quant. Methods*, no. 9, pp. 35–50, 2014.

[59] P. P. Dey, S. Pramanik, and B. C. Giri, "Multi-criteria group decision making in intuitionistic fuzzy environment based on grey relational analysis for weaver selection in Khadi institution," *J. Appl. Quant. Methods*, no. 10, pp. 1–14, 2015.

[60] D. Pamucar, D. Bozanic, A. puska, and D. Marinkovic, "Application of Neuro-Fuzzy system for predicting the success of a company in public procurement," *Decision Making: Applications in Management and Engineering*, vol. 5, no. 1, pp. 135–153.

Hindawi
Complexity
Volume 2022, Article ID 9073503, 12 pages
https://doi.org/10.1155/2022/9073503

WILEY | Hindawi

Research Article

Soft Relations Applied to the Substructures of Quantale Module and Their Approximation

Saqib Mazher Qurashi,[1] **Khushboo Zahra Gilani**,[1] **Muhammad Shabir**,[2] **Muhammad Gulzar**,[1] **and Ashraful Alam**[3]

[1]*Department of Mathematics, Government College University Faisalabad, Faisalabad 38000, Pakistan*
[2]*Department of Mathematics, Quaid-e-Azam University Islamabad, Islamabad, Pakistan*
[3]*Department of Mathematics, Jahangirnagar University, Savar, Dhaka, Bangladesh*

Correspondence should be addressed to Ashraful Alam; ashraf_math20@juniv.edu

Received 2 July 2022; Revised 4 August 2022; Accepted 17 August 2022; Published 26 September 2022

Academic Editor: Zeljko Stevic

This research article offers a study on a new relation of rough sets and soft sets with an algebraic structure quantale module by using soft reflexive and soft compatible relations. The lower approximation and upper approximation of subsets of quantale module are utilized by aftersets and foresets. As a sequel of this relation, different characterizations of rough soft substructures of quantale modules are obtained. To ensure the results, soft reflective and soft compatible relations are focused and these are interpreted by aftersets and foresets. Furthermore, the algebraic relations between upper (lower) approximation of substructures of quantale module and the upper (lower) approximations of their homomorphic images with the help of quantale module homomorphism are examined. In comparison with the different type of approximations in different type of algebraic structures, it is concluded that this new study is much better.

1. Introduction

The quantale module has piqued the interest of many researchers since it was first proposed by Abramsky and Vickers [1]. The concept of a quantale module was inspired by the concept of module over a ring. Rings are replaced by quantales, while abelian groups are replaced by complete lattices. For the first time, the concept of quantale module appeared out of nowhere as the central concept in Abramsky and Vickers' unified treatment of process semantics. Mulvey [2] proposed the Quantale theory. It is defined on the basis of a complete lattice as an algebraic structure.

Pawlak developed the famous rough set theory [3], which deals with inadequate knowledge. The rough set deals with the categorization and investigation of inadequate information and knowledge. After Pawlak's work, some contributions and a new view on rough set theory were suggested by Zhu [4]. In [5], some properties and characterization of generalized rough sets were presented by Ali et al. Rough sets are now used in a variety of fields, including cognitive sciences, machine learning, pattern recognition, and process control.

Rough sets theory was brought to algebraic structures and soft algebraic structures by a number of authors. Iwinski explored rough set algebraic characteristics [6]. In Q-module [7], Qurashi and Shabir presented the concept of roughness. Xiao and Li [8] proposed the concept of generalized rough quantales (subquantales). Yang and Xu examined rough ideals (prime, semi prime) in quantales [9]. Luo and Wang [10] introduced fuzzy ideals and its type in quantales. Generalized roughness of fuzzy substructures in quantale based on soft relation was studied by Qurashi et al. [11]. Topological structures of lower and upper rough subsets in a hyperring were introduced by Abughazalah et al. [12]. In [13], criteria selection and decision making of hotels using dominance-based rough set theory were presented. Approximations of substructures in partially ordered LA-semihypergroups were presented by Yaqoob and Tang [14].

In [15], roughness of bipolar soft sets and their related applications are discussed. In [16], Feng et al. presented the relationship between soft and rough sets and proposed rough soft sets and soft rough sets. Integrated Best-Worst Method in terms of Green supplier selection based on the information system performance was suggested by Fazlollahtabar and Kazemitash [17].

Many issues emerge in different fields such as engineering, economics, and social sciences where data have some degree of ambiguity. Because well-known mathematical tools are designed for certain situations, they have numerous restrictions. Many theories exist to deal with uncertainty, such as fuzzy set theory, probability theory, rough sets, and ambiguous sets, but they are constrained by their design.

Molodtsov introduced the concept of soft set [18], which is a mathematical tool for overcoming the problems that plague the above theories. Soft set theory is a general mathematical technique for dealing with items that are unclear, imprecise, or not precisely defined. Many authors offer different set operations and attempt to unify the algebraic aspects of soft sets like Maji et al. [19]. A new and different idea of operations was presented by Ali et al. [20]. Soft sets and algebraic structures were combined in various ways by researchers like soft intersection semigroups [21]. Soft linear programming and applications of soft vector spaces were presented in [22]. Khan et al. applied uni-soft structures to ordered Γ-Semihypergroups [23]. Complex intuitionistic fuzzy algebraic structures in groups were introduced by Gulzar et al. [24]. Development of a rough-MABAC-DoE-based metamodel for supplier selection in an iron and steel industry was introduced by Chattopadhyay et al. [25].

The central theme and objective of soft sets is to capture the essence of parametrization, which has been adapted to the creation of soft binary relations (SBRs), which are a parameterized collection of binary relations on a universe of interest. This mentioned the problem of complicated objects that can be interpreted differently from different perspectives.

By using aftersets and foresets and then notions associated to soft binary relation (SBR), a new method of approximation space is widely utilized these days. By using generalized approximation space based on SBR, different soft substructures in semigroups were approximated by Kanawal and Shabir [26]. Motivated by the idea in [26], soft substructures in quantale module are defined and the aftersets and foresets are employed to construct the lower approximation and upper approximation of soft substructures. Since we are dealing with approximation of soft subsets of quantale, further soft substructures are employed for further characterization.

A new generalized approximation space is commonly used these days by utilizing the aftersets and foresets notions related with soft binary relations. Kanawal and Shabir [26] approximated different soft substructures in semigroups using a generalized approximation space based on soft binary relations. Roughness of intuitionistic fuzzy sets by soft relations was discussed by Anwar et al. [27]. Roughness of Pythagorean fuzzy sets based on soft binary relations was proposed in [28] by Bilal and Shabir. Using soft relations, soft substructures were defined by Zhou et al. [29] and these were approximated by soft relations. Soft substructures in quantale modules are defined in this paper, and aftersets and foresets are used to construct the lower and upper approximation of substructures, respectively.

The following scheme is for the remainder of the paper. Section 2 connects some key explanations about quantale modules, their substructures, soft substructures, and their relevant sequels. Section 3 discusses the concept of crisp sub sets approximations over quantale module created by soft binary relations. In Section 4, generalized soft substructures are defined and further fundamental algebraic properties of these phenomena are investigated utilizing these ideas. In Section 5, we also extend this research by defining the relationship between homomorphic images of substructures in quantale module and their approximation by soft binary relations.

2. Preliminaries

In this section, we will review some fundamental concepts related to quantale module and its substructures, soft sets, and rough sets.

2.1. Definition (see [2]). A quantale K_d is a complete lattice equipped with an associative, binary operation $\circledast$ distributing over an arbitrary joins. That is for any $r \in K_d, r_i, s_i \in K_d, (i \in I)$. It holds $r \circledast (\vee_{i\in I} s_i) = \vee_{i\in I} (r \circledast s_i)$ and $(v_{i\in I} r_i) \otimes s = v_{i\in i} (r_i \otimes s)$.

Let $X_i, X, Y \subseteq K_d\, (i \in I)$. Then, the followings are defined:

$$\begin{aligned} X \circledast Y &= \{x \circledast y | x \in X, y \in Y\}; \\ X \vee Y &= \{x \vee y | x \in X, y \in Y\}; \\ \vee_{i\in I} X_i &= \{\vee_{i\in I} x_i | x_i \in X_i\}. \end{aligned} \tag{1}$$

Throughout the paper, quantales are denoted by K_d.

2.2. Definition (see [1]). Let K_d be a quantale and M be a $S_{up}-$ lattice equipped with a left action $\oplus : K_d \times M \longrightarrow M$. Then, M is called left K_d-module over the quantale K_d if for any $a_i, a, b \in K_d, x \in M, \{x_j\} \subseteq M, (i \in I), (j \in J)$, we have

$$(\vee_{i\in I} a_i) \oplus x = \vee_{i\in I} (a_i \oplus x); \tag{2}$$

Right quantale modules can be defined in the same way. For the rest of the paper, K_d-module M will stand for a left quantale module over the quantale K_d. The symbol T will denote the top element and $\perp$ will stand for the bottom one for quantale module, unless stated otherwise.

2.3. Example. The following are the examples of K_d-modules M:

(1) Let $K_d = \{0, r, s, 1\}$ be a complete lattice where 0 is the bottom element and 1 is the top element of K_d, as shown in Figure 1 and the operation $\circledast$ on K_d is

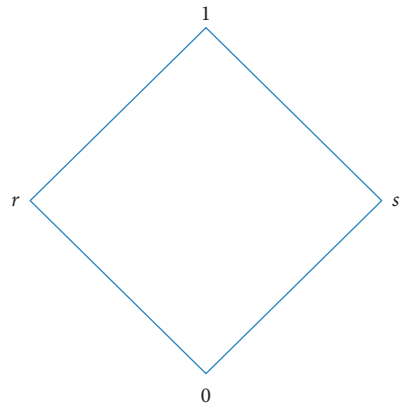

Figure 1: Illustration of k_d.

shown in Table 1. Then, it is straightforward to verify that $(K_d, \circledast)$ is a quantale. Let $M = \{\perp, x, \mathrm{T}\}$ be a $S_{up}-$ lattice. The order relation of M is given in Figure 2 and let $\oplus: K_d \times M \longrightarrow M$ be the left action on M as shown in Table 2. Then, it is straightforward that M is a K_d-module.

(2) Every quantale K_d is certainly a K_d-module over K_d.

2.4. Definition (see [1]). Let M be a K_d-module. A subset $M_1 \subseteq M$ is called a sub-K_d-module of M if for any $r \in M_1$, $\{s_i\} \subseteq M_1$, $k \in K_d$, it holds that $\vee_{i\in I} s_i \in M_1$ and $k \oplus r \in M_1$.

2.5. Definition (see [1]). Let M be a K_d-module and $\varnothing \neq I \subseteq M$. Then, I is a K_d-module ideal of M.

(1) If $r_i \in I\,(i \in I)$, then $\vee_{i\in I} r_i \in I$

(2) $r \in I$ and $c \leq r$ implies $c \in I$

(3) $r \in I$ implies $a \oplus r \in I, \forall a \in K_d$

2.6. Definition (see [1]). Let M be a K_d-module. A binary relation Γ on M is called congruence on M if it is an equivalence relation on M; for any given$\{m_i\}$, $\{n_i \subseteq M\}, m, n \varepsilon M$, and $q \in K_d$, it satisfies the following conditions: for all$i \varepsilon I, m_i \Gamma n_i$implies$\Delta_{i\in I} m_i \Gamma \Delta_{i\in I} n_iandm \Gamma n$ implies$q \Delta m \Gamma q \Delta n$.

2.7. Definition (see [1]). Let M_1 and M_2 be two K_d-modules. A map $\Omega: M_1 \longrightarrow M_2$ is a K_d- module homomorphism if it is a sup-lattice homomorphism which also preserves scalar multiplication. That is,

$$\begin{aligned} \Omega\left(\vee_{i\in I} r_i\right) &= \vee_{i\in I} \Omega\left(r_i\right), \\ \Omega\left(b \oplus r\right) &= b \oplus \Omega\left(r\right), \end{aligned} \tag{3}$$

for any $b \in K_d$, $r \in M_{,,}$ $\{r_i\} \subseteq M\,(i \in I)$

A K_d-module homomorphism $\Omega: M_1 \longrightarrow M_2$ is called an epimorphism if Ω is onto M_2 and Ω is called a monomorphism if Ω is one-one. It is an isomorphism, if Ω is bijective.

Table 1: Binary operation subject to $\otimes$.

$\otimes$	0	r	s	I
0	0	0	0	0
r	0	r	0	r
s	0	0	s	s
I	0	r	s	I

Figure 2: Illustration of M.

Table 2: Binary opreation subject to $\oplus$.

$\oplus$	$\perp$	x	T
0	$\perp$	$\perp$	$\perp$
r	$\perp$	x	T
s	$\perp$	x	x
I	$\perp$	x	T

2.8. Theorem (see [1]). Let M_1 and M_2 be two K_d-modules. If $\Omega: M_1 \longrightarrow M_2$ is a K_d-module homomorphism, then $\mathrm{Ker}\,(\Omega) = \{(a, b) \in M_1 \times M_1 : \Omega(a) = \Omega(b)\}$ is a congruence of K_d-modules.

2.9. Definition (see [18]). A pair (F, C) is called soft set over M if $F: C \longrightarrow P(M)$ where C is a subset of E (the set of parameters).

2.10. Definition (see [20]). Let (F, C_1) and (H, C_2) be two soft sets over M. Then, (F, C_1) soft subset (H, C_2) if the following conditions are fulfilled:

(1) $C_1 \subseteq C_2$

(2) $F(c) \subseteq H(c)$, $\forall\, c \in C_1$

2.11. Definition (see [30]). Let (Γ, C) be a soft set over $M \times M$, i.e., $\Gamma: C \longrightarrow P(M \times M)$. Then, (Γ, C) is called a soft binary relation (SBYR) over M.

2.12. Definition. Let (Γ, C) be a soft set over quantale module M. Then,

(1) (Γ, C) is called a soft sub-K_d-module over M iff $\Gamma(c)$ is a sub-K_d-module of $M \forall\, c \in C$

(2) (Γ, C) is a called soft K_d-module ideal over M iff $\Gamma(c)$ is K_d-module ideal of M, $\forall c \in C$

2.13. Definition (see [3]). Let $M \neq \varnothing$ be a finite set and Γ be an equivalence relation on M. Let $[t]_\Gamma$ denote the equivalence class of the relation Γ containing $t \in M$. If a subset of M is expressed as a union of equivalence classes of M, then that is said to be definable set in M. Let a subset R of M cannot be expressed as a union of equivalence classes of M. Then, we say it is undefinable set. However, we can approximate that undefinable set by two definable sets in M. The first one is called Γ-lower approximation $(\Gamma - L_{AP})$ of R, and the second is called Γ-upper approximation $(\Gamma - U_{AP})$ of R. They are defined as follows:

$$\underline{\Gamma}(R) = \{t \in M:\ [t]_\Gamma \subseteq M\} \text{ and } \overline{\Gamma}(R) = \{t \in M:\ [t]_\Gamma \cap M \neq \varnothing\}. \tag{4}$$

A rough set is the pair $(\underline{\Gamma}(R), \overline{\Gamma}(R))$; if $\underline{\Gamma}(R) = \overline{\Gamma}(R)$, then R is definable.

3. Approximation of Subsets of Quantale Module by Soft Binary Relation

In this section, applications of soft relation on quantale module are discussed. A subset of quantale module M can be approximated by soft relations in two ways. Aftersets and foresets are applied to approximate a subset of M. Two sets named as soft set corresponding to each subset are called the lower approximation (L_{AP}) and the upper approximation (U_{AP}) with respect to the aftersets and foresets, respectively.

3.1. Definition (see [11]). Let $\Gamma : C \longrightarrow P(M \times M)$. Then, (Γ, C) is a soft binary relation on a set M, where $\phi \neq C \subseteq E$ (set of parameters). For $\phi \neq S \subseteq M$, $(\underline{\Gamma}^S, C)$ and $(\overline{\Gamma}^S, C)$ of S with respect to aftersets are basically the two soft sets over M, defined as follows:

$$\underline{\Gamma}^S(u) = \{k \in M | k\Gamma(u) \subseteq S\} \text{ and } \overline{\Gamma}^S(u) = \{k \in M | k\Gamma(u) \cap S \neq \varnothing\} \tag{5}$$

Further, $({}^S\underline{\Gamma}, C)$ and $({}^S\overline{\Gamma}, C)$ of S with respect to foreset are basically the two soft sets over M, defined as follows: ${}^S\underline{\Gamma}(u) = \{k \in M | \Gamma(u)k \subseteq S\}$ and ${}^S\overline{\Gamma}(u) = \{k \in M | \Gamma(u)k \cap S \neq \varnothing\}$.

For all $u \in C$, $k\Gamma(u) = \{r \in M:\ (k, r) \in \Gamma(u)\}$ is called afterset of k and $\Gamma(u)k = \{r \in M:\ (r, k) \in \Gamma(u)\}$ is called foreset of k. Moreover, L_{AP} and U_{AP} are defined as $\underline{\Gamma}^S : C \longrightarrow P(M)$ and $\overline{\Gamma}^S : C \longrightarrow P(M)$ for aftersets. ${}^S\underline{\Gamma} : C \longrightarrow P(M)$ and ${}^S\overline{\Gamma} : C \longrightarrow P(M)$ for foresets for each $S \in P(M)$. Generally, $k\Gamma(u) \neq \Gamma(u)k$, $\underline{\Gamma}^S(u) \neq {}^S\underline{\Gamma}(u)$, and $\overline{\Gamma}^S(u) \neq {}^S\overline{\Gamma}(u)$. However, they are equal if $\Gamma(u)$ is a symmetric relation. This is justified in the next example.

3.2. Example. Let $K_d = \{\bot, r, s, T\}$ and $C = \{u_1, u_2\}$. Define $\Gamma : C \longrightarrow P(M \times M)$ by $\Gamma(u_1) = \{(\bot, \bot), (r, r), (s, s), (T, T), (\bot, r)\}$ and $\Gamma(u_2) = \{(\bot, \bot), (r, r), (s, s), (T, T), (r, T)\}$

Thus, the aftersets of elements M are as follows. $\bot\Gamma(u_1) = \{\bot, r\}$, $r\Gamma(u_1) = \{r\}$, $s\Gamma(u_1) = \{s\}$, $T\Gamma(u_1) = \{T\}$ and $\bot\Gamma(u_2) = \{\bot\}$, $r\Gamma(u_2) = \{r, T\}$, $s\Gamma(u_2) = \{s\}$, and $T\Gamma(u_2) = \{T\}$, and the foresets of elements of M are as follows: $\Gamma(u_1)\bot = \{\bot\}$, $\Gamma(u_1)r = \{\bot, r\}$, $\Gamma(u_1)s = \{s\}$, $\Gamma(u_1)T = \{T\}$ and $\Gamma(u_2)\bot = \{\bot\}$, $\Gamma(u_2)r = \{r\}$, $\Gamma(u_2)s = \{s\}$, $\Gamma(u_2)T = \{r, T\}$. Let $S = \{\bot, T\}$. Then, L_{AP} and U_{AP} of $S \subseteq M$ with respect to aftersets and foresets are as follows: $\underline{\Gamma}^S(u_1) = \{T\}$, $\underline{\Gamma}^S(u_2) = \{\bot, T\}$ and $\overline{\Gamma}^S(u_1) = \{\bot, T\}$, $\overline{\Gamma}^S(u_2) = \{\bot, r, T\}$, ${}^S\underline{\Gamma}(u_1) = \{\bot, T\}$, $\underline{\Gamma}^S(u_2) = \{\bot\}$ and ${}^S\overline{\Gamma}(u_1) = \{\bot, r, T\}$, ${}^S\overline{\Gamma}(u_2) = \{\bot, T\}$. This shows that $(\underline{\Gamma}^S, C) \neq ({}^S\underline{\Gamma}, C)$ and $(\overline{\Gamma}^S, C) \neq ({}^S\overline{\Gamma}, C)$.

3.3. Definition. A SBR Γ on a quantale module M is called soft compatible relation (SCRE), if it satisfies the following conditions: $\forall i \in I$ if $r_i\Gamma s_i \Rightarrow (\vee_{i\in I} r_i)\Gamma(\vee_{i\in I} s_i)$ and $r\Gamma s \Rightarrow (k \oplus r)\Gamma(k \oplus s)$ for any $r, s \in M, \{r_i\}, \{s_i\} \subseteq M$, $(i \in I)$ and $k \in K_d$.

3.4. Example. Let $K_d = \{\bot, r, s, T\}$ be a complete lattice as shown in Figure 3, and the operation $\circledast$ on K_d is $a \circledast b = \bot$. Then, it is easy to verify that $(K_d, \circledast)$ is a quantale. Let $\oplus : K_d \times M \longrightarrow M$ be the left action of K_d on M as shown in Table 3. In this case, $M = K_d$. Then, it is easy to check that K_d is a K_d-module over K_d and represented by M. Let $C = \{u_1, u_2\}$. Define $\Gamma : C \longrightarrow P(M \times M)$ by

$$\begin{aligned} \Gamma(u_1) &= \{(\bot, \bot), (r, r), (s, s), (\mathrm{T}, \mathrm{T}), (s, \mathrm{T})\}, \\ \Gamma(u_2) &= \{(\bot, \bot), (r, r), (s, s), (\mathrm{T}, \mathrm{T}), (r, \mathrm{T})\}. \end{aligned} \tag{6}$$

Then, (Γ, C) is a soft compatible relation (SCRE) and soft reflexive relation (SRRE) on M.

3.5. Remark. Let (Γ, C) be a SCRE on a K_d-module M. Then, it is easily verified that $k \oplus s\Gamma(u) \subseteq (k \oplus s)\Gamma(u)$ and $r\Gamma(u) \vee s\Gamma(u) \subseteq (r \vee s)\Gamma(u)$ for all $r, s \in M$ and $k \in K_d$.

3.6. Example. Let $(K_d, \oplus)$ be a K_d-module M as given in example 3.4 and let $C = \{u_1, u_2\}$. Define $\Gamma : C \longrightarrow P(M \times M)$ by $\Gamma(u_1) = \{(\bot, \bot), (r, r), (s, s), (\mathrm{T}, \mathrm{T}), (s, \mathrm{T}), (\mathrm{T}, s), (r, \mathrm{T}), (\mathrm{T}, r)\}$ and $\Gamma(u_2) = \{(\bot, \bot), (r, r), (s, s), (\mathrm{T}, \mathrm{T})\}$. Then, (Γ, C) is a SCRE and SRRE on M. The aftersets calculated by the elements of M are as follows:

$$\bot\Gamma(u_1) = \{\bot\}, r\Gamma(u_1) = \{r, \mathrm{T}\}, s\Gamma(u_1) = \{s, \mathrm{T}\}. \tag{7}$$

$\mathrm{T}\Gamma(u_1) = \{r, s, \mathrm{T}\}$. Thus, we have $r\Gamma(u_1) \vee s\Gamma(u_1) = \{r, \mathrm{T}\} \vee \{s, \mathrm{T}\} = \{\mathrm{T}\} \subseteq \{r, s, \mathrm{T}\} = (r \vee s)\Gamma(u_1)$. Hence, $r\Gamma(u_1) \vee s\Gamma(u_1) \subseteq (r \vee s)\Gamma(u_1)$ Also, similarly we can check that $k \oplus x\Gamma(u) \subseteq (k \oplus x)\Gamma(u) \forall k \in K_d, x \in M \forall u \in C$.

3.7. Remark. If (Γ, C) is a SCRE on a K_d-module M, then $k \oplus \Gamma(u)s \subseteq \Gamma(u)(k \oplus s)$ and $\Gamma(u)r \vee \Gamma(u)s \subseteq \Gamma(u)(r \vee s)$ with respect to foresets.

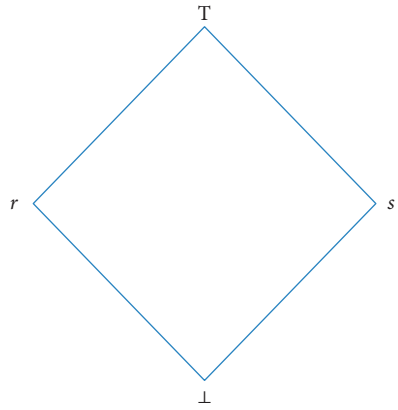

Figure 3: Illustration of M.

Table 3: Binary operation subject to ⊕.

⊕	⊥	r	s	T
⊥	⊥	r	s	T
r	⊥	r	s	T
s	⊥	r	s	T
T	⊥	r	s	T

3.8. Definition. A SCRE (Γ, C) on a K_d-module M is called soft join-complete with respect to to aftersets if $p\Gamma(u) \vee q\Gamma(u) = (p \vee q)\Gamma(u)$ and is called soft complete with respect to $\oplus$ if $k \oplus p\Gamma(u) = (k \oplus p)\Gamma(u) \forall k \in K_d p, q \in M \forall u \in C$.

A SCRE (Γ, C) which is both join-complete and $\oplus$-complete with respect to aftersets is called soft complete relation (SCTR) with respect to aftersets.

3.9. Example. Let $(K_d, \oplus)$ be a K_d-module M as given in example 3.4 and let $C = \{u_1, u_2\}$. Define Γ: $C \longrightarrow P(M \times M)$ by

$$\begin{aligned} \Gamma(u_1) &= \{(\perp, \perp), (r, r), (s, s), (\mathrm{T}, \mathrm{T}), (s, \mathrm{T}), (r, \mathrm{T})\} \\ \text{and } \Gamma(u_2) &= \{(\perp, \perp), (r, r), (s, s), (\mathrm{T}, \mathrm{T})\}. \end{aligned} \tag{8}$$

Then, (Γ, C) is a SCRE and SRRE on M. The aftersets calculated by the elements of M are as follows: $\perp\Gamma(u_1) = \{\perp\}, r\Gamma(u_1) = \{r, \mathrm{T}\}, s\Gamma(u_1) = \{s, \mathrm{T}\}, \mathrm{T}\Gamma(u_1) = \{\mathrm{T}\}$. It is easily checked that $p\Gamma(u_1) \vee q\Gamma(u_1) = (p \vee q)\Gamma(u_1)\ \forall p, q \in M$ That is, $r\Gamma(u_1) \vee s\Gamma(u_1) = \{r, \mathrm{T}\} \vee \{s, \mathrm{T}\} = \{\mathrm{T}\} = (r \vee s)\Gamma(u_1)$ etc. Further, we can check that $k \oplus p\Gamma(u_1) = (k \oplus p)\Gamma(u_1) \forall k \in K_d, p \in M \forall u \in C$.

So, (Γ, C) is a SCTR with respect to aftersets.

3.10. Definition. A SCRE (Γ, C) on a K_d-module M is called soft join-complete with respect to foresets if $\Gamma(u)p \vee \Gamma(u)q = \Gamma(u)(p \vee q)$ and is called soft complete with respect to $\oplus$ if $k \oplus \Gamma(u)p = \Gamma(u)(k \oplus p) \forall k \in K_d p, q \in M \forall u \in C$.

A SCRE (Γ, C) which is both join-complete and $\oplus$-complete is called SCTR with respect to foresets.

3.11. Remark. It has been observed that if we have SCTR for aftersets, not need it is SCTR for foresets. This is demonstrated in the following example.

3.12. Example. Let $(K_d, \oplus)$ be a K_d-module M as given in example 3.4 and let $C = \{u_1, u_2\}$. Define Γ: $C \longrightarrow P(M \times M)$ by $\Gamma(u_1) = \{(\perp, \perp), (r, r), (s, s), (\mathrm{T}, \mathrm{T}), (s, \mathrm{T}), (r, \mathrm{T})\}$ and $\Gamma(u_2) = \{(\perp, \perp), (r, r), (s, s), (\mathrm{T}, \mathrm{T})\}$. Then, (Γ, C) is a SCRE and SRRE on M. The aftersets and foresets calculated by the elements of M are as follows: $\perp\Gamma(u_1) = \{\perp\}, r\Gamma(u_1) = \{r, \mathrm{T}\}, s\Gamma(u_1) = \{s, \mathrm{T}\}, \mathrm{T}\Gamma(u_1) = \{\mathrm{T}\}$, $\Gamma(u_1)\perp = \{\perp\}$, $\Gamma(u_1)r = \{r\}, \Gamma(u_1)s = \{s\}, \Gamma(u_1)\mathrm{T} = \{r, s, \mathrm{T}\}$. It is observed that $r\Gamma(u_1) \vee s\Gamma(u_1) = \{r, \mathrm{T}\} \vee \{s, \mathrm{T}\} = \{\mathrm{T}\} = (r \vee s)\Gamma(u_1)$. Likewise, we can check that $k \oplus p\Gamma(u_1) = (k \oplus p)\Gamma(u_1) \forall k \in K_d, p \in M, \forall u \in C$ So, (Γ, C) is a SCTR with respect to aftersets. But, $\Gamma(u_1)r \vee \Gamma(u_1)s = \{r\} \vee \{s\} = \{\mathrm{T}\} \neq \{r, s, \mathrm{T}\} = \Gamma(u_1)(r \vee s)$ So, (Γ, C) is not a SCTR with respect to foresets.

In ref [31], the following theorems are helpful for our further study.

3.13. Theorem (see [31]). Let $\varnothing \neq S, \varnothing \neq R$ be the subsets of K_d-module M and (Γ, C) and (γ, C) be SRRE on M. Then, the following hold for all $u \in C$:

(1) $\underline{\Gamma}^S(u) \subseteq S \subseteq \overline{\Gamma}^S(u)$
(2) $S \subseteq R \Rightarrow \underline{\Gamma}^S(u) \subseteq \underline{\Gamma}^R(u)$
(3) $S \subseteq R \Rightarrow \overline{\Gamma}^S(u) \subseteq \overline{\Gamma}^R(u)$
(4) $(\underline{\Gamma}^S, C) \cap (\underline{\Gamma}^R, C) = (\underline{\Gamma}^{S \cap R}, C)$
(5) $(\overline{\Gamma}^S, C) \cap (\overline{\Gamma}^R, C) \supseteq (\overline{\Gamma}^{S \cap R}, C)$
(6) $(\underline{\Gamma}^S, C) \cup (\underline{\Gamma}^R, C) \subseteq (\underline{\Gamma}^{S \cup R}, C)$
(7) $(\overline{\Gamma}^S, C) \cup (\overline{\Gamma}^R, C) = (\overline{\Gamma}^{S \cup R}, C)$
(8) $(\Gamma, C) \subseteq (\gamma, C) \Rightarrow (\underline{\Gamma}^S, C) \supseteq (\underline{\gamma}^S, C)$
(9) $(\Gamma, C) \subseteq (\gamma, C) \Rightarrow (\overline{\Gamma}^S, C) \subseteq (\overline{\gamma}^S, C)$

3.14. Theorem (see [31]). Let $\varnothing \neq S, \varnothing \neq R$ be the subset of K_d-module M and (Γ, C) and (γ, C) be SRRE on M. Then, the following hold for all $u \in C$:

(10) ${}^S\underline{\Gamma}(u) \subseteq S \subseteq {}^S\overline{\Gamma}(u)$
(11) $S \subseteq R \Rightarrow {}^S\underline{\Gamma}(u) \subseteq {}^R\underline{\Gamma}(u)$
(12) $S \subseteq R \Rightarrow {}^S\overline{\Gamma}(u) \subseteq {}^R\overline{\Gamma}(u)$
(13) $({}^S\underline{\Gamma}, C) \cap ({}^R\underline{\Gamma}, C) = ({}^{S \cap R}\underline{\Gamma}, C)$
(14) $({}^S\overline{\Gamma}, C) \cap ({}^R\overline{\Gamma}, C) \supseteq ({}^{S \cap R}\overline{\Gamma}, C)$
(15) $({}^S\overline{\Gamma}, C) \cup ({}^R\overline{\Gamma}, C) \subseteq ({}^{S \cap R}\overline{\Gamma}, C)$
(16) $({}^S\overline{\Gamma}, C) \cup ({}^R\overline{\Gamma}, C) = ({}^{S \cup R}\overline{\Gamma}, C)$
(17) $(\Gamma, C) \subseteq (\gamma, C) \Rightarrow ({}^S\underline{\Gamma}, C) \supseteq ({}^S\underline{\gamma}, C)$
(18) $(\Gamma, C) \subseteq (\gamma, C) \Rightarrow ({}^S\overline{\Gamma}, C) \subseteq ({}^S\overline{\gamma}, C)$

3.15. Theorem (see [31]). Let $\varnothing \neq S, \varnothing \neq R$ be the subsets of K_d-module M and (Γ, C) and (γ, C) be SRRE on M. Then, the following hold for all $u \in C$:

(1) $((\overline{\Gamma \cap \gamma})^S, C) \subseteq (\overline{\Gamma}^S, C) \cap (\overline{\gamma}^S, C)$

(2) $(\underline{(\Gamma \cap \gamma)}^S, C) \supseteq (\underline{\Gamma}^S, C) \cup (\underline{\gamma}^S, C)$
(3) $({}^S\overline{(\overline{\Gamma \cap \gamma})}, C) \subseteq ({}^S\overline{\Gamma}, C) \cap ({}^S\overline{\gamma}, C)$
(4) $({}^S\underline{(\Gamma \cap \gamma)}, C) \supseteq ({}^S\underline{\Gamma}, C) \cup ({}^S\underline{\gamma}, C)$

3.16. Theorem. Let (Γ, C) be SRRE and SCRE with respect to the aftersets on a K_d-module M. Then, for non-empty subset S and R of M, we have $k \oplus \overline{\Gamma}^S(u) \subseteq \overline{\Gamma}^{k \oplus S}(u)$ and $\overline{\Gamma}^S(u) \vee \overline{\Gamma}^R(u) \subseteq \overline{\Gamma}^{S \vee R}(u) \forall\ u \in C$.

Proof. Let $x \in k \oplus \overline{\Gamma}^S(u)$ Then, $x = k \oplus p$ where $p \in \overline{\Gamma}^S(u)$ such that $p\Gamma(u) \cap S \neq \varnothing$. Thus, there exist $a \in p\Gamma(u) \cap S$ such that $a \in S$. That is, $(p, a) \in \Gamma(u)$. Since (Γ, C) is SCRE, we have $(k \oplus p, k \oplus a) \in \Gamma(u)$ and $k \oplus a \in k \oplus S$, $\Rightarrow k \oplus a \in (k \oplus p)\Gamma(u) \cap k \oplus S$,
$\Rightarrow \varnothing \neq (k \oplus p)\Gamma(u) \cap k \oplus S \Rightarrow k \oplus p \in \overline{\Gamma}^{k \oplus S}(u)$. So, $x \in \overline{\Gamma}^{k \oplus S}(u)$. Thus, $k \oplus \overline{\Gamma}^S(u) \subseteq \overline{\Gamma}^{k \oplus S}(u)$

Let $y \in \overline{\Gamma}^S(u) \vee \overline{\Gamma}^R(u)$. Then, $y = p \vee q$ where $p \in \overline{\Gamma}^S(u)$ and $q \in \overline{\Gamma}^R(u)$ such that $p\Gamma(u) \cap S \neq \varnothing$ and $q\Gamma(u) \cap R \neq \varnothing$. That is, $a \in p\Gamma(u) \cap S$ and $b \in q\Gamma(u) \cap R$. So, $a \in p\Gamma(u)$, $a \in S$ and $b \in q\Gamma(u)$, $b \in R$, $\Rightarrow (p, a) \in \Gamma(u), a \in S$ and $(q, b) \in \Gamma(u), b \in R$. Since (Γ, C) is SCRE, we have $(p \vee q, a \vee b) \in \Gamma(u)$and $a \vee b \in S \vee R \Rightarrow a \vee b \in (p \vee q)$ $\Gamma(u) \cap S \vee R$, $\Rightarrow \varnothing \neq (p \vee q)\Gamma(u) \cap (S \vee R) \Rightarrow (p \vee q) \in \overline{\Gamma}^{S \vee R}(u)$ So, $y \in \overline{\Gamma}^{S \vee R}(u)$. Thus, $\overline{\Gamma}^S(u) \vee \overline{\Gamma}^R(u) \subseteq \overline{\Gamma}^{S \vee R}(u)$. □

3.17. Example. Let $(K_d, \oplus)$ be a K_d-module M as given in example 3.4 and let $C = \{u_1, u_2\}$. Define Γ: $C \longrightarrow P(M \times M)$ by $\Gamma(u_1) = \{(\perp, \perp), (r, r), (s, s), (\mathrm{T}, \mathrm{T}), (r, \mathrm{T})\}$ and $\Gamma(u_2) = \{(\perp, \perp), (r, r), (s, s), (\mathrm{T}, \mathrm{T})\}$. Then, (Γ, C) is a SCRE and SRRE on M. The aftersets calculated by the elements of M are as follows: $\perp\Gamma(u_1) = \{\perp\}, r\Gamma(u_1) = \{r, \mathrm{T}\}$, $s\Gamma(u_1) = \{s\}, \mathrm{T}\Gamma(u_1) = \{\mathrm{T}\}$, $\perp\Gamma(u_2) = \{\perp\}, r\Gamma(u_2) = \{r\}$, $s\Gamma(u_2) = \{s\}, \mathrm{T}\Gamma(u_2) = \{\mathrm{T}\}$. Let $R = \{s\}$ and $S = \{\mathrm{T}\}$. Then, $\overline{\Gamma}^R(u_1) = \{s\}, \overline{\Gamma}^S(u_1) = \{r, T\}$, and $\overline{\Gamma}^R(u_1) \vee \overline{\Gamma}^S(u_1) = \{T\}$. Now, $S \vee R = \{T\}$and $\overline{\Gamma}^{S \vee R}(u_1) = \{r, T\}$. So, $\overline{\Gamma}^S(u_1) \vee \overline{\Gamma}^R(u_1) \subseteq \overline{\Gamma}^{S \vee R}(u_1)$. Similarly, we can prove that $k \oplus \overline{\Gamma}^S(u) \subseteq \overline{\Gamma}^{k \oplus S}(u)$.

3.18. Theorem. Let (Γ, C) be SRRE and SCRE with respect to the foresets on a K_d-module M. Then, for non-empty subset S and R of M, we have $k \oplus {}^S\overline{\Gamma}(u) \subseteq {}^{k \oplus S}\overline{\Gamma}(u)$ and ${}^S\overline{\Gamma}(u) \vee {}^R\overline{\Gamma}(u) \subseteq {}^{S \vee R}\overline{\Gamma}(u) \forall u \in C$.

Proof. The proof is similar to the proof of Theorem 3.16. □

4. Approximation of Substructures in Quantale Module

In this section, foresets and aftersets are applied to different type of substructures in quantale module through soft relations to discuss their lower and upper approximations. These are then characterized by soft reflexive and soft compatible relations to present different characteristics of them.

4.1. Definition. Let $\varnothing \neq S \subseteq M$ and (Γ, C) be a SBR on a K_d-module M. Then, S is said to be generalized upper soft sub K_d-module of M with respect to aftersets if $(\overline{\Gamma}^S, C)$ is a soft sub-K_d-module of M.

4.2. Theorem. Let (Γ, C) be a SRRE and SCRE on a K_d-module M. Then, S is said to be generalized upper soft sub K_d-module of M with respect to aftersets if S is a soft sub-K_d-module of M.

Proof (1) Suppose that $r_i \in \overline{\Gamma}^S(u)$ for $u \in C$ and for some $i \in I$. Then, $r_i\Gamma(u) \cap S \neq \varnothing$. There are $x_i \in r_i\Gamma(u) \cap S$ such that $x_i \in r_i\Gamma(u)$ and $x_i \in S$. That is, $(r_i, x_i) \in \Gamma(u)$ and $x_i \in S$, $\forall i \in I$. Since S is a sub-K_d-module of M and $\Gamma(u)$ is a SCRE$\forall u \in C$. Thus, we have $(\vee_{i \in I} r_i, \vee_{i \in I} x_i) \in \Gamma(u)$ and $\vee_{i \in I} x_i \in S$. That is, $\vee_{i \in I} x_i \in \vee_{i \in I} r_i\Gamma(u)$ and $\vee_{i \in I} x_i \in S$. So, $\vee_{i \in I} x_i \in \vee_{i \in I} r_i\Gamma(u) \cap S$. Hence, $\vee_{i \in I} r_i\Gamma(u) \cap S \neq \varnothing$. This shows that $\vee_{i \in I} r_i \in \overline{\Gamma}^S(u)$.

(2) Let $r \in M$ such that $r \in \overline{\Gamma}^S(u)$. This shows $r\Gamma(u) \cap S \neq \varnothing$. Then, there is $y \in r\Gamma(u) \cap S$ such that $y \in r\Gamma(u)$ and $y \in S$. That is, $(r, y) \in \Gamma(u)$ and $y \in S$. Since S is a sub-K_d-module of M and $\Gamma(u)$ is a SRRE and SCRE. Thus, we have $k \oplus y \in S$ and $(k \oplus r, k \oplus y) \in \Gamma(u)$, $\Rightarrow k \oplus y \in (k \oplus r)\Gamma(u)$ and $k \oplus y \in S$, $\Rightarrow k \oplus y \in (k \oplus r)\Gamma(u) \cap S$. Hence, $(k \oplus r)\Gamma(u) \cap S \neq \varnothing$. This shows that $k \oplus r \in \overline{\Gamma}^S(u)$. Therefore, $\overline{\Gamma}^S(u)$ is a sub K_d-module of M. That is, S is a generalized upper soft sub-K_d-module of M with respect to aftersets.

It is mentioned in the next example that the converse is not true. □

4.3. Example. Suppose $K_d = \{\perp, r, s, t, T\}$ be a complete lattice as shown in Figure 4 and the operation $\circledast$ on K_d is that $a \circledast b = \perp$. Then, it is easily checked that $(K_d, \circledast)$ is a quantale. Suppose $\circledast$: $K_d \times M \longrightarrow M$ be the left action of K_d on M as shown in Table 4. In this case, $M = K_d$; then, it is easy to check that K_d is a quantale module M. Let $C = \{u_1, u_2\}$. Then, Γ: $C \longrightarrow P(M \times M)$ defined by
$\Gamma(u_1) = \{(\perp, \perp), (r, r), (s, s),$
$(\mathrm{T}, \mathrm{T}), (r, \mathrm{T}), (s, T), (\perp, T), (t, T), (r, t), (r, \perp), (t, s), (t, t)\}$
and $\Gamma(u_2) = \{(\perp, \perp), (r, r), (s, s), (t, t), (\mathrm{T}, \mathrm{T}), (T, t), (t, r)\}$.

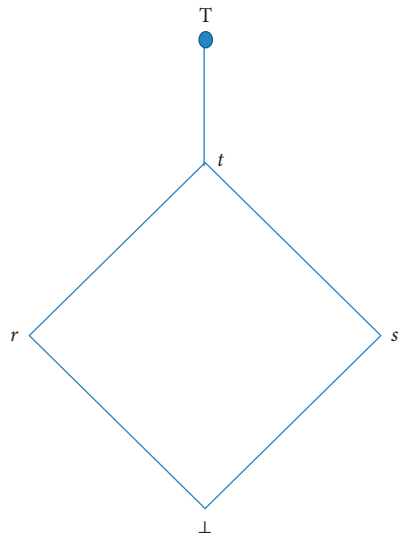

Figure 4: Illustration of M.

Table 4: Binary operation subject to ⊕.

⊕	⊥	r	s	t	T
⊥	⊥	r	s	t	T
r	⊥	r	s	t	T
s	⊥	r	s	t	T
t	⊥	r	s	t	T
T	⊥	r	s	t	T

Then, (Γ, C) is a SCRE and SRRE on M. The aftersets calculated by the elements of M are as follows:

$$\begin{aligned}
\bot\Gamma(u_1) &= \{\bot, T\}, r\Gamma(u_1)\\
&= \{\bot, r, t, \mathrm{T}\}, s\Gamma(u_1)\\
&= \{s, T\},\\
t\Gamma(u_1) &= \{s, t, T\}, T\Gamma(u_1)\\
&= \{T\},\\
\bot\Gamma(u_2) &= \{\bot\}, r\Gamma(u_2)\\
&= \{r\}, s\Gamma(u_2)\\
&= \{s\},\\
t\Gamma(u_2) &= \{r, t\}, T\Gamma(u_2)\\
&= \{t, T\}.
\end{aligned} \tag{9}$$

Let $S = \{T, r, s\}$. Then, S is not a sub-K_d-module of M. But, $\overline{\Gamma}^S(u_1) = \{\bot, r, s, t, T\}$ and $\overline{\Gamma}^S(u_2) = \{r, s, t, T\}$ are sub-K_d-module of M. Hence, S is a generalized upper soft sub-K_d-module of M with respect to aftersets.

4.4. Definition. Let $\varnothing \neq S \subseteq M$ and (Γ, C) be a SBR on a K_d-module M. Then, S is said to be generalized upper soft sub K_d-module of M with respect to foresets if $({}^S\overline{\Gamma}, C)$ is a soft sub-K_d-module of M.

4.5. Theorem. Let (Γ, C) be a SRRE and SCRE on a K_d-module M. Then, S is said to be generalized upper soft sub K_d-module of M with respect to foresets if S is a soft sub-K_d-module of M.

Proof. The proof is similar to the proof of Theorem 4.2. □

4.6. Definition. Let $\varnothing \neq S \subseteq M$ and (Γ, C) be a SRRE and SCRE on a K_d-module M. Then, S is said to be generalized lower soft sub-K_d-module of M with respect to aftersets if $(\underline{\Gamma}^S, C)$ is a soft sub-K_d-module of M.

4.7. Theorem. Let (Γ, C) be a SRRE and SCTE on a K_d-module M. Then, S is said to be generalized lower soft sub K_d-module of M with respect to aftersets if S is a soft sub-K_d-module of M.

Proof. (1) Suppose that $r_i \in \underline{\Gamma}^S(u)$ for $u \in C$ and for $i \in I$. This shows that $r_i\Gamma(u) \subseteq S$. Hence, S is a sub-K_d-module of M and $\Gamma(u)$ is SCTR $\forall u \in C$. Thus, $(\vee_{i\in I} r_i)\Gamma(u) = \vee_{i\in I}(r_i\Gamma(u))$ and $(\vee_{i\in I} r_i)\Gamma(u) = \vee_{i\in I}(r_i\Gamma(u)) \subseteq S$. Hence, $(\vee_{i\in I} r_i)\Gamma(u) \subseteq S$. This shows that $\vee_{i\in I} r_i \in \underline{\Gamma}^S(u)$.

(2) Let $r \in M$ be such that $r \in \underline{\Gamma}^S(u)$. This shows $r\Gamma(u) \subseteq S$ for $u \in C$. Hence, S is a sub-K_d-module of M and $\Gamma(u)$ is a SRRE and SCTE. Thus, we have $(k \oplus r)\Gamma(u) = k \oplus r\Gamma(u)$. So, we can write $(k \oplus r)\Gamma(u) = k \oplus r\Gamma(u) \subseteq S$. Hence, $(k \oplus r)\Gamma(u) \subseteq S$. This shows that $k \oplus r \in \underline{\Gamma}^S(u)$. Therefore, $\underline{\Gamma}^S(u)$ is a sub K_d-module of M. That is, S is a generalized lower soft sub-K_d-module of M with respect to aftersets.

Observe in the next example that the converse is not true. □

4.8. Example. Let $(K_d, \oplus)$ be a K_d-module M as given in example 4.3 and let $C = \{u_1, u_2\}$. Define Γ: $C \longrightarrow P(M \times M)$ by $\Gamma(u_1) = \{(\bot, \bot), (r, r), (s, s), (\mathrm{T}, \mathrm{T}), (r, \mathrm{T}), (s, T)\}$ and $\Gamma(u_2) = \{(\bot, \bot), (r, r), (s, s), (t, t), (\mathrm{T}, \mathrm{T}), (T, t), (r, T), (s, \bot)\}$. The aftersets calculated by the elements of M are as follows: $\bot\Gamma(u_1) = \{\bot\}, r\Gamma(u_1) = \{r, \mathrm{T}\}, s\Gamma(u_1) = \{s, T\}, \mathrm{T}\Gamma(u_1) = \{\mathrm{T}\}$, $\bot\Gamma(u_2) = \{\bot\}, r\Gamma(u_2) = \{r, T\}, s\Gamma(u_2) = \{\bot, s\}, \mathrm{T}\Gamma(u_2) = \{r, \mathrm{T}\}$. Then, (Γ, C) is a SCTR and SRRE with respect to aftersets. Let $S = \{\bot, r, s\}$. Then, S is not a sub-K_d-module of M. However, $\underline{\Gamma}^S(u_1) = \{\bot\}, \underline{\Gamma}^S(u_2) = \{\bot\}$ are sub-K_d-module of M. Hence, S is generalized lower soft sub-K_d-module of M.

4.9. Definition. Let $\varnothing \neq S \subseteq M$ and (Γ, C) be a SRRE and SCRE on a K_d-module M. Then, S is said to be generalized lower soft sub-K_d-module of M with respect to foresets if $({}^S\underline{\Gamma}, C)$ is a soft sub-K_d-module of M.

4.10. Theorem. Let (Γ, C) be a SCTR and SRRE on a K_d-module M. Then, S is said to be generalized lower soft

sub K_d-module of M with respect to foresets if S is a soft sub-K_d-module of M.

Proof. The proof is obvious. □

4.11. Remark. The results in this section related to foresets are similar to the results with respect to aftersets.

4.12. Definition. Let $\varnothing \neq S \subseteq M$ and (Γ, C) be a SRRE and SCRE on a K_d-module M if $(\overline{\Gamma}^S, C)$ is a soft K_d-module ideal M. Then, S is said to be generalized upper soft K_d-module ideal of M with respect to aftersets.

4.13. Theorem. Let $\varnothing \neq S \subseteq M$ and (Γ, C) be a SRRE, SCRE and soft join-complete relation on a K_d-module M. Then, S is said to be generalized upper soft K_d-module ideal of M with respect to aftersets if S is an K_d-module ideal of M.

Proof (1) Suppose that $r, s \in M$ such that $r, s \in \overline{\Gamma}^S(u)$ for $u \in C$. Therefore, $r\Gamma(u) \cap S \neq \varnothing$ and $s\Gamma(u) \cap S \neq \varnothing$. Then ,there are $x \in r\Gamma(u) \cap S$ and $y \in s\Gamma(u) \cap S$ such that $x \in r\Gamma(u)$, $y \in s\Gamma(u)$, and $x \in S, y \in S$. This implies $(r, x) \in \Gamma(u)$, $(s, y) \in \Gamma(u)$, and $x, y \in S$. S is a K_d-module ideal of M and $\Gamma(u)$ is a SCRE $\forall u \in C$. Hence, we have $(r \vee s, x \vee y) \in \Gamma(u)$ and $x \vee y \in S$. That is, $x \vee y \in (r \vee s)\Gamma(u)$ and $x \vee y \in S$. So, $x \vee y \in (r \vee s)\Gamma(u) \cap S$. Hence, $(r \vee s)\Gamma(u) \cap S \neq \varnothing$. This shows that $(r \vee s) \in \overline{\Gamma}^S(u)$.

(2) Let $s \in \overline{\Gamma}^S((u))$ and $r \leq s$. Therefore, $s\Gamma(u) \cap S \neq \varnothing$. Then, there is $y \in s\Gamma(u) \cap S$ such that $y \in s\Gamma(u)$ and $y \in S$. Since $\Gamma(u)$ is a SCRE and soft join-complete relation, we have $s\Gamma(u) = (r \vee s)\Gamma(u) = r\Gamma(u) \vee s\Gamma(u)$. Then, there is $u \in r\Gamma(u)$ and $v \in s\Gamma(u)$ such that $y = u \vee v$. S is a K_d-module ideal of M and $u \leq y \in S$. We have $u \in S$ so $r \in \overline{\Gamma}^S(u)$

(3) Let $k \in M$ be such that $r \in \overline{\Gamma}^S(u)$. This shows $r\Gamma(u) \cap S \neq \varnothing$. Then, there are $y \in r\Gamma(u) \cap S$ such that $y \in r\Gamma(u)$ and $y \in S$. That is, $(r, y) \in \Gamma(u)$ and $y \in S$. S is a K_d module ideal of M and $\Gamma(u)$ is a SRRE and SCRE. We have $k \oplus y \in S$ and $(k \oplus r, k \oplus y) \in \Gamma(u) \Rightarrow k \oplus y \in (k \oplus r)\Gamma(u)$ and $k \oplus y \in S$, $\Rightarrow k \oplus y \in (k \oplus r)\Gamma(u) \cap S$. Hence, $(k \oplus r)\Gamma(u) \cap S \neq \varnothing$. This shows that $k \oplus r \in \overline{\Gamma}^S(u)$. Therefore, $\overline{\Gamma}^S(u)$ is a K_d-module ideal of M. That is, S is a generalized upper soft K_d-module ideal of M with respect to aftersets.

It is observed in the next example that the converse is not true. □

4.14. Example. Let M be the quantale module as given in example 4.3 and $C = \{u_1, u_2\}$. Then, $\Gamma(u_1) = \{(\perp, \perp), (r, r), (s, s), (\mathrm{T}, \mathrm{T}), (r, \mathrm{T}), (s, T), (\perp, T), (t, T), (r, t), (r, \perp), (t, s), (t, t)\}$ and $\Gamma(u_2) = \{(\perp, \perp), (r, r), (s, s), (t, t), (\mathrm{T}, \mathrm{T}), (T, t), (t, r)\}$.

The aftersets calculated by the elements of M are as follows:

$$\begin{aligned}
\perp\Gamma(u_1) &= \{\perp, T\}, r\Gamma(u_1) \\
&= \{\perp, r, t, \mathrm{T}\}, s\Gamma(u_1) \\
&= \{s, T\}, t\Gamma(u_1) \\
&= \{s, t, T\}, \mathrm{T}\Gamma(u_1) \\
&= \{\mathrm{T}\}\perp\Gamma(u_2) \\
&= \{\perp\}, r\Gamma(u_2) \\
&= \{r, T\}, s\Gamma(u_2) = \{s\}, \mathrm{T}\Gamma(u_2) \\
&= \{\mathrm{T}\}, t\Gamma(u_2) \\
&= \{t\},
\end{aligned} \tag{10}$$

then (Γ, C) is a SCRE and SRRE and soft join-complete relation with respect to aftersets on M. Let $S = \{T, t, s, \perp\}$. Then, S is not a K_d-module ideal of M. However, $\overline{\Gamma}^S(u_1) = \{\perp, r, s, t, T\}$ and $\overline{\Gamma}^S(u_1) = \{\perp, r, s, t, \mathrm{T}\}$ are K_d-module ideal of M. Hence, S is a generalized upper soft K_d-module ideal of M with respect to aftersets.

4.15. Definition. Let $\varnothing \neq S \subseteq M$ and (Γ, C) be a SRRE and SCRE on a K_d-module M if $({}^S\overline{\Gamma}, C)$ is a soft K_d-module ideal M. Then, S is said to be generalized upper soft K_d-module of M with respect to foresets if S is a K_d-module ideal of M.

4.16. Theorem. Let $\varnothing \neq S \subseteq M$ and (Γ, C) be a SRRE, SCRE, and soft join-complete relation on a K_d-module M. Then, S is said to be generalized upper soft K_d-module ideal of M with respect to foresets if S is an K_d-module ideal of M.

Proof. The proof is obvious. □

4.17. Definition. Let $\varnothing \neq S \subseteq M$ and (Γ, C) be a SRRE and SCRE on a K_d-module M if $(\underline{\Gamma}^S, C)$ is a soft K_d-module ideal M. Then, S is said to be generalized lower soft K_d-module of M with respect to aftersets.

4.18. Theorem. Let $\varnothing \neq S \subseteq M$ and (Γ, C) be a SRRE and SCTR on a K_d-module M. Then, S is said to be generalized lower soft K_d-module ideal of M with respect to aftersets if S is an K_d-module ideal of M.

Proof (1) Suppose that $r, s \in M$ such that $r, s \in \underline{\Gamma}^S(u)$ for $u \in C$. This shows $r\Gamma(u) \subseteq S$ and $s\Gamma(u) \subseteq S$. Hence, S is a K_d-module ideal of M and $\Gamma(u)$ is SCTR $\forall u \in C$. So, we have $(r \vee s)\Gamma(u) = r\Gamma(u) \vee s\Gamma(u)$ and $r\Gamma(u) \vee s\Gamma(u) = (r \vee s)\Gamma(u) \subseteq S$. Hence, $(r \vee s)\Gamma(u) \subseteq S$. This shows that $(r \vee s) \in \underline{\Gamma}^S(u)$.

(2) Let $s \in \underline{\Gamma}^S(u)$ and $r \leq s$. Therefore, $s\Gamma(u) \subseteq S$. For $w \in r\Gamma(u)$, we have $(r, w) \in \Gamma(u)$. Since $(r, w) \in \Gamma(u)$ is a SRRE and SCRE, we have $(r \vee s, w \vee s) \in \Gamma(u)$. That is, $(s, w \vee s) \in \Gamma(u)$. Thus,

$(w \vee s) \in S$. Since S is a K_d-module ideal of M, we have $w \in S$. Thus, $r\Gamma(u) \subseteq S$ and $r \in \overline{\Gamma}^S(u)$.

(3) Let $k \in M$ be such that $r \in \underline{\Gamma}^S(u)$. This shows $r\Gamma(u) \subseteq S$ for $u \in C$. Hence, S is a K_d-module ideal of M. Then, for all $k \in M$, we have $k \oplus r\Gamma(u) \subseteq k \oplus S \subseteq S$. Also given that $\Gamma(u)$ is a SRRE and SCTE. Thus, we can write $k \oplus r\Gamma(u) = (k \oplus r)\Gamma(u) \subseteq S$. Hence, $k \oplus r\Gamma(u) = (k \oplus r)\Gamma(u) \subseteq S$. This shows that $k \oplus r \in \underline{\Gamma}^S(u)$. Therefore, $\underline{\Gamma}^S(u)$ is a K_d-module ideal of M. That is, S is a generalized lower soft K_d-module ideal of M with respect to aftersets.

Observe in the next example that the converse is not true. □

4.19. Example. Let $(K_d, \oplus)$ be a K_d-module M as given in example 3.4 and let $C = \{u_1, u_2\}$. Define Γ: $C \longrightarrow P(M \times M)$ by $\Gamma(u_1) = \{(\perp, \perp), (r, r), (s, s), (\mathrm{T}, \mathrm{T}), (r, \mathrm{T}), (s, T)\}$ and $\Gamma(u_2) = \{(\perp, \perp), (r, r), (s, s), (\mathrm{T}, \mathrm{T}), (T, r), (r, T), (s, \perp)\}$.
The aftersets calculated by the elements of M are as follows:
$\perp\Gamma(u_1) = \{\perp\}, r\Gamma(u_1) = \{r, \mathrm{T}\}, s\Gamma(u_1) = \{s, T\}, \mathrm{T}\Gamma(u_1) = \{\mathrm{T}\}$,
$\perp\Gamma(u_2) = \{\perp\}, r\Gamma(u_2) = \{r, T\}, s\Gamma(u_2) = \{\perp, s\}$,
$\mathrm{T}\Gamma(u_2) = \{r, \mathrm{T}\}$. Then, (Γ, C) is a SCTR and SRRE with respect to aftersets. Let $S = \{\perp, r, s\}$. Then, S is not an ideal of K_d-module of M. However, $\underline{\Gamma}^S(u_1) = \{\perp\}, \underline{\Gamma}^S(u_2) = \{\perp\}$ are K_d-module ideal of M. Hence, S is generalized lower soft K_d-module ideal of M with respect to aftersets.

4.20. Definition. Let $\varnothing \neq S \subseteq M$ and (Γ, C) be a SBR on a K_d-module M if $({}^S\underline{\Gamma}, C)$ is a soft K_d-module ideal M. Then, S is said to be generalized lower soft K_d-module of M with respect to foresets.

4.21. Theorem. Let $\varnothing \neq S \subseteq M$ and (Γ, C) be a SRRE and SCTR on a K_d-module M. Then, S is said to be generalized lower soft K_d-module ideal of M with respect to foresets if S is an K_d-module ideal of M.

Proof. The proof is simple. □

5. Homomorphic Images of Generalized Rough Soft Substructures

The relationship between the upper and lower generalized soft substructures of the K_d- module, as well as the images of upper (lower) approximations under K_d-module homomorphism, is being discussed in this section. Further, we study some properties of these approximations.

5.1. Lemma. Let M_1 and M_2 be K_d-modules and (β_2, C) be a SBR on M_2. Let Ω: $M_1 \longrightarrow M_2$ be a surjective K_d-module homomorphism. Set $\beta_1(u) = \{(s, t) \in M_1 \times M_1 : (\Omega(s), \Omega(t)) \in \beta_2(u) \forall u \in C\}$. Then, the following holds:

(1) (β_1, C) is a SBR on M_1

(2) (β_1, C) is SRRE if (β_2, C) is SRRE

(3) (β_1, C) is SCRE if (β_2, C) is SCRE

Proof. The proof is obvious. □

5.2. Lemma. Let M_1 and M_2 be a K_d-modules and (β_2, C) be a SBR on M_2. Let Ω: $M_1 \longrightarrow M_2$ be a surjective K_d-module homomorphism. Set $\beta_1(u) = \{(s, t) \in M_1 \times M_1 : (\Omega(s), \Omega(t)) \in \beta_2(u) \forall u \in C\}$ Then, (β_1, C) is SCTR with respect to aftersets if (β_2, C) is SCTR with respect to aftersets and Ω is one-one.

Proof. Clearly $r\beta_1(u) \vee s\beta_1(u) \subseteq (r \vee s)\beta_1(u) \forall u \in C$.

Conversely, suppose that $x \in (r \vee s)\beta_1(u)$. Then, by definition of aftersets $(r \vee s, x) \in \beta_1(u)$. Thus, $\Omega(r \vee s), \Omega(x) \in \beta_2(u)$, that is, $\Omega(r) \vee \Omega(s), \Omega(x) \in \beta_2(u)$. This implies that $\Omega(x) \in \Omega(r) \vee \Omega(s)\beta_2(u)$. Since (β_2, C) is SCTR with respect to aftersets, $\Omega(x) \in \Omega(r)\beta_2(u) \vee \Omega(s)\beta_2(u)$. Then, there is $t_1 \in \Omega(r)\beta_2(u)$ and $t_2 \in \Omega(r)\beta_2(u)$ such that $\Omega(x) = t_1 \vee t_2$. As Ω is onto, we have $s_1, s_2 \in M_1, \Omega(s_1) = t_1$ and $\Omega(s_2) = t_2$. Thus, $\Omega(x) = \Omega(s_1) \vee \Omega(s_2)$. This implies, $\Omega(x) = \Omega(s_1 \vee s_2)$. As Ω is one-one, we have $x = s_1 \vee s_2$. Now, $t_2 \in \Omega(r)\beta_2(u)$, $\Rightarrow$, $\Omega(s_1) \in \Omega(r)\beta_2(u) w w$, $\Rightarrow (\Omega(r), \Omega(s_1)) \in \beta_2(u)$, $\Rightarrow (r, s_1) \in \beta_1(u)$, $\Rightarrow s_1 \in r\beta_1(u)$. Also now, $t_2 \in \Omega(s)\beta_2(u)$, $\Rightarrow$, $\Omega(s_2) \in \Omega(s)\beta_2(u)$, $\Rightarrow (\Omega(s), \Omega(s_2)) \in \beta_2(u)$, $\Rightarrow (s, s_2) \in \beta_1(u)$, $\Rightarrow s_2 \in s\beta_1(u)$. Now, $x = s_1 \vee s_2 \in r\beta_1(u) \vee s\beta_1(u)$. That is, $x \in r\beta_1(u) \vee s\beta_1(u)$. This implies that $(r \vee s)\beta_1(u) \subseteq r\beta_1(u) \vee s\beta_1(u)$. Hence, $(r \vee s)\beta_1(u) = r\beta_1(u) \vee s\beta_1(u) \forall u \in C$. Similarly, we can prove that $k \oplus r\beta_1(u) = (k \oplus r)\beta_1(u) \forall u \in C$. This show that (β_1, C) is SCTR with respect to aftersets. □

5.3. Lemma. Let M_1 and M_2 be a K_d-modules and (β_2, C) be a SBR on M_2. Let Ω: $M_1 \longrightarrow M_2$ be a surjective K_d-module homomorphism. Set $\beta_1(u) = \{(s, t) \in M_1 \times M_1 : (\Omega(s), \Omega(t)) \in \beta_2(u) \forall u \in C\}$. Then, (β_1, C) is SCTR with respect to foresets if (β_2, C) is SCTR with respect to foresets and Ω is one-one.

Proof. The proof is obvious. □

5.4. Lemma. Let M_1 and M_2 be K_d-modules and (β_2, C) be a SBR on M_2. Let Ω: $M_1 \longrightarrow M_2$ be a surjective K_d-module homomorphism. Set $\beta_1(u) = \{(s, t) \in M_1 \times M_1 : (\Omega(s), \Omega(t)) \in \beta_2(u) \forall u \in C\}$ Then, $\Omega(\overline{\beta}_1^S(u)) = \overline{\beta}_2^{\Omega(S)}(u)$ for $S \subseteq M_1$ and $\forall u \in C$.

Proof. Let $s \in \overline{\beta}_2^{\Omega(S)}(u)$. Then, $s\beta_2(u) \cap \Omega(S) \neq \varnothing$. Then, there is $r \in s\beta_2(u) \cap \Omega(S)$ such that $r \in s\beta_2(u)$ and $r \in \Omega(S)$. So, $(s, r) \in \beta_2(u)$ and $r \in \Omega(S)$. Since Ω is onto, there exist $x \in S$ and $y \in M_1$ such that $r = \Omega(x)$ and $s = \Omega(y)$. Thus, $(s, r) = (\Omega(y), \Omega(x)) \in \beta_2(u)$, that is, $(\Omega(y), \Omega(x) \in \beta_2(u)$. Hence, $(yx) \in \beta_1(u)$, that is, $x \in y\beta_1(u)$ and $x \in S$. This implies $x \in y\beta_1(u) \cap S$. So, we have $y \in \overline{\beta}_1^S(u)$, $\Rightarrow \Omega(y) \in \Omega(\overline{\beta}_1^S(u))$, $\Rightarrow s \in \Omega(\overline{\beta}_1^S(u))$. This show that $\Rightarrow s \in \Omega(\overline{\beta}_1^S(u))$.

Conversely, let $z \in \Omega(\overline{\beta}_1^S(u))$. Then, there is $r \in \overline{\beta}_1^S(u)$ such that $r\beta_1(u) \cap S \neq \varnothing$ and $z \in \Omega(r)$. Thus, $x \in r\beta_1(u) \cap S$ such that $x \in r\beta_1(u)$ and $x \in S$. So, $(r, x) \in \beta_1(u)$ and $x \in S$,

$\Rightarrow \Omega(x) \in \Omega(S)$ and $(\Omega(r), \Omega(x) \in \beta_2(u)$, $\Rightarrow \Omega(x) \in \Omega(r)\beta_2(u)$ and $\Omega(x) \in \Omega(S)$. Hence, $\Omega(x) \in \Omega(r)\beta_2(u) \cap \Omega(S)$, that is, $\varnothing \neq \Omega(r)\beta_2(u) \cap \Omega(S)$, $\Rightarrow \Omega(r) \in \overline{\beta}_2^{\Omega(S)}$, $\Rightarrow z \in \overline{\beta}_2^{\Omega(S)}(u)$. This shows that $\Omega(\overline{\beta}_1^S(u)) \subseteq \overline{\beta}_2^{\Omega(S)}(u)$. Hence, $\Omega(\overline{\beta}_1^S(u)) = \overline{\beta}_2^{\Omega(S)}(u) \forall u \in C$. □

5.5. Lemma. Let M_1 and M_2 be K_d-modules and (β_2, C) be a SBR on M_2. Let Ω: $M_1 \longrightarrow M_2$ be a surjective K_d-module homomorphism. Set $\beta_1(u) = \{(s,t) \in M_1 \times M_1 : \Omega(s), \Omega(t) \in \beta_2(u) \forall u \in C\}$. Then, the following holds:

(1) $\Omega(\underline{\beta_1}^S(u)) \subseteq \underline{\beta_2}^{\Omega(s)}(u) \forall u \in C$; if Ω is one-one, then $\Omega(\underline{\beta_1}^S(u)) = \underline{\beta_2}^{\Omega(s)}(u) \forall u \in C$

(2) If Ω: $M_1 \longrightarrow M_2$ is one-one, then $\Omega(x) \in \Omega(\overline{\beta}_1^S(u))$ if and only if $x \in (\overline{\beta}_1^S(u)) \forall u \in C$

Proof (1) Let $r \in \Omega(\underline{\beta_1}^S(u))$ for $u \in C$. Then, there is $s \in \underline{\beta_1}^S(u)$ such that $s\beta_1(u) \subseteq S$ and $r = \Omega(x)$. Suppose that $y \in r\beta_2(u)$. Then, there is $x \in M_1$ such that $\Omega(x) = y$ and $\Omega(x) \in \Omega(s)\beta_2(u)$, that is, $(\Omega(s), \Omega(x)) \in \beta_2(u)$. Hence, $(s,x) \in \beta_1(u)$ by definition of aftersets $x \in s\beta_1(u)$. Hence, $s\beta_1(u) \subseteq S$ and $x \in S$. So, $\Omega(x) \in \Omega(S)$ using above $\Omega(x) = y$, $\Rightarrow y \in \Omega(S)$. Thus, $r\beta_2(u) \subseteq \Omega(S)$. Hence, $r \in \underline{\beta_2}^{\Omega(s)}(u)$which shows that $\Omega(\underline{\beta_1}^S(u)) \subseteq \underline{\beta_2}^{\Omega(s)}(u) \forall u \in C$. Conversely, let $s \in \underline{\beta_2}^{\Omega(s)}(u) \forall u \in C$. Then, $s\beta_2(u) \subseteq \Omega(S)$. Suppose that Ω is one-one. Then, there is $r \in M_1$ such that $s = \Omega(r)$ and $\Omega(r)\beta_2(u) \subseteq \Omega(S)$. Let $x \in r\beta_1(u)$ by definition of aftersets, we have $(r,x) \in \beta_1(u)$. Then, $\Omega(r), \Omega(x) \in \beta_2(u)$, that is, $\Omega(x) \in \Omega(r)\beta_2(u)$. Since $\Omega(r)\beta_2(u) \subseteq \Omega(S)$, $\Omega(x) \in \Omega(S), \Rightarrow x \in S$. Thus, $r\beta_1(u) \subseteq S$, that is, $r \in \underline{\beta_1}^S(u)$, $\Rightarrow \Omega(r) \in \Omega(\underline{\beta_1}^S(u))$ since $s = \Omega(r)$. Hence, $s \in \Omega(\underline{\beta_1}^S(u))$. So,$\underline{\beta_2}^{\Omega(s)}(u) \subseteq \Omega(\underline{\beta_1}^S(u)) \forall u \in C$. Thus, $\Omega(\underline{\beta_1}^S(u)) = \underline{\beta_2}^{\Omega(s)}(u) \forall u \in C$.

(2) Let $\Omega(r) \in \Omega(\overline{\beta}_1^S(u))$. Then, there is $s \in \overline{\beta}_1^S(u)$ such that $\Omega(r) = \Omega(s)$. Since Ω is one-one, we get $r = s$. Thus, $r \in \overline{\beta}_1^S(u)$. Conversely, let $r \in \overline{\beta}_1^S(u) \forall u \in C$. Then, $\Omega(r) \in \Omega(\overline{\beta}_1^S(u)) \forall u \in C$. □

5.6. Theorem. Let $S \subseteq M_1$ and let Ω be a surjective K_d-module homomorphism on a K_d-modules M_1, M_2 and (β_2, C) be a SBR and SCTR with respect to aftersets on M_2. Set $\beta_1(u) = \{(s,t) \in M_1 \times M_1 : (\Omega(s), \Omega(t)) \in \beta_2(u) \forall u \in C\}$. Then, the following holds:

(1) $\overline{\beta}_1^S(u)$ is a K_d-module ideal of M_1 if and only if $\overline{\beta}_2^{\Omega(S)}(u)$ is a K_d-module ideal of $M_2 \forall u \in C$

(2) $\overline{\beta}_1^S(u)$ is a sub-K_d-module of M_1 if and only if $\overline{\beta}_2^{\Omega(S)}(u)$ is a sub-K_d-module of $M_2 \forall u \in C$

Proof. (1) Let $\overline{\beta}_1^S(u)$ be a K_d-module ideal of M_1. Then, we have to show that $\overline{\beta}_2^{\Omega(S)}(u)$ is a K_d-module ideal of $M_2 \forall u \in C$. By Lemma 5.4, we have $\Omega(\overline{\beta}_1^S(u)) = \overline{\beta}_2^{\Omega(S)}(u)$ for all $S \subseteq M_1$ and $\forall u \in C$.

Let $r_i \in \Omega(\overline{\beta}_1^S(u)) \forall u \in C$. Then, there is $t_i \in \overline{\beta}_1^S(u)$ such that $\Omega(t_i) = r_i$. Hence, Ω is a K_d-module homomorphism and $\overline{\beta}_1^S(u)$ is a K_d-module ideal of $M_1 \forall u \in C$. So, we have $\vee_{i \in I} t_i \in \overline{\beta}_1^S(u)$, $\Rightarrow \Omega(\vee_{i \in I} t_i) \in \Omega(\overline{\beta}_1^S(u))$. Thus, $\vee_{i \in I} \Omega(t_i) \in \Omega(\overline{\beta}_1^S(u))$. Hence, $\vee_{i \in I} r_i \in \Omega(\overline{\beta}_1^S(u))$.

Let $r \leq s$ and $s \in \Omega(\overline{\beta}_1^S(u))$. Then, there is $t \in M_1$ and $u \in \overline{\beta}_1^S(u)$ such that $\Omega(t) = r$ and $\Omega(u) = s$. Hence, $r \leq s$, that is, $\Omega(t) \leq \Omega(u)$ and $\Omega(t) \vee \Omega(u) = \Omega(u)$. Further, Ω is a K_d-module homomorphism. Thus, we have $\Omega(t \vee u) = \Omega(t) \vee \Omega(u)$, $= \Omega(u) \in \Omega(\overline{\beta}_1^S(u))$, $\Rightarrow \Omega(t \vee u) \in \Omega(\overline{\beta}_1^S(u))$. By Lemma 5.5(2), we have $(t \vee u) \in \overline{\beta}_1^S(u)$. Hence, $\overline{\beta}_1^S(u)$ is a lower set and $t \leq t \vee u$. Thus, $t \in \overline{\beta}_1^S(u)$ and $\Omega(t) \in \Omega(\overline{\beta}_1^S(u))$ so $r \in \Omega(\overline{\beta}_1^S(u))$. Hence, $\Omega(\overline{\beta}_1^S(u))$ is a lower set.

Now, we show that $k \oplus r \in \Omega(\overline{\beta}_1^S(u))$ for all $r \in \Omega(\overline{\beta}_1^S(u))$ and $\forall k \in K_d$. Let $k = \Omega(s) \in K_d$ and $r = \Omega(t) \in \Omega(\overline{\beta}_1^S(u))$. So, $\Omega(t) \in \Omega(\overline{\beta}_1^S(u))$. Then, by Lemma 5.5(2), we have $t \in \overline{\beta}_1^S(u)$. Hence, $\overline{\beta}_1^S(u)$ is an K_d-module ideal of M_1. Thus, $s \oplus t \in \overline{\beta}_1^S(u)$. Thus, $\Omega(s \oplus t) \in \Omega(\overline{\beta}_1^S(u))$. Hence, Ω is an K_d-module homomorphism. Thus, $\Omega(s \oplus t) = \Omega(s) + \Omega(t)$, that is, $\Omega(s) \oplus \Omega(t) \in \Omega(\overline{\beta}_1^S(u))$. Hence, $k \oplus r \in \Omega(\overline{\beta}_1^S(u))$. Thus, $\Omega(\overline{\beta}_1^S(u)) = \overline{\beta}_2^{\Omega(S)}(u)$ is a K_d-module ideal of $M_2 \forall u \in C$.

Conversely, suppose $\Omega(\overline{\beta}_1^S(u)) = \overline{\beta}_2^{\Omega(S)}(u)$ is a K_d-module ideal of $M_2 \forall u \in C$.

Suppose $s_i \in \overline{\beta}_1^S(u) \forall u \in C$ for some $i \in I$. Then, $\Omega(s_i) \in \Omega(\overline{\beta}_1^S(u)) \forall u \in C$. Hence, $\Omega(\overline{\beta}_1^S(u))$ is a K_d-module ideal and Ω is a K_d-module homomorphism. So, $\vee_{i \in I} \Omega(s_i) = \Omega(\vee_{i \in I} s_i) \in \Omega(\overline{\beta}_1^S(u)), \forall u \in C$. Then, by Lemma 5.5(2), we have $\vee_{i \in I} s_i \in \overline{\beta}_1^S(u)$ and $\overline{\beta}_1^S(u)$ is directed.

Let $r \leq s$and $s \in \overline{\beta}_1^S(u)$. Then, $\Omega(r) \leq \Omega(s)$ and $\Omega(s) \in \Omega(\overline{\beta}_1^S(u))$. Since $\Omega(\overline{\beta}_1^S(u))$ is a lower set, we have $\Omega(r) \in \Omega(\overline{\beta}_1^S(u))$. Thus, by Lemma 5.5(2), we have $r \in \overline{\beta}_1^S(u)$. So, $\overline{\beta}_1^S(u)$ is a lower set. Suppose $k \in K_d$ and $v \in \overline{\beta}_1^S(u)$ Then, $\Omega(k) \in K_d$ and $\Omega(v) \in \Omega(\overline{\beta}_1^S(u))$. Since $\Omega(\overline{\beta}_1^S(u))$ is an K_d-module ideal of M_2, we have $\Omega(k \oplus v) = k \oplus \Omega(v) \in \Omega(\overline{\beta}_1^S(u))$, $\Rightarrow \Omega(k \oplus v) \in \Omega(\overline{\beta}_1^S(u)) \forall u \in C$ and then by Lemma 5.5(2), we have $k \oplus v \in \overline{\beta}_1^S(u)$. By the above discussion, we have $\overline{\beta}_1^S(u)$ is K_d-module ideal of M_1.

(2) Let $\overline{\beta}_1^{\Omega(S)}(u)$ is a sub-K_d-module of $M_1 \forall u \in C$. Then, we have to show that $\overline{\beta}_2^{\Omega(S)}(u)$ is sub-K_d-module of $M_2 \forall u \in C$. By Lemma 5.4, we have $\Omega(\overline{\beta}_1^S(u)) = \overline{\beta}_2^{\Omega(S)}(u)$ for all $S \subseteq M_1$ and $\forall u \in C$.

Let $r_i \in \Omega(\overline{\beta}_1^S(u)) \forall u \in C$ Then, there is $t_i \in \overline{\beta}_1^S(u)$ such that $\Omega(t_i) = r_i$. Hence, Ω is a K_d-module homomorphism and $\overline{\beta}_1^S(u)$ is a sub-K_d-module of M_1, $\forall u \in C$. So, $\vee_{i\in I} t_i \in \overline{\beta}_1^S(u)$, $\Rightarrow \Omega(\vee_{i\in I} t_i) \in \Omega(\overline{\beta}_1^S(u))$. So, we have $\vee_{i\in I}\Omega(t_i) \in \Omega(\overline{\beta}_1^S(u))$. Hence, $\vee_{i\in I} r_i \in \Omega(\overline{\beta}_1^S(u))$.

Now, we show that$k \oplus r \in \Omega(\overline{\beta}_1^S(u))$ for all $r \in \Omega(\overline{\beta}_1^S(u))$ and $\forall k \in K_d$. Let$k = \Omega(s) \in K_d$ and $r = \Omega(t) \in \Omega(\overline{\beta}_1^S(u))$.So, $\Omega(t) \in \Omega(\overline{\beta}_1^S(u))$. Then, by Lemma 5.5(2), we have $t \in \overline{\beta}_1^S(u)$. Hence, $\overline{\beta}_1^S(u)$ is a sub-K_d-module of M_1. This shows that $k \oplus t \in \overline{\beta}_1^S(u)$. Thus, $\Omega(k \oplus t) \in \Omega(\overline{\beta}_1^S(u))$. Hence, Ω is an K_d-module homomorphism. Thus, $\Omega(k \oplus t) = \Omega(k) + \Omega(t)$, that is, $\Omega(k) \oplus \Omega(t) \in \Omega(\overline{\beta}_1^S(u))$. Hence, $k \oplus t \in \Omega(\overline{\beta}_1^S(u))$. Thus, we have that $\Omega(\overline{\beta}_1^S(u)) = \overline{\beta}_2^{\Omega(S)}(u)$ is a sub-K_d-module of $M_2 \forall u \in C$.

Conversely, suppose $\Omega(\overline{\beta}_1^S(u)) = \overline{\beta}_2^{\Omega(S)}(u)$ is a sub-K_d-module of $M_2 \forall u \in C$. Suppose, $s_i \in \overline{\beta}_1^S(u) \forall u \in C$ for some $i \in I$.Then, $\Omega(s_i) \in \Omega(\overline{\beta}_1^S(u)) \forall u \in C$. Hence, $\Omega(\overline{\beta}_1^S(u))$ is a sub-K_d-module and Ω is a K_d-module homomorphism. So, $\vee_{i\in I}\Omega(s_i) = \Omega(\vee_{i\in I} s_i) \in \Omega(\overline{\beta}_1^S(u))$, $\forall u \in C$. Then, by Lemma 5.5(2), we have $\vee_{i\in I} s_i \in \overline{\beta}_1^S(u)$.

Suppose $k \in K_d$and $v \in \overline{\beta}_1^S(u)$. Then, $\Omega(k) \in K_d$ and $\Omega(v) \in \Omega(\overline{\beta}_1^S(u))$. Since $\Omega(\overline{\beta}_1^S(u))$ is an sub-K_d-module ideal of M, we have $\Omega(k \oplus v) = k \oplus \Omega(v) \in \Omega(\overline{\beta}_1^S(u)) \Rightarrow \Omega(k \oplus v) \in \Omega(\overline{\beta}_1^S(u)) \forall u \in C$ and then by Lemma 5.5(2) we have $k \oplus v \in \overline{\beta}_1^S(u)$. From the above discussion, we get $\overline{\beta}_1^S(u)$ is sub-K_d-module of M_1. □

5.7. Remark. With similar arguments, Theorem 5.6 can be similarly proved but for the foresets.

5.8. Theorem. Let $S \subseteq M_1$ and let Ω be a surjective K_d-module homomorphism on a K_d-module M and (β_2, C) be a SBR and SCTR and with respect to aftersets on M_2. Set $\beta_1(u) = \{(s,t) \in M_1 \times M_1 : (\Omega(s), \Omega(t)) \in \beta_2(u) \forall u \in C\}$. Then, the following holds:

(1) $\underline{\beta}_1^S(u)$ is a K_d-module ideal of M_1 if and only if $\underline{\beta}_2^{\Omega(S)}(u)$ is a K_d-module ideal of $M_2 \forall u \in C$
(2) $\underline{\beta}_1^S(u)$ is a sub-K_d-module of M_1 if and only if $\underline{\beta}_2^{\Omega(S)}(u)$ is a sub-K_d-module of $M_2 \forall u \in C$

Proof. The proof is similar in view of Theorem 5.6. □

6. Comparison

Qurashi and Shabir presented the roughness in quantale modules with the help of congruence relation [7]. Furthermore, generalized roughness of fuzzy substructures in quantale with respect to soft relations in quantale was defined in [11]. It is clear that equivalence relation is a hurdle while evaluating roughness. In order to avoid this this hurdle, soft binary relations are presented in this paper. Since suitable soft binary relations are easy to find out, it is an easy approach to observe soft rough properties to discuss different characterizations of soft rough substructures in quantale modules with the help of aftersets and foresets. Different characterization of soft substructures in semigroups and their approximation based on soft relation was discussed by Kanwal and Shabir [26]. We are actually motivated from the paper roughness in quantale module and taken help from [11] to develop the idea of this paper.

7. Conclusion

In this paper, we have suggested a new relation of substructures of quantale module with rough set and soft sets. The properties of rough soft substructures in quantale module are discussed for the first time. On the one hand, we have presented different characterizations for soft relations to approach quantale module subsets, as well as the use of aftersets and foresets in this regard. Structural features of soft relations under aftersets and foresets are discussed. Furthermore, in the quantale module, foresets and aftersets are applied to various types of substructures using soft relations to explore their lower and upper approximations. The following work can be done in future:

(1) Soft relations applied to the fuzzy substructures of quantale module and their approximations
(2) Some studies of soft substructures of quantale module and their approximations

Data Availability

The paper includes the information used to verify the study's findings.

Conflicts of Interest

The authors state that they have no conflicts of interest.

Authors' Contributions

All authors have contributed equally to this paper in all aspects. All authors have read and agreed to the published version of the manuscript.

References

[1] S. Abramsky and S. Vickers, "Quantales, observational logic and process semantics," *Mathematical Structures in Computer Science*, vol. 3, no. 2, pp. 161–227, 1993.
[2] C. J. Mulvey, "Rendiconti del Circolo Matematico di Palermo," *Computers & Mathematics with Applications*, vol. 12, no. 2, pp. 99–104, 1986.
[3] Z. Pawlak, "Rough sets," *International Journal of Computer & Information Sciences*, vol. 11, no. 5, pp. 341–356, 1982.
[4] W. Zhu, "Generalized rough sets based on relations," *Information Sciences*, vol. 177, no. 22, pp. 4997–5011, 2007.
[5] M. I. Ali, B. Davvaz, and M. Shabir, "Some properties of generalized rough sets," *Information Sciences*, vol. 224, pp. 170–179, 2013.

[6] T. B. Iwinski, "Algebraic approach to rough sets," *Bulletin of the Polish Academy of Sciences - Mathematics*, vol. 35, pp. 673–683, 1987.
[7] S. M. Qurashi and M. Shabir, "Roughness in quantale modules," *Journal of Intelligent and Fuzzy Systems*, vol. 35, no. 2, pp. 2359–2372, 2018.
[8] Q. Xiao and Q. Li, "Generalized lower and upper approximations in quantales," *Journal of Applied Mathematics*, vol. 2012, pp. 1–11, Article ID 648983, 2012.
[9] L. Yang and L. Xu, "Roughness in quantales," *Information Sciences*, vol. 220, pp. 568–579, 2013.
[10] Q. Luo and G. Wang, "Roughness and fuzziness in quantales," *Information Sciences*, vol. 271, pp. 14–30, 2014.
[11] S. M. Qurashi, R. S. Kanwal, M. Shabir, and K. Ali, "Generalized roughness of fuzzy substructures in quantales with respect to soft relations," *Journal of Intelligent and Fuzzy Systems*, vol. 40, no. 6, pp. 1–18, 2021.
[12] N. Abughazalah, N. Yaqoob, and K. Shahzadi, "Topological structures of lower and upper rough subsets in a hyperring," *Journal of Mathematics*, vol. 2021, pp. 1–6, Article ID 9963623, 2021.
[13] H. K. Sharma, A. Singh, D. Yadav, and S. Kar, "Criteria selection and decision making of hotels using dominance based rough set theory," *Operational Research in Engineering Sciences: Theory and Applications*, vol. 5, no. 1, pp. 41–55, 2022.
[14] N. Yaqoob and J. Tang, "Approximations of quasi and interior hyperfilters in partially ordered LA-semihypergroups," *AIMS Mathematics*, vol. 6, no. 8, pp. 7944–7960, 2021.
[15] R. Gul, M. Shabir, M. Naz, and M. Aslam, "A novel approach toward roughness of bipolar soft sets and their applications in MCGDM," *IEEE Access*, vol. 9, pp. 135102–135120, 2021.
[16] F. Feng, X. Liu, V. Leoreanu-Fotea, and Y. B. Jun, "Soft sets and soft rough sets," *Information Sciences*, vol. 181, no. 6, pp. 1125–1137, 2011.
[17] H. Fazlollahtabar and N. Kazemitash, "Green supplier selection based on the information system performance evaluation using the integrated Best-Worst Method," *Facta Universitatis – Series: Mechanical Engineering*, vol. 19, no. 3, pp. 345–360, 2021.
[18] D. Molodtsov, "Soft set theory—first results," *Computers & Mathematics with Applications*, vol. 37, no. 4-5, pp. 19–31, 1999.
[19] P. K. Maji, R. Biswas, and A. Roy, "Soft set theory," *Soft set theory, " Computers & Mathematics with Applications*, vol. 45, no. 4-5, pp. 555–562, 2003.
[20] M. I. Ali, F. Feng, X. Liu, W. K. Min, and M. Shabir, "On some new operations in soft set theory," *Computers & Mathematics with Applications*, vol. 57, no. 9, pp. 1547–1553, 2009.
[21] A. S. Sezer, N. Çağman, A. O. Atagün, M. I. Ali, and E. Türkmen, "Soft intersection semigroups, ideals and bi-ideals; a new application on semigroup theory I," *Filomat*, vol. 29, no. 5, pp. 917–946, 2015.
[22] M. I. Ali, N. Mehmood, J. Zhan, and N. Shah, "Soft linear programming: an application of soft vector spaces," *Journal Of Information And Optimization Sciences*, vol. 41, no. 3, pp. 679–704, 2020.
[23] A. Khan, M. Farooq, and N. Yaqoob, "Uni-soft structures applied to ordered Γ-semihypergroups," *Proceedings of the National Academy of Sciences, India, Section A: Physical Sciences*, vol. 90, no. 3, pp. 457–465, 2020.
[24] M. Gulzar, M. H. Mateen, D. Alghazzawi, and N. Kausar, "A novel applications of complex intuitionistic fuzzy sets in group theory," *IEEE Access*, vol. 8, pp. 196075–196085, 2020.
[25] R. Chattopadhyay, P. P. Das, and S. Chakraborty, "Development of a rough-MABAC-DoE-based metamodel for supplier selection in an iron and steel industry," *Operational Research in Engineering Sciences: Theory and Applications*, vol. 5, no. 1, pp. 20–40, 2022.
[26] R. S. Kanwal and M. Shabir, "Approximation of soft ideals by soft relations in semigroups," *Journal of Intelligent and Fuzzy Systems*, vol. 37, no. 6, pp. 7977–7989, 2019.
[27] M. Z. Anwar, S. Bashir, M. Shabir, and M. G. Alharbi, "Multigranulation roughness of intuitionistic fuzzy sets by soft relations and their applications in decision making," *Mathematics*, vol. 9, no. 20, p. 2587, 2021.
[28] M. A. Bilal and M. Shabir, "Approximations of pythagorean fuzzy sets over dual universes by soft binary relations," *Journal of Intelligent and Fuzzy Systems*, vol. 41, no. 1, pp. 2495–2511, 2021.
[29] H. Zhou, S. M. Qurashi, M. U. Rehman, M. Shabir, R. S. Kanwal, and A. M. Khalil, "Soft substructures in quantales and their approximations based on soft relations," *Computational Intelligence and Neuroscience*, vol. 2022, pp. 1–11.
[30] F. Feng, I. Ali, and M. Shabir, "Soft relations applied to semigroups," *Filomat*, vol. 27, no. 7, pp. 1183–1196, 2013.
[31] M. Shabir, R. S. Kanwal, and M. I. Ali, "Reduction of an information system," *Soft Computing*, vol. 24, no. 14, pp. 10801–10813, 2020.

Hindawi
Complexity
Volume 2022, Article ID 2782811, 8 pages
https://doi.org/10.1155/2022/2782811

Research Article

Mathematical Modeling of Multiattack Behavior Discrimination in the WSN Based on Incidence Matrix

Yu Shuai-Jing and Wang Peng-Fei

Yiwu Industrial & Commercial College, Yiwu, Zhejiang 322000, China

Correspondence should be addressed to Yu Shuai-Jing; 20150810106@m.scnu.edu.cn

Received 24 July 2022; Revised 25 August 2022; Accepted 8 September 2022; Published 22 September 2022

Academic Editor: Zeljko Stevic

The current WSN is vulnerable to a variety of malicious attacks, resulting in the decline of its comprehensive performance. Multihop routing involves a number of safety and privacy issues. Problems such as snooping, sinkhole, manipulation, cloning, wormhole, spoofing, and so on affect the integrity, availability, and confidentiality of the WSNs. Therefore, this paper mainly studies the mathematical modeling of WSN multiattack behavior discrimination based on the incidence matrix. The WSN node model is used to collect relevant data and mark and map the disguised data, so as to determine the characteristics of multiattack behavior and establish the WSN multiattack behavior discrimination model based on the incidence matrix. The experimental results show that the designed multiattack behavior discrimination model can distinguish the attack type according to the characteristics, has high recognition ability, can spend a short time to effectively distinguish the attack behavior, has a low false positive rate, and can effectively improve the antiattack ability of the WSN.

1. Introduction

The wireless sensor network (WSN) has a large number of data nodes in the network, which can be used in different application fields, such as temperature and humidity detection, air pollution monitoring, water quality monitoring, body temperature monitoring, and chemical composition attack in military field [1]. The WSN layer utilises multihop communication systems to route the packets to destination, the black hole attacks, selective forwarding, the symbolic attack, the Hello flood attack, the wormhole attack, and the replicative attack of identity. Compared with the wired network, it has stronger flexibility, can collect and analyze all nodes in the network, and has higher coverage. It can cover all types of data nodes and can use and analyze network nodes flexibly. However, due to the large number of nodes in the WSN, the network structure is more complex, the signal is difficult to maintain stability in the process of wireless transmission, and the information transmission is incomplete. At the same time, WSNs are more vulnerable to malicious attacks. In the process of security research on WSNs, it is found that they are vulnerable to attacks, among which the black hole attack, DoS attack, and selective forwarding attack are the most important attack methods [2–4]. In order to improve the ability of network security and ensure the security of network environment, scholars at home and abroad have carried out relevant research on multiattack behavior. Privalov et al. built a random network contour model by simulating the superposition of the attack and legal effect on the signal by using the extreme value filtering method, detected the WSN attack behavior, and obtained the measurement index characterizing the network attack, which can effectively distinguish the attack behavior [5]. Internal attacks are initiated by nodes that have been compromised or taken. In order to assault behavior, the data are removed, replayed, manipulated, and forged, and fake routing information is provided. Since these malicious nodes are transmitted by the network and by holding the key, the internal attacks are harder, and traditional encryption and other safety mechanisms have no effect. Chi et al. used the detection and defense algorithm based on distance vector jump to analyze the WSN attack behavior and used the DV-

hop algorithm to calculate the average value of the minimum hop node distance under the WSN node, so as to improve the security of WSN nodes [6]. The WSNs are independent and spatially distributed. As there is no central government, the WSN is prone to safety threats because of the random deployment of the nodes on the network. WSN attacks are well-known and are malicious. The algorithm for the localization of DV-Hop is a spanning algorithm based on the protocol on the distance vector routing [7, 8]. However, the above methods have the problems of weak recognition ability, high missing rate of attack behavior, and long discrimination time. Therefore, this paper proposes a mathematical modeling of multiattack behavior discrimination in the WSN based on incidence matrix. The incidence matrix is a rational matrix for the relationship in math, which is usually called an occurrence relationship, between two classes of objects. The incidence matrix offers a great capability for comprehensive evaluation. To express the quantitative and direct evaluation relationship, a different matrix can be used in place of the specific value of the evaluation index. It has the traits of a clear distinction between data nodes. In order to make the discriminating process of attack behavior simple, obvious, and tangible, it can mathematically quantify the characteristics of complicated multiattack behavior in the form of a matrix and analyze the data results acquired by discrimination.

The primary focus of this paper is on the mathematical modeling of WSN multiattack behavior discrimination based on incidence matrix. The WSN node model is used to collect relevant data, mark and map the disguised data, so as to determine the features of multiattack behavior, and construct the WSN multiattack behavior discrimination model based on incidence matrix. The experimental results show that the designed multiattack behavior discrimination model can distinguish the attack type according to the characteristics, has high recognition ability, can spend a short time to effectively distinguish the attack behavior, has a low false positive rate, and effectively improves the antiattack ability of the WSN.

2. Feature Modeling of Multiattack Behavior in WSNs

2.1. The WSN Node Model. The WSN is composed of three parts. The composition of sensor nodes is the basis of the WSN node model, which has the functions of data node receiving and operation; the sink node and the management node are components of auxiliary network node construction, and their main function is to connect external networks and receive external information data nodes [9]. Four key components such as the sensor unit, processing unit, transceiver unit, and power unit are used as a sensor node. The sensor architecture of the WSN multiattack behavior discrimination model based on the incidence matrix is composed of four modules, as shown in Figure 1. Each row in the matrix corresponds to a node of the graph. Each row has nonzero entries such as +1 and −1 depending upon the orientation of branch at the nodes. The entries in all other columns of that row are zero.

According to Figure 1, the wireless communication module adopts DH600 data collector to transmit and receive various sensor node information of the WSN and to efficiently collect and exchange node information. The sensor module uses AlphaProx technology to realize the conversion from nonelectric quantity to electric quantity, collect and convert the information in the monitoring area, and improve the discrimination ability of multiattack behavior. The new AlphaProx inductive distance measuring sensors offer more than accurate measurement technology with the Baumer IO-Link interface. The processor module is mainly responsible for storing and processing the data information of sensor network nodes. Another significant advantage of AlphaProx high sensitivity sensors is the quick and easy installation and operation of sensors through the innovative teach-in method. WSN's monitor conditions, such as temperature, sound, and pressure, are either physical or environmental. Modern networks are two-way, both data collection and sensor activity control. Military applications like battleground monitoring were the reason for development of those networks. The W25Q64JVSSIQ memory is selected to expand the storage range and strengthen the embedded operation ability. The energy supply module usually selects Tenda PoE30G-AT Gigabit high-power PoE power supply to provide the required energy for the operation of sensor nodes [10]. Military applications such as combat field monitoring were behind the development of sensor networks. Such systems are used for manufacturing and processing applications such as the monitoring and control of manufacturing applications and device health monitoring. The sink node is the main node connecting the current sensor network with the external network. It can collect and analyze the information of any location at any time and can fully analyze and process the external network data nodes. At the same time, the energy supply is provided by the sink node to provide greater storage space for the WSN and ensure the stable operation of the data node. By detecting the data node, the effective data are transmitted to the management node, and the monitoring task of identifying multiple attacks is issued [11]. With the support of several control and monitoring applications, wireless sensor networks (WSNs) have gained popularity among the research community. These simple and low-priced networks enable remote, real-time, and minimal human intervention monitoring processes.

The management node is a node in the communication transmission network. It can effectively monitor, calculate, and analyze all sensor network data nodes, judge whether the data nodes have multiple attacks, and report and process them in time. The management node can be used in various environments such as shell. It is easy to configure and has strong portability. It supports about 300 nodes and can effectively meet the needs of the cluster.

2.2. Preprocessing of Multiple Attacks in the WSN. WSNs have a large number of nodes and are vulnerable to many kinds of attacks. Therefore, the discrimination of the WSN has great complexity, and it needs to spend more time to

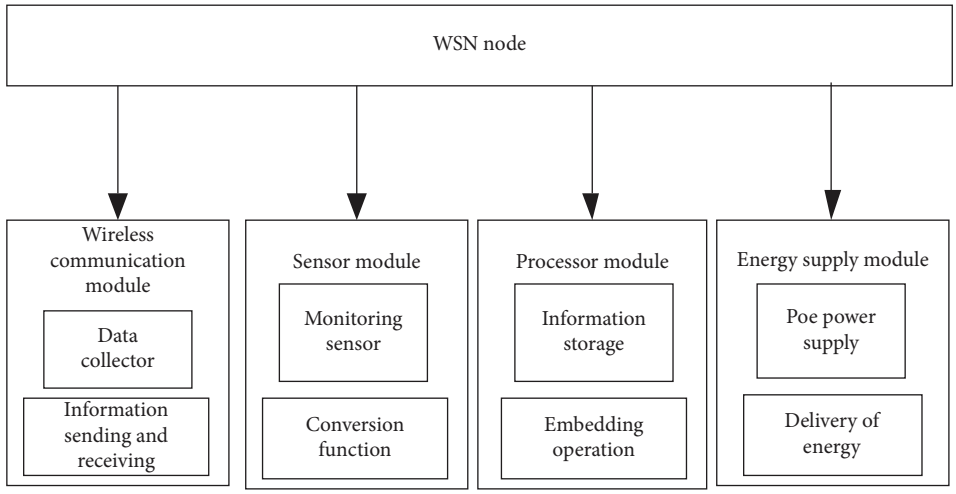

Figure 1: Composition of the sensor network.

distinguish them effectively. Therefore, preprocessing the multiattack behavior of the WSN in advance can effectively shorten the discrimination time and provide convenience for subsequent processing. High demand for bandwidth, high power consumption, service quality (QoS), data processing and compression technologies, and cross-layer design are the challenges of the WSN. Physical environment. Mobile nodes are capable of sensing, calculating, and communicating as still nodes.

2.2.1. Marking Processing of Camouflage Data Samples in Multiattack Behavior. The premise of judging the multiattack behavior of the WSN is to classify the types of the multiattack behavior, and the behavior can be effectively classified according to the characteristics of multiattack behavior [12]. Therefore, in the process of preprocessing, the attack behavior characteristics of WSN nodes are mainly considered, and the detection model of the attack behavior injection is constructed. Imperva Camouflage Data Masking permits institutions, without revealing sensitive data, to secure the way to use data for business operations. The specific process is as follows.

It is assumed that before and after the WSN is attacked, the node dataset distribution is as follows:

$$X = \{x_1, x_2, x_3, \ldots, x_n\}. \tag{1}$$

Mark the attack behavior on the node dataset and transform the original node data composed of N data into a matrix [13], with the expression

$$\mathbf{x} = \begin{bmatrix} x_{11} & x_{12} & x_{13} & \cdots & x_{1m} \\ x_{21} & x_{22} & x_{23} & \cdots & x_{2m} \\ \vdots & \vdots & \vdots & \ddots & \vdots \\ x_{n1} & x_{n2} & x_{n3} & \cdots & x_{nm} \end{bmatrix}. \tag{2}$$

The matrix is used as the input of data in the WSN. The matrix is used to mark the attack behavior. Assuming that the camouflage data sample of the WSN subjected to multiple attacks is x', the whole sample set is preliminarily trained, and the marked node data results of the attack behavior are as follows:

$$x' = \begin{cases} -x_{nm}, & a \neq 1, \\ x_{nm}, & a = 1, \end{cases} \tag{3}$$

where a represents the attack system of camouflage data injection. If $a = 1$, it means that the node data are not attacked; if $a \neq 1$, it indicates that the node data have been attacked. At this time, the node data are marked as negative. The Imperva Camouflage Data Masking solution provides protection against theft and ensures compliance with regulations and international policies that govern the privacy and transportation of data. A static data masking software that protects data forever and decrease the exposure to compliance requirements is the Imperva Camouflage Data Masking solution. Thus, the camouflage data marking of WSN data is completed, which paves the way for the follow-up.

2.2.2. Mapping Processing of Camouflage Data. The camouflage data of multiple attacks in the WSN have the function of discrimination. The camouflage sample data in the preset time are collected and effectively distinguished according to the time threshold. When the behavior of camouflage sample data is consistent with the normal nodes of the network, it can effectively distinguish the category of the attack behavior, detect, and output data results at the same time. When it is consistent with the normal behavior, it is necessary to collect and judge the data nodes again in the camouflage sample database in the WSN. The specific process is shown in Figure 2.

The detection of the camouflage attack in the WSN is a data mapping process [14]. In the discrimination process, it is necessary to effectively distinguish the unknown behavior of data nodes, summarize them into known categories after detection and analysis, and set the mapping process as $f: A \longrightarrow B$, where A is the node to be detected and B is the

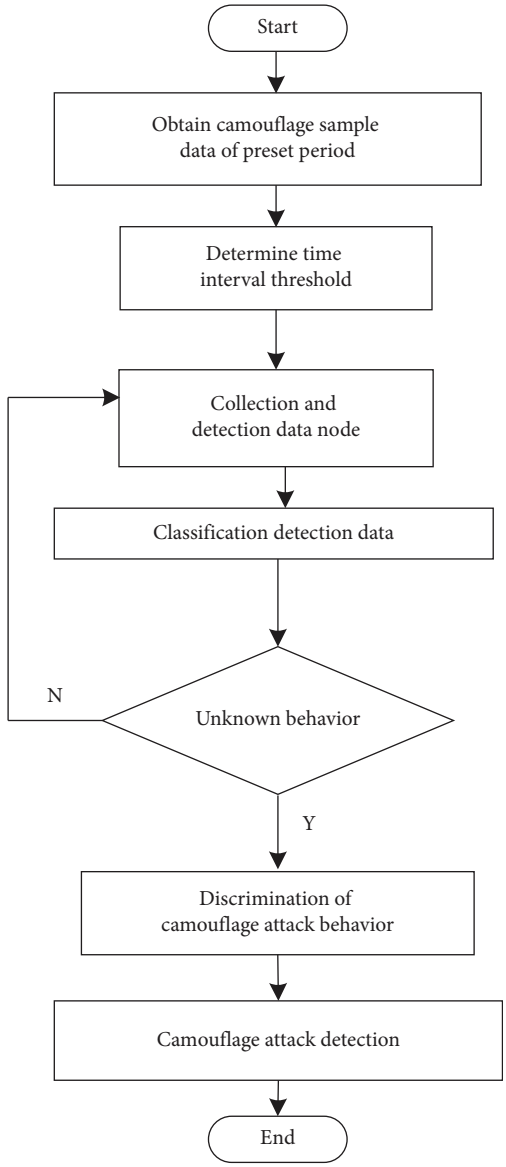

Figure 2: Camouflage data mapping processing flow.

known node category database. According to different data node information, it is summarized and sorted, so as to judge the new behavior category. Network mapping understands the physical connections between different network devices. The attack surface represents the sum of the system's vulnerabilities. They come in two different types: the software vulnerability digital attack surface and the hardware vulnerability physical attack surface.

2.3. Determine the Multiattack Behavior Characteristics of the WSN. Suppose that in the WSN, after the attack, the packet loss rate threshold of the whole WSN in the communication process is I, and A, B are used to represent the abnormal node dataset under the attack behavior [15]. In the WSN, a node for transmitting data information is set every t second. In order to reduce the false detection rate of multiattack behavior feature detection in WSNs, the wormhole attack mode is used to judge the attack status of nodes [16]. Set the number of surrounding nodes of node i to H, so that each node can detect and judge by itself by using the following formula:

$$\frac{K_1Q_1 + K_2Q_2}{H \cdot T} > I, \tag{4}$$

where K_1 and K_2 are the data test nodes in the wireless network, Q_1 and Q_2 are the information transmission nodes, and T is the transmission time of the data node. If node i meets the conditions of formula (4), the node is judged as an abnormal node. Formula (4) is the self-judgment feature of the multiattack behavior, which can effectively distinguish nodes, improve the preprocessing ability of the multiattack behavior of the WSN, and strengthen the antiattack ability of the WSN. A complex network-theory on the antiattack model is presented in this paper. The mechanism of this model is based on P2P's networks on dynamic compensation and reverse percolation.

3. Discriminant Modeling of the Multiattack Behavior in the WSN Based on the Incidence Matrix

3.1. The Incidence Matrix of Data Node States in the WSN. The incidence matrix method [17] has strong comprehensive evaluation ability when applied to WSN nodes. A separate matrix can be used to replace the specific value of the evaluation index to express the quantitative and direct evaluation relationship. It has the characteristics of concise discrimination of data nodes. It can mathematically quantify the characteristics of the complex multiattack behavior in the form of a matrix and analyze the data results obtained by discrimination, so as to make the discrimination process of attack behavior simple, clear, and concrete. This paper mainly uses the matrix form to express the relationship between multiple attack behaviors and different node states. The construction of the incidence matrix is shown in Table 1. The attack categories and object attributes of the attacked object in the WSN are represented by the matrix [F, C]. The object attributes include the number of communication link channels, link bandwidth, and device memory. The incidence matrix A of an undirected graph has a row for each vertex and a column for each graph's edge.

3.2. Matrix Modeling of Multiattack Behavior in the WSN. Taking the attributes and attack modes of multiple attack behaviors as matrix elements [18], the attributes of attack behaviors include the number of attack packets, the port number attacked, and the attack link and IP address. The specific methods include administrator identity intrusion, modifying configuration information, and consuming links. Similar to the matrix modeling of the data node state, the incidence matrix of the multiattack behavior can be constructed. However, due to the need to distinguish the multiattack behavior, the incidence matrix of the multiattack behavior is matrix-modeled. Thus, the correlation matrix between the attack method, attack path, and the process under multiple attack behaviors is obtained as follows:

Table 1: The incidence matrix of data node status.

	C_1	C_2	C_3	...	C_n
$F(1)$	(f_1, c_1)	(f_1, c_2)	(f_1, c_3)	...	(f_1, c_n)
$F(2)$	(f_2, c_1)	(f_2, c_2)	(f_2, c_3)	...	(f_2, c_n)
$F(3)$	(f_3, c_1)	(f_3, c_2)	(f_3, c_3)	...	(f_3, c_n)
...	...	...	...	...	...
$F(n)$	(f_n, c_1)	(f_n, c_2)	(f_n, c_3)	...	(f_n, c_n)

$$\mathbf{Z} = \begin{bmatrix} zx_{11} & zx_{12} & zx_{13} & \cdots & zx_{1m} \\ zx_{21} & zx_{22} & zx_{23} & \cdots & zx_{2m} \\ \vdots & \vdots & \vdots & \ddots & \vdots \\ zx_{n1} & zx_{n2} & zx_{n3} & \cdots & zx_{nm} \end{bmatrix}. \quad (5)$$

Formula (5) can be used to describe the attack path and the attack mode of attackers using each node and link between the WSN. In this formula, zx_{nm} represents an attack on the x_{nm} node data object.

3.3. Matrix Modeling and Analysis of the Overall Attack Process under Multiattack Behavior. After constructing the incidence matrix of data node state and the matrix model of the multiattack behavior in 3.1 and 3.2, respectively, the overall attack process is matrix-modeled [19], which is used to describe the attack path and attack process and provide further proof for judging the kind of the attack behavior. At the same time, the model can describe the state change of WSN data nodes after being attacked. The modeling framework of the WSN under multibehavior attacks is shown in Figure 2.

The state changes of information communication nodes after network attack are described, and a corresponding correlation model for the analysis and modeling of the power grid information physical system facing network attack [20] is provided. The attack behavior is calculated and analyzed according to the network attack model framework in Figure 3, where $p^{t_1 k_1}$ represents the occurrence and duration of the A network attack, which can be represented by $p^{t_1 k_1}$ pure delay link; t_1 indicates the moment when a network attack occurs; and k_1 indicates the duration of the attack. Considering that the attacker's attack on the target system is completed step-by-step, multiple interactions between the information communication network matrix model and the attack matrix model are designed in the modeling, and the logical correlation of the interaction is mainly reflected in the algorithm of the specific model application. So far, multiattack behavior discrimination modeling and multiattack behavior discrimination mathematical modeling of the WSN based on the association matrix are completed. The term learning discrimination refers to links between various stimuli and corresponding results or behavioral patterns. It allows animals to choose various reactions to other stimuli.

4. Experimental Verification

In order to verify the accuracy and efficiency of the proposed multiattack discrimination method, a large number of experiments are carried out under different conditions. The

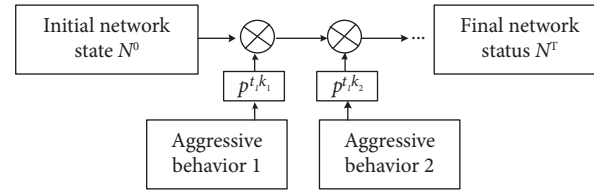

Figure 3: The network attack model framework.

experimental environment is a MATLAB simulation platform, and 200 beacon nodes and 500 ordinary nodes are randomly deployed to effectively distinguish their attack behavior. Among the 200 beacon nodes, each attack corresponds to 20 beacon nodes. Repeat the above steps 1000 times to collect the training dataset and test dataset, in which the training dataset contains the attacked data of 12000 beacon nodes and the normal data of 3000 beacon nodes. In the experimental process, the attack characteristics of three attack behaviors, the relationship between the number of malicious nodes and the recognition rate, and the discrimination results are used as experimental indicators to verify the feasibility of the discrimination model. Once an abnormal behavior detection technology has been developed, intruder detection systems are used for analysing and alarming abnormal behaviors that have a significant variation to the statistical probability modeling of expected behaviors.

4.1. Comparison of Attack Characteristics. Three attacks are understood from the level of the network layer attack as follows: the black hole attack nodes only receive data nodes and do not send data nodes, which will cause the loss of data nodes; DOS attacking nodes will cause other nodes in the network to only receive the data nodes sent by themselves and constantly send receiving requests, which is easy to cause network congestion; selective forwarding attack nodes only send node data within a specific time, but it is destructive in the selection of node information, which will disrupt the integrity of network data. The specific attack characteristics are shown in Table 2. A denial-of-service attack (DoS attack) in the computer is an attack by a cyber, in which the perpetrator attempts, by interrupting services of a host connected to the Internet, to make a machine or network resource unavailable.

4.2. Relationship between Number of Malicious Nodes and Recognition Rate. This paper analyzes the effective discrimination behavior of the configuration to the attack after several nodes in the beacon node are attacked maliciously. The experiment assumes that when the number of beacon nodes attacked by malicious attacks is 10, 15, 20, 25, 30, and 35, respectively, the model has an effective recognition rate of the black hole attack, DoS attack, and selective forwarding attack. The results are shown in Figure 4. A denial-of-service attack (DoS) is an attack that aims to shut down a machine or a network to prevent its intended users from accessing it. The congestion control is a particularly important area

Table 2: Information table of three attack characteristics.

Type of attack	Attack characteristics
The black hole attack	Only receives data, do not forward data to the base station, and do not send any collected data
The DOS attack	Keeps sending packets, resulting in network congestion
The selective forwarding attack	Sends data packets or forward fusion data to the base station in a specific time period

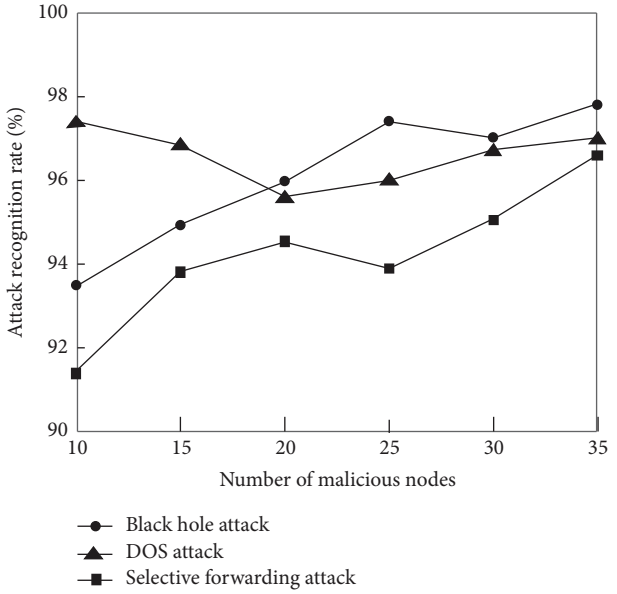

Figure 4: Relationship between number of malicious nodes and recognition rate.

within WSNs, in which traffic becomes greater than the total or individual capacities of the underlying channels.

According to Figure 4, when the number of beacon nodes attacked by malicious attacks increases, the recognition rate of the algorithm for attack types sometimes increases and sometimes decreases. Therefore, there is no obvious correlation between the attack recognition rate and the number of beacon nodes attacked because this paper fully considers the characteristics of the three attack behaviors in the feature selection stage. Although the number of malicious nodes increases and changes the network topology and other information, the recognition model can still judge the attack type according to the characteristics, and the average recognition rate of the three attack behaviors in this experiment reaches 95.4%.

4.3. Comparison of Discrimination Results under Multiple Aggressive Behaviors. In order to further analyze the reliability of the model discrimination in this paper, the identification rate of the attack behavior can be distinguished by this method, the reference [5] method, and the reference [6] method. The higher the average identification rate is, the better the stability of the model discrimination.

Table 3: Recognition rate analysis.

	Black hole attack (%)	DOS attack (%)	Selective forwarding attack (%)	Average recognition rate (%)
This method	96.7	95.8	93.7	95.4
The reference [5] method	94.8	93.7	91.2	93.2
The reference [6] method	95.3	94.1	92.6	94.1

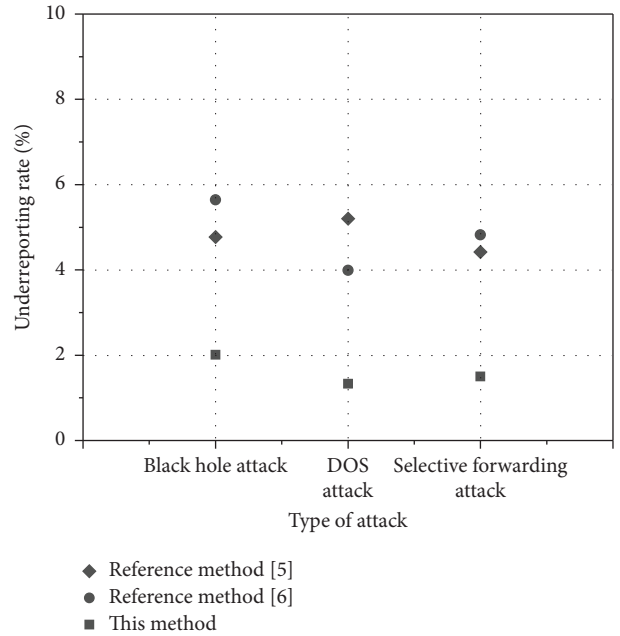

Figure 5: Discrimination results of the false alarm rate.

Compare the attack recognition rates of the three methods, and the test results are shown in Table 3.

According to the model recognition rate analysis in Table 3, it can be concluded that the method in this paper has certain advantages in judging the attack behavior, with an average recognition rate of 95.4%, which is higher than 93.2% of the reference [5] method and 94.1% of the reference [6] method. Therefore, in order to verify the actual situation of the model under the multiattack behavior of the WSN, this paper compares and analyzes the method in this paper with the reference [5] method and the reference [5] method and obtains the specific results of the missing report rate and discrimination time of the attack behavior. The test results are shown in Figure 5 and Figure 6.

According to Figure 5, the average miss rate of the three attack behaviors in this method is 1.86%. Because this paper uses the incidence matrix algorithm to build a model to effectively analyze the characteristics of the attacked behavior of sensor network nodes, it can effectively distinguish

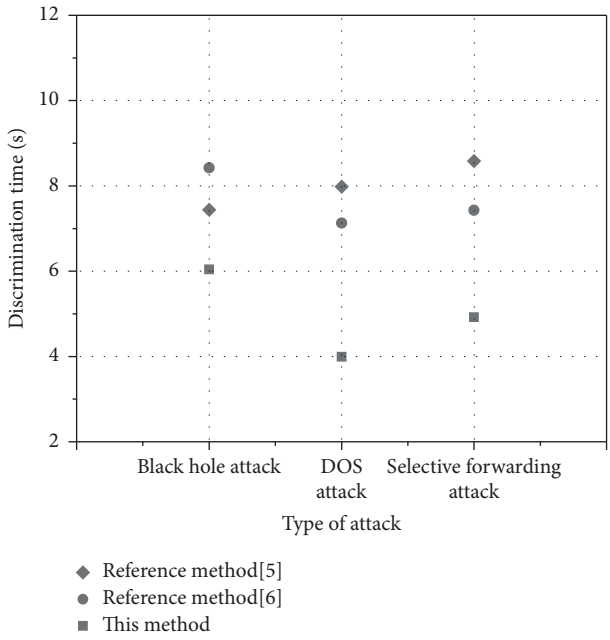

Figure 6: Discrimination of the attack time.

multiple attack behaviors in the WSN and greatly reduce the miss rate of attack behaviors. The missing reporting rates of the reference [5] method and the reference [6] method were 4.54% and 5.12%. The incidence matrix is a Boolean matrix of two dimension in which the vertices and columns represent each side of the incidence matrix. The entries show if the vertex in a line occurs at the edge of a column. One way to display a graph is by the incidence matrix.

According to Figure 6, the discrimination time of this method for the multiattack behavior is short, and the average time is only 5 s, while that of the reference [5] method is 8 s and that of the reference [6] method is 7 s. This shows that the model designed in this paper has strong discrimination ability to attack behavior and can effectively improve the antiattack ability of the WSN.

5. Conclusion

In this paper, a mathematical model of multiattack behavior discrimination in the WSN based on the incidence matrix is designed. Compared with the traditional WSN attack behavior analysis method, the incidence matrix method has a better antiattack ability in the process of data node acquisition and identification. Finally, through experimental verification, in the case of the black hole attack, DoS attack, and selective forwarding attack, the effective recognition rate of data nodes is 95.4%, the false alarm rate of multiattack behavior is 1.86%, and the discrimination attack behavior is 5 s. It is proved that the multiattack behavior discrimination model of the WSN constructed by this method has a good application effect.

Data Availability

No data were used to support the findings of this study.

Consent

Not applicable.

Conflicts of Interest

The authors declare that there are no conflicts of interest.

References

[1] J. Kim, D. Lee, J. Hwang, S. Hong, D. Shin, and D Shin, "Wireless sensor network (WSN) configuration method to increase node energy efficiency through clustering and location information," *Symmetry*, vol. 13, no. 3, pp. 390–401, 2021.

[2] G. Amudha, "Dilated transaction access and retrieval: improving the information retrieval of blockchain-assimilated Internet of things transactions," *Wireless Personal Communications*, vol. 2021, pp. 1–21, 2021.

[3] B. M. Sahoo, H. M. Pandey, and T. Amgoth, "GAPSO-H: a hybrid approach towards optimizing the cluster based routing in wireless sensor network," *Swarm and Evolutionary Computation*, vol. 60, Article ID 100772, 2021.

[4] N. T. Tam, V. T. Dat, P. N. Lan, H. T. Thanh Binh, L. T. Vinh, and A. Swami, "Multifactorial evolutionary optimization to maximize lifetime of wireless sensor network," *Information Sciences*, vol. 576, pp. 355–373, 2021.

[5] V. M. Kuthadi, R. Selvaraj, S. Baskar, P. M. Shakeel, and A. Ranjan, "Optimized energy management model on data distributing framework of wireless sensor network in IoT system," *Wireless Personal Communications*, vol. 2021, pp. 1–27, 2021.

[6] X. Chi, Y. Wang, J. Gao et al., "Study of photoluminescence characteristics of CdSe quantum dots hybridized with Cu nanowires," *Luminescence*, vol. 31, no. 7, pp. 1298–1301, 2016.

[7] S. J. Achar, C. Baishya, and M. K. A. Kaabar, "Dynamics of the worm transmission in wireless sensor network in the framework of fractional derivatives," *Mathematical Methods in the Applied Sciences*, vol. 45, no. 8, pp. 4278–4294, 2022.

[8] H. Zhao, Z. Liu, X. Yao, and Q. Yang, "A machine learning-based sentiment analysis of online product reviews with a novel term weighting and feature selection approach," *Information Processing & Management*, vol. 58, no. 5, Article ID 102656, 2021.

[9] N. T. Nguyen, B. H. Liu, V. T. Pham, and T. Y. Liou, "An efficient minimum-latency collision-free scheduling algorithm for data aggregation in wireless sensor networks," *IEEE Systems Journal*, vol. 12, no. 3, pp. 2214–2225, 2018.

[10] Z. Xi, X. Kan, L. Cao et al., "Research on underwater wireless sensor network and MAC protocol and location algorithm," *IEEE Access*, vol. 7, pp. 56606–56616, 2019.

[11] C. Thomson, I. Wadhaj, Z. Tan, and A. Al-Dubai, "A mobility aware duty cycling and preambling solution for wireless sensor network with mobile sink node," *Wireless Networks*, vol. 27, no. 5, pp. 3423–3439, 2021.

[12] S. A. B. Danique, B. B. Erik, F. S. B. E. Barbara, B. Jan, and V. Robbert-Jan, "Associations of multiple trauma types and MAOA with severe aggressive behavior and MAOA effects on training outcome," *European Neuropsychopharmacology*, vol. 30, no. 6, pp. 66–74, 2020.

[13] K. Sekar, K. Suganyadevi, and P. Srinivasan, "Energy efficient data gathering using s-temporal compressive sensing for WSNs," *Wireless Personal Communications*, vol. 117, no. 2, pp. 1279–1295, 2021.

[14] J. Leopold, B. Mcmillin, R. Stiffler, and N. Lutes, "Comparison of design-centric and data-centric methods for distributed attack detection in cyber-physical systems," *Critical Infrastructure Protection XIV*, Springer, New York, NY, USA, 2020.
[15] P. Wanda and H. J. Jie, "DeepFriend: finding abnormal nodes in online social networks using dynamic deep learning," *Social Network Analysis and Mining*, vol. 11, no. 1, pp. 1–12, 2021.
[16] S. Kumar and V. K. Chaurasiya, "A multisensor data fusion strategy for path selection in Internet-of-Things oriented WSN (WSN)," *Concurrency and Computation: Practice and Experience*, vol. 30, no. 18, pp. e4477.1–e4477.14, 2018.
[17] W. Lim, G. Khemka, D. Pitt, and B Browne, "A method for calculating the implied no-recovery three-state transition matrix using observable population mortality incidence and disability prevalence rates among the elderly," *Journal of Population Research*, vol. 36, no. 3, pp. 245–282, 2019.
[18] M. Hassani, "105.24 Conditional 2 × 2 matrices with three prime elements and given determinant," *The Mathematical Gazette*, vol. 105, no. 563, pp. 305-306, 2021.
[19] W. Xiong, E. Legrand, O. Åberg, and R. Lagerstrom, "Cyber security threat modeling based on the MITRE Enterprise ATT&CK Matrix," *Software and Systems Modeling*, vol. 21, no. 1, pp. 157–177, 2021.
[20] M. Kumar Ashok, M. Sethumadhavan, and K. V. Lakshmy, "Holistic analytics of digital artifacts: unique metadata association model," *International Journal of Digital Crime and Forensics*, vol. 13, no. 5, pp. 78–100, 2021.

Hindawi
Complexity
Volume 2022, Article ID 3486100, 10 pages
https://doi.org/10.1155/2022/3486100

Research Article

The Application of Clothing Intelligent 3D Display with Uncertainty Models Technology in Clothing Marketing

Zhonglin Xu[1] and Trip Huwan[2]

[1]*Suzhou University, Suzhou, Anhui 234000, China*
[2]*Research Center of Environmental Science and Engineering, Bishkek, Kyrgyzstan*

Correspondence should be addressed to Trip Huwan; dr.tribhuwan@mail.cu.edu.kg

Received 20 July 2022; Revised 7 September 2022; Accepted 12 September 2022; Published 21 September 2022

Academic Editor: Zeljko Stevic

As a result of the development of new technologies such as satellite communication, digitalization, and multimedia computer networks, new media such as blogs, online magazines, and wireless network media have sparked a lot of interest. This study uses 3D clothing display technologies to improve the customer experience of online clothing marketing, aid in the improvement of online clothing marketing efficacy, and extensively discuss the digital clothing anthropometric model. Furthermore, this study employs the convex hull approach and NURBS fitting technology to address concerns with digital clothing anthropometric measurement and provides a practical solution for measuring straight line length, circumference length, and curve length. Furthermore, this research incorporates 3D intelligent technology to develop an online fitting system as well as an intelligent display system for garments. The simulation experiment investigation revealed that the smart clothing 3D display system proposed in this work has a substantial impact on growing online e-commerce clothing marketing as well as improving clothing marketing effectiveness.

1. Introduction

The Internet has gradually become a huge information exchange platform, and the influence of emerging media such as electronic magazines and blogs on this basis has rapidly become prominent. Moreover, mobile phones have broken through the single function of interpersonal communication tools and increasingly have the characteristics of mass media, and more new media have been born under the impact and fusion of old and new media [1]. These new information carriers compete for people's limited attention, change people's work and lifestyle, and also change the marketing methods, marketing scope, and communication effects of enterprises. In today's information dissemination pattern, the competition for marketing information dissemination extends to different terminals, and the fragmentation of the advertising market has become a trend. The emergence of new media enhances the audience's initiative. The audience no longer unilaterally accepts the information provided by the traditional media but can selectively accept the information and release the information, becoming an important information or information source for the traditional media [2]. At the same time, the emergence of the Internet and mobile phones has brought many new concepts to marketing communication and has also established a good communication and exchange platform for fashion designers, consumers, and enterprises. Therefore, research and analysis of various new media to find a new way suitable for clothing marketing communication have positive practical significance for the construction, promotion, and communication of clothing brands [3].

New retail will integrate online and offline, while traditional retail will separate online and offline. For new retail, the boundaries between online and offline tend to be blurred. Online and offline prices are the same, data is shared, and traffic is drawn from each other. A common strategy is that when consumers place an order and buy a product online, they can arrange for a physical store nearby to ship it. And no

matter which channel consumers purchase through, the data generated will become a reference for marketing plans of various channels. For example, when a consumer purchases a piece of clothing in a physical store through mobile payment, the in-store system will send the consumer to the store. The frequency of purchases, items purchased, and the address of the store are recorded into a registered consumption, and the consumer's consumption habits are accurately pushed in the future. Although traditional retail also has multiple sales channels through physical stores and virtual stores, the two are not directly related, and when the online product resources are insufficient, it is a violation of the rules to take supplements offline. Due to the lack of cooperation between the responsible teams of the two channels and the differences in key performance indicators, they have formed differences in price and even supply.

This paper combines 3D clothing display technology to improve the customer experience of online clothing marketing and assist in improving the marketing effect of online clothing.

2. Related Work

Currently, there are several different understandings of the concept of visual merchandising. It can be mainly divided into the following three categories: the first type of view is that visual marketing uses the planning of color, shape, sound, and other aspects of the displayed products to make them have a strong impact on consumers, thereby attracting consumers to enter the store and generating transactions. This kind of point of view focuses more on the visual impact brought by the display and display of goods, so as to promote the sales of goods [4]. The second view integrates visual presentation techniques, merchandise display techniques, and marketing strategies. Emphasizes the importance of visual expression and merchandise display must be combined with marketing strategies [5]. The definition of marketing during this period still stayed within the scope of "commodity terminal store". The last category of views is to extend visual marketing from the scope of "commodity terminal stores" to other scopes on the basis of the first two views, and conduct in-depth research on the psychological impact of consumer purchases [6]. Literature [7] regards the reflection of the psychological phenomenon of "vision" on the individual attributes of commodities as the main factor affecting consumer behavior, and combines visual presentation technology and commodity display technology to formulate a marketing mix strategy that is different from other marketing concepts. Visual marketing uses the visual elements of the terminal store, such as LOGO, store design, advertising, windows, store props, color, lighting, and other visual communication systems to transmit the brand's products, brand positioning, brand culture, and brand connotation to target consumers or potential consumers, thereby achieving good communication between brands and consumers. Visual merchandising reproduces the life and consumption needs of target consumers so as to achieve the purpose of promoting commodity sales and establishing a brand image. Therefore, visual merchandising is one of the most effective strategies for the design system of end stores [8].

Visual marketing covers a wide range, it involves marketing, brand visual identity design, product mix, and display, terminal store design and display, window design, exhibition design, fashion photography, visual design in event promotion, visual design in advertising and other aspects of knowledge [9]. Visual merchandising is built on the basis of marketing and is a new marketing strategy and model. Compared with marketing, visual marketing pays more attention to product design, brand dissemination, and the design and display of terminal stores, emphasizing the influence mechanism of vision on marketing. That is to say, under the guidance of marketing, visual marketing organizes the three visual elements of product function, visual symbol design, and visual language association to convey the brand value of the enterprise to target consumers [10]. Of course, visual marketing also applies the visual marketing process to brand information and visual communication with consumers, and provides goals in product packaging, styling, store layout, merchandise display, advertising, marketing planning, and even overall corporate identification management. For consumer visual impact refer [11]. As a part of marketing, in the process of practice, visual merchandising has been extended from the application of various offline physical stores, such as physical stores, department store retail, and shopping mall, to the industry of network information dissemination and sales; from the visual presentation of technology and products The application of display technology in the field of sales has developed and expanded to include space design, communication planning, and even image recognition of the entire enterprise [12].

Literature [13] defines a brand as six connotations, namely product attributes, users, personality, interests, values, and culture. What can highlight the brand most is the brand's culture, brand personality, and brand value. In the process of consumers understanding the brand, they first experience the attributes of the brand, that is, the function of the product. In the experience, they are gradually attracted by the culture and personality of the brand, thereby further generating recognition for the brand [14]. Ultimately, consumers identify with the value of the brand and form the same values as the brand. For example, when consumers buy clothing, they first try on the clothing to understand the silhouette, color, and style of the clothing product, and then carry out the visual perception of the store image and communication with the store clerk during the try-on process. Understand, and then feel the psychological satisfaction brought by purchasing the brand's clothing and identify with the value of the brand [15]. In the brand building of enterprises, the whole process should be extended in reverse [16]. First of all, enterprises should take the brand's value orientation as the core and use it to shape the brand's culture and personality. On this basis, the target consumers of the brand are positioned, starting from the brand culture and brand personality, to design the product attributes that conform to the consumer group and the benefits the product can provide. Only by placing the value of the brand at the core can the brand achieve good results in its construction and management [17].

The main purpose of visual marketing is to reflect and enhance the brand image in the terminal store, shape the

brand style, strengthen the brand connotation, and make consumers leave a deep impression on the brand. Therefore, clothing companies need to use visual marketing strategies to establish a link window with consumers at the store terminal and establish a unique and personalized image to distinguish them from other brands [18]. The core of visual marketing is to display and display the terminal of the store so that the store image can get the best visual effect, so as to attract and infect consumers, achieve consumers' purchasing behavior, and convey the culture and connotation of the brand in a deeper level [19].

3. Clothing 3D Digital Technology

B-spline curve is an extension of Bezier curve, and its general expression is

$$Q(u) = \sum_{k=0}^{n} B_{k,p}(u) P_k u_{\min} \le u \le u_{\max}, \quad 1 \le p \le n+2. \tag{1}$$

In the above formula, P_k is the control point, p is the curve order, and $p-1$ is the curve order. We define the curve to have a continuity of order $p-2$ at the junction. $B_{k,p}(u)$ is the p-order ($(p-1)$-order) basis function, which is a piecewise polynomial function. $B_{k,p}(u)$ is defined as

$$B_{k,0}(u) = \begin{cases} 1 & u_i \le u \le u_{i+1} \\ 0 & \text{other} \end{cases},$$

$$\mathrm{B}_{k,p}(u) = \frac{u - u_k}{u_{k+p} - u_k} \mathrm{B}_{k,p-1}(u) + \frac{u_{k+p+1} - u}{u_{k+p+1} - u_{k+1}} \mathrm{B}_{k+1,p-1}(u) p > 1, \tag{2}$$

$T = (u_0, \ldots, u_m)$ is the node vector,

$$\sum_{k=0}^{n} B_{k,p}(u) = 1, \tag{3}$$

$m = n + k$, and generally, we take the node vector h as $T = (\underbrace{a, a, \ldots a}_{k}, a_1, \ldots, a_{n-k+1}, \underbrace{\beta, \beta, \ldots \beta}_{k})$.

NURBS is the abbreviation of nonuniform rational B-spline, which is specifically explained as follows:

Nonuniform: it means that the distance between each node is indeterminate (uniform or nonuniform), so the range of influence of each control vertex can be changed.

Rational: it means that control points are allowed to be weighted, and each NURBS object can be represented by a unified mathematical expression.

B-spline: it refers to a B-spline as a basis function.

Model point: that is, the point on the curve and surface. Curves and surfaces are usually obtained by interpolation through known value points.

Control points: points that control the shape of curves and surfaces. Usually, the control point and the model point do not coincide, and the control point is generally not on the curve or surface.

Node: the node vector directly affects the B-spline basis function, so the node concept is an important concept in NURBS curves and surfaces. According to whether the nodes are equally spaced, B-splines can be divided into uniform B-splines and nonuniform B-splines.

$$P(u) = \frac{\sum_{i=0}^{n} w_i P_i N_{i,p}(u)}{\sum_{i=0}^{n} w_i N_{i,p}(u)} = \sum_{i=0}^{n} P_i B_{i,p}(u),$$
$$B_{i,p}(u) = \frac{w_i N_{i,p}(u)}{\sum_{j=0}^{n} w_j N_{j,p}(u)}. \tag{4}$$

In the formula, P_i is the control vertex, $i = 0, 1, \ldots, n$. $B_{i,p}(u)$ is the p-order ($p+1$-order) basis function.

w_i is the weighting factor corresponding to P_i, and the first and last weighting factor is $w_0, w_n > 0$ and the rest are $w_i > 0$ to prevent the denominator from being zero and to preserve the convex hull property, the curve does not degenerate to a point due to weighting factors.

The node vector is $U = [u_0, u_1, \ldots, u_m]$, and the number of nodes m is $n + p + 1$.

For aperiodic NURBS curves, the repetition degree of the nodes at both ends is often taken as $p+1$, and have $U = [\underbrace{a, \ldots, a}_{p+1}, u_{p+1}, \ldots, u_n, \underbrace{\beta, \ldots, \beta}_{p+1}]$. In practical applications, $a = 0, \beta = 1$ is often taken.

The $B_{i,p}(u)$ basis function has the following properties:

(1) Nonnegativity, $B_{i,p}(u) \ge 0$;

(2) Normative, $\sum_{i=0}^{n} B_{i,p}(u) = 1, u \in [u_0, u_n]$;

(3) Locality, $\sum_{i=0}^{n} B_{i,p}(u) = 0, u \notin [u_i, u_{i+p+1}]$;

(4) Differentiability. In the node interval, when the denominator is not 0, $B_{i,p}(u)$ is infinitely continuously differentiable;

At the node, if the repetition degree of the node is m, then $B_{i,p}(u)$ is differentiable of order $p - m$.

(5) If $w_i = 0$, then $B_{i,p}(u) = 0$; if $w_i = +\infty$, then $B_{i,p}(u) = 1; B_{j,p}(u) = 0 (i \ne j)$.

Since, what is measured is the shape point on the curve, not the control vertex of the curve control polygon, the control point of the curve should be inversely calculated according to the existing data points on the curve. This process is called the inverse calculation of the curve, and the obtained curve is the interpolation curve. Through $n+1$ type-valued points Q_k, the P-th degree NURBS curve equation of $k = 0, 1, \ldots, 11$ can be written as

$$P(u) = \sum_{i=0}^{g} P_i R_{l,f}(u), \quad u \in (0, 1). \tag{5}$$

The corresponding parameter u_k of the type value point QK is substituted into the above formula in turn, and the interpolation conditions should be satisfied:

$$Q_k = P(\overline{u_k}) = \sum_{i=0}^{n} P_i R_{i,\rho}(\overrightarrow{u_r}), \quad k = 0, 1, \ldots, n. \tag{6}$$

It is written in matrix form as

$$\begin{bmatrix} Q_0 \\ Q_1 \\ \vdots \\ Q_n \end{bmatrix} = \begin{bmatrix} R_{0,p}(\overline{u}_0) & R_{1,p}(\overline{u}_0) & \cdots & R_{n,p}(\overline{u}_0) \\ R_{0,p}(\overline{u}_1) & R_{1,p}(\overline{u}_1) & \cdots & R_{n,p}(\overline{u}_1) \\ \vdots & \vdots & \ddots & \vdots \\ R_{0,p}(\overline{u}_n) & R_{1,p}(\overline{u}_n) & \cdots & R_{n,p}(\overline{u}_n) \end{bmatrix} \begin{bmatrix} P_0 \\ P_1 \\ \vdots \\ P_n \end{bmatrix}, \tag{7}$$

The element of the coefficient matrix in the above formula is the value of the B-spline basis function at the parameter u_k, which only depends on the parameter u_k and its position in the node vector U.

Parameterization refers to determining a parameter segmentation for a set of ordered data points, that is, the calculation of the parameter u_k. There are several ways to parameterize data points:

(1) Uniform parameterization method is

$$\overline{u}_0 = 0, \overline{u}_n = 1 \overline{u}_k = \frac{k}{n} \quad k = 1, 2, \ldots, n-1. \tag{8}$$

This parametric method only works when the sides (or chords) of the data point polygon are close or equal.

(2) Accumulated chord length parameter method:

$$\overline{u}_0 = 0, \overline{u}_n = 1$$

$$\overline{u}_t = \overline{u}_{k-1} + \frac{|Q_k - Q_{k-1}|}{\sum_{j=1}^{n} |Q_j - Q_{j-1}|} \quad k = 1, 2, \ldots, n-1. \tag{9}$$

This parameterization method faithfully reflects the distribution of data points according to the chord length, and overcomes the problem of uniform parameterization when the data points are unevenly distributed according to the chord length.

(3) Centripetal parameterization:

$$\overline{u}_0 = 0, \overline{u}_n = 1,$$

$$\overline{u}_k = \overline{u}_{k-1} + \frac{|Q_k - Q_{k-1}|^{1/2}}{\sum_{j=1}^{n} |Q_j - Q_{j-1}|^{1/2}} \quad k = 1, 2, \ldots, n-1. \tag{10}$$

This method has a good effect on the parameterization of nonuniform value points, so based on this consideration, this paper intends to use this method to determine the parameter uk corresponding to the type of value point Q_k.

After the parameter u_k is determined, the node vector U needs to be further determined. In order to inversely solve the same number of control point vectors from $n+1$ type-valued points, avoid supplementary boundary conditions, and in order to reflect the distribution of the parameter uk corresponding to the type-valued point Q_k in the parameter domain, the algebraic average method is used to construct the node vector U.

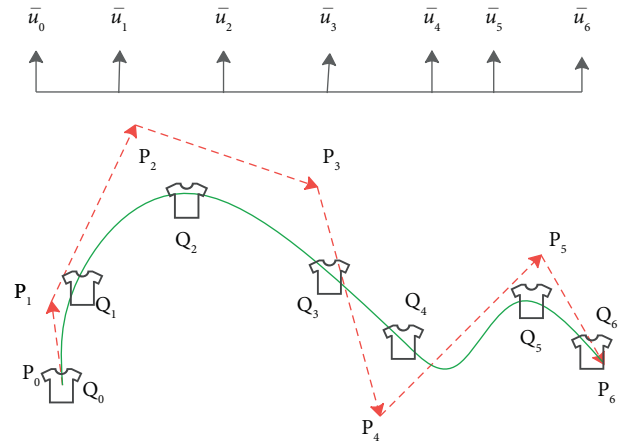

Figure 1: Control point, shape point, and node vector of cubic curve.

$$u_0 = \cdots = u_\rho = 0, u_{m-p} = \cdots = u_m = 1,$$

$$u_{j+p} = \frac{1}{p} \sum_{i=j}^{+\beta+1} \overline{u}_i \quad j = 1, \ldots, n-p. \tag{11}$$

The node vector is $U = \{0 = u_0 = \cdots u_p,\ u_{j+p}, u_{m-p} = \cdots = u_{m=1}\}$, $m = n + p + 1$.

Figure 1 shows the control points, parameters, and nodal vectors of a cubic NURBS curve interpolating 7 data points.

The measurement method for the straight line length is as follows: it first finds two reference points and their three-dimensional coordinates needed to determine parameters on the digital clothing human body, and then, obtains the parameter values by calculating the horizontal distance, vertical distance or straight-line distance between the two points. The definition of horizontal, vertical, and oblique straight line lengths in the three-dimensional coordinate system is shown in Figure 2. For example, for the human body parameter "milk distance" (definition: the horizontal distance between two breast peak points), it is necessary to locate the three-dimensional coordinates $P_1(x_1, y_1, z_1)$, $P_2(x_2, y_2, z_2)$ of the two "milk peak points" on the digital clothing human body, and then, calculate the horizontal straight-line distance $|x_1 - x_2|$ between the two points.

For the concave section on the human body surface of digital clothing, what needs to be measured is a closed convex hull (closed convex envelope), ignoring the concave part. In the previous method, the length of the curve of the concave part is also included in the circumference, which produces an error, and the error will further expand with the increase and enhancement of the concave part of the cross-section. Taking the female thoracic section as an example, Figure 3(a) shows the outline of the thoracic section. Compared with the correct bust measurement reference line shown in Figure 3(b), it can be seen that there is an obvious depression in the middle of the chest, and there is also a certain depression in the spine of the back. If this cross-

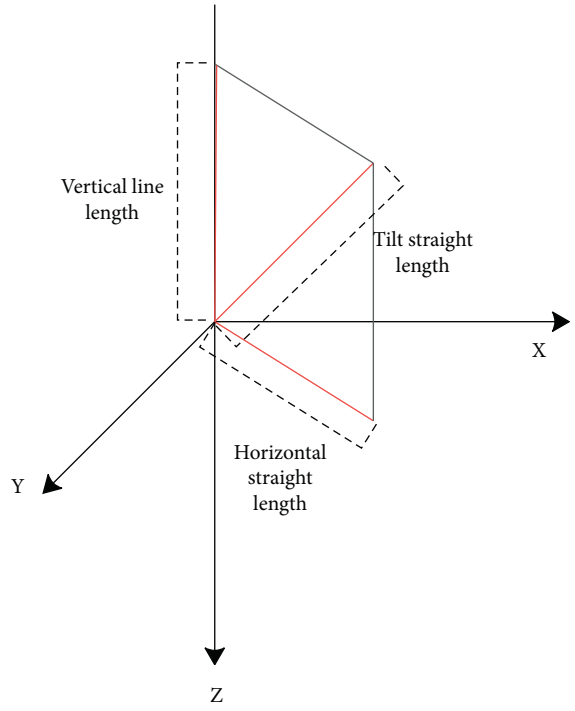

Figure 2: Definition of horizontal, vertical, and oblique straight line lengths.

sectional profile is used as the measurement benchmark for the bust, a large error will occur.

In view of this, this paper introduces the convex hull algorithm to correct the cross-section after NURBS fitting, so as to remove the influence of the concave parts of the human body on the circumference measurement.

Concept of convex envelope: the convex hull of a point set Q refers to a minimum convex polygon that satisfies the points in Q either on the polygon edge or within it, as shown in Figure 4.

In order to facilitate the measurement, this paper modifies the Graham scanning method according to the actual requirements of the measurement. The initial point sequence is sorted according to the polar angle, so that the remaining point sequence after the convex hull algorithm is still in the original order.

The specific method is as follows:

(1) The algorithm determines the point with the largest y-coordinate value in the cross-section point column after NURBS fitting as the starting point P_0. If there is more than one, the algorithm takes the point with the smallest x-coordinate value as the starting point P_0, and renumbers the remaining points in turn: $P_0, \ldots, P_i, \ldots, P_{n-1}$.

(2) The algorithm pushes the first three points P_0, P_1, P_2 into the stack.

(3) For the remaining points, the algorithm calculates the cross product $(P_i - P_{i-1}) \times (P_{i-1} - P_{i-2})$, $(3 < i < n)$ in turn. If > 0, the algorithm pushes P_i onto the stack. If < 0, the algorithm removes P_{i-1} from the stack, calculates $(P_i - P_{i-2}) \times (P_{i-2} - P_{i-3})$ again, and repeats step 3.

(4) Finally, after all the points are calculated, the remaining points in the stack are the point set $P_0, \ldots, P_{m-1}'$, $(m <= n)$ after removing the concave points.

We assume that the inclined contour line passes through m horizontal sections, and each section is represented by 30 type-valued points, that is, there are m point columns: $S_0, \ldots, S_{m-1}$, and each point column includes 30 points: $P_0, \ldots, P_i, \ldots, P_{29}(x, y, z)$. We need to use these m point columns to construct a point column to characterize the desired sloped contour, denoted by Sm.

Next, the three-dimensional coordinate point column S: $P_0, \ldots, P_i, \ldots, P_{29}(x, y, z)$ is transformed into the two-dimensional coordinate point column S': $P_0', \ldots, P_i', \ldots, P_{29}'(x', y')$. The coordinate transformation relationship is as follows:

$$\begin{cases} x' = x \\ y' = \pm \sqrt{y^2 + (z - z_0)^2} \end{cases}. \tag{12}$$

If $y > 0$, it is positive; if $y < 0$, it is negative.

Among them, z_0 is the z-coordinate of the center point of the section (the x-coordinate value and the y-coordinate value are both 0).

After obtaining the two-dimensional coordinate point series, the method of measuring the horizontal girth is used: first use the NURBS fitting technique, and then use the convex hull algorithm to correct the measurement, and then the parameter data of the oblique girth can be obtained. For the above methods, we can also make some optimizations by adjusting the steps. The method is as follows: then, after determining m point columns: $S_0, \ldots, S_{m-1}$, the algorithm first performs NURBS fitting on them, and then, after obtaining S', the girth, can be directly calculated. This can improve part of the accuracy, but at the same time, $m - 1$ times of NURBS fitting will be used more, which increases the overhead of the system. The effect of neck circumference measurement is shown in Figure 5.

The length of the curve refers to the length of the curve from one point to another point on the human body of the digital clothing. Similar to the measurement of the length of a straight line, it also needs to first determine the two endpoints of the parameter and their three-dimensional coordinates $P'(x_1, y_1, z_1), P''(x_2, y_2, z_2)$. The measurement methods of horizontal, vertical, and inclined curve lengths are discussed separately below.

Since, the horizontal circumference is a closed curve (special curve), any horizontal curve on the digital clothing body is a part of the contour line on the same section as it. That is, for any horizontal curve on the digital clothing human body, there is a contour line on the same section, and there is a many-to-one relationship between them. If the point column of a curve corresponding to the contour line is $P_0, \ldots, P_i, \ldots, P_{29}$, and the positions of the two endpoints of the curve in the contour line point column are:

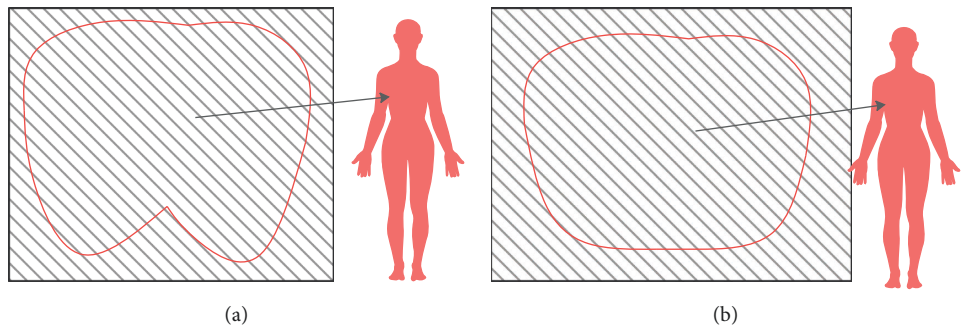

(a) (b)

Figure 3: The outline of the thoracic section. (a) Thoracic section outline. (b) Bust line.

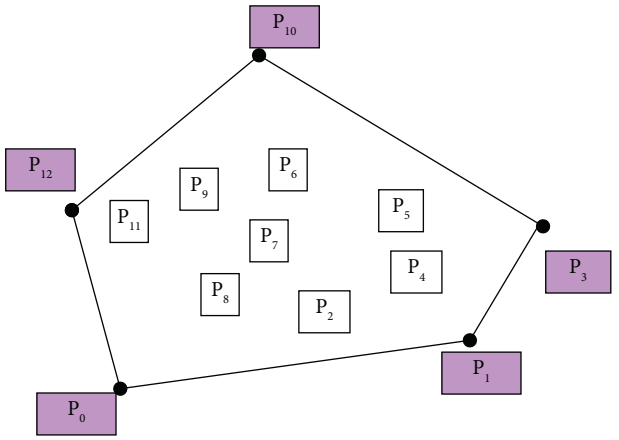

Figure 4: Definition of convex envelope.

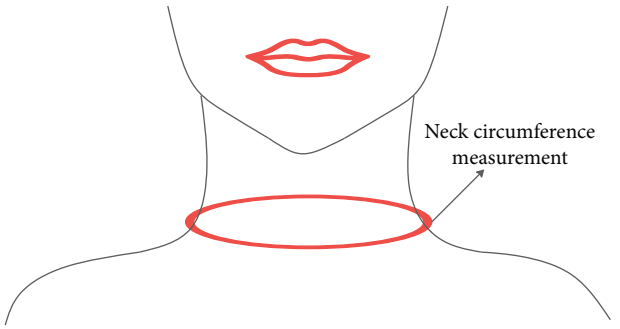

Figure 5: Neck circumference measurement chart.

$\begin{cases} P' = P_j \\ P'' = P_k \end{cases}$ $(0 < = j < k < = 29)$. Then, we only need to use NURBS fitting for each point in between $P_j \sim P_k$, and then selectively use the convex hull algorithm as needed to calculate the length of the curve $(P_j \sim P_k)$.

First, the algorithm needs to determine the starting point $P'(x_1, y_1, z_1)$ and the ending point $P''(x_2, y_2, z_2)$ of the vertical curve. Then, the algorithm sequentially determines the points of the vertical curve on each section it passes through. We assume that the vertical curve passes through m horizontal sections, each section is represented by 30 type-value points, that is, there are m point columns: $S_0, \ldots, S_{m-1}$, and each point column includes 30 points: $P_0, \ldots, P_i, \ldots, P_{29}(x, y, z)$. Moreover, we need to use the points in the m point columns to construct a point column to characterize the vertical curve, which is represented by S.

For the parameters of the front and back of the digital clothing human body, the x-coordinate of P' is consistent with the x-coordinate of P''. We can find a point in each point column of the m horizontal cross-section point columns that the vertical curve passes through to form S. The criteria for selecting points in the point column are as follows: the x-coordinate is closest to the x-coordinate of $P\prime$, and the y-coordinate and the y-coordinate of P' are both positive and negative (function: determine whether the point is on the front or the back). After finding these points, the algorithm changes the x-coordinates of these points to the x-coordinates of P' to keep them vertical, then uses NURBS fitting, and then optionally uses the convex hull algorithm as needed, and finally gets the length of the vertical curve. As shown in Figure 6(a), it is the orthographic projection of the length of the vertical curve on the front and back. Figure 6(b) is the side projection of the vertical curves on both sides.

For the parameters on both sides of the human body of the digital clothing, the y-coordinate of P' is consistent with the y-coordinate of P'', and we can find a point in each point column of the m horizontal cross-section point columns that the vertical curve passes through to form S. The criteria for selecting points in the point column are as follows: the y coordinate is closest to the y coordinate of P', and the x coordinate and the x coordinate of P' are the same positive and negative (function: determine whether the point is on the left or right side). After finding these points, the algorithm changes the y-coordinates of these points to the y-coordinates of P' to keep them vertical, then, uses NURBS fitting, and then optionally uses the convex hull algorithm as needed, and finally gets the length of the vertical curve.

The measurement of the length of a sloped curve is very similar to the measurement of the length of a vertical curve, but there are differences. The x-coordinate of P' and the x-coordinate of P'' or the y-coordinate of P'' and the y-coordinate of are no longer equal, so the criteria for selecting points in the m horizontal cross-section point columns that the inclined curve passes through have changed. The line connecting P' and P'' has an intersection with each section it passes through (Figure 6(c)).

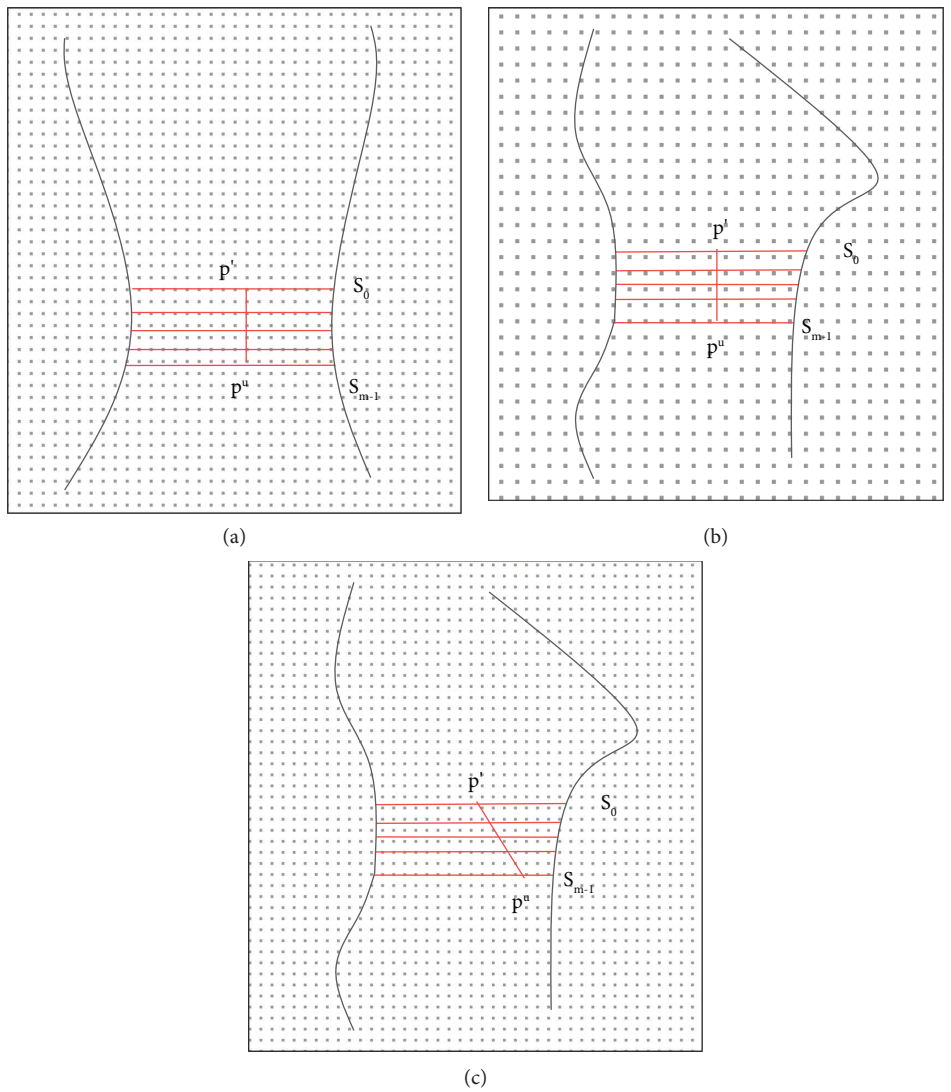

Figure 6: Projection of digital clothing human body. (a) Orthographic projection of the length of the front and back vertical curves. (b) Side projection of vertical curves on both sides. (c) Side projection of the length of the inclined curve.

For the parameters of the front and back of the digital clothing human body, the criteria for selecting points in the point column are as follows: the x-coordinate is closest to the x-coordinate of the intersection of the line and the section, and the y-coordinate and the y-coordinate of the intersection are the same positive and negative (role: determine whether the point is on the front or the back). After finding these points, the x-coordinates of these points are changed to the x-coordinates of the intersection, so that their slopes remain the same. The following steps are the same as for the measurement of the vertical curve length.

For the parameters on both sides of the human body in digital clothing, the criteria for selecting points in the point column are as follows: the y-coordinate is closest to the y-coordinate of the intersection of the line and the cross-section, and the x-coordinate and the x-coordinate of the intersection are both positive and negative (function: determine whether the point is on the left or right). After finding these points, the y-coordinates of these points are changed to the y-coordinates of the intersection, so that their slopes remain the same. The following steps are the same as the measurement of the vertical curve length.

For the measurement of vertical curves and inclined curves, it is also possible to perform NURBS fitting on each cross-section profile point column that the curve passes through to improve part of the accuracy, but also to increase the system overhead. In addition, it should be noted that the measured curve must pass through at least 3 or more cross-sections. The reason for this is that NURBS fitting requires at least three control points. Considering that such short parameters are rarely found in natural anthropometric measurements, the impact on digital clothing anthropometric measurements is not significant.

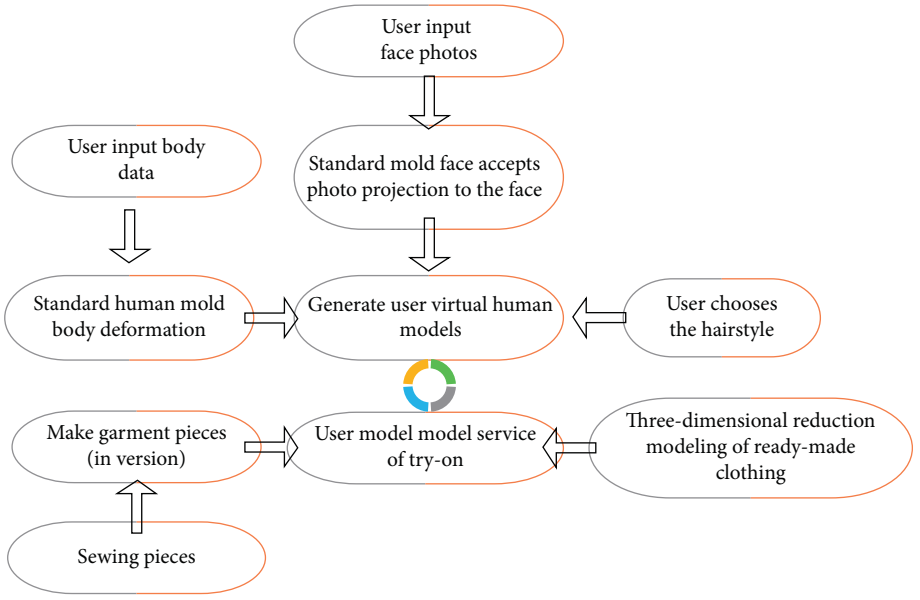

Figure 7: The interactive process of the 3D virtual fitting system.

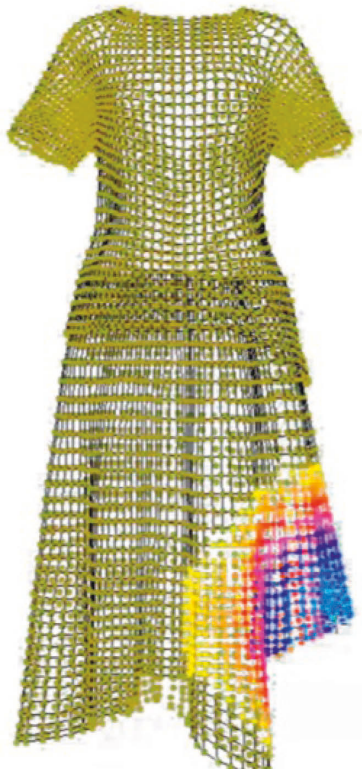

Figure 8: Schematic diagram of smart 3D clothing display.

4. Application of Clothing Intelligent 3D Display Technology in Clothing Marketing

This paper combines intelligent 3D display technology to construct a clothing marketing system that can not only display clothing but also have the function of fitting. The interactive process of the 3D virtual fitting system is shown in Figure 7.

Figure 8 shows the schematic diagram of smart 3D clothing display.

After the above system is constructed, the clothing display function and online fitting function of this system are

Table 1: Verification of clothing display effect.

Num	Fashion show
1	79.350
2	75.380
3	71.406
4	72.418
5	70.938
6	82.348
7	82.050
8	73.013
9	70.764
10	74.884
11	71.676
12	84.746
13	68.860
14	73.617
15	74.395
16	81.480
17	79.173
18	74.229
19	69.612
20	68.856
21	81.495
22	83.289
23	72.842
24	80.815
25	76.738
26	85.352
27	77.633
28	74.273
29	70.009
30	84.026
31	86.666
32	82.729
33	69.661
34	68.226
35	84.942
36	79.536
37	84.715
38	67.344
39	82.139
40	67.822
41	68.731
42	75.762
43	72.036
44	69.388
45	71.753
46	71.623
47	86.238
48	72.837
49	69.780
50	67.995
51	81.069

Table 2: Functional verification of online fitting.

Num	Online fitting
1	65.510
2	65.457
3	74.324
4	68.890
5	60.927
6	71.183
7	67.949
8	67.758
9	64.360
10	73.887
11	64.207
12	66.932
13	78.858
14	70.275
15	64.457
16	60.851
17	79.989
18	61.076
19	60.530
20	60.544
21	77.139
22	72.075
23	64.711
24	68.105
25	73.945
26	79.365
27	80.740
28	64.559
29	60.964
30	74.236
31	75.028
32	64.977
33	68.655
34	72.523
35	63.403
36	75.182
37	72.234
38	72.136
39	76.951
40	63.589
41	76.474
42	74.941
43	78.450
44	76.956
45	62.036
46	75.778
47	66.953
48	68.916
49	67.550
50	78.488
51	69.860

tested and evaluated in combination with simulation experiments, and the results shown in Tables 1 and 2 are finally, obtained.

From the abovementioned research, it can be seen that the smart clothing 3D display system proposed in this paper can effectively improve the effect of clothing marketing and has an important role in promoting online e-commerce clothing marketing.

5. Conclusions

The new retail operation approach places an emphasis on "scenario triggering," in contrast to the more traditional method of retail operation, which frequently keeps marketing material and the scene apart from one another. Consumers who are in a physical store and see a favorite article of clothing but do not have a size that is suitable for

them at the moment have two options: they can scan the QR code to search for inventory, or the relevant brand app can send personalized push notifications to target consumers who are in close proximity to the physical store using location-based service technology. With this strategy, it is possible to achieve mutual draining between online and offline activities in an effective manner.

The purpose of this paper is to improve the customer experience of online clothing marketing by utilizing 3D clothing display technology. Additionally, this paper will assist in increasing the marketing effect of online clothing. As a result of the simulation test research, it has been established that the smart clothing 3D display system that has been proposed in this article has the potential to significantly enhance the effect of clothing marketing and that it plays an important part in the promotion of clothing marketing through online e-commerce.

Data Availability

The data used to support the findings of this study are included within the article.

Conflicts of Interest

The authors declare that they have no conflicts of interest.

Acknowledgments

This work was supported by the Anhui Philosophy and Social Sciences Planning Youth Project, "Research on Inheritance, Innovation, and Development of Huizhou Traditional Women's Clothing Decoration Technology" (Project No. ahskq2019d102).

References

[1] Q. Xu, H. Liu, Y. Liu, and S. Wu, "Innovative design of intangible cultural heritage elements in fashion design based on interactive evolutionary computation," *Mathematical Problems in Engineering*, vol. 2021, Article ID 9913161, 11 pages, 2021.

[2] S. Bogović, Z. Stjepanovič, A. Cupar, S. Jevšnik, B. Rogina-Car, and A. Rudolf, "The use of new technologies for the development of protective clothing: comparative analysis of body dimensions of static and dynamic postures and its application," *Autex Research Journal*, vol. 19, no. 4, pp. 301–311, 2019.

[3] M. Man-Lok Lam, E. P. Li, E. Yee-Nee Lam, and W. S. Liu, "Aesthetic experiences and design creativity: an ethnographic study of a wool felting design workshop," *International Journal of Fashion Design, Technology and Education*, vol. 14, no. 3, pp. 375–386, 2021.

[4] X. Zhang and C. Yang, "Application of Multipopulation Genetic Algorithm in Industrial Special Clothing Design," *Wireless Communications and Mobile Computing*, vol. 2022, Article ID 1632063, 9 pages, 2022.

[5] B. E. Jin and D. C. Shin, "The power of 4th industrial revolution in the fashion industry: what, why, and how has the industry changed?" *Fashion and Textiles*, vol. 8, no. 1, pp. 31–25, 2021.

[6] S. Starkey, S. Alotaibi, H. Striebel, J. Tejeda, K. Francisco, and N. Rudolph, "Fashion inspiration and technology: virtual reality in an experimental apparel design classroom," *International Journal of Fashion Design, Technology and Education*, vol. 14, no. 1, pp. 12–20, 2021.

[7] S. Saleh Alghamdi, S. John, N. Roy Choudhury, and N. K. Dutta, "Additive manufacturing of polymer materials: progress, promise and challenges," *Polymers*, vol. 13, no. 5, p. 753, 2021.

[8] D. Kodžoman, "The psychology of clothing: meaning of colors, body image and gender expression in fashion," *Textile & Leather Review*, vol. 2, no. 2, pp. 90–103, 2019.

[9] C. Black, C. Freeman, and A. Rawlings, "Problem-based learning: design development of female chef's jackets," *International Journal of Fashion Design, Technology and Education*, vol. 11, no. 1, pp. 123–128, 2018.

[10] Y. Zhao, "Manufacturing personalization models based on industrial big data," *Journal of Discrete Mathematical Sciences and Cryptography*, vol. 21, no. 6, pp. 1287–1292, 2018.

[11] S. Kolose, T. Stewart, P. Hume, and G. R. Tomkinson, "Cluster size prediction for military clothing using 3D body scan data," *Applied Ergonomics*, vol. 96, Article ID 103487, 2021.

[12] J. Park, K. Park, B. Lee, H. You, and C. Yang, "Classification of upper body shapes among Korean male wheelchair users to improve clothing fit," *Assistive Technology*, vol. 31, no. 1, pp. 34–43, 2019.

[13] S. Miell, S. Gill, and D. Vazquez, "Enabling the digital fashion consumer through fit and sizing technology," *Journal of Global Fashion Marketing*, vol. 9, no. 1, pp. 9–23, 2018.

[14] S. Y. Kim and J. Ha-Brookshire, "Evolution of the Korean marketplace from 1896 to 1938: a historical investigation of Western clothing stores' retail and competition strategies," *Clothing and Textiles Research Journal*, vol. 37, no. 3, pp. 155–170, 2019.

[15] P. Milošević and S. Bogović, "3D technologies in individualized chest protector modelling," *Textile & Leather Review*, vol. 1, no. 2, pp. 46–55, 2018.

[16] T. Maxmudjon, "The figurative expression of the composition of costume," *Innovative Technologica: Methodical Research Journal*, vol. 2, no. 10, pp. 38–42, 2021.

[17] J. Louis-Rosenberg and J. Rosenkrantz, "Anti-entrepreneurs using computation to unscale production," *Architectural Design*, vol. 90, no. 2, pp. 112–119, 2020.

[18] S. K. Seo and C. Lang, "Psychogenic antecedents and apparel customization: moderating effects of gender," *Fashion and Textiles*, vol. 6, no. 1, p. 19, 2019.

[19] A. Ihsan, N. Fadillah, and C. Rizka Gunawan, "Acehnese traditional clothing recognition based on augmented reality using hybrid tracking method," *Indonesian Journal of Electrical Engineering and Computer Science*, vol. 20, no. 2, pp. 1030–1036, 2020.

Hindawi
Complexity
Volume 2022, Article ID 3444856, 13 pages
https://doi.org/10.1155/2022/3444856

Research Article

Analysis of Mutual Influence Relationships of Purchase Intention Factors of Electric Bicycles: Application of DEMATEL Taking into Account Information Uncertainty and Expert Confidence

Ching-Te Lin,[1,2] **Jen-Jen Yang**,[3,4] **Wen-Jen Chiang**,[5] **Jen-Jung Yang**,[6] **and Chin-Cheng Yang**[6]

[1]*General Education Center, Chaoyang University of Technology, Taichung, Taiwan*
[2]*Department of Business Administration, National Yunlin University of Science and Technology, Yunlin County, Taiwan*
[3]*Department of Business Administration, Chaoyang University of Technology, Taichung, Taiwan*
[4]*Department of Industrial Education and Technology, National Changhua University of Education, Changhua, Taiwan*
[5]*Graduate School of Technological and Vocational Education, National Yunlin University of Science and Technology, Yunlin County, Taiwan*
[6]*Department of Leisure Service Management, Chaoyang University of Technology, Taichung, Taiwan*

Correspondence should be addressed to Chin-Cheng Yang; ccyang.author@gmail.com

Received 28 July 2022; Revised 31 August 2022; Accepted 3 September 2022; Published 13 September 2022

Academic Editor: Zeljko Stevic

As the negative environmental impacts of transportation systems become more severe, governments and environmental groups are seeking more sustainable transportation options, such as replacing fuel-powered vehicles with electric vehicles and expanding public transportation systems to reduce the number of people driving on their own, in order to reduce the environmental impacts of transportation systems. At present, the rapid expansion of public transportation systems is not an easy task and requires a long period of time to plan for expansion and construction, so people are increasingly looking to find means of transportation that meet sustainable conditions as solutions. In this context, electric bicycles are one of the solutions that people can choose, with benefits such as energy saving, carbon reduction, effective air pollution reduction, and simple and labor-saving riding. However, in Taiwan, despite the many benefits of electric bicycles, their popularity is not high. Therefore, this study focuses on the factors that affect the purchase of electric bicycles in Taiwan. The Influential Network Relation Map (INRM) generated by the *Z*-based Decision-making Trial and Evaluation Laboratory (*Z*-DEMATEL) technique is used to describe the influence relationships among the factors and to establish the key evaluation criteria of electric bicycle purchase intention. The results indicate that vehicle price, safety, motor performance, battery life, and battery durability are the most important factors in purchasing electric bicycles. Furthermore, the power of motor is considered as the factor that most significantly affects other criteria, while safety and price are most likely to be affected by other criteria. This study has contributed to academia and industry, for the dependency weights of these factors are set to provide a scientific and systematic way to show how consumers think in the decision-making process and to provide more reliable information and management implications for the electric bicycle industry.

1. Introduction

Since the twentieth century, the world has been facing environmental pollution problems caused by harmful emissions from conventional fuels, such as hydrocarbons, nitrogen oxides, carbon monoxide, and suspended particulates, due to advances in transportation and communication technologies resulting in the proliferation of public transportation vehicles [1]. As environmental protection issues have gained attention and awareness of the energy crisis has risen, countries around the world have developed sustainability agreements such as the Sustainable Development Goals (SDGs) and the Convention on Biological Diversity (CBD) to persuade companies to move

toward sustainable development. The purpose of sustainable development is "to meet people's needs and future development while maintaining environmental balance and sustainability in the direction of investment, technological development, resource development, and institutional change, with benefits that meet societal expectations" [2].

More than 128 countries in the world have declared that they will achieve "net-zero carbon emissions" by 2050, hoping to effectively reduce carbon emissions to achieve net-zero carbon emissions [3, 4]. Governments around the world have begun to formulate improvement plans for transportation, looking for sustainable public transportation that reduces environmental pollution and low energy consumption, and are actively moving toward the goal of achieving zero carbon emissions in transportation [1]. Sustainable electric vehicles are considered to have a significant positive impact on the environment, effectively replacing traditional gasoline and diesel vehicles that cause serious environmental pollution, for example, by reducing air pollution and noise [5–8]. The awareness of sustainability has led to a boom in electric vehicle manufacturing-related industries, among which electric bicycles have become the mainstream focus of today's green transportation [9].

In recent years, electric bicycles have been the fastest growing industry in the transportation market [10, 11], especially in highly congested urban areas, where they are more comfortable than other eco-transit vehicles such as conventional bicycles. Compared with automobiles and motorcycles, electric bicycles have relatively low purchase cost and convenience for short-distance travel, which increases the overall demand in urban areas and makes electric bicycles the preferred means of transportation for the public [12, 13]. According to the Confederation of the European Bicycle Industry (CONEBI), more than 22 million electric bicycles have already been sold in Europe in 2020, generating a value of over 18.3 billion Euros, a significant 40% increase in electric bicycle sales compared with 2019. In the United States, the epidemic has created a huge demand for personal commuting. With the difficulty of predicting when the epidemic will abate, and with the government discouraging public transportation, American commuters are turning their attention to convenient electric bicycles [14]. The United States Department of the Interior in October 2018 announced that electric bicycles could be ridden on regular bicycle trails, etc., which boosted the public's willingness to buy electric bicycles, and gradually increased the demand for electric bicycles in the United States (U.S.) market. In urban transportation systems in Europe and the U.S., the increasing reliance on the role of electric bicycles with the use of renewable energy sources has led to their widespread use [11, 15]. Governments have also been liberalizing the use of electric bicycles in public spaces, and electric bicycles are often legally defined as bicycles, and therefore face less oversight and regulation than gasoline-powered models [16].

In response to this trend, electric bicycles are more in short supply in the market. Taiwan is the kingdom of producing bicycles and electric bicycles, so the sales of bicycles and electric bicycles in Taiwan have been increasing. Electric bicycles are in line with the trend of sustainable development with the advantages of energy saving and carbon reduction which can effectively reduce air pollution, boost simple and effortless riding without a driver's license It is gradually becoming the new choice of human mobility. Electric bicycles are regarded as the rising star of the bicycle industry [17]. Electric bicycles have a speed limit of 24 km/h, which can avoid speeding, and is more secure for the elderly in terms of speed control and safety. In addition, compared with electric motorcycles/scooters, they are exempt from license tax and the riders' helmets are not required in Taiwan. These are all beneficial to the future of electric bicycles. Besides, the Taiwan government is also actively promoting the relevant subsidy policies for the purchase of electric bicycles. Therefore, the research objectives can be described as follows.

(i) Firstly, it is to explore the purchase intention factors of electric bicycles in Taiwan, and which reasons are the main considerations of electric bicycle purchase in Taiwan, so as to establish the purchase intention factors.

(ii) Next, what is the importance of each of these purchase intention factors? What is their ranking?

(iii) Besides, what are the mutual influence relationships among the purchase intention factors?

The above questions are typical Multiple Criteria Decision-Making (MCDM) issues. The MCDM methodologies are effective in dealing with multiple complex and constrained criteria, and it is possible to identify criteria weights through expert interviews and soft computing techniques. MCDM overcomes several assumptions in the use of traditional statistical theory (e.g., the sample data needs to conform to a normal distribution, and the assumption that variables are independent of each other). MCDM allows the use of a small sample of expert interview data to generate reliable analytical results through consistency or consensus testing [18–20]. In this study, we have three main implementation stages. The first stage is to propose a framework for evaluating electric bicycle purchase intention factors in a model that aggregated 10 main purchase intention factors through extensive literature and expert interviews. In the second stage, the Z-based Decision-making Trial and Evaluation Laboratory (Z-DEMATEL) [21] is used to identify the mutual influence relationships of the intention factors and generate dependency weights. This technique not only takes into account the uncertainty of the information sources, but also measures the reliability of the experts in the evaluation. In the third stage, the Influential Network Relation Map (INRM) is plotted to present visualized results to discuss management implications and give appropriate strategies for decision-makers to follow.

Common weight determination methods include Analytic Hierarchy Process (AHP) [22], Best-Worst Method (BWM) [23], Full Consistency Method (FUCOM) [24], Level-Based Weight Assessment (LBWA) [25], Interpretative Structural Modeling (ISM) [26], DEMATEL [27], etc. These methods are popular and frequently used [28].

However, some methods, such as AHP, BWM, FUCOM, and LBWA, treat the criteria as independent. In other words, they assume that the criteria do not interact with each other. Such an assumption is not in line with the actual situation. On the contrary, DEMATEL is a technique for identifying criteria dependencies, which improves the shortcomings of ISM, for it can only identify influence with variables 0 and 1. DEMATEL has been widely used in various industries to evaluate the dependence of factors, and many studies have confirmed its effectiveness and usefulness [29–33]. On the other hand, in order to effectively conduct an evaluation in an uncertain environment and measure the confidence of experts in evaluation, this article introduces Z sets theory to replace the general fuzzy theory. Z-DEMATEL is different from other fuzzy DEMATEL techniques (e.g., general fuzzy DEMATEL, intuitionistic fuzzy DEMATEL, Pythagorean fuzzy DEMATEL, and Fermatean fuzzy DEMATEL), which constructs the confidence of experts by integration, and then combines the confidence into the fuzzy evaluation value, so that the evaluation value covers a wider range of information. Many studies have confirmed the practicality of Z sets theory [21, 34].

This study takes the development of electric bicycles in Taiwan as an example and invites experts from the electric bicycle industry, cultural and creative industries, and government agencies to form a decision-making team to use their experience and skills as the basis for data construction. The study scientifically and systematically shows the decision thinking of electric bicycle purchase intention and provide more reliable information and management implications for electric bicycle operators. The specific features and contributions of this article are summarized as follows.

(i) This study adopts the MCDM concept to construct a framework for evaluating the purchase intention factors of electric bicycles.

(ii) DEMATEL-based approach is used to identify the influential relationship among the factors and their influence weights.

(iii) The introduction of Z sets theory reflects uncertainty and expert confidence.

(iv) The research is reproducible. Other products or industries can be analyzed following the same research process.

The rest of the article is organized as follows: Section 2 introduces the literature review of electric bicycle purchase intention and identifies the criteria for electric bicycle purchase intention evaluation. Section 3 describes the basic concepts of Z-numbers and illustrates the Z-DEMATEL calculation process. Section 4 introduces the case study and discussion of electric bicycle purchase intention in Taiwan and presents the feasibility and practicality of the proposed model. Section 5 concludes the full discussion and gives conclusions, and finally provides future research directions.

2. Literature Review

This section presents the literature on electric bicycle intentions and describes the proposed framework.

2.1. Electric Bicycle Purchase Intention. With global warming, the awareness of sustainable transportation for energy saving and carbon reduction has been increasing day by day. The use of electric bicycles is growing steadily around the world. Electric bicycles are a relatively environmentally friendly means of transportation, especially for short to medium distances, the use of electric bicycles can help reduce traffic congestion [1, 5]. Numerous studies have contributed to the electric bicycle purchase intention [35–40].

For example, Bigazzi and Berjisian [35] explored the impact of government incentives on electric bike purchase intentions. Considerations include product price, demand, subsidies, and the allowable price elasticity for consumers. The results show that incentive policies can actually improve consumers' purchase intention. Sałabun et al. [13] used the Characteristic Objects Method (COMET) to discuss the relationship between electric bike features and purchase intention. The evaluation factors include battery capacity, battery charging time, number of gears, vehicle weight, price, etc. In the following year, Shekhovtsov et al. [36] used the same evaluation factors to select different types of e-bikes. Simsekoglu and Klöckner [37] took Norway as an example to study the indicators that affect the intention to buy electric bicycles, which considers factors including age, gender, experience, benefits, safety, environment, etc. Their study applied multiple regression and principal component analysis to identify the influence of indicators. The results show that age, benefits, other people's opinions, and familiarity significantly influence purchase intent. Herberz et al. [40] pointed out that most consumers agree to use environmentally friendly means of transportation. Their study used regression models to measure the impact of environmental factors on electric bike purchase intentions. Emitting less carbon dioxide, reducing the potential damage to the environment, and being environmentally friendly are important factors when people purchase an electric bike.

Most of the above literature uses statistical methodology as an analytical tool. Few studies have explored the interaction of purchase intention with the concept of MCDM. Beyond that, they have not considered the uncertainty of the assessment environment. In order to overcome the abovementioned issues, this study uses Z-DEMATEL to effectively identify the relationship among factors, and determine the confidence of experts in the assessment. We reviewed the extensive literature and integrated the judgments of multiple

experts to construct an evaluation framework. Section 2.2 presents the proposed factors and their definitions.

2.2. Proposed Framework. Based on past academic literature and discussions among experts from industry, government, and academia, the initial evaluation factors of electric bicycle purchase intention were established and the more important criteria were selected to be included in the evaluation system to highlight the characteristics and meaning of electric bicycle purchase intention. The main factors consist of 10 criteria, including price (C_1), battery life (C_2), battery durability (C_3), charging time (C_4), power of motor (C_5), and external influences are after-sales service (C_6), infrastructure (C_7), safety (C_8), government regulations (C_9), and government policy (C_{10}).

Price (C_1) aims to measure the reasonable price of electric bicycles that consumers can accept, and to increase consumers' purchase intention by setting a reasonable selling price [13, 35, 36]. In addition to price, the battery of an electric bicycle is the main source of power supply for the vehicle, and battery life (C_2), battery durability (C_3), charging time (C_4), and power of engine (C_5) are included in the evaluation framework. Battery life (C_2) evaluates the time from good to bad during battery use. Repeated charging of batteries may cause shortened battery life. If there is good research and development (R&D) technology or patents, it will extend the battery life and increase the intention of consumer consumption [13, 36]. Battery durability (C_3) evaluates the distance that a single charge of the battery can be ridden. Under normal riding conditions, the higher the battery durability, the longer the riding distance, and the more beneficial it is to reduce the number of battery recharges [13, 36, 38]. Charging time (C_4) mainly evaluates the time required to charge the vehicle battery from no power at all to a full charge. Besides, the length of the charging waiting time affects the convenience of reusing the electric bicycle [13, 36]. Finally, power of engine (C_5) evaluates the performance of the vehicle's power, whether it provides a high-performance motor with multiple functional modes to meet the needs of consumers in any situation [13, 36].

This study not only discusses the performance of the electric bicycle itself, but also discusses external influences, mainly evaluating the influence of various factors in the external environment on the purchase intention. Among the factors, after-sales service (C_6) aims to evaluate the services related to the purchase of the electric bicycle, including warranty, repair and maintenance, etc., to protect the consumer's rights after the purchase with the help of comprehensive after-sales service. Infrastructure (C_7) examines whether there is a well-planned electric bicycle system that provides a good cycling environment for riders, as well as convenient charging facilities, battery swapping stations, and repair shops [39, 40]. Safety (C_8) aims to measure the safety of road traffic, the lives of riders operating electric bicycles, the availability of adequate safety regulations, manuals, and the riding environment [40]. The last two are government regulations (C_9) and government policy (C_{10}) for examining whether the government has adequate regulations to protect the right to purchase electric bicycles and whether the government provides incentives and subsidies to encourage consumers to purchase electric bicycles [35].

Table 1: Evaluation scales of *Z*-DEMATEL and corresponding membership functions [21].

Linguistic variable (F, R)	Z-numbers
(N, VL)	(0, 0, 0.316)
(N, L)	(0, 0, 0.548)
(N, M)	(0, 0, 0.707)
(N, H)	(0, 0, 0.837)
(N, VH)	(0, 0, 0.949)
(L, VL)	(0, 0.316, 0.632)
(L, L)	(0, 0.548, 1.096)
(L, M)	(0, 0.707, 1.414)
(L, H)	(0, 0.837, 1.673)
(L, VH)	(0, 0.949, 1.897)
(M, VL)	(0.316, 0.632, 0.949)
(M, L)	(0.548, 1.096, 1.644)
(M, M)	(0.707, 1.414, 2.121)
(M, H)	(0.837, 1.673, 2.510)
(M, VH)	(0.949, 1.897, 2.846)
(H, VL)	(0.632, 0.949, 1.265)
(H, L)	(1.096, 1.644, 2.192)
(H, M)	(1.414, 2.121, 2.828)
(H, H)	(1.673, 2.510, 3.347)
(H, VH)	(1.897, 2.846, 3.795)
(VH, VL)	(0.949, 1.265, 1.265)
(VH, L)	(1.644, 2.192, 2.192)
(VH, M)	(2.121, 2.828, 2.828)
(VH, H)	(2.510, 3.347, 3.347)
(VH, VH)	(2.846, 3.795, 3.795)

3. Research Approach

The research approach used in this article is based on the *Z*-DEMATEL proposed by Hsu et al. [21] for data analysis. In this section, the basic concepts of *Z*-numbers are first introduced and the conversion rules of the linguistic variables, which overcome the shortcomings of fuzzy theory sets by increasing the reliability measure for experts in the evaluation, so that uncertain information can be described more clearly. Then, the detailed calculation procedure of *Z*-DEMATEL is given and the INRM is plotted to present the mutual influence relationships of the purchase intention factors. And this can help the decision-makers to quickly identify the main factors of the electric bicycle purchase intention.

3.1. Concepts of Z-Numbers and Conversion Rules for Linguistic Variables. Zadeh [41] proposed a method of augmenting fuzzy theory called *Z*-number, which consists of two fuzzy parameters, one for the uncertainty of the evaluated information and the other for the reliability of the

expert at the time of evaluation. A Z-number can be denoted as $Z = (\widetilde{F}, \widetilde{R})$, where $\widetilde{F}$ is the rating given by the expert in the evaluation event and $\widetilde{R}$ is the reliability given $\widetilde{F}$. Both $\widetilde{F}$ and $\widetilde{R}$ are triangular fuzzy numbers with a value range between 0 and 1, and $\widetilde{F}$ and $\widetilde{R}$ can be written as $\widetilde{F} = (f, \mu_{\widetilde{F}}) | x \in [0,1]$ and $\widetilde{R} = (x, \mu_{\widetilde{R}}) | x \in [0,1]$. In the Z-number processing program, $\widetilde{R}$ (reliability) can be converted into a crisp value, as shown in (1).

$$\alpha = \frac{\int^{x} \mu_{\widetilde{R}} \mathrm{d}x}{\int^{\mu_{\widetilde{R}}} \mathrm{d}x}. \tag{1}$$

Next, the reliability weight α is added to the evaluated value $\widetilde{F}$. The weighted Z-numbers are as in (2).

$$Z^{\alpha} = \left\{ \left(x, \mu_{\widetilde{F}^{\alpha}} \right) | \mu_{\widetilde{F}^{\alpha}}(x) = \alpha \mu_{\widetilde{F}}(x), x \in \sqrt{\alpha}\, x \right\}. \tag{2}$$

Here, it is assumed that an evaluation system has n criteria/alternatives, $c_i = (c_1, c_2, \ldots, c_n)$. For these criteria/alternatives, pairwise comparisons must be conducted to explore the mutual influence, i.e., to evaluate the degree of influence of c_i on c_j. The evaluation scales include "No influence (N)," "Low influence (L)," "Medium influence (M)," "High influence (H)," and "Very high influence (VH)." These linguistic variables are converted into the corresponding membership functions (fuzzy numbers). Next, the experts are asked to evaluate the level of confidence in their answers, i.e., the reliability of the evaluation. The evaluation scales include "Very low (VL)," "Low (L)," "Medium (M)," "High (H)," and "Very high (VH)." Therefore, a total of 25 combinations of Z-numbers can be obtained, and in the same way, the linguistic variables of Z-numbers and their membership functions can be obtained, as shown in Table 1.

3.2. Z-DEMATEL Technique. The DEMATEL technique identifies the mutual influence relationships between factors and helps decision-makers understand which factors are the primary affecting factors on others and which are the affected factors by others through a structured INRM [42]. In an evaluation environment that is complex and full of uncertainties, it is difficult for the experts to use crisp values to reflect their true feelings. Many fuzzy theoretical approaches have been combined with DEMATEL to consider uncertainties, but unfortunately, these approaches ignore the degree of confidence that the experts have in their evaluations. In this study, Z-numbers are introduced into DEMATEL to not only know the reliability of the decision-making team in the evaluation, but also to preserve the triangular fuzzy number form for computation to avoid information loss. Through the improvement of this study, the influential weights of a set of criteria/factors can be obtained by Z-DEMATEL, and the detailed steps of the Z-DEMATEL technique are as follows.

Step 1. Develop a set of evaluation criteria/factors

A group of experts formed a decision-making team to develop a set of appropriate evaluation criteria/factors (c_i). In this study, we consider the factors of development trends as criteria, $c_i = \{c_1, c_2, \ldots, c_n\}$.

Step 2. Build the direct relation matrix $\mathbf{A}$ of the group

Here, there are n development factors that need to be evaluated for their influence. Each expert evaluates the degree of direct influence of the factor i on the factor j and measures the expert's confidence in the rating. This step introduces the concept of Z-numbers into the Z-DEMATEL questionnaire.

The opinions of all experts are averaged to integrate a group of direct relation matrix $\mathbf{A}$, as shown in equation (3).

$$\mathbf{A} = \left[Z\left(a_{ij}\right) \right]_{n \times n} = \begin{bmatrix} Z(a_{11}) & Z(a_{12}) & \cdots & Z\left(a_{1j}\right) & \cdots & Z(a_{1n}) \\ Z(a_{21}) & Z(a_{22}) & \cdots & Z\left(a_{2j}\right) & \cdots & Z(a_{2n}) \\ \vdots & \vdots & \ddots & \vdots & \ddots & \vdots \\ Z(a_{i1}) & Z(a_{i2}) & \cdots & Z\left(a_{ij}\right) & \cdots & Z(a_{in}) \\ \vdots & \vdots & \ddots & \vdots & \ddots & \vdots \\ Z(a_{n1}) & Z(a_{n2}) & \cdots & Z\left(a_{nj}\right) & \cdots & Z(a_{mn}) \end{bmatrix}_{n \times n}, \quad i = j = 1, 2, \ldots, n, \tag{3}$$

where $Z(a_{ij}) = (a_{ij}^{L}, a_{ij}^{M}, a_{ij}^{U})$.

Here, Z-DEMATEL requires the diagonal elements in matrix $\mathbf{A}$ to be 0, i.e., $Z(a_{ij}) = 0$ (when $i = j$).

Step 3. Obtain the normalized direct relation matrix $\mathbf{X}$

Since the range of values of $Z(a_{ij})$ is 0 to 4, we can convert this evaluation to 0 to 1 through normalization (4) and (5).

$$\mathbf{X} = \left[Z\left(x_{ij}\right) \right]_{n \times n} = \varepsilon \cdot \left[Z\left(a_{ij}\right) \right]_{n \times n}, \quad i = j = 1, 2, \ldots, n, \tag{4}$$

where $Z(x_{ij}) = (x_{ij}^{L}, x_{ij}^{M}, x_{ij}^{U})$.

$$\varepsilon = \min \left\{ \frac{1}{\max_i \sum_{j=1}^{n} a_{ij}^{U}}, \frac{1}{\max_j \sum_{i=1}^{n} a_{ij}^{U}} \right\}. \tag{5}$$

Step 4. Generate the group total influence matrix $\mathbf{T}$

The normalized direct relation matrix $\mathbf{X}$ (4) can be integrated into a total influence matrix $\mathbf{T}$ by the computation of (6). This step sums up all direct and indirect influence relationships from the power of $\mathbf{X}$ to the power of infinity. Since the operation procedure of (7) is cumbersome, a faster solution equation can be derived from (8).

$$\mathbf{T} = \left[Z\left(t_{ij}\right) \right]_{n \times n}, \quad i = j = 1, 2, \ldots, n, \tag{6}$$

where $Z(t_{ij}) = (t_{ij}^{L}, t_{ij}^{M}, t_{ij}^{U})$.

$$\mathbf{T}= \mathbf{X}+\mathbf{X}^2+\cdots+\mathbf{X}^{\infty}, \tag{7}$$

$$\begin{aligned}\mathbf{T} &= \mathbf{X}+\mathbf{X}^2+\cdots+\mathbf{X}^{\infty} = \mathbf{X}\left(\mathbf{I}+\mathbf{X}+\mathbf{X}^2+\cdots+\mathbf{X}^{\infty-1}\right)\\ &= \mathbf{X}\left(\mathbf{I}-\mathbf{X}^{\infty}\right)(\mathbf{I}-\mathbf{X})^{-1}\\ &= \mathbf{X}(\mathbf{I}-\mathbf{X})^{-1},\end{aligned} \tag{8}$$

where $\mathbf{X}^{\infty} = [0]_{n\times n}$ and $\mathbf{I}$ is the unit matrix.

Step 5. Create an INRM to identify the mutual influence relationships of the development factors

In (9) and (10), $Z(\mathbf{r})$ is obtained by summing up each column of the total influence matrix $\mathbf{T}$. Similarly, in (11) and (12), $Z(\mathbf{s})$ is obtained by summing up each row of the total influence matrix $\mathbf{T}$.

$$\begin{aligned}Z(\mathbf{r}) &= \left[Z(r_i)\right]_{n\times 1}\\ &= \left(Z(r_1), Z(r_2), \ldots, Z(r_i), \ldots, Z(r_n)\right),\end{aligned} \tag{9}$$

$$\left[Z(r_i)\right]_{n\times 1} = \left[\sum_{j=1}^{n} Z\left(t_{ij}\right)\right]_{n\times 1}, \tag{10}$$

$$\begin{aligned}Z(\mathbf{s}) &= \left[Z\left(s_j\right)\right]_{1\times n}\\ &= \left(Z(s_1), Z(s_2), \ldots, Z\left(s_j\right), \ldots, Z(s_n)\right)^{T},\end{aligned} \tag{11}$$

$$\begin{aligned}\left[Z\left(s_j\right)\right]_{1\times n} &= \left[\sum_{i=1}^{n} Z\left(t_{ij}\right)\right]_{1\times n}\\ &= \left[Z(s_i)\right]_{n\times 1}^{T},\end{aligned} \tag{12}$$

where the symbol "superscript T" represents the matrix transposition, in addition, $Z(r_i) = (r_i^L, r_i^M, r_i^U)$ and $Z(s_i) = (s_i^L, s_i^M, s_i^U)$.

$Z(r_i) + Z(s_i)$ is the index of the strength of influences given and received. On the other hand, $Z(r)_i - Z(s_i)$ represents the net influence; the larger the $Z(r_i) + Z(s_i)$, the greater the degree of influence of factor i on the evaluation system. If $Z(r)_i - Z(s_i) > 0$ (a positive value), it means that factor i has a significant effect on other factors and is called a causal factor; conversely, if $Z(r_i) - Z(s_i) < 0$ (a negative value), it means that factor i is more affected by other factors and is called an affected factor.

Here, the centroid method is used to defuzzify fuzzy values (e.g., $Z(\lambda) = (\lambda^L, \lambda^M, \lambda^U)$) to obtain the crisp values (λ), as in (13).

$$\lambda = \frac{\lambda^L + \lambda^M + \lambda^U}{3}. \tag{13}$$

Next, r_i and s_i are obtained for $Z(r_i)$ and $Z(s_i)$ by the defuzzification procedure of (13). The relative coordinate positions of each factor are clearly plotted by using $r_i + s_i$ as the horizontal axis and $r_i - s_i$ as the vertical axis. The total influence matrix $\mathbf{T}$ is used to identify the influence between each factor, and the arrows (indicating the direction of influence) are plotted to generate a systematic INRM.

Step 6. Obtain the influence weights of the development factors

Here, $r_i + s_i$ reflects the total influence of the factors on the evaluation system, so the influence weights $w_i = \{w_1, w_2, \ldots, w_n\}$ of the factors can be constructed by (14). Here, the total weight is required to be 1.

$$w_i = \frac{(r_i + s_i)}{\sum_{i=1}^{n}(r_i + s_i)}. \tag{14}$$

4. Empirical Analysis and Results

This section introduces the background of the case, the data collection process, and the Z-DEMATEL implementation procedure.

4.1. Background Description and Data Collection. Nowadays, the public is gradually aware of the importance of air quality, causing the gradual elimination of gas and diesel from public transportation systems and the active use of non-emission electric systems. The most common means of transportation, such as trains, buses, automobiles, motorcycles/scooters, and bicycles, have been gradually transformed to be powered by electric systems. Especially in recent years, with the development of electric bicycles, they have gradually become one of the new transportation options in Taiwan because of their high energy efficiency, high power, and license exemption. Although electric bicycles have the advantage of less environmental pollution, they are not yet as popular as motorcycles/scooters in Taiwan. In order to investigate the related problems, this study uses a literature review to establish the criteria related to electric bicycles assessing what causes the low popularity of electric bicycles? What are the reasons that affect consumers' willingness to purchase electric bicycles? What are the most critical and likely factors that influence consumers' purchase intentions? How do the criteria influence each other? The answers to these questions will help improve the business model of electric bicycle operators and increase the popularity of electric bicycles in Taiwan. Therefore, in order to identify the most critical criteria in electric bicycles, this study invited 15 experts in the electric bicycle industry to form an expert team, who come from academic researchers, industry department heads, and senior industry employees, all of whom have expertise in electric bicycles. The study compiles the background information of the 15 experts and presents the results in Table 2.

In this study, structured interviews were conducted in a face-to-face format. The advantages of structured interviews are as follows: the entire interview process is highly

Table 2: Background introduction of 15 experts.

Expert code	Industry	Work experience	Highest degree
Expert 1	Academic research institutes	10 years or more	PhD
Expert 2	Academic research institutes	5–10 years	PhD
Expert 3	Bicycle manufacturing	More than 10 years	Associate bachelor
Expert 4	Bicycle manufacturing	More than 10 years	Master
Expert 5	Bicycle manufacturing	More than 10 years	Bachelor
Expert 6	Electric vehicle manufacturing	5–10 years	Associate bachelor
Expert 7	Recreational sports industry	2–3 years	Bachelor
Expert 8	Recreational sports industry	More than 10 years	Master
Expert 9	Bicycle components manufacturing	2–3 years	Bachelor
Expert 10	Bicycle components manufacturing	More than 10 years	Bachelor
Expert 11	Transportation-related ministries	2–3 years	Master
Expert 12	Transportation-related ministries	More than 10 years	Master
Expert 13	Transportation-related ministries	4–5 years	Master
Expert 14	Energy-related ministries	3–4 years	Associate bachelor
Expert 15	Energy-related ministries	10 years or more	Bachelor

standardized, the return rate of the questionnaire is higher, and the responses are more complete. These facilitate subsequent recording and analysis. In this study, 15 experts were invited to an office of the company to explain the survey process. First, all experts were asked to sign a consent form to ensure that the experts' basic information and survey results would not be leaked. Next, the meaning of each criterion was explained and the process of filling out the *Z*-DEMATEL questionnaire was presented. The presentation and demonstration of the questionnaire content took 15 minutes, and the average time for the experts to complete the questionnaire was 60 minutes, for a total of approximately 75 minutes for one questionnaire.

4.2. Z-DEMATEL Implementation. After collecting *Z*-DEMATEL questionnaires from 15 experts, to ensure a high degree of consistency among the experts' responses, this study used the consensus check formula used by Hsu et al. [21] to calculate the consensus among experts' responses to the *Z*-DEMATEL. The greater the consensus, the more the experts' agreement. The results show an average difference of 3.2% in consensus among experts, which means a 96.8% confidence level. This also indicates that the 15 *Z*-DEMATEL questionnaires have a high degree of consensus.

Taking the *Z*-DEMATEL questionnaire of Expert 1 as an example, as in Table 3, Expert 1 considered the influence of C_1 on C_2 to be very great and was highly confident in the evaluation, so the linguistic variables were filled in as (VH, H). All other criteria were evaluated in the same way, and a matrix of direct influence relationships for the 15 linguistic variables was obtained for all expert evaluations. The *Z*-number-based matrix of direct influence relationships was obtained using the *Z*-number conversion rule, as in Table 4. Similarly, taking the direct influence of C_1 on C_2 as an example, (2.19, 3.06, 3.47) were the *Z*-numbers of C_1 on C_2.

After generating the initial group direct influence relationship matrix **A**, through the normalization process, the elements in the normalized direct influence matrix number are scaled between 0 and 1, so that the units of the elements in the matrix can be unified without changing the original data distribution, and the normalized direct influence matrix **X** is obtained. Next, considering the direct influence relationships and the indirect influence relationships, the normalized direct influence matrix **X** is accumulated and multiplied multiple times to obtain the total group influence relationship matrix **T**, as shown in Table 5.

The final step is to sum the total influence matrix in the horizontal and vertical directions to produce $Z(\mathbf{r})$ and $Z(\mathbf{s})$. The total influence $(Z(\mathbf{r}) + Z(\mathbf{s}))$ and the net influence $(Z(\mathbf{r}) - Z(\mathbf{s}))$ can be obtained by adding and subtracting $Z(\mathbf{s})$ from $Z(\mathbf{r})$, respectively. Take C_1 as an example, its $Z(r_1) + Z(s_1)$ values are (0.99, 2.78, 10.74) and its $Z(r_1) - Z(s_1)$ values are (1.11, 3.01, 11.18), and $r_1 + s_1$ and $r_1 - s_1$ can be obtained by the defuzzification procedure. The total and net influences of all criteria can be obtained by following this procedure to C_{10}. Table 6 presents the results of the *Z*-DEMATEL analysis, in which the total influence $(r + s)$ is used to calculate the weight of the criteria, and the top five criteria with the highest weight values are C_1, C_8, C_5, C_3, and C_2, where C_8 and C_1 ranked first with a weight of 0.109.

The elements of the matrix **T** can be used to investigate the strengths of the criteria and their mutual influence. There $r + s$ is set as the horizontal axis and $r - s$ is set as the vertical axis. Each criterion is labeled with nodes according to its corresponding position, and then the numerical values of the elements of the matrix **T** are used to determine the influence strengths by drawing the influence arrows to create an INRM. The influence relationships of the criteria are shown in Figure 1. By visualizing the INRM, we can quickly understand which criteria are highly influential and consider them as the main causes, while on the other hand, criteria that are more significantly affected are considered as the effects. The criteria with stronger mutual influence are C_1, C_2, C_3, C_5, and C_8, and with the identification, it is beneficial to the subsequent formulation of management and improvement strategies.

5. Discussion

According to the *Z*-DEMATEL results, the top five most important criteria for electric bicycles are price (C_1) with a

Table 3: Direct relation matrix of expert 1 (linguistic variables).

	C_1	C_2	C_3	C_4	C_5	C_6	C_7	C_8	C_9	C_{10}
C_1	—	(VH, H)	(VH, VH)	(VH, VH)	(VH, VH)	(M, VH)	(M, VH)	(H, VH)	(M, H)	(N, H)
C_2	(VH, H)	—	(VH, VH)	(VH, VH)	(VH, VH)	(M, VH)	(L, VH)	(H, VH)	(L, H)	(L, H)
C_3	(VH, H)	(VH, H)	—	(VH, VH)	(VH, VH)	(M, VH)	(N, VH)	(L, VH)	(N, H)	(N, H)
C_4	(VH, H)	(VH, H)	(VH, VH)	—	(H, VH)	(N, VH)	(L, VH)	(H, VH)	(N, H)	(N, H)
C_5	(VH, H)	(VH, H)	(VH, VH)	(VH, VH)	—	(L, VH)	(L, VH)	(M, VH)	(L, H)	(L, H)
C_6	(M, H)	(H, H)	(H, VH)	(H, VH)	(M, VH)	—	(N, VH)	(M, VH)	(N, H)	(N, H)
C_7	(M, H)	(L, H)	(L, VH)	(N, VH)	(M, VH)	(L, VH)	—	(M, VH)	(L, H)	(L, H)
C_8	(M, H)	(H, H)	(H, VH)	(VH, VH)	(M, VH)	(M, VH)	(L, VH)	—	(M, H)	(M, H)
C_9	(L, H)	(M, H)	(M, VH)	(M, VH)	(M, VH)	(M, VH)	(M, VH)	(M, VH)	—	(H, H)
C_{10}	(M, H)	(N, H)	(N, VH)	(N, VH)	(M, VH)	(N, VH)	(L, VH)	(M, VH)	(M, H)	—

Table 4: Direct relation matrix of the group (Z-numbers).

	C_1	C_2	C_3	C_4	...	C_{10}
C_1	(0.00, 0.00, 0.00)	(2.19, 3.06, 3.47)	(2.26, 3.15, 3.56)	(1.02, 1.73, 2.50)	...	(0.89, 1.51, 2.23)
C_2	(2.19, 3.05, 3.38)	(0.00, 0.00, 0.00)	(2.00, 2.90, 3.32)	(1.82, 2.60, 3.09)	...	(0.85, 1.59, 2.28)
C_3	(2.14, 3.03, 3.44)	(2.42, 3.33, 3.65)	(0.00, 0.00, 0.00)	(1.75, 2.56, 3.13)	...	(0.83, 1.53, 2.24)
C_4	(1.67, 2.50, 3.09)	(2.21, 3.13, 3.56)	(1.89, 2.83, 3.33)	(0.00, 0.00, 0.00)	...	(0.66, 1.31, 2.08)
...	...	...	...	...	...	...
C_{10}	(1.19, 1.87, 2.60)	(0.75, 1.26, 1.96)	(0.87, 1.51, 2.22)	(0.71, 1.36, 2.19)	...	(0.00, 0.00, 0.00)

Table 5: Group total influence matrix.

	C_1	C_2	C_3	C_4	...	C_{10}
C_1	(0.06, 0.24, 1.07)	(0.13, 0.32, 1.14)	(0.13, 0.33, 1.17)	(0.08, 0.25, 1.04)	...	(0.06, 0.20, 0.88)
C_2	(0.13, 0.32, 1.13)	(0.05, 0.21, 0.99)	(0.12, 0.31, 1.12)	(0.10, 0.26, 1.02)	...	(0.06, 0.19, 0.85)
C_3	(0.13, 0.33, 1.17)	(0.13, 0.32, 1.14)	(0.05, 0.22, 1.05)	(0.10, 0.27, 1.05)	...	(0.06, 0.20, 0.87)
C_4	(0.11, 0.30, 1.13)	(0.12, 0.30, 1.10)	(0.11, 0.30, 1.12)	(0.04, 0.18, 0.93)	...	(0.05, 0.18, 0.84)
...	...	...	...	...	...	...
C_{10}	(0.08, 0.24, 0.98)	(0.06, 0.21, 0.93)	(0.07, 0.22, 0.95)	(0.05, 0.19, 0.87)	...	(0.02, 0.11, 0.67)

Table 6: Z-DEMATEL results.

	$Z(\mathbf{r}) + Z(\mathbf{s})$	$Z(\mathbf{r}) - Z(\mathbf{s})$	$r+s$	$r-s$	Weight	Rank
C_1	(0.99, 2.78, 10.74)	(1.11, 3.01, 11.18)	8.901	−0.249	0.109	1
C_2	(0.88, 2.59, 10.29)	(1.01, 2.79, 10.78)	8.430	−0.250	0.103	5
C_3	(0.93, 2.70, 10.64)	(0.99, 2.84, 11.02)	8.664	−0.184	0.106	4
C_4	(0.84, 2.53, 10.33)	(0.78, 2.40, 10.05)	7.961	0.151	0.097	7
C_5	(1.00, 2.83, 10.92)	(0.95, 2.73, 10.76)	8.693	0.100	0.106	3
C_6	(0.89, 2.60, 10.48)	(0.87, 2.59, 10.57)	8.299	−0.011	0.102	6
C_7	(0.81, 2.46, 10.20)	(0.81, 2.43, 10.10)	7.922	0.035	0.097	8
C_8	(0.98, 2.79, 10.94)	(1.07, 2.96, 11.22)	8.931	−0.178	0.109	1
C_9	(0.79, 2.34, 9.71)	(0.63, 2.08, 9.12)	7.269	0.317	0.089	9
C_{10}	(0.69, 2.08, 8.97)	(0.57, 1.87, 8.43)	6.646	0.269	0.081	10

weighting of 0.109, safety (C_8) with a weighting of 0.109, power of engine (C_5) with a weighting of 0.106, battery durability (C_3) with a weighting of 0.106, and battery life (C_2) with a weighting of 0.103. This shows that the public's electric bicycle purchase considerations are mostly performance-oriented. The results are in line with Johnson and Rose's [43] study. The study mentioned that the motivation for purchasing an electric bicycle is to save labor 53.6%, replace a car 50.7%, maintain health and fitness 42.0%, climb mountains 40.6%, rehabilitate 34.8%, and environmental benefits 5.8%, all of which are needed for a better performance electric bicycle to meet the needs of consumers. In addition, optimizing the top five important criteria can effectively increase consumers' willingness to purchase electric bicycles. The top five criteria will be discussed separately. First, the criterion with the highest weight is the price of the vehicle (C_1), which echoes Kazemzadeh and Bansal's [44] study, in which the Swedish government began subsidizing electric bicycles in 2018 in order to achieve a sustainable transport subsidy. The government subsidizes 25% of the price of an electric bicycle for consumers in purchase. This shows that consumers are most sensitive to

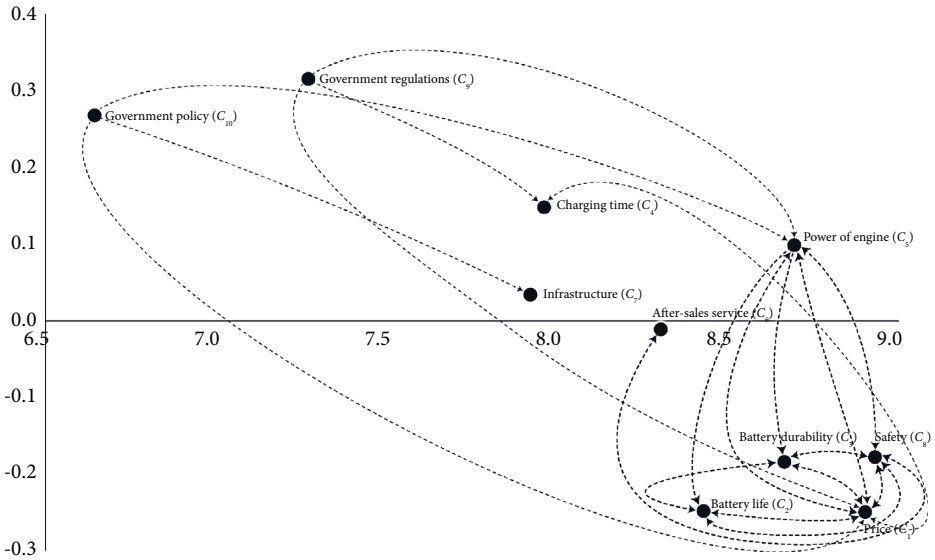

Figure 1: INRM of purchase intention factors of electric bicycles.

the price of the vehicle, and when the price of the vehicle is lowered or supported by government subsidies, consumers will be more willing to buy. At present, there are more than 500,000 electric bicycles in Taiwan. Apart from the elderly and children, the largest group of electric bicycle riders are foreign migrant workers. The price of electric bicycles in Taiwan is generally between NT$20,000 and NT$50,000, which is relatively cheap and easy to purchase compared with motorcycles, and does not require additional driving license and registration. For foreign migrant workers, electric bicycles are their first choice of transportation. If the price of electric bicycles can be lowered and there are government subsidies to purchase them, it will increase the popularity of electric bicycles in Taiwan and the willingness to purchase them.

The second most important criterion is safety (C_8), which is consistent with previous studies by Pejhan et al. [45]. Safety in driving and the operation of vehicles have always been one of the reasons why consumers value them. The study focused specifically on the vulnerability of riding electric bicycles on the road and the safety of user operation. Johnson and Rose [43] mention that the reason why electric bicycles are heavier than traditional bicycles is because of the difference in battery and component location planning. In addition, in accelerating, the speed will exceed the accidental speed, which will cause danger to the elderly and children. Therefore, in the planning and setting of electric bicycles, it is necessary to pay special attention to the user experience, in order to reduce user error and reduce the occurrence of man-made accidents. In Taiwan, since there are no specific regulations for electric bicycles, most users will modify them to pursue faster speeds. In terms of safety, the balance and speed of electric bicycles, modification restrictions, and regulations are needed to ensure the safety of road users. The third most important criterion is power of engine (C_5), which is the main power source of the electric bicycle and is used to assist the riding to save effort. Sałabun et al. [13] suggest that a good motor has multiple modes to meet the needs of consumers in any situation, such as providing good riding assistance, proper motor positioning for overall bicycle stability, and good motor maintenance services. The fourth most important criterion is battery durability (C_3) and the fifth most important criterion is battery life (C_2). Oeser et al. [46] mention that batteries need to meet stringent criteria, such as long durability and a battery life of at least 10 years. Longer battery life can effectively reduce replacement and maintenance costs. Most of the batteries used in today's electric bicycles are mainly lithium batteries. Compared with nickel and lead batteries, lithium batteries produce more electricity, being lighter, and enjoying a longer service life. In addition, using the original charger, not overcharging the battery, and keeping the battery dry will ensure that the lithium battery is active and will last longer [47].

In addition, the plotted INRM shows that the power of engine (C_5) is found to be a key factor, with the main characteristics located in the upper right corner of the INRM, indicating that this factor has high degree of influence and high association and should be listed as a priority object. It affects price (C_1), safety (C_8), battery durability (C_3), and battery life (C_2). The relationships will be explained separately. The first is the effect of power of engine (C_5) on price (C_1). There are three main components that affect the price of an electric bicycle: motor, battery, and electronic control system, of which the motor is the most expensive. Its high cost also highlights its importance in electric bicycles. Obviously, the higher the manufacturing cost of the motor with better performance, the more likely to affect the price of the electric bicycle [35, 36]. Second, regarding the effect of power of engine (C_5) on safety (C_8), nowadays, in order to ensure safety, the maximum output power of engine is only 400 watts and the maximum riding speed is limited to 25 km/h, and the motor has a 3-second automatic power supply stop setting to provide safety to

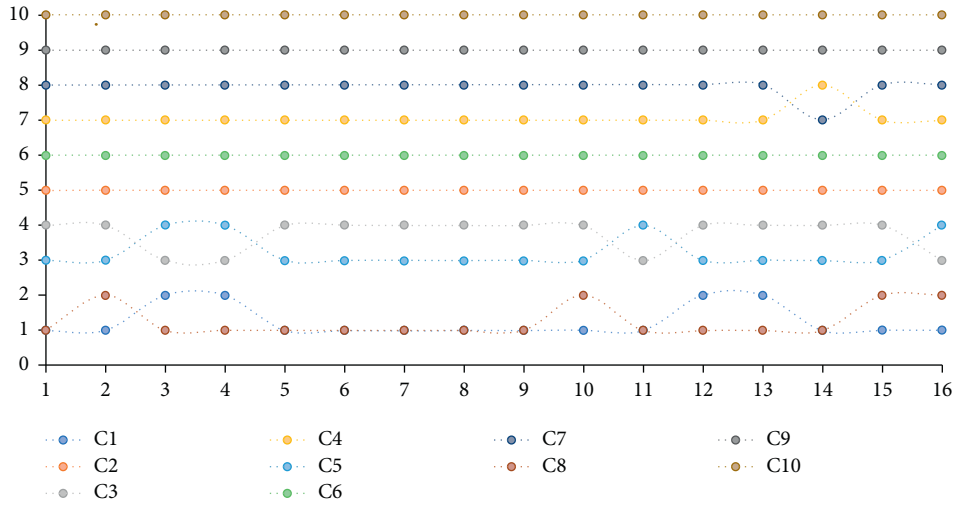

Figure 2: The 16 runs sensitivity analysis results.

users when the speed exceeds the speed limit, braking situation, short circuit, or malfunction of signal system [36, 48]. In terms of the effect of power of engine (C_5) on battery durability (C_3), the motor requires electricity to operate, and the speed can be effectively controlled by regulating the voltage level. Therefore, the longer the battery life, the more power the motor can use, which in turn will provide a constant flow of power [13]. Power of engine (C_5) has an influence on battery life (C_2), and the relationship between the motor and the battery is extremely close. The motor needs to operate efficiently for a long time, and the battery life must be long enough to effectively match the motor operation [13, 36].

Power of engine (C_5), safety (C_8), and after-sales service (C_6) have mutual influence on each other. Motor is the core element of electric bicycle and can be regarded as the heart of electric bicycle. When the motor is poorly designed or often damaged, it not only causes safety concerns, but also requires consumers to go to electric bicycle service stations for repairs, which increases the workload of the service stations and easily raises the cost of after-sales service, as well as risking consumer dissatisfaction with the after-sales service. Therefore, ensuring that the motor is not easily damaged can help reduce the impacts on after-sales service [13, 36]. Other mutual influence relationships can be examined one by one through INRM for their intended management implications.

Furthermore, government policy (C_{10}) and government regulations (C_9) can be found to have a moderate influence on the other factors. Government policy (C_{10}) and government regulations (C_9) in the upper left corner can be considered as secondary factors with high influence and low association, and are the second priority for improvement. Therefore, improving government policy (C_{10}) and government regulations (C_9) is also helpful in increasing consumer purchase intentions. It is primarily the role of government through a series of comprehensive plans and arrangements. Government commitment and public trust are often based on the integrity of regulations and institutions [49], so having clear policy support and regulations in place will help to ensure consumer safety on electric bicycles. Principles such as well-planned electric bicycle lanes, electric bicycle modification regulations, riding speed limits, and compliance with electric bicycle operators' vehicle safety inspection standards and related safety factors should be examined [50]. In addition, government policy and regulations can also protect consumers from purchasing electric bicycles at reasonable prices, avoid malicious price hikes by electric bicycle manufacturers, and establish a fair-trading environment for consumers [35]. When consumers purchase electric bicycles, the government provides friendly policies and regulations to subsidize consumers and operators, helping to increase the popularity and purchase rate of electric bicycles [17].

In order to check whether the individual subjective opinions of experts can affect the overall analysis results, a sensitivity analysis is therefore performed. After deleting the judgment of one expert, we perform Z-DEMATEL and record the ranking results of factors. A total of 16 replicates were performed (including the initial analysis, and the sequential exclusion of 15 experts). The ranking of factors is shown in Figure 2. It can be seen that the ranking change of each factor does not change significantly, despite a small change of 1 unit. In addition to ensuring expert representation through the Z-DEMATEL consensus test, sensitivity analysis can also be used to determine whether the personal judgments of these experts will significantly affect the results.

6. Conclusion

This article uses the MCDM concept to propose a purchase intention factors framework for electric bicycles. In order to effectively conduct an evaluation in an uncertain environment and measure the confidence of experts in evaluation, we introduce Z sets theory into the DEMATEL technique. Z-DEMATEL is used to identify the influential relationship among the factors and their influence weights. Our research

procedure is reproducible. Other products or industries can be analyzed following the analysis process.

The results of this study echo the results of many previous studies on electric bicycles. The DEMATEL-based approach neither require too many pre-determined assumptions to perform the calculation process, nor does it require a large sample size to conduct the survey as in statistical analysis, and the results obtained from interviewing only a few experienced experts in the field can provide good analytical information [51–53]. Overall, this study provides an appropriate electric bicycle purchase intention evaluation system to support consumers and practitioners in developing their strategies accurately. The importance of electric bicycles as environmentally friendly, relatively inexpensive, and suitable for all ethnic groups as a part of future urban transportation cannot be overlooked. This study provides an evaluation of the purchase intention of electric bicycles, which can help the industry to better understand the most important criteria for consumers to purchase electric bicycles and make adjustments to their management strategies:

(i) The electric bicycle purchase intention factors can be divided into two aspects: internal influence and external influence, with a total of ten criteria. The *Z*-DEMATEL method provides a clear ranking of the weight of the ten criteria. The top five important criteria are price (C_1), safety (C_8), power of engine (C_5), battery durability (C_3), and battery life (C_2), which show that consumers are most concerned about the performance of electric bicycles. Improvements to these five criteria will help increase consumer purchase intention.

(ii) *Z*-DEMATEL generates a visualized influential network relation map that can be used to identify the influence relationships among electric bicycle criteria. This shows that power of motor (C_5) is considered as the factor that most significantly affects other criteria, while safety (C_8) and price (C_1) are most likely to be affected by other criteria.

(iii) The current electric bicycle riding group in Taiwan is mainly foreign migrant workers, so if the price can be reduced and if the government subsidies are available, the sales volume of electric bicycles will increase.

Future research can consider criteria based on the perspective of sustainability to explore the development trend of electric bicycles, and incorporate economic, environmental, and social criteria into the evaluation. This will enable decision-makers to develop the electric vehicle market with a sense of sustainability. In the end, only 15 experts participated in this research, and we expect to interview more foreign scholars, practitioners, and electric bicycle experts in the future to increase the number of samples. In terms of methodology, there are other novel techniques for defining criterion interaction relationships, e.g., heterogeneous influence and strength attenuation (HISA) [54]. In the future, more data can be collected for analysis and comparison of multiple methods.

Nomenclature

Acronym:	Nomenclature
SDGs:	Sustainable development goals
CBD:	Convention on biological diversity
CONEBI:	Confederation of the European bicycle industry
U.S.:	United States
MCDM:	Multiple criteria decision-making
Z-DEMATEL:	*Z*-based decision-making trial and evaluation laboratory
INRM:	Influential network relation map
ISM:	Interpretative structural modeling
AHP:	Analytic hierarchy process
BWM:	Best-worst method
FUCOM:	Full consistency method
LBWA:	Level-based weight assessment.

Data Availability

All data generated or analyzed during the study are included within the article.

Conflicts of Interest

The authors declare that they have no conflicts of interest.

Authors' Contributions

Ching-Te Lin contributed to preparing the original draft; Jen-Jen Yang contributed to the methodology; Wen-Jen Chiang contributed to the conceptualization; Jen-Jung Yang contributed to the investigation and data curation; Chin-Cheng Yang performed the review and editing work.

References

[1] N. B. Hung and O. Lim, "A review of history, development, design and research of electric bicycles," *Applied Energy*, vol. 260, Article ID 114323, 2020.

[2] J. J. Yang, Y. C. Chuang, H. W. Lo, and T. I. Lee, "A two-stage MCDM model for exploring the influential relationships of sustainable sports tourism criteria in Taichung City," *International Journal of Environmental Research and Public Health*, vol. 17, no. 7, p. 2319, 2020.

[3] L. C. Vieira, M. Longo, and M. Mura, "Are the European manufacturing and energy sectors on track for achieving net-zero emissions in 2050? An empirical analysis," *Energy Policy*, vol. 156, Article ID 112464, 2021.

[4] P. M. Forster, A. C. Maycock, C. M. McKenna, and C. J. Smith, "Latest climate models confirm need for urgent mitigation," *Nature Climate Change*, vol. 10, no. 1, pp. 7–10, 2020.

[5] K. Kazemzadeh and P. Bansal, "Electric bike level of service: a review and research agenda," *Sustainable Cities and Society*, vol. 75, Article ID 103413, 2021.

[6] G. Oeschger, P. Carroll, and B. Caulfield, "Micromobility and public transport integration: The current state of knowledge," *Transportation Research Part D: Transport and Environment*, vol. 89, Article ID 102628, 2020.

[7] J. Chibwe, S. Heydari, A. F. Imani, and A. Scurtu, "An exploratory analysis of the trend in the demand for the London

bike-sharing system:From London Olympics to Covid-19 pandemic," *Sustainable Cities and Society*, vol. 69, Article ID 102871, 2021.

[8] P. Carroll, B. Caulfield, and A. Ahern, "Modelling the potential benefits of increased active travel," *Transport Policy*, vol. 79, pp. 82–92, 2019.

[9] J. E. Bourne, A. R. Cooper, P. Kelly et al., "The impact of e-cycling on travel behaviour: a scoping review," *Journal of Transport & Health*, vol. 19, Article ID 100910, 2020.

[10] E. Salmeron-Manzano and F. Manzano-Agugliaro, "The electric bicycle: worldwide research trends," *Energies*, vol. 11, no. 7, p. 1894, 2018.

[11] E. Fishman and C. Cherry, "E-bikes in the mainstream: reviewing a decade of research," *Transport Reviews*, vol. 36, no. 1, pp. 72–91, 2016.

[12] M. Patil and B. B. Majumdar, "Prioritizing key attributes influencing electric two-wheeler usage: a multi criteria decision making (MCDM) approach–A case study of Hyderabad, India," *Case Studies on Transport Policy*, vol. 9, no. 2, pp. 913–929, 2021.

[13] W. Sałabun, K. Palczewski, and J. Wątróbski, "Multicriteria approach to sustainable transport evaluation under incomplete knowledge: electric bikes case study," *Sustainability*, vol. 11, no. 12, p. 3314, 2019.

[14] J. F. Teixeira, C. Silva, and F. Moura e Sá, "The motivations for using bike sharing during the COVID-19 pandemic: insights from Lisbon," *Transportation Research Part F: Traffic Psychology and Behaviour*, vol. 82, pp. 378–399, 2021.

[15] E. Fishman, *Bikeshare: Barriers, Facilitators and Impacts on Car Use (Doctoral Dissertation*, Queensland University of Technology), Brisbane, Australia, 2014.

[16] C. R. Cherry, H. Yang, L. R. Jones, and M. He, "Dynamics of electric bike ownership and use in Kunming, China," *Transport Policy*, vol. 45, pp. 127–135, 2016.

[17] K. Kazemzadeh and E. Ronchi, "From bike to electric bike level-of-service," *Transport Reviews*, vol. 42, no. 1, pp. 6–31, 2022.

[18] Ž. Stević, D. K. Das, and M. Kopić, "A novel multiphase model for traffic safety evaluation: a case study of South Africa," *Mathematical Problems in Engineering*, vol. 2021, Article ID 5584599, 22 pages, 2021.

[19] D. Pamučar, A. Puška, Ž. Stević, and G. Cirovic, "A new intelligent MCDM model for HCW management: the integrated BWM–MABAC model based on D numbers," *Expert Systems with Applications*, vol. 175, 114862, 2021.

[20] Ž. Stević, S. Miškić, D. Vojinović, E. Huskanović, M. Stanković, and D. Pamučar, "Development of a model for evaluating the efficiency of transport companies: PCA–DEA–MCDM model," *Axioms*, vol. 11, no. 3, p. 140, 2022.

[21] W. C. J. Hsu, J. J. Liou, and H. W. Lo, "A group decision-making approach for exploring trends in the development of the healthcare industry in Taiwan," *Decision Support Systems*, vol. 141, 113447, 2021.

[22] T. L. Saaty, "What is the analytic hierarchy process?" in *Mathematical Models for Decision Support*, pp. 109–121, Springer, Berlin, Heidelberg, 1988.

[23] J. Rezaei, "Best-worst multi-criteria decision-making method," *Omega*, vol. 53, pp. 49–57, 2015.

[24] D. Pamučar, Ž. Stević, and S. Sremac, "A new model for determining weight coefficients of criteria in mcdm models: full consistency method (fucom)," *Symmetry*, vol. 10, no. 9, p. 393, 2018.

[25] M. Žižović and D. Pamucar, "New model for determining criteria weights: level Based Weight Assessment (LBWA) model," *Decision Making: Applications in Management and Engineering*, vol. 2, no. 2, pp. 126–137, 2019.

[26] J. N. Warfield, "Toward interpretation of complex structural models," *IEEE Transactions on Systems, Man, and Cybernetics*, vol. SMC-4, no. 5, pp. 405–417, 1974.

[27] E. Fontela and A. Gabus, *The DEMATEL Observer (DEMATEL 1976 Report)*, Battelle Geneva Research Center, Geneva, 1976.

[28] M. Subotić, B. Stević, B. Ristić, and S. Simić, "The selection of a location for potential roundabout construction–a case study of Doboj," *Operational research in engineering sciences: Theory and Applications*, vol. 3, no. 2, pp. 41–56, 2020.

[29] Y. C. Chuang, S. K. Hu, J. J. H. Liou, and H. W. Lo, "Building a decision dashboard for improving green supply chain management," *International Journal of Information Technology and Decision Making*, vol. 17, no. 05, pp. 1363–1398, 2018.

[30] H. W. Lo, C. C. Hsu, B. C. Chen, and J. J. Liou, "Building a grey-based multi-criteria decision-making model for offshore wind farm site selection," *Sustainable Energy Technologies and Assessments*, vol. 43, Article ID 100935, 2021.

[31] H. B. Ahmadi, H. W. Lo, P. Pourhejazy, H. Gupta, and J. J. Liou, "Exploring the mutual influence among the social innovation factors amid the COVID-19 pandemic," *Applied Soft Computing*, vol. 125, Article ID 109157, 2022.

[32] G. Koca and S. Yildirim, "Bibliometric analysis of DEMATEL method," *Decision Making: Applications in Management and Engineering*, vol. 4, no. 1, pp. 85–103, 2021.

[33] N. Osintsev, A. Rakhmangulov, and V. Baginova, "Evaluation of logistic flows in green supply chains based on the combined DEMATEL-ANP method," *Facta Universitatis – Series: Mechanical Engineering*, vol. 19, no. 3, pp. 473–498, 2021.

[34] D. Božanić, D. Jurišić, and D. Erkić, "LBWA–Z-MAIRCA model supporting decision making in the army," *Operational Research in Engineering Sciences: Theory and Applications*, vol. 3, no. 2, pp. 87–110, 2020.

[35] A. Bigazzi and E. Berjisian, "Modeling the impacts of electric bicycle purchase incentive program designs," *Transportation Planning and Technology*, vol. 44, no. 7, pp. 679–694, 2021.

[36] A. Shekhovtsov, V. Kozlov, V. Nosov, and W. Salabun, "Efficiency of methods for determining the relevance of criteria in sustainable transport problems: a comparative case study," *Sustainability*, vol. 12, no. 19, p. 7915, 2020.

[37] Ö. Simsekoglu and C. Klöckner, "Factors related to the intention to buy an e-bike: a survey study from Norway," *Transportation Research Part F: Traffic Psychology and Behaviour*, vol. 60, pp. 573–581, 2019.

[38] S. Haustein and M. Møller, "Age and attitude: changes in cycling patterns of different e-bike user segments," *International journal of sustainable transportation*, vol. 10, no. 9, pp. 836–846, 2016.

[39] K. Kazemzadeh and T. Koglin, "Electric bike (non) users' health and comfort concerns pre and peri a world pandemic (COVID-19): a qualitative study," *Journal of Transport & Health*, vol. 20, Article ID 101014, 2021.

[40] M. Herberz, U. J. Hahnel, and T. Brosch, "The importance of consumer motives for green mobility: a multi-modal perspective," *Transportation Research Part A: Policy and Practice*, vol. 139, pp. 102–118, 2020.

[41] L. A. Zadeh, "A note on Z-numbers," *Information Sciences*, vol. 181, no. 14, pp. 2923–2932, 2011.

[42] A. Gabus and E. Fontela, *World Problems, an Invitation to Further Thought within the Framework of DEMATEL*, pp. 1–8, Battelle Geneva Research Center, Geneva, Switzerland, 1972.
[43] M. Johnson and G. Rose, "Extending life on the bike: electric bike use by older Australians," *Journal of Transport & Health*, vol. 2, no. 2, pp. 276–283, 2015.
[44] K. Kazemzadeh and P. Bansal, "Electric bike navigation comfort in pedestrian crowds," *Sustainable Cities and Society*, vol. 69, Article ID 102841, 2021.
[45] S. Pejhan, M. Agelin-Chaab, M. Yusuf, and D. Eng, "Analysis of ebike dynamics and cyclists' anxiety levels and interactions with road vehicles that influence safety," *Accident Analysis & Prevention*, vol. 159, Article ID 106272, 2021.
[46] D. Oeser, A. Ziegler, and A. Ackva, "Single cell analysis of lithium-ion e-bike batteries aged under various conditions," *Journal of Power Sources*, vol. 397, pp. 25–31, 2018.
[47] J. X. Weinert, A. F. Burke, and X. Wei, "Lead-acid and lithium-ion batteries for the Chinese electric bike market and implications on future technology advancement," *Journal of Power Sources*, vol. 172, no. 2, pp. 938–945, 2007.
[48] F. H. Huang, "Exploring the factors influencing e-bike road safety: a survey study based on the experiences of Taiwanese cyclists," *International Journal of Industrial Ergonomics*, vol. 89, Article ID 103292, 2022.
[49] B. Lin and L. Shi, "Do environmental quality and policy changes affect the evolution of consumers' intentions to buy new energy vehicles," *Applied Energy*, vol. 310, Article ID 118582, 2022.
[50] Y. Ruan, C. C. Hang, and Y. M. Wang, "Government′ s role in disruptive innovation and industry emergence: the case of the electric bike in China," *Technovation*, vol. 34, no. 12, pp. 785–796, 2014.
[51] C. N. Huang and H. W. Lo, "A hybrid Z-based MADM model for the evaluation of urban resilience," *Mathematical Problems in Engineering*, vol. 2021, Article ID 9474753, 17 pages, 2021.
[52] F. C. Kao, S. C. Huang, and H. W. Lo, "A rough-fermatean DEMATEL approach for sustainable development evaluation for the manufacturing industry," *International Journal of Fuzzy Systems*, pp. 1–21, 2022, (In press).
[53] C. F. Liaw, W. C. J. Hsu, and H. W. Lo, "A hybrid MCDM model to evaluate and classify outsourcing providers in manufacturing," *Symmetry*, vol. 12, no. 12, p. 1962, 2020.
[54] Q. Wang, G. Jia, and W. Song, "Identifying critical factors in systems with interrelated components: a method considering heterogeneous influence and strength attenuation," *European Journal of Operational Research*, vol. 303, no. 1, pp. 456–470, 2022.